FSTC-HT-23-496-71

AD 742425

ARMY MATERIEL COMMAND

U.S. ARMY
FOREIGN SCIENCE AND TECHNOLOGY CENTER

BASIC THEORIES OF AIR CUSHION VEHICLES

by

Yu. Yu. Benya and V. K. D'yachenko

D D C

RECEIVED
MAY 31 1972

B

COUNTRY: WORLDWIDE

Approved for public release; distribution unlimited.

437

craft in England, France, Russia and the U.S.A. The design features of the more well-known craft in each of these countries are presented in detail, as well as a look at some experimental ACV's.

The remainder of the book deals with the major hydro-aerodynamic problem and theories, concerning these craft, and is aimed at the technical engineer or student of naval architecture. The physical features and characteristics of ACV's and the external forces which act on them are discussed in Chapter II. Static stability is the main topic of Chapter III, with some results given from the testing of operational ACV's for this quality. Speed and the forces of resistance to movement are probably the most important factors in the design of an ACV and its propelling agents--both are discussed in Chapter IV. Because of the nature of these type craft (riding on air cushions), maneuverability is quite different from conventional craft. The many problems surrounding this are examined in Chapter V. The obstacles incurred by a vessel on the open sea are many--roiling, pitching, decreases in speed due to increases in resistance, spray formation, etc. These, and other difficulties, are investigated in Chapter VI in connection with the seaworthy capabilities of various ACV's.

After finishing the book, a reader will hopefully want to delve deeper into certain subjects pertaining to air cushion vehicles. In anticipation of this, the authors have provided an excellent list of available reading matter from which they drew in writing the book. If, after this, the reader has any questions or suggestions concerning the subject, he is invited to write to the publishers of the book for further information.

ENGLISH TITLE: Basic Theories of Air Cushion Vehicles

FOREIGN TITLE: Osnove Teorii Sudov na Vozdushnoy Podushke

AUTHOR: Yu. Yu. Benya, V. K. D'yachenko, et al.

SOURCE. BASIC THEORIES OF AIR CUSHION VEHICLES

Translated for FSTC by Techtran

NOTICE

Foreword

Air cushion vehicles (ACV) have become, in a number of countries, a comfortable and profitable means of transportation. In connection with this growing interest, shipbuilders are concerned about questions of design and theoretical problems connected with the creation of an air cushion vehicle.

Over the past years, many works have been published which were devoted to questions of the speed, stability, maneuverability, and seaworthiness of the ACV. Basically, these were articles in journals, popular science pamphlets, and the reports of scientific conferences and symposiums. Some monographs were devoted to theories on the seaworthy quality of the ACV, which had not been created until recent times.

The idea, underlined in such monographs, belongs to Yu. Yu. Benya, but his untimely death did not allow him to complete the task that he had begun. Work on the book by Yu. Yu. Benya was continued by the co-authors.

In current treatises, as well as in basic local and foreign published materials by research writers, basic questions regarding theories of the seaworthy quality relevant to theories on vessels (speed, stability, control, seaworthiness) are summarized. The term "ship theory" may also be applied to air cushion vehicles. The authors entitled the monograph "Basic Theories of Air Cushion Vehicles."

In regard to the incomplete explanation in literature concerned with historical questions, the authors combined a necessary amount of sufficiently detailed historical information and gave consideration to its roles in local studies by engineers in the development of the ACV.

-1-

Taking into account the absence in contemporary literature of systematized data on the structure and design features in the construction of the ACV, the authors were forced to insert into the monograph a special chapter, from which a reader may draw information about ACV designs.

In writing the monographs, the authors sought to weigh the results of a test model and an actual ACV. They made use of the numerous foreign and local materials which dealt with the subject.

The historical information (introduction) and Chapter I was written by I. V. Ozimov, Chapters II and IV by V. K. D'yachenko, Chapter III by S. A. Smirnov, Chapter V by V. A. Litvinenko, Chapter VI by B. A. Kolyzaev. The materials of Yu. Yu. Benya were also used in the monographs.

The authors which to express their gratitude to book reviewers, Prof. A. N. Shmyrev and Candidate of Technical Science, E. F. Selyuzhenka, for providing their enormously helpful observations in reviewing the manuscripts.

The monographs represent the first attempt to systematize the complex theoretical problems concerning the seaworthy capabilities of the ACV, and the authors would greatly appreciate any observations by readers to be sent to this address: "Shipbuilding" Publishing House, D-65, 8 Gogol Street, Leningrad.

Principal Symbols

L - length of ACV.
B - width of ACV.
b - nozzle width.
H - hull height of ACV.
L_n - length of air cushions.
B_n - width of air cushions.
S_n - area of air cushions.
$h_{r \cdot o}$ - designed height of skirt.
$h_э$ - lift height of the hull above the screen.
$h_в$ - lift height of the hull above calm shallow water, while standing still.
h_V - lift height of the hull above calm shallow water, while moving.
h - lift height or increased clearance between the base of the skirt and the base surface of the water.
II - perimeter of the air cushions.
S - area of hull and skirt projections from midship surface.
$S_{бок}$ - area of hull and skirt projections from diametrical surface.
F - area of the propeller shaft.
F_r - area of the fan shaft.
α - cornering.
$α_1$ - coefficient of stop screw.
β - drift angle.
$δ_p$ - roll attitude.
θ - roll.
ψ - trim difference.
φ - yaw angle.
$φ_c$ - pitch angle.
Q - volume of expended air.
$\vec{V}$ - velocity at craft's center of gravity.
$\vec{V}_j$ - speed of air flow through areas of increased pressure.
$\vec{V}_a$ - absolute speed.
$\vec{V}_r$ - relative speed.
$\vec{w}$ - turning speed near center of gravity.
$\vec{r}$ - radius-vector points.
ρ - mass density of air.
ν - specific weight of water.
λ - lengthening of the foils or hull.
g - acceleration of forces of gravity.

q - rate of pressure.
dσ - element surfaces.
dU - element volume.
t - time.
ν - coefficient of kinematic viscosity.
G - weight of the ACV.
R_i - vector forces.

X_i, Y_i, Z_i - projection of the vector R_i on axial coordinates.

M_i - vector at the moment.

M_{xi}, M_{yi}, M_{zi} - projections of the vector M_i on axial coordinates.
cij - coefficients of force.
mij - coefficients at the moment.
$cij = dcij/dr$ - derived coefficient of forces.
$miy = dmij/dr$ - derived coefficient at the moment.
P - stop screw.
R - radius of circulation in the ACV.
T - draught.
T_c - kinetic energy.

H_p - total pressure for the fan.

p - pressure in ideal fluid.
P_p - full surplus pressure in the bag.

P_n - static surplus pressure in the air cushion.

$Fr = \dfrac{V}{\sqrt{gL_n}}$ - Froude number.

0, xg, yg, zg - fixed system coordinate.
0, x0, y0, z0 - mobile system coordinate, at beginning of movement over
            a calm surface.
0, x, y, z - mobile system coordinate, rigidly connected to the hull and
            at the beginning of its center of gravity.
0_1, x, y, z - mobile system coordinate, rigidly connected to the hull and
            at the beginning of the basic flatness of the hull.
0, x_1, y_1, z_1 - high speed system coordinate.

x_1, y_1, z_1 - current coordinates.

m - mass, tonnage.

Introduction. Development of the Structural Design of the ACV.

The development of a high speed transport craft which combines superior seaworthiness with a new principle of propulsion is gaining great attention.

At the present time, there are two basic directions in which to go to solve the problems in the creation of a high speed transport craft.

The first direction is in the application of hydrofoils, mounted on posts under the hull. The force created by the movement of the foils completely lifts the craft from the water, decreasing resistance to the craft's movement caused by waves striking the hull. This permits higher speeds and superior seaworthiness for the hydrofoil, compared to the usual displacement and gliding quality of conventional craft.

The second direction is in the use of air cushions, i.e., layers of compressed air, created under the hull with the aid of special force pumps or running an air stream over the water or land surface (and supporting the hull).

A craft in which the lifting force for the total rate of movement is created by special force pumps is called a craft with static air cushions, or simply an air cushion vehicle (ACV).

A craft in which the lifting force for the basic rate of movement at the screen is created by running an air stream under high speed pressure is called a screenplane, or aerodynamic air cushion vehicle. The possibility of a hybrid type of craft has not been excluded.

In the aerohydrodynamics of the screenplane, however, there are a great number of features which distinguish it from the static air cushion craft, and so, in this present work, it is not considered.

When the hull of the ACV does not make contact with the water, or its contact is at a minimum, the resistance of friction and wave resistance is sharply decreased since lifting the hull above water under the influence of air cushions weakens the blows of the waves. Because of this, the possibility exists for creating an ACV with a speed of about 100 knots.

The first area has been studied sufficiently well at the present time, and many hydrofoils are now successfully operating on rivers and on the seas. Investigation of problems connected with the creation of hydrofoils have been covered by special literature.

The second area has been studied to a somewhat lesser degree, although after 50 years, it now attracts the attention of many scientific research organizations. For the past decade, both in our country and abroad, large successes in the areas of theoretical and experimental research into questions of aerohydrodynamics and the durability of the ACV have been attained through the construction of many comparatively large experimental test craft and devices. In the last 2-3 years, in England, construction of a series of small passenger craft and cargo transports led to the creation of the first large ACV of similar design with a displacement up to 168 tons (the SRN4). Design studies show a technical possibility of creating an ACV with a displacement of up to 1,000 tons and more. However, in contrast to hydrofoils, the ACV is in the early stages of development, in which many scientific and technical problems must be resolved.

The reason for the lag in development of the ACV, as opposed to that of the hydrofoil, is that the creation of the ACV was found to be a more technically complex task and became possible only after progress was made in associated fields of engineering, particularly in mechanical engineering, automation, and others. With the creation of hydrofoils, it was found possible to utilize the already perfected practical forms of hydrofoil bodies and the basic propelling agent, propeller screws. Therefore, the number of possible technical decisions were restricted to fundamental selections of hydrofoil systems, with an arrangement of propelling agents and methods of transmission that would begin operating simultaneously with the engines.

The ACV required a totally new form of body, which would be able to create and retain the air cushions beneath it. In connection with this design, where the hull interacts with the water's surface by way of an air cushion, new solutions are needed for problems of stability, control, durability, etc. For this reason, the number of possible technical solutions are great and the choice of an optimum type of ACV itself presents a complex task.

In regard to the weight of the ACV, there arises the necessity to create light and simple construction materials for the body construction, a force pump to be installed for creating the air cushions, light highly--economical engines with various methods of transmission of power to the propellers and force pumps, new types of engines, etc. Construction of a practical ACV requires the creation of new fields in shipbuilding, just as the creation of the helicopter did in aviation.

The idea of using air to decrease resistance to the craft's movement is over 200 years old. In 1716, a Swedish scholar, Emmanuel Swedenborg, proposed the construction of a device, supported over a base surface with the aid of an air cushion (Figure 1). The apparatus was to have a dome-shaped, elliptical form and a body consisting of a light wood frame, covered with sail-cloth. The author proposed to force under the body of the apparatus the air needed to propel it with the aid of two paddles revolving on a horizontal axis and powered by men. The crew of the apparatus would be placed in an open cabin in the center of the dome. Swedenborg noted that the muscle-energy of man was insufficient to create air cushions under the apparatus and indicated that his idea might be realized in conjunction with the future development of engineering. Emmanuel Swederborg's apparatus might be looked upon as the prototype of the contemporary ACV [68].

Around 1853, lvanov, an architect in charge of the Archangel provincial Construction and Roads Commission, proposed the creation of a "tri--keel air boat" - a craft "which, with the aid of air machines, would force air under its bottom and it could float along with considerable speed against the wind and thrust of water." As to the quality of the force pump in the design, it was suggested that two pairs of "cylindrical bellows," pumped by two men, be utilized. In essence, this was the first known proposal of "air lubrication," that is, the creation of a thin gaseous layer on the bottom of the craft. Ivanov's proposal was declined by project departments and cast aside; realization of this plan, without a corresponding force pump and engine, was deemed impossible.

In 1865 Scott Russell, in his book "Current Systems of Naval Architecture," and ten years later, William Froude, also proposed the use of air lubrication on a craft. William Froude considered it especially expedient to employ air lubrication of a craft being much wider or circular in form such as Russian ships of the "Popovka" class.

The first patent for the use of air lubrication on a craft was issued in England to a Swedish engineer, Gustav Lavalle, in 1882. Based on Lavalle's proposal, a small test craft with an air-lubrication design, was constructed. The air under the bottom moved across numerous openings in the stem, but failed to achieve a uniform distribution of air layers beneath the hull with practically no decrease in the resistance of friction to the craft and a speed which did not exceed 12 kilometers per hour. Construction of a second launch, in which a more powerful engine would have been provided, was never completed by Lavalle.
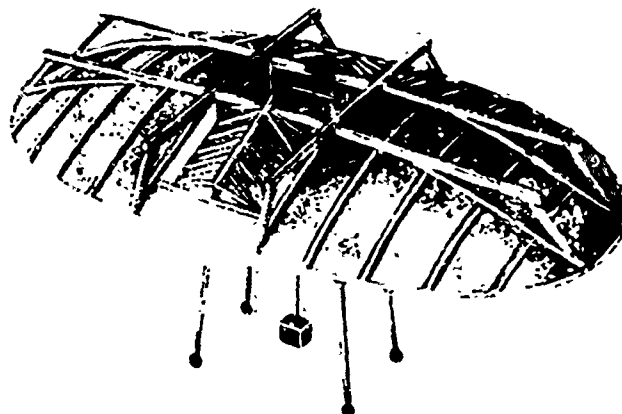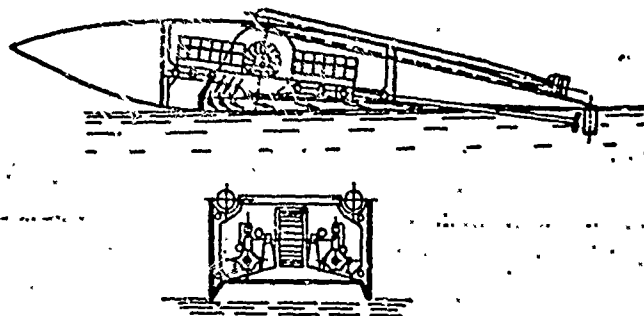
Figure 1.   The Apparatus of E. Swedenborg

Figure 2.   An Air-Cushioned Motor Torpedo Boat by D. M. Von Tomamhul.

In the following years, inventors and scientists at home and abroad repeatedly turned to the idea of using air lubrication on their craft to decrease the resistance of friction and increase the speed. Leslie Heyward, author of the pamphlet "History of Air Cushioned Vehicles," circulated in London in 1963, contended that more than 100 patents existed for designs of air-lubrication craft. During the late 19th and early 20th century, many experimental craft which utilized the air-lubrication

DOCUMENT CONTROL DATA - R & D

(Security classification of title, body of abstract and indexing annotation must be entered when the overall report is classified)

1. ORIGINATING ACTIVITY (Corporate author)	2a. REPORT SECURITY CLASSIFICATION
Foreign Science and Technology Center US Army Materiel Command Department of the Army	Unclassified
	2b. GROUP

3. REPORT TITLE

BASIC THEORIES OF AIR CUSHION VEHICLES

4. DESCRIPTIVE NOTES *(Type of report and inclusive dates)*

Translation

5. AUTHOR(S) *(First name, middle initial, last name)*

Yu. Yu. Benya, V. K. D'yachenko, et al.

6. REPORT DATE	7a. TOTAL NO. OF PAGES	7b. NO. OF REFS
October 1971	423	N/A

8a. CONTRACT OR GRANT NO.	9a. ORIGINATOR'S REPORT NUMBER(S)
b. PROJECT NO.	FSTC-HT-23-496-71
c. T702301 2301	9b. OTHER REPORT NO(S) (Any other numbers that may be assigned this report)
d. Requester Dibbern/AMXST-GET	

10. DISTRIBUTION STATEMENT

Approved for public release; distribution unlimited.

11. SUPPLEMENTARY NOTES	12. SPONSORING MILITARY ACTIVITY
	US Army Foreign Science and Technology Center

13. ABSTRACT

This is a unique book, considering the textbook title, because the authors have succeeded in blending general information about air cushion vehicles (background information such as history, basic features of designs, and prospects for their development by the major sea powers of the world) with detailed studies of the major hydro-aerodynamic problems encountered by design engineers (concerning theories in the areas of speed, stability, maneuverability and seaworthy capabilities of these strange, new craft). The result is a combination formal-informal guide which will enthuse, as well as inform, both students and technical engineers of the shipbuilding industry.

The preface serves to introduce the reader to the reasons for writing this book, and to acknowledge the work of the many people who made the book possible. Following this, there is an explanation of the principal symbols used in the theories concerning air cushion vehicles and their features.

The authors give a short history of air cushion vehicles in Chapter 1. The important thing to note here is that they are quick to weed out hydrofoils, monorail trains, and other craft which employ air cushion systems, so that they might concentrate strictly on naval craft which employ plenum chambers, peripheral flexible skirts, or captured air bubble systems. The reader can appreciate this limitation as the authors dig into the development of these type

14. KEY WORDS	LINK A		LINK B		LINK C	
	ROLE	WT	ROLE	WT	ROLE	WT
Air Cushion Vehicle						
Aircraft R and D						
Aerodynamics						
ACV Flexible Skirt						
Aircraft Engine Auxiliary Equipment						
Aircraft Design						
Aeronautic Engineering						
Hydrodynamics						
Shipbuilding Engineering						
Ocean Transportation						
Test Model						
Combatant Hydrofoil						
Ship Structural Component						
Structure Form						
Shipbuilding R and D						
Navigation Equipment						
Air Transport						
ACV Lift Fan						
Fluid Mechanics						
Aerodynamic Force						
Aircraft Maneuverability						

COSATI Subject Code: 01, 13, 20, 21
Country Code: UR, UK, FR, SZ

system were built. In the Soviet Union, investigation into this area occupied the minds of N. N. Kabachinski, L. M. Lapshin, L. G. Loitsyanski, K. K. Fedyaevski and others. Until modern times, however, air-lubricated craft were not widely accepted, apparently because of the small gains in overcoming the full resistance on the craft in calm waters and especially in waves. Soviet scientists, through investigation, established that by making the most efficient use of the craft's hull, the system of air lubrication worked well enough to reduce the resistance of friction on the bottom up to 60%. Data from a tested model showed that, in barges with a freight-carrying capacity of 3,000 tons and in waves of state 3 sea conditions, full resistance was decreased 23-26% at speeds of 16-18 kilometers per hour [3].

In contrast to the air-lubricated craft, the ACV is supported above the water by a layer of compressed air of considerable thickness, which permits the reduction of not only resistance to friction, but also wave resistance. In regard to speeds attainable, the ACV can reach much higher speeds than air-lubricated craft.

One of the first ACV's, a motor torpedo boat, was built in 1916 by D. M. Von Tomamhul for the Austrian Navy (Figure 2). Essentially, Tomamhul's torpedo boat is a hybrid type, combining air lubrication with the so-called chamber method of forming an air cushion. A chamber is formed by the flat bottom, the side walls, and the bow lines. The height of the chamber, however, was still not very great, considering what possibly might wash against the bottom in waves. A centrifugal fan and four engines, with a total of 480 horsepower to drive the screw propellers, were installed on the launch to create the air cushion. During tests, the craft developed a speed of 40 knots, but further development of Tomamhul's design was not made. The costly construction of the launch was probably the basic reason for stopping work on it. The craft was not very seaworthy, when one considers the loss of speed in the waves, the lack of the necessary engines and testing of the boat's construction.

Shortly thereafter, in 1921, a French inventor, M. A. Gamben, proposed a large barge to be operated on an air cushion (Figure 3). The fans were arranged in the bow sections and permitted the pressure head of the accumulated air stream to be utilized. To improve lift above waves and to protect the fan from the blows of the waves, a special buoyancy in the bow was provided. To improve the distribution of the air stream in the chamber and for stability, Gamben suggested the installation of fore and aft keels along the whole length of the chamber. Gamben maintained that his craft could be operated on unnavigable rivers and in shallows, but his proposal was never realized. The insufficient design of Gamben's craft was similar to that of Tomamhul's. An interesting patent was issued to V. F. Casey of the

-9-

United States of America, in 1925 (Figure 4). An air chamber under the craft's hull was separated by fore and aft keels, which improved the craft's stability. Air in the chamber was pumped by the centrifugal fans through a transverse nozzle in the bow, creating an air gate from the air cushions in the craft's stern section. Since the air was recirculated, the power of the engines could be lower for creating the air cushion. V. F. Casey was one of the first to propose the use of a system of recirculation in creating an air cushion.
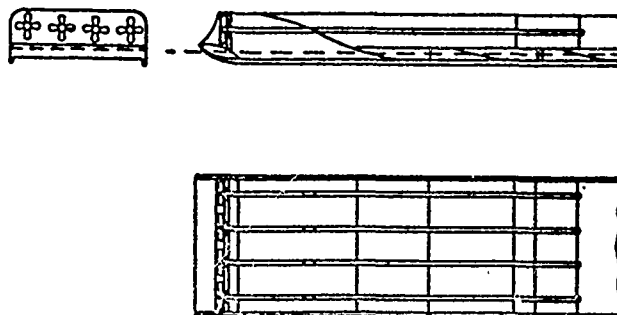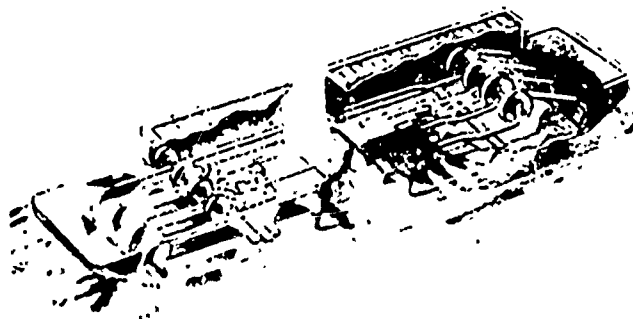

Figure 3.   The ACV Design of M. A. Gamben

Figure 4.   The ACV Design of V. F. Casey

A large contribution in the development of the ACV was made by the noted Russian scientist K. E. Tsiolkovski, who for the first time, in 1927, substantiated theoretically the principle of moving on an air cushion, in his work "Air Resistance and the Express Train" [54]. K. E. Tsiolkovski submitted a design for a train which would ride on a cushion

of air along a special type of strip and expressed a formula for determining the power necessary to create the air cushion and movement (depending on the wieght of the train, the pressure in the cushion, and the height of the lift) which is still basic to current theories on ACV's.

Further development of K. E. Tsiolkovski's ideas and their practical application for designing and building an ACV was made by another Soviet scientist, Professor V. I. Levkov of the New Circassian Institute [4, 40]. Beginning by testing models in the aerodynamic laboratory of the New Circassian Polytechnical Institute in 1927, V. I. Levkov later became head of the construction bureau for designing ACV's and held that post until 1941. Under the direction of V. I. Levkov, several craft were developed, the largest of which had a displacement of about 15 tons. The first ACV, the L-1, was powered by two 140 horsepower piston engines and was successfully tested in 1934-35 over water, snow, and land.

A distinctive speed record was set in 1937 by the L-5 ACV (Figure 5). Bearing a weight of about 9 tons, it reached the unprecedented speed for its day of about 73 knots in trials over a measured mile.
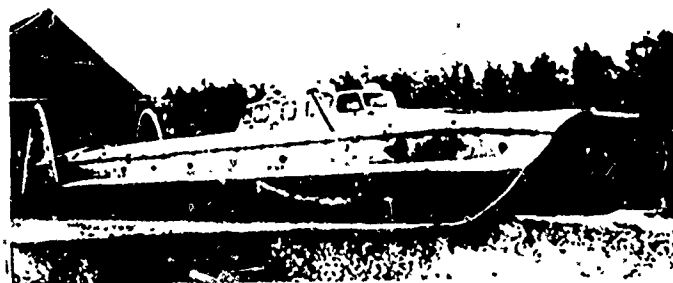

Figure 5. The L-5 ACV of Professor V. I. Levkov

The design of the craft had been devised for weights up to 30 tons, but the war prevented its realization. Work on the problem was interrupted and the launch was lost during a trial run on the Baltic.

Thus, it is to V. I. Levkov and the association which he headed that the merit for creating the first native ACV must be given; their investigations, long before those in the west, showed the prospects of utilizing ACV principles in shipbuilding.

The heavy blow of the war to the national economy of the Soviet Union, the insufficient development of the power base in the prewar and initial postwar years and, in particular, the lack of a vented-steam gas turbine, a transmission for cornering, special pumps, etc. stopped V. I. Levkov from going ahead with the creation of a large-scale ACV.

The distinctive features of V. I. Levkov's ACV were: the under-
-dome space (air chamber) for high elevation, formed by the flat bot-
tom and side profiles of the hull, the buoyancy pro-
vided to the launch, its stability in moving on a cushion of air.

The craft was a catamaran type, with an open flow of air through
the cushions in the bow and stern. The hull of the launch was made of
duraluminium; piston aircraft engines were used; the pumps served
twin-bladed screws -- the propelling agents; and rotary shutters were
arranged under the pumps.

A number of considerable deficiencies were revealed in the trial
run of the launch. In particular, there was the insufficient sea-
worthiness of the craft due to the wake of the aircraft engines and
blows by the waves set up by the shutters, which brought the engines
to a halt and broke the shutters. Optimum performance was at state
4 sea conditions; there was intensive wash on the decks and into the
wheelhouse at full-stop and at slow speeds, because of air blowing
in the bow through the open tunnel; a large sail and a strong wind drift
brought about poor control at slow speeds.

An English radio-engineer, C. Cockerell, received a patent (#854,211)
in 1955 on the design of an ACV, differing in that the cushion under the
hull of the device was protected by an air screen, flowing from a ring
(periphery) of nozzles (Figure 6). This method, named the peripheral
annular jet system, proved more effective than the chamber method and
provided for a more frugal expenditure of power in attaining more lift
(about 150-300 millimeters versus 10-20 millimeters in the chamber method).
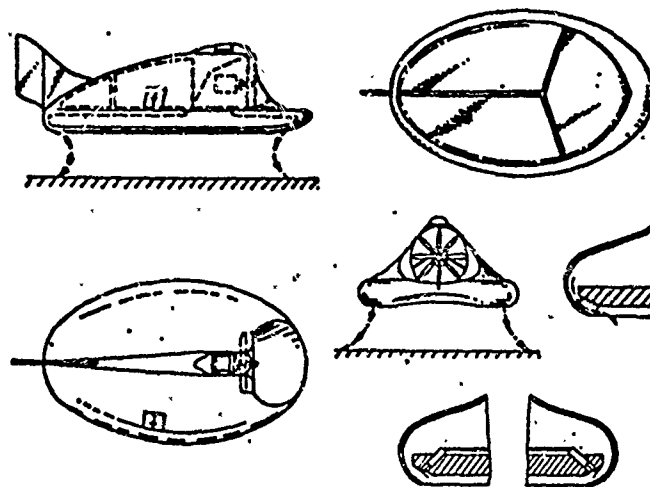
Figure 6. The Original ACV Design Proposed by C. Cockerell

We note that, two years prior to C. Cockerell's patent, G..S. Turkin of the Gubkina Oil Institute obtained an author's certificate (#6755-MRF 8 October 1953) for "A Cross-Country Air Cushion Transport Vehicle" [40]. As a follow-up to his idea, G. S. Turkin constructed a light experimental machine which utilized an annular jet system to form the air cushions. The untimely death of the inventor, however, broke off further investigations into this area until reports of work on peripheral annular jets began to appear.

Beginning in 1953, a similar investigation of peripheral annular jets was carried out in the U.S.A. in connection with studies of VTOL aircraft.

By 1959, theoretical and experimental investigation into the aerohydrodynamics of ACV's with peripheral annular jet systems had been carried out by: the N. E. Zhukovski Central Institute of Aerohydrodynamics in the Union of Soviet Socialist Republics, in the D. Taylor Test Basin and the Langley Aerodynamic Laboratory in the U.S.A., the National Physics Laboratory in England, the National Science Research Commission (ONERA) in France, and other organizations.

In England, in 1959, the first experimental ACV, with dual-contour annular jets, was built according to C. Cockerell's design -- the SRN1. The search for a design, which would solve the problem of creating air cushions while decreasing the expenditure of power, had ended just in time. The basic concept would decrease the loss, connected with air flowing into the atmosphere and would reduce the expenditure of air through the fans and then ejected into the atmosphere. To cope with the first problem, the inventors had proposed various systems of recirculation and an intricate filtration system; in dealing with the second problem, an ejection mechanism would be used. A large number of patents on recirculation systems were obtained by C. Cockerell. Some diagrams of jets designed for various systems of recirculation are shown in Figure 7.

A Swiss engineer, Karl Wyland, obtained a patent in 1957 for an ACV design which had an intricate filtration system. Two self-propelled craft, with more intricate filtration systems, were built by K. Wyland in 1959 -- bearing the name "Ilen." It measured 10 × 9.2 meters, weighed about 7.5 tons, had two 700 horsepower engines, and six fans installed vertically on the craft's bow oriented to meet the oncoming stream of air. During the trials on Lake Zurich, the craft reached speeds of 52 knots and was purchased by the U.S. Navy for research purposes. Its future is unimportant. Another of K. Wyland's crafts was operated during a storm.
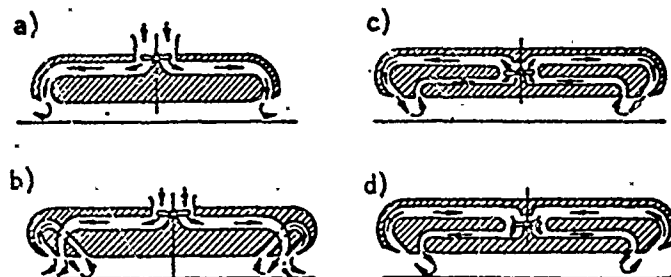
Figure 7. Diagrams of Nozzle Mechanisms with Various
Systems of Recirculation: a, a simple single-con-
tour jet; b, a system with circulation through an
open-curve contour (80% circulation); c and d,
systems with circulation through a closed-curve
contour (100% circulation) in various directions.

Testing of the recirculation system in models, under laboratory
conditions, showed that it decreased significantly the loss of power
in creating air cushions (in an efficient design, almost 1/2). How-
ever, practical applications of recirculation systems, intricate
filtration systems, and also ejection mechanisms, were never found
for contemporary ACV's. First of all, their designs were too complex
and their operation, in natural conditions, too unreliable; second,
the appearance of skirts in design changes made a system of
recirculation useless.

The trial runs of the first experimental ACV's, particularly the
SRN1, showed that the basic inefficiency of the annular-jet type craft
seemed to be its small degree of seaworthiness. During operation over
waves, an increase in resistance to movement was observed. This was
due to the sharp blows of the water against the hull, the wave heights
being 0.6 meters and the height of the air cushions only 0.3 meters.
Investigation showed that, for normal operation of a high-speed craft
over high waves, the lift of the hull over the surface must be perfectly
level with the wave height. In statistics, for example, in the English
Channel wave heights never exceed 1.2-1.5 meters 90% of the time during
a given year. Consequently, for an ACV to operate in the English Chan-
nel, or in coastal regions, the minimum possible lift of the hull must
be 1.2-1.5 meters. It was shown that to provide such lift by means
of a chamber or annular-jet system was impossible because of the sharp
increase in power necessary to create the air cushions. A search was
begun for new ways to increase lift height. Further development of
the ACV branched into two basic directions and two classes of craft
emerged, Class A and Class B.

Separating ACV's into two classes is conventional, to a degree, and reflects our present-day handling of the development of these new means of transportation. This proposed separation might be changed in the future by new, original designs, or by hybridization of present designs -- the concept is still quite young.

Class A. The invention of flexible "skirts" for ACV's was the primary technical solution to the problem of seaworthiness of light-weight ACV's. Practical work on the creation of the skirts was begun in 1959 by the English firm of Westland Aircraft. The Westland firm now holds a large number of patents on skirt designs. Extensive work in this area was also done by another English firm, Vickers-Armstrong, who also hold a number of original patents. In general outline, development of the flexible skirt may be presented in the following form. Originally, the flexible skirt appeared as a massive strip, establishing a perimeter around the air cushions (Figure 8a). The flow of air from the air cushions took place under the lower edge of the barrier. The height of a barrier, of the type fixed on the ACV SRN1, never exceeded 15 centimeters and not prove very seaworthy. Providing stability while increasing height was impossible.

The next advance was the invention of flexible skirts, consisting of two strips, and appearing as a continuous wall of riged nozzles (Figure 8b). The shape of the flexible jets was maintained with the help of a diaphragm and a chain drive in the lower part and its inclination in a vertical plane, with the assistance of corresponding guy-wires to the bottom. The height attained by the barrier was 0.6 meters. This design ensured the flow of air from the cushions, permitting an increase in hover gap. A drawback to this design was the large amount of hydraulic waste connected with increasing the length of the jets; it was impossible to create barriers with large heights, because stability was difficult to ensure and there was little pliability to the barriers when moving over waves, causing an increase in resistance and a drop in speed.

Further improvement in the designs of flexible skirts brought about the creation of flexible bags, ending in short flexible jets (Figure 8c). Such a design allowed the profile of rigid jets to be discarded; flexible jets of great length were also no longer necessary, thus avoiding hydraulic waste. The design ensured stability, while increasing the height (e.g., up to 1.2 meters). It ensured the flow of air from the cushions and, consequently, attained an acceptable hover gap.

Deficiencies in this type of barrier were: difficulty in repair or replacement of damaged sections of the skirt and, as in the previous case (Figure 8b), very little pliability in moving over waves.
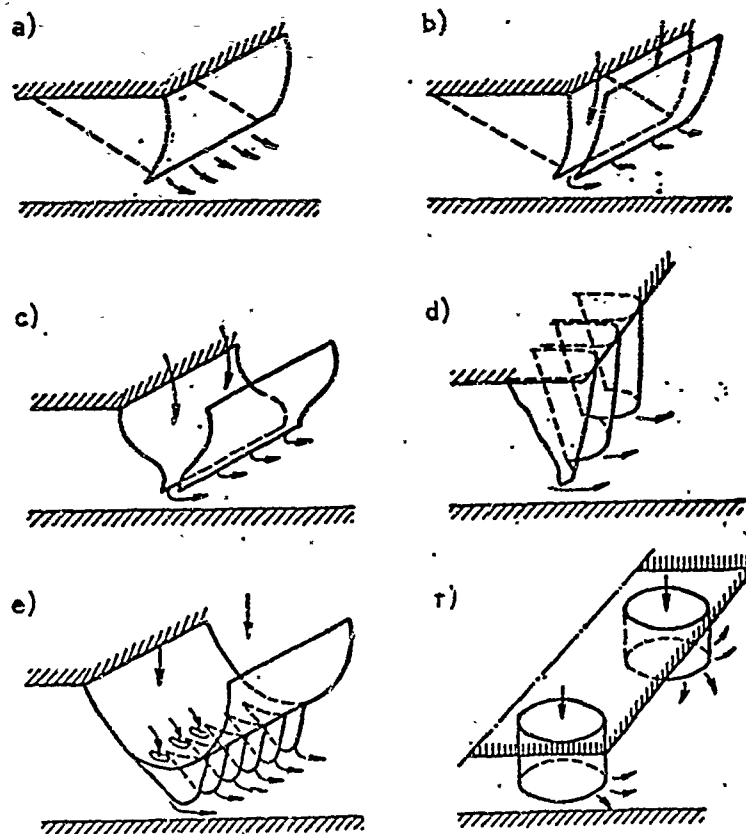
Figure 8.: Principal Diagrams of Flexible Skirts.

The next stride in the development of flexible skirts was an attempt to remove these deficiencies. This led to the creation of a segmented skirt (Figure 8d). This skirt was made up of separate elements, allowing quick replacement in case of damage, and possessing great pliability in contact with water. Difficulties again arose, however, in ensuring stability.

Later, easily removable fingers were installed on the flexible bags (Figure 8e), which permitted consolidation into one design of such qualities as: decreased hydraulic waste, stability and, therefore, an increase in height, an acceptable hover gap, quick replacement of damaged elements and, finally, a good performance quality in the craft.

The increased heights also demanded new solutions in design to ensure stability and, through exploitation of the flexible skirt design, distribution of air cushions into sections (one of the types is shown in the lower portion of Figure 32).

Flexible skirts increased the seaworthy quality and amphibious capability so much that soon after their development, the English firm of Westland Aircraft was able to move on to construction of the SRN5/SRN6 series of ACV's, with a seaworthy capability in state 3-4 sea conditions and, finally, the 168 ton SRN4, with a seaworthy capability in state 4-5 sea conditions.

An original design of a flexible skirt, in the shape of a series of closed cylindrical chambers with air in each chamber below the water mark, was worked out by the French firm Bertin (Figure 8f). A line of experimental small craft and ACV's with flexible skirts of this type was created.

Contemporary designs of flexible skirts, apparently, are still far from perfect. In future development of designs and materials, as well as through research, there lies a good chance for improving the performance and seaworthiness of all ACV's.
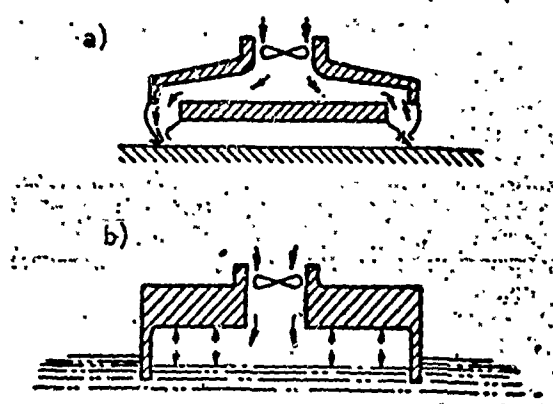

Figure 9. The Principal ACV Designs: a, Class A; b, Class B.

All ACV's with a peripheral skirt design fall into Class A (Figure 9a). The maximum displacement for craft in this class is difficult to determine at the present time. It is possible that, in the near future, craft of this class with displacements of about 500 tons and a seaworthiness in state 4-5 sea conditions will be created.

Class B. The replacement of skirts throughout a craft of any great size, designed for sea and oceanic navigation, added to the already complex problem. A craft capable of moving over waves in about state 6 sea conditions means replacement of skirts 4-6 meters high. This made it necessary to create highly durable, elastic materials -- -- a problem which was difficult to solve. ACV's with skirts required high-powered instrumentation (about 70-100 horsepower per ton), which also posed a problem in craft of great weight. Proposals were made, therefore, to increase the speed and maintain seaworthiness with a minimal expenditure of air. Lower resistance was ensured because of the decrease in drag from wetting, and seaworthiness was increased because of the lift over water. To ensure minimal expenditure of air and a decrease in the power necessary for lift, the cushion was confined by partially-submerged rigid (pliable) walls or narrow hulls (keels)[1], and were constrained at the two ends by flexible skirts or by rigid mechanical flaps of various designs. The greater the lift height while moving, the larger the size of the craft could be. The power output necessary at speeds of 40-50 knots, in this respect, was 35-40 horsepower per ton.

Essentially, craft of this type were merely modifications of the craft created by V. I. Levkov, which utilized a plenum chamber to form the air cushions. They differed from V. I. Levkov's craft in that, the lateral wall (keel) was not completely lifted above the water's surface, i.e. in ideal conditions there was an absence of air flow from the cushions. In regard to this, the designers deliberately decreased the maximum speed and the amphibious capabilities, in order, to decrease the power necessary to create the air cushions and to make it possible to replace the screw propellers or water-jet system.

An ACV with a partial-lift design (or, as a craft of this type is sometimes called, with partial-transfer of air cushions for lift) was worked out and thoroughly tested in the Soviet Union by an engineer, B. P. Ushakov, in 1939-41. Realization of this project was prevented by the war.

During the postwar years, work on this type of craft and craft with full-lift capabilities was undertaken by V. I. Levkov (until his death in 1953), Yu. Yu. Benya and, in succeeding years, a group from the N. E. Zhukovski Central Aero-hydrodynamic Institute (I. P. Lyubomirov, V. I. Khanzhonkov and others), the Central Technical Design Bureau of the Ministry of the River Fleet (chief designer -- V. A. Lipinski), the "Volga-Baltic Ship Project" Design Bureau (chief designer -- V. K. Zoroastrov), and others in the Soviet Union.

---

[1] This is sometimes referred to by foreigners as skegs, and a craft of this type, as skeg-type or sidewall vessel.

In England, rigid side-wall craft were built by the Denny firm in 1959, and by Hovermarine Ltd. in 1966.

In the U.S.A., immersed-sidewall ACV's called CAB vehicles (captured air bubble) were investigated by the Booz-Allen Applied Research Company, and scientific research was carried out by the Naval-Air Center in the D. Taylor Test Basin. One should note that, in the U.S.A., design work on crafts with displacements up to 5,000 tons has been completed and programs for the development of CAB type craft have been put together, which permit the creation of experimental craft of the CAB type with a displacement of 500-1,000 tons by the 1970's (a program is being directed by the Merchant Marine, but the U.S. Navy also has a program) [83].

Publications with similar information, for dissemination abroad, are often sensational and should be reviewed critically.

Craft with rigid and flexible immersible sidewalls, partial lift, and equipped at the ends with flexible skirts or rigid mechanical flaps of various designs fall into Class B (Figure 9b).

In aiming for a craft of this class, development of the Class A craft is lagging behind. This lag is explained by the advantages of the Class B craft: high speed (40-50 knots) with a moderate expenditure of power, an increase in the seaworthy capability, and voyages of any great distance could only be made by craft with large displacements.

The creation of such craft is, in itself, a complex scientific-technical task which requires solutions to many problems now being studied.

Chapter I. Design Features of Air Cushion Vehicles

§1. The SRN1 and SRN 2

The first experimental ACV, the SRN1 (Figure 10), was built in
England in 1959, according to the design of engineer C. Cockerell, by
the Saunders-Roe Division of Westland Aircraft. Five years of testing
and research on peripheral annular jets, used by C. Cockerell for
creating and maintaining air cushions, was being realized. The SRN1
was destined to become the forerunner of a whole series of craft, with
the first two letters designating the name of the firm's division
[80]. All of these ACV's are regarded as Class A craft. The ex-
perience gained in the building and testing of the SRN1 was used by
all foreign firms in constructing their ACV's.

The Westland firm soon became a large producer of these
craft. Meanwhile, other English firms were working toward creation
of an ACV, e.g. Vickers-Armstrong, Britten-Norman, and Denny Hovercraft.

In 1966 a new company, British Hovercraft Corp., was formed by
stockholders such as Westland Aircraft and Vickers and the National
Corporation for Research and Development. The company was created
for the purpose of channeling all the economical and technical re-
sources of British industry into one area -- the creation of
air cushion devices, doing away with unnecessary
duplication of efforts. Craft designs put out by the new company
bore the designator BH as the first two letters of their names.

The hull of the SRN1 was an oval platform, 9.2 meters long and
7.6 meters wide, with a vertical cylindrical shaft set in the center.

A six-bladed fan with a diameter of 3.1 meters was located inside the shaft and was powered by a 435 h.p. Olvis Leonides piston aircraft engine. Compressed air, flowing under the bottom through the dual--contoured peripheral jet, created two concentrated air gates to protect the air cushion. The jets were inclined at 30° angles to the base. Originally, the propellers maintained side air channels, permitting the use of a jet-traction of the compressed air coming from the fan. Utilization of this system allowed speeds of 25 knots for a fully loaded craft of 3.9 tons.

The hull of the craft was made light, yet strong, by using rivets and spot-welds. A cabin for the driver and one passenger was situated in the bow area. Control of the craft was accomplished with the aid of vertical rudders, working in the air-flow from the air channels.

Figure 10. The SRN1 Crossing the English Channel in 1959.

The ACV SRN1 first crossed the English Channel in 1959, covering the distance of 48 kilometers in about two hours. The test of the SRN1 showed the possibility to shipbuilders of using the air-cushion principle in their craft. There were, however, a number of serious deficiencies in the design. Among these deficiencies were: a small degree of seaworthy capabilities, very little jet-traction of the compressed air, a general lack of accommodations, etc. Various skirt designs, with heights up to 1.2 meters, were worked out in later years which increased the seaworthy capabilities of the ACV. Problems, with regard to lightness, stability, control, etc., were also investigated.

A turbo-jet engine, with a draught of up to 680 kilograms of force, was installed which brough the weight of the SRN1 up to 7.0 tons and the speed up to 62 knots. Additional scientific research, plus the results from testing the SRN1, permitted the firm to proceed with the creation of the first experimental passenger ACV -- the Class A SRN2, which was completed in January of 1962 (Figure 11). The main reason for designing the SRN2 was to study the operational qualities of the new type craft and to smooth out the fan and engine units, the control system, the skirts, etc.
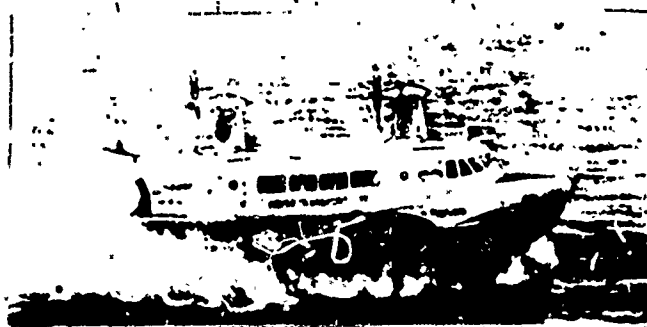

Figure 11. The Air-Cushion Vehicle SRN2.

The hull of the SRN2 was oval with a pointed bow, which improved the seaworthy capability of the craft. The full weight of the craft was 27 tons, with accommodations for passengers in the mid-section of the craft (seats for 70 people) or 6.5 tons of freight could be transported. The basic characteristics of the SRN2 are given in Table 1.

The wheelhouse was located in the bow section of the craft. In the stern section was the machinery compartment, in which the four main engines (two pair of Blackburn A-129 Nimbus helicopter gas turbines, with a maximum power of 970 h.p. and a rated power of 815 h.p.) were mounted. Each pair of engines led to a fan and an air screw. The drive was accomplished through a general reduction gear, a horizontal and vertical shaft and an angular reduction system of the transmission. A diagram of a similar gear is shown in the lower portion of Figure 15 for the SRN3 A mechanical drive, worked out for the SRN2 in the same form as a helicopter's, proved successful and was utilized in all the following craft.

Air to all the engines entered the machinery compartment through special filters arranged along the sides, which separated the sea water and spray from it.

TABLE 1. PERFORMANCE AND TECHNICAL FEATURES OF EXISTING ACV's.

English Craft

Performance and Technical Features	SRN2	SRN3	SRN4	SRN5	SRN6	BH-7	BH-8	BH-9	D-2M*	HM-2	HM-4	VT-1
Length, m	19,7	23,5	39,7	11,8	14,8	23,5	29,3	—	25,5	15,5	48,8	29,1
Width, m	9,0	9,3	23,5	7,0	7,0	13,9	17,0	—	5,9	6,1	20,7	13,6
Air Cushion height, m	6,4	9,8	13,0	3,9	4,6	10,1	9,8	—	—	3,7	9,1	9,5
Weight, tons: empty	—	—	103,1	4,1	5,2	31,0	—	—	—	—	—	50,8
full	27,0	37,5	167,6	6,7	9,1	48,0	91,4	25	29,0	16,0	127,0	77,0
maximum	—	42,5	187,9	7,7 (9,1)**	10,5 (12,8)**	50,8	101,2	—	—	16,4	—	86,2
Seating capacity, people	70	—	670	18	38	180	280	—	70	60—70	350 (+6 Automobiles)	322
Cargo capacity, tons	6,5	14,0	До 85	2	3	~15	35,6	9—14	5	5	60	21,3
Air cushion area, $м^3$	75,4	112	682	48,3	62,5	—	—	—	~110	—	—	335
Pressure in cushions, kg/m^2	366	335	245	138	147	220	—	—	~260	244	—	230
Skirt height, м	1,2	1,2	2,1	1,2	1,2	1,7	—	—	—	—	—	1,7
Mechanical power h.p.: maximum	4×970	4×1050	4×4250	1×1050	1×1050	1×4250	2×4250	2×1050	2×270 2×180	2×320 1×185	—	2×2000
cruise	4×815	4×900	4×3400	1×900	1×900	1×3400	2×3400	2×500	2×180 2×120	2×280 1×160	—	2×1850
Speed over calm water at weights of, tons:	—	37,5	167,6	6,7	10,5	48,0	91,4	—	29,0	16,0	—	77,0
maximum, knots	70	70	65	66	60	65	75	—	30	40	40	48
cruise, knots	—	60	50—55	62	52	—	—	—	28	35	40	40
Take-off speed, knots	45	50	30—40	40	30—35	35—50	45—55	—	—	35	—	15
in high waves, m	0,9—1,2	1,5	2,4—3,0	1,2—1,5	1,2—1,5	1,2	1,2—1,5	—	—	0,9	0,9	3,0—3,7
Distance capability, miles	170	240	175	205	200	~200	400—500	—	125	140	—	320
Cost of building, in thousands, at factory cost	325,7	450,6	1450	75,6	97,5	700	—	—	75,0	75,0	550,0	390,0

* In the chart, "D-2M" represents data about the D-2.003M after modernizing.

** In the brackets for the SRN5 and SRN6 is the maximum weight for cargo transfer.

Note: In the line "seating capacity" there is one variation for cargo also.

-23-

Performance and Technical Features	England			USA					France		USSR		
	CC-7	HD-1	HD-2	SKMR-1	SK-5	SK-6	SK-9	SK-10	N-300	N-500	"Neva"	"Sormo-vich"	"Gorkov-chanin"
Length, m	7,8	15,2	9,4	20,7	11,8	14,8	17,0	24,4	24,0	41,0	17,3	29,2	22,3
Width, m	4,6	7,0	5,8	9,8	7,2	7,2	10,0	14,6	10,5	—	6,6	10,0	4,05
Air Cushion height, m	2,4	4,1	5,3	8,25	4,9	4,9	5,0	8,2	7,5	—	2,6	7,0	3,1
Weight, tons: empty	1,4	8,0	—	20,4	4,5	5,2	—	60,3	14,0	—	—	23,0	7,2
full	2,3	9,1	4,1	30,6	7,7	10,0	21,3	120,0	27,0	200—220	12,45	32,0	14,0
maximum	—	10,4	5,0	31,6	9,1	11,3	23,6	133,8	80—100	400—500	—	34,0	—
Seating capacity, people	8—10	—	6	—	16	33	90	480	—	—	38	50	48
Cargo capacity, tons	0,7	—	—	5	—	—	—	—	11—13	—	3,8	5,0	5,0
Air cushion area, m²	21,4	—	~38	—	—	—	8—10	60	160	—	87,0	190	67,0
Pressure in cushions, kg/m²	106	—	107	~180	—	—	—	—	—	—	143	160	180
Skirt height, m	0,6	0,76	0,6	1,2	1,2	1,2	1,5	1,5	2,0	—	—	1,0	—
Mechanical power h.p.: maximum	1×390	1×310 1×145 2×85	3×146	4×1060	1×1000	1×1150	2×1250	2×6000	2×1500	—	2×225 1×285	2×2540	1×235
cruise	—	—	—	—	—	—	—	—	—	—	—	1×2100	—
Speed over calm water at weights of, tons	2,3	9,1	2,7	28	7,9	—	21,7	133,8	27	—	11,4	32,0	~14,0
maximum, knots	50	37	50	70	60	56	60	80	57—62	75	30,6	~65	18,9
cruise, knots	—	30	—	30	40	30—35	40	60	43—48	—	—	50	—
Take-off speed, knots	—	—	—	—	—	—	—	—	—	—	—	—	—
in high waves, m	—	—	—	0,9	1,4	1,2—1,5	1,2—1,5	1,2—1,5	—	—	—	—	—
Distance capability, miles	100	100	75	~250	175	160	180	100	~150	1500	~120	320	~220
Cost of building, in thousands, at factory cost	30,0	—	—	2,02 million dollars	—	—	—	—	—	—	—	—	—

Note: In the line "seating capacity" there is one variation for cargo also.

Centrifugal fans with drive-wheels 3.8 meters in diameter and with 12 aviation-type fixed blades were installed on the SRN2. The blades of each wheel were of riveted construction, finished with sheets of light alloys, and fastened to a cast hub. Air from the atmosphere was gathered by the fans, by means of two air-compressors installed on the pylon foundations, then combined under the pylons into a common air-water mixture. From the fan, air went to the peripheral flexible nozzles and internal jets and separated the air cushion into sections.

The SRN2, in contrast to the SRN1, developed another method of sectioning the air cushions: a peripheral nozzle was provided inside the fore and aft pneumatic keel, and diagonal nozzles which ensured better characteristics of stability than in the dual-contour annular jet.. Two air screws which regulated the pitch in the rotating pylons, with a turning radius of 30° on each side, were installed to improve the quality of movement. The 4-bladed screws had diameters of 3.0 meters, were built of light alloys, and had hydraulic mechanisms for changing the screw pitch. Redistribution of power from each pair of turbines, between the screws and the fans, was ensured by altering the corner mountings of the screw blades. In suspension rate, i.e. in the absence of speed, about 90% power could be given to the fans, and at great speeds about 50% power or more could be given to the screws.

In addition to the screws, a draught in the SRN2 was created because of the reactions in the jet flow, which made about 20% of the total draught. Control of jet flow in the stern was attained by using deflector blades in the rigid jets and inclining the diaphragm 20-30° in the flexible nozzles. During movement, with an inclined jet in the stern, there was a trim difference and an aerodynamic lifting force on the hull, which made up about 10% of the total lift force for the SRN2.

Resistance to movement, at operating speeds of the SRN2, occurred only over 10-20% of the entire craft.

Control of the movement of the SRN2 was brought about by: changes of screw pitch, turning of the pylons, horizontal stabilizers and rudders. Various combinations of positions for the organs of control were ensured with the aid of a steering column.

On the original SRN2, a flexible skirt was attached, with a height of 0.6 meters and having flexible jets, the design of which is shown in Figure 8b.

A flexible skirt with a height of 1.2 meters was installed on the ACV, at the end of 1963, composed of a flexible bag with flexible jets. The design features of this flexible skirt were briefly examined in the introduction.

The necessary navigational and communications equipment were installed on the SRN2, in particular, a navigational radar to avoid collisions with ships and buoys during the testing phase. During 1962-63, the SRN2 with flexible skirts of 0.6 meters underwent testing in the Solent Spithead (where steep, short waves up to 1.2 meters prevail) and in the open sea (with wave heights up to 2 meters).

Later, the SRN2 was operated in trial runs in the Solent Spithead, in the Bristol Channel, made several lengthy sea crossing along the coast of England, and also was demonstrated in Canada and other countries. Today, the craft has served its purpose.

§2. The SRN3

The general composition of the SRN3 was not successful, because of the small area for a passenger salon. In connection with this, the Westland firm made modifications to the craft and changed the designation to SRN2Mk2. By lengthening the salon 3 meters, it increased the seating capacity to 150 people.

Construction of the craft was begun on the Isle of Wight in November, 1962. In March, 1963, the English Ministry of Aviation contracted the firm to create a test military ACV, some changes were made to the SRN2Mk2 and the military version was designated SRN3 [84, 97]. In testing the craft, it had to be evaluated in open coastal waters for use in anti-submarine patrols, as a landing craft, in mine-sweeping operations, and for coastal patrols. Construction of the SRN3 was completed in October, 1963. In July, 1964, having been factory tested, the SRN3 was turned over to the armed forces unit (IHTU) which tests all ACV's in a special program. This unit also carried out control of designing and construction of the SRN3, and observance of the special requirements. The SRN3 could transport 70 soldiers with full field packs or four cross-country vehicles of the LandRover type, or various other military equipment. A general view of the SRN3 is shown in Figure 12 and 13, with the basic characteristics in Table 1.

The design of the SRN3 was identical to that of the SRN2.

The basic differences between them consisted in the following. The increased hull length was due to extra central sections of 3.2 meters; the height of the cargo area was increased to 2.1 meters for the storing of military equipment, as opposed to 1.8 meters in the SRN2, rounding the sides provided bigger loading ramps with hydro-drive for lifting and lowering; the design of the wheelhouse was changed; to improve the main engines, they were replaced with the more powerful Gnome gas turbines of the Bristol--Siddeley firm; Rover auxiliary gas turbines with Shottel lifting turbo-fin complexes were installed, ensuring in the movement of the

craft a displacement rate, maneuverability (accomplished by an aft stabilizer), and mechanical contact for suspension of its rudder; stationary auxiliary stabilizers were mounted on the right and left sides; the fuel tank capacity was increased; changes in the hydraulic system and electrical power system were made, and radio-navigational and special apparatus were installed.
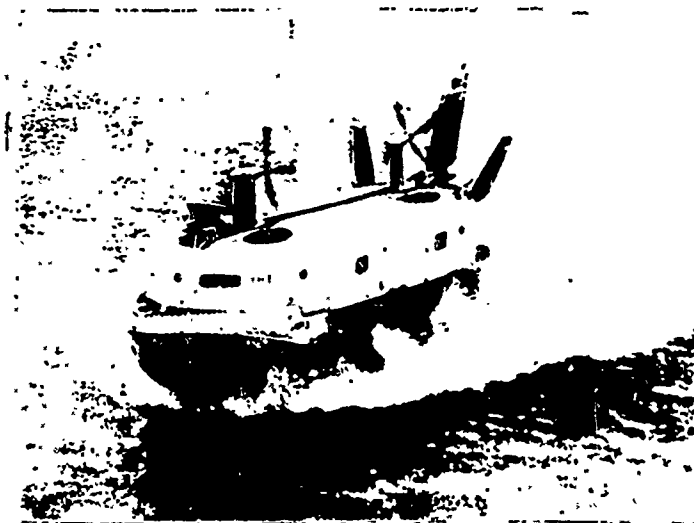

Figure 12. The Air Cushion Vehicle SRN3.

The principal diagram for creating air cushions in the SRN3 is shown in Figure 14.

A feature of the SRN3 was the use of flexible skirts of an improved design to attain a height of 1.2 meters. The skirts, composed of a flexible bag with flexible jets, provided the possibility of lift inside the hull to aid the lines and hydraulic systems.

It was assumed that, by lifting the flexible skirts to decrease resistance and to increase speed in the displacement rate of the moving craft, the operable time would be increased considerably (a valuable quality for a military ACV). The operable time of the SRN3, at full speed, is about three hours due to the great expenditure of fuel by the gas turbines and the limited reserves. By lifting the skirts, however, a considerable increase in the speed of the SRN3's displacement was not realized because of the poor hydrodynamic by-pass. In operating the twin auxiliary Rover 25/150 gas turbines and the Shottel screw--rudder complex and in raising the flexible skirts, the required speed for displacement rate equalled 8 knots in calm water and 6 knots over waves. Maximum power for each of the Rover 25/150 turbines was 150 h.p. The screw-rudder complexes did the lifting and were equipped with movable flexible screws of nylon, with diameters of 0.76 meters.
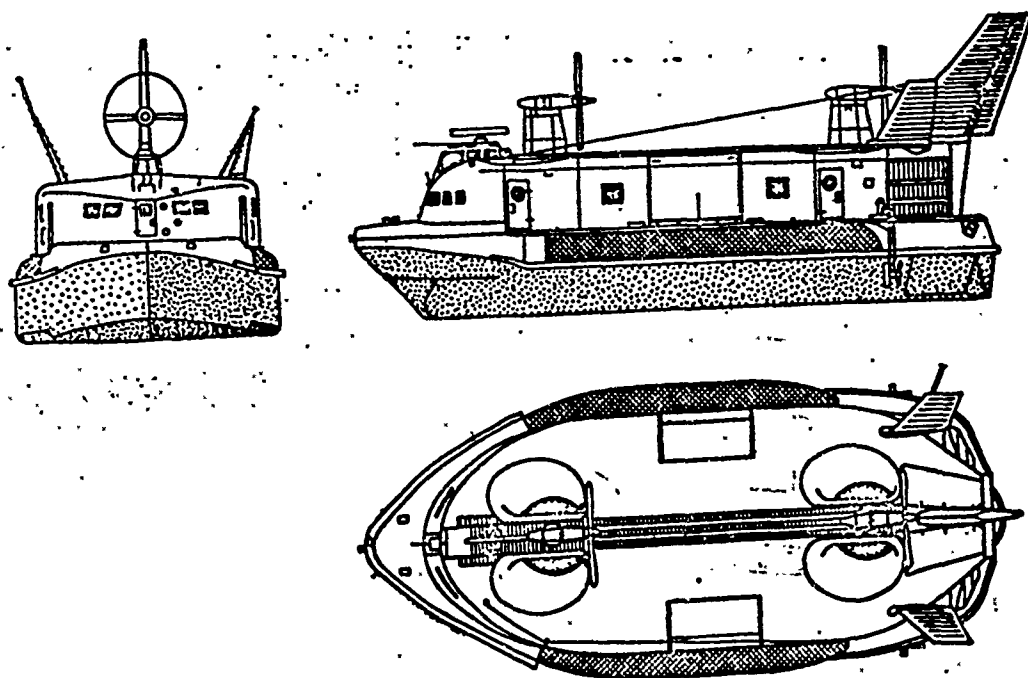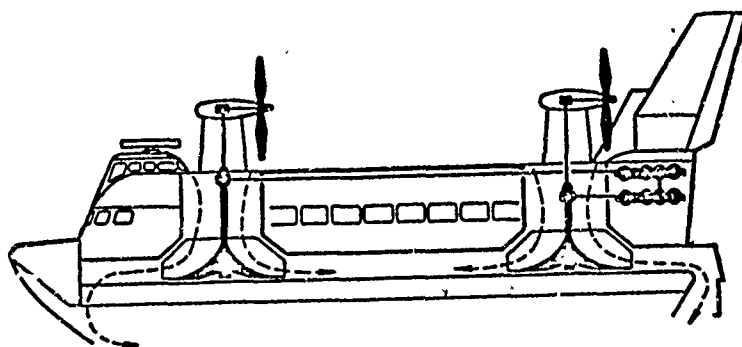
-27-

Figure 13. Structural Design of the SRN3.

Figure 14. Principal Diagram for Creating Air Cushions in the SRN3.

In joining the separate sections of flexible skirts onto the SRN3, as was done in all following models, the builders considered adhesives and rivets and fastened the upper edges of the skirts to the bottom and the thwart riser to aid the joint pin and ensure quick replacement of separate skirt elements. The skirt's material was a corded rubber--proofed substance.

To the bottom of the hull were fastened eight steel landing cushions, with rubber shock absorbers, ensuring the craft's landing on dry land without damaging the flexible skirts. For ferrying the craft across land, supports were provided on which wheel-chassis were fixed.

To ensure a 360° field of vision, the wheelhouse was placed high on the superstructure. Besides improving the field of vision, the location of the wheelhouse was dictated by the necessity of placing special equipment and military posts in the bow section.

The crew of the SRN3 consisted of 6-8 people.

Four converted helicopter Gnome gas turbine engines from the Bristol--Siddeley firm represented the main engines. At maximum power, each engine had 1050 h.p. and an expenditure of 284 grams of fuel per h.p. per hour, which ensured a rated speed of about 70 knots, and at prolonged speeds -- 900 h.p. and a fuel consumption of 295 grams per h.p. per hour, with a speed of about 60 knots. In Figure 15, there is a diagram of the transfer of power from one pair of engines to the fan--screw complex, with reduction gear producing a stepped decrease to 1750 RPM's of the screw shaft and 550 RPM's for the fan shaft. As in the SRN2, there were two engines on the right side which led across to the horizontal shaft, the stern fans and screws, and on the left -- a pair of engines led to the bow fans and screws. There was no connection between the engine shafts on the right and left sides. The centrifugal fans and screws on the SRN3 were like those on the SRN2, except that on the SRN3 the diffusion rings around the fans were relinquished.

The air screws had a turning radius of the fixed blades of +35 to -30.°. The turning radius of the pylon was ±30°. In turning the rear pylon, thanks to mechanical contacts, the stabilizer was turned simultaneously by suspending the rudder. Maximum corner deviation of the stabilizer was ±20°; maximum corner deviation of the rudder twice as much..

The turning gear of the pylons and stabilizer was electro-hydraulic.

In the SRN3, in addition to the basic turn stabilizers mounted along the side, there were two stationary stabilizers in the stern, with an outside under the corner incline of 25°.
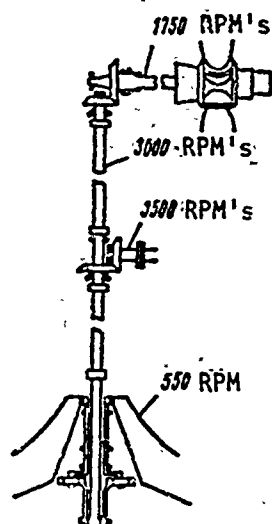
1750 RPM's

3000 RPM's

3500 RPM's

550 RPM

Figure 15. The Drive System of the Screw and Fan in the SRN3.

In the craft's hydrualic system, the fluid DTD-585 was used for operating at pressures of 210 kilogram forces per cm². Each pair of main engines started a hydro-pump, which served an automatic hydro-system for turning its own pylon. Each auxiliary engine started a hydro-pump which served independent hydro-systems for turning stabilizers and rudders, lifting and lowering the flexible skirts and ramps, and for the screw-rudder complex. If necessary, these hydro-systems could duplicate each other. The auxiliary engines also started a 12 kilowatt generator.

In such a way, one of the Rover auxiliary gas turbines ensure that the generator and the hydro-systems were working, and acted to momentarily prepare the craft for take-off.

The driver's controls were like those used in aircraft including, as in the SRN2, a steering column with a steering wheel, a control lever for screw pitch in all ranges (the column allowed one to alter the screw pitch not more than 1/3 of the maximum). In contrast to the SRN2, the SRN3 had foot pedals for controlling the turning of the rudder. On the instrument panel, situated in front of the driver, were indicators for screw pitch, turning of pylons, trim difference, corner incline of the stabilizers, relative nautical and air speeds, turbine and auxiliary engines' RPM's, turning of the column, and others.

The navigational equipment and means of radio-communication provided in the SRN3 were: a Decca 969 navigational radar, gyro-compass and magnetic-compass, a shortwave radio sets (with sets working in the 10 meter band and reserve/emergency VHF set), and a Doppler

effect gauge for relative air speeds of the ACV. During the testing of the SRN3 as an antisubmarine ship, a hydro-acoustical station was installed.

In operating the SRN3, it was possible to alter the weight of the craft from 25 to 42.5 tons. This depended on changes in the weight and speed of the craft, its lift height over the support surface. So, at a weight of 37.5 tons and with main engine power at 4X900 h.p., clearance was increased between the flexible skirts and the support surface by 0.23 meters and the lift height of the bottom, by 1.45 meters. With engine power of 4X1050 h.p., clearance was increased by 0.32 meters. In normal operating conditions and at speeds of about 70 knots, clearance was increased by 0.15 meters.

In conditions of irregular waves, where wave heights reached 1.5 meters, operation of the craft was possible if the speed was decreased. Moving along the coast, the SRN3 ably overcame heights of 1.2 meters at speeds of more than 18 knots, and trough widths of 6.1 meters and 0.8 meters deep at speeds of more than 10 knots. Tests of the SRN3 proved the possibility of its operation in state 3-4 sea conditions and permitted the Westland firm to begin work on an ACV with a larger displacement, the SRN4.

§3. The SRN4

The SRN4 was a Class A ACV, with a total weight of 167.6 tons and was one of the largest ACV's built in current times [85, 98]. It was the first ACV with a higher seaworthy capability, built for operation in the open sea with wave heights up to 4.0 meters. The SRN4 was designed to transport cargo/passengers across the English Channel. Planning of the SRN4 was begun in December, 1964. In June, 1965, the two Swedish firms of Swedish Lloyd and Swedish American Lines signed contracts with the Westland firm for a 5-year lease on two SRN4's and two SRN6's for operation in the English Channel between Ramsgate and Calais, a distance of 27 miles. In compliance with these contracts, the Westland firm began construction of the two SRN4's. In January, 1966, still another order was received for an SRN4, from the English firm of British Rail Hovercraft, which planned to operate it from Dover to Calais.

The first SRN4 was built on the Isle of Wight at the end of 1967, the second one in the beginning of 1969. A general view of the craft and a construtive diagram of it are shown in Figure 16 and 17, with its basic characteristics shown in Table 1.

In constructing the hull, a honeycomb construction was used extensively. The deck and the bottom of the hull were composed of panels made from two sheets of light alloys, between which were placed honeycombs of packed foil. The panels were manufactured with dimensions of 1.2 × 2.4 meters, and the thickness of the packing was 38 millimeters.

-31-
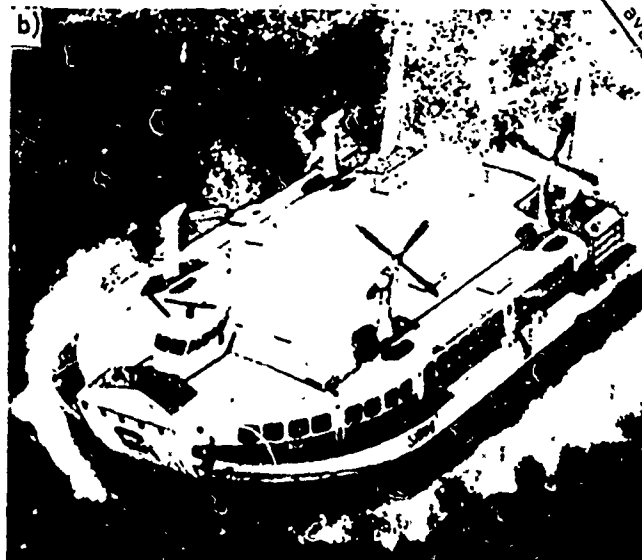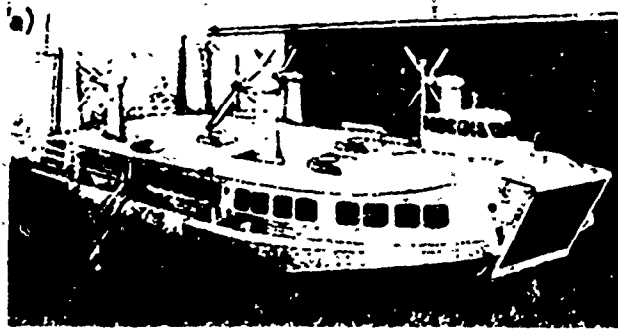
Figure 16. The Air-Cushion Vehicle SRN4.

The bonding of the honeycomb packing to the sheets of planking was accomplished with the aid of special adhesives.

Bonding the rigid ribs and the roof panels of the superstructure also was accomplished with adhesives.

The hull was divided into 24 watertight compartments. Each compartment was formed from several panels. The panels were joined by bolts and rivets into larger sections.

The total size of the hull, more than 550 m³, created a buoyancy of 250%.

At the bottom stood 5 landing cushions, with heights of 0.5 m, used to land the craft on ground. The cushions were made of highly--durable, light-weight alloys and had rubber shock absorbers. The lift height was insufficient inspection and repair of the skirts. Therefore, six supports were provided on the craft ensuring its lift to greater heights by installing hydraulic jacks.
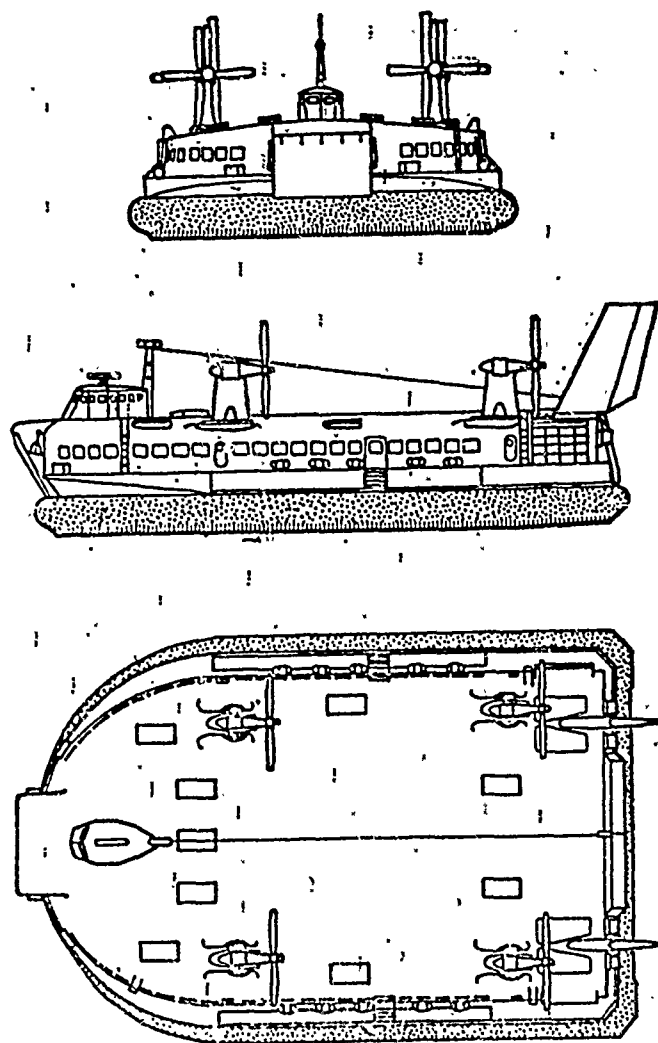
Figure 17. Structural Design of the SRN4.

On the cargo deck, up to 30 cars could be accommodated. The lateral
sections of the deck, between the air-conducting fans, could be outfitted
as passenger cabins with lightweight bulkheads (Figure 18). The central
part of the cargo deck was 4.9 meters wide and meant for accommodating
buses or vehicles that weight up to 9 tons with maximum cargo on the
axles of 5.9 tons and having corresponding supports. The remaining part
of the deck permitted places for cars with loads no greater than 2.0 tons.
The deck had a non-slip covering. The height of the mid-deck area was
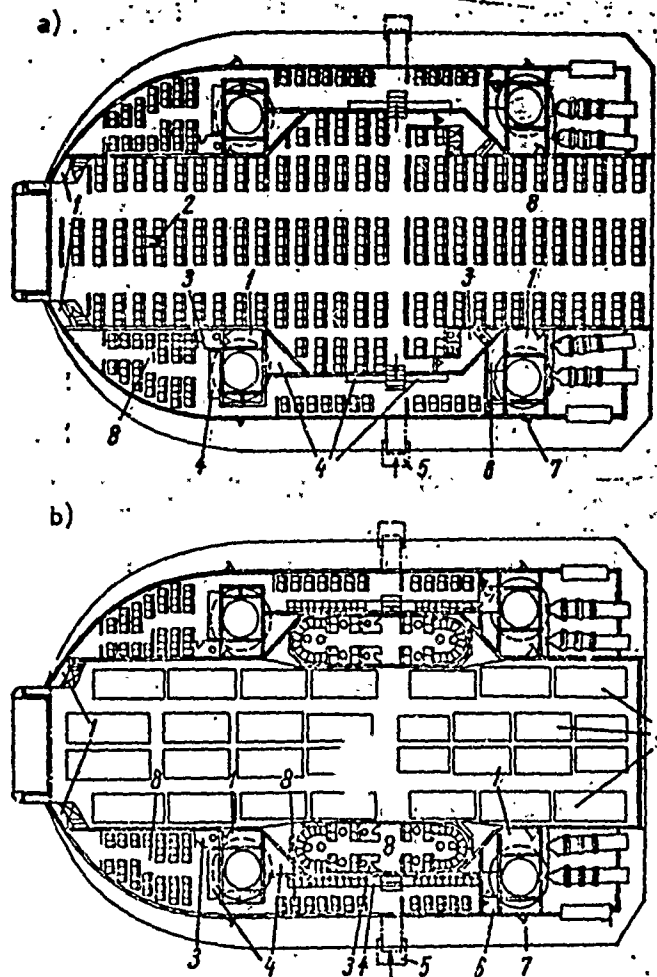3.4 meters.

Figure 18. The General Layout of the SRN4: a, passenger version;
   b, cargo/passenger version.
   Key: 1, store-room; 2, ladder to the deckhouse; 3, lavatory;
   4, baggage compartment; 5, main entrance; 6, electrical equip-
   ment; 7, crew entrance; 8, passenger accommodations; 9, auto-
   mobiles.

To speed up the loading and unloading of automobiles, the SRN4 was equipped with bow and stern ramps. The former had a width of 5.5 meters and a height of 3.5 meters; the latter had a width of 9.45 meters and was 3.5 meters high. Loading of cars took place in the stern and unloading, in the bow; both loading and unloading could be done simultaneously.

Passengers were accommodated in cabins along the sides and in the front extremities of the craft. The passenger deck was set 0.8 meters above the cargo deck and was attached to the hull by means of tubular pillars. As in the SRN3, the receiver for the fans was in the lower deck area.

The wheelhouse, situated in the bow extremity of the craft, had a tear-drop shape and was raised above the roof of the superstructure to ensure a 360° view. The wheelhouse accommodated three crew members: the commander (who was also the pilot), the engineer-mechanic (who was also the radio operator), and the navigator (who was also the radar operator). In accordance with this arrangement, there were three chairs in the wheelhouse and an extra one for a co-pilot.

A design for flexible skirts, like those used in earlier craft, was used by the company. Some changes in the design of the skirts consisted in the flexible jet, previously joined to the flexible bag, being changed in the bow and lateral sections to diametrically-distributed elements of an open type which made up 1/3 of the skirt's height.

There was a lower tier of skirts in the stern section and the skirts which separated the air cushion into sections were composed of cone-shaped elements (diametrically-distributed closed type elements) of greater rigidity. The material for the flexible skirts was standard, with the lower tier of skirts composed of material less thick than the flexible bag. The elements of the skirts were bonded together by adhesives and rivets with metal washers.

The four main engines of the SRN4 were converted aircraft gas turbines, with an independent Proteus turbine from the Bristol-Siddeley firm, used for the first time in an ACV. At a maximum power of 4250 h.p., the expenditure of fuel was 272 grams per h.p. per hour; with the engine power at 3400 h.p., the expenditure was 290 grams per h.p. per hour. The important advantage of the engines was the possibility of their operating on diesel fuel, considerably lowering the danger of fire. The dry weight of the engine was 1410 kilograms, with a resource of 1500-2000 hours. The engines were arranged into twin stern units, with two on each side. Each engine operated a fan-screw complex, composed of a centrifugal 12-bladed fan with fixed blades, 3.5 meters in diameter, and a 4-bladed air screw with variable pitch, 5.8 meters in diameter.

The screw blades of the SRN4 were made entirely of aluminium alloys, and their front edges were nickel-plated for protection from corrosion.

The layout of the SRN4's drive screws and fans was similar to that of the SRN2, except that each complex worked off of one engine instead of two. Redistribution of power between the screws and fans aided in giving variable pitch to the screws. Typical distribution of the power of one engine consisted of: 2000 h.p. for the screw and '150 h.p. for the fan, with the remaining 250 h.p. spent in driving he auxiliary units, loss in the transmission, etc.

The drive shafts of the engines were components with flanges connected to a pipe of lightweight alloys, about 2.3 meters in length. The drive shafts to the stern fan-screw complexes were relatively short, while those to the bow reached 18.3 meters. At such a length, the shaft conductor could change in form under operating conditions. To avoid this deformation, self-centered sleeves and bearings were used. The design of the vertical shafts were similar to the horizontal ones, however, the shafts which turned the screws were steel, as they had to transfer greater torque. Through the basic reduction gear, the auxiliary cog-type transmission was aided by taking power to drive the oil pump and hydro--pump, which ensured shifting of the pylons and putting the helm over. All engines and mechanisms were easily accessible for inspection, servicing, and easy dismantling. Even the operational drive wheel of the fan could be dismantled and unloaded onto the cargo deck.

To operate the craft with one of the engines stopped, speed had to be decreased to maintain the air cushions. In such an event, air leakage from the cushions through the idle fan was prevented by covering the aperture with a special roof, which could be put in place from the wheelhouse by a hydraulic drive. In day-to-day servicing, these roofs were utilized for approaching and inspecting the upper reduction gear in fairing the screw.

The fuel was stored in 12 fuel tanks, located in the area of the fans and separated into four groups, with three tanks in each group. Such distribution of the fuel satisfied the requirements for its maximum extraction from the cargo deck, and also its utilization to improve the ballast in the trim-difference system. Each group had one pump attached to a main engine, and two larger independent pumps which could be utilized for trimming or for feeding fuel to the engines in case the basic pump went out. Refueling could be accomplished in 6 minutes.

Special attention, in planning and building the SRN4, was given to the problem of noise. To solve this, speed was decreased in the screws (to 0.6 Ma, instead of 0.8-0.85 Ma as in previous craft), and the internal noise was reduced, thanks to the well-planned placing of basic equipment.

Air moved through two air-gates, situated along the sides, to the engines. To decrease the noise-level, the area of the air-gate was increased, and effective filtration of air from sand and spray was ensured with the help of a cotton gauze filter. A special system of baths was provided to remove the salt deposits from the engines.

The quality of electrical energy sources for the craft was enhanced by mounting two AC generators (200 volts, 400 cps, with 55 kilowatt amps of power) in the machinery compartments on the right and left sides, which drove the two auxiliary Rover 15/90 gas turbine engines. The generators worked independently of each other, each in its own tyre. In the event that one went out, the other could feed both tyres. The ventilation system and network of lighting were the basic AC consumers. A DC system, with tension of 28 volts and 112 volts, was aided by rectifiers. The current tension of 28 volts was used to feed the control-measuring instruments and for sub-loading the 24-volt storage batteries, which were adapted for the engine thrust of the Rover 15/90. The 112-volt current tension was used for the main engine thrust. Transfer of energy from sources on the shore was also possible.

A bilge system was provided to ensure draining of any compartment, or all compartments simultaneously. Drainage pipes from each compartment led to one of four tanks, serviced by an electrical pump.

To attain high reliability in control of the craft, several independent hydraulic systems were employed. One of them ensured operation of the bow ramp, the special roofs of the fans, and the passenger gang-plank on the right side, the other -- operation of the stern ramp, the special roofs of the fans, and the gang-plank on the left side. Each pylon had its own electrohydraulic movement system with drive from an independent hydro-pump. This was how the electrohydraulic systems were used for turning the rudder and changing the screw pitch.

The control system did not differ greatly from that of the SRN3. The control organs of the craft were: the four movalbe pylons with variable-pitch air screws and two stabilizers and rudders operating in the slip-stream. Movement of the pylons was ±35°, ±30° for the stabilizers, and ±40 for the rudders.

The necessary radio and navigational equipment were installed in the craft, including: shortwave and VHF radio stations, an inter-com system, Decca navigational radar, a gyrocompass and a magnetic compass, relative water and air speed indicators, turn-speed indicator, etc. Two Doppler gauges for measuring speed and drift were probably mounted in the stern along the left side of the SRN4.

§4. The SRN5 and SRN6.

The proven design and operation of the SRN1, SRN2, and SRN3 craft permitted the Westland firm to set about creating a small Class A ACV -- -- the SRN5 (full weight 6.7 tons) and, subsequently, its modification -- -- the SRN6 (full weight 9.1 tons) [86, 87]. The goal was to build a multi-purpose speedy craft, which could move in coastal waters and straits, and could be used for first-class passenger or cargo service, search and rescue missions, landing and disembarking, as a fire or medical craft, and also for coastal patrols. Today, these craft are turned out in variants for passanger, cargo, and military use. The firm sought to create a series, sufficiently inexpensive and reliable, which would be of interest to a wide cross-section of buyers. A general view of the SRN5 and its constructive design are shown in Figures 19 and 20, with its basic characteristics appearing in Table 1.
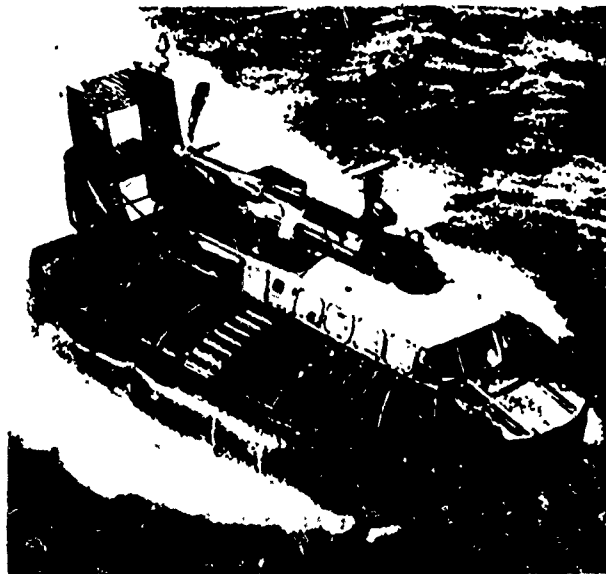
Figure 19. The SRN5 Air Cushion Vehicle.

The first SRN5 was built in April, 1964. The ninth craft of this series was a modified version, which was designated SRN6. The basic difference consisted in the hull being lengthened by 2.95 meters. The SRN5 and SRN6 series, when completed, will consist of 60 craft.

The first trial run of the SRN5 was in the Solent Spithead in July, 1964. Today, a number of English companies (Hovertravel, British Rail Hovercraft, Hoverlloyd) and companies in other countries are using these craft in regular passenger service. In two years of operation, more than a million passengers were transported on these craft.
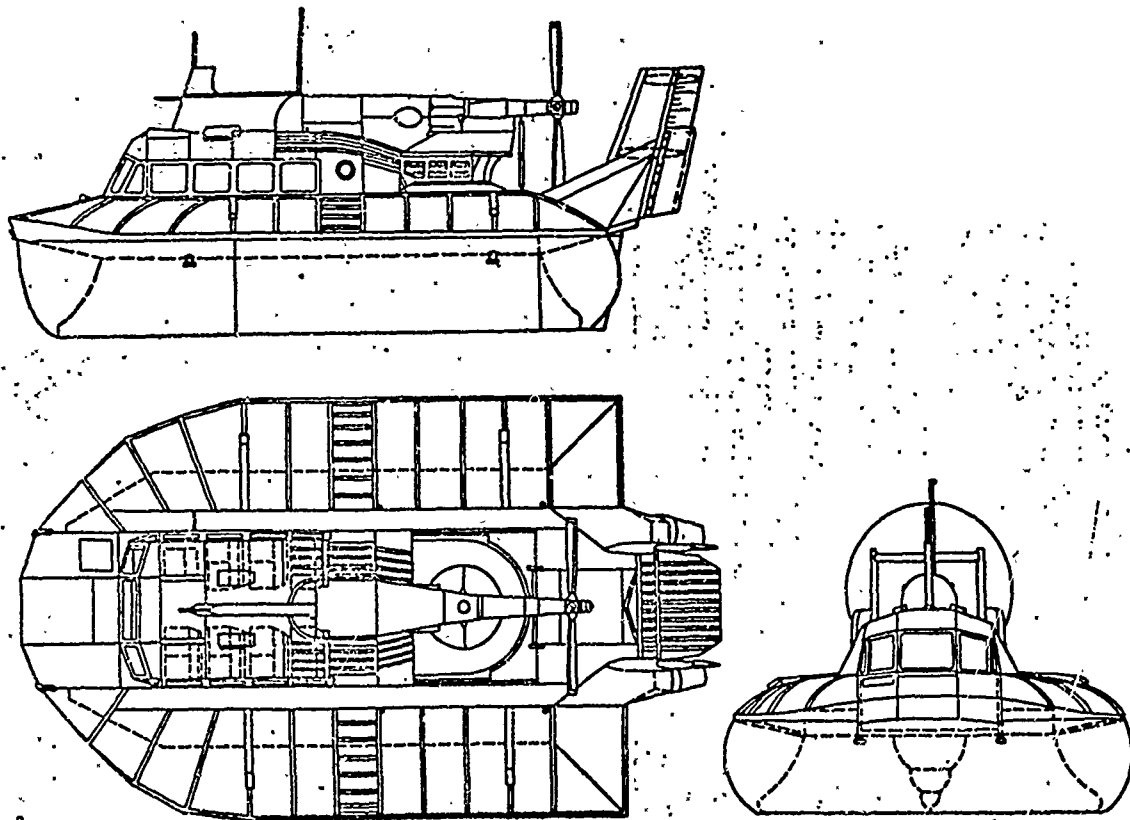
Figure 20. The Constructive Design of the SRN5.

A great deal of interest in the SRN5 and SRN6 was shown by the armed forces of England and the U.S.A. Three SRN5 craft were turned over to them for testing and evaluation of their potential for military uses by the armed forces unit referred to earlier as the IHTU.

In England, in 1967, the first unit of military ACV's was formed, consisting of four SRN6's intended for use as transport-landing craft. A similar unit was proposed for the Navy.

Three of the seven ARN5 craft, purchased by the Bell Airsystems firm, were turned over to the U.S. Navy which, after installing American-made GELM-160 gas turbines in them, changed the designation to SK-5. These craft, called patrol ACV's, were armed and took part in the aggressive war in Vietnam from 1967-68. They then underwent modifications for heavier armament, were armor-plated and in 1968, they were again sent to Vietnam.

The body of the SRN5 and SRN6 was composed of a central compartment for buoyancy and two removable side sections. The width of the central compartment, in which a salon and the main engine were located, was 2.5 meters permitting the craft to be transported, in disassembled form, on aircraft and by railway. The body and the superstructures were riveted together, using the anodized light alloy L-72. For the air-gates, fans, and small sections of the superstructures, glass reinforced plastic was used. Below the waterline, the compartments were divided into a number of watertight compartments. To ensure watertightness, the space between them and the salon was filled with a layer of foam. The reserve buoyancy of the SRN5 was 350% and, by flooding the salon -- 150%.

The passenger salon was situated in the bow section of the central compartment and had the following measurements: 3.7 meters in length, 2.3 meters wide, and 1.8 meters high in the SRN5; the width and height in the SRN6 was the same, but the length was 6.6 meters.

Ventilation in the salon of the SRN5 was natural; in the SRN6 it was artificial. An air conditioning system was available for installation on the SRN6. Pressurization of the salon ensured elimination of condensation in windows and doors.

The passengers' baggage was stowed astern in two areas with a capacity of 2.1 m^3.

In the military version of the SRN5, 15 armed personnel could be accommodated. The military and cargo versions of the SRN6 differed from the passenger version by the presence of a hatch on the salon's roof (2.1 meters long and 2.3 meters wide), and increase of 1.3 meters in the width of the bow ramp, and also a strengthening of the deck's side sections, ensuring the transfer of long items weighing up to 0.5 tons. For the military version lightly armored engines and electrical equipment were provided, as well as accommodations for the landing party (bulletproof armor for 7.62 millimeter projectiles). The military and cargo versions of the SRN6 ensured transfer of 30 armed assault troops, evacuation of the wounded, transfer of a 105 millimeter cannon with its gun crew, and patrol of the seacoast with a 120 millimeter anti-tank weapon and its crew, etc.

In the stern sections of the central compartment, separated from the salon by a transverse partition, the fan and gas turbine with reduction gear and screw were situated, as well as a shield made of light alloys for the additional elastic fuel tank with a capacity of 1200 liters. On the compartment deck a framework, consisting of a pipe made of light alloys and supported by light planking, was installed which formed a cavity for placing the fan. A plastic air-gate was joined to the planking above.

The side sections formed additional compartments for buoyancy and had an external framework of light-alloy piping, used for strengthening the flexible skirts. Near the central compartment the sections were strengthened by hinging.

-40-

On the SRN5 and SRN6, as on the SRN3, the main engine was a Marine Gnome gas turbine, manufactured by the Bristol-Siddeley firm, with a maximum power of 1050 h.p., converted to operate in sea conditions with a resource of 1000 hours of power. In contrast to the SRN3, however, these craft did not have special machinery compartments. The turbine was installed in the central compartment on twin tubular tripods with four auxiliary posts for supporting one of the tooth-gears. Additional support for strength came from the foundation of the partition of the salon, and the bars which supported the screw shaft.

The gas turbine ran the screw and the fan at the same time. The power, used for both lift and movement, could be redistributed depending on operating conditions to aid in altering the screw pitch. At maximum power, the turbine produced 1050 h.p. and 20,960 rpm's, and fan and screw had a turning speed of 950 and 2000 rpm's respectively. Decelleration was accomplished through a system of reduction gears. The 12--bladed centrifugal fan, produced by the Westland firm, had a diameter of 2.1 meters and was manufactured from light alloys. The design of the 14-bladed reversible screw with a diameter of 2.74 meters, from the firm of Doughty Rotol, was similar to that design used in the SRN2 and SRN3. A hydrosystem was used to alter the screw pitch.

The fuel used by the turbines was kerosene, however it could also operate on light diesel fuel. Expenditure of fuel at 1050 h.p. was 284 grams per horsepower per hour and 295 grams per h.p. per hour at 900 h.p. The fuel was fed from the storage tanks to an engine by an electric pump which put it through a water-separator. The fuel flowed from the tank through a branch pipe in the superstructure by gravity. An additional 90 liters of reserve fuel in the SRN5 and 230 liters in the SRN6 was used in place of ballast for trim difference, by placing it into two different tanks of equal capacities situated in the bow and stern.

Air for the gas turbines passed through three air filters, fixed on the side of the craft in the region of the fan's air-gate, which eliminated the sea spray. The gas turbines, the gears, and the screw's drive shaft were encased in housings of light alloys. The location of the mechanical installations ensured easy access to it from the decks and made it possible for fast replacement.

Aboard the SRN5 a generator was installed which had alternating current and rectifiers to ensure a constant current of power of 60 amps and tension of 27.5 volts. A 24-volt battery, with a capacity of 40 ampere hours, was used to start the engine. On the military version of the SRN6, a 6.5 h.p. diesel generator was also installed for use when the craft was moored and the main engine was shut off.

The flexible skirts were made of Terylene, a corded rubberized cloth one to five millimeters thick, able to withstand 500 kilogram forces per centi-

meter. They were 1.2 meters high and made up of sections 1.2 to 5.2 meters long. The sections were bonded together with an adhesive and doubled in a row of rivets, attached to a leaning beam and the edge of the compartment by hinges of removable pintles. This reinforcement of construction ensured fast replacement of damaged skirt sections. Design-wise, the flexible skirts consisted of a periphery of flexible skirts (in the first version, a type of flexible receiver with jets; in the final version, a type of flexible receiver with transverse open-formation elements), with stern skirts in the form of bags, and with longitudinal and transverse flexible-pneumatic keels to ensure sectionalization of the air cushions.

After two cases of an SRN5 capsizing because the flexible skirts in the bow section were washed off at high speeds, vertical breakaway ribs were installed which consisted of two rows of apertures with diameters of 25-50 millimeters in 100 millimeter degrees to ensure air lubrication of the lower parts of the skirts from the outside.

This, together with other elaborate measures, excluded the possibility of the SRN5 and SRN6 ever capsizing in operable conditions. The life of the flexible skirts was about 1000 hours, although individual sections were changed every 200 hours. The design of the flexible skirts, plus their height, ensured the craft's overcoming vertical obstacles up to 1.1 meters high and sand bars up to 1.8 meters high.

The SRN5 and SRN6, in contrast to the SRN2, SRN3 and SRN4, had only one screw. This greatly complicated solving the problem of control. Control was aided by: two vertical rudders with stabilizers; a horizontal rudder; jet rudders -- consisting of two flat air-hydro drives attached to the receiver, and a strip of exterior overhead vertical rudders turning with them; and the lift systems of the flexible skirts. The lift systems ensured lift for the skirts in each of the four air cushions to a length of about 1.8 meters, and consisted of four hydro-cylinders with wires leading to parts of the flexible skirts and hydrosystems with hydraulic pumps. Moving the control stick forward brought about lift of the flexible skirts in the two front quarters and gave momentary trim to the bow. Moving the handle back or to the side brought about trim to the stern or momentary lift, accordingly. This system was used to eliminate drift and to control the craft at low speeds, in circulation for creating an inside heel, etc.

These craft did not have a special wheelhouse. The control panel and a chair for the commander were situated on the right side, and a chair for the navigator was located on the left side in the bow part of the cabin. On the right side of the commander's chair there was a lever to alter the screw pitch, with a handle to alter the engine's power, which permitted the commander to control the lift height and the speed with one hand. The other hand would be used to move a lever to control the angle of the transverse horizontal rudders. The commander could manipulate the transverse vertical rudders with the aid of foot-pedals. The lever for controlling the lift system for the flexible skirts was mounted in front of the commander.

-42-

The typical set-up of the navigational and communications equipment aboard the SRN6 was: Calvin Hughes Type 17 navigational radar with circular antenna, a Sperry G4B gyrocompass, a Bendix magnetic compass, turn-speed indicator, a Doppler-effect speed gauge, VHF radio, etc.

Tests of the SRN5 and SRN6 showed that, at speeds of 60 knots the minimum turning radius of the SRN5 was 640 meters and 230 meters at 50 knots, while the SRN6 took 350 meters. However, in using the lift systems of the flexible skirts, the radius could be reduced considerably -- -- for example, the SRN6 would only have a turning radius of 150 meters at a speed of 40 knots.

As far as the craft's inertia properties were concerned, the stop distance of the SRN5 after cutting the engines at 70 knots was 500 meters with a braking time of 33 seconds; for the SRN6, it took 240 meters to stop after cutting the engines at 50 knots. This was decreased considerably by controlling the flexible skirts and reversing the fan. The stop distance for the SRN5 at 60 knots was 140 meters, while the SRN6 managed to stop in 110 meters at 50 knots. The SRN5 developed speeds up to 65 knots in 76 seconds; the SRN6 attained 50 knots in 41 seconds.

§5. The BH-7, BH-8 and Other British Hovercraft Designs

The amalgamated company of British Hovercraft, created in 1966, continued to work out Class A ACV designs. On the basis of the fundamental elements of design in the SRN4, new craft were created (the BH-7 and BH-8) [80]. These craft were the intermediate links between the 9-ton SRN6 and the 168-ton SRN4.

The BH-7 was designed as a cargo/passenger variant for fast ferrying, and also as a type of fast patrol and military transport craft. The firm received orders for the delivery of one BH-7 to the English Navy and two to the Iranian Navy.

The BH-8 was designed as a military transport craft and also as a cargo/passenger variant. Overall views of the BH-7 and BH-8 are shown in Figures 21-23. The designs of the fans, screws, train of gears and drive shafts of both craft were identical to those of the SRN4. They also utilized the same Proteus gas turbines for main engines as in the SRN4, one in the BH-7 and two in the BH-8.

At the end of 1969, the first BH-7 for the English Navy was completed (of the four being built at the factory). It had one turning pylon. The main engines were placed in the machinery compartment. To improve control jet air-propelled rudders were installed. The wheelhouse was raised above the top of the superstructure and ensured at 360° field of vision.

The cargo/passenger version of the BH-7 was equipped with a bow ramp 4.2 meters wide and 2.4 meters high. The clearance height between

-43-

decks was 2.4 meters. The deck area was 93 m^2 with two fore-and-aft
bulkheads separated by the cargo area (in the center of the craft) and
the passenger area along the sides.

The military transport version of the BH-7, besides having a bow ramp
4.2 meters wide, had a cargo hatch in the top of the superstructure wide
enough to be used for non-entensive loads (e.g. a 4-5 ton truck or other
machine of equal height). The BH-7 could accommodate: two armored
carriers or one 4-5 tons truck or two jeeps and 60 soldiers or 170 soldiers
with their weapons. The wheeled-vehicles and armament were placed on the
cargo deck; the soldiers with their weapons in the side compart-
ments. On the initial BH-7, there was no bow ramp or cargo hatch.
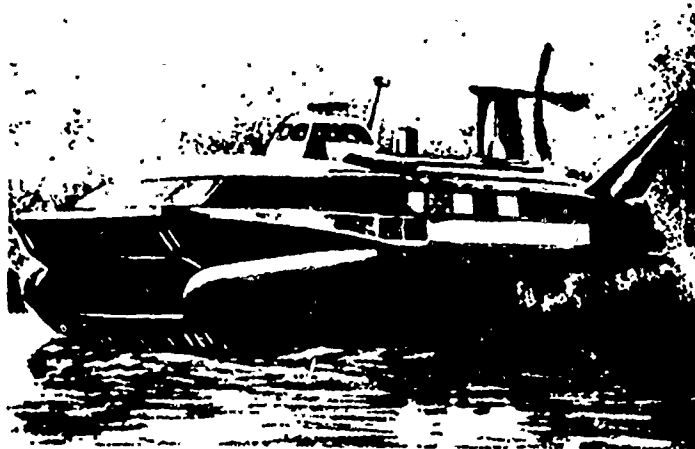

Figure 21. The BH-7 Air Cushion Vehicle (a drawing).

On the patrol craft variant of the BH-7, rapid-fire automatic artillery
could be mounted with a control system for firing and a firing mechanism
for anti-aircraft rockets or surface-to-surface missiles. The craft could
operate for as long as 10 hours over a distance of 500 miles. Since a
craft of this type was self-sustaining for several days, living quarters
for the crew were provided.

The typical features of the BH-8 craft were: bow and stern ramps,
ensuring a through-passage for automobiles (equipment) and the possibility
of loading and unloading at the same time; engines installed in gondolas
atop the superstructure to avoid the use of pylons; use of pneumatic,
multi-tiered flexible skirts, aided by a width which could be increased to
17.0 meters to ensure the necessary transverse stability for moving on an
air cushion. The width of the rigid hull of the craft was 12.2 meters,
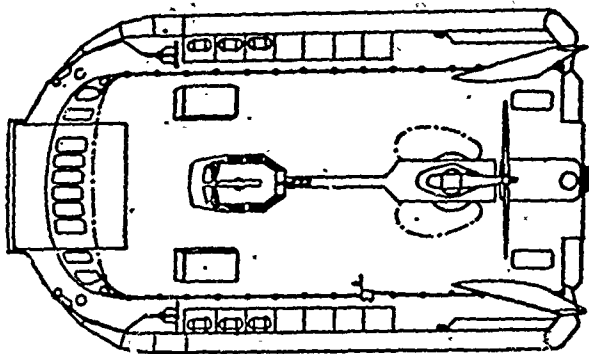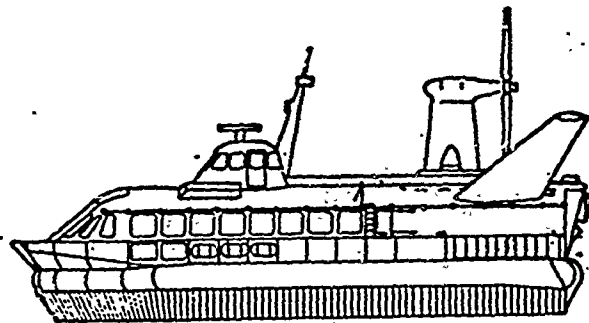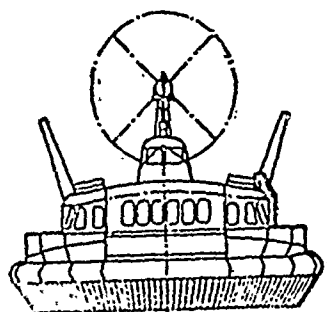which met the requirements for its transfer of landing and transport craft.
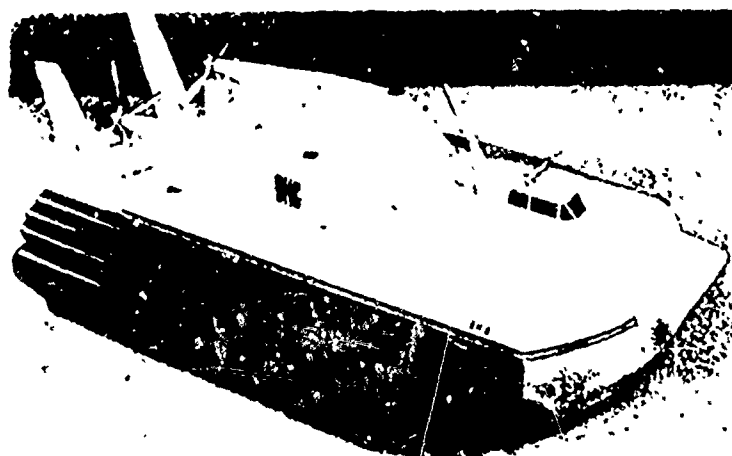
Figure 22.   Design of the BH-7.

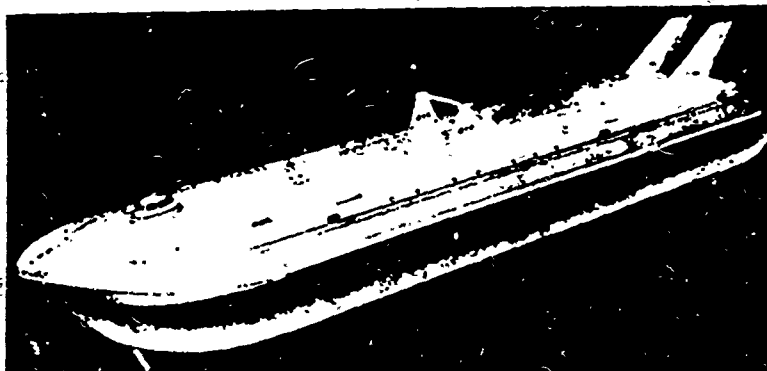Figure 23.   A Model of the BH-8 Air Cushion Vehicle.

Figure 24. Model of a 4000-ton Cargo Air Cushion Vehicle.

The BH-7, BH-8 and BH-9 ACV's were designed for transporting large landing and transport craft. The BH-9, designed by British Hovercraft, was the logical continuation of the SRN5, SRN6 series and used elements of their designs, but in contrast to them was equipped with two Gnome gas turbine engines. The full weight of the BH-9 was 25 tons, having a freight-carrying capacity of 9-14 tons and a design worked out by modifying the landing and passenger craft.

Future plans of the British Hovercraft company, for craft based on the SRN4 design, includes a 300-400 ton displacement, 50-60 knot craft.

A design was worked out from one of these versions for an anti-submarine ACV, which received the approval of the Ministry of Defense. In the opinion of a company spokesman, the ship could be created by 1970.

By the mid-70's, there is a possibility of creating an ACV with a displacement of approximately 1000 tons. In current times, British Hovercraft built an ACV which had a displacement of 168 tons. Building a craft with a larger displacement was restricted by the technical capabilities of industry at the time.

Nevertheless, the company introduced an ACV design for greater displacement. This design called for a cargo-type ACV with a displacement of 4000 tons, a model of which was shown in a British exhibition in 1966 (Figure 24). The chief dimensions of the craft were: 146 meters in length, 44 meters in width, and 214 meters in heighth. The craft was designed to transfer cargo in containers. With a payload totalling 2600 tons, cargo would account for 1,600 tons, with a capacity for 64

containers measuring 2.4 × 2.4 × 9.1 meters. Eight Olympus gas turbines engines which would be designed by the British Navy would be needed, with a maximum power of 27,200 h.p.. Its speed over calm water would be 50 knots, with a range of 1000 miles in the open sea. This cargo vessel was designed in two variants: with flexible skirts and with immersible rigid sidewalls. Higher interest has been shown in the latter design in England.

§6. Air Cushions Vehicles With Sidewalls

At the same time that ACV's with flexible skirts were being developed in England and the U.S.A., ACV's were being created which did not completely leave the water's surface, but had immersible sidewalls (hulls) representative of Class B ACV's.

One of the first to begin research in this direction was the English firm of Denny, which in 1961 built a self-propelled, inhabitable model, the D-1, which weighed about 4.5 tons. The hull of this model was constructed of woods and veneers, had a right-angled plane to its form, two longitudinal sidewalls 0.3 meters high and 0.15 meters wide, and transverse jets in the bow and stern to create air curtains that would surround the air cushion. The preliminary form of encirclement and the sidewalls had been worked out in a test basin on small models. The greatest success was in the upright encirclement of a body with a flat bottom and sidewalls composed of right-angled sections. The walls gradually narrowed from the middle to the bow and ended in a sharp stem that improved the seaworthy capabilities of the models.

The length of the D-1 was 19.2 meters and the width was 3.0 meters. Four centrifugal fans were mounted on the D-1 -- two in the bow and two in the stern, driven by two 25 h.p. engines for creating the air curtains. The total output of the fans was about 2.4 m^3 per second, with pressure in the air curtain set at 85 kilograms of force per m^2. In the two suspended Mercury 500 engines was a power of 50 h.p. for operating the screws, which allowed the D-1 to develop a speed of 20 knots.
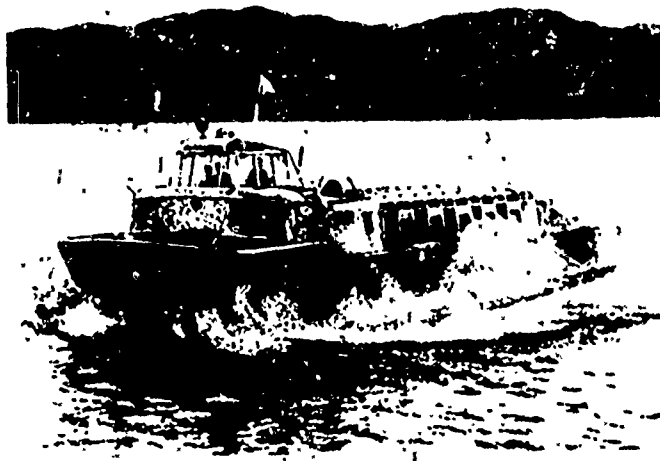

Figure 25. The D-2 Air Cushion Vehicle Before Modification.

Results of testing the D-1 during 1961-62 gave hope for a higher speed than ordinary craft, an insignificant amount of splash, very little noise, good control, the absence of wave formation at designed speeds, and a number of other positive qualities.

In light of this, the firm made the decision to build a series of four test passenger craft with rigid sidewalls and designated them D-2 (Figure 25) [103]. The first craft, the D-2.001 was built in July, 1962; the second craft was completed at the end of 1963. The full weight of these craft was about 25 tons, with an operating speed of 25 knots, and was designed to transport 70 passengers along riverways. The passenger salon was situated in the middle of the craft. The machinery compartments were located in the bow and stern, and the wheelhouse was in front of and above the superstructure.

The power plant for these craft consisted of four Caterpillar diesels with a total of 700 h.p. Two of these served to drive the Shottel screw--rudder complexes with their twin propeller screws, having a turning radius of 360° on a horizontal plane; the other two drove the eight centrifugal fans, four in the bow and four in the stern, to create the air curtains. The air pressure in the cushion was 250 kilograms of force per m^2. The material selected for the hull was choice glass reinforced plastic, however, to speed up construction, the first craft was manufactured with planking of multi-layered veneers.

Lift above the water's surface at 25 knots was about 20 centimeters. Flexible skirts were installed in the extremities. Maximum wave heights of about 0.6 meters could be overcome without decreasing speed. Over larger waves, the speed was dropped.

Test runs of D-2 craft on the Thames showed that they were vulnerable where the propeller screws were uncovered and were often damaged by floating objects. To check out the seaworthy capabilities of the D-2.002 in natural conditions, the craft made an 820 mile voyage from Dumbarton to London, doubling the eastern seaboard of England.

Later, the Denny firm worked out the design for the D-3 ACV which could transport 600 passengers at speeds of 40 knots. The craft had a full weight of 135 tons, a length of 45.8 meters, and a width of 15.3 meters. The use of diesels for main engines and to drive the fans was envisioned in the design. Variations of both rigid and flexible side-walls with flexible skirts in the bow and stern were considered. In working out the D-3 model designs, the results of the D-2 test were studied to eliminate the sharp blows to the bow and the heavy amount of splashing. The bows of the models were given more seaworthy forms, significantly improving its characteristics over waves.

On the whole, the testing of the D-2 on the Thames was not successful due to: enclosed accommodations for passengers, a lack of air conditioning,

parts of the screws being damaged, intensive splashing at low speeds, and a small degree of seaworthiness, which did not permit these craft to compete with the average pleasure boat. The advantage of speed in this case was not as large an influence as in ACV's with flexible skirts.

As a result, the Denny firm, after having built four D-2 craft, discontinued further construction, and interest in ACV's with sidewalls declined in England for a while.

In 1966-67, the newly-formed firm of Denny Hovercraft made modifications to the D-2.002, seeking to improve its seaworthy capabilities and to increase the life of the screws [99]. The screw-rudder complexes were replaced with propeller screws, installed in the sidewalls with the shafts going inside each wall. Semi-balanced rudders were suspended for the screws. The form of the bow was changed and transverse, segmented flexible skirts were installed to improve the seaworthy capabilities of the craft. The D-2.003 and D-2.004 craft had eight fans with greater output.

Such modifications permitted an increase in speed of the D-2.002M to 34 knots (versus 25 knots in the D-2.002) and up to 30 knots for the D-2.003M, which was three tons heavier than the D-2.002M.

Following these modifications, the craft could develop its greatest speed over waves up to 0.6 meters high. Over higher waves, the speed had to be decreased to avert blows on the hull by the waves. Over wave heights of 1.2 meters, the craft could not exceed 10 knots.

These modifications did not help to increase the seaworthy capabilities of the D-2, however. This could be explained by its failure to increase the lift height of the sidewalls -- a considerable increase which would require increasing the geometric measurements of the craft itself to ensure stability. It is recalled, in comparison, that the seaworthy capabilities of the SRN6, weighing considerably less, permitted its operation over waves up to 1.5 meters high at speeds of 40 knots, thanks to flexible skirts 1.2 meters high.

In 1965 a new boost in the development of ACV's with sidewalls in was provided by the joint efforts of Denny Hovercraft, Hovermarine, and Hovercraft Development in creating a number of interesting designs for craft weighing 8 to 300 tons. In providing these designs, it was ascertained that a demand existed also for small craft with sidewalls, because they were able to attain greater speeds than displacement or glider craft could with equal expenditure of power (Figure 26), and were considerably less expensive and simpler in design than craft with flexible skirts. On orders from the firm of British Rail, Hovermarine built two 60-seat HM-2 craft in 1967-68, weighing 16.3 tons (Figure 27) and intended for passenger-ferry service in the Solent Spithead [92]. Construction of the HM-2 series was complete with the ninth unit.
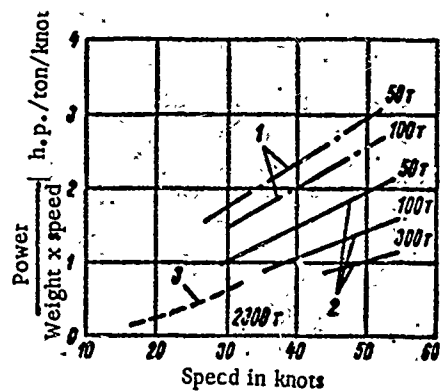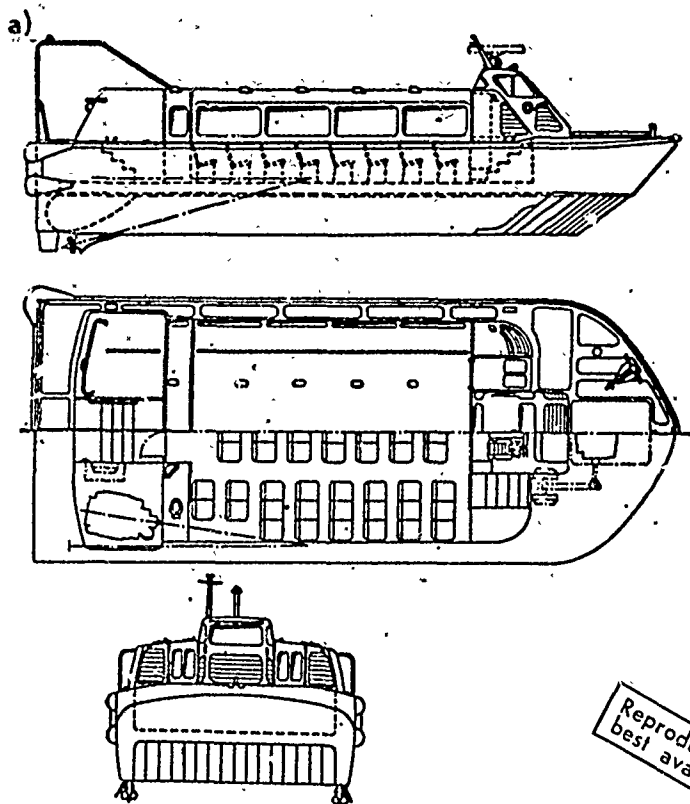
-49-

Figure 26. Equal Expenditure of Power in Craft with Various Rates of Movement. 1, glider craft; 2, ACV's with sidewalls; 3, displacement-type frigates.

a)

b)

Figure 27. The HM-2 Air Cushion Vehicle: a, constructive diagram; b, in movement.

Hovermarine created a series of relatively inexpensive craft, suitable for mass exploitation, using equipment found also in displacement-type craft. The projected speed of the craft was in the range of 25-60 knots. The range of speed in most cargo/passenger craft, possessing diesel power plants, was 35-45 knots. Craft with higher speeds could be created for special or military purposes by using converted gas turbines for the main engines. For larger craft, hydro-drive systems could be utilized.

Besides the afore-mentioned HM-2, Hovermarine had worked out designs for 30, 100 and 350-seat craft with sidewalls, designated HM-1, and HM-4. Also designed were: a patrol helicopter carrier with a displacement of 56 tons and a speed of 37 knots, a fast-moving fire-fighting craft, and a hydrographic survey craft based on the HM-2. The first hydrographic survey craft was built in 1968.

The greatest interest lay in the design of the 127-ton HM-4 craft, built to transport 350 passengers and six automobiles or other cargo weighing up to 60 tons (Figures 28 and 29) [80]. It had a length of 48.8 meters, a width of 20.7 meters, and was 9.1 meters high from the roof of the wheelhouse to the cushion.

The designers sought to create a sufficiently large seaworthy catamaran-type craft, suitable for operation in sea conditions. To accomplish this, the lift height of the hull above the water's surface was increased considerably (up to 4 meters) in moving on the air cushions. In order to lower the center of gravity to ensure stability, all the basic compartments (including the passenger compartment, the machinery compartment, and fuel tanks) were placed in the side bodies, which were well-suited for this purpose. The width of the hull, in the bottom part, was one meter.

The central part of the body served basically to join the hull together, to accommodate some equipment (the centrifugal fans and their engines), and also to take in the lift forces for the air cushions. In view of the transverse contacts (piping with a diameter of about 2.2 meters) with the light elastic elements, the pressure of the air cushions could be taken in by the central part of the body.

Transverse-segmented flexible skirts more than 4 meters high were provided in the bow and stern extremities. The wheelhouse was situated in the bow and ensured a 360° field of vision. The passenger compartments were placed in the side body on two decks, the width of the upper one being about 4.5 meters and the lower one -- 2.5 meters. The hull was made of glass reinforced plastic or light alloys. The main engines were situated in the hull and were highly-reversible diesels or gas turbines which drove the hydro-drive system, having water-gates in the bottom of the side bodies.

-51-

Disembarking of passengers and the unloading of automobiles and other cargo were accomplished through the stern door. In addition, a door was provided on each side of the bow for entrance into the passenger compartment.

The draught of the HM-4, in moving on the cushion, was about 0.6 meters. In accordance with its design, the HM-4 could attain a speed of 40 knots over waves 0.9 meters high.

Obviously, the design problems of the HM-4 were: ensuring stability, creation of optimum design in flexible skirts, difficulty in ensuring normal operation of the hydro-drive system due to the small amount of draught, the possibility of baring the bottom to waves, etc.
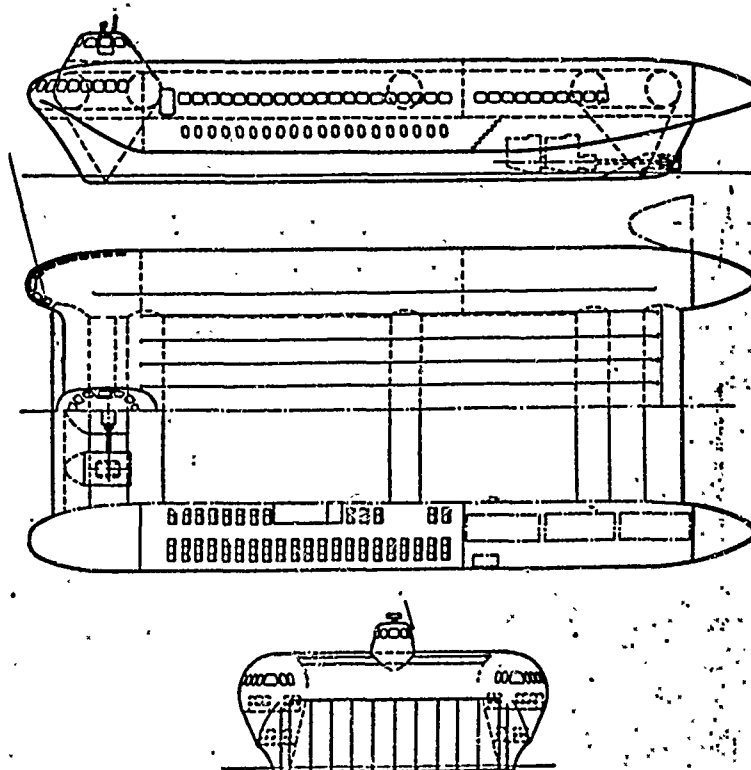

Figure 28. Constructive Diagram of the 127-ton Cargo/Passenger ACV -- the HM-4.

The HM-1, HM-3, and the helicopter-carrier patrol craft had less displacement than the HM-4. The range of their speeds was 35-45 knots. They had improved seaworthy capabilities compared to the seaworthiness

of the D-2, thanks to an increase in the height of the sidewalls (in the little HM-1, alone, it equalled 0.76 meters), and they improved the form of the bow extremity by using flexible skirts. The HM-3 craft was put out in two variants: for navigation on rivers and on the sea. In the latter case, the sidewall height was increased by 0.6 meters in contrast to the first version. The seaworthy capabilities of the HM-3 and the power of its engines ensured its movement over waves 1.2 meters high at a speed of 30 knots and over waves 1.8 meters high at a speed of 20 knots. The HM-2 could develop a speed of 35 knots over waves 0.9 meters high.

In the construction of the craft, Hovermarine used plastics and reinforced fiberglass extensively in forming the hull, while the bottom compartments were packed with layers of foam to ensure buoyancy.

The work of the Hovermarine firm, supported by the Ministry of Aviation and coordinated with Hovercraft Development, could be considered as the first phase in exploiting ACV's with greater displacements.
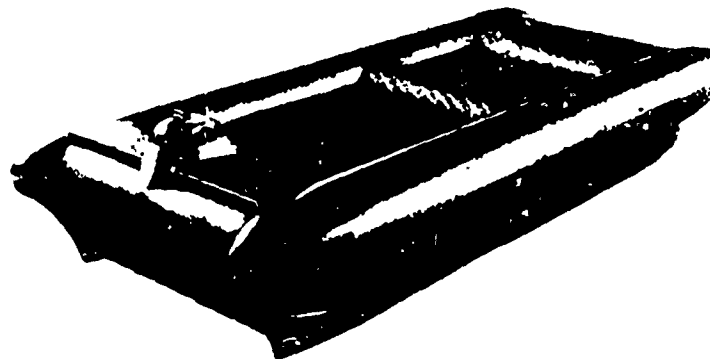
Figure 29. A Model of the HM-4 ACV.

A design was worked out for an anti-submarine ACV with a displacement of 300-400 tons and with sidewalls, in which prolonged operation at a displacement rate with economical speeds of about 25 knots and at a speed of about 90 knots on air cushions could be ensured.

As is generally known, craft with flexible skirts have a short duration of operation on cushions because of the large expenditure of fuel, and at displacement rate their speed is low (8-10 knots) because of the presence of skirts and poor hydrodynamic surroundings.

Design research of a large English ACV, mentioned earlier, with a weight of 4000 tons was completed in two variants: with flexible skirts

-53-

and with sidewalls. The possibility of creating flexible skirts for ACV's of such weights seemed doubtful. Research by British Hovercraft confirmed the possibility of creating a large ACV with sidewalls and a speed of 50 knots, yet the specific power of 40 h.p. per ton would be decreased.

In the U.S.A., serious attention was given to the development of an ACV with sidewalls, which was designated CAB type craft and placed in Class B. After several years, research on CAB craft led to scientific investigation by the Naval Aviation Center at Jonesville [100]. An experimental craft was built at the Center in 1963, the XR-1, which was 15.9 meters long and weighed 10 tons. An interesting solution was found to the problem of containing the air cushion in the bow and stern of this craft. This was accomplished by rigid flaps, fastened on hinges to the sidewalls. In the lower sections, the flaps are joined by glider skis. The craft glided along the water's surface on the skis, with the flaps overlapping the underdome area between the sidewalls to prevent air flowing from the cushions. Constant contact of the skis with the water's surface was maintained either by pressure from the air cushions on the flaps or by special springs. Stability could be ensured, it was figured, by dividing the width of the craft into sections with the flaps and skis. Stability in the XR-1 was insufficient, however, and it over-turned in testing.

A design worked out by Booz-Allen Applied Research utilized the new bow and stern skirt developed in the U.S.A. The creation of such a design, which would ensure the durability of skis and flaps in conditions of dynamic ascendancy over waves, was an extremely difficult task.

The performance of the XR-1 in tests showed great promise, and in Jonesvills, under the direction of G. Chaplin, a CAB type craft was designed with a displacement of up to 12,000 tons, the results of which confirmed the adviseability of building a CAB type ACV with a greater displacement [90]. A great amount of design research into CAB type ACV's in the U.S.A. was also accomplished by the Booz-Allen Applied Research firm on orders from the the Merchant Marine [76]. ACV's with weights from 1-10,000 tons were envisioned for trans-Atlantic transfer of cargo.

The creation of such craft was itself a complex scientific-technical task and required solutions to many problems. In connection with ensuring stability and control, systems of control were worked out; to attain greater seaworthy capabilities, the firm worked out scientifically valid norms of durability and methods of calculating durability, created optimum designs and materials for the hull and skirts and highly economical gas turbines with an aggregate power of up to 30,000 h.p., transmissions for them, optimum propelling agents, etc.

-54-

Regardless of the task, work on creating CAB type ACV's with large displacements was carried out in the U.S.A. both by the Department of the Navy and, in particular, by the Merchant Marine. The Merchant Marine envisioned the design and construction of an ACV weighing 500-1000 tons in the first phase of its program. The cost of this first phase, including the building of an ACV weighing 500-1000 tons in the mid-70's was put at 20 million dollars, and together with a program of expenditures for the completion of a project for a craft weighing 5000 tons would run 100 million dollars.

Designs for CAB type ACV's with greater displacements also were worked out by Bell Airsystems, which played a leading role in the building of this type of ACV.

§7. The Air Cushion Vehicles of Bell Airsystems

The American firm of Bell Airsystems began creating ACV's in 1958. On orders from the U.S. Navy in 1960, the firm built an experimental launch for its first test run -- the XHS-3 "Hydroskimmer" which weighed less than a ton and employed single contour peripheral jets. The total power of the engines was 145 h.p. and the craft developed a speed of 32 knots.

The Bell firm's most serious work was the design and construction, on orders from the U.S. Navy (on a competitive basis), of a tested ACV -- -- the Class A SKMR-1 (Figure 30) [91]. Construction of the craft took a year and was concluded in May, 1963. The cost of the contract was 2.02 million dollars. The SKMR-1 was built to conduct tests and work out results in specifications required for seaworthiness, stability, maneuverability, durability, etc., as well as for estimations of the suitability of the ACV as a landing craft for troops, an anti-submarine and patrol craft, a minesweeper, a rescue craft, and a supply ship, The SKMR-1 initially had a length of 20 meters, was 8.24 meters wide and 7.2 meters high. Its full weight was 20.4 tons.

The air-cushion was created by four master fans 1.98 meters in diameter. Each fan supplied air to one-fourth of the cushion. Thrust was ensured by two screws 3.05 meters in diameter.

The fans and screws were run by four Solar Saturn gas turbines, placed in the bow and stern on both sides of the craft, with power of 1080 h.p. The cargo compartment was in the central part of the craft and measured 2.4 × 5 meters.

A peripheral nozzle, and latitudinal and transverse nozzles to ensure stability, divided the craft into four sections. These buoyant sections were the basic elements of the body. Air in the jets acted on the flat receiver, the decks of the superstructure, and over the surface of the sections for buoyancy. The total area of the air cushions was 114 m^2. The jets for stability were vertical and the peripheral jets were inclined at a 45° angle.
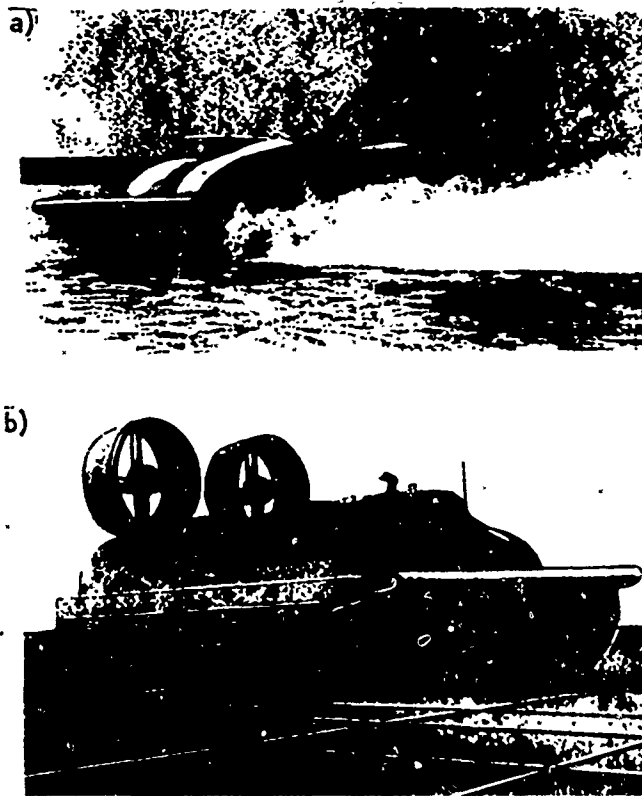
-55-

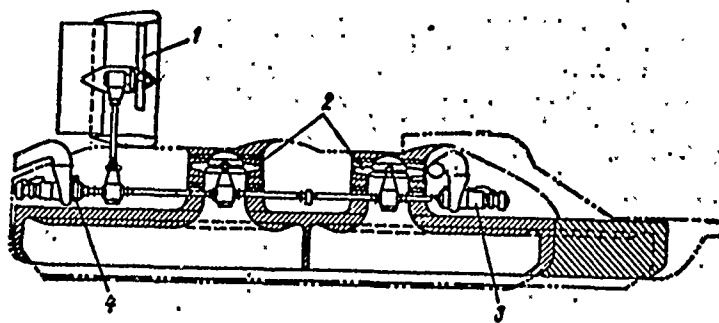Figure 30. The SKMR-1 Test Air Cushion Vehicle: a, without flexible skirts; b, with flexible skirts.

Figure 31. Principal Diagram of the Lift System on the SKMR-1: 1, the screw; 2, the fans; 3, the bow engine; 4, the stern engine.

Two Solar Saturn engines were connected to one common shaft, to the reduction gear of two fans, and to one screw on each side of the craft (Figure 31). Redistribution of power between the lift system and the motive system was carried out by varying the pitch of the air screws.

The fans were made of glass reinforced plastic and had blades to regulate the entrance of air and a wheel with 10 fixed blades.

The 3-bladed, variable pitch air screws were made of aluminium alloys. The stationary annular jets of the screws provided an increase of up to 50% of the total thrust at low speeds and up to 1/3 at high speeds.

The jets also ensured course stability for the ACV. Suspension of the jets in the flow of the screw rudders ensured control of the craft at high speeds.

The estimated durability of the hull was brought about as an out-come from situations of operating the craft at speeds of up to 50 knots in state 3 sea conditions. The basic contacts of the hull and the planking were made of light alloys, and the superstructure -- from glass reinforced plastic. The SKMR-1 had dual aircraft-type controls. In front of the commander's chair were: a steering column, pedals for rudder control, a throttle, two levers for the air pitch screws, and control gauges used to control the engines, the various systems, and movement. In contrast to the British-made ACV's the SKMR-1 craft had reversible shields in the peripheral jets, which were used to alter the flow of air in the jets on either side and to create side forces. Control of these shields was accomplished by declining the columns to the side. A similar system also was provided for control of trim difference, but proved ineffective after flexible skirts were installed.

Fuel for the engines was placed in four tanks, with a capacity of 1820 liters each, one in each compartment of the buoyant section. This supply of fuel ensured 14 hours of operation. Four generators with a power of 15 kilovolts and storage batteries for starting the engines were installed on the craft.

The SKMR-1 was designed to appraise several ways of skirting air cushions: with jets and a flat bottom, with sidewalls 0.4 meters high, and with flexible skirts.

Operational and seaworthy tests of the SKMR-1, without flexible skirts and with skirts 0.6 meters high, were conducted during 1963-64 on Lake Erie. After the flexible skirts of the SRN5 and SRN6 were worked out by the Westland firm, they were installed on the SKMR-1. The skirt design is shown in Figure 32.

The skirt height was increased to 1.2 meters. The full weight of the craft stood at an even 30.6 tons, the maximum -- 31.6 tons.
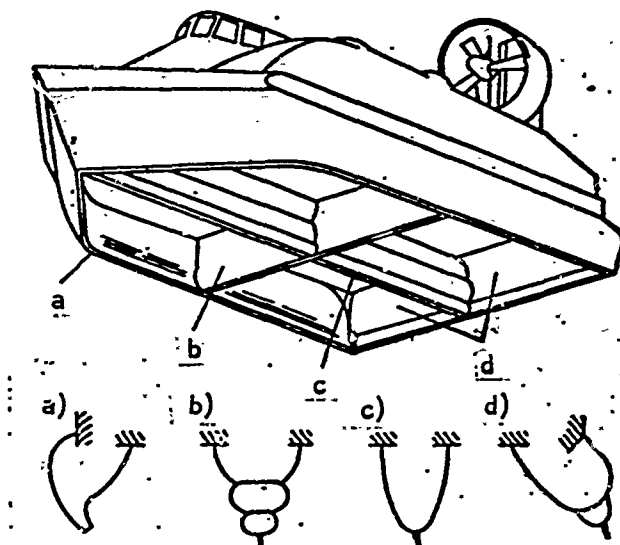
Figure 32. Design of the Flexible Skirt Installed on the
SKMR-1: a, periphery; b, ensuring transverse stability;
c, ensuring longitudinal stability; d, the stern.

During 1965, tests were conducted on the SKMR-1 under a special program.

Using the test results of the SKMR-1, the Bell firm worked out an ACV design that would weigh 250 tons, but the craft was never built. The Bell firm had an agreement with the English firm of British Hovercraft to build (under license) the SRN5 and SRN6 ACV's. Today, in keeping with this agreement, Bell has built a total of seven SRN5 craft. The firm received the bodies from England and mounted American-made 7LM101PJ 101 gas turbine engines on them, with a power of 1000 h.p. Re-equipped by the firm, the SRN5 and SRN6 craft received the designators SK-5 and SK-6. Three military SK-5 craft, equipped with light armor and four machine guns, were sold to the U.S. Navy and participated in the agressive war in Vietnam, while two SK-5 passenger craft were used in Alaska [80].

In future production of SK-5 and SK-6 craft, the firm decided to make some changes in their design, in particular: to install the more powerful General Electric 7LM100PJ 102 gas turbine engines with 1150 h.p.; to increase the seating area, and to strengthen the armament.

The Bell firm worked out several original designs of Class A ACV's, in particular the SK-9 and SK-10. They planned to build a total of 65 units of SK-5, SK-6 and SK-9 craft.
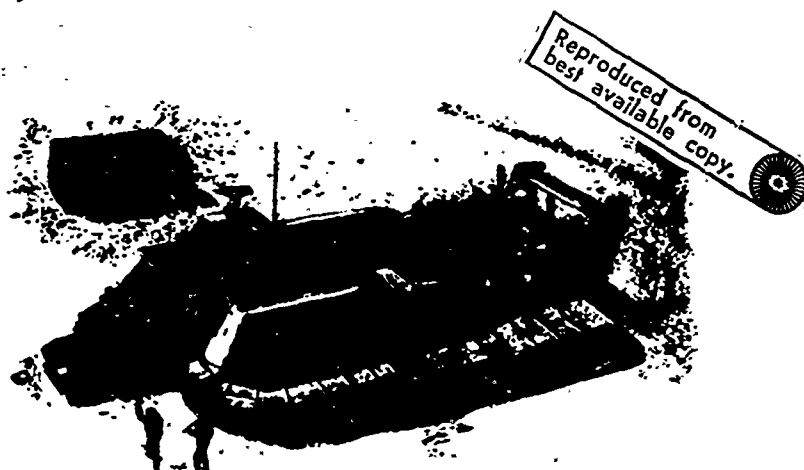
Figure 33. The 90-Seat Military ACV, SK-9 (Drawing).

Figure 34. The Landing-Assault ACV, SK-10 (Drawing).

The SK-9 (Figure 33) was a development of the SK-5/6 craft and used many of their features, in particular, securely-mounted fans and screws but, in contrast to the SK-5/6 series, the SK-9 had two engines and two screw/fan complexes. This permitted the weight to be increased

-59-

to 21.3 tons and the accommodations for passengers to 90 people with two tons of additional cargo. In essence, the SK-9 was an American version of the BH-9. The main engines were two gas turbines with 1,250 h.p., which drove two 4-bladed air screws 2.74 meters in diameter and two centrifugal fans 2.13 meters in diameter. The capacity of the fuel tanks was 2.6 m^3.

Its seaworthy capabilities ensure movement over waves 1.2-1.5 meters high at speeds of 40 knots. Its speed over calm waters was 60 knots, its operating range -- 180 miles.

The SK-10 (Figure 34) was an assault landing craft, built for landing troops and technicians from U.S. Navy landing craft.

The SK-10 could transport 60 tons of cargo over a distance of 100 miles at a speed of 80 knots over calm waters or 60 knots in state 3 sea conditions. It was equipped with flexible skirts 1.5 meters high. It had bow and stern ramps and a cargo compartment built to carry one tank or other military equipment. Additionally, the right and left sides of the superstructure could be used to transport 160 soldiers with their weapons. In using the cargo hold for transporting landing troops, 320 soldiers could be accommodated.

The general arrangement of the craft did not differ from that of the SK-9, but the main engines were two gas turbines with a total power of 12,000 h.p., leading to the 4-bladed air screws 4.4 meters in diameter and to the centrifugal fans 3.66 meters in diameter. The full weight was about 120 tons.

The firm also completed an ACV design for a 4,000 ton craft [104].

§8. Experimental ACV's

Despite the short period of the ACV's development, the creation of the basic type ACV's with flexible skirts around the entire perimeter and with immersible sidewalls (bodies) was preceded by an intensive search for design solutions which led to a large number of diverse experimental ACV's. However, some design solutions were never used, for example, water curtains for skirting the air cushions on the XHS-1 (U.S.A.), and others underwent improvements and were adapted to the design of the ACV. The last to be regarded in the way of designs for experimental Class A ACV's, the VA-2 and VA-3, were by Vickers-Armstrong and received further development by the British aircraft company.

We will dwell on design features only for those experimental ACV's which offer good prospects and are distinguished from the ACV designs already considered. It is natural that such an approach to examination of experimental ACV's appears biased to a certain extent.

The first group of experimental ACV's that we shall study belongs to the British firm of Vosper-Thorncroft [107]. This firm, engaged earlier in creating small ACV's, has specialized since 1967 in creating semi-amphibious ACV's with flexible skirts around the entire perimeter but using screw propellers for movement. In 1969 the first experimental ACV of this type was built, the VT-1, with a full displacement of 77 tons, intended for operating along coast lines with passengers and cargo (see Table 1). The design of the hull and the flexible skirts were standard, having been used on the ACV's of British Hovercraft. The central part of the deck acted as a cargo hold with through passage and ramps for accommodating automobiles or, in the passenger version, as a passenger salon. In the side compartments were the passenger and auxiliary accommodations, and in the middle of these compartments -- the machinery compartment.

In particular, the VT-1 had an original engine-propelling agent complex. It consisted of two AVCO Lycoming T-20 gas turbines with a maximum power of 2000 h.p.; a Vee-drive gearbox, inclined shafts, and Ka-Me-Wa variable pitch screws. Each turbine, besides this, drove four centrifugal fans 1.5 meters in diameter through a transfer gearbox and a larger than usual shaft which created the air cushion.

The designed maximum speed of the VT-1 over calm waters was 48 knots, with a speed of 40 knots over long voyages.

Tests of the half-scale self-propelled model VT-1 were successful.

The design of the VT-1 was an interesting test to avoid using air screws on an ACV and, yet maintain the high speed necessary for an ACV to have full separation from the water's surface (Class A). Essentially, a craft of this type used elements designed for Class A ACV's (full separation of the rigid hull from the water's surface, with flexible skirts) and Class B (submerged screw propellers). It is natural that use of screw propellers should deprive the ACV of the possibility for complete movement in coastal waters, however, it ensured the possibility of partial movement in advance preparation for disembarking passengers and automobiles in the bow extremity.

All things considered, the Vosper-Thornycroft firm's cost of building the VT-1 was lower than that of an ACV in Class A with a similar displacement.

The British firm of Britten-Norman (Cushioncraft) offered some interesting work connected with creating an ACV in Class A that would

have very little noise, which we shall place in the second group of experimental ACV's [80]. The first ACV built by Cushioncraft, in 1959, was the 3-seater CC-1. Following that, three 10-seat CC-2 craft were built. From the test analysis of the crafts' operation came the idea to create two new types of ACV's: the CC-4 and CC-5.

The experimental CC-5 was built in 1966, had a length of 8.8 meters and a width of 4.7 meters, was 1.8 meters high, and was equipped with flexible skirts 0.6 meters high. The full weight of the craft was 2.0 tons, the empty weight -- 1.45 tons. This ACV was intended for passenger transport, with room for 6 passengers or 0.45 tons of cargo. Its highest speed was 39 knots.

The CC-5 used Rolls-Royce gas engines with 240 h.p. as its main engines. They were mounted in the bow section of the ACV and led to two pairs of centrifugal coaxial fans, of which the stern pair provided thrust (70% of the power), and amidship -- created the air cushion (30% power).

This arrangement of the engines and fans gave the most advantage for centering the craft.

A feature of the CC-5 was the use of a low pressure fan-jet system, air flowing from the receiver through special openings in the stern. Use of the jet streams of air for creating thrust and the deflection by the air screws allowed Cushioncraft to work out a number of designs for ACV's with little noise. The firm considered the prospects of using this method to create thrust in an ACV of large weight.

In 1968, the firm proposed to put out a CC-7 series capable of speeds up to 50 knots and built to carry ten people. The main engines of the CC-7 were gas turbines with 390 h.p. to ensure drive of the centrifugal fans and to create the lift forces and thrust.

Seeking to improve transport of ACV's along roads and to decrease their width, the firm worked on creation of a design for an ACV with removable or pneumatic sides. The CC-7 had inflatible sides of elastic material. The width of the CC-7 with the pneumatic sides was 4.6 meters and without them -- 2.3 meters. An 18-ton ACV was designed, the CC-6, for which the CC-5 was a semi-scale model. In this ACV, the firm proposed to transport from 4 to 6 automobiles and 30-40 passengers at a speed of up to 48 knots over calm waters. Movement was also accomplished by a jet flow of air. The project was never realized due to a lack of financing.

In evaluating the work of Cushioncraft in regard to the creation of an ACV with little noise, we note that the method of movement by jet

air streams can only be used on small ACV's and at low speeds, because of the small increase in achieving thrust and by the lower coefficients of useful actions in such propelling agents. It could be used, however, to improve meaneuverability in an ACV at low speeds, in particular by the use of rudders in the streams. This method was used earlier on the experimental SRN1 (England) and the SAAB-401 (Sweden).

The third group of experimental ACV's, HD-1 and HD-2 Class A craft, was created by "overcraft Development.

In 1967, these were turned over to the National Physics Lab, which carried out research into speed and dynamics of the craft both in models in a test basin and actual craft. Special attention was given to research into the ACV's conduct over waves.

The HD-1 was built in 1963 as a basis for working out various designs of flexible skirts. The hull of the HD-1 was made of woods and veneers with a topping of nylon. The length of the modified HD-1 was 15.2 meters, the width (including the skirts) was 7.0 meters, and the full weight was 9.1 tons. Its highest speed was 37 knots; 30 knots on long voyages. For propelling agents, there were two air screws situated in the bow and stern. The bow screw had two fixed-angle blades and was driven by a Continental GJO-470A engine with 310 h.p., and the stern -- by a Rolls-Royce 145 h.p. engine.

In Figure 35 the HD-1 is shown with a variant of flexible skirts tested on it. The skirt in the bow consisted of transverse-segmented elements and the sidewalls consisted of one rigid layer of material.

At the same time that the flexible skirts of the HD-1 were being designed, research was being conducted on material from which they would be manufactured. Skirts of various light, strong-wearing materials were tested, in particular nylon with neoprene topping which weighed 0.2 to 1.0 kilograms per meter^2. The best of these were selected for further investigation.

Prolonged testing of the HD-1 showed it adviseable to research the individual problems connected with movement in small self-propelled models of the ACV, especially designed and equipped for these purposes. In regard to this, Hovercraft Development built a second experimental craft in 1967, the HD-2, intended initially for working out the problems of control and maneuverability, especially at low speeds. The HD-2 was a self-propelled model similar to the BH-8, and was equipped with two Proteus gas turbines [101]. The HD-2 had a full weight of 4.1 tons, a length of 9.4 meters, and a width of 5.8 meters. Its choice for optimum control systems on the ACV included: two air reversible screws on turning pylons with turning angles of ±90°, bow and stern jet rudders on each side, three chassis -- one for control in the bow and two non-directional ones in the stern, accounting for up to 20% of the weight of the craft (the remaining weight was taken care of by the air cushion).
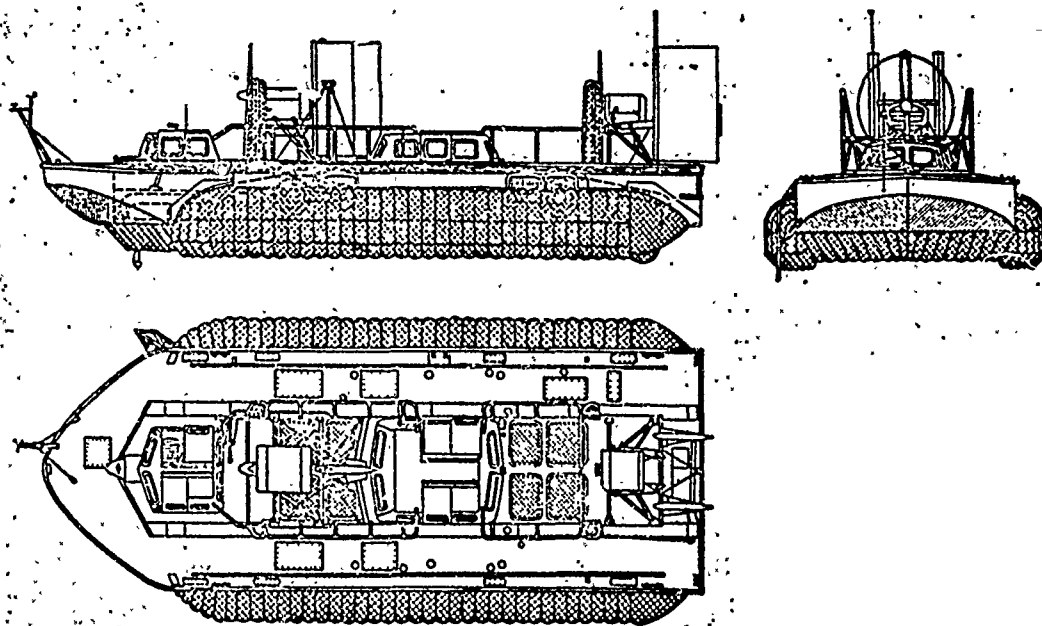
Figure 35.   Constructive Design of the Experimental ACV, HD-1.

Three Rover 2S-150A gas turbines, with 146 h.p. each, were mounted on the craft -- two of them led to the screws and one, situated in the stern, led to two 10-bladed axial fans, making an air gate in the stern. The total output of the fans was 28 m^3 per second, the pressure in the cushion of 107 kilograms of force per m^2. Effentially, this was the second case (the SRN1 was the first) of using under-dome fans on British ACV's. The fans fed air to the under-dome area, which was surrounded by transverse-segmented flexible skirts to strengthen the flexible receiver.

The fourth group of experimental ACV's in Class A were the ACV's with cylindrical flexible skirts initially created by the French firm of Bertin (see Figure 8f). The firm had worked on creating an ACV since 1957, with the first French craft (the Terraplane BC-4) being built and displayed in 1961. Later, the firm designed a whole series of similar craft, designated BC-6, BC-7, etc., which essentially were wheeled vehicles more practical in moving over land than water. A distinctive feature of all the ACV's worked out by this firm was the use of cylindrical flexible skirts, the number of which varied from 8 to 12.

The amalgamated firm of SEDAM was created in 1965, in France, by several shipbuilding and aviation firms.

The company specialized in creating ACV's, with its greatest interest being the building in 1967 of a 27-ton experimental ACV, the Naviplane N-300 (Figures 36 and 37).

The company envisioned for its craft a combined system of flexible skirts, including the cylindrical flexible skirts of Bertin, increasing the peripheral flexible skirt around the air cushions.

The advantages of cylindrical flexible skirts were: an increase in economy (i.e. a small expenditure of power to create the lift forces), high stability, stable forms in the skirts, the ability to easily overcome obstacles, simplicity in its repair, and very little cost. The N-300 was built to carry up to 100 passengers. In the summer of 1969, two N-300 craft were put into test operation along the coast of the Mediterranean Sea for 5 months.

Two Turbomeca Turmo gas turbine engines with a total of 1500 h.p. were mounted on the N-300 and drove two air screws 3.5 meters in diameter, which were situated amidship, and four fans 2.2 meters in diameters. The fans forced air to the eight cylindrical flexible skirts two meters high for a massive peripheral flexible skirt. This height of the flexible skirts, installed on all ACV's of this weight in the future, provided higher seaworthy capabilities' in the craft.

The experimental N-300 acted as a prototype for a series of much larger ACV's, the first of which was the N-500 with a weight of 200-220 tons and due to be put into service in 1972. It was designed to carry 400-500 passengers or 40 automobiles and 300 passengers at maximum speeds of about 75 knots.
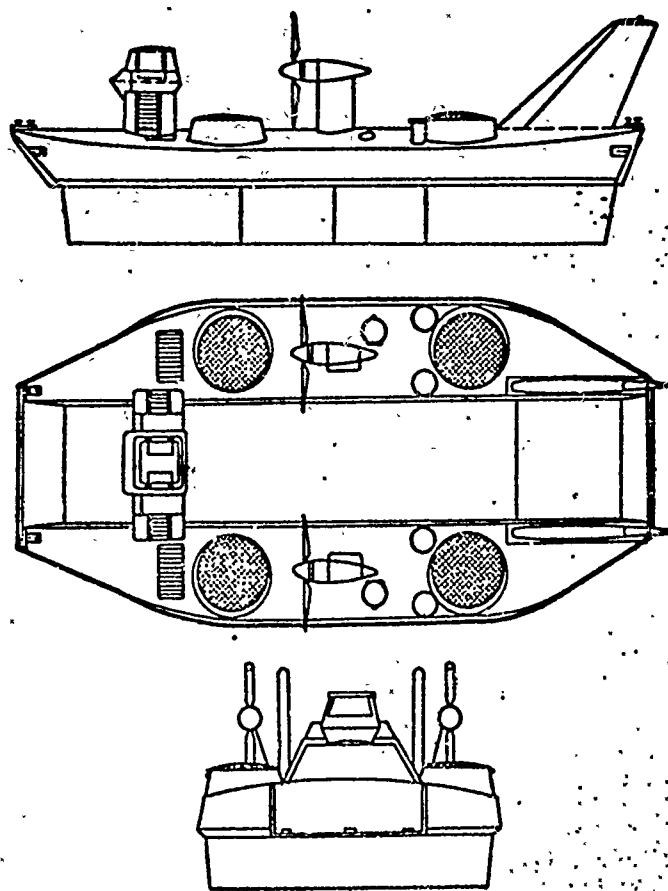
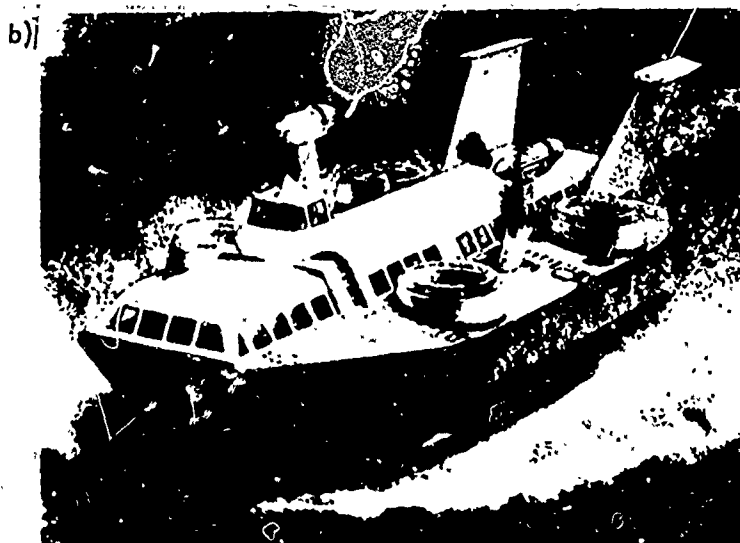Figure 36. Constructive Design of the ACV, N-300.

a)

b)

Figure 37. The ACV, N-300.

Later on, the SEDAM firm was supposed to build ACV's for military purposes -- an assault landing craft, a patrol ship, a ship for anti--submarine defense, etc.

We note that the design of the flexible skirts in the form of cylinders was investigated also in other foreign countries. In particular the American firm of Bell built an experimental ACV in 1963, the "Carabao", weighting about 1.3 tons, with three cylindrical flexible skirts, which developed a speed of about 50 knots and had a total engine power of 210 h.p. Later, the Bell firm worked out designs for ACV's with greater displacement and having cylindrical skirts, but they were never built.

§9. Local ACV's

Construction of air cushion vehicles in the Soviet Union, as was noted in the introduction, was begun soon after K. Eh. Tsiolkovski theoretically substantiated the principle of moving on air cushions in 1927. Work, connected with creation of these craft, was led by Professor V. I. Levkov of the New Circassian Polytechnical Institute.

After the Great Patriotic War, work in the Soviet Union designing and building ACV's continued. The work moved in two directions: the creation of ACV's using the chamber design and their subsequent modifications -- ACV's with immersible sidewalls (Class B), and ACV's using the peripheral jet design and their later modifications -- ACV's in Class A.

We will not dwell on all the forms of ACV's built during the postwar years in the USSR, but will consider the ones which offer the greatest interest.

Representative of the first direction taken by designers is the test passenger ACV, the Neva (Figure 38), designed by the Central Technical Design Office of the Ministry of River Fleet (Russian Soviet Federative Socialist Republic) together with the N. E. Zhukovski Central Aerodynamic Institute and the Leningrad Institute of Water Transportation Engineers, and a passenger ACV, the Gorkovchanin (Figures 39 and 40), designed by the Design Office of the Volga-Baltic Ship Project together with the Gorkiy Institute of Water Transportation Engineers. The Neva was built in 1962 and testing was begun on it that year. The craft, a catamaran type, had hinged covers installed in the bow and stern to block the flow of air from the cushions. The body was welded of aluminium magnesium alloys. The air cushion was created by axial fans two meters in diameter with a total output of about 95 m^3 per second and pressures in the air cushions of about 145 kilograms of force per m^2. It had 12-bladed fans, placed in diametrical planes, and driven by two aviation piston engines with 225 h.p. A third engine, with 285 h.p., drove a 2-bladed reversible screw 2.5 meters in diameter.

The passenger compartments were situated along the right and left sides of the craft and the wheelhouse was located in the bow section. The steering gear consisted of two aerodynamic rudders suspended on the air screw fitting

-68-

and operating in the stream of the screw, and two collapsible hydro-
-rudders mounted for transom of the boat. The bow and stern covers, con-
trolled by pneumo-hydro-drive, regulated the flow of air from the cushions.

The full weight of the Neva was 12.45 tons, with a seating capacity
of 38 passengers or 3.8 tons of cargo. The maximum lift height, while
fully loaded over a concrete area, was 60 millimeters. The speed of the
craft, with 11.4 tons of weight, was about 30 knots.

Figure 38. The "Neva" Air Cusion Vehicle.

Problems of stability, speed, control, splashing (spray formations), etc.
were investigated in the Neva. The form of the bottom parts and the design
of the lift systems in the craft were similar to that of V. I. Levkov's.
In testing this ACV, the following deficiencies appeared: a small degree
of seaworthiness, insufficient engine traction power, a small degree of
effectiveness of the air rudders, heavy splashing, etc. which were included
on a series of Neva-type ACV's built for operating on rivers.

In the experimental plant of the Gorkovski Institute for Water Trans-
port Engineers, the passenger ACV "Gorkovchanin" was built -- an ACV with
immersible sidewalls. The craft was intended for carrying passengers on
local lines along small rivers, ensuring its unexpected mooring along the
banks. The body of the craft was put together with D16AT and D16T types
of duralumium. The full weight of the craft was about 14 tons and measured
22.3 meters long, 4.0 meters wide, with a draught of 0.3 meters while moving.
Passengers were accommodated in a passenger salon furnished with arm-chairs
(48 places); the two of the crewmen in the wheelhouse. The salon was pro-
vided with heating and ventilation systems. To form air cushions in the
stern section, a centrifugal fan with an output of 8.6 m^3 per second and a
total pressure of about 200 kilograms of force per m^2 was installed. Drive
of the fan was accomplished by a shaft leading from the main engine. The

main diesel, a 3D6N-235 235 h.p. engine, worked the waterjet system of pro-
pulsion, ensuring movement over calm waters at a speed of 18.9 knots with
180-190 h.p. The other 30 h.p. was spent driving the fan. The
rated height of the sidewalls (0.45 meters) predetermined the small degree
of seaworthiness of the craft, meant only for moving in river conditions.
A flexible skirt was installed in the bow.
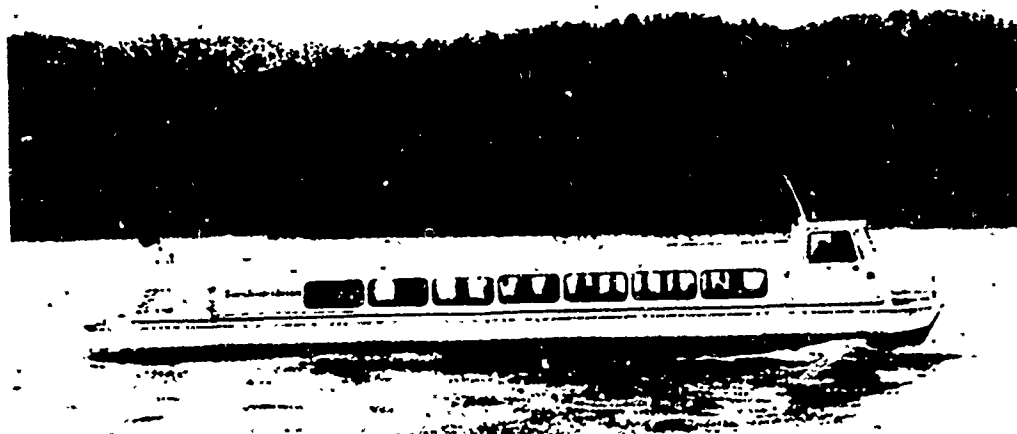
Figure 39. The ACV, Gor'kovchanin.

The Design Office of the Volga-Baltic Ship Project, in collaboration
with the Gorkiy Institute of Water Transport Engineers, had been engaged in
investigation of Class B ACV's since 1961. During this time, it built several
self-propelled models weighing up to 3 tons and put them through comprehensive
tests.

On the basis of the testing of the models, an ACV design was worked
out -- the Gorkovchanin. The Design Office complete a series of design-
-research studies, in which a number of tested river cargo/passenger ACV's
weighing about 400 tons with a payload capacity of 170 tons and speeds of
about 30 knots were studied.

The five-seat experimental ACV "Raduga" and the test passenger ACV
"Sormovich" (Figure 41) were Class A ACV's designed and built by the Design
Office at the Krasnoye Sormovo shipyard. The 30-ton experimental ACV shown
on parade in honor of Navy Day, 1967, in Leningrad is also considered a
Class A craft (Figure 42).
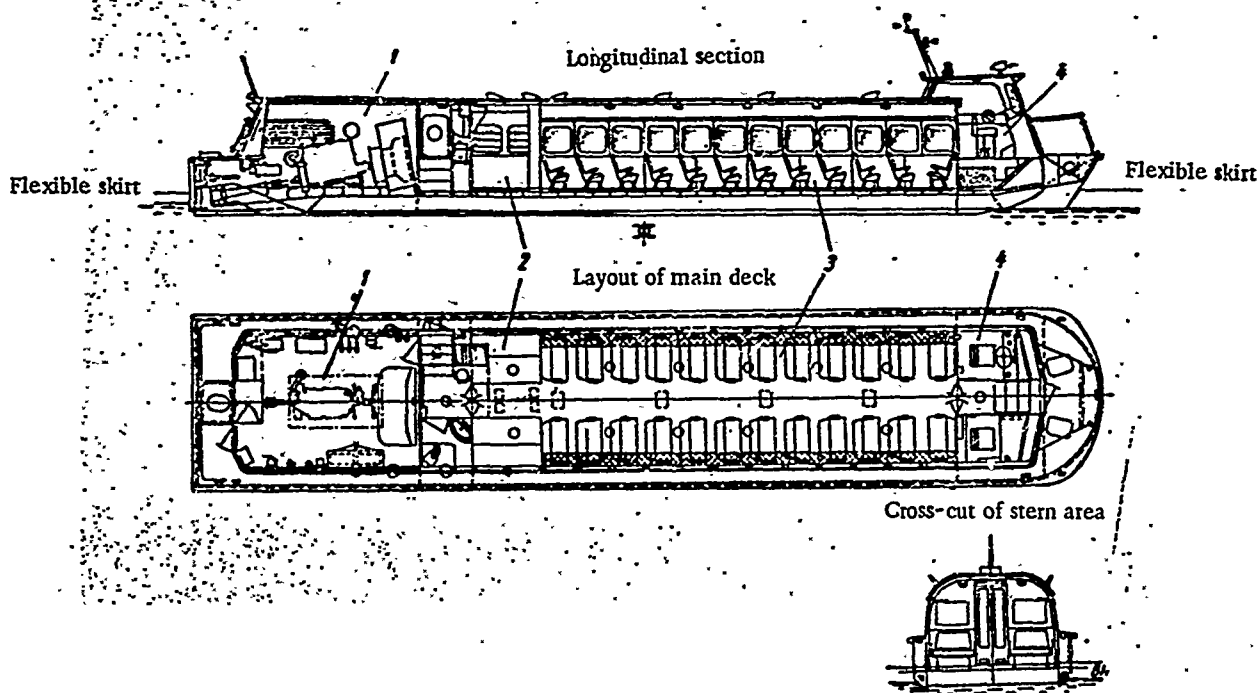
Figure 40. The General Layout of the ACV, Gor'kovchanin.
1, engine compartment; 2, baggage compartment; 3, passenger salon; 4, wheelhouse.

These ACV's were built originally as peripheral jet types , and later modified by installing flexible skirts. The Raduga was built at the Krasnoye Sormovo shipyard in 1962. In the original version of the Raduga, a peripheral jet system 75 millimeters wide, inclined downward 45°, and with two internal logitudinal jets 40 millimeters wide for forming and maintaining the air cushions was provided. The weight of the craft was three tons, the length was 9.4 meters, the width was 4.1 meters, and the over-all height was 3.5 meters.. An axial fan was mounted on it, driven by an aviation AI-14R engine with 220 h.p. A second such engine led to a 3-bladed variable pitch screw, mounted in the stern on a stationary pylon. Control of the craft was attained with the aid of air rudders, mounted in the stream of the screw.

Tests of the Raduga, carried out in 1962-63 without flexible skirts, showed that it developed a speed on the air cushions of up to 54 knots and a displacement rate of up to eight kilometers per hour.

-71-

Figure 41. THe "Sormovich" ACV.

Its speed over snow and ice was 27-32 knots, but it was restricted by safe navigation procedures. Movement over ice was accomplished by a preliminary study of the route. The seaworthy capability of the craft without flexible skirts was shown to be insufficient; if the craft advanced at maximum speed over wave heights greater than 0.3 meters, it experienced rolling, sharp bumps, and heavy splashing. Over wave heights greater than 0.5 meters, the craft was only able to maintain speeds at displacement rates. The planking in the bow section was made of sheets of aluminium alloys 1 millimeter in thickness and considerable damage was incurred by blows to to the ship moving over high waves at speeds of about 80 kilometers per hour. To avoid this damage, the bow extremity was packed with a layer of foam.

In later testing of the craft with flexible skirts, they showed that it increased the speed and seaworthy qualities and allowed them to proceed with the designing and construction of a larger passenger ACV -- -- the "Sormovich."

The Sormovich, built in 1965, also used the jet system. Its full weight, until the installation of flexible skirts, was about 22 tons. It had a length of 26.5 meters and a width of 10 meters. The draught afloat was exactly 0.32 meters. An axial 12-bladed fan driven by turbines, which had to ensure a lift height over hard surfaces of about 0.2-0.3 meters, was installed on the Sormovich. As was shown in test operations, however, this height also was insufficient to ensure high seaworthy capabilities, and installation of flexible skirts was required and later completed. The main engines of the Sormovich were AI-20DK gas turbines with 2540 h.p., which drove the fan and the two 4-bladed regulated pitch screws. The passenger salon was situated in the bow section, isolated from the machinery compartment, and had an excellent view. Fifty easy chairs were placed in the salon. The estimated speed of the craft was about 65 knots over calm waters and 27-43 knots over waves. Its range was believed to be 400 kilometers.
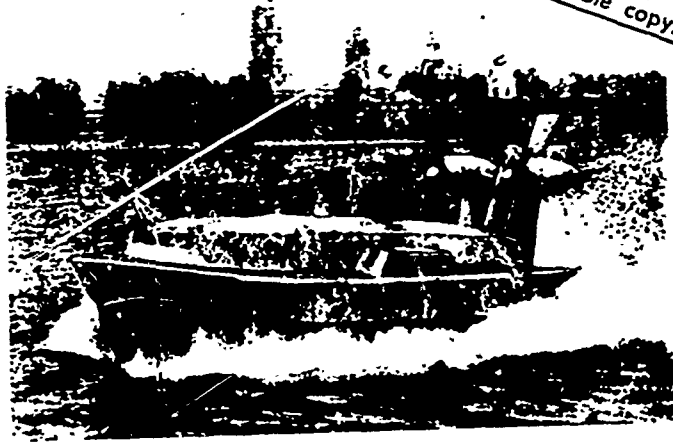
Figure 42.   A 30-Ton Experimental Air Cushion Vehicle.

To provide control of the craft, there were four air rudders with hydro-drive from the wheelhouse suspended on the screw's fitting.

Also in the Sormovich were: a ballast system for control of trim, a bilge system, and a system of fire extinguishers.   In the construction, of the hull, light alloys and glass reinforced plastic were used extensively.

Today, tests are being continued with trial runs of the Sormovich cn the Volga.

We have examined several forms of ACV's built in the Soviet Union. Further research is being carried out on small, self-propelled and non- -self-propelled models, in order to create larger ACV's with higher sea- worthy capabilities and speeds.

Chapter II. Basic Features in the Hydro-Aeromechanics of ACV's

§10. Physical Features and Characteristics of ACV's

In bringing forth and solving the problems in the hydro-aeromechanics of ACV's, it is necessary to consider the basic features of these craft and their distinction from usual vessels and aircraft.

Hydro-aeromechanics of ACV's is one of the complex divisions of applied mechanics, embracing problems of statics and dynamics of both water and air.

In the majority of problems concerned with hydro-aeromechanics of vessels and aircraft, the movement of a rigid body in boundless uniform fluids is examined. In contrast to this, the hydro-aeromechanics of ACV's are determined by the joint solution of 3 problems concerning movement in dense environments of varying density in 3 area (water, receiver and cushion, external air space surrounding the ACV) with complex border conditions of surface division. The ground speed of water and the ground speed of air inside the air cushions are connected by physical conditions equal to the normal speeds and pressures of the border division of water and air.

Theoretical determination of ground speeds and pressures inside the air cushions, according to the given law of distribution for the normal make-up of the border division, is sufficiently complex.

The difficulty of a theoretical solution is made worse by the necessity of solving this problem by means of consecutive approximation, since the ground speed of the moving water and, consequently, the border conditions (law of distribution for normal speeds of border division) depend on fields of air pressure on the surface of the division. Therefore, to solve the problem practically, one has to use a purely experimental method of determining the external forces acting on the ACV - testing models in a basin.

In the majority of problems concerned with the hydro-aeromechanics of vessels and aircraft, the movement of a body that is impervious to surrounding environments is examined. One of the basic features of an ACV is its permeability, which leads to the appearance of specific external forces of an inertial nature: impulse resistance, Coriolis forces in movements of circulation and rotations relative to longitudinal and transverse axes.

In the majority of problems concerned with the hydro-aeromechanics of vessels and aircraft, the movement of bodies with fixed geometric forms is examined. A significant feature of an ACV with flexible skirts is the deformation of these skirts during contact with water, i.e. there arises the problem of determining the external hydrodynamic forces acting on the body, the form of which depends upon the quantity of these hydrodynamic forces.

The whole complex of hydro-aeromechanical problems may be divided roughly into three groups.

The first group encompasses those problems, resolved in static formulations, in which fixed rates of water and air flow (during suspension of an ACV over a site) without translational movement are examined.

The second group includes those problems in which fixed flow during an ACV's movement is examined.

Those problems which require the calculation of transient movement of an ACV before they may be solved belong to a third group.

Typical problems of statics of an ACV are those problems for determining lift characteristics and static stability of an ACV.

In determining the parameters of the air cushions of a planned craft, it is necessary to ensure the completion of 3 basic conditions:

1) The force maintaining the craft's air cushions must be equal to the weight of the craft. This requirement determines the geometric dimensions (area) of the cushions and the quantity of excess pressure inside the cushions.

2) The quantity of air, entering the ACV through the fans, must be equal to the quantity of air escaping from the regions of excess pressure under the ACV's hull.

3) The scheme for distribution of excess pressure and air flow inside the cushions must ensure a stable balance of lift height, list angle, and trim for the ACV.

A solution for these problems has been sought by designers since the initial appearance of ACV's. Many interesting ideas have emerged while working on effective ways of skirting the air cushions to ensure the greatest lift height at given expenditures of power.

A great deal less attention was given to the problems of air moving along inside the air conductors in the ACV's hull, a rational choice of types of fans, their influence on expended-pressure characteristics of static stability of lift height, list angle, and trim.

Until recently, there has been little investigation of such problems as the influence of static stability of the basic parameters of air cushions: the pressure in the cushions, air expenditure, overflow of pressure between the receivers and the cushions, as well as the influence of mechanical characteristics and rigidity of materials of the flexible skirts on the lift characteristics and stability of an ACV. Meanwhile, test work with models and actual ACV's shows that many of these factors may be highly essential.

Added to the number of problems in the second group are the problems of maintaining and retaining the ACV's air cushions, and problems connected with the determination of resistance to the ACV's movement.

A feature of ACV's, in comparison to other type craft, is the commensuration of external forces of aerodynamic and hydrodynamic natures. This leads to the necessity of having to consider such phenomena as aerodynamic clearance of the craft in movement due to aerodynamic lift forces on the hull. In a number of instances, the aerodynamic lift force may reach 10-15% of the craft's weight. This changes the under-dome pressure in the air cushions, the quantity of air expenditure, wave resistance, etc.

A typical feature of the ACV is its catching and moving great volumes of air.

The flow of air from the air cushions occurs in the form of streams, usually distributed along the perimeter unevenly, due to the actions of corresponding forces on the craft. The longitudinal make-up of this reaction creates additional resistance to movement or draught. The lateral make-up of the reaction leads to the craft becoming lopsided, to drift, which leads to the appearance of hydrodynamic forces of resistance to drift.

One of the essential aerodynamic features, arising from the ACV's movement, is the interaction of the air stream escaping from the air cushions meeting with the rising flow of air outside. Investigations show that ACV's with annular, single-duct, flow screens have 3 rates of movement, characterized by sharp distinctions in distribution of air flow escaping from the air cushions (Figure 43). At low speeds, due to the interactions of skirting streams of air with the onrushing flow in the bow section, there arose rarefied zones, air from the air cushions being directed into these zones, and static pressure on the bottom part of the ACV's bow was decreased (Figure 43b).

As far as increases in speed of counter-flow, the bow stream is diverted to the sides and back. Subsequently, the speed of pressure becomes equal to the static pressure in the air cushions. The bow stream is divided in two: part of the air continues to flow in front, part is diverted back (Figure 43 c). Finally, at super-critical speeds, when the speed of pressure exceeds the total pressure of the stream, all of the air from the jet is diverted back, and the counter-flow is divided in two, with part of its flowing between the vehicle and the base surface (Figure 43d).

-76-
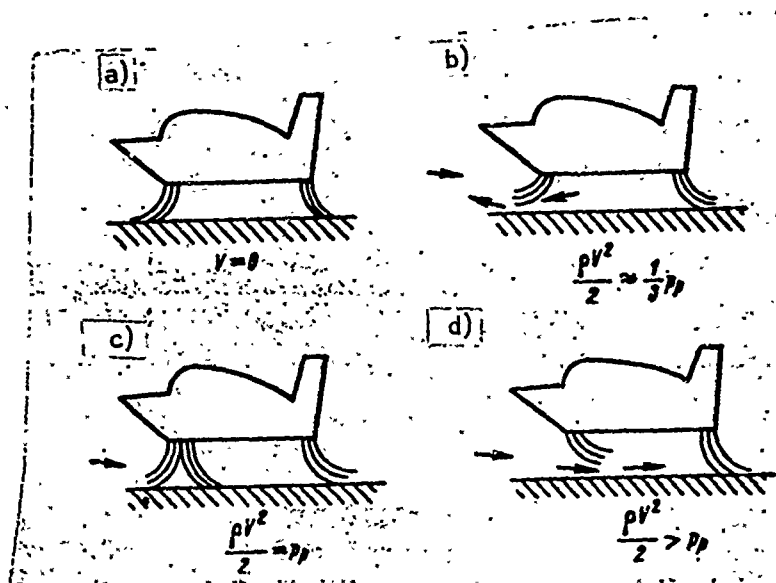
Figure 43. Diagrams of the Interactions of Streams Flowing From the Air
Cushions with the Onrushing Air Stream: $a - V = 0$;

$$b - \rho \frac{V^2}{2} \approx \frac{1}{3} p_p; \quad c - \frac{\rho V^2}{2} = p_p; \quad d - \rho \frac{V^2}{2} > p_p.$$

In the operation of modern ACV's, the second and third rates of flow
are not attained, as a rule, because the pressure in the cushions greatly
exceeds the speed of pressure. The distribution of air flow, characteristic
of the first rate, apparently is realized as a result of an appreciable de-
crease in the static pressure on the bottom, occurring during fulfillment
of the conditions

$$\frac{\rho V^2}{2} \approx \frac{1}{3} p_p,$$

where P_p - quantity of excess pressure in the receiver;

ρ - mass density of the air.
i.e. at velocty V, conforming to the speeds of modern ACV's.

It is necessary to view these critical phenomena, in order to avoid the
possibility of emergency situations when the craft is moving at high speeds
with very little under-dome pressure.

The effect of the zones of increased pressure (cushions) on the free
surface of the water is the appearance of waves on the water's surface. The
intensity of this wave formation essentially depends on two factors: the
excess pressure in the cushions and the speed of the ACV.
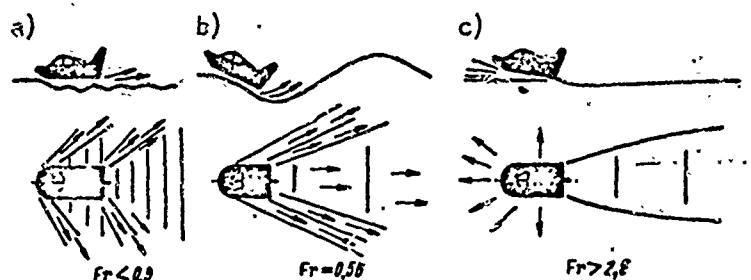
Figure 44. Diagrams of Wave Formation and Escape of Air From the Air Cushions at Various Froude Numbers: a - Fr < 0.5; b - Fr = 0.56; c - Fr > 2.5.

The qualitative characteristic of wave formation, during the movement of an ACV, leads to the following. During suspension of an ACV, without translational movement (at "stop"), a depression is formed in the water under the ACV, the mid depth of which is equal to the amount of excess pressure in the air cushions P_p/γ millimeters (Figure 44).

During translational movement, the depression is deformed, the rear wall becomes more sloped than the front, and a wave system appears behind the craft. Just as during movement of displacement-type craft, the wave system distinctly is marked, varying about 18° in angle to the diametric planes of the craft, and is a system of transverse waves (Figure 44a). Where Fr < 0.5 of the length of the air cushions, it is confined to a few transverse waves. With an increase in speed, the length of the air cushions is roughly 1/2 the length of the transverse waves. In regard to this, the bow part of the air cushions concides with the peak of the first half-waves, and the stern part with the depression of these half-waves. The amplitude of the transverse waves attains maximum meaning, and the ACV acquires significant trimming of the hull (Figure 44b).

With further increases in speed, the wave amplitude decreases, but their length increases. At large Froude numbers, deformation of the free surface vanishes, and movement of the ACV over water is the same as over a hard screen.

As a result of the deformation of the water's surface during movement, there is a redistribution of the pressure inside the air cushions which changes embarkation of the craft (suspension height, list angle, and trim difference), and causes additional external forces of hydrodynamic nature. The longitudinal make-up of these forces is called wave resistance. The transverse make-up of forces, together with the longitudinal and transverse make-up of hydrodynamic moments, have considerable influence on the degree of stability of the craft, effecting list, trim difference, and yaw.

Problems pertaining to the third group include: rolling of the ACV, dynamic stability, course stability and maneuverability, as well as some problems of speed during transient rates of movement (momentum and braking).

In a majority of cases, during movement of the ACV, there is direct contact between various sections of the hull or flexible skirts and the water. This leads to the appearance of additional hydrodynamic forces, which are very substantial at high speeds. In connection with this, it is necessary to note still another feature characteristic of ACV's with flexible skirts. The force of resistance to movement depends on the rigidity of the flexible skirt and its deformation during wash--off, i.e. on the mechanical properties of the material and the con-struction of the flexible skirt.

At high speeds, the forces of contact hydrodynamic origin are so great that in some cases buckling occurs - a loss of stability for the flexible skirt in the bow and its being sucked under the hull. The center for the application of forces to maintain the air cushions is shifted sharply to the stern, the craft is trimmed in the bow and is sharply braked, which might lead to an emergency situation. If the craft moves along a curvilinear trajectory or with drift, the list angle of the outside also is sharply increased. There are several known cases of the English SRN5 ACV capsizing during sudden gyrations at high speeds, because the flexible skirts buckled under the contact of water. To prevent similar occurrences special structural arrangements were worked out which would ensure a decrease in hydrodynamic forces during the flexible skirts' contact with water.

One of the most complex problems of hydroaerodynamics of ACV's is stabilization of the craft's movement on its course and during maneuvers. For an amphibious ACV that doesn't have a mechanism for control in the water, stabilization is attained by aerodynamic means, i.e., by using those of aerodynamic origin (wash-off of the flexible skirts, blows from the waves, etc.). Considering that the density of water is 800 times greater than air, it is necessary to counter the perturbation forces by increasing the area of the stabilizer. However, this leads to an undesirable increase in the area of the sails on the whole, intensifying the amount of side drift in cross winds. Besides that, during movement in choppy sea conditions its speed often is less than with a fair wind. In these conditions, the unnecessarily developed tail unit is a de-stabilizing factor and only hampers control of the craft.

Control of an air cushion vehicle in strong winds is itself a complex problem and requires a certain amount of skill.

On the other hand, many modern ACV's are equipped with a complex of controls which permit completion of maneuvers too difficult for other type craft.

To the number of little-studied problems of an ACV's hydroaerodynamics, the problems of rolling in choppy sea conditions must be added. A specific distinction of ACV's, in comparison with other type craft, is the relationship of rolling and acceleration in choppy sea conditions to the basic

parameters of the air cushions (pressure and expenditure of air). Therefore, in designing an ACV, there are problems as to choice of the basic parameters and, consequently, the power equipment of the craft responsible for providing these parameters by the most direct form in connection with seaworthiness, which the planned craft must have. This feature allows regulation, to a certain degree, of an ACV's seaworthy qualities by altering the expenditure of air in relation to the state of the sea's surface, and may also be used for automatic stabilization of an ACV's movement on choppy seas.

Another specific distinction of an ACV is the relationship of the rolling characteristic to the parameters of the internal system of air ducts and the expended-pressure characteristic of the fans.

In those instances where the pressure between the cushions and the receivers is very insignificant in the static condition of overflow, fluctuation of pressure in the cushions during movement on choppy seas overflows to the receiver, which leads to a change in the rate of the fan's operation and may lead to engine overload.

In reviewing the basic features of an ACV's hydroaerodynamics, one should not omit such phenomena as intensive spray formation which, in a number of instances, impedes the operation of the ACV. A large amount of spray and small water droplets, flying out with the streams of air from the air cushions, hampers the view from the wheelhouse and makes it necessary to install special filter-separators where the air enters the engines, using special structural measures to protect the blades of the air screws from corrosion. Sometimes the force from the interaction of the spray stream with the hull is quite substantial. This is examined in more detail in Chapter IV.

§11. External Forces Which Act on ACV's

Passing on to the amount of external force which acts on an ACV during its movement, it is necessary to assume a working hypothesis which allows a simplified solution of the problem.

The hypothesis assumed in the current chapter consists of the following. The influence of wave formation on the free surface only leads to deformation of the water's surface directly in the zone of excess pressure (the cushions) under the craft, i.e. the wake of the craft does not lead to considerable redistribution of ground speed and the air pressure in the space surrounding the craft.

This hypothesis proves correct according to the above-stated observations, and may be confirmed by experimental means, it allows one to acquire, for theoretical examination, almost all categories of experimental work with models and ACV's.

A diagram of the ACV's movement is set forth in Figure 45.
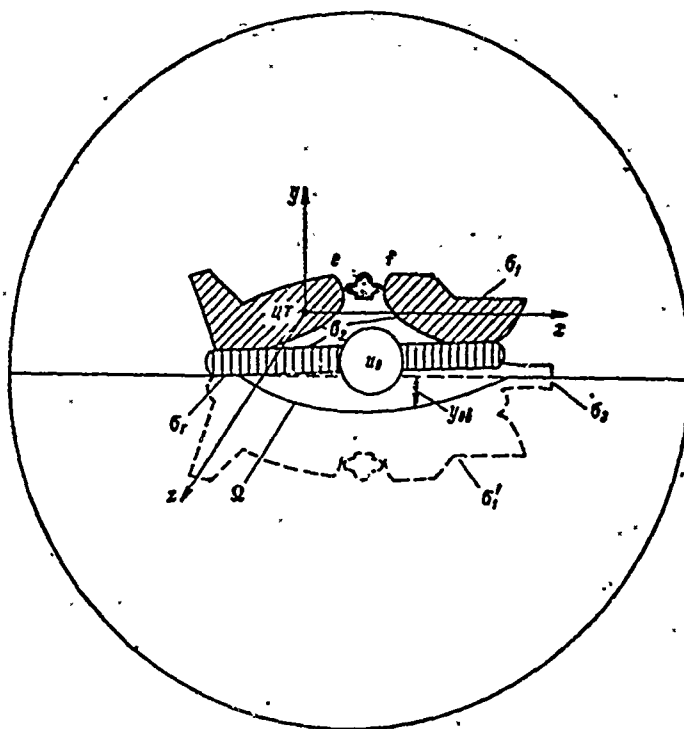
Figure 45. Diagram of an ACV's Cross-Sections for Determination of
External Forces.

The air enters the hull of the ACV through the fan and flows from
the air cushions in the form of streams. Deformation of the water's free
surface, in the regions of increased pressure, is determined by the
equation (Figure 45)

$$y_0 = y_{08}(x, z).$$ (1)

Various sections of the hull or flexible skirts are in direct contact
with the water. The speed $\vec{V}_a$ of a craft, like any solid body in a fixed
system of coordinates, is determined by the law

$$\vec{V}_a = \vec{V}(t) + \vec{\omega} \times \vec{r}.$$ (2)

In the observed moment t, the initial points of mobile and fixed
systems of coordinates coincide with the center of gravity of the ACV.

The quantity of external forces $d\vec{R}$, applied to the element $d\sigma$ of the hull's surface with the side-surrounding environs, equals

$$d\vec{R} = -\vec{p'}d\sigma, \qquad (3)$$

where $\vec{p'}$ - vector of the density of distribution of surface forces (tension) [31].

The vector $\vec{p'}$ may be presented as the sum of three vectors

$$\vec{p'} = p\vec{n} + \Delta p\vec{n} + \varepsilon\vec{\tau}, \qquad (4)$$

where $\vec{n}$ - normal vector to the ACV's surface;

$\vec{\tau}$ - a single vector, in line with the intersection of planes, containing vectors $\vec{p'}$ and $\vec{n}$, with a tangent plane (Figure 46);

p - quantity of aerodynamic pressure, acting on part of the surface in the absence of viscosity;

Δp - an addition to the quantity of pressure of conditional viscosity;

ε - amount of projection of vector $\vec{p'}$ to the tangent plane, i.e. the elementary force of friction.

To calculate the total forces, acting with the side-surrounding environs, it is necessary to integrate the quantity $d\vec{R}$ along all surfaces σ of the ACV's hull, which come into contact with water and air. Calculation of this integral is easy to carry out by breaking the surface integrals into the following parts:

$$\sigma = \sigma_a + \sigma_g,$$

where σ_a - external surface of the ACV and flexible skirts;

σ_g - that part of the surface bounded by water.

In its own way, the surface σ_a also is divided into two parts

$$\sigma_a = \sigma_1 + \sigma_2,$$

where σ_1 - external surface of the ACV and flexible skirts;

σ_2 - internal surface of the ACV, bounded by the flow of air, i.e. the surface of the receiver, the bottom, and the inside surface of the flexible skirts.

Figure 46. Diagram of the Force, Acting on the Surfaces of an ACV's Element.

In addition, there is the surface of the normal profile of the air stream σ_3, escaping along the perimeter of the air cushions, and part of the water's surface bordered by the air cushions Ω.

The external force, acting on the ACV with side-surrounding environs may be presented as types of force: aerodynamic and hydrodynamic

$$\vec{R} = \vec{R}_a + \vec{r}, \qquad (5)$$

where

$$\vec{R}_a = -\int\int_{\sigma_a} \vec{p'} d\sigma;$$

$$R_r = -\int\int_{\sigma_r} \vec{p'} d\sigma.$$

The aerodynamic force $\vec{R}_a$, in its own way, may be presented as two types of force, acting on the external $\vec{R}_a^*$ and internal $\vec{R}_a^{**}$ parts of the hull's surface of the ACV,

$$\vec{R}_a = \vec{R}_a^* + \vec{R}_a^{**}, \qquad (6)$$

where

$$\vec{R}_a^* = -\int\int_{\sigma_1} \vec{p'} d\sigma; \quad \vec{R}_a^{**} = -\int\int_{\sigma_2} \vec{p'} d\sigma.$$

To calculate the integral of the surface forces, applying to the internal surfaces of the ACV, one uses the theorem of quantitative movement conforming to the control surface, bordered by the volume U_0, of air in the receiver and air cushions. This control surface is stationary in systems of coordinates connected with vessels. Therefore, the equation of quantitative movement for relative speeds $\vec{V}_r$ [31] is in the form of

$$\int\int_{\sigma_2+\sigma_3+b} \vec{p'} d\sigma + \rho\int\int\int_{U_0} \vec{R}_m dU -$$

$$- \rho\frac{\partial}{\partial t}\int\int\int_{U_0} \vec{V}_r dU = -\rho\int\int_{\sigma_2+\sigma_3+\Omega} \vec{V}_r V_{rn} d\sigma, \qquad (7)$$

-83-

where $\vec{R}_m$ - vector of the mass force of air.

Due to this scheme for control surfaces, the normal make-up of V_{rn} for relative speeds is

$$V_{rn} = 0$$

anywhere, with the exception of normal profiles σ_z of the air streams, escaping from the cushions, the base surface Ω, and that part of the surface σ_2, of which the air flows into the ACV's hull. It is assumed furthermore, that division of the external and internal parts of the flow of air along the face of the fan agrees with those parts of the surface σ_1 and σ_2. It follows that one should look upon this as normal to the surfaces, in each case being directed inside the areas, i.e. to the part σ_2 inside the receiver, and to the part σ, outside.

A special symbol "σ_v" is used for this part of the surface (σ_2).

On the basis of formula (7), the quantity of internal aerodynamic forces $\vec{R}_a^{**}$ may be written as

$$\vec{R}_a^{**} = -\iint_{\sigma_s} \vec{p'} d\sigma = \iint_{\sigma_s+\Omega} \vec{p'} d\sigma + \rho \iiint_{U_o} \vec{R}_m dU - $$
$$ - \rho \frac{\partial}{\partial t} \iiint_{U_o} \vec{V}_r dU + \rho \iint_{\sigma_s+\sigma_s} \vec{V}_r V_{rn} d\sigma + \rho \iint_{\Omega} \vec{V}_r V_{rn} d\sigma. \tag{8}$$

In calculating the external aerodynamic forces $\vec{R}_a^*$, it is expedient to divide it into the forces, acting in ideal fluids $\vec{R}_{1d}^*$ and forces $\vec{R}_{a1}$, produced by viscosity of air. With this in mind, the quantity $\vec{p}'$ appears in the integral as the sum of three terms, in accordance with formula (4). A substitute for this calculation is

$$\vec{R}_a^{\cdot} = \vec{R}_{u\pi}^{\cdot} + \vec{R}_{a1}. \tag{9}$$

where
$$\vec{R}_{u\pi}^{\cdot} = -\iint_{\sigma_1} p\vec{n} d\sigma; \quad \vec{R}_{a1} = -\iint_{\sigma_1} (\Delta p \vec{n} + \varepsilon \vec{\tau}) d\sigma.$$

To calculate the first term on the right-hand side of the formula, one should apply Kirkhof's method for determination of the hydrodynamic reactions in the movement of bodies of arbitrary form in boundless ideal fluids [26]. The quantity of force, arising with the flow of air from the surrounding area to the hull of the moving ACV, is calculated by using the concepts of N. E. Zhukovski [20] which determine the reactions to the intake of fluids[1].

We use this Kirkhof-Zhukovski method to calculate the forces, acting on a body in boundless fluids. In order to consider the influence on a free surface, we should examine the movement of twin bodies in boundless fluids. Skirting these bodies are: the hard surfaces of σ_1 (with the exception of σ_v, which is a permeable surface) and σ_3, and the symmetry of their surfaces relative to the free surface of the water. Due to the symmetry of the bodies, the flow will be symmetrical to the points, situated in symmetry relative to the planes of the free surface of the water. Therefore, the force acting on the upper half of the twin bodies is equal to half the forces acting on the whole body.

Regarding what was just said, it is possible to present the quantity of forces $\vec{R}^*_{1d}$ as the sum of two quantities

$$\vec{R}^{\cdot}_{\text{нд}} = -\frac{d}{dt} \iint_{\sigma_1 + \sigma_3} \rho \psi_0 \vec{n} d\sigma + \rho \iint_{\sigma_1 + \sigma_3} \vec{V}_a V_{rn} d\sigma, \tag{10}$$

where ψ_0 - potential air flow in the area surrounding the craft.

In accordance with this concept, $V_{rn} \neq 0$ only on surface σ_v. There= fore, i. formula (10)

$$\rho \iint_{\sigma_1 + \sigma_3} \vec{V}_a V_{rn} d\sigma = \rho \iint_{\sigma_3} \vec{V}_a V_{rn} d\sigma. \tag{11}$$

---

[1]Kirkhof's method cannot be applied for determining the reactions of liquids flowing out, so the formula of Ostrogradski-Gauss is used in the process of transformation, but it may be applied often on examination of functions with continuous derivatives. As much as the flow of air from the cushions bears a stream characteristic and the ground speed of the air is broken in the confines of the streams, we, following N. E. Zhukovski [20], determine the reaction of the fluids flowing out with the aid of quantitative theorems of movement, and the total reaction of air from the sides we find as the sum of forces applicable to the external and internal surfaces of the ACV.

To calculate the total quantity of forces $\vec{R}$, acting on an ACV, it is necessary to add to formulae (5) and (6) the equations (8) and (9) with the quantity of hydrodynamic forces $\vec{R}_r$. Substituted next in the right-hand side of (9) is $\vec{R}^*_{id}$, calculated by formula (10) with the calculation of (11), we get (from calculating the normal attitudes on surface σ_v)

$$\vec{R} = -\iint_{\sigma_1}(\Delta p \vec{n} + s\vec{\tau})ds - \rho\frac{d}{dt}\iint_{\sigma_1+\sigma_2}\varphi_0\vec{n}d\sigma +$$
$$+ \rho\iint_{\sigma_2}(\vec{V}_a - \vec{V}_r)V_{rn}ds + \iint_{\Omega}\vec{p'}ds + \rho\iint_{\sigma_2}\vec{V}_r V_{rn}ds + \rho\iiint_{U_0}\vec{R}_m dU + \quad (12)$$
$$+ \rho\iint_{\Omega}\vec{V}_r V_{rn}ds - \rho\frac{\partial}{\partial t}\iiint_{U_0}\vec{V}_r dU + \iint_{\sigma_2}\vec{p'}ds + \vec{R}_r$$

We observe the physical meaning of the integrals received in the determination of the separate components of external forces of an aerodynamic nature:

1) $$\vec{R}_{a1} = -\iint_{\sigma_1}(\Delta p \vec{n} + s\vec{\tau})d\sigma, \qquad (13)$$

$\vec{R}_{a1}$ - the aerodynamic force, due to force of viscosity of the air. By composing it along the axis, the speed system of coordinates is:

a) A force of aerodynamic resistance (along axis x), in numbers of inductive resistance;

b) Aerodynamic lift force on the hull (along axis y);

c) Aerodynamic side force on the hull of an ACV, its rudder, stabilizer, etc. (along axis z).

2) $$\vec{R}_{a2} = -\rho\frac{d}{dt}\iint_{\sigma_1}\varphi_0\vec{n}d\sigma, \qquad (14)$$

$\vec{R}_{a2}$ - a force of inertial nature, acting on an ACV in transient movement.

3) $$\vec{R}_{a3} = \rho\iint_{\sigma_2}(\vec{V}_a - \vec{V}_r)V_{rn}d\sigma, \qquad (15)$$

R_{a3} - reaction of the incoming air, an additional force of inertial nature, acting on an ACV with side masses of air carried into movement.

With $\vec{V}_a = \vec{V} + \vec{V}_r$ (movement without torque, $\omega = 0$) $R_{a3} = \rho \vec{V} \int_{\sigma_v} \int V_{rn} d\sigma =$ $= -\rho \Omega \vec{V}$, the so-called force of impulse resistance is

4)
$$\vec{R}_{a4} = \int\int_{\Omega} \vec{p}' d\sigma, \qquad (16)$$

$\vec{R}_{a4}$ - the integral of surface forces along the base surface Ω.

Thus, for the aerodynamic force, in the general movement of an ACV, this vector has three compoenets: along the axis x - wave resistance, along axis y - a supporting force for balancing the basic part of the ACV's weight, and along axis z - a side force.

5)
$$\vec{R}_{a5} = \rho \int_{\sigma_v} \int \vec{V}_r V_{rn} d\sigma, \qquad (17)$$

$\vec{R}_{a5}$ - reaction of the air stream, escaping from the area of the air cushions.

This force, in projection of axis x, makes for additional resistance or draught. The vertical make-up of speed in the streams, with the ACV suspended over water, is directed upward. This leads to a decrease of the forces maintaining the ACV on the water in comparison to the forces for maintaining an ACV over a flat hard screen. During movement or stationary suspension of the ACV with list, the reaction of the air streams also has a lateral make-up - a projection of axis z.

6)
$$\vec{R}_{a6} = \rho \int\int_{U_0} \int \vec{R}_m dU, \qquad (18)$$

$\vec{R}_{a6}$ - the resultant mass of forces, acting on the internal surfaces of the ACV. From these forces, there are usually significant inertial forces in the take-off of an ACV and Coriolis forces in the ACV's movement in a curved linear trajectory. These forces are calculated for solving problems of maneruverability of an ACV.

7)
$$\vec{R}_{a7} = -\rho \int_{\Omega} \int \vec{V}_r V_{rn} d\sigma, \qquad (19)$$

$\vec{R}_{a7}$ - a force, caused by the redistribution of fields of air pressure in the cushions due to fluctuation of the water's base surface. On the right-hand side of formula (12), there are two terms, considering the external aerodynamic forces, acting on the ACV.

8)
$$\vec{R}_{a8} = -\rho \frac{\partial}{\partial t} \int\int_{U_0} \int \vec{V}_r dU \qquad (20)$$

arises due to the transience of ground speed inside the ACV and in the air cushions.

The forces $\vec{R}_{a7}$ and $\vec{R}_{a8}$ show a considerable effect on rolling of the ACV.

The force $\vec{R} = \{_{\sigma_v} \int \vec{p}' d\sigma$, in practice, usually is not considered due to the small quantity of surface σ_{ya} compared to the surfaces σ_1 and Ω.

9)
$$\vec{R}_r = -\iint_{\sigma_r} \vec{p}' d\sigma, \qquad (21)$$

$\vec{R}_r$ - the force of the interactions of the ACV with water, due to wash-off on the hull or flexible skirts.

We pass on to examination of those moments, acting from the side surrounding environs, without making repeated inferences to the list of external moments and remarks concerning them. They all may be stated as analogous to the basic theorems for moments of quantitative movement:

$\vec{M}_r$ - moments of hydrodynamic force

$$\vec{M}_r = \iint_{\sigma_r} (\vec{r} \times \vec{p}') \, d\sigma; \qquad (22)$$

$\vec{M}_{a1}$ - moments of external aerodynamic forces, caused by the viscosity of fluids

$$\vec{M}_{a1} = -\iint_{\sigma_t} [\vec{r} \times (\Delta p \vec{n} + \mathbf{e}\vec{\tau})] \, d\sigma; \qquad (23)$$

$\vec{M}_{a2}$ - moments of associated masses of air

$$\vec{M}_{a2} = -\rho \frac{d}{dt} \iint_{\sigma_t} \varphi_0 (\vec{r} \times \vec{n}) \, d\sigma; \qquad (24)$$

$\vec{M}_{a3}$ - moments, acting on an ACV, due to the air being carried into movement with the ACV,

$$\vec{M}_{a3} = \rho \iint_{\sigma_a} [\vec{r} \times (\vec{V}_a - \vec{V}_r) V_{rn}] \, d\sigma; \qquad (25)$$

$\vec{M}_{a4}$ - moment of surface force on the base surface of the water

$$\vec{M}_{a4} = \iint_{\Omega} (\vec{r} \times \vec{p}') \, d\sigma; \qquad (26)$$

$\vec{M}_{a5}$ - reactive moment of the air stream

$$\vec{M}_{a5} = \rho \iint_{s} (\vec{r} \times \vec{V}_i) V_n \, ds; \tag{27}$$

$\vec{M}_{a6}$ - moment of internal mass aerodynamic force

$$\vec{M}_{a6} = \rho \iiint_{U} (\vec{r} \times \vec{R}_m) \, dU; \tag{28}$$

$\vec{M}_{a7}$ - moment of force due to the redistribution of air pressure during fluctuation of the base surface

$$\vec{M}_{a7} = -\rho \iint_{s} (\vec{r} \times \vec{V}) V_n \, ds; \tag{29}$$

$\vec{M}_{a8}$ - moment of internal force of a transient nature

$$\vec{M}_{a8} = -\rho \frac{\partial}{\partial t} \iiint_{U_k} (\vec{r} \times \vec{V}_i) \, dU. \tag{30}$$

The list of forces and moments set forth represents the entire number of external forces of hydroaerodynamic nature which act on an ACV. Methods for the practical calculation of external forces will be examined late in a special chapter devoted to the problems of speed, control, and stability of an ACV.

§12. Some Situations Connected With Research on ACV's With the Aid of Model Experiments

As was noted above, some categories of external forces which act on an ACV cannot be found at present, theoretically, and to determine them it is necessary to set up a model experiment.

The means of conducting the model experiment and the laws of similarity in duplicating the hydrodynamic characteristics of an ACV without flexible skirts are worked out in sufficient detail.

The use of flexible skirts for improving the seaworthiness of an ACV posed a number of new problems connected with duplication of the deformation of the flexible skirts in the simulation of external forces, i.e. the question was raised concerning the duplication of characteristics and structural materials of the flexible skirts. This side of the problem still has not been solved satisfactorily. Therefore, in speaking about the influence of mechanical properties of flexible skirts on the hydrodynamic characteristics of an ACV, one may state only those preliminary results which have no bearing on its systematic character.

In contrast to the average structural materials, materials which are used in the manufacture of flexible skirts are not isotropic and do not obey Hook's law.

In order to characterize the deformation of materials under stress, a complex of diagrams are utilized to represent the normal characteristics of the materials. It includes, first of all, two diagrams showing stress (with the dependence of the relative length ε, on the linear load R_T in kilograms of force per meter) in one direction with a fixed linear load in a transverse direction; secondly - a group of diagrams of stress for a given size load's shift.

It is easy to see that it is practically impossible to select two such materials (one for models, the other for full-size craft) which would be suitable for all mechanical parameters: thickness, specific weight, module of elasticity with tension along the base, module of elasticity with tension along the cleat, module of elasticity with shift for all size loads, etc.

Besides this, at least some types of deformation may depend not only on the normal characteristics of materials, but also on the structure, i.e. the number of layers of rubber which line the base of the material, thickness of the layers and type of adhesive, frequency of the materials netting, etc.

Therefore, for an approximate calculation of the influence of the mechanical properties of the flexible skirts' material on the hydrodynamic characteristics of an ACV, one should strive to duplicate one set form or another of the deformation of the flexible skirts and to maintain similarity according to the parameters for determining this type of deformation.
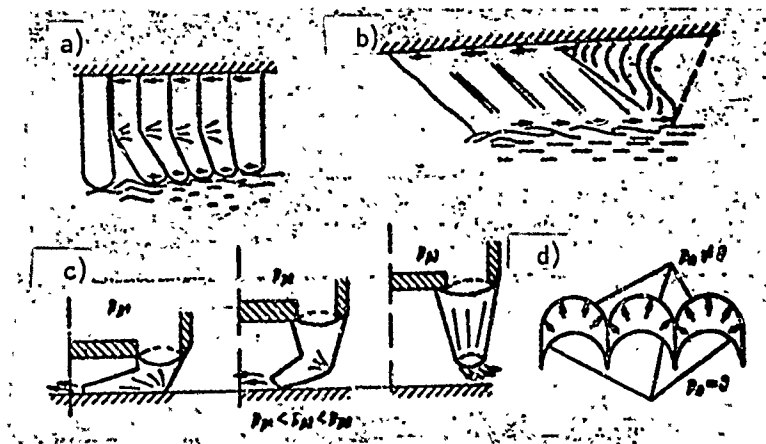

Figure 47. Diagrams of the Deformation of Flexible Skirts: a - Buckling Upon Contact With Water; b - Shift Upon Contact With Water; c - Straightening-Out of a Section Upon Increasing Pressure in the Receiving; d - Stress of a Section Upon Increasing Pressure in the Receiver

-91-

$$\Pi_5 = \frac{G}{\rho V^2 L^2} = Eu$$ - Eiler number, proportionate in relativity of under-dome pressure in the cushions to the velocity of air pressure. This parameter determines the similarity of the processes of air-escaping from the air cushions and direction of take-off for the spray stream, as well as characterizing the rate of the fan's operation;

$$\Pi_6 = \frac{\gamma}{\rho g}$$ - relationship of the mass density of water and air;

$$\Pi_7 = \psi$$ - angle of trim difference;

$$\Pi_8 = \frac{\alpha_w g}{\gamma V^2 L}$$ - Weber number, determining the similarity of the process of spray formations and quantity of spray drop;

$$\Pi_9 = \frac{E \cdot \delta \cdot g}{\gamma V^2 L^2}$$ - Koska number, determining the similarity of the bending of the flexible skirt's elements by the forces of water and air pressure;

$$\Pi_{10} = \frac{\gamma \cdot L^2}{G}$$ - parameter, characterizing the similarity of the deformation of the flexible skirts by gravitational forces.

During investigation of the lift height of an ACV with flexible skirts (suspended over a screen without translational movement), some of the above parameters proved to be non-existent (speed of movement, physical properties of the water).

In contrast to this, parameters, characterizing different forms of deformation of the flexible skirts, acquire great significance.

Non-dimensional lift height may be presented in the form of the following function:

$$\frac{h_3}{L} = \Phi(\Pi_{11}, \ldots \Pi_{13}), \tag{32}$$

where

$$\Pi_{11} = \frac{E \cdot \delta \cdot L^2}{\rho Q^2}$$ - parameter, characterizing the similarity of "straightening" the flexible skirts by the force of pressure of air exhaust for the flexible skirts (Figure 47c);

$$\Pi_{12} = \frac{G L^3}{\rho Q^2}$$ - parameter, determining the similarity of the processes of air escaping from the air cushions, i.e. a change in quantitative movement on the outskirts of the air stream under the effect of excess pressure in the cushions;

$$\Pi_{13} = \frac{E \cdot L}{G}$$ - parameter, determining the similarity of deformation of tension without bending the flexible skirts under the effect of excess pressure in the cushions (Figure 47d). This parameter is most characteristic of the sectioning of flexible skirts, since it determines the quality of condensation for the air cushions;

-93-

$$\Pi_{14} = \frac{E \cdot \delta \cdot}{G}$$ - parameter, characterizing the rigidity of the flexible skirts, in relation to the ACV's weight without flexible skirts;

$$\Pi_{15} = \frac{T'' l^2}{G}$$ - parameter, determining the deformation of the flexible skirts under the effect of the forces of weight.

In practice, two of the last parameters usually prove to be immaterial, as in the parameter Π_{10} with modelling of resistance.

To investigate lift height over water, it is necessary to introduce additional parameters: a Weber number, Π_6, and a Froude number (in moving).

To examine problems of stability for an ACV, with typical, independently-measured, physical parameters, one must introduce additionally: pressure in the receiver P_p, variable quantity of pressure in the air cushions p_d (x,z), the area of the air cushions S_d, and the width of the air cushion B_d.

The relationship between the quantity of non-dimensional restored moments and typical non-dimensional parameters is presented in the form of

$$\frac{M}{GB_n} = \Phi \left(\Pi_1, \Pi_2, \Pi_3, \Pi_4', \Pi_5', \Pi_6, \Pi_7', \Pi_8, \Pi_{16}, \Pi_{17} \right), \tag{33}$$

where, in addition to the known designators, the following new designators are implemented:

$$\Pi_4' = \frac{Q}{\sqrt{\frac{4 S_n G}{\pi \rho}}}$$ - parameter, determining the similarity of the quantity of air expenditures

$$\Pi_5'' = \frac{p_p S_n}{G} \text{ or } \Pi_5' = \frac{p(x, z)}{G/S_n}$$ - analog of Eiler numbers;

$$\Pi_7' = \psi_0$$ - angle of trim difference for an ACV hovering without translational movement (at stop);

$$\Pi_{16} = \theta_0$$ - list angle for an ACV hovering without translational movement (at stop);

$$\Pi_{17} = \frac{G}{\rho g S_n^{3/2}}$$ - parameter, determining the similarity of the load weight of models and actual-size craft.

The influence of the remaining factors (spray formation, mechanical properties, and rigidity of materials in the flexible skirts) was not taken into account in examining the problems of stability.

Upon examining the makeup of the parameters for a model (set forth on page 114) it was proven that, using modern methods for conducting the experiment, it is impossible to meet the requirement for constancy of numerical meaning of all parameters under actual and model conditions simultaneously, i.e. it is impossible to provide total similarity of the physical processes involved in model and actual conditions.

For example, to fashion a model using Froude numbers, it is necessary to decrease the geometric dimensions by decreasing the speed of movement and, using Reynolds numbers - by increasing the speed of movement. This contradiction is solved by means of isolating the total amount of resistance to movement from forces of friction on water, the main form depending on Reynolds numbers and the remaining parts on Froude numbers, i.e. by evaluating the amount of resistance in actual proportion to the cube of the linear scale. For calculating the resistance of a fast-moving glider craft, the resistance of friction usually is not isolated, but the total amount of resistance in models is evaluated in actual proportion to the cube of the linear scale. In principle, this will lead to an excess of resistance in an actual-size launch, therefore the Reynolds number is increased and the coefficient of friction on water is decreased during transition from model to actual-size.

It has been shown in practice that such evaluation gives satisfactory results without excesses of natural resistance. This is connected, apparently, with the fact that some additional resistance increases faster than according to the cube of the scale.

Today, considering the total physical processes, it is expedient to carry out an evaluation of the hydrodynamic makeup of resistance in both ACV's and glider-type craft according to the cube of the scale, maintaining throughout the test an equality of Froude numbers in the actual-size and model craft and disregarding friction on water for the model.

However, modelling according to Froude numbers does not allow one to determine forces of resistance of aerodynamic nature. The hulls of ACV's are usually poorly-streamlined bodies, which accounts for a great deal of profile resistance. To determine this resistance, it is necessary to conduct tests at great Reynolds numbers, exceeding the critical mark $Re_{kp} = 10^6$.

It is possible to conduct such a test only in a wind tunnel, because the speed of a model's movement relative to the air in a test basin is many times less than the speed of air flow in a wind tunnel.

A specific feature in determining resistance to an ACV's movement is that, in a model experiment, it is necessary to carry out the test in two stages: in a test basin and in a wind tunnel.

Division of the experiment into two stages involves additional outlining and distortion of the physical conditions in movement which, naturally, serves as a source for additional errors. Testing in a wind tunnel omits consideration of deformation of the base surface under the craft, wave formation and additional forces involved in the contact with water, changes in the angle of trim difference and the lift height of models. Conditions for testing models in a wind tunnel are approximate to conditions of an ACV moving without any contact with water at very high speeds, exceeding the average speeds of modern ACV's.

In testing model ACV's in a wind tunnel, it is possible to provide modelling principally according to parameters II_2, II_4, II_5, i.e. to model the processes of flow along the external surfaces of the ACV as well as inside the hull. There is a special interest in this so-called modelling process concerning the interaction of external and internal flow of air, i.e. the influence of air intake through the fans on resistance to movement and of the lift force on the hull of the ACV, as well as the interaction of the air stream escaping from the air cushions and the flow of air outside. However, this big possibility has not been realized in current times because of the insurmountable technical difficulties. No one has succeeded in placing in model ACV's (bound by dimensions) fans and engines which would provide the output and air pressure necessary for aerodynamic similarities of air flow on the outside and inside of the model's hulls. In Table 2 results of calculations are set forth which illustrate this contradiction in the example of the English SRN3 ACV.

Table 2. Estimation of Reynolds Numbers in Accordance With the Conditions of Modelling External and Internal Air Streams

V, m/sec	$\rho \dfrac{V^2}{2}$, kg forces/m²	$p_n = \Pi_5 \rho \dfrac{V^2}{2}$,	$G = p_n S_n$, kg	$Q = \Pi_4 D_n^2 V$, m³/sec	$N = \dfrac{Q p_n}{75}$, h.p.	$10^{-5} R_1 = \dfrac{\Sigma Q}{\pi D_n v_1} \times \times 10^{-5}$
20	25,5	98,5	117	1,78	2,34	1,98
30	56,3	222	264	2,67	7,92	2,98
40	100	394	469	3,56	18,7	3,97
50	156	615	731	4,45	36,5	4,96
60	225	885	1050	5,34	63,0	5,95
70	307	1210	1440	6,23	100	6,95

From Table 2 it is clear that, to ensure critical Reynolds numbers for the air flow inside the models, it is necessary to use engines of such power and weight and loads of such aerodynamic weights that this experiment would currently be unrealistic.

Therefore, mock-ups (without internal air ducts and without fans) are presently being tested in wind tunnels as models of the ACV's. This permits measuring forces and moments during testing to determine the main forms of external aerodynamic flow, without calculating the influence of interactions with internal aerodynamic flow. In addition to these forces there are: aerodynamic profile resistance, lift force on the hull, moment of pitching, stabilizing forces and moments when the model is blown to a slanting position, as well as revolving derivatives.

Besides this, testing of a mock-up permits avoiding the principal difficulties connected with modelling the reactive makeup of resistance in an ACV.

After conducting tests in a wind tunnel and test basin, it is necessary to sum up the results which were received. If all the forces are of an aerodynamic nature, including profile and impulse resistance and reaction forces received during tests made in the wind tunnel, it is necessary to eliminate them from the forces of resistance for tow-type models so that they will not be taken into account twice. The force of impulse resistance may be calculated according to the theoretical formula of N. E. Zhukowski [20] in order to find the total amount of measured resistance. The force of aerodynamic resistance for tow-type models is determined approximately by measuring resistance in models suspended on a cart with the fans not working. Consequently, this force also may be calculated from the amount of tow-type resistance. However, to distinguish the reaction force of the air stream from the total amount of tow-type resistance is impossible in principle. Therefore, it is necessary to determine the reaction forces in the makeup of forces of hydrodynamic resistance and to test a mock-up in a wind tunnel without modelling the air cushions.

In completing the examination of the problem of carrying out tests on model ACV's in a wind tunnel, one more circumstance should be noted. Aerodynamic forces and moments, acting on an ACV, essentially depend on the proximities of the borders of air flow to the base surface. Therefore, tests of models often are carried out in the presence of a screen, imitating the base surface. Due to the manner of movement, the surrounding condition of the base surface is broken. The flow of air in the wind tunnel moves in relation to the screen, a surrounding layer forms on the screen - the thickness of which is commensurate with the height of clearance between the model's hull and the screen. In actual conditions, the air is stationary in relation to the base surface and this surrounding layer does not appear.

An investigation was carried out on the influence of this phenomenon on the distribution of pressure along the hull of a model ACV. To approximate natural conditions, the base surface was in the form of conveyer belts which could shift with the speed of the air in the wind tunnel. Comparison of results from measuring pressure during movement and at rest of the conveyer belts shows that breaks in the surrounding condition (on a free surface) appear in the base of parts of the hull, converting immediately to the screen, but on other parts of its surface this influence is non-existent.

In carrying out tests of tow-type ACV models in a test basin one must keep in mind that hydrodynamic resistance in an ACV usually depends very strongly on the craft's landing, i.e. on the angle of operating trim difference. However, it is difficult to provide similarity in the landing of models and actual-size ACV's for the following reason. The angle of trim difference of an ACV, while moving at a constant speed, is determined by the balance of the ACV being subjected to all the external forces and moments caused by the draught of the propelling agent. It was shown above that, in principle, it is impossible go provide similarity of hydrodynamic and aerodynamic forces simultaneously. Therefore, the balance of a full-size ACV differs from the balance of a tow-type model - the angles of operating trim difference in positions of balance are not equal. Additional and more considerable error is brought about by attempting to duplicate the influence

of draught of the propelling agent on the ACV's trim difference by shifting the center of gravity.

In carrying out a test in basin, the resistance to a full-size ACV's movement and, consequently, the draught of the propelling agent are unknown beforehand. Therefore, an accurate calculation of the moments of draught on the screws is impossible. In practice, they usually disregard the change in the amount of trimming moments of draught and substitute approximate moments of draught according to the average meaning of the moments, due to the transfer of cargo which leads to inaccuracy in duplicating the ACV's landing.

This inaccuracy may be eliminated by means of some increases in volume for testing tow-type craft. A method for calculating an ACV's resistance will be stated below. It permits the trimming moments of the propelling agent's draught to be taken into account and calculation of the angle of operating trim difference for a full-size ACV. To calculate this, it is necessary to have the results from testing the tow-type model in 3-4 positions for the center of gravity along the length. The test results are conveniently presented in the form of the parametric relationship of non-dimensional coefficients of hydrodynamic resistance and hydrodynamic moments (as well as the angle of trim difference) to the quantity $x_d = x_d/L$, where x_d is the

distance along the length from the model's center of gravity to the center of gravity in the area of the air cushions. These graphs are based on a fixed amount of Froude numbers.

To carry out testing of the tow-type model ACV in a test basin, it is necessary to have the possibility of a scale effect combined with a breach in similarities according to Weber's numbers.

Spray formation may have considerable influence on resistance to movement. In natural conditions, the physical picture of the interaction of the stream of water on the hull may differ greatly from that of model conditions.

To observe the geometric similarity in the lingth of the stream during the transition from model to full-size craft, increases must be proportionate to a first degree scale. The speed of water particles in the stream, during duplication according to Froude numbers, is increased in proportion to the square root of the linear scale.

But from Rayleigh's work [39] it is known that at high speeds the length of the stream (until its destruction) varies inversely in proportion to the speed of the water particles in the stream. Consequently, during transition from models to full-size craft, the length of part of the stream (up to destruction) is not increased, but decreased.

A natural stream disintegrates into droplets faster than the stream of a model. Therefore, there may not be such a strong influence on the hull as is the case when carrying out an experiment. It is necessary to consider this circumstance when, in conducting a model experiment, it is discovered that there is a very strong interaction between the stream of spray and the hull of the model ACV.

-98-

In the beginning of this section, it was said that the rigidity of the flexible skirts on an ACV renders an influence on the hydrodynamic characteristics of lift height, resistance to movement, and stability. Ignorance of this factor may also lead to the appearance of a scale effect during duplication. In the excellent illustration shown in Figure 48, relationships are set forth which characterize the influence of rigidity of materials on the lift height of model ACV's with flexible skirts. Although the structure of the flexible skirts was constant, the lower part of the flexible skirts was manufactured from two materials with different thicknesses and possessing a module of elasticity during tension. Since both materials had only a single layer of material, it may be supposed that the module of elasticity during tension was sufficient to take into account the bending of rigid materials at increased pressure during tests.
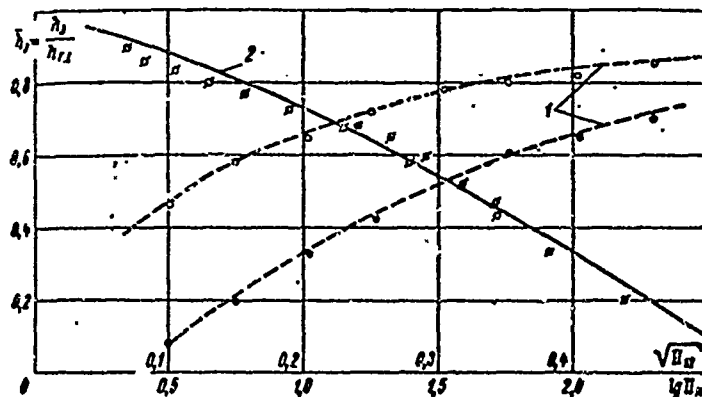

Figure 48. Relationship of Non-Dimensional Lift Heights of ACV's Over a Screen to Typical Parameters

— — — — — relationship of lift height to expenditure of air;

— — — — — relationship of lift height to combined parameters, allowing for both air expenditure and rigidity of the flexible skirt's material

In Figure 48 we see that the quantity of air expenditure (parameter Π_{12}) does not define merely the lift height of a model over a screen. On the contrary, the relationship of lift height to the parameter Π_{11}, considering the rigidity of the materials, actually has the same value for both materials in the flexible skirts.

From investigations of the static characteristics of ACV's based on tests of model and actual-size craft, it may be stated that a first approximation of the characteristics of static stability for ACV's depends on the following quantities:

-99-

in the rate of suspension of an ACV over a screen or over water

$$\frac{\dot{h}_{3s}}{\sqrt{S_n}} = \Phi(\Pi_4', \Pi_6', \Pi_{17}); \\ \frac{M}{GB_n} = \Phi(\Pi_4', \Pi_5', \Pi_{17});$$ (34)

in the rate of movement over water the calculation is made according to formula (34), but with the addition of a Froude number:

$$\Pi_1 = \frac{V}{\sqrt{gL_n}}.$$ (35)

All the basic experimental and calculated bits of data for the work are set forth in the functions of the complexes (34) and (35).

As for the basic non-dimensional static characteristics of ACV's and models, the following were received:

$\frac{\partial h_3}{\partial Y}$ - coefficient of stability for lift height;

$\frac{\partial M}{\partial \theta}$ - initial transverse metacentric height (non-dimensional);

$\frac{\partial M}{\partial \psi}$ - initial longitudinal metacentric height (non-dimensional).

Comparison of the results of measurements made during the testing of similar type ACV's and models verifies the lack of a noticeable scale effect in the simulated statics of Class A ACV's. Any deviations may be explained by some differences of non-dimensional parameters Π_4, Π_5, and Π_{17} for ACV's and models, as well as by differences in the construction and rigidity of the flexible skirts.

In planning the real-size ACV's, experiments with the models in choppy sea conditions are considered essential since testing of the models permits one to study their movements on average and extremely choppy seas at various speeds and with various courses relative to the waves. In these tests the influence of wave height and length on the parameters of moving models is investigated, as well as the relationship of the ACV's seaworthy qualities to the volume of air expended, the center of the craft, structure, materials and dimensions of the flexible skirts. Also checked during testing of the models are the accuracy of the design architectural solutions and the correlation of the main dimensions.

The scales of models may vary from 1/20 to 1/2. Not only geometric similarity is maintained in creating models, but similarity of distribution of mass, similarity of air pressure in the receiver and air cushions, and similarity of the volume of air expended through the fans as well.

Tests are carried out in tow-type or self-propelled models. The simulation is carried out with observance of equality of Froude numbers for models and actual-size craft. A difference in Reynold's numbers is not particularly significant since the resistance of friction from the interaction of the ACV's flexible skirts and the water is small in comparison with the total resistance. Similarity of Weber numbers (characterizing spray fromation) is not provided for in the simulation.

Since three degrees of freedom are provided in the testing of tow-type models, there is a possibility of fluctuation along the vertical and around the axes O_x and O_y. Self-propelled models have six degrees of freedom, therefore their tests are given the most attention.

In conducting seaworthy tests of large-scale, self-propelled models and actual-size ACV's, specific problems appear which, in order to be solved, require the creation of special measuring devices and the development of particular techniques for measuring. The first problem is the drop in speed. An ACV's speed relative to water and relative to air, under actual conditions, are different. Since the aerodynamic forces which act on an ACV (including impulse resistance) depend on speed relative to air, and the hydrodynamic forces depend on speed relative to water, it is necessary to know the meanings of these speeds to determine the forces. The measuring device must determine the amount and direction of the wind for speeds relative to water and air.

In seaworthy tests, speed relative to water is determined according to the Doppler index, fixing the speed of the ACV's progressive movement along the axes O_x and O_y. The speed also may be determined with the aid of systems of external measuring: coastal motion-picture theodolite posts, by leading, by synchronous survey of the ACV's trajectory of movement, or by air-photo survey of the ACV's shift relative to a fixed point on the water.

Considering the great influence of an ACV's angle of drift relative the water's surface on the amount of force which acts on the craft, it is necessary to execute the drop in the angle of drift with great precision. It is generally accepted that, in speed trials, a driver must endure an angle of drift within the limits of $\pm 2 \div 5°$.

Chapter III. Statics of ACV's

In this chapter we will consider the methods of approximate determination of the parameters characterizing the ACV balanced in space (under control), the degree of static stability of such a position under calculated operating conditions, and an attempt will be made to establish the critical significance of these parameters.

It is assumed that the ACV has an absolutely rigid hull and a flexible skirt either along the entire perimeter of the air cushion (class A, see Introduction), or along part of the perimeter (class B).

Included in this calculated instance of ACV operation are assumptions of uniform straightforward movement of the vehicle over the surface of calm, deep water with an absence of wind.

§13. Equalizing the Balance of an ACV

The calculation of the parameters determining the balance of an ACV in space--the lift height h, list angle θ and trim difference ψ, as well as the static stability of this position - $\partial h/\partial G$, $\partial \theta/\partial M_{list}$ and $\partial \psi/\partial M_{trim}$, is carried out by determining the systems for equalizing the balance of forces and moments acting upon the ACV, among which are the external hydroaerodynamic forces and moments considered in Chapter 2, as well as forces of another nature – gravity G and propeller draught P.

In problems of statics it is more convenient to arrange in the beginning in the ACV a combined system of coordinates 0_1xyz on the fundamental plane. Then characteristic measurements (for example, $h_{r,o}$) will enter into the equalization of balance and the rise of the center of the mass above the fundamental plane (y_G), in the obvious form, so that it simplifies the analysis of their influences on the static characteristics of the ACV. We will direct axis 0_1x to the bow along the base line of the ACV, axis

O_1y upwards in the diametrical plane through the center of the mass of the ACV, axis O_1z normally towards the plane xo_1y on the starboard side.

We will determine the moments and forces in the mobile system of coordinates $ox_oy_oz_o$, where the horizontal plane Ox_oz_o coincides with the undisturbed surface of the water, axis θX_o is collinear with the speed vector of the ACV $\vec{V}$, and axis Oy_o is directed vertically and passes through the beginning of the combined system of coordinates O_1xyz, but axis Oz_o is normal, relative to plane x_oOy_o and makes up, with the remaining axes, the right hand system. In designating the projections of forces and moments the index "0" will be omitted in order to simplify the writing.

Equalization of balance consists of equalization of forces described by the balance of the center of the mass and the equalization of moments depicted by the position of the ACV relative to the center of the mass.

In conforming to the conditions set up in the problem, these equations are written in the following form:

$$\sum \vec{R} = \vec{R}_{a1} + \vec{R}_{a3} + \vec{R}_{a4} + \vec{R}_{a5} + \vec{R}_{a7} + \vec{R}_r + \vec{P} + \vec{G} + d\vec{G} = 0; \qquad (36)$$

$$\sum \vec{M} = \vec{M}_{a1} + \vec{M}_{a3} + \vec{M}_{a4} + \vec{M}_{a5} + \vec{M}_{a7} + \vec{M}_r + \vec{M}_P + \qquad (37)$$
$$+ \vec{M}_G + \vec{M}' = 0,$$

where $d\vec{G}$ and $\vec{M}'$ represent additional force and moment.

Using the expressions arrived at in Chapter 2 for external forces and moments acting upon the ACV, we will write these equations in the form:

$$\sum \vec{R} = \int\int_{\sigma_i} (\Delta p\vec{n} + \vec{\epsilon\tau})\, d\sigma + \rho Q\vec{V} + \int\int_{\Omega} \vec{p'}\, d\sigma + \rho \int\int_{\sigma_3} \vec{V}_r V_{rn}\, d\sigma + \qquad (38)$$
$$+ \rho \int\int_{\Omega} \vec{V}_r V_{rn}\, d\sigma + \int\int_{\sigma_r} \vec{p}_r\, d\sigma + \vec{P} + \vec{G} + d\vec{G} = 0;$$

$$\sum \vec{M} = \int\int_{\sigma_i} [\vec{r} \times (\Delta p\vec{n} + \vec{\epsilon\tau})]\, d\sigma + \rho \int\int_{\sigma_3} [\vec{r} \times (\vec{V}_a - \vec{V}_r)]\, d\sigma + \qquad (39)$$
$$+ \int\int_{\Omega} (\vec{r} \times \vec{p'})\, d\sigma + \rho \int\int_{\sigma_3} (\vec{r} \times \vec{V}_r) V_{rn}\, d\sigma + \rho \int\int_{\Omega} (\vec{r} \times \vec{V}_r) V_{rn}\, d\sigma +$$
$$+ \int\int_{\sigma_r} (\vec{r} \times \vec{p}_r)\, d\sigma + (\vec{r}_P \times \vec{P}) + (\vec{r}_G \times \vec{G}) + \vec{M}' = 0.$$

-103-

Equations (38) and (39) in their overall form cannot be solved due to the complexity of dependences involved. Therefore, we'll simplify them by taking out the part most essential to the engineer's solution of the problem.

For this purpose we will first write out separately the systems for equalization of balance for several particular instances. Considering that, for Class A ACV's, the rate of hovering over the water and over a screen are in a certain sense limited cases of a rate of movement over water, we will try to determine the unknown parameters for these two rates specifically, and then we will find the dependence of change of the unknown parameters on the speed of the ACV. For a Class B ACV the quality of the initial data in determining known parameters in the calculated rate will be considered significant of the parameters, found for the rate of hovering over water.

Secondly, in considering the balanced position of the ACV, we will isolate the problem of the balance of vertical forces and show that using the results of its solution will greatly simplify the solution of the overall problem.

Thirdly, in considering hovering rates, rather than the spacial problem, we will solve the problem for the transverse plane (where ψ = const), and the solution of the longitudinal plane problem is analogous, but the solution of the spacial problem where there are small angles of inclination of the ACV is arrived at by combining the results of the solutions of transverse and longitudinal problems. Strictly speaking, such division is impossible for a rate of movement, but in this case it is possible to arrive at an approximate solution by a similar method.

In this way we will get the sum total of the following simplified systems of equalization of balance for an ACV with little significance for the moment of list $\vec{M}' = M_{list}$ and $G = G + dG$.

Class A ACV

1. Rate of movement over water

$$\sum X = X_{a1} + X_{a3} + X_{a4} + X_{a5} + X_{a7} + X_{r1} + X_p = 0; \tag{40}$$

$$\sum Y = Y_{a1} + Y_{a4} + Y_{a5} + Y_{a7} + Y_{r1} + Y_p - G_2 = 0; \tag{41}$$

$$\sum Z = Z_{a1} + Z_{a3} + Z_{a4} + Z_{a5} + Z_{a7} + Z_{r1} + Z_p = 0; \tag{42}$$

$$\sum M_x = M_{x a1} + M_{x a4} + M_{x a5} + M_{x a7} + M_{x r1} +$$
$$+ M_{a0} + M_{1 list} = 0; \tag{43}$$

$$\sum M_y = M_{ya1} + M_{ya4} + M_{ya5} + M_{ya7} + M_{ri} + M_{yP} = 0; \qquad (44)$$

$$\sum M_z = M_{za1} + M_{za3} + M_{za4} + M_{za5} + M_{za7} + M_{zri} + \\ + M_{zP} + M_{zO} = 0. \qquad (45)$$

2. Rate of hovering over water (transverse plane problem) - movement broadside (drift)

$$\sum Y = Y_{a4} + Y_{a7} - G_{\Sigma} = 0; \qquad (46)$$

$$\sum Z = Z_{a1} + Z_{a3} + Z_{a4} + Z_{a5} + Z_{a7} + Z_{r1} = 0; \qquad (47)$$

$$\sum M_x = M_{xa1} + M_{xa4} + M_{xa5} + M_{xa7} + M_{xr1} + \\ + M_{xO} - M_{list} = 0. \qquad (48)$$

3. Rate of hovering over a screen while moored (with the absence of any contact of the screen with the rigid body of the ACV)

$$\sum Y = Y_{a4} - G_{\Sigma} = 0; \qquad (49)$$

$$\sum Z = Z_{a4} + Z_{a5} - Z_m = 0; \qquad (50)$$

$$\sum M_x = M_{xa4} + M_{xa5} + M_{xO} + M_m - M_{list} = 0. \qquad (51)$$

Class B ACV

4. Rate of movement over water

$$\sum X = X_{a1} + X_{a3} + X_{a4} + X_{a5} + X_{a7} + X_{r1} + X_{r2} + X_P = 0; \qquad (52)$$

$$\sum Y = Y_{a1} + Y_{a4} + Y_{a5} + Y_{a7} + Y_{r2} + Y_P - G_{\Sigma} = 0; \qquad (53)$$

$$\sum Z = Z_{a1} + Z_{a3} + Z_{a4} + Z_{a5} + Z_{a7} + Z_{r1} + Z_{r2} + Z_P = 0; \qquad (54)$$

$$\sum M_x = M_{xa1} + M_{xa4} + M_{xa5} + M_{xa7} + M_{xr1} + M_{xr2} + \\ + M_{xO} - M_{list} = 0; \qquad (55)$$

$$\sum M_y = M_{ya1} + M_{ya4} + M_{ya5} + M_{ya7} + M_{yr1} + \\ + M_{yr2} + M_{yP} = 0; \qquad (56)$$

$$\sum M_z = M_{za1} + M_{za3} + M_{za4} + M_{za5} + M_{za7} + M_{zr1} + \\ + M_{zr2} + M_{zO} + M_{zP} = 0. \qquad (57)$$

5. Rate of hovering over water (with drift)

$$\sum Y = Y_{a4} + Y_{a7} + Y_{r2} - G_{\Sigma} = 0; \qquad (58)$$

$$\sum Z = Z_{a1} + Z_{a3} + Z_{a4} + Z_{a5} + Z_{a7} + Z_{r2} = 0; \qquad (59)$$

$$\sum M_x = M_{xa1} + M_{xa4} + M_{xa5} + M_{xa7} + M_{xr2} + \\ + M_{xO} - M_{list} = 0. \qquad (60)$$

In equations (40) - (60) is designated $(X_i + Y_i + Z_i = R_i)$:

$\vec{R}_{a1-7}$ - aerodynamic forces (see Chapter 2);

$\vec{R}_{r1}$ - hydrodynamic force, caused by contact of the flexible skirt with the water;

$\vec{R}_{r2}$ - hydrodynamic force, caused by contact of the rigid hull or structures with the water;

$\vec{R}_m$ - mooring reaction force, keeping the ACV from shifting horizontally in its rate of hovering over a screen;

$\vec{P}$ - draught force of the ACV propeller;

$M_{list} = M'_x = M'$ - moment of list.

Calculations and experiments show that the lift height as well as the stability characteristics of an ACV are to a significant degree considered according to the rate of work of the lifting system of the ACV (but for Class A, this rate is excluded, therefore we will first consider the parameters characterizing the rate of work of the ACV's lifting system and their interdependency.

§14. Tilt Height and the Degree of Static Stability of an ACV Relative to Vertical Shifts

A typical structural feature of air cushion vehicles is the special lifting system creating and maintaining under the hull of the vehicle an area of air under high pressure. Generally, the lifting system is the sum total of technical means, which include:

air scoops (air gates);

air superchargers (fans, compressors, injectors, etc.);

air hoses and receivers

nozzle devices in the rigid hull of the ACV;

skirts for high pressure areas;

means for controlling the air currents within the lifting system.

The rate of work of the lift system is usually characterized by the following values:

Q - expenditure of air;

H_p - full pressure for the fan;

h - average lift height of the rigid hull of the ACV over a base surface.

Depending on the case under consideration, usages indicate the lift height in the following manner:

h_3 - lift height of ACV in a hovering rate, over a screen;

h_h - lift height of ACV in a hovering rate, over water;

h_v - lift height of ACV in a rate of movement, with velocity V, over water

The values Q, H_p, h_3, $_h$, $_v$ may be designated as the lift characteristics of an ACV. The lift characteristics depend on the characteristics of all elements of the lift system, but the deciding influence on them are the characteristics of the air superchargers and the air cushion skirts.

During research and development these characteristics usually turn up in the form of the following non-dimensional values:

$$\overline{Q} = \frac{Q}{\sqrt{\frac{4S_n \cdot G}{\pi \rho}}}$$ - relative expenditure of air;

$$\overline{p} = \frac{p_p \cdot S_n}{G}$$ - pressure coefficient (relation of pressure in receiver p_p to average pressure $p_n = G I S_n$);

$$\overline{h}_3 = \frac{h_3}{\sqrt{S_n}}$$ - relative lift height in the ACV's hovering rate, over a screen.

In designing the fan (supercharger) for an ACV the basic calculated rate must be set up first of all, i.e., air expenditure and the fall of pressure are determined, both of which must be provided for by the fan. The selection of air expenditure and the form of expended pressure are characterics of the fan and locations of "working points" on it are basically determined by the requirements for seaworthiness. The dependence for seaworthy qualities of an ACV on the expenditure of air will be examined in Chapter 4.

In determining the calculated fall of pressure, the starting point is the value of the average static excess air pressure in the air cushion, determined by the weight of the ACV and the area of the air cushion S_n, $p_n = \frac{G}{S_n}$.

In the early stages of development of the ACV, when it was a popularized nozzle-type vehicle without a flexible air cushion skirt, the lift characteristics had the following tentative meanings: $0.05 < \overline{Q} < 0.08$; $1.5 < \overline{p} < 2.5$; $0.005 < \overline{h}_3 < 0.010$.

With the development of flexible skirts, the operational qualities of the ACV were sharply improved and their lift characteristics at present are within the limits: $0.015 < \overline{Q} < 0.03$; $1.25 < \overline{p} < 1.5$; $0.1 < \overline{h}_3 < 0.2$ (class A). Class B air cushion vehicles with immersible side barriers (walls, shells, hulls) have the following lift characteristics: $0.0015 < \overline{Q} < 0.015$; $\overline{p} \approx 1$ (due to the absence of a receiver).

Improvement of the seaworthiness of the class A ACV evidently is leading to some increase in the relative expenditure of air $\overline{Q}<0.030$, but the quantitative limit of Q has not been set at this time.

The structural form of air superchargers does not influence the hydro-aerodynamic qualities of an ACV, since the lift characteristics depend solely on the expended pressure characteristics of the air supercharger H (Q). However, in designing, a reasonable selection of structural elements for the fan plays a substantial role. In the first place, this concerns the selection of the diameter and the number of revolutions of the fan. As a result of the general location and the provision for weight characteristics, it is expedient to decrease the diameter of the fan and increase the number of rotations, but doing this causes an increase in the portion of dynamic pressure and a decrease in the static efficiency.

In those instances where the general arrangement of the air gates in an ACV entails altering the air stream 90°, it is expedient to use a centrifugal fan, in which such alteration is accomplished by means of the aerodynamic set-up and, consequently, succeeds in avoiding complications in hull design. Recently, effective designs of centrifugal fans have been worked out for ACV's, [71] permitting the achievement of static efficiency $n_{st} \approx 0.7\text{-}0.8$ and total

efficiency $7=0.9$. The non-dimensional expended pressure characteristics of such a fan are set forth in Figure 49.

The expended pressure characteristic H (Q) determines the change of the parameters of the air stream, depending on the given conditions, for example, the weight of the ACV. The location of it's working points must satisify definite conditions. The following must be assured:

conformity of meaning for H_p and Q according to the maximum relationship of 7 (Q) (Figure 50);

sufficient margin for H_p and Q where n_B = const, which permits preservation of the designed characteristics of the lift systems in the greatest possible range of external conditions;

a great enough difference in the derivatives $\partial H/\partial Q$ and $\partial p_p/\partial Q$, which provides the necessary degree of stability for the ACV.

The first and second conditions are determined by the requirement for maximum efficiency of the lift systems and stability for the ACV relative to vertical shift.

The third condition is determined by the requirement for the form of the fan's characteristics which, as far as possible, must not have an area of $\partial H/\partial Q>\partial p_p/\partial Q>0$.

The overflow of pressure in the fan must exceed the static pressure in the cushion by the amount of pressure lost in the ACV's internal air conductors.
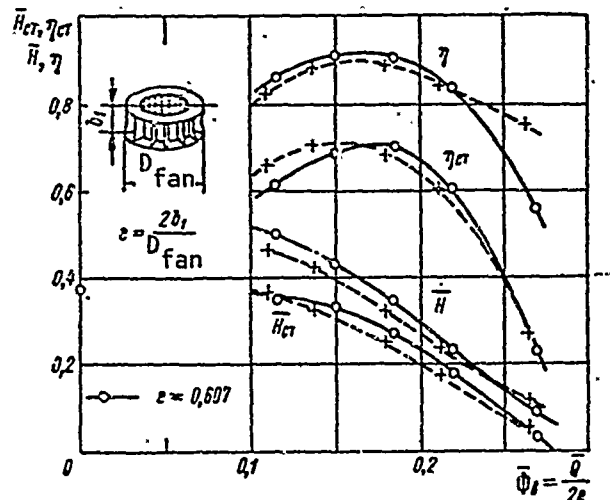
Figure 49. Expended-Pressure Characteristics of the Centrifugal Fan Mounted on the CC-2 ACV [71]

$\overline{H}$, $\overline{H}_{c+}$ - coefficients of pressure (full and static).; $\overline{\Phi}_B$ - coefficient of expenditure; η, η_{CT} - efficiency of the fan (full and static)

———o——— Type E1 fan;

--------+------- Type G1 fan

A graph is set forth in Figure 51 which gives a qualitative illustration of the distribution of the total pressure during the movement of air inside the ACV's hull. According to the graph, the overflow of the total pressure is equal to

$$H = p_n + \Delta p_1 + \Delta p_2 + \Delta p_3 + \Delta p_4,$$ (61)

where $\Sigma \Delta p_i$ there are the following losses of pressure:

Δp_1 - at the entrance to the fan's shaft;

Δp_2 - during expansion of the air in the fan's diffusor;

Δp_3 - during expansion of air in the receiver;

Δp_4 - in passing from the receiver to the air cushion.

Losses for Δp_1 depend on the structure of the air gates and the ratio of the ACV's speed to the air speed in the fan's shaft (influence of these factors is illustrated in Figure 102).

Losses in the diffusor are determined by the ratio of static to dynamic makeup of the total pressure and by the ratio of the area of the shaft's section at the entrance to the diffusor to its exit-way. A continuous movement of air in the diffusor which would create a minimum loss of pressure may be provided only by a fixed ratio of the size of the area of the diffusor section at the entrance-way to the exit-way. The purpose of the diffusor is the transformation of the dynamic makeup of pressure to static with the aim of decreasing the speed and loss of pressure with air passing from the shaft to the receiver. In an ideal variant there would be total transformation of dynamic pressure to static, i.e. an inhibition of air flow at the entrance-way to the receiver of almost zero. However, the analysis of numerous investigations, devoted to the problems of air inhibition, leads us to the conclusion that even in a uni-dimensional flow, reduction of speed without removal of the surrounding layer is possible for only up to 60% of the initial amount. In such a case, the large degree of success in braking the flow (up to 40% of the initial speed) is due to the surrounding layer being very thin during initial movement. Thus, when deceleration of the flow is added to its turning, the effectiveness of the diffusor is even less since the turning of the flow leads to an increase in the ground speed of the flow. Experimental research of radial and combined diffusors $l_{DIF} \approx 0.4 \ D_{FAN}$ in the length showed that the

loss factor of pressure is between 0.6 and 0.8 on the average, in some cases reaching 1.0 to 1.26 [9]. In [16], a method was set forth to calculate the loss in a curvilinear diffusor with detached flow.
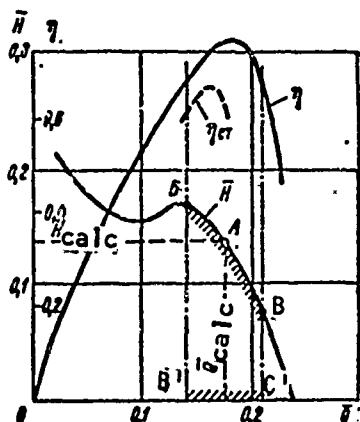

Figure 50. Diagram of the Selection of Calculated Parameters for the Fan

A - operating point $(\overline{Q}_{calc}, \overline{H}_{calc})$;

BC - operating section

Pressure losses from air movement in the receiver are determined by the speed of movement, i.e. by the area of a cross-section or size of the receiver and blockage of the section by various parts of the hull's structure, which sets up resistance to air movement. For this reason, the size of the receiver is determined in consideration of the general design.

Special consideration is usually given to the choice of the amount of overflow of pressure between the receiver and the air cushion. To decrease power expenditure during lift, it is logical to try to decrease this overflow.

-110-

However, a number of other reasons hinder maintaining such an overflow within certain limits, namely:

overflow of pressure between the receiver and the cushion must provide the necessary stability for a Class A ACV, which is achieved either by sectioning the cushion with air streams sufficiently high in kinetic energy or by an increase in pressure to the sections (with chamber-type air flow), where expenditure is decreased;

high enough overflow of pressure between the receiver and the cushion facilitates an even distribution of air to various sections of the air cushion and pneumatic elements of the flexible skirt;

increase of overflow of pressure, i.e. provision of considerable hydraulic resistance between the receiver and the cushion, necessary to dampen the fluctuation of pressure in the receiver during considerable changes of pressure in the cushion while moving in choppy sea conditions. This is necessary to protect the engine from overload and allows the fan to work with more stability.
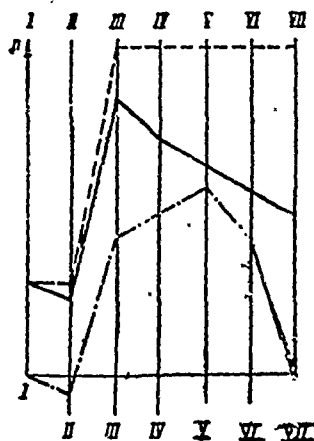

Figure 51. Diagram of the Distribution of Surplus Pressure Along the ACV's Internal Air Ducts.
I - I in meeting the air flow; II - II in front of the fan; III - III leaving the fan; IV - IV leaving the diffusor; V - V in the receiver; VI - VI in the air cushion; VII - VII in meeting the stream flowing from the area of surplus pressure.

- - - - without any loss (ideal)
——— full pressure
-- • -- static pressure

After determining the basic calculated parameters of the fan (overflow of pressure H_β and amount of expenditure Q), the problem arises as to choice of structural elements of the air-supercharger, i.e. its diameter, number of RPM's, and structural type (centrifugal, axial, etc.).

The normal operating rate of the air-supercharger represents a constant number of RPM's of the drive wheel (rotor), therefore, the relationship between air expenditure and pressure for the fan will be regarded later on, under expended-pressure characteristics, as the constant number of RPM's of the fan's drive-wheel.

In addition to the fan's characteristic, the ACV's lift characteristic considerably influences the expended-pressure characteristics for skirting the air cushion (including sectioned skirts).

There are many known types of air cushion skirts. One might consider the following plan for classifying the basic types of skirts, based on various aerodynamic parameters of air flow (Figure 52).

Skirts, for Which Air Flow is Provided for From an Area of Increased Pressure (During Suspension of the ACV), Figure 52 I

1) Air-stream skirts (Figure 52a): peripheral jets of various configurations - 1; recirculation systems of various types - 2.

2) Hydro-jet skirts (and combined, Figure 52b): hydro-jet curtain - 3; combination hydro and air-jets - 4; combination water curtain and flexible panels - 5.

3) Mechanical skirts (Figure 52c):

rigid, fixed curtains (panels, side walls, shells, etc.) with a chamber-type setup for air flow - 6;

rigid rotary flaps, a jointed curtain of rigid elements, etc. - 7;

rigid skirts with nozzles of various configurations - 8;

flexible, massive and vertically-arranged skirts (panels, pneumatic fingers with no air flow, pneumatic keels, etc.) - 9;

flexible, diagonally-arranged skirts (open and closed types) - 10;

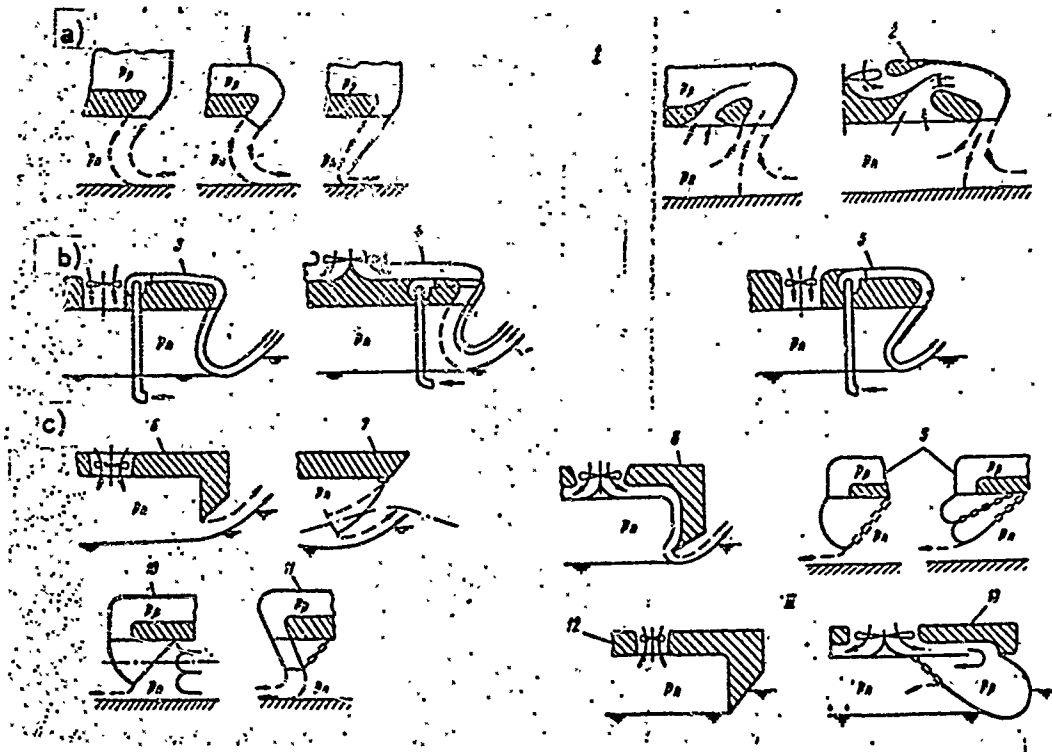and flexible nozzles (massive and diagonally-arranged) - 11.

Figure 52. Classification of Skirts for Air Cushions

Skirts Which Do Not Permit Air Flow From an Area of Increased Pressure (During Suspension of the ACV), Figure 52 II

1) Rigid structures (side barriers: walls, hull, shells, working in continuous contact with water, etc.) - 12.

2) Flexible structures (massive panels; pneumatic closed, massive and diagonally-arranged structures, submerged in the water) - 13.

To a great degree, the above classifications reflect the variety of type of skirts for air cushions. Besides this, it is necessary to take into account that, first of all, the skirt is usually a combination of various elements along the perimeter of the area of increased pressure and various designs are used to separate the air cushions into sections. Secondly, in operating conditions, one of these elements may switch from one classification category to another depending on the angle of the ACV's incline or the interaction of the skirts with the agitated surface of the water, etc. Thus, it is obvious that the problem of determining the expended-pressure characteristics of skirts for air cushions is complex and many-sided.

To simplify matters, only two variants will be examined in the aerodynamic arrangement of skirts: air-stream (nozzle) and chamber-type, considering that all the remaining types are in between these two.

In any type of skirt, approximation of its lower edge to the base surface (with no incline of the ACV) induces an increase of hydraulic resistance with air flowing into the atmosphere. This feature explains the increase in lift forces with increase of the ACV's weight, and ensures its stability with respect to vertical shift.

The forms which the expended-pressure characteristics of the air-cushion skirts take depend both on the aerodynamic arrangement of air flow and deformation of the base surface, over which the ACV is suspended. The standard base surfaces are an absolutely rigid screen and the surface of calm, deep water.

We note that the basic expended-pressure characteristics of skirts:

the coefficient of pressure

$$\bar{p} = \frac{p_p \cdot S_n}{G},$$ (62)

and the coefficient of expenditure

$$\bar{q} = \frac{Q}{f_c \sqrt{2 p_p \rho^{-1}}}$$ (63)

(f_c equals the area of the ducted section of the nozzle) depend on the height of suspension of the nozzle's cut-off (or edge of the chamber) over the base surface and the kind of base surface involved.

1. Air-stream Curtain Above a Screen

Using theoretical models with air-stream curtains (2-dimensional), flowing onto the screen from nozzles with parallel walls, and considering that the air is combined with ideal imcompressible fluid, we are able to discover the distribution of speed in the stream in relation to the given parameters: the width of the nozzle b, the distance of the nozzle's cut-off from the screen h_{sc}, and the nozzle's angle of incline.

This problem was completely solved by Strand and Stenton-Jones (exponential theory [108]). The border conditions were formulated by the following means. Pressure on the inside and the outside of areas in relation to the stream began accordingly: p_n along CD and $p_o = 0$ along BA_o (Figure 53). Along BC, the vector speed is co-linear with axis Cy. Then the potential speed ϕo along BC is constant and may be assumed as equal to zero. The angle 0_c is determined by the direction of the vector speed $\vec{V}$ in a polar system coordinate, along BC equals zero, and along DA_o^1 — $(\frac{\pi}{2} + \phi_c)$. Assuming that the function of current $\psi = a$ along BA, one may assume that $V_o b_o = a$, where b_o equals the thickness of the stream to infinity and V_o equals the constant of speed along BA_o, determined from Bernoille's equations.

Thus formulated, the border conditions permit us to find the function of the current and the potential speed by means of the following consecutive

transformations which were accomplished accordingly. The plane of the complex variable $w = \phi_0 + i_\phi$ (Figure 54) is transferred to the first quadrant of the plane ξ by means of Shwartz--Kristoffel transformation:

$$\xi = \mathrm{ch}\left(\frac{\pi w}{2a}\right).$$
(64)

Then a rectangle containing the field of flow and its smooth reflection in the plane of the hodograph $Q_c = \ln (V_0/V + i\theta_c)$, as well as being reflected in the first quadrant of the plane ξ according to the following formula of Shwärtz-Kristoffel is:

$$Q_c = M \int_0^\xi \frac{dt}{\sqrt{(1-t^2)(1-k^2t^2)}} + N,$$
(65)

where M, N and k equal constant, fixed outcomes of the conditions of transformation.

By excluding ξ from equations (64) and (65), one may assume

$$Q_c = \frac{\frac{\pi}{2} + \varphi_c}{K'} \int_0^{\mathrm{ch}\left(\frac{\pi w}{2a}\right)} \frac{dt}{\sqrt{(1-t^2)(1-k^2t^2)}},$$
(66)

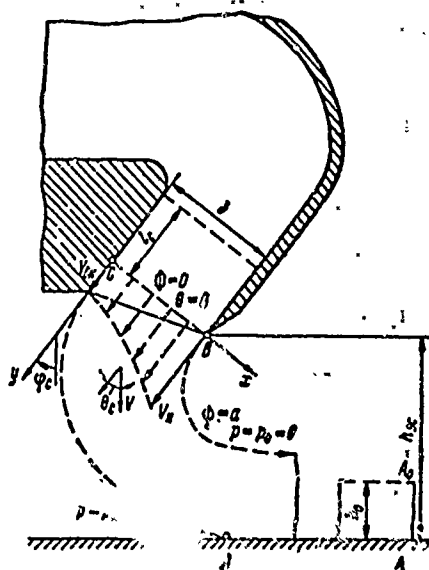where K' equals the elliptical integral of the first kind, appearing in the course of determining the constants.

Figure 53. Diagram of the Plane of the Stream's Flow

-115-

The last expression completely characterizes the air flow in the stream and allows one to find out the ground speed according to the potential speed and function of the current. As a result, the answer is determined by the amount of the coefficient of pressure and expenditure, as well as some other amounts. To get the answer, there are no restrictions in the correlation between the width of the nozzle, the height of suspension, and the dimensions of the bottom of the ACV. It was shown that the answer may be used to observe the flow created by an axisymmetric nozzle system in a circular arrangement.

As a result, the following relationships for the coefficient of pressure and expenditure were obtained:

$$\bar{p}_{\ni} \approx \frac{e^{Cx}}{e^{Cx}-1}; \qquad (67)$$

$$\bar{q}_{\ni} \approx \frac{e^{x}-1}{xe^{x}}; \qquad (68)$$

where

$$x = \frac{b}{h_{\text{эс}}}(1+\sin\varphi_{\text{c}}); \qquad (69)$$

C equals the coefficient received in accordance with the exponential theory, equal to two.

Experimental data [74] shows that, in actual cases, more accurate results are received, when C = 1.67.

An almost accurate answer was given by Professor G. Yu. Stepanov [43], who received the following correlation between the average speed in the jet $V_{aver.}$ and the stream bordering a section of the jet.
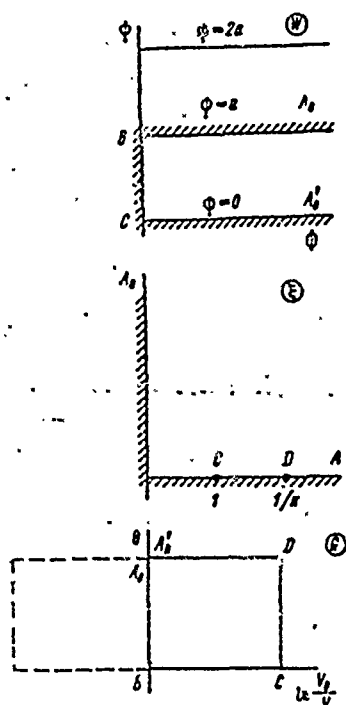
$$V_{\text{cp}} = \sqrt{V_{\text{н}} \cdot V_{\text{вн}}}. \qquad (70)$$

As a result, the following equation was received:

$$\frac{h_{\text{эс}}}{h} = 2\sqrt{\bar{p}_{\ni}}\sqrt{\bar{p}_{\ni}(\bar{p}_{\text{v}}-1)} + \left[\sqrt{\bar{p}_{\ni}(\bar{p}_{\ni}-1)} + \bar{p}_{\ni} - 1\right]\sin\varphi_{\text{c}}. \qquad (71)$$

Some other approaches, used by M. A. Grechin for determining the correlation between $b/h_{\text{эс}}$ and $\bar{p}_{\ni}$ (where $b/h_{\text{эй}}' < 1$) and discovering the coefficient of expenditure $\bar{q}_{\ni}$, permitted the following formulae to be obtained [15]:

$$\left.\begin{aligned}
\bar{p}_{\ni} &= \left(\frac{h_{\text{эс}}}{b}+\sin\varphi_{\text{c}}\right)\left[(1+\sin\varphi_{\text{c}})\left(2-\frac{1+\sin\varphi_{\text{c}}}{\frac{h_{\text{эс}}}{b}+\sin\varphi_{\text{c}}}\right)\right]^{-1}; \\[2mm]
\bar{q}_{\ni} &= \frac{\frac{h_{\text{эс}}}{b}-1}{1+\sin\varphi_{\text{c}}}\ln\frac{\frac{h_{\text{эс}}}{b}+\sin\varphi_{\text{c}}}{\frac{h_{\text{эс}}}{b}-1},
\end{aligned}\right\} \qquad (72)$$

From L. F. Kalitievski's work on "thin" streams (where $b/h_{\textrm{эc}} \ll 1$), the following expression was obtained [22]:

$$\bar{p}_{\textrm{э}} = \frac{\left(1 + \dfrac{b}{h_{\textrm{эc}}} \sin \varphi_c\right)^2}{2\dfrac{b}{h_{\textrm{эc}}}(1 + \sin \varphi_c) - \left(\dfrac{b}{h_{\textrm{эc}}}\right)^2 \cos^2 \varphi_c}. \tag{73}$$

Figure 54. Diagram of the Conforming Transformation.

In Figure 55, a comparison is set forth of the results, calculated according to formulae (67) - (73) for $\phi_c = 45°$, between its own and the experimental data obtained by V. I. Khanzhonkov [53]. It is obvious from the graphs that the results closest to that of the experimental data is the calculations of $\bar{p}_{\textrm{э}}$ according to formula (67) with C = 1.67 and of $\bar{q}_{\textrm{э}}$ according to formula (68).

Tests showed that the length of the nozzle l_c (Figure 53) must be about $2 \ll l_c/b \ll 2.5$. With a shorter nozzle, the stream does not develop, and a longer nozzle causes great losses of pressure due to the development of a border layer.

Thus are the expended-pressure characteristics determined for an air-stream curtain, and the same geometry applies to a nozzle-type device, including the height of the nozzle's cut-off above the screen along all perimeters of the air cushion, assuming that the pressure found is the average excess pressure in the air cushion. The possibility is minimal that there will be dissimilar geometry in the nozzle or the distance of its cut-off from the screen (along the perimeter) of pressure. For example, with an inclined position over a screen, the nozzle device is constant along the perimeter of the configuration and the pressure is determined by the element of the stream, flowing from the nozzle to the most remote point from the screen (with $x = x_{\textrm{min}}$).

Thus, using the hypothesis of the plane of the section (i.e. the cross-current of air from section to section is not considered), it is possible to determine the total air expenditure as the total elementary expenditure according to the geometry of the separate parts of the curtain

$$Q = \oint_{\textrm{л}} dQ = \sqrt{\frac{2p_{\textrm{p}}}{\rho}} \oint_{\textrm{п}} \bar{q}_{\textrm{э}}(\lambda_{\textrm{к}}) d\lambda_{\textrm{к}}, \tag{74}$$

-117-

where λ_k equals the curvilinear coordinate of that part of the air cushion's contour which has been noted.
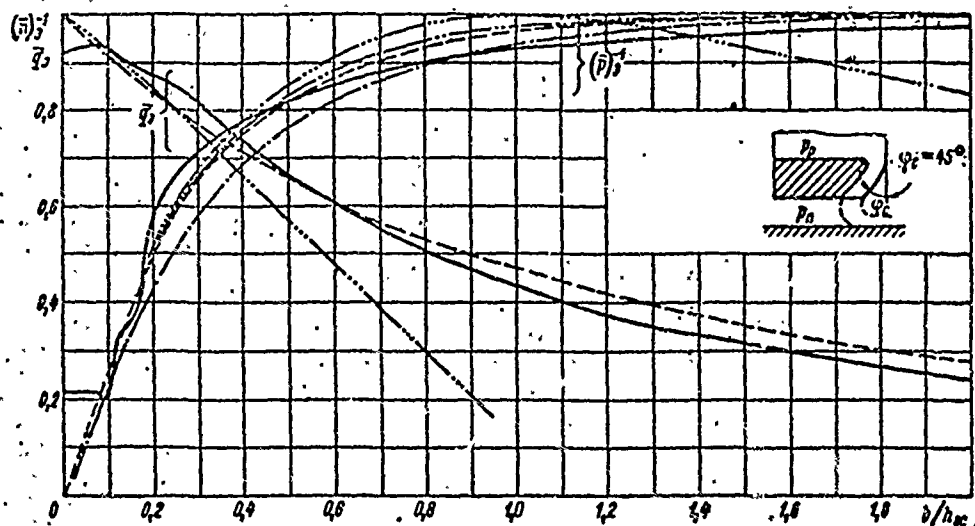

Figure 55. Expended-Pressure Characteristics of the Air Stream in the ACV's Skirts in Suspension Above the Screen

———————————— Central Institute of Aerohydrodynamics Experiment

Calculations

‐ ‐ ‐ ‐ by formulae (67) and (68) where C = 2;

— • — by formula (67) where C = 1.67;

— •• — by formula (71);

— ••• — by formulae (72) and (73)

A more exact approach is possible, in which the redistribution of expenditure along the separate part of the air cushion's contour (due to division of the stream) is taken into account, but for practical purposes it is sufficient to use the method set forth above.

2. Chamber Variant of Air Flow Above a Screen

In the chamber variant of air flow from the under-dome area, under the action of pressure p_Π, expenditure is also determined by using the hypothesis of the plane of the section

$$Q = \sqrt{\frac{2p_\Pi}{\rho}} \oint_{\Pi} \varkappa(\lambda_\varkappa)\, h_{\ni\varkappa}(\lambda_\varkappa)\, d\lambda_\varkappa, \tag{75}$$

-118-

where $x(\lambda_k)$ equals the local coefficient of the narrowing of the stream and $h_{\ni k}(\lambda_k)$ equals the clearance between the skirt and the screen in the section noted.

The coefficient of the narrowing of the stream is determined by the geometry for the edge of the air cushion's skirt.

For rounded edges $x(\lambda_k) = 1$ is usually adopted, and for sharp edges it is possible to use the expression (Figure 56)

$$x(\lambda_k) \approx 0{,}50 + 0{,}05 \left(\frac{\pi}{2} - \varphi_c \right)^2 ; \tag{76}$$

which shows the connection between the coefficient of the narrowing and the angle of incline of the edge toward the screen, where $0 < \phi_c < \frac{\pi}{2}$.

3. Jet Variant of Air Flow Over Water

Let us examine the inleakage for a flat air-stream curtain, of a single width, on the water's surface (Figure 57). We will consider both fluids as ideal, incompressible, and the stream as not mixing with the surroundings. We will suppose that the innermost border of the curtain, at the point of contact with the surface of the depression, has a horizontal direction of connecting. For simplification of analysis, we will compute the radius of the internal border of the stream as R_c = const. Then, designating the angle of takeoff for the stream as ϕ_B, from a geometric standpoint we get

$$h^* = h_{ac} + \frac{G}{\gamma S_n} = R_c (1 + \sin \varphi_c) - b \sin \varphi_c,$$

where

$$R_c = \frac{h^* + b \sin \varphi_c}{1 + \sin \varphi_c}. \tag{77}$$

In accordance with the data set forth by V. V. Klichko [23], one may consider that the expended-pressure characteristics of the air-stream curtain are as uniform over water as they are over a screen, but it is necessary to take into account the deformation of the base surface which is expressed in the case given by the additional reason $G/\gamma S_\pi$. Then the coefficient of pressure will equal

$$\bar{p}_a \approx \frac{e^{Cr}}{e^{Cr} - 1}; \tag{78}$$

and the coefficient of expenditure is

$$\bar{q}_a \approx \frac{e^{x^*} - 1}{x^* e^{x^*}}. \tag{79}$$
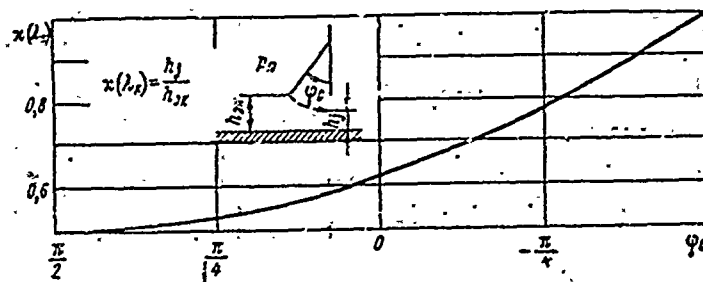
-119-

Figure 56. Relationship of the Coefficient of the Narrow Stream During Flow From a Chamber Over a Screen

By designating the distance from the outside edge of the jet's cutoff to the internal border of the stream during takeoff from the water as h^*_B, we get the expression for the index x^*

$$x^* = \frac{b}{h^*_B}[1 + \sin(\varphi_c + \varphi_a)].$$

(80)

The amount h^*_B is equal to

$$h^* = R_c[1 + \sin(\varphi_r + \varphi_a)] - b\sin(\varphi_c + \varphi_a).$$

(81)

Substituting R_c according to formula (77) in the expression (81) and then in (80), we get

$$x^* = \left[\frac{\frac{h^*}{b} + \sin\varphi_c}{1 + \sin\varphi_c} - \frac{\sin(\varphi_c + \varphi_a)}{1 + \sin(\varphi_c + \varphi_a)}\right]^{-1}.$$

(82)

The amount ϕ_B may also be found as the result of the geometric calculation

$$\cos\varphi_a = \frac{R_c - \frac{G}{\gamma S_n}}{R_c} = 1 - \frac{(1 + \sin\varphi_c)G}{\left(\frac{h^*}{b} + \sin\varphi_c\right)b\gamma S_n}.$$

(83)

The approximate expressions received may be used for numerical calculation with $b/h^* \ll 1$. Besides this, their structure permits one to establish the inter-dependency for determining the parameters.

It is obvious from expressions (82) and (83) that deformation of the base surface is calculated by the factor $G/b_\gamma S_\pi$, consequently the coefficient of pressure $\overline{p}_B$ and the coefficient of expenditure $\overline{q}_B$, in the case of the ACV suspended over water, depend on two parameters: b/h^* (or the equivalent parameter of b/h_{ac}) and $(./b_\gamma S_\pi$. An example of the relationship of $\phi_c = 45°$,

-120-

according to the calculations of V. V. Klichko, is set forth in Figure 58.
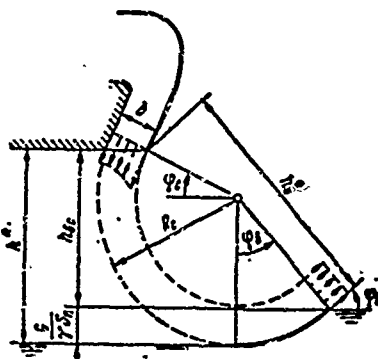

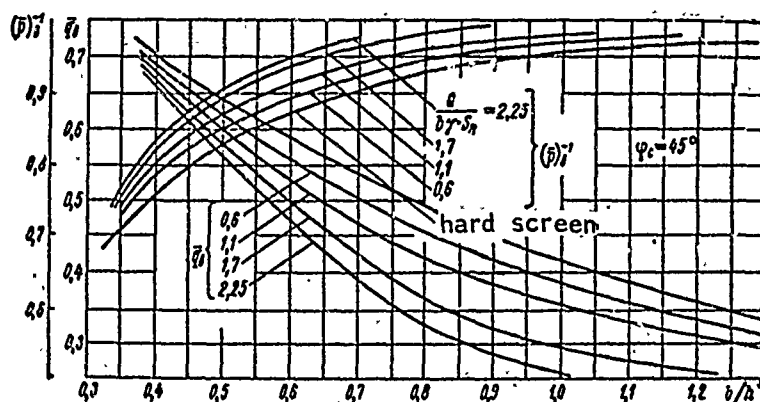Figure 57. Diagram of Inleakage of the Air Stream on Surface Waters.

Figure 58. Expended-Pressure Characteristics of the Air Stream Surrounding an ACV During Suspension Over Water (Estimated)

4. Chamber Variant of Air Flow Over Water

The plane problem concerning air flow from a chamber over water was dealt with by Jones [69]. It was shown in his work that the lift characteristics of a chamber-type ACV are functions of non-dimensional parameters

$$\Gamma = \frac{p_n V_{cp}}{8\gamma Q} = \frac{p_n}{8 x_{B}\gamma l (h_{aK} + \Delta h)};$$

the designations are shown in Figure 59.

To determine the coefficient of a narrow stream over water (x_B), Jones took into account that

$$\frac{x_B}{x_s} \approx 0.7. \tag{84}$$

-121-

This assumption was not taken into account by all experimenters but, apparently, it may be used for engineering calculations.

The amount Δh is calculated according to the formula

$$\Delta h = \frac{p_n}{2\gamma}\left[1 + \frac{1-\cos \varphi_a}{2\Gamma}\right]$$ (85)

Calculations showed that when $\Gamma > 0.2$, the amount $\frac{\Delta h \gamma}{p_n} \approx 0.6 \div 0.7$. All amounts of interest to us may be determined in this way.

The relationships given make it possible to calculate the ACV's lift characteristics for a given weight and size.

Experimental research into the distribution of pressure along the area of the air cushion provides a basis for calculating the amount p_n (x, z) for even distribution. Sharp changes in pressure are only observed along the border of the air cushion and in the area where the air is fed in. With sectioning of the area of increased pressure to provide stability for the ACV, overflows of pressure occur in the border sections and is not distributed evenly p_n (x, z), but inside each section the pressure is distributed evenly.

In Figure 60 the results are set forth of the measurements made during research into distribution of pressure along the area of a sectioned air cushion. The sketch of a model (see Figure 71 below) shows an air cushion consisting of three sections (flexible chamber-type). In the side sections (number 1 and 3) air was drawn from the receiver and the middle section received air from the sides. The graph shows that the amount

$$\frac{\Delta p S_n}{G} = \frac{[0.5(p_1 + p_3) - p_2]S_n}{G},$$

characterizing a degree of unevenness of distribution of pressure along the area of the cushion, is decreased first of all by the increase in the relative load

$$\overline{G} = \frac{G}{S_n^{3/2}\rho g}.$$

and secondly due to the suspension of the model over water. This amount is decreased in comparison with its meaning above a screen, due to the deformation of the base surface.

The calculated meaning of the average pressure in the air cushion, in each specific case, is selected according to the design calculations, the general disposition of the craft and other requirements, but it is possible to point out general relationships which facilitate the selection of this amount to the first approximation.
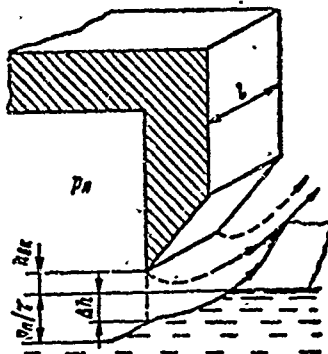
-122-

Figure 59. Diagram of Air Flow From a Chamber During Suspension of an ACV Above Water

The well-known English designer of high-speed craft, P. Du Cane [63], proposed the following method for determining the designed meaning p_Π for passenger-type ACV's, in which the amount of pressure is calculated as the sum of the individual parts of pressure:

$$p_\Pi = p_{pass} + p_{hull} + p_{mech} + p_{fuel} + p_{eqpt}, \qquad (86)$$

where p_{pass} — that part of the pressure necessary for lifting the passengers (or any payload);

p_{hull} — that part of the pressure necessary for lifting the ACV's hull;

n_{mech} — that part of the pressure necessary for lifting the ACV's mechanical gear;

p_{fuel} — that part of the pressure necessary for lifting the fuel;

p_{eqpt} — that part of the pressure necessary for lifting the equipment, systems, etc.

These components may be determined thusly. Let us suppose that the weight of a passenger with his baggage is 100 kilograms, for example, and that he takes up 0.5 meters^2 of space, we get (with regard to the area of the passenger's accomodation) S_Π equal to K_Π,

$$p_{pass} = \frac{100}{0.5} K_\Pi = 200 K_\Pi \text{ kilograms (of force) per meter}^2. \qquad (87)$$

It is possible to get the amount p_{hull} by using the statistical data for the weight of the hull structure equal to, for example, 100 kilograms (of force) per

-123-

meter^2

$$p_{hull} = 100 \text{ kilograms (of force) per meter}^2. \qquad (88)$$
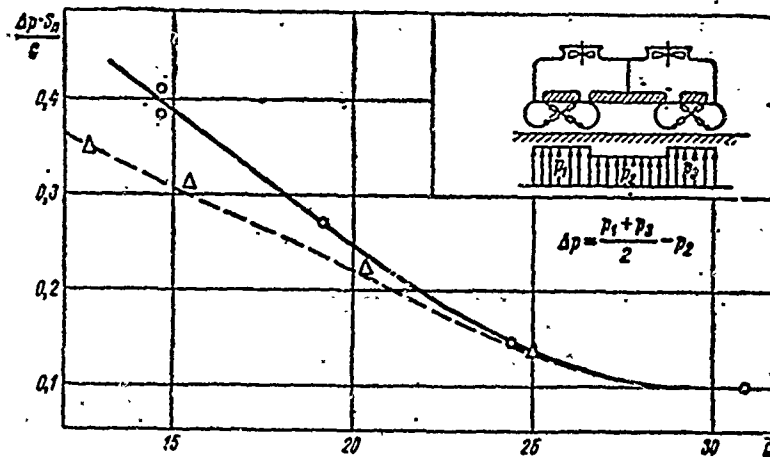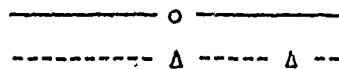

Figure 60. Relationship of the Degree of Unevenness of Distribution of Pressure Along the Air Cushion to the ACV's Relative Weight and the Nature of the Base Surface

———————— o ————————

———————— Δ ————— Δ ——

It is suggested that the pressure p_{mech}, necessary for lift by the ACV's mechanical equipment, be written in the form

$$p_{mech} = C_1 \left(\frac{N_e}{VG}\right) p_\Pi V, \qquad (89)$$

where C_1 equals the weight of the mechanical equipment and the ACV's transmission, using 1 h.p. of power.

As a component of the pressure in lift, the fuel is expressed similarly:

$$p_{fuel} = C_2 \left(\frac{N_e}{VG}\right) p_\Pi R', \qquad (90)$$

where C_2 equals the specific fuel expenditure, in kilograms (of force) per h.p. hour and R' equals the distance of the ACV's voyage.

The weight of the equipment and the systems, as well as the weight of the hull, may be determined by calculation or according to statistical data. For our purposes, let us assume that

$$p_{eqpt} = 50 \text{ kilograms (of force) per meter}^2. \qquad (91)$$

-124-

Hence

$$p_n = 200K_n + C_1 \frac{N_e}{VG} p_n V + C_2 \frac{N_e}{VG} p_n R' + 150. \tag{92}$$

Optimum meanings of the parameter N_e/VG are determined according to the data set forth in [63] and the graph (Figure 61), where meanings are received for the efficiency of the lift system $\eta_{\text{п.c}}$ = 0.7 and 1.0 and the incline angle of the nozzle ϕ_c = 45°. For quality in the relative lift height, we adopt the parameters $h_{sc} \sqrt{\pi/2} \sqrt{S_n} = 0.887\ \bar{h}_{s c}$. By substituting the meaning N_e/VG, which we found in Figure 61, into the expression (92) it is possible to get the relationship p_n to the relative lift height, the distance of the voyage, the speed, and the relationship K_n.
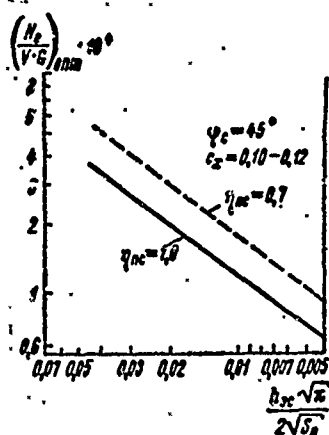

Figure 61. Relationship of the Parameter $(\frac{N_e}{V \cdot G})_{opt}$ to the Relative Lift Height of the ACV.

Set forth in Figure 62 is a graph of the relationship for K_n = 0.5; C_1 = 2 kilograms (force) per h.p. and C_2 = 0.6 kilograms (force) per h.p. hour. Also set forth is the relationship of the payload to the total weight of the ACV - the coefficient of utilization of displacement. With the aid of a similar graph, it is possible to find the pressure in the air cushion p_π in accordance with the design plan.

A projected estimate of the coefficient of the pressure for the lift system of a Class A ACV

$$\bar{p} = \frac{p_p S_n}{G} \approx \frac{H_p}{p_n}$$

may be accomplished both on the basis of the calculation of the sum of the coefficient of loss in pressure according to formula (61) and according to the statistical data. Analysis of the latter shows that the quantity $\bar{p}$ is basically determined by the requirement for static stability of the ACV and, with ineffective sectioning of the lift system, may reach $1.7 \leqslant \bar{p} \leqslant 2.5$. Sectioning of the skirt makes for, as a rule, a lower coefficient of pressure up to 1/6 - 1.5 and, in a number of cases, even up to 1.2 - 1.3.
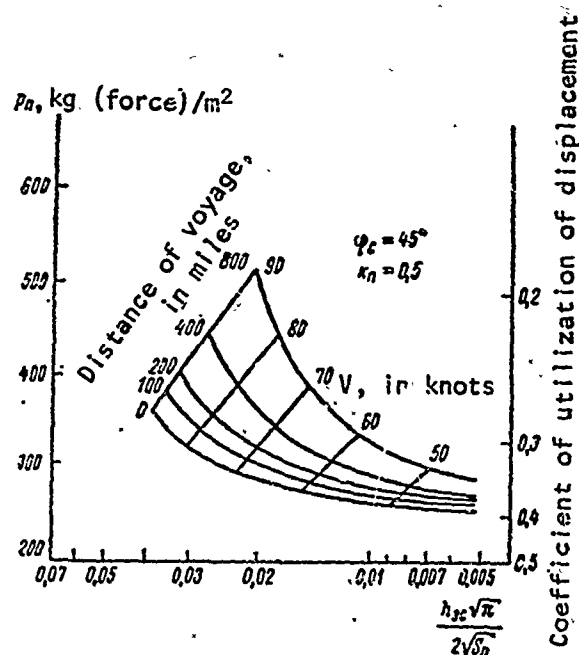
Figure 62. Regarding the Selection of Pressure in the Air Cushion

The height of the ACV's suspension above water (for a workable load of $10 \leqslant \bar{G} \leqslant 30$) is less than above a screen. It is possible to roughly determine h_B according to the formula

$$h_{\scriptscriptstyle 3} \approx h_{\scriptscriptstyle 3} - \frac{G}{\gamma S_{\scriptscriptstyle \Pi}}. \qquad (93)$$

The quantity $G/\gamma = U_{B0}$ may be computed as equal to the size of the depression formed in the water from the increased pressure, where $V = 0$. It is well-known that, as the ACV's speed is increased, the size of the depression in the water is decreased and where

$$Fr = \frac{V}{\sqrt{gL_{\scriptscriptstyle \Pi}}} > 1{,}2 \div 5$$

U_B becomes negligible. It follows from this that, with such meanings for the Froude number, the ACV's lift height (moving over water) becomes almost equal to the lift height above a screen. Calculation of the relationship of the size of the depression (following the contour of the air cushion) to the Froude number may be accomplished with the help of the formulae set forth earlier for determination of the ordinate of the water's surface where there were regions of air at increased pressure (Figure 63). Figuring, roughly, that the average change in the ACV's lift height is equal to

$$\frac{U_{\scriptscriptstyle 3}}{S_{\scriptscriptstyle \Pi}} = \frac{1}{S_{\scriptscriptstyle \Pi}} \iint\limits_{S_{\scriptscriptstyle \Pi}} y_{\scriptscriptstyle 3} \,(p_{\scriptscriptstyle \Pi},\ x,\ y,\ z,\ Fr)\,dx\,dz,$$

A diagram of this theoretical relationship is set forth in Figure 64, where experimental relationships are also shown which were published by P. duCane in his work [70]. For comparison of the curved equation, there are the final meanings ($h_\ni$ and h_B). The graph shows that in some decreases of lift height in the area of the "hump" wave resistance to the ACV, and then -- of the

-126-

increase h_v up to a meaning equal to $h_э$, which is attained when Fr = 1.2 ÷ 5. Lesser meanings of critical Froude numbers conform to lesser relative loads $\bar{G}$.

$$h_v \approx h_э - \frac{1}{S_n} \iint\limits_{S_n} y_a\,(p_n,\ x,\ y,\ z,\ \text{Fr})\,dxdz. \tag{94}$$
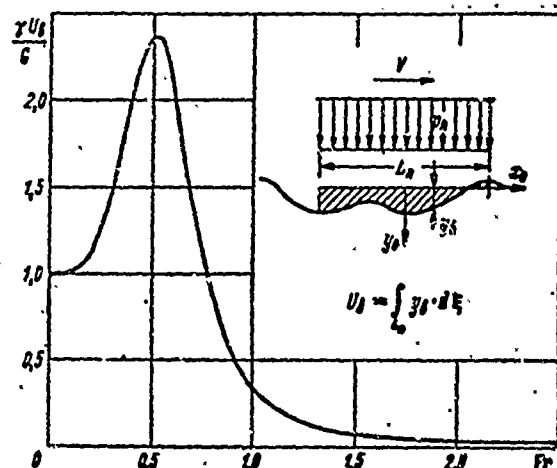
Figure 63. Dependence of the Relative Lift of the Cavities in Shallow Waters to the Speeds of the ACV
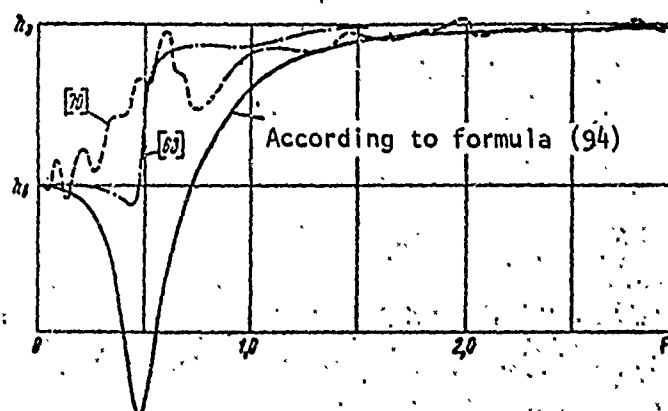
Figure 64. The Change in Lift Heights of an ACV in the Dependence on Speed of Movement Over Water.

A practical arrangement for calculating the power of the lift systems $N_{\text{п.c}}$, necessary for maintaining the ACV, is set forth in Table 3. Initial data for the calculation consists in the amounts G, $S_{\text{п}}$, n_B, D_{fan}, and the geometric dimensions of the air ducts.

TABLE 3. ARRANGEMENT FOR CALCULATING THE POWER $N_{\text{п.c}}$, NECESSARY TO MAINTAIN AN ACV ON AN AIR CUSHION.

	Formula	Numerical Amount	Comment
1)	$p_a = \dfrac{G}{S_s}$		
2)	$\Delta p_1 + \Delta p_2 + \Delta p_3 + \Delta p_4$		Calculated according to well-known hydraulic methods.
3)	$H_p = p_a + \sum\limits_{i=1}^{4} \Delta p_i$		
4)	$\bar{Q} = \dfrac{Q}{\dfrac{\pi D_{\text{fan}}^2}{4} U_{\text{fan}}}$		Non-dimensional expended-pressure characteristic is selected by calculating the requirements enumerated in Section 13.
5)	$\bar{H} = \dfrac{H_p}{\rho U_{\text{fan}}^2}$		
6)	$\eta_{cr} = f(\bar{Q}, \bar{H})$		
7)	$N_{\text{п.c}} = \dfrac{QH_p}{75\eta_{cr}}$ (in h.p.)		

Some interest has been shown in the method for quantitative estimate of power loss from the air flow which moves along the air duct of the lift system [74]. Disregarding the compressibility of air, the authors of this work sought to estimate the efficiency of each element of the lift system in the following manner.

The efficiency of the air-gate is

$$\eta_R = 1 - \frac{\zeta_R \cdot 2}{\rho V^2};\qquad\qquad (95)$$

efficiency of the fan is

$$\eta_{\text{fan}} = 1 - \frac{\zeta_{\text{fan}}}{p_p} = \frac{\left(H_p - \frac{\rho V^2}{2}\right) Q}{N_{\text{fan}}};$$

(96)

efficiency of the air duct is

$$\eta_d = 1 - \frac{\zeta_d}{H_p} = \frac{p_p}{\eta_R \frac{\rho V^2}{2}\left(H_p - \frac{\rho V^2}{2}\right)};$$

(97)

and efficiency of the stream is

$$\eta_l = 1 - \frac{\zeta_l}{p_p}.$$

(98)

The total efficiency of the lift system is

$$\eta_{\text{л.с}} = 1 - \frac{\zeta_R + \zeta_{\text{fan}} + \zeta_d + \zeta_l}{H_p^{\text{ideal}}}.$$

(99)

In these formulae:

$\zeta_R, \zeta_{\text{fan}}, \zeta_d, \zeta_l$ — equal the coefficients of loss in the air-gate, fan, air duct and during flow of air from the area of increased pressure accordingly; and

H_p^{ideal} — equals the total pressure created by the fan with no loss at the entrance and exit-way of the fan.

According to the data set forth in Thompson's article [75], the total efficiency for the SRN6 ACV was $\eta_{\text{л.с}} = 0.49$. These figures may be adopted as the standard characteristics of the effectiveness of a well-designed ACV lift system. They also establish indices of specific power for a lift system, according to the total weight of the ACV: 28 h.p. per ton for the SRN6 and 25 h.p. per ton for the SRN4.

Experimental research, carried out by the Aviation Institute in Bedford (England) [71], showed that even with a high efficiency rate for the fan ($\eta = 0.9$; $\eta_{\text{aT}} = 0.7$) and retention of a wide range for lift height ($2 < h/b < 5$), the efficiency of the lift system does not exceed 0.5 with $h/b = 1.5$, but with an increase in lift height--it decreases: $\eta_{\text{л.с}} = 0.4$ with $h/b = 3.7$ and $\eta_{\text{л.с}} = 0.28$ with $h/b = 6$.

Everything above may apply to ACV's with rigid bodies or with flexible skirts, their deformation from changes in air pressure or during slight contact with the water being negligible. In the latter case, the ACV's lift height is determined by calculation of the constant height of the flexible skirt (e.g., for Class A ACV's with flexible jets) according to the formula:

$$h_s \approx h_{r.o} + \bar{h}_{sc};$$
$$h_s \approx h_{r.o} + h_{sc} - \frac{G}{\gamma S_n};$$
$$h_v \approx h_{r.o} + h_{sc} - \frac{U_s(Fr)}{S_n}.$$

However, the basic characteristic of flexible skirts is the capacity for considerable deformation from comparatively small forces of a specific direction. The height of the skirt, therefore, depends on its structure, materials and amounts of external and internal forces.

By analyzing the dimensions of the actual skirt height (see Chapter II), it is possible to establish that there is a great influence on the rigidity of the flexible skirt's material (during suspension over a screen), characterized by the non-dimensional parameter $\Pi_{11} = \dfrac{E\delta_{r.o}^{l^2}}{\rho Q^2}$ of Kosh numbers, where $\delta_{r.0}$ equals the thickness of the material;

l equals the typical dimension; and

E equals the module of elasticity of the skirt's material.

Besides this, the parameter connected with air expenditure has a considerable influence on the ACV's lift height above a screen

$$\Pi_{12} = \frac{\rho Q^2}{G l^2}.$$

During suspension over water, the influence on the skirt's rigidity decreases, but the influence on the expenditure increases.

During the Class A ACV's movement over water, with lengthy contact between the flexible skirt and the water's surface, there is considerable deformation in the bow and side sections of the skirt, a decrease in the skirt's height and, consequently, in the ACV's lift height. The amount of deformation depends both on external conditions and characteristics of the ACV (stability and control). This phenomenon is called "dumping" and will be examined in more detail in the appropriate section.

The methods set forth for determining the ACV's lift height yield still another important characteristic--the degree of static stability for an ACV in relation to vertical shift, expressed in the form of the derivative from the relationship of lift forces to lift height. In non--dimensional form, this characteristic may be set forth as:

$$\overline{K}_y = \frac{\partial Y}{\partial h}\bigg| \cdot \frac{1}{\gamma S_n}.$$

(100)

As with the lift height, $\overline{K}_y$ basically depends both on the form of the characteristic H (Q) of the air pump and on the characteristic of the skirted air cushion. Using as the basic equation for balance of a Class A ACV

$$G = p_n S_n = Y \text{ with the calculation } p_n = p_p \sqrt{\overline{p}},$$

and for Class B

$$G = p_n S_n + \gamma U_k = Y \text{ with the calculation } \overline{p} = 1 \text{ } (U_k \text{ equals the}$$

submerged portion of the ACV's hull), we get for

for Class A
$$\overline{K}_y = \frac{\left(\frac{\partial p_p}{\partial h}\right)\overline{p} - p_p\left(\frac{\partial \overline{p}}{\partial h}\right)}{\gamma (\overline{p})^2};$$

(101)

for Class B
$$\overline{K}_y = \frac{\frac{\partial p_n}{\partial h}S_n + \gamma \frac{\partial U_\kappa}{\partial h}}{\gamma S_n} = \frac{\partial p_n}{\gamma \partial h} + \frac{\partial U_\kappa}{S_n \partial h}.$$

(102)

The derivative $\partial \overline{p}/\partial h$ is ι rmined according to the skirt characteristics set forth above.

The derivative $\partial U_k/\partial h$ is determined by methods, familiar in statics of ships, according to the ACV's cargo space.

Determination of the derivative $\partial p_n/\partial h$ for Class A ACVs and the derivative $\partial p_n/\partial h$ for Class B ACV's introduces a number of simplifications which are set forth below.

Let us consider that the operational part of the expended-pressure characteristics for the fan is approximately linear, i.e.,

$$H_{cт} = H_{cт}^{max}\big|_{Q=0} - \frac{\partial H}{\partial Q}Q.$$

(103)

131-

We note that the pressure in the receiver is composed of static pressure and parts of dynamic pressure developed by the fan, i.e.,

$$p_p = H_{cr} + x_H H_{\text{дин}};$$ (104)

where $x_H < 1$;

$$H_{\text{дин}} = \frac{\rho v_{\text{вых}}^2}{2} = \frac{\rho}{2}\left(\frac{Q}{F_\text{в}}\right)^2,$$

$F_\text{в} = \frac{\pi}{4}\left(D_{\text{вент}}^2 - d_{\text{стуn}}^2\right)$ access area of the fan.

Hence,

$$p_p = H_{cr} + x_H \frac{\rho}{2}\left(\frac{Q}{F_\text{в}}\right)^2.$$ (105)

By substituting Q here, according to formula (63), we get

$$p_p = H_{cr} + x_H (\bar{q})^2 p_p \left(\frac{f_c}{F_\text{в}}\right)^2 =$$

$$= H_{cr}^{max} - \frac{\partial H}{\partial Q} \bar{q} f_c \sqrt{\frac{2 p_p}{\rho}} + x_H (\bar{q})^2 p_p \left(\frac{f_c}{F_\text{в}}\right)^2,$$

or

$$p_p \left[x_H (\bar{q})^2 \left(\frac{f_c}{F_\text{в}}\right)^2 - 1 \right] - \frac{\partial H}{\partial Q} \bar{q} f_c \sqrt{\frac{2}{\rho}} \sqrt{p_p} + H_{cr}^{max} = 0.$$

We designate

$$x_H (\bar{q})^2 \left(\frac{f_c}{F_\text{в}}\right)^2 - 1 = L; \quad \frac{\partial H}{\partial Q} \bar{q} f_c \sqrt{\frac{2}{\rho}} = M.$$

Then

$$L p_p - M \sqrt{p_p} + H_{cr}^{max} = 0;$$

$$p_p = \frac{M^2}{2L^2} - \frac{H_{cr}^{max}}{L} \pm \frac{M}{2L^2} \sqrt{M^2 - 4LH_{cr}^{max}}.$$

By uncovering the meanings of L and M and differentiating according to h the relationship $p_p(h)$ which was received, we discover the meaning of the derivative $\partial p_p/\partial h$.

The amount for Class B ACVs $\partial p_n/\partial h$ is similarly determined.
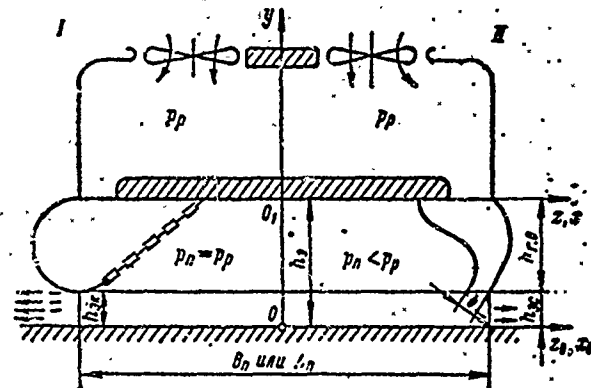
-132-

, Figure 65. Diagram of the Structure of ACV
Variants, Adopted for Calculation. I, Chamber
variant; II, Jet variant.

The practical application of the correlation received is shown in a
numerical example. We will calculate according to the following data,
given for a Class A ACV: L_n = 7.50 meters, B_n = 8.75 meters, S_n =

= 65.6 meters^2 (the form of the air cushion in the plan is right-angled),

and $h_{r.0}$ = 0.70 meters (Figure 65). For a first-rate pneumatic super-

charger, we note that there are two fans in two versions: type DV-1k and
type Ts7-29. The non-dimensional characteristics of these fans are set
forth in Figure 66. As a result of calculating the dimensional relation-
ship of H(Q), we get two groups of characteristics, corresponding to the
"incline" characteristic of the DV-1k and the "decline" characteristic of
the Ts7-29.

Calculation of lift height during suspension of the ACV above a
screen also is accomplished for the two variations of flexible skirts:
chamber and flexible jet (b = 0.100 m). For practical purposes, let's
use a range of relative weights where $15 \leqslant \overline{G} \leqslant 30$. The skirts are cal-
culated according to nondeformation, but a comparison of the results of
calculations from experimental tests made on model ACVs (chamber variant,
fan-type DV-1k) shows some kind of "extenuating" relationship $\overline{h}_{\mathfrak{a}}(\overline{G})$ in

the models due to skirt deformation, which characteristically approximates
the experimental relationship to the calculation made for chamber-type
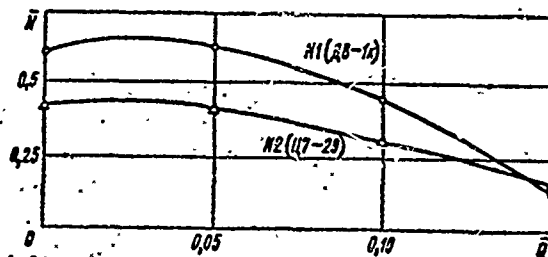ACV's with fans--the Ts7-29.

'Figure 66. Flow Rate-Pressure Characteristics
of Fans Used for Calculation.

Using the relationship h (G) (Figure 67), we discover the function
Ky(G) for all the ACV variants (Figure 68). The graphs clearly illustrate
the role of each factor in creating vertical stability for an ACV:

increased weight leads to a higher degree of vertical stability;

in conforming with formulae (101) and (102), an increase in the
"uphill" characteristic of the fan leads to a comparable increase in degree
of vertical stability;

a chamber-type barrier creates a higher degree of vertical stability
than does the jet-type.

The problems of vertical stability in the ACV were examined by N. K.
Walker [78] (U.S.A.) and P. Quine [102] (France). For the jet-type ACV,
N. K. Walker proposed the formula (in our designations):

$$
\overline{K}_y = \frac{p_p}{\gamma h_{\mathit{ac}}} \left[\frac{\frac{\partial \overline{q}}{\partial h}}{\overline{q}_\bullet} \frac{1}{\frac{p_p}{Q}\left(\frac{\partial Q}{\partial H}\right) - \frac{1}{2}} + \frac{\overline{p}}{\frac{\partial \overline{p}}{\partial h}} \right].
\tag{106}
$$

The results acquired from formula (106), and shown in Figure 68, approximate
the characteristic proposed, but quantitatively some are separate due to
the difference between the graphs of V. I. Khanzhonkov and the values of
the derivatives in formula (106) obtained according to exponential theory.
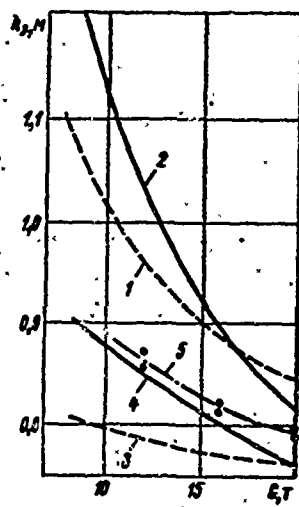
Figure 67. Relationship of an
ACV's Lift Height to Weight,
Type of Fan (Nos. 1 and 2) and
Type of Air Flow Where N_B = const.

1, No. 1, Jet-type, estimated;
2, No. 2, jet-type, estimated;
3, No. 1, chamber-type, estimated;
4, No. 2, chamber-type, estimated;
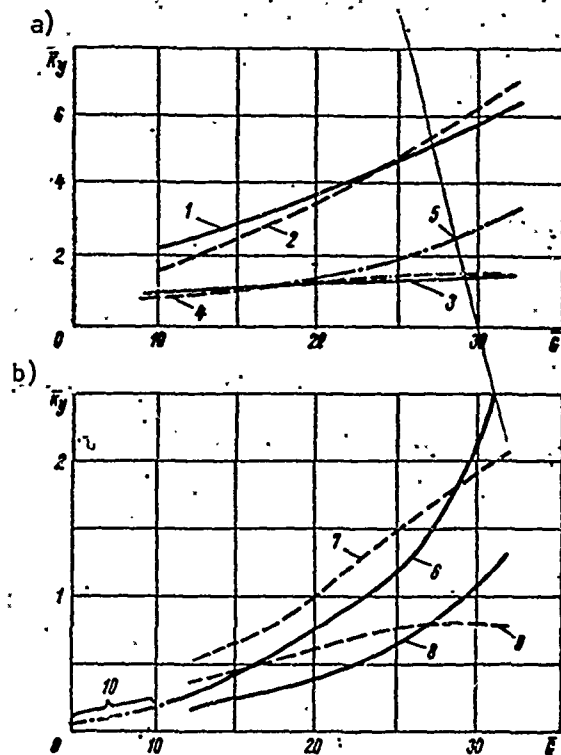5, No. 1, chamber-type, tested.

Figure 68. Dependence of Degree
of Vertical Static Stability of an
ACV in Suspension Above a Screen
From a Fan (#1 and 2), Variants of
Air Flow and Weight of the Craft:
a, Chamber version; b, Nozzle version.
1,6, #1 Calculated by the formula
(100); 4, #2 calculated by formula (107); 5, Model experiment (fan
#1); 7, #1 calculated by formula (106); 8, #2 calculated by formula
(100); 9, #2 calculated by formula (106); 10, Model experiment on
the ACV, CC-2.001.

For the chamber-type ACV, Walker and Quine proposed the same formula

$$\bar{K}_y = \frac{G\left[\frac{p_n}{Q}\left(\frac{\partial Q}{\partial H}\right) - \frac{1}{2}\right]}{S_n \gamma h_{эк}}. \qquad (107)$$

The results of formula (107) also are set forth in Figure 68, and substantiate the good qualitative and quantitative convergence of data acquired by various methods.

A calculated estimate of the degree of vertical static stability for an ACV suspended over water may be made, in principle, by methods similar to the above, however, for practical purposes, fairly reliable results may be obtained by the following simple method.

Let us suppose that, during suspension over water, the derivatives $\partial \bar{p}/\partial \bar{h}$ retain their meanings, as well as during suspension above a screen, but that the flexible skirt has not yet been deformed. Then the ACV's vertical shift ∂h_B, during changes in loads, will result in only two types of shift being formed:

a) ACV shift relative to depressions under the bottom

$$\partial h^{\flat} \approx \frac{\partial G}{\overline{K_y} \gamma S_n};$$

b) ACV shift coupled with bottom depressions due to changes of loads on the water

$$\partial h^{\flat} = \frac{\partial G}{\gamma S_n}.$$

$$\partial h_{\mathbf{a}} = \partial h^{\flat} + \partial h^{\flat}$$

Hence

$$\overline{K_{\nu^*}} \approx \frac{\partial G}{\partial h_{\mathbf{a}}} \cdot \frac{1}{\gamma S_n} = \frac{\overline{K_y}}{\overline{K_y}+1}. \tag{108}$$

Thus, to estimate the degree of vertical static stability for an ACV suspended over water, all one needs to know is this characteristic for suspension above a screen.

In spite of the roughness of the approach, experimental data coincides with the calculations (Figure 69).

The relationship of the degree of vertical static stability of an ACV to its speed in calculating the previous formula for h_v (Fr) may be estimated by the equation

$$\overline{K_{\nu V}} \approx \frac{1}{2}\left[(\overline{K_\nu} + \overline{K_{\nu a}}) - (\overline{K_\nu} - \overline{K_{\nu a}})\cos\frac{\pi \, Fr}{Fr^{\kappa p}}\right], \tag{109}$$

where $Fr^{kp} \approx 1.2\text{-}5$ in accordance with experimental data.

Figure 69. Relationship of Degree of Vertical Static
Stability for an ACV Suspended Above Water to Fan-Type
(Nos. 1 and 2), Type of Air Flow and Weight of the Craft.
1, No. 1, chamber-type, estimated; 2, No. 2, chamber-
-type, estimated; '3, No. 1, chamber-type, model experi-
ment; 4, No. 1, jet-type, estimated; 5, No. 2, jet-type,
estimated.

§15. Static Stability of an ACV

Stability for an air cushion vehicle, as understood in ship theory,
is a feature of the craft resulting from external forces for balance
returning again after having stopped [44].

Stability is provided by forces and moments arising when the craft
deviates from a position of balance, in relation to the amount of
deviation, it is possible to observe stability in non-linear form in the
final deviation to balance and stability in linear approximation, or
initial stability when there is little deviation in balance.

As to the amount of deviation from balance (shift), usually list
and trim difference are observed (transverse and longitudinal stability).
These shifts may be static, produced for example by changes in the center
of gravity for the ship, or dynamic, appearing during the ship's rolling
on the waves, maneuvering, etc.

At first glance the physical phenomena characterizing the stability
of the ACVs are similar to the analogous phenomena examined in the
theory of stability of high speed cutters (floating and on hydrofoils).
In either case a lateral force develops during roll, and the quantitative
characteristics of stability depend largely on the speed of the vessel.
At the same time the theory of ACV stability is more complex, since it
examines the various conditions of operation--hovering and motion above
the water and above a rigid screen, the more complex mechanism of formation

-137-

of recovery forces and moments which include, in addition to hydrodynamic components, forces and moments produced by the list system of the ACV through interaction of air currents and air cushion enclosures with the deformed bearing surface (water).

Since the ACV is a high speed vessel, straight-line uniform travel at high speed over the surface of calm, deep water should be considered as characteristic mode of operation for analysis of its stability. The external load that acts on the ACV under these conditions may be static when the time of change of load from zero to the design magnitude is several times greater than the period of listing of the ship, and dynamic when the time of change of the load is commensurate with the period of listings, or when the action of this load is of a pulsed character. In accordance with the character of action of external forces and the behavior of the ACV stability can be classified as static and dynamic.

In this chapter we will examine only static stability. The basic problems of the theory of ACV stability are the following:

development of methods of calculation of the quantitative characteristics of the static stability of the ACV under normal operating conditions (travel over water, hovering above water and above a screen);

development of a system of design and operational measures related to insuring optimal stability characteristics of the ACV;

development of stability standards, compliance with which should insure safe ACV operation without capsizing.

Methods of Insuring ACV Stability

As was shown in Chapter I, the evolution of the design types of ACVs led to the appearance of a great diversity of designs and constructions of these vehicles. Examination of ACV stability, however, shows that nearly all of them can be placed in two basic classes, depending on the method used for producing the recovery moment when the vehicle is listing:

Class A--the hull of the ACV separates completely from the bearing surface. The vessel, as a rule, is equipped with a flexible air cushion inclosure and receiver, which distributes the air flow among the sections of the cushion.

The recovery moment is created by redistribution of pressure over the area of the sectioned air cushion when the ACV is in a listing position (Figure 9).

-138-

Class B--the protruding parts of the ACV, attached to the rigid hull and designed to insure stability (side bodies, hydrofoils, etc.) come into partial contact with the water. The recovery moment is created through the action of hydrostatic or hydrodynamic forces on these parts. As a rule there is no receiver, air is delivered to a common sub-cupola chamber and there is practically no pressure redistribution when the ship is listing (Figure 9).

In individual cases it is possible to have combinations of these two methods of producing the recovery moment.

We will examine in greater detail the physical phenomena that occur during sloping of Classes A and B ACV and the mechanism of influence of the parameters of the ACV lift system on the magnitude of the recovery moment.

Class A ACV

The initial stability of the ACV in the over-water travel mode depends substantially on the velocity of the vehicle, but after some velocity has been reached the stability ceases to change with further increase in velocity. It is natural to assume $V = 0$ as the lower bounds of velocity, i.e., the case when the vehicle is hovering over the water. The upper bounds of the examined velocity range can be determined on the basis of a combination of two conditions. The first condition is the practically total disappearance of deformations of the water surface, caused by high-pressure air passing over it (see Chapter II). This condition is satisfied when $Fr > Fr^{kp}$ and corresponds to the mode of ACV travel over a solid screen.

The second condition is that the velocity should not exceed the value at which the air flow begins to have a notable effect on the distribution of pressures in the air cushion, i.e.,

$$V \leqslant k_j V_j = k_j \sqrt{\frac{2p_p}{\rho}},$$

where V_j is the velocity at which the air flows from the receiver into the atmosphere.

It has been established theoretically and experimentally that $Fr^{kp} \approx 1.2\text{-}5$, $k_j \approx 1/2$, and consequently the upper bounds of the examined velocity range of ACV can be assumed approximately

-139-

$$(1,2 \div 5)\sqrt{gL_n} \leqslant V_m \leqslant \frac{1}{2}\sqrt{\frac{2p_p}{\rho}}. \qquad (110)$$

Tests have established that when an ACV travels above a screen its static stability remains practically constant in a broad range of velocities [5], therefore the travel of an ACV over a screen can be equated to hovering over the screen, i.e., the conditions during travel of an ACV over water at a velocity close to V_m can be assumed to correspond approximately to the conditions of hovering over a screen.

Thus, during examination of the interaction of the high pressure region with the water surface, the general case of ACV travel over water can be considered intermediate between the cases of hovering over water and hovering over a screen. This notion considerably simplifies the methods of determining ACV stability characteristics, since it is essential to determine these characteristics only in two cases of hovering, (over water and over a screen) and also to establish between these characteristics the relationship that depends on the velocity of the ACV.

During ACV hovering over a screen, regardless of the type of air cushion enclosure, the pressure within it changes as a function of the elevation of the ACV, specifically: pressure increases as the hull of the ACV approaches the screen and conversely. This phenomenon is the basis of the principle of sectioning of the air cushion to create the recovery moment when the ACV is in a listing position. In this case the pressure in each section changes as a function of the distance between the sections and the screen. Moreover, the air flow rate through the various portions of the air cushion enclosure also changes as a function of the distance between the lower edge of the enclosure and the screen. The quantitative characteristics of change in pressure and flow rate as functions of elevation depend on the type of air cushion enclosure, operating parameters of the lift system and hydraulic interaction among the air cushion sections.

There are many variations of air cushion sectioning, but all of them can be placed in three substantially different groups (Figure 70):

Experience shows that the second group, which produces the greatest recovery moments, other conditions being equal, is the most effective.

Sectioning of the air cushion is accomplished by means of jets (a nozzle system) or mechanical (rigid and flexible) enclosures analogous to the peripheral enclosures.
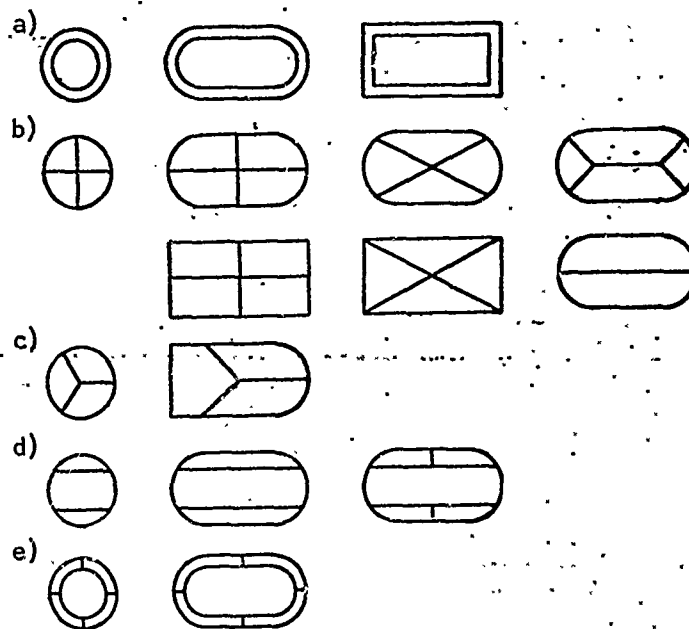
Figure 70. Diagrams of Sectioning of Air Cushions of Class A ACVs: a, Concentric sectioning; b, c, d, Radial sectioning; 3, Combined sectioning.
1, Concentric sectioning (type a in Figure 70);
2, Radial sectioning (type b, c, d); 3, Combined sectioning (type e).

We will list the basic requirements on sectional skirts:

the skirts of maximum pressure.drops among the sections during listing of the ACV;

required stability of the form of sectional skirts during action upon them of possible pressure drops;

minimal use of power by the lift system for the creation of boundaries of the sections;

minimal additional drag.

-141-

Other parameters of the lift system (design of lift system, form of characteristic H(Q), etc.) also influence pressure change in the sections when the ACV is tilted in addition to the characteristics of the air cushion enclosures. By way of example we will examine the pressure change in some section of the air cushion, attributed to displacement of the nozzle exit by the magnitude δh in two different cases:

a) for constant receiver pressure p_p = const, which corresponds to a common receiver, which distributes the air flow among all sections of the air cushion;

b) for fan operation separately in that section of the receiver connected exclusively to the examined air cushion section.

In case a) the pressure in the air cushion section approaches a constant pressure p_p and its maximum h is increased. Here, the reduction of the air flow rate through the section of the lower side is compensated by an increase in the flow rate through the opposite section, with the result that p_p and Q remain constant.

In case b) the reduction of flow rate as the nozzle approaches the screen causes p_p to increase in accordance with fan characteristic H(Q) $\approx$ $\approx p_p(Q)$. Consequently, as in case a) the reduction of pressure coefficient p as h increases, i.e., as x is increased (see equation (69)), leads to a sharper increase in pressure in the air cushion section.

Consequently, the partitioning of only the air cushion into sections can insure initial stability of the ACV if the pressure coefficient $\overline{p}$ is sufficiently large. In this case, when the ACV is in a listing position the fan operates practically in a constant mode and the pressure in the section of the air cushion located beneath the lower side can reach the magnitude of the pressure in the receiver. This substantially limits the recovery moment.

In the case, however, of partitioning of the receiver of the ACV into parts in such a way that each section of the receiver is connected only to its air cushion section, as the pressure in the air cushion section increases and as the air flow rate decreases correspondingly, the pressure in the receiver also rises, i.e., in this case the fan operates according to this characteristic and the recovery moment at this angle of list is much larger. Calculations carried out on the basis of data on several ACVs show that partitioning of the receiver and some alteration of internal flexible enclosures may yield a 2-2.5 fold increase in initial stability.

In this case, maximum stability is achieved when fan characteristic $H(Q)$ has the maximum possible "curvature" of $\partial H/\partial Q$, and the location of the working point on it ensures sufficient pressure reserve $H(Q = 0)/ H_{calc} > 1.15$. In addition, a lift system of this design affords the possibility of controlling the position of the ACV through actions on the air flow parameters in the sections. The control devices are usually various types of rotating flaps located in the air intakes, receiver and rigid nozzles. Certain ACVs, among them SRN5, SRN6 and SRN3, are equipped with methods of control by flexible enclosures. The means of control of the operation of components of the lift system include remote control of the position of the vanes of the fan and dried vanes at the fan intake, and also control of fan rpm.

Experimental studies of the dependence of the degree of ACV stability--

--dimensionless initial metacentric height $\overline{m}_x$ (see equation (117))--on the

pressure coefficient revealed that this dependence is, in most cases,

linear and can be characterized quantitatively by the product $\partial \overline{m}_x^\theta / \partial \overline{p}$,

which determines the increment of metacentric altitude as the pressure coefficient increases, i.e., the capacity of a specific lift system to create initial ACV stability. Comparison of various ACVs in terms of

$\partial \overline{m}_x^\theta / \partial \overline{p}$ gives a more complete idea of their stability under identical con-

ditions, but experimental data are often insufficient for evaluation of

$\partial \overline{m}_x^\theta / \partial \overline{p}$. Therefore comparison of ACV stability is usually limited to the

value $\overline{m}_x^\theta$.

In the hovering mode of Class A ACV over water, the recovery moment is created in the same way as in the mode of hovering over a screen, but the quantitative characteristics differ considerably from those of the mode of hovering over a screen. This is caused primarily by the capacity of the bearing surface (water) for deformation under the influence of surface pressure. It has been established theoretically and experimentally that at the relatively low air flow rate characteristic of contemporary ACVs the elevation of the vehicle above the water, assuming other conditions to be equal, exceeds the elevation above the screen. At the same time the character of change of pressure and air flow rate as a function of elevation remains practically the same as above the screen.

Consequently, the functions obtained for the mode of hovering above the screen, with corrections that allow for deformation of the water surface, and also experimental data can be used for approximate determination of ACV stability characteristics in the mode of hovering over water.

The pliability of the bearing surface is easily considered by introducing the corresponding coefficients obtained either through calculations or experimentally. Calculations and tests of ACVs and models indicate that ACV stability in the water-hovering mode is always less than in the screen-hovering mode. The converse may be true only in the case of exceedingly high relative air flow rates and relatively low altitudes, when large spray streams packed on the ACV's hull, causing additional forces and moments [32].

The mode of travel of Class A ACVs over water is characterized by the gradual change in stability parameters as a function of the travel velocity and change of deformations of the bearing surface [63, 72], (see Chapter II). The elastic properties of the air cushion are considered here to be constant. Tests of ACVs and models indicate that the initial stability during travel changes from the value corresponding to the water-hovering mode (for $V = 0$) to the value corresponding to the mode of hovering over a screen (for $V_i < V_m$).

Class B ACV

The nature of forces that ensures a stability of Class B ACVs and the physical phenomena related to them differ substantially from those examined above. For example, the stability of a catamaran type ACV is insured in the water-hovering mode basically by hydrostatic forces, and in the high speed travel mode by hydrodynamic forces on the side bodies in contact with the water. Consequently, the system of forces that ensure stability of Class B ACVs is more complex and can be calculated comparatively simply only for the hovering mode.

Hovering over water. During heeling of catamaran type ACVs, in contrast to Class A ACV, the hull, as it enters the water, discharges some of the air cushion, and therefore pressure in the sub-cupola part decreases as list increases. In accordance with fan characteristics, as the roll angle increases air flow rate Q increases. The distribution of pressures over the air cushion area during the process of listing of the ACV remains practically uniform, and therefore the moment from the air cushion comprises a small fraction of the total recovery moment. Most of the recovery moment is created by a moment of hydrostatic nature, generated by the hull as it enters the water.

In the mode of travel of Class B ACVs over water the hull interacts with the wavy surface, which at low speed (Fr ≤ 1.0) generally leads to a 15 to 25% decrease in the initial stability of the vessel from the value corresponding to hovering over water.

When Fr ≈ 1.0-1.1, the initial stability returns to the original value, and when Fr = 1.5-1.7, it becomes maximum. In this case, obviously, a combination of the magnitude of hydrodynamic pressures acting on the hull of the ACV and of the submerged surfaces of the hull is optimal.

With a further increase in velocity of the ACV the stability decreases due to a reduction of the submerged area of the hull and reduction of the trim of the ACV. This phenomenon is similar to the loss of longitudinal stability of a cutter traveling at high speed and may occur in those ACVs whose hulls have hydroplaning surfaces. If the hulls are built in the form of side walls with a large keel, changes in stability as a function of velocity should be less sudden, since the vertical component of the hydrodynamic forces is much smaller in this case than in the preceding case.

Approximation of Static Stability of ACV

Class. A. Hovering Over Screen

The equations of equilibrium of ACV are

$$\sum Y = \sum p_{ni} S_i - G = 0; \tag{111}$$

$$\sum Z = P_6 - Z_w = 0; \tag{112}$$

$$\sum M_x = M_{xn} + M_6 + M_{x0} - M_{kp} = M_\theta - M_{kp} = 0. \tag{113}$$

In these equations:

p_{ni} -- the average excess pressure in the i section of the air cushion;

S_i, z_i -- the area and ordinate center of gravity in the area of the i section of the cushion;

Z_w, Y_w -- the force of resistance of the ACV's side drift or reaction to contact, keeping the ACV from horizontal shift during list, and the coordinate point applicable to the craft;

P_6, y_6 -- the side force or reaction to the air stream, flowing from the area of increased pressure during incline of the ACV, and its coordinate in connection with the craft's coordinate system;

G, y_G -- the weight and coordinate of the ACV's center of gravity;

θ -- the ACV's list angle;

M_{kp} -- the external list moment, applicable to the ACV;

-145-

M_θ -- the restored moment, with $M_0 = M_{x\pi} + M_6 + M_{xG}$;

M_{xG} -- the moment of weight, with $M_{xG} = Gy_G \sin\theta$;

$M_{x\pi}$ -- the moment specified by the redistribution of pressure along the air cushion

$$M_{x\pi} = \sum p_{\pi i} S_i z_i$$

M_6 -- the moment specified by the action of horizontal reaction

$$M_6 = P_6 (y_m + y_6) \cos\theta.$$

The equations may be solved relative to $M_0 = M_{kp}$, if the relationships are determined beforehand.

To determine $p_{\pi i}(\theta)$, the following are used: equation (111), the equation for continuous flow in the lift system, the characteristics of peripheral and sectioned skirts and the characteristic H(Q) of the fan, as well as the equation for kinematic contact with shift for various points of the hull and skirt of the ACV affecting the list angle and lift height of the ACV. The non-linearity characteristic of the skirt (see formulae (67) and (68) for example) and the characteristics of the fan force the ACV to seek some kind of balance with vertical shift by means of the calculation $p_{\pi i}(h)$ with θ fixed. To attain this, a number of meanings for $p_{\pi i}$ are calculated, with several meanings for lift heights of $h\big|_{\theta=0}$ and less, solved each time according to the equation for continuous flow in the lift system. Thus, we get for the lift height h_θ, which satisfies the equation for vertical forces (111). Results of calculations and experimental data provides evidence that the average lift height for an ACV, as a rule, has a maximum meaning when $\theta = 0$ and is decreased with the increase of list angle. Deviation from this ratio will occur only when there is a small relative load with $\overline{G} \lessgtr 15$ and a meaning of θ in the surrounding area. Because of the materials for the test model's lift system (shown in Figure 71), Figure 72 was constructed to illustrate this relationship. The quantity of air expenditure obtained is used throughout various parts of the skirted air cushion for determination of reactive horizontal force P_6 according to formula (114), as a projection of the vector quantity of the movement of the stream, flowing from the area of increased pressure at axis Oz

-146-

$$P_6 = n p_{02} \rho \oint_{\Pi} \int_{h_j} V_j^2 \, dy \, d\Omega_\kappa,$$

(114)

where h_j equals the clearance between the screen and the skirted air cushion. Thus are the components of the restored moment found which, according to equation (113), equal

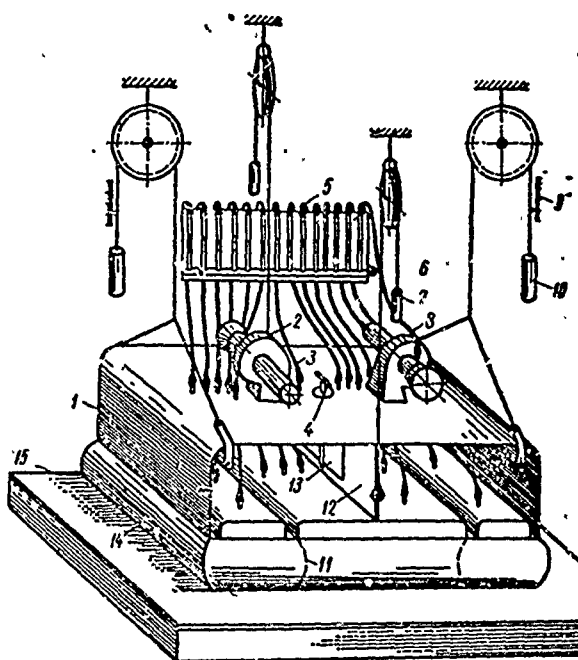$$M_\theta = \sum p_{ni} S_i z_i + P_6 (y_m + y_6) \cos \theta - G y_0 \sin \theta.$$

(115)

Figure 71. Sketch of a Model Lift System for a Class A ACV.
1, Hull of model; 2, Fan; 3, Gauge for pressure in receiver;
4, Steering lever; 5, Pressure gauge; 6, Gauge for pressure in
in air cushion sections; 7, Discharge; 8, Gauge for air expenditure; 9, Lift and list scale; 10, List-ballast; 11,
Sectioned flexible skirt; 12, Partition in receiver; 13, Flap;
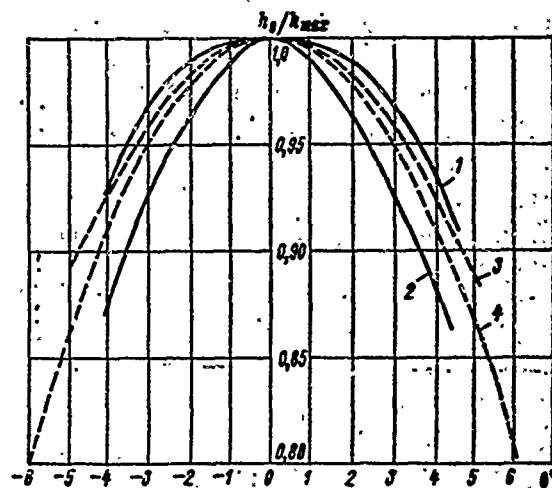14, Flexible skirt; 15, Screen-tank.

Figure 72. The Relationship of a Class A ACV's Lift Height to Its List Angle. 1, Divided receiver, above a screen; 2, Non-divided receiver, above a screen; 3, Divided receiver, above water; 4, Non-divided receiver, above water.

The calculation is complete with the determination of the transverse initial metacentric height according to the formula

$$m_x^\theta = \frac{\partial M_\theta}{\partial \theta}\bigg|_{\theta=0} \cdot \frac{1}{\alpha} \cdot \tag{116}$$

For comparing the primary stability of various ACVs, it is convenient to express the amount m_x^θ in non-dimensional form

$$\overline{m}_x^\theta = \frac{m_x^\theta}{B_\Pi} \cdot \tag{117}$$

where B_Π equals the width of the air cushion.

A similar calculation may be performed by determining the relationship of the longitudinal restored moment to the angle of trim difference ψ and the longitudinal primary metacentric height m_z^ψ. In such a case, the following designations are used:

-148-

$$M_\phi = \sum p_{ni} S_i x_i + \dot{P}_{np}(y_m + y_{np}) \cos\psi - G y_G \sin\psi; \qquad (118)$$

$$P_{np} = n p_{ax} \rho \oint_{\Pi} \int_{h_i} V_j^2 dy d\lambda_x; \qquad (119)$$

$$m_z^\psi = \frac{\partial M_\phi}{\partial \psi}\bigg|_{\psi=\psi_0} \cdot \frac{1}{G L_n}, \qquad (120)$$

where x_i = absciss center of gravity of the area i in the air cushion;

L_n = length of the air cushion; and

P_{np}, y_{np} = longitudinal reactive force and its coordinates.

Let us observe in somewhat more detail the relationship $P_{np}(\psi)$. Since reactive forces are functions of the amount of movement of air streams, i.e., the flow created in the ACV's lift system, their amount may exceed some meanings set by expenditure Q and pressure in the receiver p_p. The upper limits of P_6 and P_{np} may be determined by the following expression (in conditions where the total air flow is directed to one side):

$$\bar{P}_6 = \frac{P_6}{G} = \frac{\rho Q V_l}{G} \leqslant \frac{\rho}{G} \bar{Q} \sqrt{\frac{4 S_n G}{\pi \rho}} \sqrt{\frac{2G}{\rho S_n}} = $$
$$= \bar{Q} \sqrt{\frac{8}{\pi}} = 1.60 \bar{Q}. \qquad (121)$$

Using the value $\bar{Q}$, set forth earlier, we get the value for $\bar{P}_6$:

$$\bar{P}_6 \leqslant 0.05. \qquad (122)$$

Calculations and experiments show that $\bar{P}_6$ attains its maximum significance with a list angle of $2° \leqslant \theta \leqslant 8°$, and then is reduced according to the ease in list angle.

Because of the smallness of $\bar{P}_6$, its effect on the recovery moment can only be roughly approximated. During tests of ACVs or models, they are usually secured with flexible couplings located at the level of the center of gravity of the vessel. Therefore, we may assume that $y_{ш} = y_G$.

-149-

The magnitude of y_6 is approximated as follows:

$$y_6 \approx \frac{h_\bullet - 0.5B_n \sin\theta - h_{r.0}\cos\theta}{2}.$$

(123)

In such an approach, obviously, deformations of the flexible skirts, caused by pressure changes in the air cushion sections, are not taken into account.

The results of calculations carried out by the above-examined method agree satisfactorily with the experimental data in the case when the skirts are not deformed during listing of the vessel. If the skirts have a high capacity for deformations, a special method should be used, whereby the values can be refined and the calculations simplified.

The part of the flexible enclosure that comes into contact with the bearing surface is assumed to have infinite flexibility, and the part that does not come into contact is assumed to be rigid. We will consider the position of an ACV in which these features are most completely realized, i.e., we will determine the maximum low angle at which the rigid hull of the ACV does not come into contact with the screen:

$$\theta_{p\bullet c\imath} \approx \arctan\frac{h_\bullet}{B_n}.$$

(124)

Here the flow of air through one section of the air cushion is terminated and the pressure within it becomes p_p. Proceeding from the flow design in the lift system, we can determine the pressures in the other air cushion sections that satisfy equation (111). Otherwise the calculation is carried out by the above-described procedure.

Calculations done by equations (111)-(115), (117) with consideration of estimate (122), expression (123) and condition (124) for the ACV models whose diagram is illustrated in Figure 71, for $\bar{G} = 24.6$ and $\bar{y}_G = y_G/$

$/\sqrt{S_n} = 0.272$ yielded the value $\bar{m}_x^\theta = 2.57$. The experimental value was

$\bar{m}_x^\theta = 2.48$ (see Figure 75).

Calculations for other ACVs and models with asymmetric shape with respect to the midframe, "to oval", revealed a certain discrepancy between the results and experimental data. The calculated values of m_x^θ are 10-15% higher than the experimental, and therefore it is advisable to introduce the correction factor $k_\theta = 0.90-0.85$ into equation (117). The final expression for calculation of $\bar{m}_x^\theta$ is

-150-

$$\overline{m}^{\bullet}_x \approx k_{\bullet} \frac{\sum p_{ni} S_i z_i + 0{,}05 G\,(y_O + y_6) - G y_O \sin\theta}{G B_n \theta} \qquad (125)$$

For the purpose of clarifying the problem we will assume that the lift system of some hypothetical ACV consists of an even number of partitioned sections, located on the side (Figure 73). The hull of the ACV is assumed to be connected to these sections by ball joints located on the same vertical as the CG of each section, which as the hull of the ACV,lists causes vertical displacement of the separate sections of the lift system. Examination of such a conditional model (nearly corresponding to one of the ACVs built by the French firm Berten) yields the following advantages for theoretical analysis of the static stability of an ACV:

a) There is no lateral reaction due to the asymmetric air flow during listing of this model;

b) The expressions derived in the preceding section can be used for analyzing ACV stability;

c) The type of air cushion skirt and the characteristics of the fan may be arbitrary.

The model has one disadvantage: the numerical results obtained during its analysis pertain only to a completely sectional lifting system. This disadvantage can, in principle, be eliminated by introducing some coefficient or function that takes into account the actual means of sectioning of the lift system.

If we disregard the aerodynamic coupling between the sections of the conditional model, caused by the interaction of colliding jets from the adjacent sections, we can write the equations of equilibrium of the system

for list θ

$$\sum Y = p_1 S_1 + p_2 S_2 - G = 0; \qquad (126)$$

$$\sum M_x = p_1 S_1 z_1 + p_2 S_2 z_2 - G y_O \sin\theta - M_{\kappa p} = 0. \qquad (127)$$

The list angle of the system is determined according to the vertical displacements of the section

$$\tan\theta \approx \theta = \frac{y_2 - y_1}{2 z_{1,2}} = \frac{\partial y}{z_{1,2}}. \qquad (128)$$

-151-

The recovery moment of the system is

$$M_\theta = \partial p S_{1,2} z_{1,2} - G y_G \sin\theta,$$ (129)
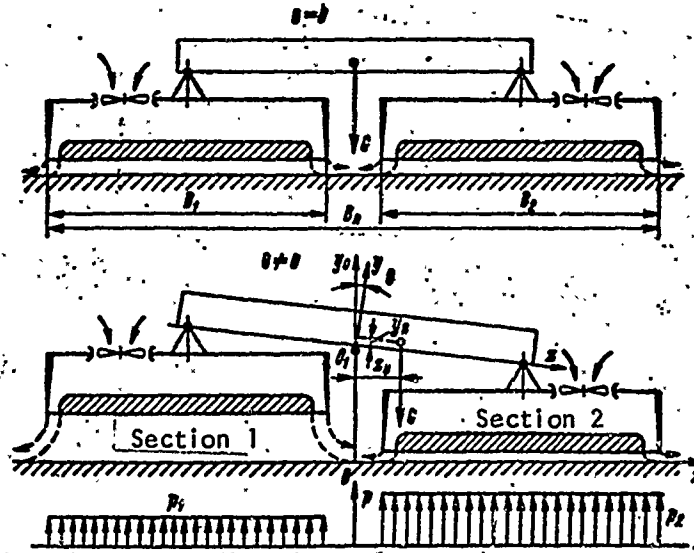
where $\partial p = p_1 = p_2$.

Figure 73. Conventionally Designed Model ACV
With an Entirely Separate Lift System.

The initial metacentric height is

$$\overline{m}_x^\theta = \frac{M_\theta}{GB_n\theta} = \frac{2\partial p S_{1,2} z_{1,2}^2}{\partial y GB_n} - \frac{y_G \sin\theta z_{1,2}}{\partial y B_n}$$

or considering that $\partial p/\partial y = \gamma \overline{K}_y$ and $2S_{1,2} = S_n$, we obtain

$$\overline{m}_x^\theta = \overline{K}_y \frac{\gamma S_n z_{1,2}^2}{GB_n} - \frac{y_G z_{1,2} \sin\theta}{\partial y B_n}.$$ (130)

for small list angles $z_{1,2} \sin\theta/\partial y \approx 1$.

Denoting $\bar{y}_G' = \bar{y}_G/B_\Pi$, we obtain, finally

$$\overline{m}_x^\theta = \overline{K}_y \frac{\gamma S_\Pi}{G} \cdot \frac{z_{1,2}^2}{B_\Pi} - \bar{y}_{G'} \qquad (131)$$

The first term in equation (131), corresponds to "stability of form" and the second to "stability of mass," which are known in the statics of the vessel. The expression obtained,

$$\overline{m}_x^\theta + \bar{y}_G' = \overline{K}_y \frac{\gamma S_\Pi}{G} \cdot \frac{z_{1,2}^2}{B_\Pi} \qquad (132)$$

makes it possible to analyze the influence of both structural and operational factors on initial ACV stability.

The dependences of $\overline{m}_x^\theta + \bar{y}_G'$ on $\overline{G}$, computed for those versions of the fans and flexible skirts examined in the preceding section, are depicted in Figure 74. It is obvious from the graph that maximum stability is achieved, other conditions remaining equal, with the chamber version of air flow from the high pressure region and with a "steep" fan characteristic. Other combinations give smaller values of $\overline{m}_x^\theta + \bar{y}_G'$, and as $\overline{G}$ increases the stability of the chamber version drops somewhat and that of the nozzle version increases.
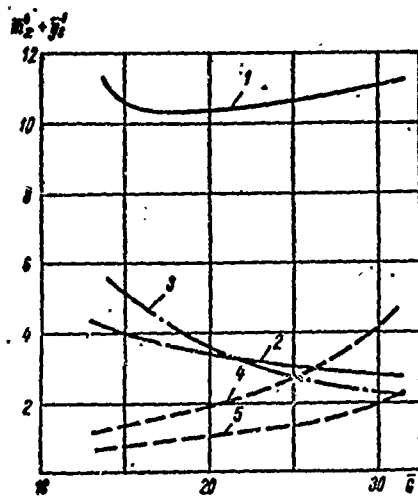

Figure 74. Initial Stability of Conditional Model as Function of Type of Fan (Nos. 1 and 2), Version of Air Flow and Relative Weight of the Vehicle While Hovering Over Screen. 1, No. 1, chamber version (theoretical); 2, No. 2, chamber version (theoretical); 3, No. 1, chamber version (experimental); 4, No. 1, nozzle version (theoretical); 5, No. 2, nozzle version (theoretical).

-153-

The appropriate corrections, which to some degree lower the values obtained, should obviously be introduced to these results, depending on the "rigidity" of the flexible skirts.

Furthermore, in converting to real lift systems, a number of corrections must be introduced, depending on the actual form of fan characteristics, design and degree of partitioning of the receiver, interaction of the air cushion sections, etc., which means that experiments must be undertaken in order to obtain design data. The first laboratory experiments were conducted on circular and rectangular models with non-partitioned receivers and different air cushion skirts. After discovering the instability of ACV models freely hovering on an air cushion with respect to list, the researchers began to use various methods of sectioning the air cushion.

In. the early stages of ACV development high air flow rates were used, which led to a relatively high elevation without the use of flexible air cushion skirts and also to considerable lateral forces during ACV listing. Some lack of of definition in the localization of these lateral forces forced the researchers to assume that the problems of ACV stability do not yield to simulated physical testing.

Further ACV development led to design improvements and to improvements in their economic characteristics. The relative flow rate was decreased to $\bar{Q} \leqslant 0.03$, and therefore the importance of the moment contributed by the lateral force in the formation of the recovery moment was sharply reduced, and even the approximation of this value yielded good results during analysis of experimental data. Moreover, during the first tests a system of characteristic paces of ACV operation, i.e., those modes for which it is essential to determine the stability characteristics, was developed.

Tests of the systematized model described below (Figures 71 and 96) in the mode of hovering over a screen verified the qualitative dependences obtained above. Graphs of $\bar{m}_x^\theta$ as a function of model way $\bar{G}$ are illustrated in Figure 75. Although comparison of these results in terms of fan characteristics should be made between the experimental curve and the top theoretical graph, the effect of final "rigidity" of the flexible skirts and of interaction of the air cushion sections led to a substantial reduction of the initial stability of the model and made the results of the experiment and calculation carried out for the conditional model with a comparable "hollow" fan characteristic.
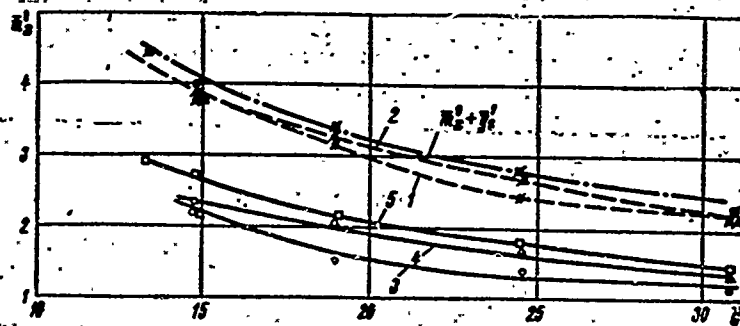
Figure 75. Transverse Metacentric Height $\bar{m}_x^{\theta}$ as a Function of Relative Mass of Model of Lift System for ACV. 1. Sectional receiver; throat area of rigid nozzles $\bar{f}_c = \bar{f}_c/S_\Pi = 0.069$; 2, Sectional receiver, $\bar{f}_c = 0.051$ and 0.038; 3, Non-sectional receiver, $\bar{f}_c = 0.069$; 4, Non-sectional receiver, $\bar{f}_c = 0.051$; 5, Non-sectional receiver, $\bar{f}_c = 0.038$.

Class A. Hovering Over Water

Deformations of the water surface have a double-edged effect on ACV stability characteristics:

The pliability of the bearing surface decreases stability, other conditions being equal;

The interaction of the water surface with the air jets and mechanical enclosures of the air cushion and its sections causes redistribution of pressures among the sections compared to pressures in the mode of hovering over a screen.

The equations of equilibrium in the given case are formally simplified somewhat because the effect of horizontal reactive forces P_6 and $P_{\text{пр}}$ practically vanishes. In fact, full scale ACVs are tested for stability in the mode of hovering over water in the free state, and therefore the resistance to lateral drift, which during slow movement of the ACV along axis OZ_0 is of a hydrodynamic character, can be assumed to be applied practically on the same level as the lateral force. Consequently, $M_6 \approx$ ≈ 0 and the equations of equilibrium acquire the form

-155-

$$\sum Y = \sum p_{ni} S_i - G = 0; \tag{133}$$

$$\sum M_x = M_{xn} + M_{xG} - M_{xp} = 0, \tag{134}$$

where M_{xn} and M_{xG} are calculated with the same expressions as for the solution of the system (111)-(113).

Determination of $p_{ni}(\theta)$ in the examined case involves great difficulties, since pressure p_{ni} is affected by deformations of the water surface, which are themselves functions of pressures p_{ni}. As an example of a calculation model we will examine an approximate method of determining the initial stability of a Class A ACV, equipped with flexible nozzles, (Figure 76). We will make the following assumptions:

The flexible skirt in tilted positions retains the shape it acquired during hovering without list;

Change in air pressure in the side section of the air cushion is basically the result of change in hydrostatic pressure on the jet skirt of the outboard nozzle;

An increase in hydrostatic pressure on the jet skirt of the descending side is equivalent to a reduction of the height of this jet skirt by the magnitude of the column of water corresponding to the increment of the depth of submersion of the skirt during list, i.e., by the magnitude $0.5\,B_n\theta$. For simplicity we will assume that the pressure prior to the flow of air into all the flexible nozzles is p_p = const.

Denoting the pressure coefficient in the outboard section of the descending side $\bar{p}_{1\theta}$, and in the section of the rising side $\bar{p}_{3\theta}$, we obtain

$$\bar{p}_{1\theta} = \frac{e^{cx_1^*}}{e^{cx_1^*} - 1}; \tag{135}$$

$$\bar{p}_{3\theta} = \frac{e^{cx_3^*}}{e^{cx_3^*} - 1}, \tag{136}$$
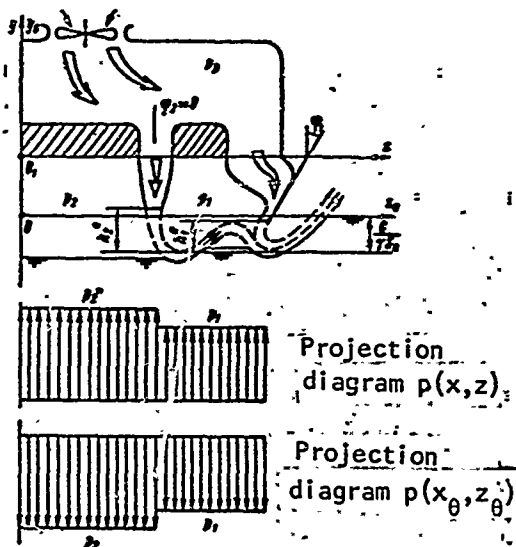
where x_1^* and x_3^* are computed by equation (82).

Figure 76. Calculation Model of Air Jet During
Hovering of ACV With Flexible Nozzles Over Water.

Tests of ACV models indicate that elevation h_θ^* is less than elevation h^* in the mode of hovering without list, and that it is a function of weight G, flow rage Q and method of sectioning of the lift system. Change of this value as a function of the list angle θ is illustrated in Figure 72. Considering the above-expressions for determining the lift created by the outboard sections of the air cushion, we can use the equations

$$Y_1 = p_p S_n \frac{\overline{S_1}}{\overline{p_{10}}};$$

(137)

$$Y_3 = p_p S_n \frac{\overline{S_3}}{\overline{p_{30}}}.$$

(138)

The recovery moment created by the air cushion can be represented as follows:

$$M_{xn} = Y_1 z_1 - Y_3 z_3 = z_{1,3} p_p S_n \frac{\overline{S_{1,3}}(\overline{p_{10}} - \overline{p_{30}})}{\overline{p_{10}}\overline{p}} k_p,$$

(139)

where $k_n = \dfrac{\displaystyle\int_{-0,5L_n}^{0,5L_n}(p_1 - p_j)\,dl}{(p_1 - p_3)\,l_n}$ is the completeness factor of the pressure

difference diagram through the length of the air cushion. This coefficient falls within the range [36]

-157-

$$0.5 < k_y < 1.0.$$

In the mode of hovering and free drift of an ACV over water the moment from horizontal forces is negligibly small, and therefore, for determination of $\bar{m}_{xB}^\theta$ the following equation can be used:

$$\bar{m}_{xB}^\theta = \frac{M_{xn} - Gy_0 \sin\theta}{GB_n^A}$$ (140)

Determination of the transverse initial metacentric altitude of a Class A ACV while hovering over water by the above-described method (by calculating the pressure distribution among the air cushion sections) involves computational difficulties, even in the case of rather coarse simplifications, and therefore we will examine a method by which it is possible to bypass the difficulties. Using equations (108), (131) and (140) for determination of $\bar{m}_{xB}^\theta$ of a systematized ACV model, consisting of two independent lift sections, connected by a swivel beam, we obtain (Figure 73)

$$\bar{m}_{xB}^\theta + \bar{y}_0 = \bar{K}_{yn} \frac{\gamma S_n}{Q} \frac{z_{1.s}^2}{B_n}.$$ (141)

We will find the new value

$$k_m = \frac{\bar{m}_{xn}^\theta + \bar{y}_0'}{\bar{m}_x^\theta + \bar{y}_0}$$

and analyze its dependence on basic factors

$$k_m = \frac{\bar{K}_{yn}}{\bar{K}_y} = \frac{1}{\bar{K}_y + 1}.$$ (142)

In view of equation (142) we may conclude that $k_m < 1$, and consequently, assuming other conditions to be equal, the initial stability of a Class A ACV in the mode of hovering over water is less than in the mode of hovering over a screen.

The values of k_m are calculated for two types of $H(Q)$ characteristics, two versions of air flow--chamber and nozzle--and range of values of relative ACV mass $15 \leq \overline{G} \leq 30$, which corresponds to the range of $\overline{G}$ of contemporary ACV.

The results of the calculations are presented in Figure 77. The graphs of the dependence $k_m(\overline{G})$ show the following. First, as $\overline{G}$ increases k_m decreases; secondly, the nozzle version of air flow retains the initial stability over water closer to its value over the screen than is possible with the chamber version, although due to the smaller value of $\overline{m}^\theta_x$ in the nozzle version the absolute value of $\overline{m}^\theta_{xB}$ for $\overline{G} \approx 30$ only, approximates $\overline{m}^\theta_{xB}$ of the chamber version.
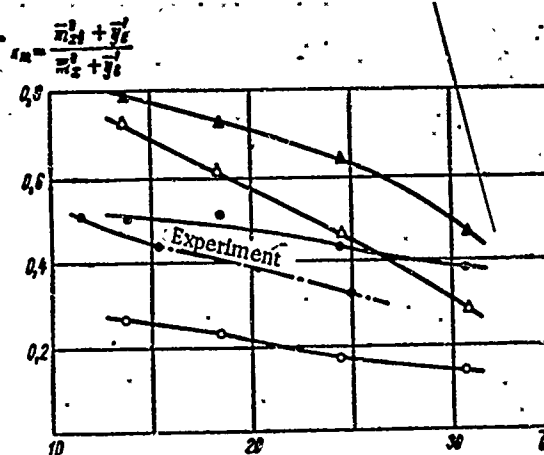

Figure 77. Relationship of the Coefficient k_m to the Type of Fan, Variant of Air Flow, and Relative Weight of a Class A ACV. $O, \triangle$, Fan No. 1; $\bullet, \blacktriangle$, Fan No. 2; $O, \bullet$, Chamber variant; $\triangle, \blacktriangle$, Jet variant.

The experimental curve plotted in Figure 77 confirms the character of the function $k_m(\overline{G})$, obtained through calculation and is quantitatively close to the theoretical values obtained from analysis of the chamber version with fan No. 1, although even in this case the effect of the natural rigidity of the flexible inclosures apparently increases as $\overline{G}$ increases, and this results in quantitative discrepancies.

-159-

The analyzed results can be used for approximating the k_m of __an ACV in__ various design stages. Considering that the theoretical graphs illustrated in Figure 77 pertain to a conditional ACV model with completely isolated lift chamber sections, the corresponding correction factors must be introduced to the theoretical value $\overline{K}_y$ during calculation of the k_m of a real ACV. In view of the lack of experimental data, we recommend at this time the following corrections to $\overline{K}_y$ in the form of the sum of co-efficients $\chi_p + \chi_n$:

$\chi_p = 0.5$ for total isolation of receiver sections from each other;

$\chi_p = 0$ for a common receiver;

$\chi_n = 0$ for an integral air cushion;

$\chi_n = 0.5$ for partitioning of the air cushion by means of flexible nozzles that extend to the peripheral flexible enclosure with nozzle exits at the level of the edges of this enclosure.

Then the final form of the equation (142) becomes:

$$k_m = \frac{1}{(\chi_p + \chi_n)\overline{K}_y + 1}$$ (143)

Class A. Travel Over Water

The stability of an ACV, both while hovering over water and in the traveling mode, depends largely on the character of interaction of high pressure region with the water surface. If the elastic properties of the air cushion in the absence of contacts between the flexible enclosure and the water is practically independent of speed, deformations of the water vary notably as a function of the speed of the ACV. In the case of contact between the flexible enclosure of the air cushion and the water surface there are additional hydrodynamic forces that influence ACV stability.

Experimental studies of the change of initial stability of Class A ACVs as a function of the speed indicated first of all that the ACV has minimal transvere and longitudinal stability while hovering over water, and second, that the initial stability increases monotonically as the speed of the ACV increases. Therefore, it is natural to suppose that when

some speed is reached, when deformations of the water surface practically disappear, the stability of the ACV approaches the value that it has in the travel mode or while hovering over a screen. Hence, the following conclusions can be made:

1. The initial static stability of Class A ACVs should be characterized by the following set of values:

initial transverse metacentric altitude m_{xB}^{θ} corresponding to hovering of the ACV over water;

initial transverse metacentric altitude m_x^{θ} corresponding to hovering of the ACV over screen;

initial transverse metacentric altitude m_{xV} corresponding to travel of the ACV over water at velocity V.

The value of m_x^{θ} can be determined approximately by calculation, and then $m_{xB}^{\theta} = k_m \cdot m_x$ can be determined using equation (143) or on the basis of the experimental characteristics of a similar prototype. The last step is the determination of the dependence of m_{xV}^{θ} on V. The following empirical formula is presently used for this purpose:

$$\overline{m}_{xV}^{\theta} \approx \frac{1}{2}\left[(\overline{m}_x^{\theta} + \overline{m}_{xB}^{\theta}) - (\overline{m}_x^{\theta} - \overline{m}_{xB}^{\theta})\cos\frac{\pi Fr}{Fr^{kp}}\right]. \qquad (144)$$

Fr^{kp} depends on k_m, but tests of ACV models indicate, on the average, that with some reservation it may be assumed that $Fr^{kp} = 4$-5.

The static stability of a Class A ACV at finite list angles while hovering over water is calculated in like manner as the stability of a floating vessel, but with corrections that take into account the effect of the working lift system. These corrections have different significance in different ranges of list angles of ACVs.

Calculations have shown that most complex is the introduction of corrections in the range of list angles from approximately 5-15°, when it is essential to consider both the forces and the moments created by the air cushion, and the lift in corresponding moments produced by the forcing out of water from the receiver as it passes through the actual water line.

It is not necessary to consider the effect of the air cushion in the
range of list angles of $15° \leqslant \theta \leqslant 25°$, but when the receiver is located
around the periphery of the vessel's hull and has a substantial volume
it is essential to consider the forcing of water from it by pressure p_p.

The calculation is carried out to the angle of flooding of penetrable
hatches or air intakes. If the flooding angle is not yet reached for
$\theta > 25°$ further calculation is carried out by the usual method, taking
into account the flooding of the penetrable parts of the hull.

Class B. Hovering Over Water

By way of example we will examine the calculation of the diagram of
transverse stability of an ACV of the catamaran type. We will assume one
hull to be submerged in water and the escape of air to be blocked on one
side. The recovery moments produced by partial vacuum on the lower side
is neglected because of its smallness. The bottom edges of all enclosures
of the air cushion (side hulls, bow and stern) are assumed to be located
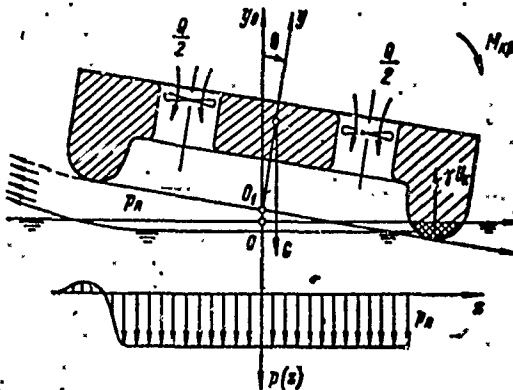on the primary plane of the vessel XO_1Z (see Figure 78).

Figure 78. Diagram of Forces Acting on Class B ACV
During List.

Consequently the recovery moment is assumed to be produced basically
by the force of buoyancy of the hull immersed in water. Here, as the
list angle changes, the distribution of lift between the aerodynamic
and hydrostatic components is altered, which in turn influences the landing
of the ACV (h_B, θ).

The equations of equilibrium of ACVs are:

$$\Sigma Z = P_6 - Z_{r2} = 0; \tag{145}$$

$$\Sigma Y = p_n S_n + \gamma U_k - G = 0; \tag{146}$$

$$\Sigma M_x = p_n S_n z_n + P_6(y_6 + y_G) + \gamma U_k z_k + G y_G \sin \theta - M_{\kappa p} = 0. \tag{147}$$

The equations are based on the following assumptions:

1.   Distribution of the under-dome pressure along the area of the cushion was obtained for all meanings of θ evenly

$$p_k = \frac{1}{S_n} \int_{S_n} p(x, z, \theta) \, ds = f_p(\theta). \tag{148}$$

2.   Abatement of the water-level by the under-dome pressure, the influence of spray and wave formation, and the increased flow of air are insignificant in calculating forces and moments. As a matter of fact, the greatest relative error in this assumption shows very little list angle (up to 10-12°) when the forces and moments are small, but with an increase in list the under-dome pressure falls sharply (Figure 79), decreasing the influence of the enumerated factors of the calculated amounts. It is possible to estimate the influence of non-calculated drops in the water-level under the action of p_p on the amount of hydrostatic force γU_k

according to the formula (see Figure 80):

$$\delta(\gamma U_\kappa) \approx \frac{p_n^2 L_n}{2\gamma^2 U_\kappa}. \tag{149}$$

To examine the example below, the following relationship of error in the amount $\gamma \overline{U}_k = \gamma U_k / S_n^3 {}^2 \rho g$ to the ACV's list angle (Table 4) was received.

3.   Trim difference is considered constant and equal to zero for all angles of list. Calculation of initial trim difference may result in considerable corrections to the calculated amounts. Calculation of free trim difference for an asymmetrical, relatively plane, mid-frame type hull is carried out by methods of ship statics [44].
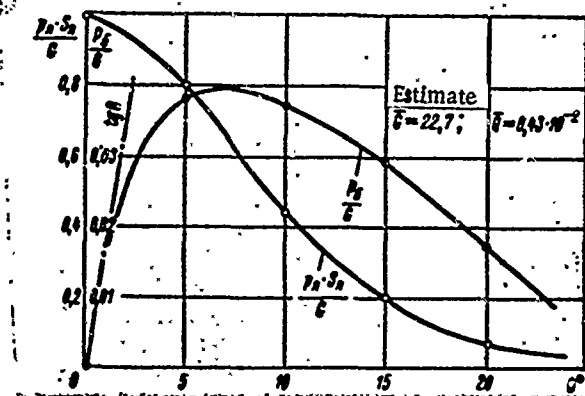
-163-

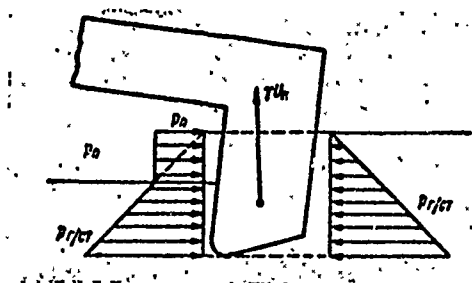Figure 79. Relationship of Side Force and Under--Dome Pressure of a Class B ACV to List Angle.

Figure 80. Diagram for Calculating Errors to Determine the Restored Hydrostatic Moment. $P_{г/ст}$ = hydrostatic moment.

4. The perimeter of air flow from the under-dome area is equal to $L_п$ · $B_п$. The plausibility of this assumption is confirmed by the insignificant amount h_B received in the calculation and the small amount of influence of the air flow in the bow and stern on the estimated forces and moments.

5. The number of rpms of the fan does not change in relation to the list angle, which corresponds in operation of the ACV and makes it possible to use this in calculating the similar relationship H(Q).

6. The amount of under-dome space is great enough to compute the air speed in it to almost zero.

7. The ACV's speed of drift in reaction to the air, asymmetrical in escaping from the under-dome space, is very small.

-164-

TABLE 4. RELATIONSHIP OF ERROR IN CALCULATING DISPLACEMENT OF
A BOAT TO LIST ANGLE OF AN ACV.

List angle $\theta°$	Relative error, %, $\delta(\gamma U_k)$	Relative hydrostatic lift force $\gamma \overline{U}_k$	Absolute error for $\gamma \overline{U}_k$ $\dfrac{\delta(\gamma \overline{U}_\kappa)\gamma \overline{U}_\kappa}{100}$
5	11,6	4,5	0,52
10	1,4	12,5	0,18
15	0,2	18,1	0,04
20	0,02	20,6	0
25	~0	22,7	0

Note: Commas indicate decimal points.

8. Forces of resistance to drift are hydrodynamic in nature and are used in half droughts by the hull penetrating the water.

9. The coefficient of the narrowing stream, with the air flowing from the under-dome space into the atmosphere is equal to the unit, corrected by rounding off the hull's frame.

Calculation is made in the following sequence:

Determination of the components of lift forces according to equation (146) and calculation of the fan's characteristic H(Q) according to the given list angle θ.

1) Computation of the relationship is

$$\gamma \ddot{U}_\kappa = f_U(\theta, h_s).$$

As ·a result, we get a set of curves similar to that set forth in Figure 81, where θ = the parameter.

-165-

2) Computation of the relationship $h_B = f_h(p_n)$ is performed according to the equation for continuity and makes it possible to calculate the linearization of the fan's characteristic

$$Q = Q_0 - \frac{\partial Q}{\partial p} p_n \tag{150}$$

The calculated formula is

$$h_s = \frac{Q_0 - \frac{\partial Q}{\partial p} p_n}{(L_n + B_n)\sqrt{\frac{2p_n}{\rho}}} - \frac{B_n}{2}\sin\theta. \tag{151}$$

Also as a result is the set of curves $h_B = f_h(p_n)$ where θ equals the parameter.

3) The structure of the graph's function is $h_B = f_h(p_n)$ where θ is the parameter.

4) Determination of the balanced state is in accordance with the equation (146), i.e., where Y = G for each value of θ. The values h_B and p_n in relation to θ are determined with this.

Determination of the relationship $M_\theta = f_M(\theta)$ is according to the formula

$$M_\theta = \gamma U_\kappa(\theta) z_\kappa(\theta) + $$
$$ + p_n(\theta) S_n \frac{tg\,\theta}{2}\left(\frac{B_n}{2}\sin\theta + h_s\right) - $$
$$ - G y_0 \theta. \tag{152}$$

As shown by practical calculation and comparison with results of experiments and with the influence of side forces and moments created by them, it may be disregarded if the relative expenditure is $Q \leqslant 0.05$.

The results, calculated according to the data and compared with the results of actually testing two ACVs, are shown in Figures 82 and 83.
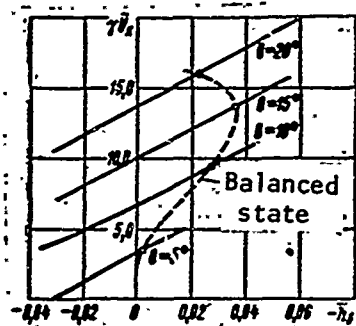
Figure 81. Hydrostatic Lifting Force on Hull Entering Water Versus Altitude of ACV and Angle of List.
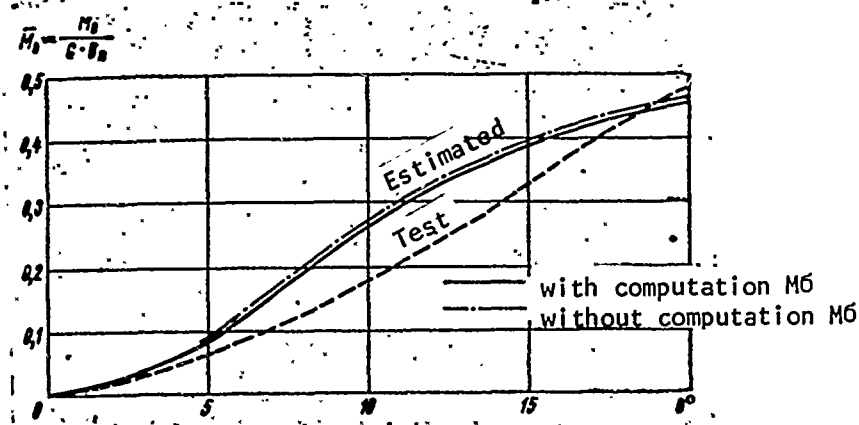

Figure 82. Diagram of Static Stability of a Class B ACV (Type I).

A comparison of the estimated and experimental graphs in Figure 82 shows the following:

a) the calculated relationships of $\overline{M}_\theta = M_\theta/GB_\Pi$, computed with the estimated moment, the created side forces, and without estimation of this moment are practically coincidental;

b) the greatest deviations of the estimated and experimental values are in the range of $7° \leqslant \theta \leqslant 15°$ which, apparently is produced by some conventional calculation.

Shown in Figure 83 are the results of estimated and actual tests of the "Neva" ACV, made both during suspension of air cushion, and during navigation of the craft where $\theta = 0$.
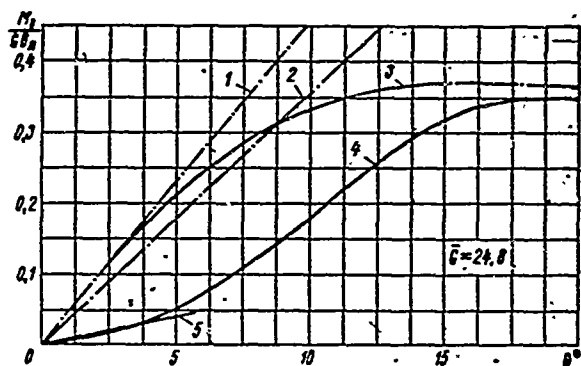
Figure 83. Diagram of Static Stability of a Class B ACV
(Type II). 1, Computation $\bar{m}_{xB}^{-\theta}$ = 2.64 (afloat, Q = 0);
2, Experiment $\bar{m}_{xB}$ = 2.06 (afloat, Q = 0); 3, Computation $\bar{M}_\theta$
(afloat, Q = 0); 4, Computation $\bar{M}_\theta$ of the air cushion
($\bar{Q}$ = 3.2·10^{-2}); 5, Experiment $\bar{m}_{xB}^{-\theta}$ = 0.46 (of the air cushion,
$\bar{Q}$ = 3.2·10^{-2}).

It is clear from the graph that lift of a moving ACV leads to a sharp decrease of initial stability of the craft and a decrease in area of designed static stability. The decrease M_θ disappears when $\theta > 20°$,
i.e., with those list angles when the lift force begins to be completely provided by a good deal of the hull being immersed in the water. Verification of the calculated corrections of designed static stability, carried out by various methods, may serve well for convergence of their results where $\theta > 20°$. Conditions of the experiment did not permit large enough list angles to be obtained, therefore, a comparison of the estimated and experimental data is only made for small angles. This comparison shows that calculated initial stability of the craft during suspension is close to the test examples, with the same errors as during navigation (Q = 0).

§16. Features of the Experimental Investigation of Statics and Some
      Results of Test Operation of an ACV

Currently, it is possible to use the following set method for experimental determination of static stability in ACVs or models.

Sequence for Conducting the Experiment

The ACV is carefully suspended, the center of gravity is determined, and the weight and center of gravity coordinates are adjusted to set values.

Then we determine:

a) the lift characteristics--air expenditure, pressure in the receiver, lift height at various rpms of the fan, during suspension above a screen. With this data, we begin to check the lift system for all other tests;

b) the ACV's stability characteristics during suspension above a screen. The results of these tests are basic for evaluation of initial stability for Class A ACVs, since measurements during suspension above a screen are complete and reliable;

c) the lift characteristics during the ACV's suspension over water;

d) the initial stability characteristics during the ACV's suspension over water;

e) a change in the characteristic of static stability and lift height during the ACV's straight, steady movement over calm water.

Tests, shown in paragraphs a) and b), were made only on Class A ACVs. These craft are restrained by flexible braces from horizontal shift. The hawsers are secured so they are not hindered by vertical and angular (list, trim) shift of the ACV.

List (trim) is provided by means of shifting the ballast and measurement of the ACV's incline angle. The most accurate results are obtained when there is an angle change by balance of great enough length and by measurement of lift height of the four extreme points of the ACV's hull batten.

In the tests, shown in paragraphs c, d, and e, the ACV moves freely along the water's surface, but a non-self-propelled model is kept from drifting by moorings. Measurement of the angle is carried out with the aid of balances and gyroscopic instruments.

Errors in measurement of angle by balance and by batten usually do not exceed 0.05-0.1°, but by gyroscopic means 0.2-0.5° where the incline angle is ± 2-8°, i.e., relative errors are in the range of ± 5-10%.

The basic static characteristics of the ACV usually are expressed in the non-dimensional form:

$$\bar{h} = \frac{h}{\sqrt{S_n}};$$

$$\bar{p} = \frac{p_p S_n}{G};$$

$$\bar{m}_x^\vartheta = \frac{\partial M_3}{\partial \vartheta}\bigg|_{\vartheta=0} \cdot \frac{1}{GB_h};$$

$$K_y = \frac{\partial Y}{\partial h} \cdot \frac{1}{qS_n} \quad \text{etc.}$$

A model experiment was conducted on the CC-2 ACV [71, 93]. Tests of a variant without flexible-skirted air cushion (CC-2.001) were made with an average weight of 2.070 kg during suspension above a screen. The craft was kept from horizontal shift by lines, in which dynamometers were incorporated. The lift characteristics obtained depended on lift height in relation to the ACV's weight at various rpms of the fan n_B (Figure 84).
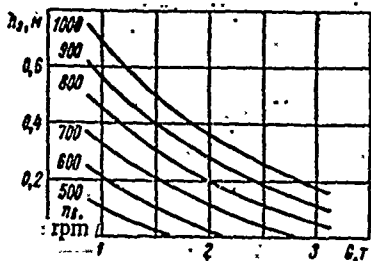

Figure 84. Lift Characteristics of the CC-2.001 ACV During Suspension Over a Screen.

Transverse stability was investigated with h_3 = 0.239 meters, which permitted sufficient list angle up to ±5.5°, and longitudinal with h_3 = 0.206 meters, which corresponded with the trim angle up to ±2.8°. During inclination the ACV rotated on longitudinal and transverse axes, lying on a flat plane, therefore the change in angle of incline had practically no influence on the average lift height of the ACV.

In Figure 85, diagrams of longitudinal and transverse stability of an ACV, received during testing, are set forth as well as relationships of longitudinal and transverse reactive forces to list angle and trim difference.

Working out the results showed that, due to the relatively great expenditure of air $\bar{Q}$ = 8.3·10^{-2}, there was a higher amount of side forces $\bar{P}_6$ = 1.64% in degree of list. The non-dimensional lift height of the CC-2.001 ACV consisted of $\bar{h}_3$ = 0.04.
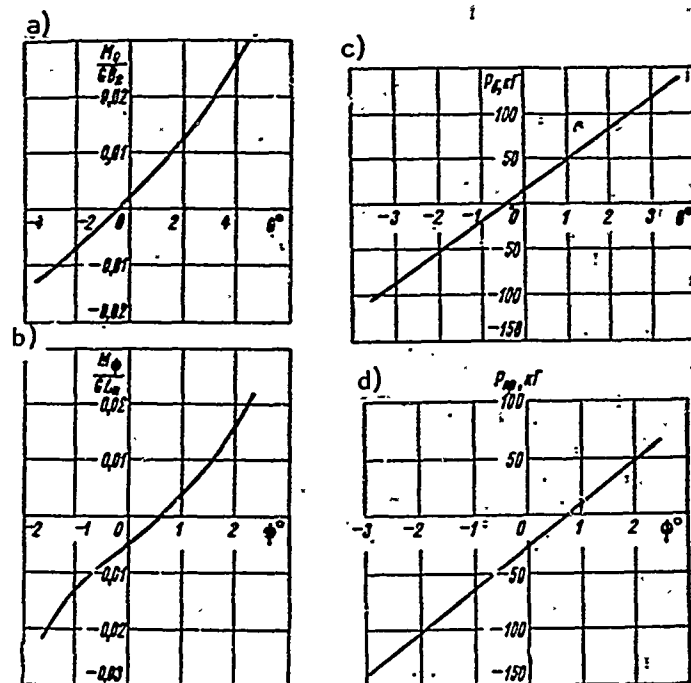
-170-

Figure 85. Diagrams of Static Stability and the Relationship
of the Horizontal Reactive Forces of the CC-2.001 ACV to the
Angle of Incline During Suspension Over a Screen, G, 1,1.8:
a, Transverse stability; b, Longitudinal stability; c,
Side force; d, Longitudinal force.

In spite of the presence of jet stability, the latter proved comparatively low

$$\overline{m}_x^{\theta} = 0{,}30;$$
$$\overline{m}_z^{\psi} = 0{,}54.$$

This may be explained by the relatively small weight of the ACV

$$G = 10.0\text{-}12.0,$$

which doesn't provide sufficiently high coefficient for vertical stability
of the craft

$$\overline{K}_y = 0.2,$$

while the coefficient for pressure

$$\bar{p} = 1.24$$

is sufficiently high. This ACV's lift system was designed apparently, without considering requirements for stability and therefore had a low meaning for the derivative

$$\frac{\partial \bar{m}_x^{\xi}}{\partial \bar{p}} = \frac{0.30}{1.24 - 1.00} = 1.25$$

For comparison, we note that the model of another ACV with a similar design of sectioned air cushions and a non-divided receiver had an observed rate of $\bar{G} = 21.2$ and $\bar{Q} = (2-3) \cdot 10^{-2}$ with derivative

$$\frac{\partial \bar{m}_x^{\bullet}}{\partial \bar{p}} = 2.22,$$

and $\bar{m}_x^{\theta} = 1.00$ with $\bar{p} = 1.45$.

The final figures are considerably close to the conditions of an ACV's normal operation.

The arrangement of the flexible skirt (type CG-2.002, Figure 86) on the CC-2 ACV led to a sharp decrease in longitudinal initial stability and, as shown in the diagram for static stability, essentially changed its form (Figure 87). The longitudinal non-dimensional initial meta-centric height was equal to $\bar{m}_z^{\psi} = 0.02$, which led to a high response of trim in the ACV from the action of the multi-natured differential moment in the range of $-2° < \psi < 2°$. For the extent of this range, the ACV has a sufficiently high stability.

On the basis of results from testing stability in a number of models and actual-size ACVs, it is possible to get the relationship of the derivative $\partial \bar{x}_G / \partial \psi$ (or $\partial \bar{z}_G / \partial \theta$) to the relative lift height of the ACV $\bar{h}_L = h/L_\Pi$ or $\bar{h}_B = h/B_\Pi$ for the longitudinal and transverse stability, in that order (Figure 88 and Table 5). Also plotted in Figure 88 are the average limits with the truest meaning for these derivatives and the mean curve proposed by Stenton-Jones.
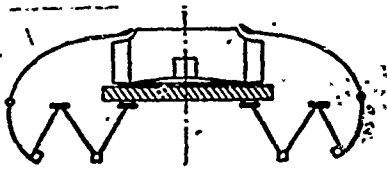
Figure 86. Diagram of the
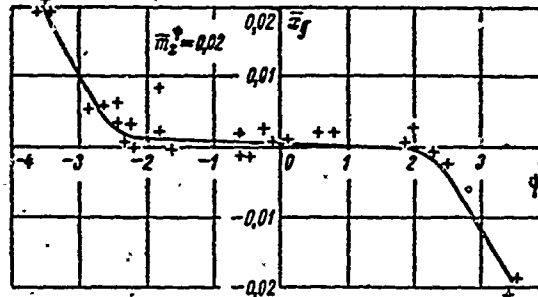Flexible Skirts on the
CC-2.002 ACV.

Figure 87. Diagram of the Longitudinal
Static Stability of the CC-2.002 ACV.

$$\bar{x}_g = x_g/L_n.$$ relative shift of the craft's center of gravity

$$\bar{x}_g = \frac{M_\psi}{Q \cdot L_n} = \bar{M}_\psi$$

In this first class example, we see the test results of the SKMR-1 (U.S.A.) ACV [66, 96]. Testing began in 1963. In the first series of tests, the peripheral skirt consisted of an air-jet curtain. Using a similar curtain, the cushion was sectioned off into four equidimensional parts (the jet was arranged in a diametric plane, in the region of the ship's mid-frame--Figure 89, type BGO). To test the second series of ACVs, 0.6 meter high flexible jets were installed-peripheral and sectioned (Figure 90, type GS-0.6).

In testing the third series, the height of the flexible jets on the ACVs was 1.2 meters (type GS-1.2). The sectioned cushions were provided by closed, massive skirts mounted on the sectioned-off jet (Figure 91). Set forth below are some characteristics of the tested SKMR-1 ACV (Table 6).

TABLE 5. DIAGRAMMED SECTIONS ADOPTED FOR TESTING NATURAL ACVS AND THEIR MODELS.

| Diagrammed sections	Conventional designation in Fig. 88	Firm	ACV Model	Type of stability
	▼		SRN1, ACV	Longitudinal
	⧌		SRN1, ACV	Transverse
	△		SRN1, model #13	Longitudinal
	●	Westland	SR, model 130	Longitudinal
	✕		SR, » 130	Transverse
	⊙		SR, model 51	Longitudinal
	✚		SR, » 51	Transverse
	▣	Langley	Model	Longitudinal
	☐			
	▲	Boeing	Model	Longitudinal
	∅		CC-2.001, ACV	Longitudinal $\Big\}\, t_{\text{вн}} = t_{\text{н}}$
	○		CC-2.001, ACV	Transverse
	⍉	Britten-Norman	CC-2.002, ACV	Longitudinal $\Big\}\, t_{\text{вн}} = 0{,}75 t_{\text{н}}$
	◼		CC-2.002, ACV	Transverse
	✳		CC-5, ACV	Longitudinal
	�֎		CC-5, ACV	Transverse
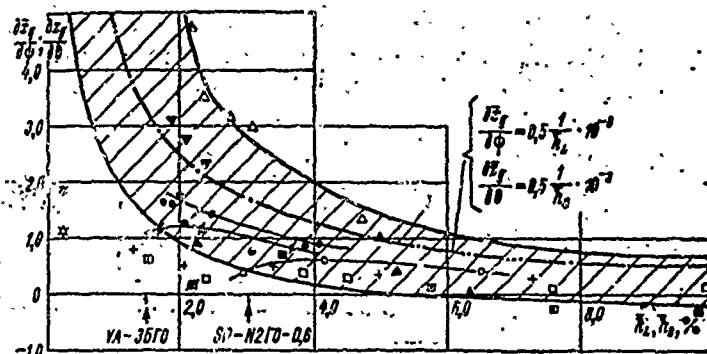
Figure 88. Matching Diagram of the Relationship of the Value $\partial \bar{x}_g/\partial \psi$ to $h_L = h_{_9}/L_\pi$ and $\partial \bar{z}_g/\partial \theta$ to $\bar{h}_B = h_{_9}/B_\pi$

According to the Results of Testing the SRN1 ACV, the CC-2.001, the CC-2.002, the CC-5, and Several Models.

$\partial \bar{x}_g/\partial \psi$ and $\partial \bar{z}_g/\partial \theta$ are in % of one degree of incline angle. Conventional designators are set forth in Table 5. 1, Mean curve according to Stenton-Jones.

$$\left(\frac{\partial \bar{x}_g}{\partial \psi} = 0.5 \frac{1}{\bar{h}_L} \cdot 10^{-3}; \quad \frac{\partial \bar{z}_g}{\partial \theta} = 0.5 \frac{1}{\bar{h}_B} \cdot 10^{-3} \right)$$
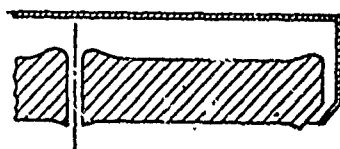

Figure 89. Layout of the Jet Apparatus of the SKMR-1 ACV (Type BGO).
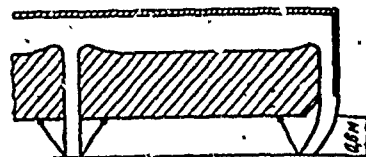

Figure 90. Layout of the Flexible Jet of the SKMR-1 ACV (Type BGO).

TABLE 6. BASIC CHARACTERISTICS OF THE SKMR-1 TYPE ACV

Characteristic	Test Series,		--
	1st (BGO)	2nd (GS-0.6)	3rd (GS-1.2)
Weight of the tested ACV G = tons	20.4-26.5	28.4	27.1-31.8
Air expenditure Q = meters^3/sec	396.4	350	154
Fan rpms n_B = rpm	2,580	2,580	1,406
Air cushion dimensions: Area S_n = meters^2	113	113 (arbitrary)	113
Length L_n = meters	17.4	17.4	17.4
Width B_n = meters	7.25	7.25 (arb.)	7.25
Center of gravity increase y_G, m	1.55	1.68	1.6*
Lift height h = meters	0.46	1.0	1.30
Relative weight $\bar{G}$	15.7-20.4	21.9	20.8-24.4
Relative expenditure $\bar{Q} \cdot 10^2$	8.2- 7.2	6.1	2.8- 2.5
Relative lift height $\bar{h}_a$	0.043	0.094	0.123

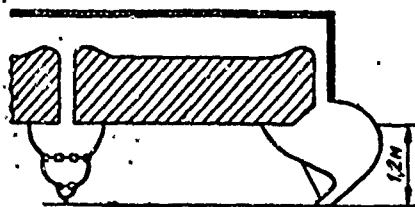Figure 91. Layout of the Flexible Jet and the Inflated Sectioned-Off Keel of the SKMR-1 ACV (Type GS-1.2).

Diagrams of static stability in the BGO type ACV are presented in Figure 92 and one may clearly follow the influence on stability of wide sectioned jets and the nature of the base surface. After increasing the width inside the jet by 2% B_n, the stability of the ACV above a screen changes very little.
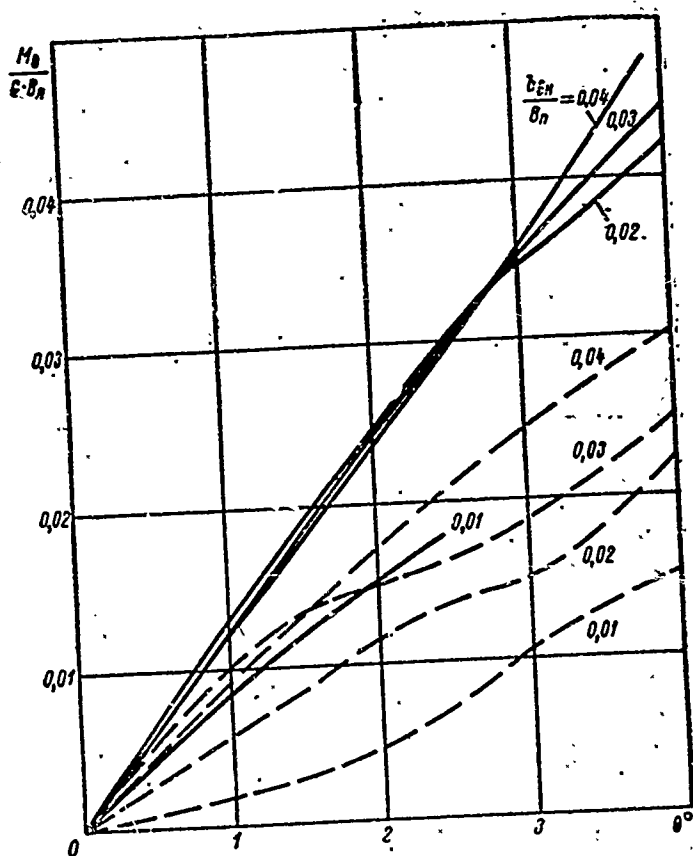
-176-

Figure 9.2. Diagrams of the Transverse Static Stabilities of the ACV, SKMR-1 (BGO Version). ————, Above the screen; - - - -, Above water; b_{BH}, Widths of the sectioned nozzles.

Changes of stability in the diagrams of $\theta > 3°$ actually cause a loss of stability in the form of sectioned streams of air, but during suspension over water, stability is increased with the growth of b_{BH}. This may be connected with the influence of the moment created by the stream of spray hitting against the ACV's bottom.

Diagrams of the static stability noted in actual testing of the GS-0.6 type ACV are set forth in Figure 93. The tests showed that static stability in the BGO type craft above water is considerably less than over a screen, but both diagrams on the GS-0.6 craft's stability are identical. This result, contradicting theory in an overwhelming majority of experiments, may explain the high air expenditure, the creation of powerful streams of spray acting on the ACV's bottom, and the additional restored moments which it causes.
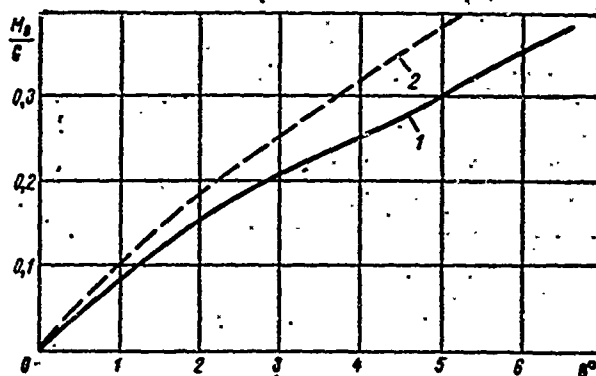
-177-

Figure 93. Diagrams of Transverse Static Stability
of the SKMR-1 ACV (Type GS-0.6). —————, Above a
screen; - - - -, Over water.

Along with the SKMR-1, the SK-5 and VA-3 ;ACVs were tested.
Comparative tests established that, for normal operation of the ACV,
the transverse metacentric height during suspension over water must be
no less than $\bar{m}_{zB}^{\theta} \geqslant 0.35$-$0.40$, the longitudinal--$\bar{m}_{zB}^{\psi} \geqslant 1.00$, and during

suspension above a screen--$\bar{m}_{x}^{\theta} > 1.0$.

There is a great deal of interest in the results of investigating
the possibility of regulating the ACV's stability by the French firm of
Bertin [61]. The first type of lift system built, consisted of even-
-numbered annular flexible chambers with vertical axes and air fed into
each chamber individually, which corresponds to the conventional ACV
model mentioned above (Figure 73). In relation to the method of feeding
the air, the characteristics of the air pump and the fundamental rigidity
of the material of the flexible skirt, a value of $m_x = 4.6$-8 was obtained
, which was close to the value that we calculated earlier. Apparently,
these characteristics were accepted as excessively high and to lower the
stability in the design, an annular panel was introduced, which encompas-
sed a group of four primary rings for a "combined skirt" (Figure 94).

In regaru to the shift Δh of the lower edges of the external rings,
being relatively level, passing across the lower edges of the initial·
(internal) rings, the following values were obtained:

Δh, мм	0	5	10
$\bar{m}_x^{\theta}$	2,9	1,7	1,0

-178-

The tests were conducted in the BC-8 model ACV, with a scale of 1:5. Brought into this, for comparison, is the characteristic of stability for an ACV with peripheral annular flexible jets and cross-shaped panels, and a sectioned-off air cushion where $\overline{m}_x^{\theta} = 0.9$.
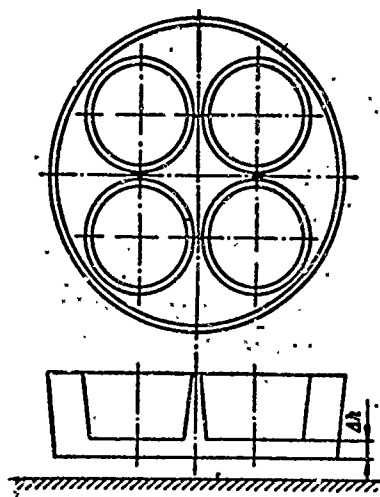

Figure 94. Combined Skirt in the Form of Combined Annular Flexible Chambers of Various Diameters (Bertin Firm).

The data produced from this confirms the tendency of experimenters to take the initial metacentric height of $\overline{m}_x^{\theta} \geqslant 1.0$ (above a screen), but, at the same time, the value $\overline{m}_x^{\theta} \approx 2\div3$ is recognized as excessively high.

Test operation of a number of ACVs, with flexible skirts showed that, with no contact of the edges of the flexible skirt with water, the ACV's stability while moving doesn't undergo a sharp change (in the range of speed examined.)

Nevertheless, it is known that in a number of cases, when the flexible skirt made contact with the water during movement, a peculiar phenomenon occurred called "digging in" (plow-in). It occurs when the stability of the ACV during movement is changed considerably for a comparatively short time (just several seconds): trim becomes negative, lift height is decreased considerably, and in a number of cases there is a spontaneous turn and significant list. This is connected with the drawing closed of parts of the flexible skirt inside the air cushion, due to the contact with the running water and the braking forces of the contacting parts.

The flexible skirt, coming into contact with the water, suffered considerable deformation and the ACV, braking, caused additional forces of contact. As a result, there was a destablizing moment M_{r1} (Figure 95).

$$M_{r1} = M'_{r1} + M''_{r1},$$

-179-

where $M'_{r1} = G\delta x_n$ is the destabilizing moment, causing a shift in the center of gravity of the air cushion with a value of δx_n due to deformation of the flexible skirt;

$M''_{r1} = X_{r1}(y_G + h_{r.0}$ is destabilizing moment, causing braking of the ACV from the force X_{r1}.
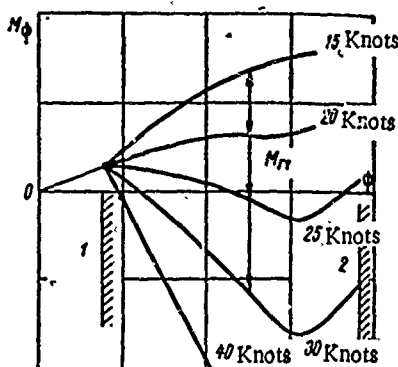

Figure 95. Change in Diagrams of a Class A ACV's Static Stability During the Flexible Skirt's Contact with the Water. 1, Angle of contact of the skirt's lower edge with the water; 2, Angle of contact of the ACV's rigid hull with the water.

"Plow-in" of the ACV may have two effects: disruption of stability in movement, followed by restoration of it; the ACV capsizing.

In spite of relatively little testing in operating ACVs there are well-known cases currently of capsizing because of "plow-in," and in a number of instances, of craft just about to capsize.

In the "plow-in" process the ACV experiences sharp braking, lift height is considerably decreased, and there is list and trim difference.

These phenomena were encountered during testing of the SRN5 and SKMR-1 ACVs. There are three known cases of the SRN5 capsizing and one for the CC-5 (England).

The Westland Firm, builders of the SRN5, had conducted a broad investigation of the "plow-in" process, its cause and its associated phenomena. Model and actual tests were conducted during movement and an analysis made of the cases of capsizing. The operation of the separate elements of the ACV's lift system during "plow-in" took the following form. In the SRN5, air is drawn in by one fan to a large control duct and then to a flexible "bag," having a compact aperture (jet) in the lower section. One can see from this that the pressure is in the bag from both sides almost equally. If the pressure in the bag and the width of the aperture are constant, then the pressure in the cushion depends on the height of the jet's shear above the base surface. Therefore, under

normal conditions, the craft has favorable stability thanks to sectioning of the air cushion by the pneumatic thick massive skirts in a diametric plane and in the middle. In the event of a sudden maneuver, the flexible skirt may make contact with the water, which causes frictional forces as was noted above.

"Plow-in," as a result of the flexible skirt making contact with the water, occurred at high speed on calm water with all ACVs with flexible skirts, starting with the SRN1. On this basis, it was concluded that it is necessary to avoid letting the bow skirt section make contact with the water and to trim the bow. The first type of skirt on the SRN5 showed a tendency to "plow-in" at speeds above 55 knots, although it may attain 60 knots safely, if the ACV is correctly trimmed. However, this was found to be unacceptable and tests were made to remove this feature, to remove its formation to limit the range of speed. The tests showed that installation of an additional gib in the bow section of the skirt decreased the influence of wash at high speeds.

Let's look at the basic factor--the influence of wash on the flexible skirt. Let's suppose that the ACV is moving right along with constant trim. Then the work being transferred below by the controls may lead to the bow section's skirt making contact with the water.

Device for control of pitch screw. An increase in thrust creates trim of the bow. Usually, this is neutralized by shifting the horizontal rudder or adjusting the ballast. As a result of increase in screw pitch, there is a decrease in engine rpms and, consequently, those of the fan. The general decrease in lift height also causes the skirt edge to dip close to the water.

The rudder. Operation of the rudder creates not only moments of yaw, but also moments of list, causing static list and vibration.

Horizontal rudder. It is used when turning to counteract changes in trim.

Device for lifting the flexible skirt. Each quarter of the skirt may be lifted by turning the control lever, which permits compensation for undesirable incline of the craft.

Other causes of "plow-in" or external list during the craft's turning may be: incorrect adjustment of ballast, a sudden change (reduction) of passengers, wind from the center of circulation, etc.

Let us look at a basic factor for counteracting "plow-in."

Stability, provided by redistribution of pressure in sections of the air cushion, is determined by its division into four parts. The pressure in each quarter increases as the sections approach the water, which also creates formation of restored moments.

For the flexible skirt design of the SRN5 ACV, a thorough evaluation of a number of design measures was made for preventing deformation of the skirt from wash. It was estimated that these measures would provide the necessary values of the restored moments.

Skirt collapses in contact with water. The additional lift force is approximately equal to the difference in the pressure produced in the bags and the air cushion in the area of collapse.

Flexible skirt design. The smooth, even, rounded surface coming into contact with the smooth water's surface creates great forces of resistance to movement. The mounting of gibs on the skirts of the SRN5.001 and 007 decreased this resistance.

Model tests showed that trimming of the ACV has stable curves of resistance and momentary curves of up to $\psi = -1°$, when the skirt edge contacts the water. After this, the curve form $M_\psi(\psi)$ is changed in relation to the craft's speed. This relationship has a critical characteristic. The greater the speed, the more clearly expressed is the instability of the pattern of moments and the greater the resistance to movement (see Figure 95). At the "hump" of wave resistance (about 10 knots) usually there is local contact of the skirt with water. The basic forces blocking "plow-in" are created by increased pressure between the walls of the flexible skirts and the bow section of the air cushion.

Three types of tests were conducted:

1) At a fixed rate of movement, "plow-in" was caused by changing the horizontal rudder, lifting of the skirt, and increase in screw pitch.

2) At a fixed rate of movement, shifting of the rudder created a drift angle of 20-30°, then "plow-in" was caused by horizontal rudder shift, increased screw pitch, and lifting of the skirt.

3) In stable coordinated turning at a constant speed (drift angle up to 20°), "plow-in" was caused in turning around by a quick shift of the horizontal rudder, increasing screw pitch, and lifting of the skirt.

Over 60 planned "plow-ins" of three models with flexible skirts were carried out: with vertical strips in the bow section (basic variant); with vertical ribs and two rows of openings, situated in enclosed sections and provided air-expenditure of about 3.5% of the total; with vertical ribs, two rows of openings, and with additional openings in the ribs' mid-section. Air expenditure made up about 5% of the total.

Tests showed that, if before the introduction of an air layer turning in uncoordinated at speeds of $V \leqslant 35$ knots could lead to "plow-in", then, after introduction of the layer, even at speeds of 40 knots there were safe drift angles up to 45° with rough control of the craft.

Besides this, tests showed the following:

An ACV with the first type of skirt may be controlled up to $V = 55$ knots and "plow-in," under these conditions, it is still not a threat. A simultaneous shifting of all control levers forward leads to trim of the bow up to 3-3.5° and to contact with the water by the rigid hull.

With $V = 36$ knots and the control levers for screw pitch, horizontal rudder, and skirt lift by shifting the rudder in the wrong position, there was a threat of capsizing with water rising 0.30-0.45 meters above the rigid hull and immediate correction was required. The drift angle reached 70-80°.

In a set turn, where $V = 25$-45 knots and $\beta = 20$-30°, skirt lift and turning of the horizontal rudder led to an increase of 60-80°, which also required immediate correction.

In testing the second type of skirt, incorrect position of control levers created a controlled soft "plow-in", which didn't influence movement and was considered absolutely safe up to speeds of 36 knots. In a set turn, where the speed is 36 knots, correction is not mandatory. The craft continues turning, although drift angle is increased to 90°. If the lever positions are incorrect for 4-5 seconds, then correction is necessary.

A series of tests on the third type of skirt showed that "plow-in" could occur at all speeds and the beneficial influence of additional devices was decreased. In spite of additional air expenditure, resistance to movement is increased somewhat because of the additional openings.

Then testing was repeated on the second type of skirt with wind speeds of 6-9 meters per second and wave height about 0.3 meters. They showed that "plow-in" occurs not only on clam water. Moving on rough seas, there was vibration of the ACV before "plow-in." The speed at the beginning of "plow-in" was almost the same as on clam water.

. In testing the SKMR-1 ACV, a number of cases of "plow-in" were also observed [66]. The first four cases were recorded at speeds of 50-60 knots and with initial trim of +1°. In the process of "plow-in", the bow of the craft is immersed up to -4° for four seconds. Changing screw pitch to zero, the pilot corrected the craft to its initial position in three seconds. Braking of about 0.5 g's was noted with maximum negative trim, which corresponds to the force $X_{\Gamma 1}$ = 13.6 tons. Clearance under the flexible skirt, before "plow-in," was 75 millimeters.

Let us look at the conditions which resulted in capsizing from "plow-in" for the SRN5 and CC-5 ACVs.

1) The SRN5.001 capsized on 8 April 1965, in the area of Alesund (Norway) during a sharp maneuver at high speed over calm waters. Immediately prior to the capsizing, there was a rupture of the flexible pneumatic--stabilized keel. The craft sustained minor damage. The capsizing occurred during demonstration of a 180° turn of the ACV, with vigorous braking by the screw as the stern moved out front ("pirouette"). In the first phase of the maneuver, the speed was lowered from 50 to 38 knots and the rudder was shifted. Reaching a drift angle of about 65°, the height above water was sharply decreased on the left side of the bow. For 2-3 seconds, the speed dropped 8-10 knots, the list increased to 12° and a bow wave formed, rising above the rigid hull. The craft then slowly turned over. At that point the drift angle was 100°. People on the ACV (10 persons) were thrown through the 3 windows and the bow door was knocked out during the accident [81].

2) The SRN5.007 capsized under similar conditions on 11 May 1965, in San Francisco Bay (U.S.A.). There was no rupture of the stabilized keel. The accident occurred during acceleration of the ACV. With a drift angle of 35-45° and a speed of about 35 knots, "plow-in" began, resistance to movement increased, and the speed dropped 8 knots, but the drift angle increased to 60-70°. After a sharp increase in list, the craft slowly capsized [81].

3) The SRN5 capsized on 8 July 1966 in the Solent Spithead (England) under similar conditions during a demonstration of braking (pirouette) at a high speed. The craft had a flexible-skirted air cushion, specially modified to avoid similar phenomena [82].

4) The CC-5 capsized on 12 November 1966, in the Solent Spithead (England) in rough seas, 0.6-1.2 meters high, during the test of an improved rudder mechanism [82].

Similar phenomena also were observed in Class B ACV tests.

5) During tests in 1961 of the Aqua-GEM craft, due to a sharp turn to the side after moving along shallow water (parallel to deep water) wound up almost capsizing. List reached 45° and one researcher was thrown from the craft [87].

6) The XR-1 experimental craft (U.S.A.) capsized during testing [106].

Class B ACV stability is provided in the form of side vessels or boats having, as a rule, a shallow waterline and minor collapse of the frame in the bow section occurs, with considerable collapse in the stern. In testing the ACV at high speeds without drift, or at moderate speeds, but with drift (in turning around) a tendency of the craft to tilt "diagonally" was observed, i.e., the bow and side simultaneously. Coincidental notes of the process of side roll and pitch in rough seas also show that, on the basis of the rocking, they result in "diagonal" tilt.

Analysis of these phenomena is complicated, but in ACV tests they are observed quite often.

Hence, it may be concluded that there is a necessity for detailed investigation of ACV stability and measures should be worked out in order to avoid their capsizing during movement.

One of the most efficient design measures is increased initial stability of the ACV. Regarding this idea, interest has been shown in results of tests of planned model lift systems for ACVs with flexible--skirted air cushions. A diagram of the model is shown in Figure 96. Special construction permitted experiments to be conducted during suspension above a screen made of organic glass, and over water (an over-turned box-like screen filled with water). The maximum value of the support moment was $0.2 \, GB_{\text{п}}$, maximum list angle for the model was up to 9-10°.
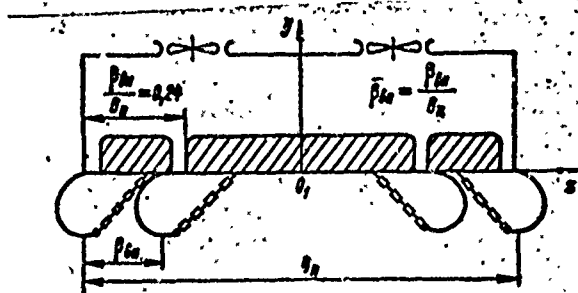

Figure 96. Diagram of a Model Lift System for Class A ACVs.

The model was made of wood and organic glass, drained along the bottom and formed by two centrifugal electric fans. In the bottom section, there were two side and two subdivided jets. At the bottom was support for the massive flexible skirt, made of rubberized material. The design of the flexible skirt and the receiver allowed tests to be conducted on two types of lift systems: one fully divided into sections and one with a common receiver, as well as with various locations of the subdivided skirt on the model's bottom.

The total weight of the model and support moments were regulated by the load, acting on the model through flexible lines. List angle and lift height were determined on a millimeter scale, the pressure-by a U-shaped manometer. The model was tested in a range of relative weight of $11.8 \leqslant G \leqslant 30.8$; lift height was $0.094 \leqslant h_{\ni} \leqslant 0.110$ and $0.044 \leqslant h_B \leqslant$ $\leqslant 0.099$.

As a result of the tests, the relationship of the derived $\partial \overline{m}_x^{\theta}/\partial \overline{p}$ to the arrangement of the internal skirt section (Figure 97) is obtained. This relationship shows, first of all, that division of the receiver 1.5-2 times increases initial stability of the ACV with the rest of the equal conditions and, secondly, that the arrangement of a sectioned-off skirt inside from the rigid jet ($\overline{\beta}_{BH} \geqslant 0.24$ in the given situation) allows a value for the derived example twice as high as the usual air supply to be obtained for all three cushion sections.

Thus, it might be said that there are considerable reserves of surplus initial stability for the designed ACV that are not used in known designs of craft and a number of design measures may be worked out to allow a decrease of external forces at the onset of "plow-in" by the ACV. However, if design measures are provided for, this does not exclude the necessity to stipulate in the instructions (for the craft's pilot) the conditions for safe operation and a sequence of maneuvers for the threat of capsizing. In particular, it is sometimes expedient to introduce restrictions on permissible drift angles [105] in relation to speed of the craft (Figure 98), as well as restrictions on the amount of yaw. For control of the ACV, on the pilot's panel are: a speed indicator, a trim meter, drift angle indicator and angle of yaw indicator.

On the basis of results of tests and analysis, the following recommendations may be made for regulating the decrease in probable capsizing for Class A ACVs during movement.

1. The ACV must have a high enough initial stability. Minimum values of non-dimensional initial metacentric height are

$$\overline{m}^\theta_{xB} \geqslant 0{,}35 \div 0{,}40;$$

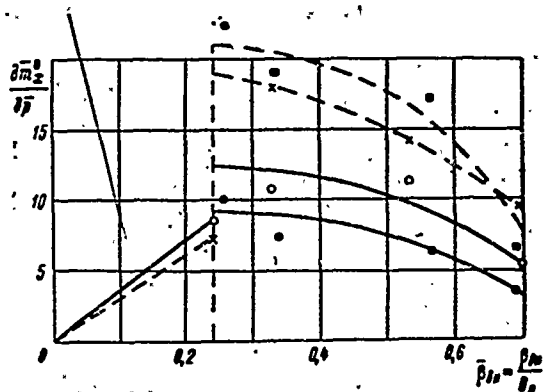$$\overline{m}^\theta_{zB} \geqslant 0{,}90 \div 1{,}00.$$

Figure 97. Relationship of Derivative $\partial \overline{m}^\theta_x / \partial \overline{p}$ to a Sectioned-Skirt Arrangement in a Class A ACV Model Lift System.

---X ■ , Divided receiver; - O - ● , Common receiver; X O, Suspension above a screen; ■ ● , Suspension over water.
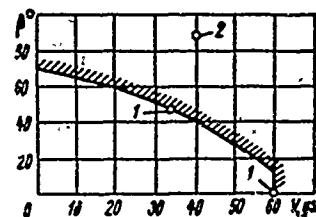
.Figure 98. Permissible Drift Angles for the SK-5 in Relation to Speed. 1, Model experiment; 2, Actual experiment.

For increase of initial stability in the ACV, the following measures may be applied:

separation of all lift systems into sections, beginning with the fan and receiver;

increase of the coefficient of pressure $\overline{p}$, which usually is essential to an undivided receiver;

use of the fan with great signifcance placed on the derived character-istic $\partial H / \partial Q$;

use of a plan for sectioned-off air cushion with parameters of $\overline{\beta}_{BH}$ = = 0.4-0.5.

It is possible that the non-dimensional longitudinal initial meta-centric height of $\overline{m}^\theta_{zB}$ = 1.0, in future tests will prove inadequate and not allow a decrease of the probability of "plow-in."

-187-

2. Design of the flexible skirt, because of the action of wash forces X_{r1}, must permit surrounding deformation in order to provide a minimum decrease in stability. In regard to this idea, skirt elements of type 1 (Figure 99) have the advantage, since their deformation from the action of X_{r1} is considerably less than deformation in type 2, which leads to less shift in the center of pressure of the air cushion during skirt wash.

The value of X_{r1} may decrease, providing for the manufacture of skirt material possessing a lower coefficient of friction during wash by a stream of water, as well as the use of various design measures (mounting of the prop; collapsible, smooth, streamlined skirt; air fed to the wash area; use of transversely-separate design for the side skirt, etc.).
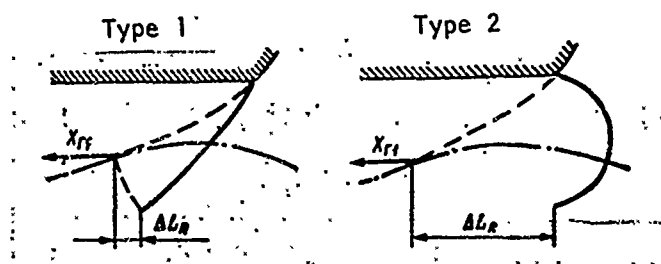
Figure 99. Comparison of Deformation of Two Types of Flexible Skirts in the ACV's Bow Sections, Resulting in Contact with Water.

3. The probability of capsizing as a result of "plow-in" may be decreased with a rational design of the ACV's rigid hull. Tightness of the hull section and external collapse of the side bow section must create hydrostatic and hydrodynamic forces, which provide a sharp increase in stability during the rigid hull's entry into water.

4. The probability of "plow-in" and capsizing depends on its direction of movement. In the craft's operating instructions, there must be information on acceptable speeds, drift angle, trim, yaw angle, etc. For example, for the SRN5 with generation of speeds of 70 knots and higher in tests, a safe operating speed is 60 knots with drift angles to 15°, but when the drift angle is more than 15°, the speed is decreased and when $\beta = 60°$, $V \leqslant 20$ knots is permissible. Practical testing established critical values of negative trim $|\psi| \leqslant 2.5\text{-}3°$ and yaw angle of $\partial\beta/\partial t \leqslant \leqslant 3\text{-}3.5°$ per second.

As the test results show, a Class A ACV's stability increases with increase in the fan's rpms, therefore, when a dangerous situation occurs it is helpful to increase the fan's rpm, which causes increased rigidity of the pneumatic sections of the flexible skirt and improves the ACV's dynamic stability, thanks to an increase of hydroscopic moment of the fan's operation.

The probability of a Class B ACV capsizing may be decreased by using design measures and providing correct control of the craft's movement.

It is recommended that design measures be applied to the design of the bow section of the hull in view of the jutting forward of the hydrofoils, having moderate pitch (Figure 100) which must be increased for longitudinal and diagonal stability.
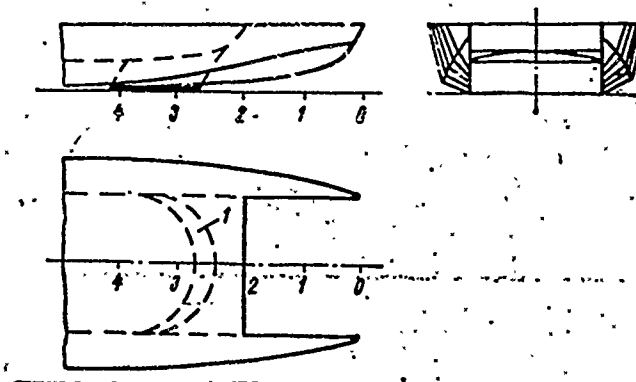

Figure 100. Outline of Class B ACV Bow Sections, Which Lessen the Probability of "Plow-In." 1, Bow flexible-skirted air cushion.

Obviously, additional investigation into the influence of the form of surroundings and the parameters of an operational lift system on the stability of a Class B ACV will allow more concrete recommendations to be made.

Chapter IV.   The Speed of ACV's

§17.   Aerodynamic Components of Resistance

In Chapter III, the basic features of the hydroaerodynamics of
ACV's are set forth and the general formula (12) for determining the
external moments of force which act on the ACV's in movement is given.
On the basis of this formula, the resistance during the ACV's movement
(as well as in other type craft) is determined to be the total of
several combined factors determined independently of each other.

It is known that such a principle gives, in practice, quite satis-
factory results in calculating the resistance for ACV's, and apparently it
is more vital. As, for example, the sucking inside the body of a great
volume of air cannot be reflected in a quantity of the aerodynamic pro-
file resistance. However, in the present chapter, questions concerning
the reciprocal actions of differently composed resistance will be touched
upon, if only superficially, as far as such a reciprocal action in strong
measures is determined by the design features of each ACV.'
General regualarities in current times are impossible to ascertain.

The aerodynamic frontal resistance X_a appears as a projection of forces
$\vec{R}_{al}$ [see formula (9)] on axis x

$$X_a = -\iint_{\sigma_1} [\Delta p \cos(n, x) + \varepsilon \cos(\tau, x)] d\sigma. \tag{153}$$

For basic parameters, determination of the quantity of the aerodynamic resistance X_a usually takes into account the coefficient of aerodynamic resistance c_a, the speed relative to the air V, and the area of the frontal sections of the ACV Symbol

The quantity of resistance X_a is computed by the formula

$$X_a = c_a \frac{\rho V^2}{2} S_{\mathfrak{M}}. \tag{154}$$

Aerodynamic resistance of the ACV appears in basic vertical resistance, i.e., resistance forms

$$X_a \approx - \iint_{\sigma_t} \Delta p \cos(n, x) \, d\sigma. \tag{155}$$

For the illustration below, calculation is made of the value of the coefficient for the resistance of friction in three models, in comparison with the coefficient for the profile resistance, obtained in a wind tunnel (see Table 7). It is obvious from the table, that, for these models, the role of friction resistance really isn't much and, consequently, the principle portion of profile resistance in the models is due to wind resistance.

TABLE 7. CALCULATION OF THE VALUE OF THE COEFFICIENT OF FRICTION RESISTANCE

Number of the Model	Coeffient of Profile Resistance of the Hull Without Tail Units, Taken to the Area Amidship in the Models c_a	Coefficient of Friction Resistance	
		Equivalent Smooth-plated Models, Taken to the Area Amidship in Super-Critical Numbers $Re(f_x tp)$	Taken to the Coefficient of the Profile Resistance $f_{x\,tp}/c_a$, %
1	0.536	0.037	6.9
2	0.536	0.039	7.3
3	0.740	0.072	9.7

The quantity of the coefficient c_a is determined by the results of testing the models in a wind tunnel. In the early stages of planning, when tests still haven't been carried out, advantage may be taken of the results of test model prototypes or other means of similar transport.

Below are meanings of coefficients of resistance from data adduced in various works, in [65] for example.

Coefficients of Aerodynamic Resistance in Some Means of Transport

Apparatus	c_a
The Volkswagen cargo automobile	0.73
A streamlined train with a special caboose	0.39
A streamlined single-decker bus	0.25
A common, mode rn-day steamship	0.68
A well-streamlined vessel	0.17
The SRN1 -- England	0.50
The SRN3 -- England	0.30
The SRN5 -- England	0.30
The VA-3 -- England	0.50

For comparison, it may be recalled that such a poorly streamlined body as a sphere in super-critical Reynold's numbers has a coefficient of resistance $c_a = 0.1$ and a squared disc has $c_a = 1.1$ in an air stream. Apparently, the hulls of all means of transport with the value c_a take up an intermediate position between these two bodies.

By such means, an ACV with a common-shaped hull might take the meaning c_a by statistical materials such as $c_a = 0.4$-0.5.

In calculating the aerodynamic resistance of a scale-size ACV, it is recommended that one implement a correction to the resistance to guard rails, Jacob's ladders, and other parts which aren't normally installed on models of ACV's. According to the standards of aircraft construction, the correction for small projecting parts make up from three to seven percent of the aerodynamic resistance.

Following this, individual computations of resistance to aerodynamic rudders, stabilizers, and other surfaces located in the air-screw's stream may be made. The speed of the moving air in the screw's stream is significantly higher than that of the ACV. Besides that, the quantity of speed in the screw's stream in many instances is changed very little in comparison to the mooring rate, even in moving at a speed of V = 50-60 knots. Therefore, forces of resistance on surfaces located in the blowing air depend little upon speed. These forces may be computed approximately by the usual formulae of hydromechanics with a calculation of the summoned speed of the air screw, resulting from preliminary values of draught, necessary for the movement of the ACV.

The quantity of impulse resistance appears as a projection of forces $\overset{\star}{R}_{a3}$ on axis x [formula (15)]. It is computed by the theoretical formula

$$X_{\mathfrak{a}} = \rho Q V.$$

<div align="right">(156)</div>

Impulse resistance appears as a strong inertia of air, drawn into movement along with the craft. The mechanism of the formation of forces of impulse resistance in a particular case -- in data from the design of the air-gate -- is illustrated in Figure 101. It is apparent from the drawing that the force of the impulse resistance appears because of the asymmetrical entry of air into the shaft of the fan at half speed -- -- part is responsible for rarefaction in the bow-section shafts and part increases pressure in the stern-section shafts (Figure 101). On this basis, it is possible to figure that the point of application of impulse resistance is found in the region of the air-gate apertures. It is natural that it may shift in relation to specially-designed ventilator shafts.

A more severe point of application of the force of impulse resistance is formed as a result of calculations of all aerodynamic moments which act on an ACV relative to axis z. Apparently, from formula (156), the quantity of this force depends on the expenditure of air and the speed of the craft. The quantity of air expenditure appears as one of the parameters determined during the designing of the ACV. However, this usually means that the quantity of the expenditure in lift without movement is, by comparison, easy to measure during the building of the craft. It is consideralby more complex to determine the quanity of the expenditure in a moving craft. At the same time, it is known that the quantity of the expenditure during movement may change considerably. This offers, first of all, a change in the characteristics of the net- work in which the craft's fans work, due to various deformations of the water's surface under the craft at various speeds, and also the beginning of the aerodynamic lift forces on the ACV's hull, decreasing the load on the water, the pressure in the air cushion and in the re- ceiver. Secondly, the velocity of the air pressure, passing through the fans, partially decreases the overall pressure created by the fans, which also leads to an increase in air expenditure. The extent to which the velocity of the air pressure is used depends on the design of the shafts of the air-gates and the correlation of the speed of movement and the air speed in the shafts.
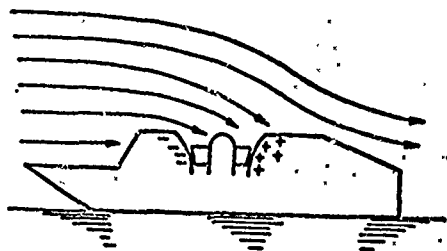

Figure 101. Diagram of the Formation of Impulse Resis-
tance.

.In Figure 102 a relationship is adduced, characterized by the degree of use of the velocity of pressure for several models of ACV's with airgates of various designs.

In some cases there is an influence due to the unloading of the ACV while moving, in which the design of the air-gates leads the quantity of air expenditure in the moving ACV to be decreased 20 to 30%.

Currently, in practical designs, these factors of resistance are not taken into consideration. However, in future investigations, accumulated tests and improved theories on ACV's, it will be necessary to consider them. Impulse resistance in modern ACV's reaches 30 to 35% of the full amount of resistance while moving at maximum speed. At low speed, the effect of this force is nil.

One kind of resistance formed in the ACV is the reaction force of the air stream, X_i, escaping from the air cushions. This force is itself a projection of the axis x forces R_{a5} [see formula (17)]. It possesses a number of specific properties.
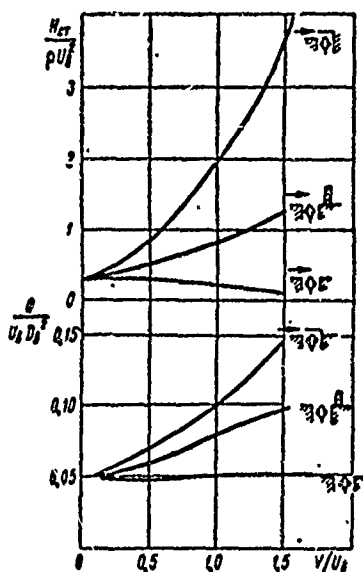
Figure 102. Effect of the Air-
gates' Design and the Head-on
Air Stream of Pressure and the
Production of the Fans of the
ACV.

U_b, peripheral speed at the tips of the fans' blades; D_b, diameter of the fans.

First of all, it usually does not equal 0 in lift of the ACV without moving (at stop).

Secondly, this force may be adverse or positive, i.e. it appears as draught or a form of resistance.

According to N. Walker [77], the quantity of resistance in model ACV's, tested over a hard screen in a wind tunnel, was formed with a relationship to

$$c = c_a + k^+ c_{u'}$$

(157)

where

    c -- non-dimensional coefficient of the full quantity of resistance, measured by a dynometer in the wind tunnel with the fan on;

    c_a -- coefficient of profile aerodynamic resistance with the fan on;

    -- coefficient of impulse resistance to the models;

    k^+ -- experimental coefficient, changing in range from -0.3 to +2.3 depending on the speed of the blowing wind and the design of the air-gates' shafts.

Consequently, according to our terminology, for these models the quantity of the coefficient of reaction forces c_i is composed of

$$-1,3c_u < c_i < 1,3c_u.$$

The greatest quantity of reaction force may be acquired in the escape of all air from the cushions on one side, in the bow or in the stern, that occurs close to the implementation in type B craft. In this case, the maximum possible quantity of reaction is:

    $X_i = pQVr$ -- in escape from the stern;

    $X_i = -pQVr$ -- in escape from the bow.

In nozzle-type craft and ACV's with flexible skirts, the escape of air along the perimeter usually occurs uniformly on all sides and this uniformity is broken only during inclination of the ACV relative to support on the water's surface or a screen. In case of a significant incline relative to support on the surface, the reactive force may reach 50% or more of the maximum possible quantity (Figure 103), however, more often it does not exceed 20 to 30%.

In practice, the escape of air from the cushions occurs, basically, on the side where resistance to escape is least. In particular, during lift over a hard screen, the quantity of reaction force depends considerably on the trim difference ψ, and the force itself on direction to the side of the sunken extremity, since the escape of air occurs on the side of the raised extremity.

This result is illustrated by experimental materials (Figure 103). For a craft with a flat bottom to be suspended over a screen with little trim difference ψ is well confirmed by the formula

$$X_i = G \tan \psi. \qquad (158)$$

There is an analogous relationship to its movement along the water, however, in this the quantity of reaction force turns out to be proportional not to the trim difference ψ, but to the average incline angle relative to the deformation of the water's surface

$$\psi = a ,$$

where a -- average incline angle of support on the water's surface to the horizon under the influence of a system of transferring pressure to the air cushion.
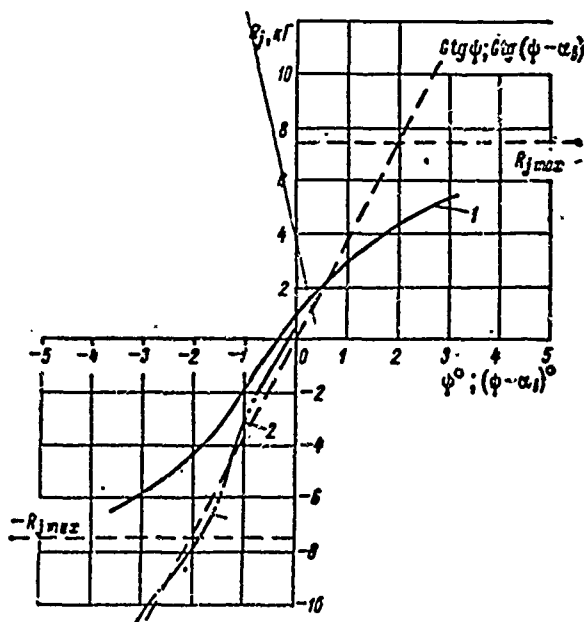
Figure 103. Relationship of the Relative Reaction Force of Air Streams to the Incline Angle in Support on the Surface in Free Trim Difference of an ACV.
1, in suspension over a hard screen; 2, in movement over water.

A practical quantity of wave incline angle may be found proceeding from the following correlation (Figure 104). Wave resistance

$$X_s = \iint_\Omega p_n \cos(n, x_0) d\sigma.$$ (159)

The weight of the craft (without calculating the lift forces on the hull and jet stream)

$$G = -\iint_\Omega p_n \cos(n, y_0) d\sigma.$$ (160)

In calculating the small quantity of the angle (n, y_0), one gets

$$G \approx -\iint_\Omega p_n d\sigma.$$ (161)

$$\angle(n, x_0) = a_s + \frac{\pi}{2};$$

The angle is

where a -- is the local angle of incline to the horizon of the free water's surface (see Figure 104).

Substituted in the integral (159) by the formula $\angle(n, x_0) = a_s + \frac{\pi}{2}$ and using the theory of averages, we get

$$X_s = -\iint_\Omega p_n \sin a_s d\sigma \approx a_s G.$$ (162)

Figure 104. Diagram of Wave Formation During Movement in a System of Surface Pressure.

-197-

From this, there arises a formula for the practical calculation of the average wave incline angle

$$\alpha_\bullet = \frac{X_\bullet}{G}.$$ (163)

During lift over water without moving, the adduced correlation sometimes is broken because of the appearance of an additional force, called jet spray. This problem is examined in more detail in the following paragraph.
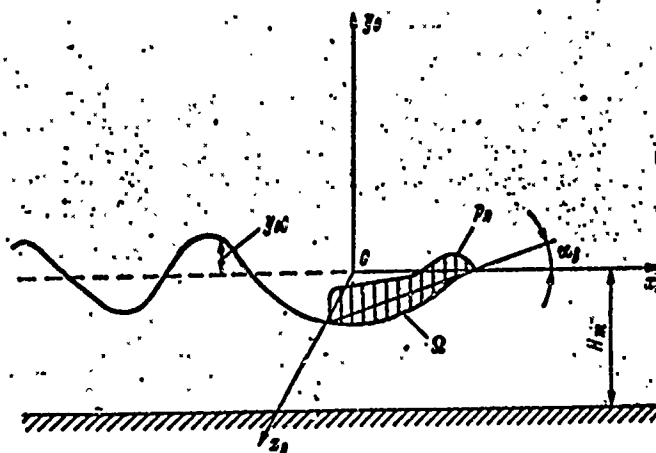
Currently, methods have not been devised for the calculation of values of reactions to the air stream. This resistance was formed solely by experimental means as a result of testing tug-type ACV models. A scheme for carrying out the experiment and a method of computing resistance are examined below.

Although experimental means exist for determining reaction force, a search for the path of its theoretical values appears urgent and the importance of resolving these problems especially exists in the early stages of planning.

To get the values of the reaction force in the air stream, it is necessary to know how the air escapes from the air cushions and by which factors this phenomenon is formed.

To such factors, apparently, may be attributed:

1) The correlation of pressure quantity in the air cushion and pressure velocity of the head-on air current;

2) A picture of the wave formation on the free water surface, in particular under the hull of the ACV., i.e., in the region of the air cushions;

3) Designed implementation of air-feed to the cushion, as well as a scheme for sectioning the air cushions.

The problems of wave formation and wave resistance are examined in detail in the following paragraph. For the characteristics of resistance, in the escape of air from the air cushions, the following two circumstances should suffice:

1) Wave cavity systems radiating waves appear as a way for the escaping air in the direction of the stern under an angle of approximately 18° to the diametrical plane of the ACV. Such a way is impossible.

2) In relation to the Froude number system, transverse waves create favorable conditions for escaping air either in the stern (Fr < 0.6), or in the bow (Fr > 1.0), which is illustrated in Figure 44.

It is evident that the direction of the basic stream of air, to a great extent, is formed by longitudinal centering and, consequently, by the trim difference of the ACV in movement. The more an ACV's trim difference in the

stern, the greater portion of air escapes in the direction of movement; the more in the bow, the greater air escapes in the opposite direction. For most, however, normally the trim difference of the craft, it seems, at low speeds (Fr < 0.6) creates more favorable conditions for escape of air in the stern, and at maximum speeds -- in the bow (see Figure 44).

The influence of still another factor, the scheme of sectioning the air cushions, in the final analysis also leads to the redistribution of the amount of air escaping along the perimeter of the air cushion, i.e. a change in the quantity of reaction force.

A great deal of attention to the given problem of air distribution, in escaping from the air cushions, isn't by chance. The quantity of resistance or draught, arising because of the escape of air, is at times comparable to the total of all remaining resistance combined. It is known that some of Professor V. I. Levkov's launches did not have special propelling agents and could go at speeds of up to V = 70 knots under the action of the jet draught.

In connection with this, it is interesting to consider the problem of most expedient direction of the air stream, escaping from the air cushions, which may be reached, for example, by way of controlling the flexible skirts by flaps, etc.

The total power expenditure, necessary for the ACV's movement, includes two basic items: the maintenance of the air cushions and the overcoming of resistance to movement.

In the ideal case quantity of engery, used every second for maintence of the air cushions, equals a second of expenditutre of kinetic engery of air in a circular stream, escaping from the air cushions

$$T_c = \iint_{\sigma_s} \frac{V_r^2}{2}\, dm = \iint_{\sigma_s} \rho\, \frac{V_r^2 V_{rn}}{2}\, d\sigma, \tag{164}$$

where V_r - relative speed of air in the stream;

V_{rn} - its normal make up (Figure 105).

Through theorum of cosines

$$V_r^2 = |V|^2 + |V_j|^2 - 2|V||V_j|\cos(V, V_j). \tag{165}$$

Taking into account that $|V_j|\cos(V, V_j) = |V| + V_{rx}$ with $|V| < |V_j|$ and $\iint_\sigma V_{rn}\, d\sigma = Q$, we get

$$T_c = -\frac{\rho V^2}{2}Q + \frac{\rho V_j^2}{2}Q + V\rho \iint_{c_i} V_{rn}V_{r_x}d\sigma, \tag{166}$$

where V_i - speed of the escaping air from the cushions during suspension (without moving);

$\rho V^2 j/2$ - the quantity of full pressure in the receiver.

The latter item in the formula (166) is numerically equal in power, and is necessary for overcoming the force of resistance (or draught) in the reaction stream

$$X_i = \rho \iint_{c_2} V_{rn}V_{r_x}d\sigma. \tag{167}$$

In such form, independently of the direction of the air stream

$$T_c + V X_i = \left(p_p - \frac{\rho V^2}{2}\right)Q = \text{const}, \tag{168}$$

i.e. the total ideal power, spent on overcoming resistance of the reaction stream X_i and on maintaining the air cushions, is the quantity constant, not dependent on distribution of air in escaping from the air cushions.

The directed air current from the cushions to meet the running flow, allows the power consumed to be lowered without decreasing the flight height of the ACV. In this, however, so much power is developed, necessary for overcoming resistance during movement, that reaction to the air, escaping in the direction of movement, creates additional resistance.
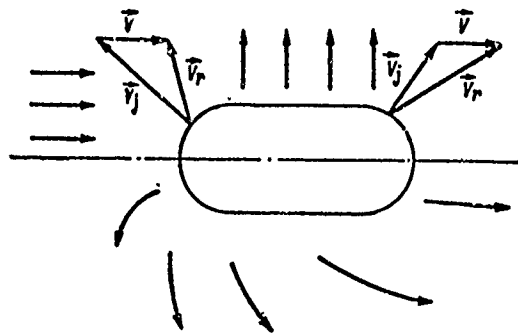

Figure 105. A Diagram for Addition of Vectors of Air Speed, Escaping from the Air Cushions, and the Head-On Stream.

This conclusion is correct in ideal conditions, when the efficiencies both in the fan and screw are equal units. In actual conditions, it is advantageous to distribute air in such a form that a large part of the power is processed by a unit with a higher efficiency. Usually the efficiency of the fan is higher than the efficiency of the air screw. Therefore, it is adviseable to lower the resistance during movement by directing the current of air in the stern, thus releasing power to transfer to the fan installation to ensure the task of flight height.

In conclusion we note that, in the number making up the forces of resistance, there appears to be still another force -- wave resistance. This force arises because of the redistribution of air pressure in the cushion, therefore its mechanism of transmission has an aerodynamic character and it acts on the ACV even in total absence of contact with the water's surface. To wit, therefore, wave resistance is looked upon as one of the forces which make up the aerodynamic nature in calculating the integral pressure of all sections of the hull's surface on an ACV.

However, the initial cause of redistribution of force of aerodynamic pressure in the cushion is the pliability of water-surface support in transferring along its system of surface pressure. In force, this wave resistance may be attributed to the category of forces of hydrodynamic nature, especially as the quantity of these forces are determined by methods of wave theory in classical hydrodynamics. In connection with this, the wave resistance of an ACV is examined, along with other problems of a hydrodynamic character, in the following paragraphs.

§18. Forces of Resistance of a Hydrodynamic Nature

Forces of a hydrodynamic nature. acting on the ACV may be divided into three groups:

1) Wave resistance;

2) Resistance due to wash, i.e. friction of water and profile resistance during immersion of part of the hull or the flexible skirts of the ACV;

3) Resistance due to spray formations.

The most studied and widely computed force is the force of wave resistance. Much research has been devoted to wave resistance of an ACV. Theoretical research into wave formation, which gave rise to a system of transferring surface pressure, was carried out at the end of the 19th and beginning of the 20th centuries by Lamb, Havelock, and Winebloom. The most common solution to these problems (for instance in a moving system of pressure along the surface of a channel, using deep skirts) was provided by M. V. Keldysh and L. I. Sedov. The investigations were of a mathematical nature and did not lead to practical, calculated methods.

In the early 1900's, in connection with the appearance of the first experimental ACV's, interest grew in computing wave resistance of an ACV. During this period, practical methods for computing wave resistance called transfer systems of surface pressure, were developed in the USSR by V. P. Bol'shakov [7] and abroad by Neuman and Poole [73] on the basis of a solution by Vegauzen. Later, a examination of the problem of wave resistance in mobile systems of pressure [17] was begun.

One of the most interesting problems is that of the mechanism of transmission of wave resistance on the ACV's hull. In this problem, two basic points of view were formed; Ya. I. Vojtkunski [11], following the method of N. E. Kochin, substitutes the moving ACV's system of sources and drains and examines the force of wave resistance as a result of the redistribution of air pressure fields around the ACV due to the rising of waves on the free water's surface under the craft. In this formula for computing resistance, the structure is similar to the well-known formula of N. E. Kochin. This method of approach is quite rigid and, in principle, cannot be called objectionable. However, practical use of this method proves unreliable for two reasons:

1) Before beginning the computations, it is necessary to know the seating, i.e. the flight height and angle of moving trim difference of the ACV in actual conditions of movement;

2) Kochin's function succeeds in determining solutions for the present only for bodies of sufficiently simple form.

Yu. Yu. Benya and V. P. Bol'shakov suggested another interpretation of the mechanism of influence of wave resistance on the ACV's hull. In this scheme, the ACV in movement acquires a trim difference equal to the average incline angle to the horizon in support of the water's surface under the craft. In this case, the resultant force of pressure in support of the water's surface Ω and on the bottom of the ACV is equal in quantity and direction of mutual opposites. The quantity of resistance, operating on the ACV, numerically is equal to the horizontal projections of the resultant force of pressure on the surface

$$X_u = \iint_\Omega p_n \frac{\partial y_{0a}}{\partial x_0} \, d\sigma. \tag{169}$$

In the actual scheme, however, they did not take into account the circumstances, which in actual conditions means that the angle of trim difference in the moving ACV could be changed to considerable limits in relation to the position of the center of gravity along the length and the quantity of moments of internal force acting on the craft.

This contradiction is cancelled out if the resultant forces of pressure along parts of the ACV's hull, bordering with the region of the air cushions, are computed using theorum of change in the amount of movement conforming to the controlled surface bordering the air cushion,

as was done in Chapter II. It may be closely computed that the force, acting on the ACV's hull from the sides of the air cushions, is the vector (by closing the triangular force) which includes the resultant force of pressure at the base of the surface and the resultant amount of movement f r one second in normal sections of the air stream escaping from the air cushions (Figure 106). Therefore, for an ACV with a flat bottom the resistance forces, acting from the sides of the air cushions, sometimes are computed according to the weight of the craft and the angle of trim difference during movement, giving the force the name "attitude resistance." The quantity of the attitude resistance is equal to the algebraic sum of the wave resistance and the horizontal projections in reaction to the air stream (Figure 106).
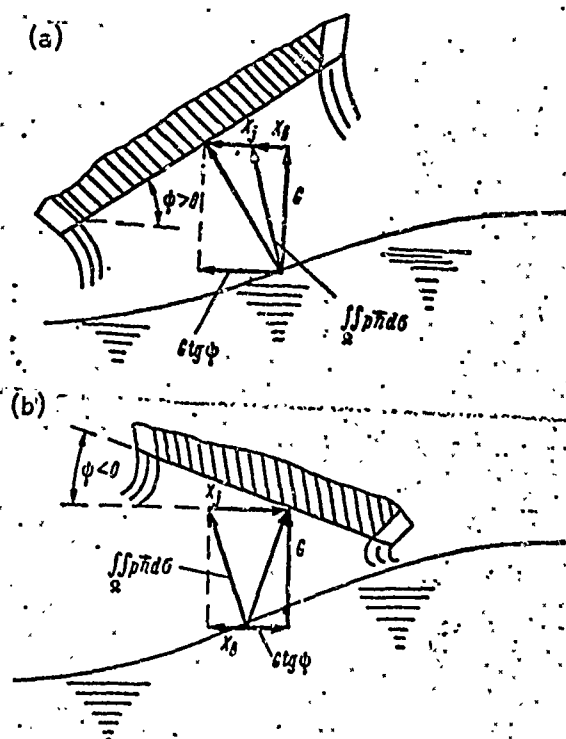

Figure 106. Diagram of the Force Which Acts on the Flat Bottom of an ACV.

. To compute wave resistance by formula (169), the so-called transfer system of surface pressure, it is necessary to know the law of distribution of ordinate wave surfaces in the region of the air cushions, i.e. the function

$$y_0 = y_{0a}(x_0, z_0).$$ (170)

This function may be found in the resulting solution of marginal problems of mathematical physics with complex boundary conditions, the conclusion of which is known in wave theory. Using the system of coordinates presented in Figure 104, these boundary conditions may be recorded for instances of mobile movement along an unrestricted wide surface in the following form:

$$\frac{\partial^2 \varphi_1}{\partial t^2} + g \frac{\partial \varphi_1}{\partial y_0} + V^2 \frac{\partial^2 \varphi_1}{\partial x_0^2} - 2V \frac{\partial^2 \varphi_1}{\partial x_0 \partial t} -$$

$$- \frac{dV}{\partial t} \cdot \frac{\partial \varphi_1}{\partial x_0} = - \frac{g}{\gamma} \frac{\partial p_n}{\partial t} + \frac{Vg}{\gamma} \frac{\partial p_n}{\partial x_0} \qquad (171)$$

$$\text{with } y_0 = 0;$$

$$\frac{\partial \varphi_1}{\partial y_0} = 0$$

$$\text{with } y_0 = -H_m,$$

where φ_1 (x_0, y_0, z_0, t) - potential speed of perturbed movement of fluid;

$\qquad$ H_m - depth of reservoir;

$\qquad$ γ - specific weight of the water.

The physical meaning of the first equation is that the free surface of fluid consists of one of those fractions and the pressure on this surface is set by the condition

$$p = p_n(x_0, y_0).$$

The physical meaning of the second equation is the absence of fluid flowing through the bottom of the reservoir.

In the case of stationary movement systems, the equation (171) is simplified and observed in the form of

$$V^2 \frac{\partial^2 \varphi_1}{\partial x_0^2} + g \frac{\partial \varphi_1}{\partial y_0} = \frac{gV}{\gamma} \frac{\partial p_n}{\partial x_0}$$

$$\text{with } y_0 = 0;$$

$$\frac{\partial \varphi_1}{\partial y_0} = 0 \qquad (172)$$

$$\text{with } y_0 = -H_m.$$

One way of solving the problem posed consists in the following. The unknown quantity of the function φ_1 (x_0, y_0, z_0, t) and the right part of

the boundary conditions (171) occurs in the form of integrals of Fourier [17]

$$\varphi_1(x_0,\,y_0,\,z_0,\,t) = \frac{1}{4\pi^2} \int_{-\infty}^{\infty} \int_{-\infty}^{\infty} \left[\dot{A}_1(t) \exp\left(-\sqrt{\alpha^2 + \beta^2}\,y_0\right) + \right.$$
$$\left. + B_1(t) \exp\left(\sqrt{\alpha^2 + \beta^2}\,y_0\right)\right] \exp\left[i\,(\alpha x_0 + \beta z_0)\right] d\alpha d\beta; \tag{173}$$

$$x\overline{V}\frac{\partial \overline{p}_n}{\partial x_0} = \frac{1}{4\pi^2} \int_{-\infty}^{\infty}\int_{-\infty}^{\infty} d\alpha d\beta \iint_{\Omega} x\overline{V}\frac{\partial \overline{p}_n}{\partial x_0} \times$$
$$\times \exp\{-i\,[\alpha\,(x_0 - x_0^{\bullet}) + \beta\,(z_0 - z_0^{\bullet})]\}\,dx_0^{\bullet}dz_0^{\bullet}, \tag{174}$$

$$x = \frac{p_{\text{ат}\text{м}}}{\gamma l}; \quad \overline{V} = \frac{V}{\sqrt{gl}};$$
$$l = \frac{1}{2}\,L_n; \quad \overline{p}_n = \frac{p_n}{p_{\text{ат}\text{м}}}.$$

Substitution of integrals (174) in the system equation (171) and solution systems after a number of transformations leads to a solution of the differential equation

$$\frac{d^2 A_2}{dt^2} + A_2 k\, \text{th}\, kH_m = \frac{\exp\left(-ik\cos\theta^{\bullet}s\right)}{1 + \exp\left(2kH_m\right)} \times$$
$$\times \iint_{\Omega} x\overline{V}\frac{\partial \overline{p}_n}{\partial x_0^{\bullet}} \exp\left[-ik\,(x_0^{\bullet}\cos\theta^{\bullet} + z_0^{\bullet}\sin\theta^{\bullet})\right] dx_0^{\bullet}dz_0^{\bullet}, \tag{175}$$

where

$$s = \int \overline{V}dt; \quad \alpha = k\cos\theta^{\bullet}; \quad \beta = k\sin\theta^{\bullet}.$$

The unknown quantity of functions A_1 (t) and B_1 (t) are formed by relationships

$$A_1 = A_2 \exp\left(ik\cos\theta^{\bullet}s\right);$$
$$B_1 = A_1 \exp\left(2kH_m\right).$$

Set by zero initial conditions (i.e. determining the problems of dispersal from the rate of suspension)

$$A_2 = 0; \quad \frac{d\overline{A}_2}{dt} = 0 \text{ when } t = 0;$$

and determination of the differential equation (175) may be obtained by the formula, forming the potential speed

-205-

$$\varsigma_1(x_0, y_0, z_0, t) = \frac{1}{4\pi^3} \int_0^\infty k\,dk \int_{-\pi}^{\pi} d\theta^* A_2 \times$$
$$\times \exp(ik\cos\theta^* s)[\exp(-ky_0) + \exp k(2H_m + y_0)] \times$$
$$\times \exp[ik(x_0\cos\theta^* + z_0\sin\theta^*)]. \tag{176}$$

Formula (176) may be used for determining deformation of the water's surface. It is known that the correlation in theories of small waves is

$$y_{0*} = -\frac{p_n}{\gamma} + \frac{V}{g}\frac{\partial \varphi_1}{\partial x_0} + \frac{1}{g}\frac{\partial \varphi_1}{\partial t}. \tag{177}$$

Substitution of formula (177) in the expression (169) after transformation leads to the concluding formula for computing wave resistance

$$X_n = p_{\text{nix}} l^2 \iint z\bar{p}_n \frac{\partial \bar{p}_n}{\partial x_0} dx_0 dz_0 -$$
$$-\frac{\pi}{4\pi^3}\int_0^\infty k\,dk \int_{-\pi}^{\pi} (ik\cos\theta^*) G(k, \theta^*) G^*(k, \theta^*) \Phi(k, \theta^*, t) d\theta^*, \tag{178}$$

where
$$\Phi(k, \theta^*, t) = \exp(ik\cos\theta^* s)[\cos\delta_1 t \times$$
$$\times \int \bar{V}\exp(-ik\cos\theta^* s)\cos\delta_1 t\,dt + \sin\delta_1 t \times$$
$$\times \int \bar{V}\exp(-ik\cos\theta^* s)\sin\delta_1 t\,dt],$$

there is
$$\delta_1^2 = k\,\text{th}\,kH_m; \tag{179}$$
$$G(k, \theta^*) = \iint_\Omega \bar{p}_n \exp[ik(x_0\cos\theta^* + z_0\sin\theta^*)]dx_0 dz_0; \tag{180}$$
$$G^*(k, \theta^*) = \iint_\Omega \frac{\partial \bar{p}_n}{\partial x_0} \exp[-ik(x_0\cos\theta^* + z_0\sin\theta^*)]dx_0 dz_0. \tag{181}$$

In formula (178), the first item takes into account static longitudinal forces, arising from gradient pressure in the cushion; the second item takes into account the additional forces of wave phenomena in the moving ACV.

The problem of wave formation in establishing moving systems of surface pressure was solved by V. P. Bol'shakov by a scheme analogous to the aforementioned.

Wave resistance in pressure-systems, transferred along the surface of extremely deep fluids (as shown in the work of [7]), is expressed by the relationship

$$X_s = \frac{g^3}{\pi \rho V^6} \int\limits_1^\infty (A^2 + B^2 + C^2 + D^2) \frac{t^4 dt}{\sqrt{t^2 - 1}}. \tag{182}$$

In systems of constant pressure, i.e. in pressure p_n = const, the coefficients A, B, C and D consist of

$$A = p_n \iint\limits_\Omega \cos(vtx_0) \cos\left(vt \sqrt{t^2 - 1}\, z_0\right) dx_0 dz_0;$$

$$B = p_n \iint\limits_\Omega \cos(vtx_0) \sin\left(vt \sqrt{t^2 - 1}\, z_0\right) dx_0 dz_0;$$

$$C = p_n \iint\limits_\Omega \sin(vtx_0) \cos\left(vt \sqrt{t^2 - 1}\, z_0\right) dx_0 dz_0; \tag{183}$$

$$D = p_n \iint\limits_\Omega \sin(vtx_0) \sin\left(vt \sqrt{t^2 - 1}\, z_0\right) dx_0 dz_0$$

V. P. Bol'shakov's concluding formula for computing wave resistance to systems of pressure, which are uniformly distributed by rectangle with correlation of sides $\mu_n = B_n/L_n$ has the form

$$X_s = \frac{16 p_n^2}{\pi \gamma} \frac{V^2}{g} \int\limits_1^\infty \sin^2 \frac{k't}{2} \sin^2 \frac{\mu_n k't \sqrt{t^2 - 1}}{2} \frac{dt}{(t^2 - 1)^{3/2}}. \tag{184}$$
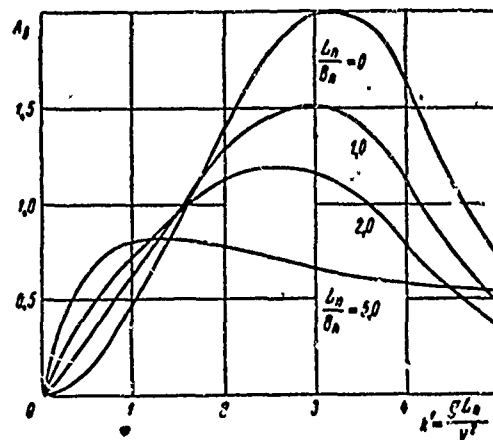

Figure 107. The Relationship of Wave Resistance to Systems of Surface Pressure in Froude Numbers.

For convient, practical use of the formulae, the meaning of the integral in formula (184) was computed on an electronic digital computer and is presented in Figure 107 in the form of a graphic relationship to the argument $k' = 1/Fr^2$ in the discrete meaning of the parameter μ_n.

-207-

Formula (184) may be obtained immediately from formula (178) by way of maximum transition at times with

$$V(t) \to const, \quad t \to \infty.$$

A greater volume of analogous calculations was accomplished by Neuman and Poole for rectangular and elliptical (in plane) systems of uniform pressure in moving in a channel.

The solution to such problems of wave formation, during movement with extremely wide regions of surface pressure, may be obtained by such a form as the solution to spatial problems. The final formulae for calculation of wave resistance, following forms.

In unsettled movement of resistance, falling into single widths,

$$X_a = p_n i \varkappa \int_{-1}^{1} \bar{p}_n \frac{\partial \bar{p}_n}{\partial x_0} \, dx_0 + \bar{V} \int_{0}^{\infty} k^2 \mathrm{Re}[\Phi \cdot G] \, dk +$$

$$+ \int_{0}^{\infty} k \frac{d}{dt} [\mathrm{Im}(\Phi \cdot G)] \, dk, \tag{185}$$

where

$$\Phi(k, t) = W_1 \exp(-iks); \tag{186}$$

$$G(k) = \int_{-1}^{1} \bar{p}_n \exp(-ikx_0) \, dx_0; \tag{187}$$

$$W_1 = \frac{1}{\delta_1} \sin(\delta_1 t) \int f \cos(\delta_1 t) \, dt - \frac{1}{\delta_1} \cos(\delta_1 t) \int f \sin(\delta_1 t) \, dt; \tag{188}$$

$$f = \exp(iks) \left[\frac{\varkappa \bar{V}}{\pi} \int_{-1}^{1} \bar{p}_n k \sin(ku) \, du - i \frac{\varkappa \bar{V}}{\pi} \int_{-1}^{1} \bar{p}_n k \cos(ku) \, du \right]. \tag{189}$$

In fixed movement of resistance in single widths, there is (Lamb's formula)

$$X_a = \frac{4p_n^2}{\gamma} \sin^2 \frac{gL_n}{2V^2}. \tag{190}$$

The results of the calculations of wave resistance according to formulae (185) and (190) are shown in Figure 108. In accordance with Lamb's formula, wave resistance in fixed movement takes a number of maximum meanings as far as increasing speeds

$$X_{am} = \frac{4p_n^2}{\gamma}$$

with the meaning of relative speeds

$$Fr = \sqrt{\frac{1}{\pi(2n+1)}}, \quad n = 0; 1; 2. \ldots$$

The last "hump" of wave resistance corresponds to $n = 0$, i.e.

$$Fr = \sqrt{\frac{1}{\pi}} = 0,563.$$

After exceeding this speed, wave resistance diminishes monotonically. The influence of mobility on the quantity of wave resistance, corresponding to Figure 108, leads to a lower amount of "hump" wave resistance with the removal of "hump" at great speeds and with an increase in resistance in comparison with stationary movement where the Froude number > 1.0. In practice, usually no more than 1-2 "humps" of resistance are displayed in the range of speed

$$0 < Fr < 0.563.$$

This, apparently, is explained by the action of the force's viscosity which is not taken into account in theory.
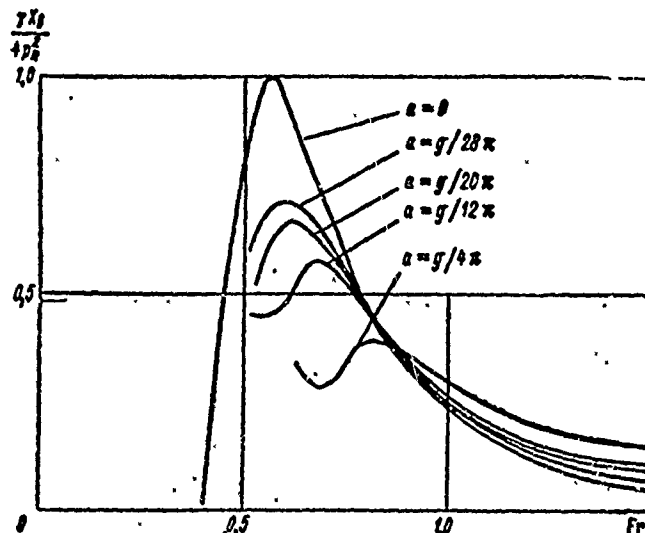

Figure 108. The Relationship of Wave Resistance of a Flat System of Surface Pressure to Froude Numbers.

-209-

The theory of waves allows the possibility to determine the profile of the deformed water surface in the region where there is higher pressure, in the air cushion.

According to [29], the profile of the free surface for the concentration of concentrated sources of pressure equals (Figure 109)

$$y_{0a} = \frac{\varkappa p_n}{\pi \gamma} \left[2\pi \sin\varkappa x_0 + \int_0^\infty \frac{m \exp(mx_0)}{m^2 + \varkappa^2} \, dm \right]$$

$$\text{with } x_0 < 0.$$

(191)

The profile of the surface in front of the sources of pressure equals

$$y_{0a} = \frac{\varkappa p_n}{\pi \gamma} \int_0^\infty \frac{m \exp(-mx_0)}{m^2 + \varkappa^2} \, dm \text{ with } x_0 > 0.$$

(192)
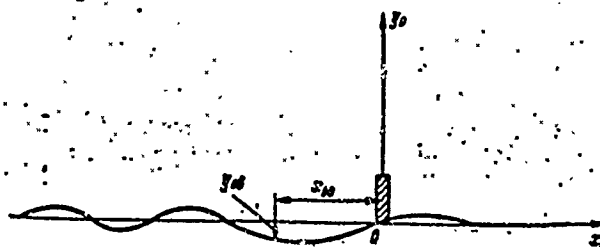
Figure 109. Diagram of Wave Formation During Movement with a Concentration of Concentrated Sources of Pressure.

At the point of the air cushions with abscissa x_{0B} the quantity of the ordinate Y_{OB} becomes the sum of the influence of sources set at point X_0 where substituted in formulae (191) and (192) the quantity X_0 in X_0-a and (191) is integrated by a in the boundary of $(X_{OB}, -1)$, and then the results of the formula are set down, taking into account the profile of the surface in the region of the surplus pressure,

$$\frac{y_{0B}}{p_n/\gamma} = -2\left[1 - \cos\varkappa(l - x_{0B})\right] -$$

$$- \frac{\varkappa}{\pi} \int_0^\infty \frac{\exp[m(l - x_{0B})]}{m^2 + \varkappa^2} \, dm + \frac{\varkappa}{\pi} \int_0^\infty \frac{\exp[-m(x_{0B} + l)]}{m^2 + \varkappa^2} \, dm.$$

-210-

Formula (193) may also be written in another form, more convenient for immediate numerical estimation,

$$\frac{y_{0\text{в}}}{p_n/\gamma} = -2[1 - \cos\varkappa(l - x_{0\text{в}})] - \frac{1}{\pi}\left\{\left[\frac{1}{2}\pi - \right.\right.$$
$$\left. - \text{Si}\,\varkappa(l - x_{0\text{в}})\right]\cos\varkappa(l - x_{0\text{в}}) + \text{Ci}\,\varkappa(l - x_{0\text{в}}) \times$$
$$\varkappa\sin\varkappa(l - x_{0\text{в}})\Big\} + \frac{1}{\pi}\left\{\left[\frac{1}{2}\pi - \text{Si}\,\varkappa(l + x_{0\text{в}})\right]\cos\varkappa(l + \right. \tag{194}$$
$$\left. + x_{0\text{в}}) + \text{Ci}\,\varkappa(l + x_{0\text{в}})\sin\varkappa(l + x_{0\text{в}})\right\},$$

where

$$\text{Si}\,(x) = \int_0^x \frac{\sin t}{t}\,dt; \quad \text{Ci}\,(x) = -\int_x^\infty \frac{\cos t}{t}\,dt,$$

The results computed according to formula (194) are given in Figure 110.

The theory of waves is also used to carry out the numerical estimations of deformation of the free water's surface for large removal of the moving belts. of pressure. Just as in the problem of plane, the values adduced naturally are attributed only to a system of transverse waves stirred up by the moving ACV. According to [29], the equation for free surfaces has the form of

$$y_{0\text{в}} = \frac{4p_n}{\gamma}\sin\frac{1}{2\text{Fr}^2}\cos\frac{x_0}{L_n\text{Fr}^2}. \tag{195}$$

For large removal in the ACV, a system of sinusoidal waves is developed. At a point remote from the center of the air cushions in the quantity

$$x_0 = L_n\text{Fr}^2(2\pi n) \quad n = 1;\ 2;\ 3\ldots$$

higher water level constitutes

$$y_{0\text{в}} = \frac{4p_n}{\gamma}\sin\frac{1}{2\,\text{Fr}^2},$$

i.e. maximum wave amplitude

$$y_{0\text{в}m} = \frac{4p_n}{\gamma}.$$

With $\text{Fr} \to \infty$ $y_0 \to 0$, i.e. at great speed of movement, the waves vanish.

The length of the waves equal $\lambda' = \mathtt{\pi L} \ Fr^2$ and is increased in light of increases in speed. The maximum angle of wave incline

$$\frac{\partial y_{\theta z}}{\partial x_\theta} = \frac{4p_n}{\gamma L_n} \cdot \frac{1}{Fr^2} \sin\frac{1}{2Fr^2} \to 0 \quad \text{при } Fr \to \infty. \tag{196}$$

Formulae (195) and (196) may be utilized for numerical estimation of deformation of free surfaces, the qualitative description of which was given in Chapter II.

In practice, the design and exploitation of the ACV is often hampered by the difficulty in overcoming the "hump" of wave resistance. The selection of power of a mechanical plant in the ACV depends, to a great extent, on the quantity of draught necessary for overcoming the "hump" resistance. Reserve draught also determines the possibilities for increasing weight, i.e. the receipt of additional cargo on the ACV.

We note that there exists a potential reserve to lower the draught, necessary to the ACV's momentum in the case of using optimum dispersal rates, i.e. optimum quantity of acceleration a.

The possibility of lowering the necessary draught is illustrated by the following example.

In the momentum of the ACV, at each moment t is the correct differential equation

$$\frac{G}{g} a = P - X_a - \Sigma X, \tag{197}$$

where ΣX - resistance to the moving ACV for elimination of the wave's composition.

We will figure that this part of the resistance doesn't depend on acceleration of momentum. In non-dimensional form, the equation (197) has the form of

$$\frac{a}{g} = \frac{P}{G} - \frac{X_a}{G} - \frac{\Sigma X}{G} \tag{198}$$

or, in brief, is written as

$$\overline{P} = \widetilde{a} + \overline{X}_a + \Sigma\overline{X}. \tag{199}$$
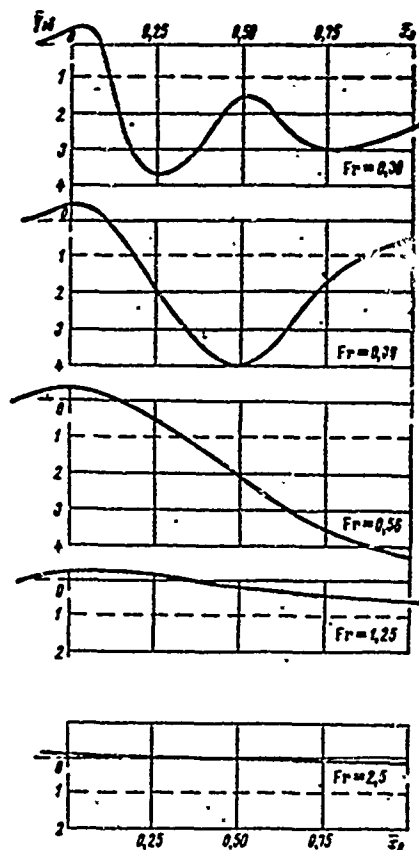
Figure 110.   Profile of the Deformed Water's Surface in the Air Cushion.

$$\bar{y}_{0n} = y_{0n}/(p_n/\gamma)$$

_____ at speed;   _ _ _ _ _ _ _ _   at "stop;"

$\bar{x}_0 = x_0/L_n$ where x_0 is figured from the front edge of the air cushion.

As shown in equation (199), in the constant meaning ΣX = const the quantity of the draught necessary for overcoming the "hump" resistance is greater than the acceleration a and the maximum meaning of the wave resistance

$\bar{X}$. But, in Figure 108, one can see that $\bar{X}$ is decreased with the increase

of $\bar{a}$. Consequently, in the right-hand portion of equation (199) is the sum of the two functions, from which one increases and the other diminishes with the increase of the quantity of acceleration. This lends to the possibility of the extreme meaning of the quantity necessary for draught P in some meanings of a, by determining the outcome of the condition

$$\frac{\partial \bar{P}}{\partial \bar{a}} = 1 + \frac{\partial}{\partial \bar{a}}(\bar{X}_{\mathit{nm}}) = 0. \tag{200}$$

We use the acquired correlation in the investigation of wave resistance of belts of pressure of single widths and lengths of $2l$ (in the direction of movement). The quantity of the lift forces of such a system equals $G = 2p_n l$, the quantity of non-dimensional wave resistance is $\bar{X}_s = \dfrac{X_s}{G} = \dfrac{X_s}{2p_0 l}$.

We denote

$$\Phi(\bar{a}) = \frac{l X_{sm}}{4 p_n^2} = \frac{\gamma l}{2 p_n} \bar{X}_{sm}(\bar{a}).$$ (201)

In fulfilling the condition of (200)

$$\frac{\partial \bar{X}_{sm}}{\partial \bar{a}} = \frac{2 p_n}{\gamma l} \frac{\partial \Phi(\bar{a})}{\partial \bar{a}} = -1,$$ (202)

i.e.

$$\frac{\partial \Phi(\bar{a})}{\partial \bar{a}} = -\frac{\gamma l}{2 p_n}.$$ (203)

A diagram of the function $\Phi(\bar{a})$, reconstructed from the diagram in Figure 108, is shown in Figure 111. Just as the curve of reversion is vivid below, the extreme meaning of draught is at a minimum.

The working out of graphic differentiation function $\Phi(\bar{a})$, using the condition in (203), may be accomplished in relation to the quantity of under-dome pressure and length of air cushions of the following quantity of relative acceleration of momentum. With p = 500 kilograms of force per m^2, $2l$ = 40 meters $\bar{a}$ = 0.015 and in lowering of the "hump" of wave resistance,

$$\frac{X_{sm\,(\bar{a}=0.015)}}{X_{sm\,(\bar{a}=0)}} = 0.7.$$

With p = 300 kilometers of force per m^2, $2l$ = 14 meters $\bar{a}$ = 0.025 and

$$\frac{X_{sm\,(\bar{a}=0.025)}}{X_{sm\,(\bar{a}=0)}} = 0.5.$$

The example illustrates the existence of the optimum rate of momentum of the ACV. The quantitative values of gain in draught and the quantity of optimum accelerations must be formed on the basis of experimental materials, since a number of factors were not taken into consideration in the adduced diagrammatic example, e.g. the spatial character of wave formation, the progression X_{BM} from Froude numbers in modifying $\bar{a}$ and the relationship of the remaining parts of resistance to acceleration.
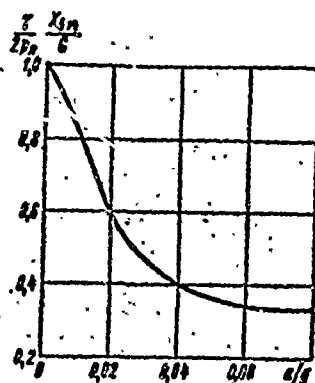
-214-

Figure 111. The Relationship of Maximum Quantity of Wave Resistance to the Relative Quantity of Acceleration of Movement.

The second resistance formed, of a hydrodynamic nature, is the force of resistance due to wash-off, i.e. the force of water friction and the profile resistance from submerging part of the hull or the flexible skirts into water. Usually, in designing the ACV, all measures are taken to eliminate the possibility of wash-off or decrease the harmful after-affects of wash-off which leads to a drop in speed.

However, solving this problem doesn't always work out satisfactorily. First of all, wash-off and additional resistance is practically inevitable in an ACV that is moving over waves. Secondly, the quantity of this portion of resistance essentially depends on the constructive type of ACV and even on details of construction of the ACV for craft of a single type.

The best possibilities for lowering resistance are in the design of an ACV with a flow of air skirting the cushions, ensuring equally great height of takeoff in soaring over a hard screen and minimal wash-off over water.

In craft with a chamber principle of air flow from the cushions, susceptibility of the influence of wash-off is significantly stronger. Finally in designing Class B ACV's, the designers deliberately keep in balance the resistance of considerably strong resistance to water, compensating the power expenditure in its overcoming by decreased expenditure of air and power consumed by the fan.

Third, in practice, this usually succeeds in ensuring total absence of contact with water only momentarily in limited range of speed of movement.

Test operation of tug-type model ACV's show that, at the moment of overcoming "hump" of wave resistance or in the area of speed close to this rate, wash-off practically always occurs in the bow section of the hull or the flexible skirts of the ACV.

This rate of curve resistance usually conforms to the additional peak of resistance, connected with the appearance of wash-off. Wash-off in the bow may be avoided successfully only by very great lift height, i.e. at a height of suspension over a screen considerably exceeding the depth of the sinking water under the craft, in suspension (without movement) at "stop." This may be attained essentially by increasing the expenditure in lift and movement of the ACV.

-215-

Usually, in connection with the overcoming of wash-off, the peak of resistance in the region of the "hump" does not require an impossible power expenditure, since this phenomenon occurs at a low speed of movement. The problem of wash-off of the hull or flexible skirts in the stern section of the craft, which often occurs at high speeds, is more difficult to solve. This resistance, by its very nature, appears as profile resistance typical to a poorly-streamlined body, since it appears as phenomenon "bevelled" from the water jets on the rigid hull or flexible skirts facing toward the oncoming flow of air (Figure 112) or other parts of the stern section's flexible skirts in the absence of air flowing out.
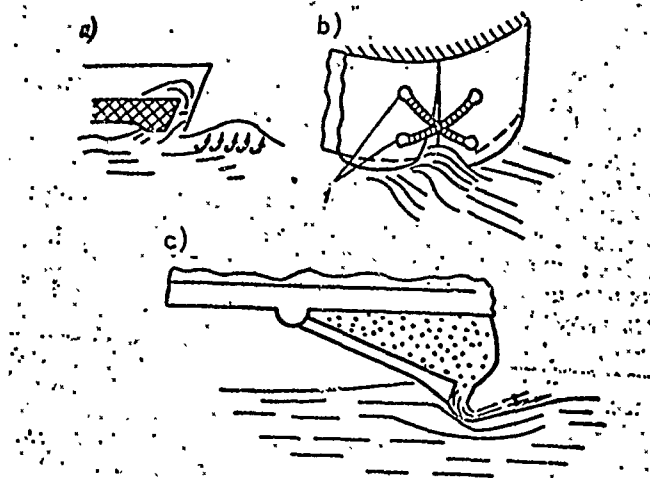
Figure 112.. Sketch of the Interaction with Water of Various Versions of Designs of Stern Sections to Skirt Air Sections:
a, rigid sidewall; b, flexible skirts with cross-sections and rubber shock absorbers; c, rigid flap with jet, absorbing shock with a section of the flexible receiver.
1, rubber shock absorbers.

The appearance of this phenomenon usually may be judged by the intensive trail of foam from the stern of a moving model or craft. In the fight against this, the designers use various constructive solutions, for example, installing rigid or soft steps in the stern part of the ACV. The hydrodynamic idea of this measure leads either to an increase in clearance between the water and the hull in the stern, or to the replacement of profile resistance with water friction. Some types of constructive designs for the stern parts of the flexible skirts are presented in Figure 112. For Class B craft with the basic type of resistance due to wash-off, there is friction in the boat or the skegs on the water.

To lower resistance in this case, well-tried glider structure methods of stepping the boat, installation of splash-guards in the bilge, etc. are used. These measures, combined with a considerable reactive draught of air, flowing out in the stern, allow for attainment in a number of cases of a very high hydrodynamic quality for ACV's of the chamber type on calm water, G/X = 25-30. However, in moving even over insignificant waves (about state 2 sea conditions) the resistance to movement is increased sharply due to wash-off on the hull.

For craft with skegs, the resistance from the friction of the hull to the water is itself the most essential component in the general balance of resistance. This part of the resistance, in the end, determines that range of speed which the application to an ACV with skegs is expedient.

Faced with the power expenditure of the ACV, the design of which provides a great expenditure of air (for example, an ACV of nozzle structure and flowing air skirting the air cushions), and an ACV with skegs leads to the conclusion that, in the initial stages of movement (at low speeds), a significant portion of energy is spent on maintaining the air cushions and the overcoming of impulse resistance. In connection with this, the quantity of impulse resistance is relative to the linear speed and this portion of energy accelerates in increased speed according to square-law. The quantity of resistance from friction of hull to water increases with the rise in speed roughly by square-law, and the power necessary for overcoming this resistance by cube-law.

So, the advantage of an ACV with skegs becomes apparent at low speeds, and an ACV with flow-through skirts, on the contrary, at high speeds. In published data [4], based on experimental research, the use of an ACV with skegs proves most expedient in the range of relative speed

$$0 < Fr < 1.$$

One of the least-studied forms of resistance is splash resistance of an ACV. The influence of spray formation on the quantity of resistance becomes apparent in two ways. First of all, the splashing water effects the flow of air from the receiver in the air cushion, which leads to a redistributed quantity of air flowing from the cushions at various points along the perimeter of the air barrier, i.e. to a change in the quantity of reactions to air flow.

In this, just as the water splashes, so also a deformation of the base surface of the water leads to a considerable change in the speed of air movement in the jets compared to the rate of lift over hard screens. The experimental results of Everst [67], illustrating this phenomenon, are shown in Table 8.

TABLE 8. RESULTS OF MEASURING THE QUANTITY OF PRESSURE AND SPEED OF AIR FLOW IN THE JETS OF MODEL ACV'S

Angle of trim difference $\psi - 2°$ in the stern, the average lift height $h = 38$ millimeters

Pressure in cushions, kilogram force per meter^2	Measured Quantities	Over screens		Over water		Over a Polyphene Film on Water	
		Bow	Stern	Bow	Stern	Bow	Stern
17,1	Pressure, kilogram force per meter^2: full static. Average speed of air flow, meters per second	28,9 3,8 20,1	24,9 2,5 18,9	50 5,8 26,5	48,7 17,8 22,2	35,5 2,5 22,9	33,5 2,5 22,2
27,3	Pressure, kilogram force per meter^2: full static. Average speed of air flowing, meter per second	— — —	— — —	96,2 7,6 37,8	91,4 29,2 31,7	98,0 2,5 39,0	94,6 7,6 37,5

On the basis of the materials presented in Table 8, the conclusion may be drawn that in lift over hard screens or polyphene films afloat on the water, the distribution of air along the perimeter of jets is more uniform than in lift over water. It is possible to assume that the splashing of water, hitting the stern section's jets, hinders air flow in the stern.

Secondly, streams of water splash and hit the craft's hull and may increase or decrease the effect on the ACV of the quantity of resistance. Such an effect was detected by Everest [67] with the aid of a periscope, allowing him to observe a picture of the internal air cushions of a nozzle-type ACV. The results of measuring longitudinal forces, acting on the ACV, are given in Figure 113. As is obvious from Figure 113, the quantity of the longitudinal forces in lift over water is considerably less than in lift over screens or in moving over water at a speed of Fr = 0.4.

From the visual observations in the periscope, it was ascertained that this was connected with the action of the spray stream, hitting on the bottom of the models and directed to the side of the rising bow extremity. In the movement of the ACV, the picture of the spray formation changed, and the forces acting on the ACV over water approximated the forces in action over a screen.

-218-

This physical phenomenon was assumed on the basis of the substitution of water surface by deformed hard screens, established in Chapter II. An additional argument for the use of the established scheme may be found in the graph in Figure 114, using the experimental materials of Everest [67].
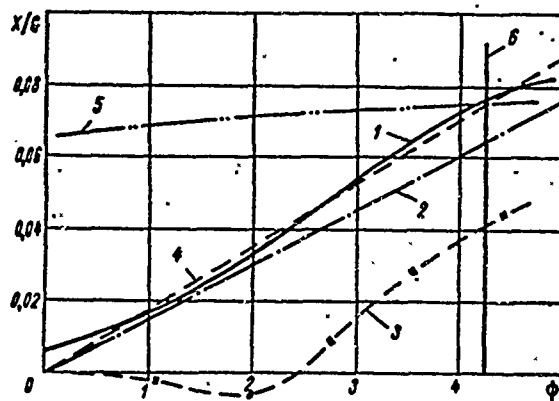
Figure 113. Relative Force of Reaction to the Air Stream in Relation to the Angle of Incline to the Base Surface in Rigidly Strengthened ACV's.
1, moving over water at Fr = 0.56; 2, suspension over a hard screen; 3, suspension over water; 4, sine ψ; 5, wave resistance during movement of the craft at Fr = 0.56, computed by the energy of the wave's wake; 6, angle of trim difference $\psi = x /G$.

One may be certain that in this graph, at a relative speed of Fr > 0.4, the quantity of the longitudinal forces acting on a model ACV in tow with a fixed angle of trim difference is close to the quantity G sine ψ, i.e. a force acting on an ACV in movement with such an angle of trim difference over a hard screen.

In the number Fr < 0.4, the quantity of the resistance differs considerably from G sine ψ, consequently a change of water surface by the screen in these conditions is incorrect.
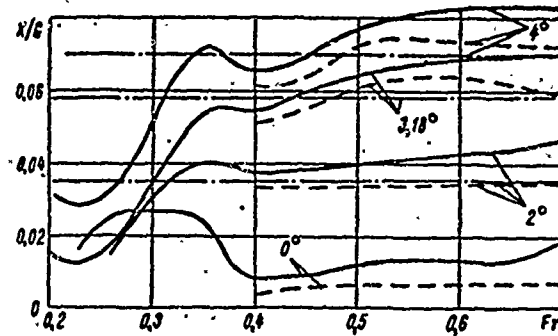
Figure 114. The Dependence of Relative Resistance in Froude Numbers
in the Tightly Secured ACV Models with the Angle of Trim Difference.
——————— tow resistance,
— — — — difference in tow resistance and total aerodynamic and
impulse resistance.
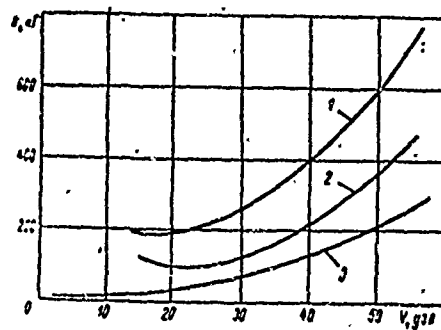
Figure 115. Resistance in Movement in
Dependence on Speed of the ACV SRN5,
G = 5700 kilograms.
1, total resistance; 2, total aerody-
namic and hydrodynamic resistance;
3, aerodynamic resistance.
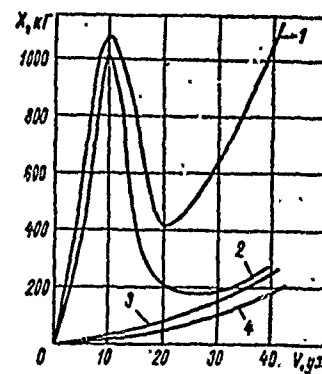
Figure 116. Resistance to Move-
ment in Dependence on Speed of
an ACV with Side Walls, G = 8500
kilograms.
1, total resistance; 2, total
wave, aerodynamic and impulse
resistance; 3, total aerodynamic
and impulse resistance; 4, aero-
dynamic resistance.

-220-

Just as in the case of reaction to air streams, there aren't any other methods of determining forces of hydrodynamic contact and spray resistance today, except those used in model experiments in test basins or on open water.

Methods of conducting testing and evaluating results in natural conditions are examined in the following paragraph. In the initial stages of design, when the testing of a model ACV still hasn't been carried out, the results of tests made on a prototype or results from the systematic testing of a towed model of the ACV may be used for estimations of resistance.

Having examined the total composition of the quantities of resistance to movement and the physical nature of the individual components of resistance, in conclusion we cite the types of curves in the relationship of resistance to movement at speeds for some ACV's and the graphs which illustrate each of the components in the general balance of resistance to movement.

These relationships are necessary, in view of the ACV's design, which permits taking the most rational constructive solutions and implementing the components from the calculations, ensuring high propulsive quality in the design of the craft (Figures 115 and 116).

§19. Practical Methods of Calculating Resistance to Movement in ACV's

In working out the design of an ACV, the resistance to movement and the speed are calculated, as a rule, more than once. The first rough calculations usually are made at the very beginning of the planning stage, allowing for resolution of the necessary power of the engine and the basic parameters of the designed craft: displacement, area of the air cushions, expenditure of air, and tentative quality of the attainable speed.

The calculations are usually made on the basis of tests accumulated in the process of designing previous ACV's. Resistance to movement is estimated by the results of tested prototype models or the systematic testing of a number of model types.

After establishing the first estimation of approximate displacement, main dimensions, forms of the hull, and the basic parameters of the planned craft, models of the designed ACV are manufactured for testing in a wind tunnel and in a test basin. During the testing phase, an argument is made for the forms of the hull, designs for flexible skirts, and the curves of aerodynamic and tow resistance are clarified.

From these results, more precise calculations of resistance to movement and speed are made, permitting the establishment of specific meanings to tactical-technical elements: speed, range, etc.

The final correction of the calculations of speed is made after conducting tests in an actual craft. In conjunction with this, such factors as interaction of the air screws and the hull of the ACV, unknown effects in evaluating the resistance of actual models, and others are specified.

In some instances, during the designing of especially complex new craft, the building of an actual ACV precedes the building and conducting of tests on self-propelled models. In this case, the calculations of the speed of the actual craft may be corrected additionally by the results of test on self-propelled models. This allows to spacify some degree beforehand part of the problems connected with the scaled translation from model to actual size, including; the influence of rigid materials for flexible skirts in resistance to movement, the influence of small waves, wind drift, etc.

Scheme of the Approximate Calculation of Resistance to Movement of an
ACV According to Table 9

1) The speed of movement "V" is given a number of meanings.

2) The quantity of the aerodynamic resistance of the hull is calculated according to the formula

$$X_a = c_a \frac{1}{2} \rho V^2 S_{\text{ж}},$$

where c_a -- is formed by the results of prototype models tested in a wind tunnel.

3) The quantity of the aerodynamic resistance of the tail units, blown by the stream from the screws, is formed by the relationship of

$$X_p = c_{xp} \frac{1}{2} \rho (V + w_a)^2 S_p, \qquad (204)$$

where c_{xp} -- coefficient of resistance to the rudders, defined by the atlas as blowing off a number of rudders;
w_a -- so-called axial speed in the screw's stream, determined by the quantity of the coefficient of the load on the screw

$$w_a = V(\sqrt{1 + \sigma_p} - 1); \quad \sigma_p = \frac{P}{\frac{1}{2} \rho V^2 \frac{\pi D^2}{4}}; \qquad (205)$$

P -- expected quantity of the screw's draught;
D -- diameter of the screw.

TABLE 9. DIAGRAM OF ROUGH CALCULATIONS OF RESISTANCE TO MOVEMENT OF AN ACV
Initial Data

$$G = \ldots \; \kappa s; \; S_n = \ldots \; \mu^2; \; p_n = G/S_n \; \kappa\Gamma/\mu^2; \; L_n = \ldots \; \mu;$$
$$S_\Omega = \ldots \; \mu^2; \; D = \ldots \; \mu; \; B_n = \ldots \; \mu; \; S_p = \ldots \; \mu^2;$$
$$Q = \ldots \; \mu^3/cc; \; \mu_n = B_n/L_n; \; \varsigma_1 = \ldots \; \mu^3$$

No. n.n.	Formula, value		Values
	ACV with flexible skirts	ACV with side walls	
1	V	V	Speed of an ACV (meters per second), a series of meanings are given
2	X_a	X_a	Profile aerodynamic resistance to the hull, kgs. of force
3	σ_p		Coefficient of loads to the screw
4	w_Ω		Rise in speed in the slip-stream, meters per second
5	X_p		Aerodynamic resistance of tailing slip-air-streams, kg. of force
6	X_H	X_H	Impulse resistance, kg. of force
7	$k' = \dfrac{gl_n}{V^2}$	$k' = \dfrac{gL_n}{2V^2}$	Parameter
8	$A = f(k', \mu_n)$	$\sin\dfrac{gL_n}{2V^2}$	(see Figure 107)

-223-

Table 9 continued

No. n.n.	Formula, Value		Value
	ACV with flexible skirts	ACV with side walls	
9.	$X_{\text{в}}$	$X_{\text{в}}$	Wave resistance, kg. of force
10	$f_{\text{r}} = f\left(\dfrac{V}{\sqrt{gL_{\text{n}}}}\right)$	—	Residual resistance in tow models, kilograms of force
11	$X_{\text{г}} = m^{3} f_{\text{r}}$	—	Residual resistance in an ACV with flexible skirts, kg. of force
12	—	$Re_{\text{з}} = \dfrac{VL}{\nu_{\text{з}}}$	Reynold's # of a side wall ACV
13	—	$f_{\text{тр}}(Re_{\text{з}})$ $$f_{\text{тр}} = 0{,}455 : (\lg Re)^{2,58} + \Delta f_{\text{roughness}}$$	Coefficient of side wall friction from registered roughness
14	—	$X_{\text{г}}$	Resistance of side wall friction, kgs. of force
15	$X = (2) + (5) + (6) + (9) + (11)$	—	Value of total resistance X, in kgs. of force. for an ACV with flexible skirts
16	—	$X = (2) + (6) + (9) + (14)$	Value of total resistance X, in kgs. of force, for an ACV with side walls

-224-

4) The quantity of the impulse resistance is calculated according to the formula

$$X_{\text{z}} = \rho Q V.$$

5) The quantity of the coefficient k' is found by the relationship

$$k' = \frac{g L_n}{2V^2}.$$

6) The quantity of the wave resistance is calculated by the formula

$$\dot{X}_{\text{a}} = A\,(k',\ \mu_n)\,\frac{p_n^2 V^2}{\pi \gamma g}. \qquad (206)$$

Wave resistance to movement of the craft with sidewalls is due to the flat characteristic of movement of fluids between the sidewalls, expediently computed according to Lamb's formula

$$X_{\text{B}} = \frac{4 p_n^2 B_n}{\gamma}\,\sin^2\frac{g L_n}{2V^2}. \qquad (207)$$

7) The quantity of the remaining resistance, including reaction to the air stream, resistance from wash-off, and spray resistance for a craft with flexible skirts, is evaluated by prototypes or is determined by graphs of systematic testing of tow models with flexible skirts close to those designed.

The quantity of the resistance to movement of a craft with sidewalls (water friction) is calculated by the formula

$$X_r = f_{\text{тр}}\,(\text{Re}_2)\,\frac{\gamma V^2}{2g}\,\Omega_1, \qquad (208)$$

where $f_{\text{тр}}$ -- coefficient of friction; is formed by the graph in relation to Reynold's numbers relative to the water Re_2; Ω_1 -- wetting of the hull's surface on the ACV.

8) The quantity of the full resistance is calculated by totaling up its components

$$X = X_{\text{a}} + X_{\text{p}} + X_{\text{и}} + X_{\text{в}} + X_{\text{r}}. \qquad (209)$$

Scheme of the Precise Calculation of Resistance from the Results of the Tow Tests in a Basin and Testing Model ACV's in a Wind Tunnel

The scheme given of the calculation for construction is the outcome of the necessity of exact computation of the influence of all internal forces, including the draught of the screws, on the trim difference of an ACV at each speed. Equalization of balance in the ACV in conforming to the scheme of forces, presented in Figure 117, has the form of

$$\left.\begin{array}{l} X_a + X_x + X_r = P; \\ M_a + M_x + M_r + G\,(x_n - y_g \sin \psi) = PH_p. \end{array}\right\} \tag{210}$$

In non-dimensional form after the division of both parts of $1/2\rho V^2 S$ and $1/2 V^2 S L^2$ the equalization accordingly takes on the form

$$\left.\begin{array}{l} c_a + c_x + c_r = c_p; \\ m_a + m_x + m_r + \overline{G}\,(\bar{x}_n - \bar{y}_g \sin \psi) = c_p \overline{H}_p. \end{array}\right\} \tag{211}$$
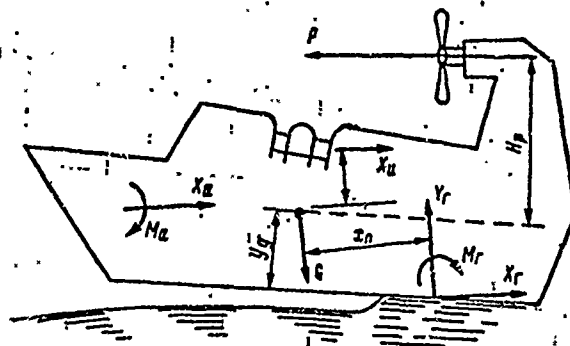

Figure 117. Diagram of the Forces Acting on an ACV.

---

[1]The quantity X_r, in the case given, includes not only the reaction flow and resistance connected with spray formation and wash-off, but also wave resistance.

[2]The quantity of the characteristic of the linear measurement L and the area S are selected arbitrarily.

The coefficients c_a, c_r, m_a, m_r may be presented in the form of linear functions of the angle of trim difference ψ by way of expansion in series of Taylor, in which to sufficiently retain two of the first terms·

$$c_a = c_a(\psi_0) + \frac{\partial c_a}{\partial \psi}(\psi - \psi_0) = a_1 + a_2(\psi - \psi_0);$$

$$c_r = c_r(\psi_0) + \frac{\partial c_r}{\partial \psi}(\psi - \psi_0) = a_3 + a_4(\psi - \psi_0). \tag{212}$$

Similarly

$$m_a = a_5 + a_6(\psi - \psi_0);$$
$$m_r = a_7 + a_8(\psi - \psi_0).$$

In substituting (212) for (211) and excluding the unknown quantity of the coefficient of draught c_p, we get the formula for determining the angle of operating trim difference ψ at given speeds

$$\psi = \psi_0 \frac{a_4 - a_2\overline{H}_p + a_5 - a_6\overline{H}_p}{a_4 - a_2\overline{H}_p + a_5 - a_6\overline{H}_p - \overline{G}\overline{y}_g} -$$
$$- \frac{a_5 - a_1\overline{H}_p + m_n - c_n\overline{H}_p + a_7 - a_3\overline{H}_p + G\overline{x}_n}{a_4 - a_2\overline{H}_p + a_5 - a_6\overline{H}_p - \overline{G}\overline{y}_g}. \tag{213}$$

The results of the tow tests are presented in the form of the relationship $c_r = c_r(\psi)$, $m_r = m_r(\psi)$ or, simpler, in the parametric form

$$c_r = f(m_g); \quad \psi = f(m_g); \quad m_r = f(m_g),$$
$$m_g = \overline{G}(\overline{x}_n - \overline{y}_g \sin \psi).$$

Similarly, results are worked out by testing models of the hull in a wind tunnel.

The structural relationships permit determination of the quantities of all coefficients a_1, a_2 ... a_7, a_8. Now the scheme of calculating resistance leads to the following (Table 10).

1) The speed "V" is given a number of meanings.

2) According to formula (213), the angle of operating trim difference is computed. The quantity ψ_0 is assigned arbitrarily, in anticipating the range of change of the angle of trim difference.

3) By computing the quantity of the angle ψ, the quantities of coefficients c_a and c_r are formed, with graphs, constructed from the test results.

4) The quantity of the coefficient of draught (equal to the coefficients of full resistance) is computed by totaling

$$c_p = c_a + c_{\text{tt}} + c_r. \tag{214}$$

5) The quantity of the resistance is found by the formula

$$X = c_p \cdot \frac{1}{2} \rho V^2 S. \tag{215}$$

§20. Propelling Agents of ACV's

Propelling agents, installed in contemporary ACV's differ considerably both in principle of operation and constructive implementation. Regarding quality, illustrations may be given in the following list of exploited propelling agents:

1) Air screws;
2) Shrouded air screws;
3) Air-jet propelling agents;
4) Air-jet propelling agents with air flow:
   a) from the receiver;
   b) from the air cushions;
5) Water-jet propelling agents; and
6) Screw propellers.

Besides this, for the different surfaces required for automatic piloted or amphibian craft, propelling agents such as wheels, caterpillars, and other means are provided, the examination of which exceeds the limits provided for the authors for the problem.

The basic features of the propelling agents, characteristic of most ACV's are:

$$X = c_p \frac{1}{2} \rho V^2 S.$$

First of all, utilization of the environment of air to ensure the amphibiousness of the ACV;

Secondly, relatively low (compared to aircraft) speeds and great quantities of draught, necessary for overcoming the "hump" of wave resistance; and

Third, constructive restrictions on the over-all dimensions of the propelling agents.

TABLE 10.   A DIAGRAM OF THE PRECISE CALCULATION OF RESISTANCE TO MOVEMENT OF AN ACV AS THE RESULT OF TESTING MODELS IN A BASIN AND IN A WIND TUNNEL.

$G = \dots$kilograms; $Q = \dots$meters^3/second; $L = \dots$meters; $S = \dots$meters; $H_p = \dots$meters; $l_i = \dots$meters; $y_g = \dots$meters; $X_n = \dots$meters; $a_1 = \dots$; $a_2 = \dots$; $a_3 = \dots$; $a_4 = \dots$; $a_5 = \dots$; $a_6 = \dots$; $a_7 = \dots$; $a_8 = \dots$;

$$\bar{l}_n = \frac{l_n}{L}; \quad \bar{H}_p = \frac{H_p}{L}; \quad c_n = \frac{2Q}{VS}.$$

Value	Method of Calculation
V	Setting a series of meanings to speed, meters/ /second
ψ	The angle of actuating trim difference calculated by Formula (213). The value ψ_0 is set arbitrarily
$c_a = c_a(\psi)$	The coefficient of aerodynamic resistance is determined by experimental data
$c_r = c_r(\psi)$	The coefficient of aerodynamic resistance is determined by experimental data
$c_p = c_a + c_i + c_r$	Coefficient of Full Resistance
$X = c_p \, \rho V^2/2 \; S$	Value of full resistance[1]

[1]The value of resistance on the aerodynamic tail unit, moving in the air screw's stream, may be calculated separately by formulae set forth in Table 9.

These features, essentially, are summarized by one typical characteristic of all ACV propelling agents - high meaning of the coefficient of load

$$\sigma_p = \frac{P}{\frac{1}{2}\rho V^2 \cdot \frac{\pi D^2}{4}} \cdot \qquad (216)$$

In theories on ideal propelling agents, a connection is established between the quantity of the coefficient of loads at rest and the quantity of the efficiency (Vetchinkin's formula).

$$\eta_i = \frac{2}{\sqrt{1 + \sigma_p} + 1} \qquad (217)$$

The quantity of the draught of ideal propelling agents may be determined from the equality of

$$P_i = \frac{75 N \eta_i}{V} ; \qquad (218)$$

These formulae allow determination of the the maximum possible (ideal) meanings of draught, set at 1 h.p. of underwater power, in relation to the speed of movement and the area of the disc-type propelling agent F. The intended quantities of the ideal draught are set forth in the graph of Figure 118. However, the adduced meanings of specific draught turn out to be practically unattainable because of the additional loss of so-called strength of viscosity of the air, the vortex formation, and methods of constructive implementation of the propelling agents.

In connection with these, it is expedient to pass on to the examination of specific types of propelling-agent designs. The first items of practical significance are the air screws. Problems of designing air screws are widely clarified in science-technical literature Therefore, an examination may begin with the uses of air screws in quality movement of ACV's compared to aircraft propellers. As a rule, each air screw designed is the result of mutual technical solutions, due to streamlined designs, to satisfy a number of contradictory requirements. The diameter of the screw and the number of revolutions are limited by the quantity of the maximum turning speed at the tip of the blades, which must not exceed the speed of sound. In a case where special requirements for the level of air noise of an ACV are produced, the maximum turning speed at the tip of the blades must not exceed M = 0.6 (M = Mach number).
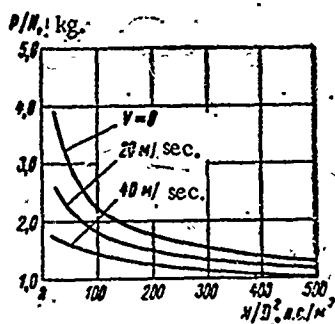
Figure 118. Relationship of Ideal Draught to the Consumption of Power and the Diameter of the Disc of the Propelling Agent.

The width of the screw blades usually does not exceed 8-10% of the diameter, and is dictated by the limited possibilities of the mechanism for turning the blades, which is situated in the bushing of the screw. Therefore, in regard to aerodynamics, the design of the screw remains two parameters, modification of which may essentially alter the draught characteristics of the screw; the profile of sections of the blades and angle of the mountings of the sections, i.e. the curve of the blades. In designing a propeller for an aircraft, these parameters are suitable also for selection by compromise optimum profiles and attack angles for the sections in conditions of take-off and flight at maximum speed are different.

In contrast to an aircraft, the ACV's screw may be considered single-rated and the selection of profile and curve of blades is optimum for conditions of take-off. This allows an increase in the draught characteristics of the screws, designed especially for the ACV, in comparison with aircraft propellers.

Other features, required for the air screws of an ACV, are the necessity of implementating of reverse and increasing the durbility of the screws. Reversing of the screws increases the maneuverability of the ACV to such an extent, that reverse appears as a necessary quality for a propelling agent of an ACV.

In contrast to aircraft, the screws of an ACV often are obscured by various superstructures on the ACV's hull, which may lead to beginnings of dangerous resonance rates of vibration in the blades and must be determined in the process of designing and elminated before exploitation.

Air screws, as a rule, operate in small amounts of water spray and splash. Because the blade edge is subject to corrosion, in some cases the blades cease operating for several hours at a time. To prolong the term of serviceability of the screws, a special coating is applied to the incoming edges of the blades.

Calculation of draught characteristics of air screws is accomplished with the aid of diagrams of aerodynamic characteristics, obtained in testing model screws in a wind tunnel.

In these diagrams are the relation of the coefficient of the screw's draught

$$\alpha_{\lambda} = \frac{P}{\rho n^2 D^4}$$

and the coefficient of power

$$\beta_1 = \frac{75N}{\rho n^3 D^5}$$

to the relative step

$$\lambda_p = \frac{V}{nD}$$
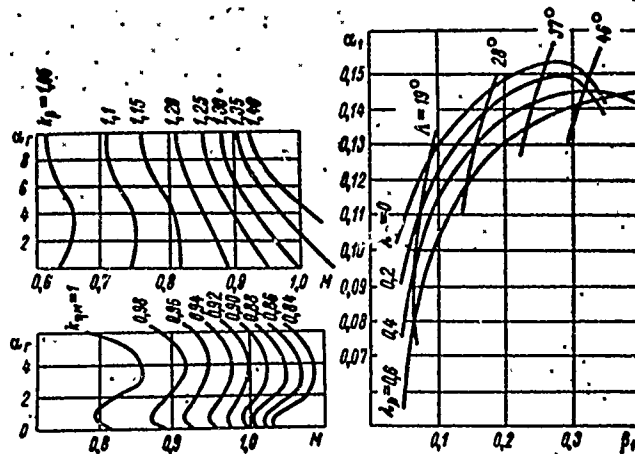
Figure 119. Aerodynamic Characteristics of Air Screw 2 SMV-3.

In some cases, there is a convenient use of the diagrams reconstructed in other co-ordinate axes. In Figure 119, the relationship of coefficient α_1 to β_1 is constructed, with constant meanings of the parameters of step λ_p and angle Λ arrangement of sections (steps) in radius $r_1 = 0.75D/2$ for screw 3 SMV-3 [27].

In calculating draught, it is necessary to take into account the influence of the engine gondolas and the air compression in aiding the construction of additional diagrams (Figure 119). Detailed schemes for calculation of draught characteristics lead to special technical literature [27]. The scheme for calculating draught is set forth in Table 11.

-232-

TABLE 11. DIAGRAM OF THE COMPUTATION OF DRAUGHT OF THE AIR SCREWS
Initial data: series of screws ... ...
D = ...meters; V = ...meters/second; N = ...horsepower.

Formula	Designation of Value
n	Number of revolutions/second in the screw
$\lambda_p = V : nD$	Relative step, where V is meters/second; n, $\frac{1}{sec}$; d, meters
$u = \pi D n$	Circumferential speed at end of blades, meters/second
$M = \dfrac{\sqrt{u^2 + V^2}}{a'}$	Final Mach number. Speed of sound a' = 340 meters/second
$\beta_1 = \dfrac{75N}{\rho n^3 D^5}$	Coefficient of power N, horsepower.
$\beta_r = \text{arctg} \dfrac{V}{0.75 u}$	Angle of air flow in radius R = 0.75 $\dfrac{D}{2}$.
$\Lambda_r = f(\beta_1, \lambda_p)$	Angle of blade setting. Determined according to graph (Fig. 119).
$\alpha_r = \Lambda_r - \beta_r$	Angle of attack of the blades in radius R = 0.75 $\dfrac{D}{2}$
$k_\beta = f(M, \alpha_r)$	Power correction factor. Determined according to graph (Fig. 119)
$\beta_p = \dfrac{\beta_1}{k_\beta}$	Computed coefficient of power
$\Lambda_p = f(k_p, \lambda)$	Designation of Value
$\alpha_1 = f(\Delta_p, \lambda_p)$	Calculated angle of fixed blades in radius R = 0.75 $\dfrac{D}{2}$. Set forth in graph (Fig. 119)
$\alpha_p = \Lambda_p - \beta_r$	Coefficient of draught
$k_{\eta M} = f(\alpha_p, M)$	Calculated angle of attack
$\alpha' = \alpha_1 k_p k_{\eta M}$	Correction factor. Set forth in graph (Fig. 119)
$P = \alpha' \rho n^3 D^4$	Draught of screw [1]

[1]
For a more precise calculation, the correction of relative dimensions of the screw and gondolas is taken into account, see [22].

A great deal of experience, accumulated by aircraft builders in the area of designing air screws, permits obtaining, in some instances, the meanings of specific draught, which are sufficiently close to the draught of proposed propelling agents (attaining quantities of 90% ideal draught). However, this has a place only in relatively small quantities of power supplied to the screw. In Figure 118 it is observed that, with quantities of ratio $N/D^2 > 200$, the specific proposed draught P_i/N aims toward constant quantity. In regard to this, the quantity of draught must be increased proportionally to the power supplied. However, any practical screw may reprocess effectively only within the limits of the quantity of supplied power. In Figure 119 it is observed that, in quantities of coefficient of power above $\beta_1 = 0.3$, the coefficient of draught α_1 ceases to increase and later on even begins to decrease, i.e. an increase in power doesn't lead to an increase of the screw's draught.

The physical logic of this phenomenon consists of the following. In the construction of a screw-type propelling agent, the principle of lift forces from wing-type blades is used for creating draught. In limiting the area of the wing (diameter and width of blades) and the turning speed (number of revolutions), the lift forces may be increased only as a consequence of increased coefficient of lift forces c_y, which is attained by means of increasing the angle of attack of the wing. However, the possibilities of increasing lift forces of the wing are not unlimited. In some critical meanings of the attack angle a_{kp}, the quantity of c_y reaches maximum meaning after the apprearance of a breaking-off of the bordering layers, interrupting the flow of the wing and the lift forces begin to decrease. A similar phenomenon arises with the increase of attack angle of the screw's blades.

After a considerable part of the blades' sweep is interrupted, the screw's draught begins to diminish, in spite of an increase in bringing power to the screw.

Today, very powerful aviation gas-turbines, which are small in size and light in weight, may be used on ACV's. However, with their use there arises a familiar problem of propelling agents, i.e. the method of reprocessing the power in draught.

The only thing to be done is to divide the power between several screws. It is natural that, in doing this, new difficulties arise: the complexity in the general arrangement of the craft in a given size, the necessity of using a large number of reduction gears and transmissions, and the calculation of mutual influences of the propelling agents.
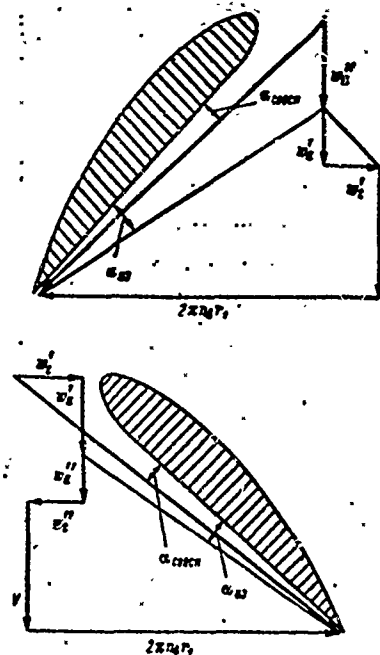
Figure 120. Polygons of Speed of Coaxial Screws with Opposite Rotations.

A successful solution, discovered by aircraft builders for large transport aircraft like the Tu-114 and the "An" series, involves coaxial screws with opposite directions of rotation. In the operation of coaxial screws in twin activity, each of the screws induces in the disc of its twin screw additional axial w'_a, w''_a and circumferential w'_t, w''_t speeds, in comparison with speeds w_a and w_t in the operation of the screw by itself (Figure 120), which leads to alteration of the angles of attack of the blade elements.

In the first place, the interruption of the flow of a considerable part of the blades' sweep is eliminated. Secondly, because of the opposite directions of rotation, circumferential speeds induced by the front and rear screws are mutually cancelled, and the flow from the disc of the rear screw creates a considerable degree of torque. Consequently, the kinetic energy of that eliminated by the propelling agent's air mass is decreased, which increases the efficiency of the coaxial-screw complex.

The specific draught of a well-designed coaxial-screw complex is almost equal to the total draught of screws working individually, but in practive it remains smaller than this total. It has been concluded that the reason for such a descrepancy is that the mass of air, flowing through the disc of each of the coaxial screws, considerably exceeds the mass which flows through each of the screws in singular activity, and because of this speeds are increased for the air flow through the discs and the calculated meaning of operable steps of the screws, which leads to lower draught.

This circumstance, essentially, is considered according to the ideal efficiency of the coaxial screw complex. To illustrate the effectiveness of the division of power or use of coaxial screws, several diagrams are set forth in Figure 119.

Let us assume that the coefficient of power in the operating screw is a speed of V = 15 meters/second, λ_p = 0.2, β_1 = 0.2. Consequently, the coefficient of draught of this screw is α_1 = 0.143. In dividing the power between the two screws, the diameter and the number of revolutions β_1 = 0.1.

For each of the screws, the coefficient is $\alpha_1 = 0.122$, consequently, the total draught is increased to m' = 0.244/0/143 = 1.7 times. In the case of dividing the power between the two coaxial screws in operable steps, the front screw will equal $\lambda_{p1} = 0.4$ and the rear screw $\lambda_{p2} = 0.27$ [1]. The coefficient of draught of the front screw of the coaxial combination is $a'_1 = 0.115$, and the rear is $a''_1 = 0.118$.
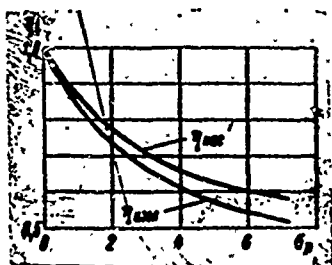

Figure 121. Relationship of the Ideal Efficiency of the Screw Complex (shrouded and isolated screws) to the Load Coefficient.

The total draught is increased, in comparison with the initial variant, 1.63 times (0.233:0.143), but is lower than the total draught of the two screws acting individually.

An important means of increasing draught of propelling agents for ACV's is the use of circular shrouds.

Propelling agent complexes, in the form of propeller screws confined in circular shrouds, are widely used in shipbuilding to increase the draught of·tow-type and other craft with heavy--duty screws. For shipbuilding tests, the use of circular shrouds stands to gain from the meaning of the load coefficient of the propelling agents $\sigma_p > 1.0$ (Figure 121).

For an ACV, the quantity σ_p in the area of speed, in accordance with the "hump" of resistance, reached 10-20 and more. Consequently, the use of a shroud in this case is even more justifiable than in a tow-type craft.

The basic reasons for the increase in draught of a shrouded screw, in comparison with an isolated screw, lie in the following. In theories of ideal propelling agents, Rankin's formula is well-known - it determines the efficiency of ideal propelling agents in that

$$\eta_u = \frac{2}{1 + \frac{V_\infty}{V}}$$

(219)

where V - speed of the craft's movement;
V_∞ - speed of the air stream of the propelling agents to infinity for craft in system-coordinates connected·with the movement of the craft.

The quantity of the draught of propelling agents is determined by the formula

$$P = \dot{m}(V_\infty - V)$$

(220)

where m - a second's expenditure of air in the propelling agent's stream, calculated by this system of coordinates.

An analysis of formulae (219) and (220) shows that, to increase efficiency for maintaining given quantities of draught, it is always expedient to increase the mass m and decrease the speed in the stream of the propelling agents.

In the operation of an isolated screw, the stream is narrow after passing through the disc and the speed to infinity for the screw is increased by the law

$$\frac{V_\infty}{V} = \sqrt{1 + \sigma_p}.$$

(221)

In the case of the shrouded screw, the stream is widened after passing through the disc, following the profile of the shroud (Figure 122). For the shroud, as with the circular foils, there arises a force of draught. Usually, that pressure in the stream flowing from the shroud is equal to the pressure to infinity, i.e. the stream of air, flowing from the propelling-agent complex, has a constant transverse
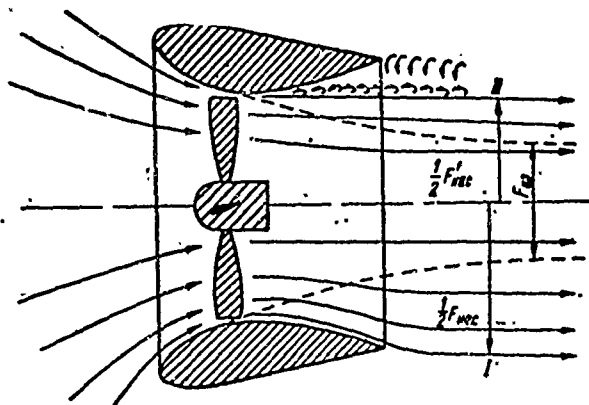
$$F_2 = F_\infty \text{ (see [28])}.$$

Figure 122. Diagram of the Line of Current in Operating a Shrouded Screw. I - Uninterrupted flow in the shroud; II - Interrupted flow in the shroud. ----- In operation of an isolated screw.

If the designation F - area of the screw's disc and $\beta_2 = F_2/F$, then in this case

-237-

Secondly, the air screw (appearing as the working agent operating in a shroud) is replaced by a fan, calling for a large quantity of the coefficient of thrust a_1 [28].

Calculation of draught of the air-jet propelling agent may be accomplished by the well-known scheme of calculations for water-jet propelling agents [28]. For the completion of a sufficiently reliable calculation, as is also the case of water-jet propelling agents, it is necessary to arrange this by the following experimental materials:

a) Characteristic of the agent operating in isolated activity;

b) Characteristic of the air-conductor route.

A special air-conductor route for the propelling agent does not appear according to the necessary conditions. In Figure 124, b and c views of ACV's in the hulls of which air (going toward the creation of jet draught) moves along a duct of the systems maintaining the ACV's. In the case of b, the jet force is created in the air flow from the receiver of the ACV; in the case of c, the air flows directly from the air cushions. These principles, in ACV configurations, are well known in practice.

The propelling agent in scheme b was used in the creation of the first English ACV, the SRN1, as well as in many other craft. the CC-5, etc.

The propelling agent c was used much earlier with great success in the first native full-size craft of chamber type, created by Prof. V. I. Levkov [4]. There are many well-known ACV's using air-jet propelling agents, the creations of which utilized schemes b and c.
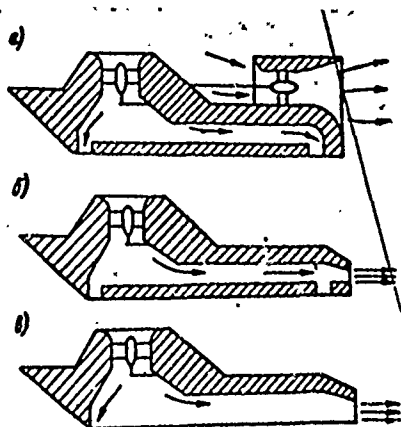

Figure 124. Constructive Type Configurations of Air-Jet Propelling Agents in the Hulls of ACV's: a, Air-jet propelling agent; b, Air flow from the receiver; c, Air flow from the air cushions.

-238-

$$\frac{V_\infty}{V} = \frac{1}{2}\left(1 + \sqrt{1 + 2\frac{\sigma_c}{\beta_2}}\right),$$

(222)

where σ_c - load coefficient from the calculated draught of the shroud.

The quantities of ideal efficiency, calculated according to formula (219) with the calculations of formulae (221) and (222)., are set forth in Figure 121 [28]. Apparently, in the operation of a shrouded screw, the ideal efficiency is higher than in the operation of an isolated screw. However, the advantages of a shrouded-screw complex, in comparison with an isolated screw, do not lead to gains in ideal efficiency.

If the designation V_s - speed of air flow through the screw's disc, then on the basis of equalization of indissolubility of the environs it is possible to write the following equality:

$$\frac{V_s}{V} = \frac{1}{2}\left(1 + \frac{V_\infty}{V}\right) \quad \text{— for an isolated screw}$$

$$\frac{V_s}{V} = \beta_2\frac{V_\infty}{V} \quad \text{— for a shrouded screw}$$

$$\frac{V_{s_{из}}}{V_{s_{исc}}} = \frac{1 + \left(\frac{V_\infty}{V}\right)_{из}}{2\beta_2\left(\frac{V_\infty}{V}\right)_{исc}}.$$

If the ideal efficiencies of the propelling agent are equal, i.e.

$$\left(\frac{V_\infty}{V}\right)_{исc} = \left(\frac{V_\infty}{V}\right)_{из} = c, \ c > 1,$$

$$\frac{V_{s_{из}}}{V_{s_{исc}}} = \frac{1 + c}{2\beta_2 c}.$$

The lower limit of the quantities is lim c = 1, and the quantity $\beta_2 >$ > 1. Therefore,

$$\frac{1}{2\beta_2} \leqslant \frac{V_{s_{из}}}{V_{s_{исc}}} \leqslant \frac{1}{\beta_2} < 1.$$

Consequently, in the equality of ideal efficiencies, the speed of air flow through the screw's disc in a shroud is greater than the speed of air flow through the disc of an isolated screw.

In this, as well as in the case of coaxial screws, a part of the blades' sweep is blocked and the draught increases. In such a way, the

use of a shrouded screw not only increases the ideal, but also the designed efficiency. For aircraft screws, the total increase of draught from a shrouded-screw complex is 100% in some instances. If the screw if specially designed for the ACV, the increase of draught of the shrouded screw is considerably less.

The possibilities of expansion of the streams after passing through the screw's disc (shrouded) is not without limits, and are formed by conditions of uninterrupted flow according to the profile of the shroud. In a given length of the shroud, the increase of the coefficient of expansion β_2 is equivalent to the increase of the angle of attack of the shroud's winged profile (Figure 122).

As was already noted, after reaching some of the critical meanings of the angle of attack, the flow of air is blocked and further expansion of the stream does not occur. In this, both the lift force of the profile and, consequently, the draught of the shroud are decreased.

Determination of optimum rates and the profile of the shrouds are connected by thorough aerodynamic calculation. After carrying out such a calculation, it usually is expedient to conduct tests of the designed shrouded-screw complex in a wind tunnel and to introduce the necessary corrections to the given parameters.

Today, application of circular-shrouds has been suspended because of the considerable design and technological difficulties of their completion. The length of the shrouds usually is 0.5-1.0 of the screw's diameters. Thickness of the profile is from 15 to 25% of the chord profile (shroud lengths).

For effective operation of the complex, it is necessary to ensure minimal clearance between the blade tips and the profile of the shroud, equal to 0.3-0.5% of the screw's diameter. For this, it is necessary to ensure a tight system of securing the screws and shrouds, which would exlcude the possibility of blows from the edges of the blades along the profile of the shroud during conditions of dynamic load in the design for wind and rolling of the ACV in sea conditions.

The shrouds of a craft with propeller screws sometimes are cast or reinforced by rigid internal framework. However, this is possible only for screws with small diameters. Diameters of air screws reach 3 to 6 meters. Naturally, the use of a cast shroud leads to an intolerable increase in weight. It is necessary, therfore, to look for the most successful design solution which would ensure rigidity at a minimal weight in construction.

Above, it was shwon that the basic gain in draught of the propelling agent, using an air-screw complex and circular shrouds, is connected with

the large quantity of load coefficient of the propelling agent. At
high speeds, the load coefficient is decreased, as is the effectiveness
of the shroud (Figure 123). At maximum speeds of modern ACV's the
effect of using shrouds is practically nil. Therefore, to acquire
the necessary reserve draught in the area of the "hump" of wave re-
sistance for ACV's, the use of shrouds is not expedient, especially if
the design difficulties in creating propelling agents of such a type
are taken into account.

As was indicated earlier, the basic deficiency of air screws,
used as quality propelling agents of ACV's, is that they are of large
dimensions. Therefore, from the very outset, the efforts of designers
were directed toward looking for propelling agents of other types,
which could be integrated into the components of the ACV. The basic
direction of this search was the use of the air-jet propelling agent
in different ways. The principal diagrams for three basic design-
-types of ACV's, which employ the air-jet propelling agent, are set
forth in Figure 124.
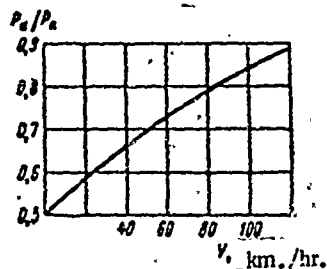
Figure 123. The Relationship
of Draught of an Isolated In-
dividual screw to the Draught
of. a Shrouded-screw Complex
in Relationship to the Speed
of Movement.

In the first case, the pro-
pelling agent of the ACV is not
connected with the system of
maintainence of the ACV. Special
air conductors were provided in
the construction of the craft,
in which the velocity of the air
mass occurs, acting from without,
due to the supply of energy neces-
sary for operation of the propelling
agent, e.g., the fan at the site
of the air conductor. This construc-
tion, in principle, is similar to
water-jet propelling agents, which are
widely used in shipbuilding, and
may be called an air-jet propelling
agent. Today, there still is not an
ACV equipped with propelling agents
of such a type, but great attention has been given to study by the
designers, with the exception of such an ACV emerging in the near future.

Streamlining to lower the transverse dimensions of the propelling
agent, in maintaining the possibility for a great quantity of draught,
leads to the use of air-jet propelling agents instead of shrouded air
screws. This transition is connected with two character-design traits.

First of all, the longitudinal, axial measurements of the propelling
agent, necessary for the effective transformation of the energy carried
to the working organ (the kinetic energy stream flowing from the pro-
pelling agent) are lengthened.

-241-

The merits of the propelling agents of the types examined are obvious: simplicity of construction, organic combination of systems of air conductors in the propelling agents and lift systems of the ACV's.

The basic dificiency of air-jet propelling agents lies in that they may be effectively used only on small ACV's with small quantities of under-dome pressure in the cushion. The quantity of draught, necessary for the ACV's movement, is formed usually by the quantity of "hump" of wave resistance. By measuring the increase in pressure in the cushion, the quantity of "hump" of wave resistance increases proportionately to the square of pressure, while the jet draught P_j is

increased proportionately to the first steps of pressure.

$$(223)$$

where F - area of outlet of the propelling agent.

To illustrate this, a graph of the calculated meanings of power necessary for overcoming the "hump" of resistance in air flowing from the receiver, in relation to the pressure in the cushion, is set forth in Figure 125.
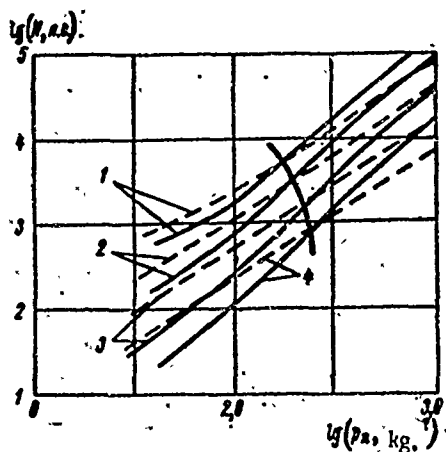

Figure 125. Comparative Curves of Power N, Necessary for Overcoming Wave "Hump", in Relation to Pressure P_n (Kilograms of force per meter^2) in the Air Cushion.
———— Air-Jet Propelling Agent;
-------- Air Screw, Developing a specific draught of 1 kilogram force per h.p.;
1 - G = 1000 meters; 2 - G = 300 meters; 3 - G = 50 meters; 4 - G = = 10 meters.

-242-

The following assumptions were obtained in this calculation:

1) The "hump" of resistance $X = 3.25\, P_n^2 B_n / \gamma$; $Fr = 0.5$;

2) $N = Q P_p / 75_{\eta c}$, where $\eta c = 0.75$;

3) $P_p / P_n = 1.3$;

4) $L_n / B_n = 2.0$; $G = 2 P_n B_n^2$.

The results of the computation are plotted by solid lines.

In increasing pressure, the quantity of power necessary for over-coming the "hump" of resistance increased sharply. In this graph, the dotted lines mark the power necessary for use of quality propelling agents of the air screw type, developing a draught of 1 kilogram force at 1 h.p. of supplied power. The advantage of the screw is seen in the large quantity of pressure, where the dotted lines go below the solid lines.

As the graph shows, the use of air-jet propelling agents is expedient only in pressure $\lg P_n < 2.2$-2.4, i.e. $P_n < 160$-250 kilograms of force per meter^2, being the lower limit corresponding to a craft of large dimensions.

Due to the condionality of the calculation in this graph, one cannot use it for quantitative value in selecting a type of propelling agent. In practice, the advantages of air screws are seen to be more considerable both in the small quantities of pressure, and in the development of draught of more than 1 kilogram force at 1 h.p.

Aviation turbojet and turbofan engines, also use as quality propelling agents for ACV's, deserve some attention. The aviation industry has organized the production of a large number of jet engines, which are precise, reliable, and widely adapted by native and foreign passenger and military aircraft.

The advantages of a propelling agent of this type are regarded as [18]: small dimensions; low weight with great power; and an insignificant drop in draught at increased speeds, compared to screws.

Regarding quality, the following deficiencies are noted: a great fuel expenditure at 1 kilogram force of draught, compared to engines of internal combustion or gas-turbine type; and the necessity of using special construction materials to prevent corrosion and salt buildup of sea conditions.

c_e, kg. of thrust per hr.
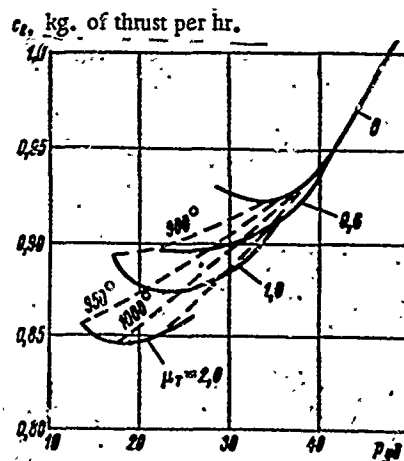
Figure 126. Specific Hourly Fuel Expenditure in Relation to the Specific Draught of an Air Jet Engine at Different Quantities of the Coefficient of Dual Induction.

Special interest has been shown in turbofan engines and particularly in twin-ducted jet engines with a great degree of dual induction μ_τ.

The relationship of the basic parameters of engines of specific fuel expenditures and specific draught to the degree of dual induction and to the temperature of the gases in front of the turbines is shown in Figure 126. The quantity of air, flowing through the engine, equals

$$G_0 = G'_\tau \frac{a^* l_0}{3600},$$

where G'_τ - quantity of fuel supplied per hour;

l_0 - quantity of air, theoretically necessary for total combustion of the fuel;

a^* - coefficient of air surplus.

It is obvious that the dimensions of the engine must be larger, the larger the expenditure of air passing through the engine. In order to decrease the dimensions, in conditions for maintaining the required draught constant, it is necessary to increase the specific draught.

In Figure 126 it is shown that, for each coefficient of dual induction there exists an optimum temperature rate corresponding to the minimum specific fuel expenditure, i.e. the most expedient rate of movement is that of economy. This rate simply corresponds to the determined quantity of specific draught, ile. the determined dimensions of the engine. The high degree of dual induction μ_τ = 2.0 the specific fuel expenditure is low, c_e = 0.84 kilograms of kilogram force of draught per hour, but in return the dimensions of the engine are great. The minimum coefficient of dual induction μ_τ = 0 (turbojet engine) means

that the dimensions of the engine are small, but there is great amounts of specific fuel expenditure c_e = 0.92 kilograms of kilogram force of draught per hour.

The optimum meanings of μ_τ lie in the limits of μ_τ = 0.7-1.2.

Turbofan engines, compared to the average turbojets, have the following advantages: less specific fuel expenditure; less weight at a given draught; a higher relation of take-off draught to cruise, which particularly is essential for ACV's; and a lower (10-15 decibels) noise level because of less speed of flow in the jet stream.

Special construction is necessary in turbofan engines to reverse draught. In this case, when the engine's fans are situated in the tail or there is a common exhaust nozzle for both ducts, they may be situated in common alignment (turning simultaneously both the air and the bases inside the duct to create reverse draught) or in moved cones [18].

A final review of the propelling agents of ACV's follows the notation concerning the special non-amphibious type craft - craft with sidewalls, in American terminology "craft using the principle of the captured air bubble" (CAB).

The elimination of amphibiousness permits the use of quality propelling agents, operating wtih water instead of air. An increase in the density of the operating environs (800 times) allow a sharp decrease in the dimensions of the propelling agent and to lower the load coefficient, i.e. to raise the efficiency of the propelling agent.

Propeller screws, semi-submerged propeller screws, and water-jet propelling agents are also used in ACV's. One ACV with propeller screws is the English D-2 craft from the Denny Hovercraft firm, pictured in Figure 25. Computations for propeller screws and water jet propelling agents of ACV's may be carried out by the well-known methods [1], [18].

CHAPTER V. THE ACV'S MANEUVERING QUALITIES

21. General Information About the ACV's Maneuvering Qualities

Air cushion vehicles are a means of transportation, occupying an intermediate position between ordinary craft and flying machines.

ACVs must possess maneuvering qualities inherent both in flying machines (for example, altitude maneuvers, movement on an air cushion and on an air bubble, and in a water displacement position) and in ordinary craft (for example, backwards movement.)

Maneuvering qualities are those which enable an ACV to change its position (at all three coordinates) at a definite period of time and speed vector (by amount and direction.)

The ACV's maneuvering qualities may be attributed to control and proper maneuverability. ·

An air cushion vehicle, having six stages of freedom along each of three fixed coordinates of axes which coincide in a suspended mode with rigidly constrained axes, the beginning of which we assume in the center of gravity[1] may perform translational (lift height, longitudinal and side drive) and fluctuating shifts, turning dsplacements (list, difference and yaw) and angles of fluctuating shift are possible relative to the center of gravity around three coordinates of axes.

The ability of the ACV to change its position in space and speed vector as a result of rotating around the center of gravity we shall call "controllability."

The ability of the ACV to change its position in space and speed vector, due to translational displacement, we shall call "maneuverability."

As has already been stated in Chapter I, the ACV may be one of two types, suitable for movement:

a) with total separation from the water and

b) with an incomplete separation from the water. i.e., craft with partial discharge.

---

[1] We also assume that the center of gravity coincides with the center of the mass.

Two extreme positions in reference to height are possible for both types of ACVs:

1) during movement without utilizing, for one reason or another, an air cushion;

2) during movement at maximum lift height.

In the first case (and for the ACV with partial discharge in the second case also), the movement of an ACV is not much different from movements of a conventional craft and its maneuvering qualities should be analyzed by methods acquired from examination of water-displaced craft. The ACV's movement with total separation from the water (in the second case) will occur in the air (with $h = 0 - h_{maximum}$, where $h_{maximum}$ is maximum lift height above water). This particular rate of the ACV's movement with total separation, will be fully covered in Chapter V.

As already stated above, the control devices are the mechanisms which allow for the creation of forces and moments, necessary to control the ACV.

The ACV's control devices are expediently divided into basic and auxiliary, taking into account the great amount of literature on patents and equipment used in experimental air cushion craft. By way of analogy, with water-displaced craft it is necessary to regard the steering gear, which provides a steady or changing course, as a basic control devices.

To the auxiliary control devices (steering gear) may be attributed equipment for creating forces and moments in a horizontal plane for controlling drift and yaw (and according to course-in supplementing the steering gear), as well as equipment for creating forces and moments in longitudinal and transverse-vertical planes for controlling suspension height by list and trim difference.

On the majority of designed craft, to have first rate steering gear, vertical aerodynamic rudders (vertical tail units) are provided.

At the present time the most widely used tail-unit arrangements on the ACV are the following:

1) The mobile part of the tail unit (rudder) is directly behind the stationary part (stabilizers) and is a direct continuation of it. The tail unit is situated to the rear of the air screws and is blown upon by a stream of air escaping from the operating propelling agent (VA-3).

2) The rudders are sitauted to the rear of the air screws in a ring ("Neva") or in a nozzle (SKMR-1) or to the rear of open air screws ("Raduga").

Besides this, different combinations and combined arrangements are possible.

In addition to the first arrangement, stabilizers may be provided, situated outside the air stream zone from the propelling agents (SRN3), and in addition to the second arrangement, stabilizers situated in the stream or outside the stream from the screws ("Sormovich").

Auxiliary surfaces may be set up besides the basic rudder and stabilizer, for example rotary (SRN2, SRN3) or stationary pylons of the propeller agents (SRN5).

Individual peculiarities may also be evident in different ACV tail unit arrangements, for example the bow stabilizer and an additional stream of air from the receiver (SRN5) over the rudders; the VA-3 bow free orienting rudders with trimmers (removed afterwards), and others.

The following primary tail unit complex may be isolated from among the numerous variants:

isolated rudder in combination with an isolated stabilizer;

a stabilizer in combination with a rudder behind the stabilizer (with a flap or without it).

The complex, as a rule, is placed in the air stream from the propelling agent.

Rotary propelling agents are employed on the English ACV, SRN4 for a first rate rudder system. Besides this, the well-known first rate rudder system of louvered propelling agents and independent jet nozzles (jet stream rudders) is used.

The size of the moment in relation to the vertical axis Oy may be modified utilizing the jet stream rudders by changing the area of the nozzle hole passage (or the speed of the jet flow). With this method of control, the following variants are possible:

1) feeding air to the jet stream rudders originates in the common receiver. In this case, effective control is possible only with great pressure in the receiver, when high speeds of air flow may be received from the nozzles and, correspondingly, great enough side force and its moments.

2) Supply of air (gas) to the jet stream rudders originates from independent fans or jet engines. In this case, changing the jet stream parameters, creating forces and moments which are necessary for control, is accomplished irrespective of the power plant operating rate to create the air cushion.

Qualitative comparison of controls of ACV models with the help of rotary screws (propelling agent) and jet-stream rudders (jet nozzles) is illustrated in Figure 127.
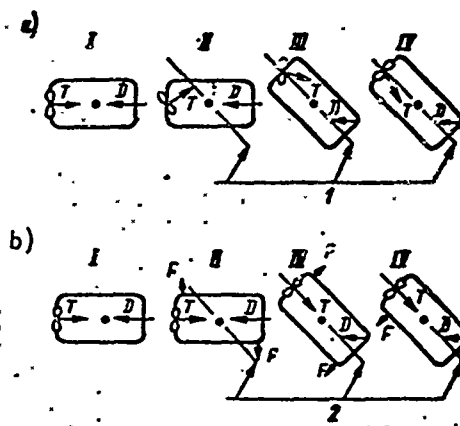
Figure 127. ACV Control with the Aid of Rotary Screws and Jet-Stream Rudders: a, Turning with the Aid of Rotary Screws; b, Turning with the Aid of Jet-Stream rudders. 1, Necessary course, turning with the aid of rotary propelling agents; 2, Necessary course, turning with the aid of lateral jet forces; T, Direction of thrust of the screws; D, Direction of aerodynamic forces; F, Direction of thrust of jet-stream rudders; I-IV; Position of the ACV at various consecutive moments of time.

While the blades are rotating to the left for executing a right turn, inertia is created for turning the ACV clockwise. After a while (Figure 127 a) the ACV model is set 45° to the right and is ready to shift to a newly given course, however, the inertai turning the ship in a clockwise direction is still there. In order for the model to cease further rotation, it is necessary to turn the blade to the left from the DP and thus remove the turning inertia around the center of gravity. But when the model's angular rotating speed around the center of gravity decreases to zero, the vector of thrust is not in the direction of the course and it is necessary to turn the blade's axis again. Thus, in order to maintain the model on course it is necessary to change the direction of the propelling agent's thrust often (for several seconds). In Figure 127 b, the model's control system is illustrated where the clockwise turn occurs due to the action of the left bow and right stern jet nozzles. It is evident from Figure 127 b that any inertia may be neutralized in this manner, creating a force of resistance during the

turn without changing the direction of thrust which immediately after the turn proceeds to a new course.

The method of control with the help of jet-stream rudders having an independent air supply is considered, theoretically, the most effective since it permits, without changing the operating mode of the main engines, provision for necessary control both during suspension and while the ship is in motion. However, adopting this method in practice has its drawbacks connected with equipment difficulties and independent systems operation not warranted in the ACV's small displacement. Of the two methods, the preference now is for control with the aid of rotary engines (SRN2, SRN3 and SRN4). Water rudders are possible for use on ACVs with chamber and other systems which create an air cushion, providing an insignificant or less than total separation from the water.

The necessity for placing additional equipment on the ACV, creating forces and moments in a horizontal plane for controlling side drift and yaw is developed on the one hand, because of absence of stability of the ACV during suspension in relation to the disturbance effected by the shift of the mass center along the longitudinal and lateral axes and rotation in relation to the mass center around the vertical axis. On the other hand, such installation is due to the appearance of horizontal forces because of the resultant reaction in air tilting of the ACV relative to the longitudinal and lateral axes causing their drift toward the incline. Besides, steering on course with aerodynamic rudders is effective only at high speeds when the inflowing air stream is great enough.

These circumstances, under certain conditions, may severely handicap the ship's steering in a horizontal plane, especially in wind and swells. That is why it is advantageous to utilize special equipment for creating forces and moments in a horizontal plane, in addition to the basic steering devices. Jet nozzles (jet streams) in particular may be utilized as first rate devices. Jet power from exhaust gas streams of gas turbine engines may be utilized along with jet nozzles for creating moments to compensate for yaw. To this effect, one may use control devices in the form of deflectors, set up in exhaust gas stream of a gas turbine engine. On an ACV having two air screws arranged symmetrically in regards to the surface diameter, the utilization of draught variances is the most effective. If they are variable pitch screws, then the draught variance may be produced in two ways: by changing the screw pitch and by changing the engine rpms of one side in relation to the screw pitch and number of engine rpms of the other side.

Of course, by mounting several rotary engines all the problems of controlling the ship in a horizontal plane may be solved, however, it is

not always advantageous to complicate the ship's design with rotary engine pylons. In this case, several methods of control in a horizontal plane are employed simultaneously on the ship.

Devices in various combinations are also specified on almost all the ACVs, for creating forces and moments in longitudinal and transverse vertical planes for controlling suspension height by list and trim difference.

Controlling suspension height may be achieved most simply and economically by changing the quantity of air being supplied to the air cushion by regulating the operating rate of the fans, the fan's blade angle or the blade angle of the controlling device.

Furthermore, in a nozzle arrangement this problem may be solved by symmetrically changing the geometric parameters of the nozzle device due to the change in nozzle width (moving one of the walls forming the nozzle, to maintain the nozzle's profile) or the incline angle of the symmetrical nozzle parts separated at the bottom into individual parts (for the ACV without flexible skirts. However, it must be noted that changing the suspension height or movement is possible within extremely insignificant limits. Shifting from a displacement position into a suspended mode above the water, the craft is raised to a height equal to the sum of immersion height of the flexible skirts, and height of clearance of the air space between the base surface and lower edge of the flexible skirts. The clearance of an ACV with a flexible-skirted air cushion changes very little and usually consists of 5-10 centimeters.

List and trim difference control may be achieved at the expense of asymmetrical changing of the geometric parameters of the nozzle device (for nozzle arrangement) and the aerodynamic parameters of the air stream directed to it. Using this method, the following variants are possible:

width control of separate parts of the nozzle device;

regulating the incline angle of asymmetrical parts of the nozzle (in the absence of flexible-skirts);

controlling the supply of air to the asymmetrical nozzle parts under a uniform nozzle width and their unchangeable incline angle;

asymmetrical change of height of the flexible skirts, etc.

Independent trim difference control, when the control devices do not affect the aerodynamic properties of the air cushion, is possible at the expense of applying horizontal aerodynamic rudders or, for example ballast-trim difference systems, etc.

-251-

Thus, as we see, there are various devices for controlling air cushion vehicles. The devices are varied and complex on constructed experimental air cushion craft. By way of an illustration, we will cite a description of devices on three ACVs, essentially different from each other: the CC-2.001, the SRN3 and the SRN5.

The ACV CC-2.001 was developed for testing without flexible skirts. The forced air equipment consists of two counter-rotating fans (bow and stern). On the ACV, there is a right-angle shaped peripheral nozzle with two longitudinal stability nozzles. ACV control devices consist of directional blades and rotating panels, mounted in the nozzles.

The rotating panels are mounted directly on the bow and stern parts of the transverse nozzles. They are able to support the width changes and nozzle covering in these parts. These same panels are provided for in the longitudinal nozzles.

Moveable control blades are mounted in both nozzles to ensure stability. They can generate an air current incline fr   )° in the bow to 50° in the stern (from the vertical). Stationar bl. s with a constant 30° incline angle in the stern are on a large part of the longitudinal periphery of the nozzles.

Draught force for the craft and its control either in the bow or stern is developed by:

utilizing stationary blades;

shifting the blades in the nozzles thereby ensuring stability;

covering the bow or stern transverse currents with panels;

trim difference through ballast.

Yaw control was intended to be ensured by tilting the moveable blades of the right and left sides in opposite directions, however, their effect proved to be insufficient. It was revealed that rotating panels in longitudinal peripheral nozzles could be utilized for yaw control. Furthermore, there was a certain tendency to yaw when using the rotating panels in transverse nozzles. All these methods were utilized while the craft was underway and in every instance an almost identical moment of yaw was provided. The craft's movement in a lateral direction was provided by the rotating panels in the longitudinal peripheral nozzles, which, when covered on one side, produced a bank toward that side.

With the necessity of ensuring the craft's suspension, a large part of the force designated for control was utilized for compensating reacting draught, making control of the craft impossible.

It appeared expedient to pitch the ship toward the stern to compensate for the draught developed by the stationary blades while in a suspended mode and while maneuvering at low speeds. But this had an adverse effect on the speed.

Control of the ACV SRN3 is achieved by the action of the screws on rotating pylons, moveable and immovable stabilizers, rudder and screw--rudder complexes (submerged in the water). The moveable stabilizer turns automatically as the stern pylon, connected mechanically to the stabilizer, rotates. The maximum turn angle of the stabilizer is $\pm20°$ and the maximum turn angle of the rudder is $-40°$. To deviate from course while in a forward motion, the pylons are rotated in various directions, and the transverse draught of the screws develops a pair of forces which turns the craft. To turn the craft while the craft is stationary, the helmsman must impart to one screw forward draught and to the other reverse draught to rotate the pylons to one side.

While the pylons rotate in one direction and the screws work in one direction, the transverse draught of the screws and the reaction of the stabilizer and rudder cause the craft to list and drift. This method of control may be utilized for counteracting a headwind or for compensating an asymmetrical load. The flexible skirt may also be raised and lowered.

The SRN5 craft is controlled with the aid of two stabilizer, as well as vertical and horizontal rudders. Horizontal rudders serve to alter the trim difference of the ship. At the first ACV trials it was established that the static stability on course was excessive. Therefore, the height of the stern stabilizers was lowered, and additional stabilizer (on the deck cabin) was mounted to the bow from the ship's center of gravity and in the stern-jet rudders consisting of two flat air ducts connected to a receiver and a portion of the external surfaces of the vertical rudders rotating with them. This additional equipment ensures yaw control at low speeds. The air flow from the air ducts does not bring about any noticeable decrease in the lift forces of the craft and develops a reacting draught (base) significantly lower than the screw base. When it becomes necessary to s p the craft fully, the reaction draught is compensated for by reversin he screw pitch. To prevent side drift, a device is mounted on the craft for lifting the flexible skirt. The lift of two sections of the flexible skirt on the corresponding side creates list and and produces a side force, impeding side drift while in a turn. The rudders are sufficiently effective during movement at high speeds, but the force developed at the bow stabilizer while in a turn produces an adequate internal list for input into a circulation which has been set up.

The test results of these three craft demonstrated that such a complex as that used for controlling the ACV CC-2.001 cannot provide the necessary control and maneuverability, especially in wind and swells. The remaining two models offer satisfactory maneuvering qualities and are roughly the same.

We shall turn to Figure 128 (the two-digit numbers in the chart = = time in seconds) for a qualitative evaluation of ACV controllability without flexible skirts in comparison with other fast moving craft.
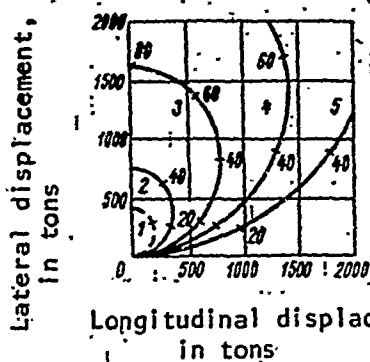
Figure 128. Comparison of Maneuver Characteristics of ACVs and Hydrofoils. 1, 40 knots; 2, 40 knots; 3, 60 knots; 4, 80 knots; 5, 100 knots. - - - -, hydrofoil craft; ———, ACVs.

Lateral displacement, in tons

Longitudinal displacement, in tons

The curve 1 in Figure 128 shows that ordinary hydrofoil craft at speeds of 40 knots make a 180° turn in 30 seconds, having a turning circle 400 meters in diameter and a side acceleration of 0.2 gs. Curves 2 to 5 are plotted for an ACV moving with a drift of 30° (which creates a centripetal force from the screw on the turning circle equal to P/G = = 0.06) and while using lateral jet nozzles with a relative thrust of P/G = 0.05. It is evident from Figure 128 that 90-180° turns for an ACV at speeds of 60-100 knots, requires an extremely large amount of space and time, and a reduction in speed is recommended when these turns are made. Attempts to improve an ACV's maneuverability with a nozzle arrangement by lowering a keel (rudder) into the water are met by difficulties because it would be necessary to install keels of excessive lengths, and also because of excessive outboard list in turns.

Using extended keels is considered expedient while operating an ACV on level water surfaces and as an emergency measure for improving the maneuverability while passing areas with large volumes of traffic. Figure 129 depicts the relationship of the turning radius of certain ACVs to speed. It follows from this figure in particular, that added control with flexible skirts significantly lowers the established turning radius (for the SRN6 more than 50%). Certain maneuverability elements of constructed ACVs are given in Table 12.
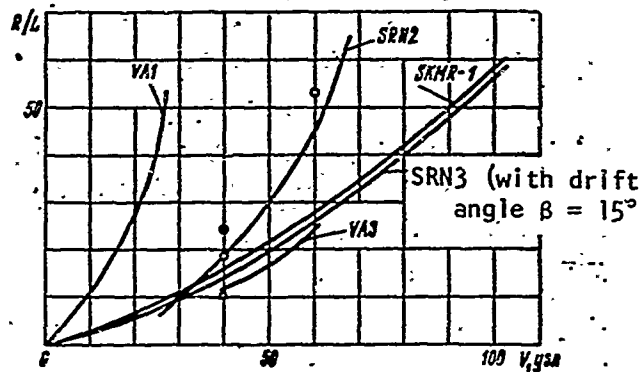
Figure 129. Relationship of an ACV's Turning
Radius to Speed. ●, SRN6; Δ, SRN6 (with
control by flexible skirts); O, SRN5.

TABLE 12. SOME ELEMENTS OF MANEUVERABILITY OF SRN5 AND
SRN6 ACVs.

ACV	Acceleration time, (sec)	Range of speed (knots)	Braking time, (sec)	Overshoot (relative)		Surmountable incline
				In normal conditions	In emergency cases	
SRN5	76	0-70	33	41.6 L	11.3 L	1:6 in a suspended mode. 1:3 in lift at an incline with primary speed of 23 knots
SRN6	41	0-50		16.1 L	7.4 L	1:9

It is considered difficult to design an ACV which can maneuver
in a lateral direction with an acceleration of more than 0.1g and
while braking 0.15-0.20g. It must be also taken into consideration
that acceleration to attain a speed of 80-100 knots must not be very
great (0.05-0.10 g).

-255-

Going over to the basic theory of studying the ACV's maneuvering qualities, we will notice that primary attention in the future will be devoted to ACV controllability inasmuch as ensuring control is precisely the most important and complex question in ACV operation.

The study of controllability, as with ordinary craft, is based on the differential equation of movement and the study of external forces, which will be examined in the following paragraphs.

For studying the ACV's behavior, we will adopt the starboard coordinate system (Figure 130).
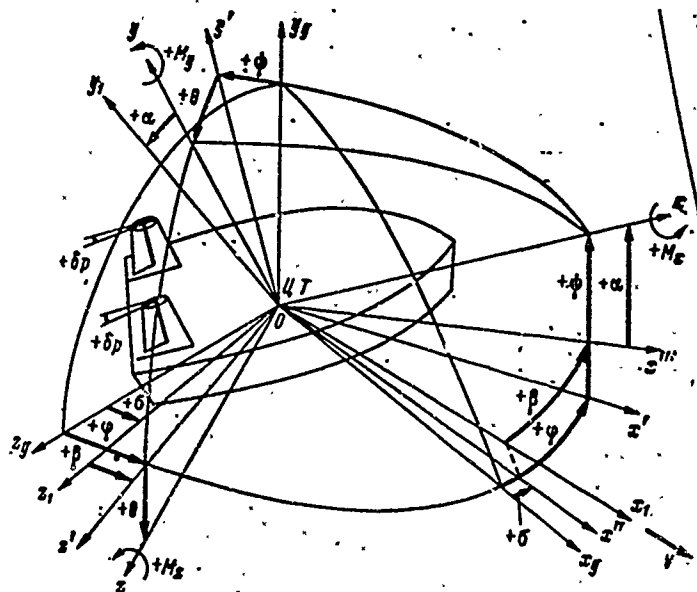
Figure 130. Systems of Fixed $(Ox_g y_g z_g)$, Rigidly Constrained by the Craft $(Ox_1 y_1 z_1)$ Coordinate Axes.

Fixed coordinates of axes (Ox_g, Oy_g, Oz_g) are connected by calm water surfaces, whereas axis Ox_g is arranged in a calm water surface plane in an arbitrary direction, axis Oy_g is directed upward vertically, and axis Oz_g is normal to the first two to produce a starboard coordinate system of axes.

For a first rate mobile coordinate system, the Oxyz system is assumed, the beginning of which coincides with the ACV's center of gravity.

Axis Ox is directed toward the bow parallel to the base and is called the longitudinal axis, axis Oy is directed upwards, perpendicular to the axis Ox in a diametric plane and is called the normal axis. Axis Oz is normally directed to the symmetrical plane xOy to starboard and is called the transverse axis.

In addition we will introduce the speed (flowing axes) coordinate axes $Ox_1y_1z_1$. The initial coordinates of this system also coincide with the ACV's center of gravity. Axis Ox_1, directed along a mobile speed vector of the ACV's center of gravity (i.e., opposite the speed of air flow), is called the speed axis. Axis Oy_1 is directed perpendicular to the Ox_1 axis directed upwards and is called the lift force axis.

Axis Oz_1, normal to the x_1Oy_1 plane, also depicts a starboard coordinate system.

In order for the ACV movement to be fully known, it is necessary to know:

a) the ACV's pole position (center of gravity) relative to the system of fixed coordinates of axes $Ox_gy_gz_g$ (translational movement);

b) the position of the axes Oxyz, rigidly constrained by the ACV in relation to the fixed axes (rotary movement).

To determine ACV turning in relation to axes $Ox_gy_gz_g$, it is necessary, as is well-known, to know the nine angles between the mobile and fixed axes. However, of the nine angles only three are independent. That is why, in order to assign the position of axes Oxyz in relation to axes $Ox_gy_gz_g$, the three independent angles (Euler's) are designated φ, ψ and θ. It is convenient to designate them, employing three consecutive turns of axes Oxyz [35]:

first turn--around axis Oy_g to angle φ (yaw angle);

second turn--around axis Oz' to angle ψ (trim angle);

third turn--around axis Ox to angle θ (list angle).

-257-

Parameters φ, ψ and θ are kinematic parameters of rotary movement.

Translational movement is assigned a speed vector of the ACV's center of gravity oriented in relation to axes Oxyz, where this vector is determined by two angles α and β, where α is the angle of attack, the angle between the projected vector speed of the ACV's center of gravity on the plane xOy (Ox''') and the direction of the longitudinal axis Ox; β is the drift angle, the angle between the direction of the speed vector of the ACV's center of gravity and the projected vector on the plane xOy. Parameters α and β, as well as speed vector $\vec{V}$ are the kinematic parameters of translational movement.

We shall examine the forces acting on the ACV in projections of axes of systems of coordinate Oxyz, rigidly constrained by the craft.

In transitory motion the projection of external forces on these axes and their moments depend on the kinematic parameters of movement examined above and on all these parameters carried out in time, however, this dependence, in the average case, is nonlinear.

In order to give the linearized analytical expressions for the questioned projections of forces onto connected axes and their moments, we will use the steady state hypothesis, i.e., we will assume that the forces and moments at some moment of time are the same during non-steady state motion as during steady state motion with the same kinematic parameters.

In the ensuing discussion, we will examine the sums of the projections of all forces and their moments acting on the ACV, i.e.,

$$\sum X_i = X; \ \sum Y_i = Y; \ \sum Z_i = Z;$$
$$\sum M_{x_i} = M_x; \ \sum M_{y_i} = M_y; \ \sum M_{z_i} = M_z.$$

In the general case forces and their moments, among which are the main, auxiliary or those preventing hovering or motion of the ACV, and artificial (control), used for altering or overriding the main forces, act on ACV with a flexible air cushion skirt.

We will examine the following main forces and moments.

1) aerodynamic forces and moments;

a) forces and moments created by the headwind on the hull of the vessel and its flexible enclosure (forces and moments of the external aerodynamics of the ACV), R_a and M_a;

b) forces and moments created by the pressure of the air cushion on the bottom of the ACV, R_p and M_p;

c) forces and moments created by the reaction of the intake and exhaust air, R_r and M_r;

d) forces and moments created by the flowing of good air through the internal ducts (forces and moments of internal aerodynamics), R_i and M_i.

2) Hydrodynamic forces and moments:

a) forces and moments caused by the interaction of the air cushion and water surface, R_v, M_v;

b) forces and moments caused by the interaction of the flexible skirt and air jets with the water surface, $R_{f.s.}$ and $M_{f.s.}$

3) Weight of the vehicle G.

We will examine, moreover, the controlling forces and moments, including:

a) forces and moments created by the rudder, R_{ru} and M_{ru};

b) forces and moments created by the working engines, R_e and M_e.

§22. Forces and Moments Unrelated to Air Cushion

We will examine the forces and moments acting on a moving ACV and unrelated to the air cushion. These forces and moments include the following:

aerodynamic forces and moments on the hull;

forces and moments created by the rudder;

forces and moments created by the engines;

weight of vehicle.

The force of weight G of the vehicle on the Oxyz axis produces the projections:

-259-

$$X_a = G \sin \psi; \tag{224}$$
$$Y_a = -G \cos \psi \cos \theta;$$
$$Z_a = G \cos \psi \sin \theta.$$

Here

$$M_{xa} = M_{ya} = M_{za} = 0.$$

Aerodynamic Forces and Moments on Hull and Rudder of ACV

The presence of the air cushion beneath the hull in ACV leads to asymmetric distribution of that component of normal stresses which develops on the hull of the ACV due to the oncoming air flow and is attributed to static air pressure.

The forces produced by this component are related to one of the basic categories of external forces acting on ACV. They comprise the principal part of external forces applied to ACV on the air cushion side, R_{a4} and M_{a4} (see §11, Chapter II).

The second component of normal stresses caused by excess dynamic pressure, and also tangential stresses that develop only during motion of the air in relation to the body, govern the action of ordinary aerodynamic forces and moments (R_{a1}, M_{a1}, see §11, Chapter II).

The problem of determining the normal and tangential stresses on the surface of a moving body has not yet been solved by hydromechanics, even for relatively simple bodies. Therefore we will use the expressions for aerodynamic forces and moments in a form reflecting geometric and dynamic similarity and making it possible to use the experiment:

Longitudinal aerodynamic force

$$X_a = c_{x_a} q S_\text{ЗП}; \tag{225}$$

Normal aerodynamic force

$$Y_a = c_{y_a} q S_n; \tag{226}$$

Transverse aerodynamic force

$$Z_a = c_{z_a} q S_{6ok};$$ (227)

Aerodynamic moment of roll

$$M_{x_a} = m_{x_a} q S_{6ok} L;$$ (228)

Aerodynamic moment of yaw

$$M_{y_a} = m_{y_a} q S_{6ok} L;$$ (229)

Aerodynamic moment of trim

$$M_{z_a} = m_{z_a} q S_{6ok} L,$$ (230)

where $q = 1/2 \rho V^2$ is dynamic pressure;

   L is the length of the vehicle;

   S_{bok} is the area of lateral projection of the hull and skirt
      projections onto diametral plane;

   $S_{\emptyset}$ is the area of projection of hull onto midplane;

   S_n is area of air cushion;

   C_{x_a} is the coefficient of longitudinal aerodynamic force;

   C_{y_a} is the coefficient of normal aerodynamic force;

   C_{z_a} is the coefficient of transverse aerodynamic force;

   m_{x_a} is the coefficient of roll moment;

   mm_{y_a} is the coefficient of yaw moment;

   m_{z_a} is the coefficient of trim moment.

Using the method of small perturbations, we will expand the aero-
dynamic forces and moments into Maclaurin series in terms of angular
velocities and we will retain only the first terms in them

-261-

$$X_{a} = X_{a\,(\omega=0)} + \frac{\partial X_{a}}{\partial \bar{\omega}_{x}} \bar{\omega}_{x} + \frac{\partial X_{a}}{\partial \bar{\omega}_{y}} \bar{\omega}_{y} + \frac{\partial X_{a}}{\partial \bar{\omega}_{z}} \bar{\omega}_{z};$$

$$Y_{a} = Y_{a\,(\omega=0)} + \frac{\partial Y_{a}}{\partial \bar{\omega}_{x}} \bar{\omega}_{x} + \frac{\partial Y_{a}}{\partial \bar{\omega}_{y}} \bar{\omega}_{y} + \frac{\partial Y_{a}}{\partial \bar{\omega}_{z}} \bar{\omega}_{z};$$

$$Z_{a} = Z_{a\,(\omega=0)} + \frac{\partial Z_{a}}{\partial \bar{\omega}_{x}} \bar{\omega}_{x} + \frac{\partial Z_{a}}{\partial \bar{\omega}_{y}} \bar{\omega}_{y} + \frac{\partial Z_{a}}{\partial \bar{\omega}_{z}} \bar{\omega}_{z};$$

$$M_{x_{a}} = M_{x_{a}\,(\omega=0)} + \frac{\partial M_{xa}}{\partial \bar{\omega}_{x}} \bar{\omega}_{x} + \frac{\partial M_{xa}}{\partial \bar{\omega}_{y}} \bar{\omega}_{y} + \frac{\partial M_{xa}}{\partial \bar{\omega}_{z}} \bar{\omega}_{z};$$ (231)

$$M_{y_{a}} = M_{y_{a}\,(\omega=0)} + \frac{\partial M_{ya}}{\partial \bar{\omega}_{x}} \bar{\omega}_{x} + \frac{\partial M_{ya}}{\partial \bar{\omega}_{y}} \bar{\omega}_{y} + \frac{\partial M_{ya}}{\partial \bar{\omega}_{z}} \bar{\omega}_{z};$$

$$M_{z_{a}} = M_{z_{a}\,(\omega=0)} + \frac{\partial M_{za}}{\partial \bar{\omega}_{x}} \bar{\omega}_{x} + \frac{\partial M_{za}}{\partial \bar{\omega}_{y}} \bar{\omega}_{y} + \frac{\partial M_{za}}{\partial \bar{\omega}_{z}} \bar{\omega}_{z},$$

where $\bar{\omega}_{i} = \omega L/V$ are dimensionless angular velocities.

The first terms in the right-hand side of (231) are positional. (translational) forces and moments, and the other terms are their rotational derivatives.

For further simplification of the problem, disregarding magnitudes of the second order of smallness, we may write these expressions in the following form:.

$$X_{a} = X_{a\,(\omega=0)};$$

$$Y_{a} = Y_{a\,(\omega=0)};$$

$$Z_{a} = Z_{a\,(\omega=0)} + \frac{\partial Z_{a}}{\partial \bar{\omega}_{y}} \bar{\omega}_{y};$$

$$M_{x_{a}} = M_{y_{a}\,(\omega=0)} + \frac{\partial M_{xa}}{\partial \bar{\omega}_{y}} \bar{\omega}_{y};$$ (232)

$$M_{y_{a}} = M_{y_{a}\,(\omega=0)} + \frac{\partial M_{ya}}{\partial \bar{\omega}_{y}} \bar{\omega}_{y};$$

$$M_{z_{a}} = M_{z_{a}\,(\omega=0)};$$

The positional forces and moments are written in the following form:

$$X_{a\,(\omega=0)} = X_{a_{\circ}} + X_{a}^{\beta}\beta + X_{a}^{\psi}\psi;$$

$$Y_{a\,(\omega=0)} = Y_{a_{\circ}} + Y_{a}^{\psi}\psi;$$ (233)

$$Z_{a\,(\omega=0)} = Z_{a}^{\beta}\beta;$$

$$M_{x_{a}\,(\omega=0)} = M_{x_{a}}^{\beta}\beta;$$

$$M_{y_{a}\,(\omega=0)} = M_{y_{a}}^{\beta}\beta;$$

$$M_{z_{a}\,(\omega=0)} = M_{z_{a_{\circ}}} + M_{z_{a}}^{\psi}\psi.$$

Later on we will examine individually the aerodynamic characteristics of the hull and aerodynamic characteristics of the rudder.

Aerodynamic Characteristics of Hull

Proceeding to the coefficients and considering the preceding equations, we obtain

$$c_{x_K} = c_{x_{K_0}} + c_{x_K}^\beta \beta + c_{x_K}^{\dot\psi} \dot\psi; \tag{234}$$

$$c_{y_K} = c_{y_{K_0}} + c_{y_K}^{\dot\psi} \dot\psi;$$

$$c_{z_K} = c_{z_K}^\beta \beta + c_{z_K}^{\bar\omega_y} \bar\omega_y;$$

$$m_{x_K} = m_{x_K}^\beta \beta + m_{x_K}^{\bar\omega_y} \bar\omega_y;$$

$$m_{y_K} = m_{y_K}^\beta \beta + m_{y_K}^{\bar\omega_y} \bar\omega_y;$$

$$m_{z_K} = m_{z_{K_0}} + m_{z_K}^{\dot\psi} \dot\psi.$$

The dependences of aerodynamic coefficients of ACV on the various parameters are more complex than those, for example, of aircraft, since in addition to everything else, the screen and artificially created air cushion have an effect on the aerodynamic characteristics of ACVs.

As shown by experience, however, the coefficient of moment of yaw m_{y_n}, created by the air cushion, is small in value. Therefore we may evaluate the aerodynamic characteristics in the first approximation without considering the influence of the air cushion, i.e., on the basis of the results of ordinary aerodynamic tests.

Aerodynamic Characteristics of Hull $c_{z_k}^\beta$, $m_{y_k}^\beta$, $c_{z_k}^{\bar\omega_y}$, and $m_{y_k}^{\bar\omega_y}$

For approximate analytical determination of these aerodynmic characteristics of the hull, we may use the theory of bodies of minimum elongation, the aerodynamic characteristics of which, given small angles of attack (drift), are proportional to the elongation λ of the body, equal to

$$\lambda = \frac{H^2}{S_{6\cdot\kappa}},$$

where H is the maximum height of the body.

-263-

Three models of the flow of air past the body were examined during the analysis of isolated bodies of minimum elongation, with rectangular shape in projection on the diametral plane:

non-circulating flow around body;

circulating flow around body with elliptical distribution of circulation with respect to span (K. Vigkhardt's linear theory) [51];

circulating flow around body with constant distribution of circulation with respect to span [46].

Using the basic requisites of the last two problems, we obtain the following expressions for the aerodynamic characteristics of the hull:

$$c_z^\beta = K\pi\lambda;$$
$$\bar{c}_z^{\omega y} = K\pi\lambda(1 - \bar{x}_g);$$
$$m_y^\beta = K\pi\lambda\bar{x}_g;$$
$$\bar{m}_y^{\omega y} = -K\frac{\pi}{4}\lambda\left[1 + (1 - 2\bar{x}_g)^2\right],$$

(235)

where $\bar{x}_g$ is the dimensionless coordinate of the center of gravity from the wing tip.

According to linear theory the coefficient is $K = 0.5$.

In accordance with the circulation theory, the outcome of constant distribution of circulation with respect to span, coefficient $K = 1$. In known investigations of ACV controllability [62], the aerodynamic characteristics of the hull are evaluated on the basis of linear theory of a detached wing of minimum elongation, in which the influence of the screen on the characteristics is not taken into account. We feel that it is more scientific to allow for the influence of the screen effect.

It should be borne in mind that the theoretical solution [47] of the problem of forces acting on the submerged part of the hull of a floating vessel, as on a body of minimum elongation in the form of an elliptical cylinder, yields the same analytical expression for linear load[1] as derived in [46] for a thin detached wing of minimum elongation,

---

[1]A linear load is transverse load (elementary hydrodynamic reaction in the transverse plane) per unit of length of the diametral plane $\Delta z/\Delta x$ for $\Delta x \to 0$.

if the span of the body, equivalent to the hull, is assumed equal to two draughts. This is indirect proof of the validity of viewing the submerged portion of the hull of a floating vessel as a body of minimum elongation with a span equal to double draught 2T and elongation $\lambda =$ $= 2T/L$, admitting the assumption that flow over a wing of minimum elongation, standing on its end, is analogous to flow over a detached wing with a conditional height 2H and conditional elongation $\lambda = 2H/L$.

Further, we will use a second assumption that an ACV with a flexible air cushion enclosure can be replaced approximately with a wing or body of minimum elongation, standing on end on a solid screen..

As elevation h increases the condition of absence of flow of the incident airstream between the screen and bottom is satisfied because of the air cushion. · Therefore, obviously, such an assumption can be made by examining motion at non-zero elevations of the vessel above the screen. Here, obviously, as elongation of the ACV we may use the value

$$\lambda = \frac{2H}{L} \times \frac{2H^2}{S_{\max}}. \qquad (236)$$

Under such assumptions it is possible to use the linear theory of (lateral) flow around a detached wing of minimum elongation, developed in [50].

We will examine the effect of the incident air flow on the lateral surface of the ACV hull as it travels in a circular trajectory. In this case the drift angles $\beta(x)$ change·in length. The drift angle is β at the center of gravity of the vehicle. Then the normal component of flow velocity at the center of gravity will be $(-V \sin \beta)$. As a result of rotation of the hull at angular velocity ω_y, an additional normal

velocity, equal to $x\omega_y$, appears at points on the side of the hull (Figure 131).
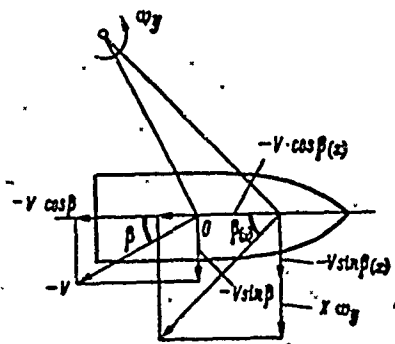

Figure 131. Effect of Incident Air Flow on Side of ACV Hull Moving in Circular Trajectory.

-265-

Then the summary normal component of velocity at arbitrary point x will be equal in absolute value to $V \sin \beta - x\omega_y$, and the longitudinal component will be $V \cos \beta$.

Hence, the local drift angle can be found from the expression

$$\tan \beta(x) = \frac{V \sin \beta - x\omega_y}{V \cos \beta} = \tan \beta - \frac{x\omega_y}{V \cos \beta} \qquad (237)$$

In the theory of probability of a surface vessel it is assumed approximately that

$$\sin \beta \approx \beta; \quad \cos \beta \approx 1; \quad \tan \beta \approx \beta, \qquad (238)$$

since drift angles do not exceed 12-15°. Therefore the character of change of the drift angle as a surface vessel travels is expressed by the following simplified relation:

$$\beta(x) = \beta - \frac{x\omega_y}{V} . \qquad (239)$$

For consideration of this law of change of drift angle, the linear load on a wing of minimum elongation can be represented by the following expression, bearing in mind that the wing span of an ACV is equal to twice the hull height $l(x) = 2H(x)$:

$$\gamma_n(x) = -\frac{\pi \rho V^2}{4} \frac{d}{dx} [\beta(x) l^2(x)] = -\pi \rho V^2 \left[2 \frac{dH(x)}{dx} H(x) \beta - \right.$$
$$\left. - 2 \frac{dH(x)}{dx} H(x) \frac{x\omega_y}{V} - H^2(x) \frac{\omega_y}{V} \right]. \qquad (240)$$

Tests have shown that compared to floating vessels, the ACV have substantially greater drift angles which, for example, in the case of steady state circulation can reach 30°.

We will examine how great will be the error in the determination of local drift if approximate expressions equation (238) are used for analysis of angles up to 30°. The greatest local drift angle will occur at the bow tip, i.e., for x = -L/2.

Assuming that

$$\omega_y = \frac{V}{R},$$

(241)

Then with a radius of circulation equal to hull length, expressions (237) and (239) become:

$$\tan \beta(x) = \tan \beta + \frac{1}{2 \cos \beta};$$

(242)

$$\beta(x) = \beta + \frac{1}{2}.$$

(243)

Calculation by equations (242) and (243) is presented in Table 13.

TABLE 13. COMPILATION OF <u>DRIFT</u> ANGLES CALCULATED USING EQUATIONS (242) AND (243).

No. of row	Functions	At angle $\beta°$		
		15	30	35
1	β, rad	0,262	0,524	0,611
2	$\tan \beta$	0,266	0,577	0,700
3	$\cos \beta$	0,966	0,866	0,819
4	$\tan \beta(x)$	0,770	1,133	1,311
5	$\beta(x)$, rad	0,762	1,024	1,111
6	$\beta°(x) = \arctan \beta(x)$	37° 36'	48° 35'	52° 40'
7	$\beta°(x) = f\beta(x)$ rad	43° 41'	58° 40'	63° 40'
8	(7) in % of (6)	116	120	121

We see in Table 13 that the use of approximate relations (238) for angles β reaching 30-35° gives, in the worst case, an error 4-5% greater than that obtained in the case of angles β of about 15°.

Considering that usually $R \gg L$, such an increase in error can be regarded as minor, and approximate expression (240) can be used in those cases when the angles go up to 30°.

As the result of integration of linear load through the length of the hull we may calculate the coefficient of summary transverse force

-267-

$$c_{z_{\text{кр}}} = \frac{Z_{\text{кр}}}{2qS_{60\text{к}}} = -\frac{\pi}{S_{60\text{x}}}\left[2\int_{L_{\text{ш}}}^{0.5L} H(x)\frac{dH(x)}{dx}\beta - 2\int_{L_{\text{ш}}}^{0.5L} H(x)\frac{dH(x)}{dx}\times\right.$$

$$\left.\times\frac{x\omega_y}{V} - \int_{-0.5L}^{0.5L} H^2(x)\frac{\omega_y}{V}\right]dx, \tag{244}$$

since

$$dZ_{\text{кр}} = \gamma_\text{в}(x)\,dx.$$

To find the solutions corresponding to flow past a wing of minimum elongation in the presence of circulation, it is necessary, as we know, to satisfy the Chaplygin-Zhukov postulate of smooth flow past the trailing edge of the wing. Jones' theory states that for this purpose the load must be located only on the leading part of the wing, between the leading edge and the section corresponding to maximum span. Therefore the integrals containing $dH(x)/dx$ entering into expression (244) are taken up to the section $H(x) = H_{\text{max}}$. In fact, the integral containing $H(x)$, is taken in terms of the length of the vessel, since it represents a load of inertial character[1].

By analogy we may also find the coefficient of the moment of yaw

$$m_{y_{\text{кр}}} = \frac{M_{y_{\text{кр}}}}{2qS_{60\text{x}}L} = -\frac{\pi}{S_{60\text{к}}L}\left[2\int_{L_{\text{ш}}}^{0.5L} H(x)\frac{dH(x)}{dx}x\beta - \right.$$

$$\left. -2\int_{L_{\text{ш}}}^{0.5L} H(x)\frac{dH(x)}{dx}\cdot\frac{x^2\omega_y}{dx} - \int_{-0.5L}^{0.5L} H^2(x)x\frac{\omega_y}{V}\right]dx. \tag{245}$$

With the consideration of the expression

$$\omega_y = \frac{V}{L}\bar{\omega}_y$$

the following expressions can be derived from (244) and (245) for translational and rotational derivatives of the coefficients of transverse force and moment of yaw:

---

[1]Inertial load is load during non-circulating motion of wing in perfect fluid.

$$c^{\beta}_{z_{\kappa p}} = -\frac{2\pi}{S_{6ox}} \int\limits_{L_{\scriptscriptstyle H}^{\circ}}^{0,5L} H(x)\frac{dH(x)}{dx}dx;$$

$$m^{\beta}_{y_{\kappa p}} = -\frac{2\pi}{S_{6ox}L} \int\limits_{L_{\scriptscriptstyle H}^{\circ}}^{0,5L} H(x)\frac{dH(x)}{dx}dx;$$

$$c^{\bar{\omega}y}_{z_{\kappa p}} = \frac{\pi}{S_{6ox}L}\left[2\int\limits_{L_{\scriptscriptstyle H}^{\circ}}^{0,5L} H(x)\frac{dH(x)}{dx}xdx + \int\limits_{-0,5L}^{0,5L} H^2(x)dx\right];$$

$$m^{\bar{\omega}y}_{y_{\kappa p}} = \frac{\pi}{S_{6ox}L^2}\left[2\int\limits_{L_{\scriptscriptstyle H}^{\circ}}^{0,5L} H(x)\frac{dH(x)}{dx}x^2dx + \int\limits_{-0,5L}^{0,5L} H^2(x)xdx\right]$$

(246)

From these expressions we will remove the correction factors that allow for the effect of form change in plan (in projection onto the diametral plane of the vessel). For this purpose we will represent the expressions for the aerodynamic characteristics in the following form:

$$c^{\beta}_{z_{\kappa p}} = \pi\lambda c_1;$$

$$m^{\beta}_{y_{\kappa p}} = \pi\lambda m_1\bar{x}_g;$$

$$c^{\bar{\omega}y}_{z_{\kappa p}} = \pi\lambda(1-\bar{x}_g)d_1;$$

$$m^{\bar{\omega}y}_{y_{\kappa p}} = -\frac{\pi\lambda}{4}\left[1+(1-2\bar{x}_g)^2\right]f_1.$$

(247)

where $\bar{x}_g = x_g/L$ is the dimensionless coordinate of the center of gravity from the bow of the ACV.

Hence, the correction factors that allow for the influence of change of height of the hull through the length of the vessel can be calculated as follows:

$$c_1 = \frac{1}{H^2_{max}} \int\limits_{L_{\scriptscriptstyle H}^{\circ}}^{0,5L} \frac{dH(x)}{dx}H(x)dx;$$

$$m_1 = -\frac{1}{\bar{x}_g H^2_{max}L} \int\limits_{L_{\scriptscriptstyle H}^{\circ}}^{0,5L} \frac{dH(x)}{dx}H(x)xdx;$$

(248)

-269-

$$d_1 \cong \frac{1}{2H_{max}^2 L (1 - \bar{x}_g)} \left[2 \int_{L_H^*}^{0.5L} \frac{dH(x)}{dx} H(x)\, x\, dx + \int_{-0.5L}^{0.5L} H^2(x)\, dx \right];$$

$$f_1 = -\frac{2}{H_{max}^2 L^2 [1 + (1 - 2\bar{x}_g)^2]} \left[2 \int_{L_H^*}^{0.5L} \frac{dH(x)}{dx} H(x)\, x^2\, dx + \int_{-0.5L}^{0.5L} H^2(x)\, x\, dx \right]. \tag{248}$$

The dependences of coefficients c_1 and m_1 on the product of the coefficient of completeness of the bow part of the diametral plane (DP) of ACV models $S_{HOC}/(L/2\ H^*)$ by the relative length of the bow taper $L_H^*/(L/2)$ are represented in Figure 132. Here S_{HOC} is the area of diametral plane of the model from midships to the bow; L_H^* is the length of the bow taper, the distance from the bow tip of the model to the rib with maximum hull height H^*.
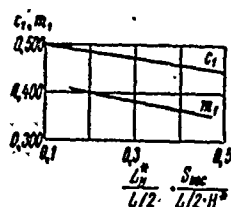

Figure 132. Coefficients c_1 and m_1, Which Take Into Account the Influence of Change of Height of the Hull Through the Length of the Vehilce on its Aerodynamic Characteristics, as Functions of the Product of the Completeness Coefficient of the Bow Section of the Diametral Plane of the ACV $S_{HOC}/(L/2 \cdot H^*)$ When Relative Length of Bow Taper $L_H^*/(L/2)$.

Analysis of the data in Figure 132 indicates that the coefficients c_1 and m_1 diminish as $L_H^*/(L/2) \cdot S_{HOC}/(L/2 \cdot H^*)$ increases. This tendency is weaker for the coefficient c_1 than for m_1. The numerical values of coefficients c_1 and m_1 differ little from each other and are closer to $K = 1/2$ than $K = 1$. This means that the linear theory of a detached wing of minimum elongation can be used for approximation of the aerodynamic characteristics of the ACV hull, but elongation of the hull must be determined with consideration of its doubled height, i.e., it must be assumed that

$$\lambda = 2\lambda_{a.\ r}, \tag{249}$$

where л.т denotes linear theory.

-270-

Equations (247) with the consideration of expressions (248) can be used for more accurate calculations of the aerodynamic characteristics of a hull as a wing of minimum elongation.

As in the theory of a wing of minimum elongation, the corporeality of the hull is not taken into account. Meanwhile, the ACVs have a large relative width (L/B ≈ 1.8-2.5), which should have a considerable effect on flow around the hull, and consequently its characteristics. In order to evaluate this phenomenon within the frameworks of linear theory we will represent aerodynamic characteristics $c_{z_k}^{\beta}$, $m_{y_k}^{\beta}$, $c_{z_k}^{\omega_y}$, $m_{y_k}^{\omega_y}$, with consideration of corporeality, in the following form:

$$c_{z_k}^{\beta} = c_{z_{\kappa p}}^{\beta} c_2 = \pi \lambda c_1 c_2; \qquad m_{y_k}^{\beta} = m_{y_{\kappa p}}^{\beta} m_2 = \pi \lambda m_1 m_2 \bar{x}_g;$$

$$c_{z_k}^{\omega_y} = c_{z_{\kappa p}}^{\omega_y} d_2 = \pi \lambda (1 - \bar{x}_g) d_1 d_2;$$

$$m_{y_k}^{\omega_y} = m_{y_{\kappa p}}^{\omega_y} f_2 = -\frac{\pi \lambda}{4} [1 + (1 - 2\bar{x}_g)^2] f_1 f_2.$$

(250)

Because they have less effect on the final result than coefficients c_2 and m_2, we will assume d_2 and f_2 to be equal to 1. Coefficients c_2 and m_2, in fact, can be determined with consideration of the results of wind tunnel tests of models.

The coefficient c_2 is shown in Figure 133 as a function of the product of the two parameters $L_n^*/\sqrt{S_{\text{об}}}$ and $\frac{L_{k\kappa}}{L/2}$ where $L_n^*/\sqrt{S_{\text{об}}}$ - is coefficient of completeness of the bow portion of the model;

$\frac{L_{Bk}}{L/2}$ is the relative length of the stern curvature of the model in plan, measured from the stern point of the model toward the bow to the rib at which the beam of the model is maximum.

The coefficient c_2, as we will see, has a tendency to decrease as the product of these parameters increases.
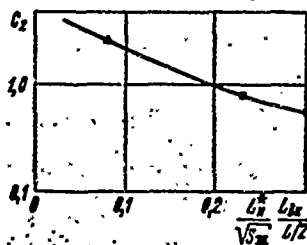
Figure 133. Coefficient c_2, Which Considers the Influence of the Corporeality of the Hull on the Value $c_{z_k}^\beta$ as a Function of the Product of the Coefficient of Completeness of the Bow Part of the ACV $L_{_H}^*/\sqrt{S_{_{\overline{\omega}}}}$ and Relative Length of the Stern Curvature of the Vehicle in Plan $L_{BK}/(L/2)$.

Figure 134 represents the coefficient m_2 as a function of the coefficient of completeness of the bow section of the model $L_{_H}^*/\sqrt{S_{_{\overline{\omega}}}}$.
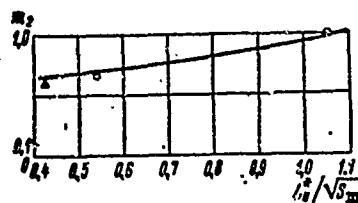
Figure 134. Coefficient m_2, Which Considers the Effect of the Corporeality of the Hull on the Value m_{yK}^β, as a Function of the Coefficient of Completeness of the Bow Section $L_{_H}^*/\sqrt{S_{_{\overline{\omega}}}}$

We see in Figure 134 that as the coefficient of completeness increases, the coefficient m_2 has a tendency to diminish.

Experience in hydrodynamic classification of bodies of minimum elongation [49] indicates that if the hull of an ACV is used not as a wing, but as a body of minimum elongation, then it is essential to consider other factors, in addition to corporeality, which influence the character of flow around the body. One of these factors, which largely determines the turbulence structure of the body, is cross-section shape.

Bodies with rectangular cross-sections fall into the category of strong lifters, whereas bodies with rounded cross-sections fall into the category of normal lifters.

Here bodies for which

$$0 < \frac{c_z^\beta}{\lambda_{_{n.\,r}}} < \frac{2}{3}\left(\frac{c_z^\beta}{\lambda}\right)_{_{n.\,r}},$$

(where l.t denotes linear theory) are called weak lifters, bodies for which

-272-

$$\frac{2}{3}\left(\frac{c_z^\beta}{\lambda}\right)_{\text{л.т}} \leqslant \frac{c_z^\beta}{\lambda_{\text{л.т}}} \leqslant \frac{4}{3}\left(\frac{c_z^\beta}{\lambda}\right)_{\text{л.т}};$$

are called normal lifters and, finally, bodies for which

$$\frac{c_z^\beta}{\lambda_{\text{л.т}}} > \frac{4}{3}\left(\frac{c_z^\beta}{\lambda}\right)_{\text{л.т}},$$

are called strong lifters.

Applying this classification to bodies located above a screen, assuming the condition of absence of flow between the body and the screen to be satisfied and considering condition (249), we may call bodies for which equation

$$0 < \frac{c_{z_{\kappa}}^\beta}{\lambda} < \frac{1}{3}\left(\frac{c_{z_{\kappa}}^\beta}{\lambda}\right)_{\text{л.т}}; \tag{251}$$

weak lifters, bodies for which equation

$$\frac{1}{3}\left(\frac{c_z^\beta}{\lambda}\right)_{\text{л.т}} \leqslant \frac{c_{z_{\kappa}}^\beta}{\lambda} \leqslant \frac{2}{3}\left(\frac{c_z^\beta}{\lambda}\right)_{\text{л.т}}; \tag{252}$$

normal lifters and bodies for which

$$\frac{c_{z_{\kappa}}^\beta}{\lambda} > \frac{2}{3}\left(\frac{c_z^\beta}{\lambda}\right)_{\text{л.т}}. \tag{253}$$

strong lifters. However $\left(\frac{c_z^\beta}{\lambda}\right)_{\text{л.т}} = \frac{\pi}{2}$, and hence conditions (251)-(253) can be written as follows, respectively:

$$0 < \frac{c_{z_{\kappa}}^\beta}{\lambda} < 0,524; \tag{254}$$

$$0,524 \leqslant \frac{c_{z_{\kappa}}^\beta}{\lambda} \leqslant 1,05; \tag{255}$$

$$\frac{c_{z_{\kappa}}^\beta}{\lambda} > 1,05. \tag{256}$$

The hull models of many ACVs are strong lifters. This complicates conditions of controllability: a very sophisticated rudder unit is required to ensure cruise stability. On the basis of controllability it is advisable to strive for an ACV hull that has the least lifting capacity. One of the ways of achieving this goal is rounding off the lines in

-273-

cross-section and giving the ACV a streamlined shape. In addition, as indicated by experience in hydrodynamic classification of bodies of minimum elongation [49], this goal can also be achieved by smoothing off the lines in the stern section and by decreasing the beam of the hull.

As regards the rotational derivatives $m_{y_k}^{\bar{\omega}y}$ and $c_{z_k}^{\bar{\omega}y}$, in connection with the absence of experimental determination of these values near the screen, such analysis of the dependence of coefficients f_1, f_2, d_1, d_2 is difficult. The coefficients $m_{y_k}^{\bar{\omega}y}$ and $c_{z_k}^{\bar{\omega}y}$ can be approximated, as mentioned above, on the basis of linear theory, i.e., assuming $f_1 f_2 = = d_1 d_2 = k = 0,5$ with consideration of (249).

Coefficient of Aerodynamic Longitudinal Force c_{x_k}. The aerodynamic longitudinal force of ACV traveling without a drift angle and angle of attack coincides numerically with the force of aerodynamic drag.

The results of wind tunnel tests of models are used for determining the coefficient of aerodynamic longitudinal force c_{x_k}.

We will examine coefficient c_{x_k} in accordance with expression (234) in the following form:

$$c_{x_к} = c_{x_{к_0}} + c_{x_к}^{\beta} \beta$$

where $c_{x_{k_0}}$ is the coefficient of aerodynamic longitudinal force at zero drift angle.(coincides numerically with the coefficient of aerodynamic profile drag);

$c_{x_k}^{\beta}$, $c_{x_k}^{\psi}$ are its derivatives in terms of drift angle and trim.

The processing of wind tunnel test results indicates that the dependence of the coefficient c_{x_k} on the drift angle is clearly nonlinear.

-274-

As a whole, c_{x_k} as a function of the angle of drift is analogous to the change of this coefficient established for the surface ships: as β increases, it first increases and then diminishes.

The relative maximums of the coefficient c_{x_k} differ for various models, and moreover these maximums are scattered in terms of drift angle.

Linearization makes it possible to construct, on the basis of wind tunnel tests of models, the approximate dependence of the coefficient $c_{x_k}^\beta$ on the product of three parameters $\dfrac{L_H^\bullet}{\sqrt{S_\infty}} \cdot \dfrac{L_{BK}}{L/2} \cdot \dfrac{L_{BH}}{L/2}$ (Figure 135).

The error from linearization for an angle of drift of 30° is about 20% of the value c_{x_k}.
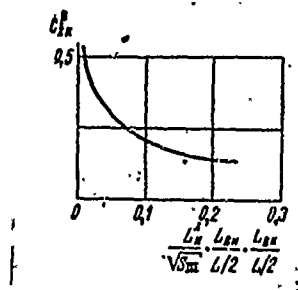
Figure 135. Derivative of Coefficient of Aerodynamic Drag of Hull in Terms of Drift Angle $c_{x_k}^\beta$ as a Function of the Product of Three Parameters: Coefficient of Completeness of Bow Section of Hull $L_H^\bullet/\sqrt{S_\infty}$, Relative Length of Stern $\dfrac{L_{BK}}{L/2}$ and Bow $\dfrac{l_{BH}}{L/2}$ Curvature of Hull in Plan.

Coefficient m_{x_k}. In accordance with expression (234), the coefficient of the aerodynamic moment of roll that acts on the hull is

$$m_{x_K} = m_{x_K}^\beta \beta + m_{x_K}^{\omega_y}\bar{\omega}_y.$$

The derivatives of this coefficient are least known. The results obtained from wind tunnel tests of models indicate that coefficient

$m_{x_k}^{\beta}$ may be both positive and negative, apparently depending on the position of the center of gravity of the model with respect to height. Derivative $m_{x_k}^{\bar{\omega}_y}$, for practical purposes, is not determined for ACVs like the other coefficients in equations (234).

Aerodynamic Characteristics of Tail Group

We will examine the forces and moments acting on the tail by means of expressions of the form (231).

Converting to coefficients related to $S_{\mathbb{Q}}$, S_n and S_{HOC}, we will have by analogy with functions (234), equations

$$
\begin{aligned}
c_{x_{on}} &= c_{x_{on}}^{\delta}\, \delta p + c_{x_{on}}^{\beta}\, \beta; \\
c_{y_{on}} &= c_{y_{on}}^{\delta}\, \delta p + c_{y_{on}}^{\psi}\, \psi; \\
c_{z_{on}} &= c_{z_{on}}^{\delta}\, \delta p + c_{z_{on}}^{\beta}\, \beta + c_{z_{on}}^{\bar{\omega}_y}\, \bar{\omega}_y; \\
m_{x_{on}} &= m_{x_{on}}^{\delta}\, \delta p + m_{x_{on}}^{\beta}\, \beta + m_{x_{on}}^{\bar{\omega}_y}\, \bar{\omega}_y; \\
m_{y_{on}} &= m_{y_{on}}^{\delta}\, \delta p + m_{y_{on}}^{\beta}\, \beta + m_{y_{on}}^{\bar{\omega}_y}\, \bar{\omega}_y; \\
m_{z_{on}} &= m_{z_{on}}^{\delta}\, \delta p + m_{z_{on}}^{\psi}\, \psi + m_{z_{on}}^{\bar{\omega}_z}\, \bar{\omega}_z.
\end{aligned} \tag{257}
$$

The aerodynamic characteristics of the detached tail assembly (vertical and horizontal) will be analyzed in the form of two components:

$$
\begin{aligned}
c_{x_{on}} &= c_{x_p} + c_{x_{cr}}; \\
c_{y_{on}} &= c_{y_p} + c_{y_{cr}}; \\
c_{z_{on}} &= c_{z_p} + c_{z_{cr}}; \\
m_{x_{cn}} &= m_{x_p} + m_{x_{cr}}; \\
m_{y_{cr}} &= m_{y_p} + m_{y_{cr}}; \\
m_{z_{on}} &= m_{z_p} + m_{z_{cr}},
\end{aligned} \tag{258}
$$

where c_{x_p}, c_{y_p}, c_{z_p}, m_{x_p}, m_{y_p}, m_{z_p} are the aerodynamic characteristics of detached rudders;

$c_{x_{cт}}$, $c_{y_{cт}}$, $c_{z_{cт}}$, $m_{x_{cт}}$, $m_{y_{cт}}$, $m_{z_{cт}}$ are the aerodynamic characteristics of detached stabilizers or other stabilizing surfaces (pylons, engine housings, etc.)

By way of example of the vertical member of the tail group we will examine the approximate equations that determine these coefficients.

After determining the coefficient $c_{x_{оп}}$ we obtain the following formulas for its components:

$$c_{x_p} = c_{x_p}^{\delta} \delta p + c_{x_p}^{\beta} \beta;\tag{259}$$

$$c_{x_p}^{\delta} = c_{x_p}^{\beta} = \sum_{1}^{n} c_{x_{pi}}^{\delta} \frac{S_{pi}}{S_{ж}}.\tag{260}$$

Here and in the ensuing discussion the values with the index i pertain to the area of the i-th rudder or stabilizer S_{r_i} and S_{st}

$$\delta p = \frac{\sum_{1}^{n} c_{x_{pi}}^{\delta} \frac{S_{pi}}{S_{ж}} \delta_{pi}}{c_{x_p}^{\delta}}.\tag{261}$$

Usually

$$\delta p = \delta p_i;$$
$$c_{x_{cт}} = c_{x_{cт}}^{\beta} \beta;\tag{262}$$

$$c_{x_{cт}}^{\beta} = \sum_{1}^{n} c_{x_{cтi}}^{\beta} \frac{S_{cтi}}{S_{ж}}.\tag{263}$$

Determining coefficient $c_{z_{оп}}$ using relations (258), we obtain

$$c_{z_p} = c_{z_p}^{\delta} \delta p + c_{z_p}^{\beta} \beta + c_{z_p}^{\bar{\omega}_y} \bar{\omega}_y,\tag{264}$$

where

$$c_{z_p}^\delta = c_{z_p}^\delta = \sum_1^n c_{z_{p_i}}^\delta \frac{S_{v_i}}{S_{6ox}}; \qquad (265)$$

$$c_{z_p}^{\bar\omega_y} = -c_{z_p}^\beta \frac{x_p}{L}; \qquad (266)$$

and also

$$c_{z_{cr}} = c_{z_{cr}}^\beta \beta + c_{z_{cr}}^{\bar\omega_y} \bar\omega_y; \qquad (267)$$

where

$$c_{z_{cr}}^\delta = \sum_1^n c_{z_{cr_i}}^\beta \frac{S_{cr_i}}{S_{6ox}}; \qquad (268)$$

$$c_{z_{cr}}^{\bar\omega_y} = -c_{z_{cr}}^\beta \frac{x_{cr}}{L}. \qquad (269)$$

Determining coefficients $m_{x_{on}}$ and $m_{y_{on}}$ using relations (258), we obtain

$$m_{(x,\,y)_p} = m_{(x,\,y)_p}^\delta \delta p + m_{(x,\,y)_p}^\beta \beta + m_{(x,\,y)_p}^{\bar\omega_y} \bar\omega_y; \qquad (270)$$

$$m_{x_p}^\delta = m_{x_p}^\beta = c_{z_p}^\delta \frac{y_p}{L}; \qquad (271)$$

$$m_{x_p}^{\bar\omega_y} = -m_{x_p}^\delta \frac{x_p}{L}; \qquad (272)$$

$$m_{y_p}^\delta = m_{y_p}^\beta = c_{z_p}^\delta \frac{x_p}{L}; \qquad (273)$$

$$m_{y_p}^{\bar\omega_y} = -m_{y_p}^\beta \frac{x_p}{L}. \qquad (274)$$

Furthermore,

$$m_{(x,\,y)_{cr}} = m_{(x,\,y)_{cr}}^\beta \beta + m_{(x,\,y)_{cr}}^{\bar\omega_y} \bar\omega_y; \qquad (275)$$

where

$$m_{x_{cr}}^\beta = c_{z_{cr}}^\delta \frac{y_{cr}}{L}; \qquad (276)$$

$$m_{x_{cr}}^{\bar\omega_y} = m_{x_{cr}}^\beta \frac{x_{cr}}{L}; \qquad (277)$$

$$m_{y_{cr}}^\beta = c_{z_{cr}}^\delta \frac{x_{cr}}{L}; \qquad (278)$$

$$m_{y_{cr}}^{\bar\omega_y} = -m_{y_{cr}}^\beta \frac{x_{cr}}{L}. \qquad (279)$$

Here x_{r_i}, x_{st_i}, y_r, y_{st} are the average distance from the center of pressure on the rudders and stabilizer to the center of gravity of the vehicle.

Thus, in order to determine the aerodynamic characteristics $c_{x_{оп}}$, $c_{z_{оп}}$, $m_{x_{оп}}$, $m_{y_{оп}}$ of a detached tail group it is necessary to know coefficients $c_{x_{r_i}}^{\delta} = c_{x_{r_i}}^{\beta}$; $c_{x_{st_i}}^{\varepsilon}$; $c_{z_{r_i}}^{\delta}$; $c_{z_{st_i}}^{\beta}$, which pertain to the

areas of the stabilizer and rudder, respectively.

We know, however, that resultant R of aerodynamic forces applied to the detached rudder or stabilizer, to simplify its determination, is usually broken down into components either on axes rigidly connected to the tail group itself (normal R_n and tangential R_i components) or, in most cases, on axes connected to the air current flowing around the gail group (lift R_y and drag R_x). Therefore, it is helpful to show the relationship between coefficients $c_{x_{r_i}}^{\delta} = c_{x_{r_i}}^{\beta}$; $c_{x_{st_i}}^{\beta}$; $c_{z_{r_i}}^{\delta} = c_{z_{r_i}}^{\beta}$; $c_{z_{st_i}}$ and the coefficients that characterize lift R_y and drag R_x on the

tail group.

For this purpose we will examine the forces acting on the tail group during lateral motion of the ACV in the general case, using flowing coordinate system xOy for the tail group (Figure 136).
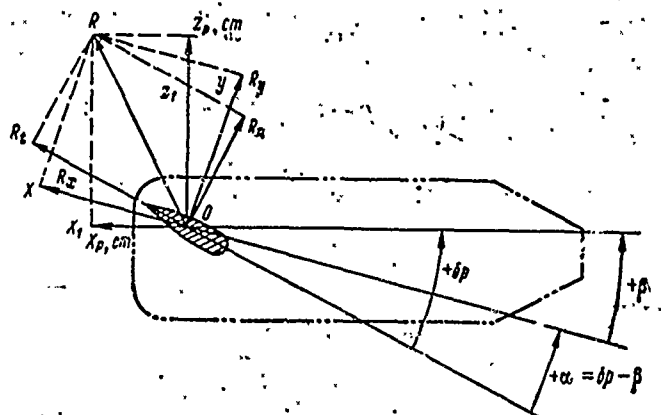

Figure 136. Components of Aerodynamic Force Acting on Tail Group During Lateral Motion of the ACV on Axes of Flowing Coordinate System (xOy) and Coordinate System (x_1Oz_1) Rigidly Connected to Fixed Tail Group.

-279-

We see in Figure 136 that the air flow strikes the rudder at an angle of attack $\alpha = \delta p - \beta$, and the stabilizer at angle of attack $\alpha = \beta$.

On the basis of this figure we obtain equations

$$X_{p,\,c\tau} = R_{x_{(p,\,c\tau)}} \cos\alpha - R_{y_{(p,\,c\tau)}} \sin\alpha; \tag{280}$$

$$-Z_{p,\,c\tau} = R_{x_{(p,\,c\tau)}} \sin\alpha - R_{y_{(p,\,c\tau)}} \cos\alpha. \tag{281}$$

In order to linearize expressions (280)-(281), the functions of the angles must be replaced by the angles themselves and the values of the second order of smallness must be discarded. Then we obtain equations

$$X_p \approx R_{x_p}; \qquad -Z_p \approx R_{y_p}; \tag{282}$$

$$X_{c\tau} \approx R_{x_{c\tau}}; \qquad -Z_{c\tau} \approx R_{y_{c\tau}}. \tag{283}$$

or, converting to the coefficients

$$c_{x_{p_l}}^{\delta} \approx c_{x_{p_l}}^{\beta} \approx c_{x_{c\tau_l}}^{\beta} \approx c_{x_{(p_l,\,c\tau_l)}}^{\alpha}; \tag{284}$$

$$c_{z_{p_l}}^{\delta} = c_{z_{p_l}}^{\beta} = c_{z_{c\tau_l}}^{\beta} \approx -c_{y_{(p_l,\,c\tau_l)}}^{\alpha}. \tag{285}$$

The analogous results can also be obtained for the horizontal stabilizer.

In the absence of data concerning wind tunnel tests of profiles of the required elongation, the coefficients of the forces acting on the tail group can be determined using the approximate analytical expressions presented below. Thus, the derivatives of the coefficient of lift on the rudder or stabilizer at angle of attack c_y^{α} can be approximated according to the so-called Prandtl interpolation equation:

$$c_y^{\alpha} = \frac{2\pi}{1 + \dfrac{2}{\lambda}}. \tag{286}$$

This equation was derived for large elongations and elliptical wing. For $\lambda < 3$ it overstates the coefficients. For elongations of the tail group greater than 2, the following empirical equation is also used:

$$c_y^{\alpha} = \frac{2\pi\lambda}{\sqrt{\lambda^2 + 4} + 2}. \tag{287}$$

-280-

As seen in Figure 137, this equation also does not completely reflect the experiment, particularly in Soviet experience. Therefore the given value may be determined according to the empirical equation

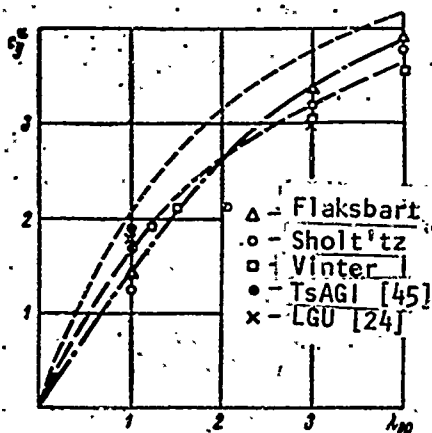$$c_y^\gamma = \frac{2\pi\lambda}{\sqrt{\lambda^3 + 2\lambda + 2}} \qquad (288)$$

Figure 137. . Derivative of Coefficient of Lift on the Attached Tail Group in Terms of Angle of Attack c_y^α on the Elongation $\lambda_{оп}$. - - -, in Equation (286); -·-·-, in Equation (287); — — —, in Equation (288).

We see in Figure 137 that this equation more accurately reflects the Soviet experiment on wings with $\lambda = 1$-4.

It follows from [24] that the critical angle of attack, after which flow breakaway occurs and the coefficient of lift drops sharply, is approximately 28-30° for $\lambda = 1$ and about 21° for $\lambda = 3$.

Considering that this angle is somewhat larger for full scale wings, we may use these angles as reference points with a safe margin of error. A further increase of 6-8° in angle of attack leads to a 35-40% reduction of the coefficient of lift c_y for $\lambda = 1$ and 45-48% reduction for $\lambda = 3$.

The dependence of coefficient c_x on the angle of attack is substantially nonlinear. Linearization of these dependences for a profile with $\lambda = 1$, with a safe margin of error up to angles of about 28-30°, yields an average of $c_x^\alpha = 0.67$, and for a profile with $\lambda = 3$, up to angles of approximately 20-21°, yields $c_x^\alpha \approx 0.53$.

By way of illustration, the aerodynamic characteristics of one variant of hull and tail group of the American ACV SKMR-1 [62] are shown in Figures 138 through 140. The aerodynamic characteristics of the hull were calculated according to linear theory, and the aerodynamic characteristics of the tail group by equation (286). The effect of the shrouds and blowing of the tail group (rudder) by the props was not taken into account. The lateral force on the rudder was assumed to be applied at 1/4 chord from the leading edge of the rudder through length and at one-half the height.
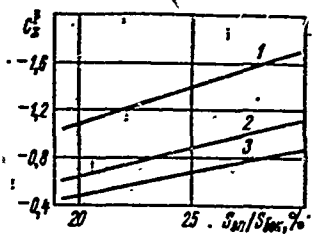
Figure 138. Effect of Relative Area of Tail Group $S_{cп}/S_{бok}$ on the Derivative of the Coefficient of Aerodynamic Lateral Force at Drift Angle $c_z^\beta = c_{z_k}^\beta + c_{z_{oп}}^\beta$ for ACV SKMR-1.

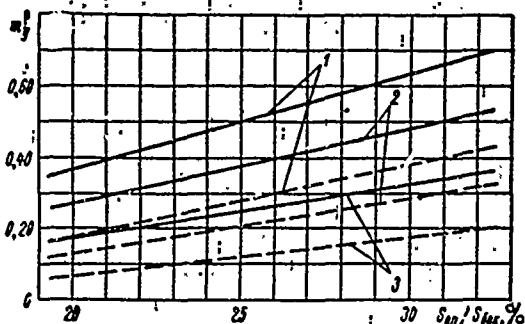$1 - b_{oп}/L = 0.0323;\ 2 - b_{oп}/L = 0.0646;\ 3 - b_{oп}/L = 0.0968$

Figure 139. The Effect of Relative Tail Group Area $S_{oп}/S_{бok}$ on Derivative of Aerodynamic Moment of Yaw at Angle of Drift $m_y^\beta = m_{y_k}^\beta + m_{y_{oп}}^\beta$ for SKMR-1.

$1 - x_{oп}/L = 0.45;\ 2 - x_{oп}/L = 0.35;\ 3 - x_{oп}/L = 0.25$
——— $b_{oп}/L = 0.0323;$
—·—·— $b_{oп}/L = 0.0646$
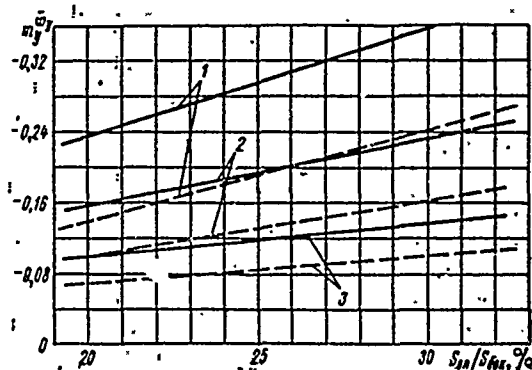
Figure 140. The Effect of Relative Tail Group Area $S_{oп}/S_{бok}$ on Derivative of Aerodynamic Moment of Yaw at Angular Yaw Velocity $m_y^{\bar\omega}y = m_{y_k}^{\bar\omega}y + m_{y_{oп}}^{\bar\omega}y$ for SKMR-1.

$1 - x_{oп}/L = 0.45;\ 2 - x_{oп}/L = 0.35;\ 3 - x_{oп}/L = 0.25$
——— $b_{oп}/L = 0.0323;$ —·—·— $b_{oп}/L = 0.646$

Figure 138 illustrates the effect of the relative chord $b_{oп}/L$ of the tail group on the derivative of the coefficient of aerodynamic lateral force at drift angle $c_z^\beta = c_{z_k}^\beta + c_{z_{oп}}^\beta$ as a function of relative area of tail group $S_{oп}/S_{бok}$. It follows from this figure that for the same tail group area an increase in its height will lead to an increase in the coefficient c_z^β in connection with the lengthening of the tail group.

-282-

Figure 139 illustrates the effect of the location of the tail group in terms of length x_{on}/L as a function of relative chord b_{on}/L and relative tail group area S_{on}/S_{60H} on the derivative of the aerodynamic moment of yaw at angle of drift $m_y^\beta = m_{y_k}^\beta + m_{y_{on}}^\beta$. It follows from this figure that the coefficient m_y^β for the same tail group area increases as the height of the tail group increases and as the tail group is placed farther toward the stern from the center of gravity of the vessel.

Figure 140 shows the effect of the location of the tail group in terms of length x_{on}/L as a function of the relative chord b_{on}/L and relative tail group area S_{on}/S_{60H} on the derivative of aerodynamic yaw moment at angular yaw velocity $m_y^{\bar{\omega}_y} = m_{y_k}^{\bar{\omega}_y} + m_{y_{on}}^{\bar{\omega}_y}$. This coefficient changes similar to coefficient m_y^β.

Also seen in these figures is the range of change of relative tail group area, which is of practical importance in ACV design.

The tail group, consisting of a stabilizer and rudder, is usually installed symmetrically relative to the axis of rotation of the prop. The aerodynamic characteristics of such a tail group are determined through equations (237). The usual expression for the angle of attack of a detached rudder is not valid for rudders behind the stabilizers. In the case of a cross-beam rudder, wing consisting of a rudder and stabilizer changes shape, and therefore the effect of the angle of rudder placement and the angle of drift can vary, and this must be taken into account in the expressions for the aerodynamic characteristics of this type of tail group.

R. Ya. Pershits analyzed several rectangular rudders placed behind the stabilizers and blown through the entire height by the propeller wash.

The coefficient of propeller thrust load σ_p varied during the tests from 0 to 5.

Using the results of these tests it is possible to establish that the derivative of the coefficient of lateral force on the tail group were the angle of cross-over of the i-th rudder depends on the thrust load coefficient σ_p and is equal to

$$-c_{z_{on_i}}^\delta = c_{y_{on_i}}^\alpha + \mu_\kappa \sigma_p. \tag{289}$$

-283-

The derivative of the coefficient of lateral force on the tail group at angle β is

$$\dot{c}^{\beta}_{z_{on}} = \dot{c}^{\delta}_{z_{on}} x_{b}.$$ (292)

$S_{o_i} = \dot{S}_{p_i} + S_{st_i}$ is the area of the complex;

$x_{b_\ell} = \dfrac{\dot{c}^{\beta}_{z_{on_\ell}}}{\dot{c}^{\delta}_{z_{o\jmath_\ell}}} \cdot$ is the coefficient that considers change in the angle

of attack on the tail group due to drift, and κ_b is its average value for the entire tail group.

The value of the coefficient κ_{b_i} is equivalent to data from the test conducted by. R. Ya. Pershits, as represented in Figure 142.
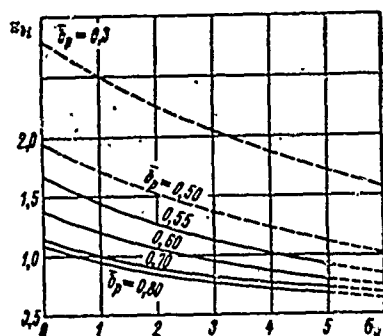
Figure 142. Coefficient κ_{b_i} that Considers the Influence of the Change of Angle of Attack on the Tail Group, Caused by Drift, on Derivative of the Coefficient of Lateral Force on Tail Group at Angle Rudder Crossover $c^{\delta}_{z_o}$, as a Function of the Coefficient of Propeller Thrust Load σ_p. The broken curves were obtained by extrapolation.

This coefficient is a function both of σ_p and of relative rudder chord $\bar{b}_p$. It is clear from Figure 142 that the ratio between rudder chord and stabilizer chord has a strong influence on the coefficient κ_{b_i} and, consequently, on the lift of the rudder behind the stabilizer in the presence of an angle of drift. As $\bar{b}_p$ decreases, i.e., as the stabilizer chord increases, the coefficient κ_{b_i} increases. When $\kappa_{b_i} > 1$ the angle of drift has a greater influence on the lift than the angle of rudder crossover. As the coefficient σ_p increases the coefficient κ_{b_i} decreases, but the effect of the relative rudder chord $\bar{b}_p$ remains the same.

The range of change of the coefficient of the load of ACV engines is much greater than that found experimentally [37] and can go up to $\sigma_p = 10$ and above.

In addition, the relative rudder chord $\bar{b}_p$ for ACV is also beyond the experimental range $\bar{b}_p = 0.56$-0.83 and usually has values $b_p \leqslant 0.5$. For approximate calculations the curves in Figure 142 were extrapolated into the range of change of σ_p and $\bar{b}_p$ customary for ACV. For accurate calculations it is necessary to find the analogous dependences on the basis of special tests of the tail group in the propeller wash.

The expression for the derivative of the coefficient of lateral force on the tail group according to dimensionless angular velocity of yaw has the form

$$c_{z_{\text{оп}}}^{\bar{\omega}_y} = - c_{z_{\text{оп}}}^{\beta} \frac{x_{\text{оп}}}{L} \tag{293}$$

The coefficient of the moment of roll on the tail group $m_{x_{\text{оп}}}$ is found using the dependences obtained on the basis of equations (257):

$$m_{x_{\text{оп}}}^{\delta} = c_{z_{\text{оп}}}^{\delta} \frac{y_{\text{оп}}}{L}; \tag{294}$$

$$m_{x_{\text{оп}}}^{\beta} = m_{x_{\text{оп}}}^{\delta} x_{\text{в}}; \tag{295}$$

$$m_{x_{\text{оп}}}^{\bar{\omega}_y} = - m_{x_{\text{оп}}}^{\beta} \frac{x_{\text{оп}}}{L}, \tag{296}$$

where $x_{\text{оп}}$, $y_{\text{оп}}$ are the coordinates of the center of gravity of the tail group area.

For the coefficient of the moment of yaw on the tail group $m_{y_{\text{оп}}}$, we obtain the expressions [see equations (257)]

$$m_{y_{\text{оп}}}^{\delta} = c_{z_{\text{оп}}}^{\delta} \frac{x_{\text{оп}}}{L}; \tag{297}$$

$$m_{y_{\text{оп}}}^{\beta} = m_{y_{\text{оп}}}^{\delta} x_{\text{в}}; \tag{298}$$

$$m_{y_{\text{оп}}}^{\bar{\omega}_y} = - m_{y_{\text{оп}}}^{\beta} \frac{x_{\text{оп}}}{L}. \tag{299}$$

If the height of the tail group is greater than the diameter of the propeller, or the tail group is displaced from the propeller axis, then for determination of the coefficients $c_{z_{on_i}}^{\delta}$ and $c_{z_{on_i}}^{\beta}$ we may use the recommendations set forth in [12].

For the coefficient $c_{x_{on}}$, in accordance with equations (257), we will have equations

$$c_{x_{on}}^{\delta} = \sum_{1}^{n} c_{x_{p_i}}^{\delta} \frac{S_{on_i}}{S_{\mathfrak{X}}}; \tag{300}$$

$$c_{x_{on}}^{\beta} = \sum_{1}^{n} c_{x_{on_i}}^{\beta} \frac{S_{on_i}}{S_{\mathfrak{X}}}. \tag{301}$$

The coefficient $c_{x_{p_i}}^{\delta}$ can be approximated using the graph illustrated in Figure 143.
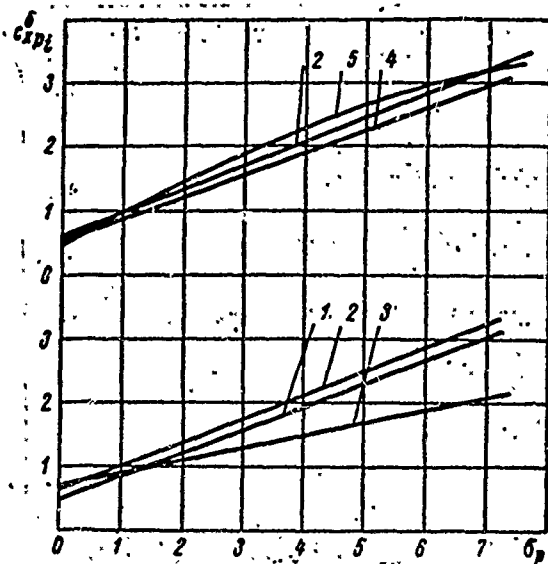
Figure 143. Derivative of Coefficient of Drag of Tail Group at Angle of Rudder Crossover $c_{x_{p_i}}^{\delta}$ as a Function of Propeller Thrust Load Factor σ_p for $\beta = 0$.

$1 - \lambda_{on} = 1.0;\ \bar{b}_p = 0.56;\ \lambda_p = 1.8;\ 2 - \lambda_{on} = 1.1;\ \bar{b}_p = 0.61;\ \lambda_p = 1.8;\ 3 - \lambda_{on} = 1.08;\ \bar{b}_p = 0.83;\ \lambda_p = 1.3;\ 4 - \lambda_{on} \approx 1.23;\ \bar{b}_p = 0.69;\ \lambda_p = 1.8;\ 5 - \lambda_{on} = 2.0;\ \bar{b}_p = 0.69;\ \lambda_p = 2.9$

Linearization to the safe limit up to $\delta p = 25°$.

-287-

In this graph are represented the results of processing of the tests [45] of rudders behind stabilizers. Linearization of the dependence of $c_{x_{p_i}}$ on the angle of crossover δp was carried out to the safe limit up to angles $\delta p = 25°$.

The coefficient $c_{x_{on_i}}^{\beta}$ can be approximated using the graph shown in Figure 144. In this graph are shown the results of processing of tests [24] and [45] of rudders behind stabilizers for a thrust load factor $\sigma_p = 0$. Unfortunately, the dependence of $c_{x_{on_i}}^{\beta}$ on σ_p for the required forms and elongations of the tail groups is not available.
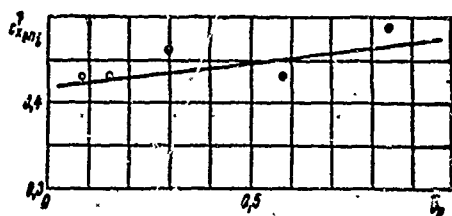
Figure 144. Derivative of Coefficient of Drag of Tail Group at Angle of Drift $c_{x_{on_i}}^{\beta}$; as a Function of Relative Rudder Chord $\overline{b}_p$. ●,TsAGI [45] O,LGU [24]; $\lambda_{on_i} = 1$.

Forces and Moments Created by Engines

Forces and Moments Created by Propeller-Shroud Engine Complex

If we denote the summary thrust of the propeller-shroud complex through P, then for the projections of the forces and moments of interest to us, created by the working engine complexes, we may write the following expressions:

$$Y_{\tau} = 0; \quad X_{\tau} = X_{\tau(\omega=0)};$$

$$Z_{\tau} = Z_{\tau(\omega=0)} + \frac{\partial Z_{\tau}}{\partial \overline{\omega}_y} \overline{\omega}_y; \tag{302}$$

$$M_{x_{\tau}} = M_{x_{\tau(\omega=0)}} + \frac{\partial M_{x_{\tau}}}{\partial \overline{\omega}_y} \overline{\omega}_y;$$

-288-

$$M_{y_\text{T}} = \dot{M}_{y_{\text{T}(\omega=0)}} + \frac{\partial M_{y_\text{T}}}{\partial \bar{\omega}_y} \bar{\omega}_y;$$

$$\dot{M}_{z_\text{T}} = M_{z_{\text{T}(\omega=0)}}$$

(302)

Here

$$X_{\text{T}(\omega=0)} = P - X_\text{H} = P + X_\text{H}^\beta \beta;$$

$$Z_{\text{T}(\omega=0)} = -Z_\text{H} = -Z_\text{H}^\beta \beta;$$

$$M_{x_{\text{T}(\omega=0)}} = -M_{x_\text{H}} = -M_{x_\text{H}}^\beta \beta;$$

$$M_{y_{\text{T}(\omega=0)}} = z_\text{T} P - M_{y_\text{H}} = z_\text{T} P - M_{y_\text{H}}^\beta \beta,$$

(303)

where z_t is the arm of action of the summary thrust from the DP;

y_t is the arm of action of the summary thrust from the CG (center of gravity);

$$P = c_{x_{\text{T}_0}} \delta\Lambda q S_\text{Ж};$$

(304)

$c_{x_{t_o}}$ is the thrust coefficient;

$\delta\Lambda$ is the propeller pitch;

$$X_\text{H} = c_{x_\text{H}} q S_\text{Ж} \quad \text{is the drag of the shrouds.}$$

(305)

Converting to the coefficients we obtain equations

$$c_{x_\text{T}} = c_{x_{\text{T}_0}} \delta\Lambda - c_{x_\text{H}}^\beta \beta;$$

$$c_{z_\text{T}} = -\left[c_{z_\text{H}}^\beta \beta + c_{z_\text{H}}^{\bar{\omega}_y} \bar{\omega}_y\right];$$

$$m_{x_\text{T}} = -\left[m_{x_\text{H}}^\beta \beta + m_{x_\text{H}}^{\bar{\omega}_y} \bar{\omega}_y\right];$$

$$m_{y_\text{T}} = c_{x_{\text{T}_0}} \delta\Lambda \frac{S_\text{Ж}}{S_\text{бок}} \frac{z_\text{T}}{L} - \left(m_{y_\text{H}}^\beta \beta + m_{y_\text{H}}^{\bar{\omega}_y} \bar{\omega}_y\right);$$

$$m_{z_\text{T}} = c_{x_{\text{T}_0}} \delta\Lambda \frac{S_\text{Ж}}{S_\text{бок}} \frac{y_\text{T}}{L}.$$

(306)

Thus, for determination of the forces and moments that are of interest to us, in addition to the thrust of the engines, it is necessary to know the coefficients $c_{x_{H_i}}^{\beta}$ and $c_{z_{H_i}}^{\beta}$. Actually, by knowing the coefficient $c_{z_{H_i}}^{\beta}$, the other coefficients of the lateral forces and moments on the shroud can be determined using the following approximate expressions:

$$c_{z_{H}}^{\bar{\omega}y} = -c_{z_{H}}^{\beta}\frac{x_{H}}{L};$$
$$S_{H_i} = \pi D_{H_i} l_{H_i},$$

$$(307)$$

where D_{H_i} is the minimal shroud diameter;

l_{H_i} is shroud length;

$$c_{z_{H}}^{\beta} = \sum_{1}^{n} c_{z_{H_i}}^{\beta}\frac{S_{H_i}}{S_{6ok}};$$

$$(308)$$

$$m_{x_{H}}^{\beta} = c_{z_{H}}^{\beta}\frac{y_T}{L};$$

$$(309)$$

$$m_{x_{H}}^{\bar{\omega}y} = -m_{x_{H}}^{\beta}\frac{x_{H}}{L};$$

$$(310)$$

$$m_{y_{H}}^{\beta} = c_{z_{H}}^{\beta}\frac{x_{H}}{L};$$

$$(311)$$

$$m_{y_{H}}^{\bar{\omega}y} = -m_{y_{H}}^{\beta}\frac{x_{H}}{L},$$

$$(312)$$

where x_H, y_H are the averaged coordinates of the center of effort of the sail area of the shrouds.

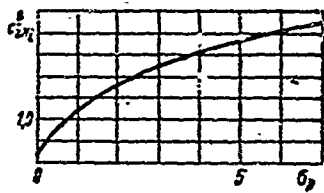Figure 145 represents $c_{z_{H_i}}^{\beta}$ as a function of v_p.

Figure 145. Derivative of Coefficient of Lateral Force on the Shroud $c_{z_{H_i}}^\beta$ as a Function of the Coefficient of Thrust Load of the Propeller σ_p.
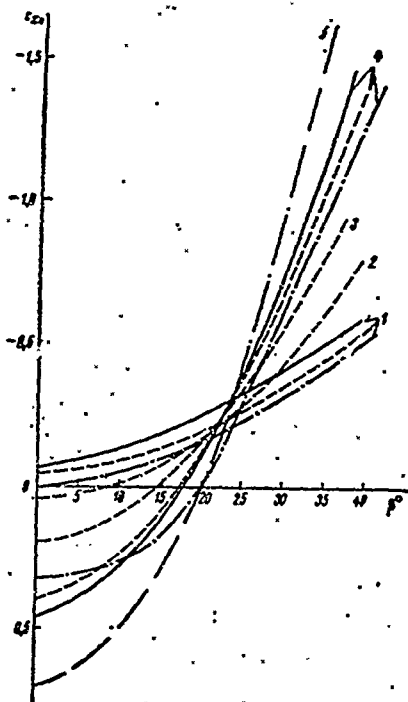

Figure 146. Coefficient of Drag of Shroud c_{x_H} as a Function of Drift Angle β for Various Relative Shroud Elongations $\bar{l}_H$ and Various Propeller Thrust Load Coefficients σ_p.

$1 - \sigma_p = 0;\ 2 - \sigma_p = 1;\ 3 - \sigma_p = 3;\ 4 - \sigma_p = 5;\ 5 - \sigma_p = 7$

$\underline{\hspace{1.5cm}}\ \bar{l}_H = 0.84;\quad \ ----\ \bar{l}_H = 0.67;$

$-\cdot-\cdot-\cdot-\ \bar{l}_H = 0.50$

The value of
The value of $c_{z_{H_i}}^\beta$ was obtained by processing data from the tests of a series of rotating shrouds [12].

The experimental series of shrouds had an aperture coefficient equal to 1.25 and an expansion coefficient of 1.12. Therefore the dependence of $c_{z_{H_i}}^\beta$ on σ_p represented in Figure 145 should be used only for geometrical elements of shrouds close to the experimental.

The test results of shrouds for propellers [12] indicated a substantial dependence of the coefficient c_{x_H} not only on the angle of drift β but also on the coefficient of load of the propeller σ_p. Up to drift angles $\beta = 22\text{-}23°$, however, the dependence of c_{x_H} on β can be used

-291-

according to the curve for $\sigma_p = 0$, assuming a safe margin of error. The dependence of the coefficient c_{x_H} for $\sigma_p = 0\text{-}7$ on shroud elongation $\bar{l}_H$ and β, determined by the processing of test results [12], is illustrated in Figure 146.

Forces and Moments Created by Rotating Engines

The thrust of rotating engines, in the presence of angle of deflection γ_i of the direction of thrust from the diametral plane, yields the following forces and moments:

$$X_T = \sum_1^n P_i \cos \gamma_i; \qquad Z_T = \sum_1^n P_i \sin \gamma_i;$$
$$M_{y_T} = z_T X_T - Z_T x_T; \qquad (313)$$
$$M_{x_T} = y_T Z_T.$$

Additional forces and moments act on rotating propellers at drift angle β, which can be expressed through the following equations:

$$\dot{Z}_{T_i} = c_{z_{T_i}}^\beta \beta q S_{\text{ок}}; \qquad (314)$$
$$M_{y_{T_i}} = m_{y_{T_i}}^\beta \beta q S_{\text{ок}} L. \qquad (315)$$

Expressions are presented in [41] for the derivatives of the coefficient of lateral force for drift angle $c_{z_{T_1}}^\beta$ and coefficient of yaw moment for drift angle $m_{y_{T_1}}^\beta$ which can be used for approximate calculations.

These forces and moments are mutually offsetting on counter-rotating propellers.

§23. Forces and Moments Created by Air Cushion and Its Flexible Skirts

We will examine the influence of the flexible skirts on the aerodynamic forces and moments acting on an ACV hull, the forces and moments created by the pressure of the air cushion on the hull of the ACV, reaction of the intake and exhaust air and its passage through the inner channels of the ACV, and also the forces and moments of hydrodynamic origin.

-292-

The flexible air cushion skirt changes the pattern of flow around the ACV hull:

1) With a flexible skirt the clearance, i.e., air space between the bearing surface and the lower edge of the flexible skirt, is sharply reduced, and this means that the area of interaction between the oncoming flow and the air cushion is reduced;

2) the height of the flexible skirt, as a rule, is much greater than the clearance of the ACV without a flexible skirt, which increases the area of the lateral projection and changes the position of the center of effort of the sail area;

3) the flexible skirt changes the area and shape of the cross-sections of the ACV, particularly at the extremities, which leads to a change in the flow around the ACV's hull as a whole;

4) the flexible skirt, compared to an air screen, is more rigid, and therefore less subject to deformations as the dynamic pressure of the oncoming air flow is increased. Visual observations of flexible skirts have not shown any substantial changes in the shape of the flexible skirt during motion, compared to the shape in the hovering mode;

5) flow from beneath the flexible skirt differs from that from beneath the bottom with an air curtain and is irregular around the perimeter, since the bottom edge of the flexible skirt has irregular rigidity.

Consideration of the influence of all these factors on the aerodynamic characteristics of ACV hulls is difficult due to the complexity of their interaction.

Comparison of the dependences of c_{z_k} and m_{y_k} on drift angle β, obtained for a hull model with flexible skirts, for changes in the angle β from 0 to $20°$, with values obtained for a model without a flexible skirt, suggests the following conclusion concerning the different character of the effect of the flexible skirt on the various coefficients. Thus, the flexible skirt increases the coefficient of lateral force c_{z_k} and the

coefficient of lateral moment on the hull in this case can be decreased or increased, depending on the specific shape and design of the flexible skirt.

An increase in the coefficient of lateral force c_{z_k} is represented by the general law in the presence of a flexible skirt, and, therefore a flexible skirt has an unfavorable effect on the bearing capacity of the hull. Analysis of the results of tests of models with flexible skirts and without a flexible skirt indicates that a change in the coefficient $c_{z_k}^{\beta}$ for models with a flexible skirt is approximately proportional to the change of elongation λ if λ and $S_{бок}$ is calculated with consideration of the area of the flexible skirt and its height. Therefore, for approximate calculations, consideration of the effect of the flexible skirt on the aerodynamic characteristics of the hull can be confined to the inclusion of the area of the lateral surface of the flexible skirt and its height in the calculation of $S_{бок}$ and λ.

Forces and Moments Created by Pressure of Air Cushion on Bottom of ACV

As was shown earlier, the presence of the air cushion beneath the hull of the ACV leads to asymmetric distribution of the component of normal stresses caused by its static pressure and acting on the hull due to the action of the boundary layer of air. The forces from this component represent the principal part of the lift of the ACV. They can be related to the center of the gravity of the ACV (origin of the fixed coordinate system) and represented in the form of resultant force $\vec{R}_{a_i}$ and moment $\vec{M}_{a_i}$. Of their projections onto the fixed axes we are interested in this section only in the lift and the moments of roll and trim created by it:

$$Y_n = c_{y_n} GB_n;$$
$$M_{x_n} = m_{x_n} GB_n;$$
$$M_{z_n} = m_{z_n} GB_n. \qquad (316)$$

We will examine the creation of moments by the air cushion by way of the example of the moment of roll. We will analyze the moment of roll from the forces of pressure in the cushion in the form of two components:

$$M_{x_n} = M_{x_n}(\theta) + M_{x_n}(\dot{\theta}), \qquad (317)$$

where

$$M_{x_{\text{п}}}(\theta) = m_{x_{\text{п}}}^{\theta}\theta G B_{\text{п}};$$ (318)

$$M_{x_{\text{п}}}(\dot{\theta}) \approx M_{x_{\text{п}}}(\bar{\omega}_x) = m_{x_{\text{п}}}^{\bar{\omega}_x}\bar{\omega}_x G B_{\text{п}}.$$ (319)

Here $M_{x_{\text{п}}}(\theta)$ and $M_{x_{\text{п}}}(\dot{\theta})$ are the recovery and damping moments of roll, respectively, from the forces of pressure in the air cushion;

$m_{x_{\text{п}}}^{\theta}$ and $m_{x_{\text{п}}}^{\bar{\omega}}$ are the derivatives of the coefficients of the recovery and moments of roll in terms of θ and $\bar{\omega}_x$, respectively.

The recovery moment of roll from the air cushion can be determined in accordance with equations presented in the chapter concerning the stability of ACV. We will examine below the problem of damping the moment of roll.

In the presence of an angular velocity of motion of the ACV in the direction of roll, the pressure in the air cushion beneath the lower side of the vessel increases, and the pressure beneath the higher side decreases. This circumstance leads to the development of a damping moment of roll from the air cushion.

If the air cushion is divided into individual sections, the method of calculation of the additional component of width from the vertical oscillations of a single contour nozzle apparatus can be employed for the approximate determination of the damping moment of roll, using it individually for each side section of the ACV.

The additional component of lift of the air cushion in the presence of vertical oscillations of the ACV arises due to the change of pressure within the air cushion, and also the change in the amount of motion of the jet of the air curtain and of the air flowing in and out of the air cushion. It depends basically on the vertical velocity and acts in the direction opposite the velocity vector. In this connection we will assume that this component is independent of the character of the screen and the presence of the flexible skirt.

We will examine the problem of vertical oscillations of an apparatus with a single contour nozzle, without a flexible skirt, hovering above a solid screen. In solving the problem we will consider the exponential distribution of velocities and pressures through the thickness of the jet.

Additionally we will make the following assumptions:

The compressibility of air is not considered;

the inertial forces are not considered (steady state motion is examined);

the principle of superposition is valid for determination of pressure increments.

As the vehicle descends at velocity V_y the volume of the air cushion decreases, and the pressure within it increases. Here the enclosing properties of the air screen change in the following manner (Figure 147). The mean velocity of the air screen jet increases at nozzle exit in relation to the bearing surface, and the mean angle of inclination of the discharge velocity vector decreases. The increase in the velocity of the air screen jet leads to an increase in the amount of its motion and thereby facilitates maintenance of higher pressure in the air cushion. A reduction of the angle of inclination of the discharge velocity vector has the opposite effect, but its influence on pressure in the air cushion is much smaller. The opposite processes take place during motion upward.
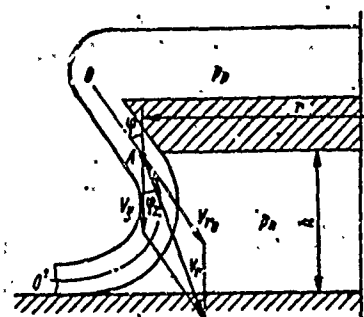

Figure 147. Summation of Velocities in a Jet During Descent of ACV.

In consideration of the above statement, the force of damping can be analyzed in the following form:

$$Y_\partial = \Delta p S_n.$$
(320)

The pressure increment Δp is found as follows:

$$\Delta p = p'_n - p_n,$$
(321)

-296-

where p'_Π is the pressure in the air cushion, resulting from the change in the amount of air it contains.

This pressure can be determined on the basis of the amount of motion of the air flowing from the air cushion (during downward motion of the ACV). In order to determine the quantity of motion it is essential to know flow rate Q and discharge velocity V_j of the air from the cushion. The flow rate is determined on the basis of the velocity of vertical motion of the ACV

$$Q = S_n V_y \tag{322}$$

The air escape velocity is determined by the excess pressure in the cushion. In this case, when a reduction of altitude is accompanied by a change in the amount of air in the cushion, p_Π can be used as the excess pressure. Hence,

$$V_j = \sqrt{\frac{2p_\Pi}{\rho}} \tag{323}$$

and the per-second rate of travel is

$$\rho Q V_j = \rho S_n V_y \sqrt{\frac{2p_\Pi}{\rho}}. \tag{324}$$

Further, constructing the equation of equilibrium of the jet, with consideration of (324) we obtain the following expression:

$$p'_\Pi = p_\Pi + \frac{\rho S_n}{h\Pi} \sqrt{\frac{2p_\Pi}{\rho}} V_y. \tag{325}$$

Hence

$$Y_\partial = \frac{\rho S_n^2}{h\Pi} \sqrt{\frac{2p_\Pi}{\rho}} V_y. \tag{326}$$

Using this equation we can calculate in the first approximation the damping force created during angular oscillations of the ACV according to the role of each section of the lowered and elevated sides. These forces will create a damping moment of roll, representing the moment of a pair of forces, equal to

$$M_{x_\Pi}(\omega_x) = 2Y_\partial z_i = \frac{2\rho z_c S_c^2}{h\Pi_c} \sqrt{\frac{2p_\Pi}{\rho}} V_y, \tag{327}$$

-297-

where Π_c is part of the perimeter of a section from which the air is discharged into the atmosphere;

S_c is the area of the section.

Further conversions lead to the following expression for $M_{x_\Pi}(\omega_x)$:

$$M_{x_\Pi}(\omega_x) = S_c z_c \frac{\sqrt{2\rho p_\Pi}}{h\Pi_c} \frac{dU}{d\theta} \omega_{x'} \tag{328}$$

with consideration of the dependence

$$2S_c V_y \approx \frac{dU}{dt},$$

where

$$U = U_1 - U_2,$$

U_1 is the volume occupied by the air under the section of the lowered side;

U_2 is the volume occupied by the air under the section of the elevated side,

$$\frac{dU}{dt} = \frac{dU}{d\theta} \frac{d\theta}{dt} \approx \frac{dU}{d\theta} \omega_{x'}$$

The value of $dU/d\theta$ for a single contour jet screen with two longitudinal nozzles is expressed as follows (according to the data of V. V. Kramer and V. G. Tabachnikov):

$$\frac{dU}{d\theta} = -2S_c z_c + 2S'h \qquad \varphi_1 - \frac{h^2 l'}{\cos^2 \varphi_1}; \tag{329}$$

where $X' = S_c + S_b$; S_b is one-half the area of the internal section;
$ l'$ is the base of the area.

Equation (329) shows that when $\varphi_1 \neq 0$, derivative $dU/d\theta$ at high hovering altitudes h becomes positive and the moment becomes an oscillating moment and not a damping moment.

This occurs for the value of h

$$h > \frac{\cos \varphi_1}{l'} \left(S' \sin \varphi_1 + \sqrt{S'^2 \sin^2 \varphi_1 - 2 S_c z_c l'} \right). \tag{330}$$

Comparing expression (319) with (328) we obtain

$$m_{xn}^{\bar{\omega}x} = \frac{S_c z_c V}{h \Pi_c L B_n G} \sqrt{2 \rho_n \rho} \frac{dU}{d\theta}. \tag{331}$$

The coefficient $m_{x_n}^{\bar{\omega}x}$, obtained on the basis of expression (331), is

compared in Figure 148 with the coefficient obtained in [25] experimentally for an ACV model with a single contour nozzle and two longitudinal nozzles while hovering over a solid screen. Shown also is the curve obtained in [25] according to the analytical expression based on linear theory.[1] It is clear from Figure 148 that the theoretical curve, calculated according to expression (331), is much closer to the experimental curve than that obtained on the basis of the analytical expression based on linear theory.
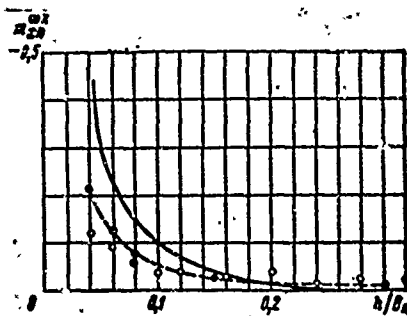
Figure 148. Derivative of Roll Moment Coefficient From Air Curtain for Angular Roll Velocity $m_{x_n}^{\bar{\omega}x}$ as a Function of Relative Hovering Altitude h/B_n.

———— , Theoretical data [25];

●-●-●- , Theoretical data [equation (331)];

O-O-O- , Experimental data [25].

Moments and Forces Created by Reaction of Intake and Exhaust Air

The force created by the reaction of the air drawn into the air receiver of the fan is

---

[1]Linear theory is the outcome of linear drop of velocities and pressures to the width of the nozzle.

$$\vec{R}_{s_3} = \vec{R}_1 = \rho Q \vec{V}, \qquad (332)$$

where Q is the flow rate of the air moved by the fan.

The projections of this force of interest to us onto the coordinate axes, rigidly fixed to the ship, with the fan located symmetrically in relation to the DP, are:

$$X_{R_1} = -\rho Q V_x \approx -\rho Q V; \qquad (333)$$
$$Z_{R_1} = -\rho Q V_z \approx -\rho Q V \beta.$$

If x_{R_1}, y_{R_1} and z_{R_1} are the coordinates of the point of application of the force relative to the center of gravity of the vessel, then its moments in relation to all the coordinate axes will be of the form

$$M_{x_{R_1}} = y_{R_1} Z_{R_1}; \qquad (334)$$
$$M_{y_{R_1}} = x_{R_1} Z_{R_1}.$$

If the ACV is rotated in relation to the center of gravity the amount of motion of the air passing through the fan air receiver will change, with the result that on the air receiver will also occur forces and moments proportional to the velocity of its angular displacements [10]

$$\Delta X_{R_1} = \rho Q \left(y_{R_1} \bar{\omega}_z - z_{R_1} \bar{\omega}_y \right) \frac{V}{L};$$

$$\Delta Y_{R_1} = \rho Q \left(z_{R_1} \bar{\omega}_x - x_{R_1} \bar{\omega}_z \right) \frac{V}{L};$$

$$\Delta Z_{R_1} = \rho Q \left(x_{R_1} \bar{\omega}_y - y_{R_1} \bar{\omega}_x \right) \frac{V}{L}; \qquad (335)$$

$$\Delta M_{x_{R_1}} = \rho Q \left[y_{R_1} x_{R_1} \bar{\omega}_y - \right.$$
$$\left. - (y_{R_1}^2 + z_{R_1}^2) \bar{\omega}_x + x_{R_1} z_{R_1} \bar{\omega}_z \right] \frac{V}{L};$$

$$\Delta M_{y_{R_1}} = \rho Q \left[x_{R_1} y_{R_1} \bar{\omega}_x - \right.$$
$$\left. - (x_{R_1}^2 + z_{R_1}^2) \bar{\omega}_y + y_{R_1} x_{R_1} \bar{\omega}_z \right] \frac{V}{L};$$

$$\Delta M_{z_{R_1}} = \rho Q \left[z_{R_1} x_{R_1} \bar{\omega}_x - (x_{R_1}^2 + y_{R_1}^2) \bar{\omega}_z + z_{R_1} y_{R_1} \bar{\omega}_y \right] \frac{V}{L}.$$

In the case of several fans $Q = \sum_1^n Q_i$

$$x_{R_1} = \frac{\sum\limits_1^n Q_i x_{R_i}}{Q};$$

$$y_{R_1} = \frac{\sum\limits_1^n Q_i y_{R_i}}{Q};$$ (336)

$$z_{R_1} = \frac{\sum\limits_1^n Q_i z_{R_i}}{Q}.$$

Of the forces and moments created by the reaction of the air discharged from beneath the lower edge of the flexible skirt $\vec{R}_{a5}$ and $\vec{M}_{a5}$ there exists

only longitudinal and lateral forces created by the horizontal component of the force of reaction during roll and trim X_{R_2}, Z_{R_2}, and also moments

relative to axes Ox and Oz, created by forces X_{R_2} and Z_{R_2}

In the presence of a flexible skirt, the reactive component of lateral force can be represented in the following form:

$$Z_{R_1} = G Z_{R_1}^\theta \theta,$$ (337)

where

$$Z_{R_1}^\theta \approx 0.54.$$

For approximate calculations Z_{R_2} during hovering of the ACV above

water can be assumed equal to the value of Z_{R_2} during hovering over a solid screen.

The moment $M_{x_{R_2}}$ from this force has arm of application y_{R_2} equal to

the distance between the center of gravity and the middle of the slit through which the air is discharged during rolling of the ship. This arm of application is practically equal to the elevation of the center of gravity above the level of the undisturbed water

$$M_{x_{R_1}} = Z_{R_1} y_{R_1}; \quad M_{z_{R_1}} = X_{R_1} y_{R_1}.$$ (338)

Longitudinal force X_{R_2}, with positive trim (on the stern) represents

a reactive component of drag, which can be depicted graphically (Figure 149). Flexible skirts, because of their wash during motion, prohibit representation of reactive drag in pure form, and therefore the reactive drag of ACV models with flexible air cushion skirts is part of the residual drag. Thus, we obtain

$$X_R = X_{R_1} + \Delta X_{R_1} + X_{R_2};$$

$$Y_R = Y_{R_1} + \Delta Y_{R_1};$$

$$Z_R = Z_{R_1} + \Delta Z_{R_1} + Z_{R_2};$$

$$M_{x_R} = M_{x_{R_1}} + \Delta M_{x_{R_1}} + M_{x_{R_2}};$$

$$M_{y_R} = M_{y_{R_1}} + \Delta M_{y_{R_1}};$$

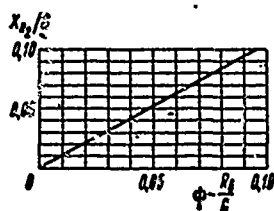$$M_{z_R} = M_{z_{R_1}} + \Delta M_{z_{R_1}} + M_{z_{R_2}}.$$

(339)

Figure 149. Relative Reactive Component of Drag X_{R_2}/G as Function of Effective Trim Angle $\psi - R_B/G$. R_B is wave drag; ψ is trim angle.

Forces and Moments from Inertia of Air Flowing Through Air Channels of ACV

The air that flows through the air channels of ACVs is a continuous medium, to which apply the laws of dynamics of a rigid system of material points [48].

If during motion of a rigid system of material points their trajectories are predeterimed by the constraints applied to the system, then to the system is applied the action from the applied constraints. The constraints that constrict movements of the material points of the system act on them by means of forces called the forces of constraint reactions.

Indeed, any force of inertia is a reaction of a system of material points applied to the constraints and developing when some acceleration is imparted to the system as a result of the constraints.

It follows from the above that in the general case of unsteady motion the ACV experiences the effect of air passing through the air channels, which should be taken into account in the differential equations of motion as one of the categories of external forces.

Determination of these forces is based on the laws of dynamics of complex motion. For the air passing through the air channels of an ACV, motion performed by an ACV in relation to systems of fixed Earth coordinate axes is translatory, and motion accomplished in relation to the vessel is relative motion; the passage of air through air ducts in relation to the system of fixed coordinate axes is absolute motion.

The forces of inertia of air flowing through the air ducts of an ACV belong to the category of forces and moments $\vec{R}_{a3}$ and $\vec{M}_{a3}$ (see §11 Chapter II) and in the general case are reduced to a force equivalent to the principal vector of inertial forces $\vec{R}_{\text{и}}$ and to a pair of forces whose moment relative to the center of reduction is equivalent to the principal moment of inertial forces $\vec{M}_{\text{и}}$.

In turn,

$$\vec{R}_{\text{и}} = \vec{R}_{\text{ип}} + \vec{R}_{\text{ик}};$$
$$\vec{M}_{\text{и}} = \vec{M}_{\text{ип}} + \vec{M}_{\text{ик}},$$

(340)

where $\vec{R}_{\text{ип}}$ is the principal vector of translatory forces of inertia;

$\vec{M}_{\text{ип}}$ is the principal moment of translatory forces of inertia;

$\vec{R}_{\text{ик}}$ is the principal vector of Coriolis forces of inertia;

$\vec{M}_{\text{ик}}$ is the principal moment of Coriolis forces of inertia of air.

If the flow-through part of the ACV is symmetrical with respect to its longitudinal and transverse axes, even if the air intake of the fans are arranged somewhat asymmetrically in relation to the center of gravity, the forces and moments of inertia that develop during translatory movement of the air can be disregarded because of their smallness.

Coriolis acceleration of air occurs during rotational translatory motion of the ACV and characterizes the change of relative velocity in translatory motion and of translatory velocity in relative motion and it is equal to twice the vector product of angular velocity of translatory motion of the ACV and relative velocity of the air in the air ducts

$$w_{\text{кор}} = 2(\vec{\omega}_{\text{пер}} \times \vec{V}_{\text{отн}})$$

or in terms of the modulus

$$|w_{\text{кор}}| = 2\,[(\omega_{\text{пер}})\,(V_{\text{отн}})]\,\sin\alpha^{*};$$

where α^* is the angle between the vectors of the angular velocity of rotational translatory motion and relative velocity of the air in the air channels.

Coriolis acceleration is perpendicular to the plane formed by the vectors of angular velocity of rotational translational motion and the relative velocity of the air and is applied in the direction to which the vector of relative velocity is deflected due to rotation.

If to the air passing through the air channels of an ACV is imparted Coriolis acceleration, then the air will develop a Coriolis force of inertia.

The Coriolis force is numerically equal to

$$R_{\text{ик}} = -mw_{\text{кор}};\qquad\qquad(341)$$

is applied in the direction opposite to Coriolis acceleration and, like any force of inertia, is applied to the constraints, i.e., directly to the ACV hull.

For an ACV with a nozzle in the form of a single contour peripheral nozzle with two longitudinal stabilizer nozzles, the projections of the Coriolis forces and moments of inertia of interest to us on rigid axes can be represented in the following form:

$$X_{\text{ик}} = -2\rho Q H_1 \bar{\omega}_z\,\frac{V}{L};\quad Y_{\text{ик}} = 0;$$

$$Z_{\text{ик}} = 2\rho Q H_1 \bar{\omega}_x\,\frac{V}{L};$$

$$M_{x_{\text{ик}}} = 2\rho Q H_1\,(y_{R_1} - l_{t_R})\,\bar{\omega}_x\,\frac{V}{L} -$$

$$-\frac{1}{2\pi}\rho Q\left[3L_n B_n + \left(\frac{L_n^2}{2} + B_n^2\right)K_2\right]\bar{\omega}_x\,\frac{V}{L};$$

$$M_{y_{\text{ик}}} = -2\rho Q H_1 x_{R_1}\,\bar{\omega}_x\,\frac{V}{L} - \frac{1}{2\pi}\rho Q\left[6L_n B_n + \left(\frac{1}{2}K_1 + K_2\right)B_n^2 + \right.$$

$$\qquad\qquad\qquad\qquad\qquad\qquad\qquad\qquad\qquad(342)$$

-304-

$$+ \left(\frac{1}{2}K_2 + K_1\right) L_n^2 \Big] \bar{\omega}_y \frac{V}{L} - 2\rho Q H_1 z_{R_1} \bar{\omega}_z \frac{V}{L};$$

$$M_{z_{\text{як}}} = 2\rho Q H_1 (y_{R_1} - h_R) \bar{\omega}_z \frac{V}{L} - \frac{1}{2z}\rho Q \Big[3L_n B_n +$$

$$+ \left(\frac{B_n^2}{2} + L_n^2\right) K_1 \Big] \bar{\omega}_z \frac{V}{L},$$

(342)

where K_1 and K_2 are form factors of the nozzle in plan;

h_R is the vertical distance between the center of gravity of the ACV and the top edge of the intake (of the air duct);

$$H_1 = y_{R_1} + h_R$$

The form factors are shown in Figure 150. In the case of steady state circulation $\bar{\omega}_x = 0$. Moreover, translatory movement of air in the air ducts (motion of the ACV itself) consists of two rotations at the same angular velocity ω_y, in the same direction. In this case the resultant motion of the ACV will be instantaneous rotation an angular velocity

$$\omega_{\text{пер}} = 2\omega_y$$

around an instantaneous axis parallel to the Oy axis. Only $M_{y_{\text{ик}}}$ is not equal to zero:

$$M_{y_{\text{як}}} = -\frac{1}{\pi}\rho Q \frac{V}{L}\Big[6L_n B_n + \left(\frac{1}{2}K_1 + K_2\right)B_n^2 +$$

$$+ \left(\frac{1}{2}K_2 + K_1\right) L_n^2 \Big]\bar{\omega}_y$$
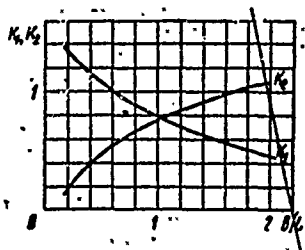
(345)

Figure 150. Form Factors in Plan K_1 and K_2 as Functions of Relative Hull Width B/L (According to K. P. Vashkevich).

It is clear from the above expressions that the Coriolis forces and moments of inertia of air, other conditions being equal, depend on the geometrical shape and distribution of the air ducts and ratio of the

-305-

principal dimensions of the ACV. Assuming that the Coriolis forces and moments of inertia depend little on the presence of a flexible skirt and that this dependence can be disregarded, then they can also be determined for ACV with a flexible skirt according to equations (342), (343)

Hydrodynamic Forces and Moments

Hydrodynamic forces and moments, as stated earlier, can be broken down into two categories:

The first category includes forces and moments caused by the interaction of the air cushion, as a system of distributed surface-pressures, with the surface of the water;

The second category includes forces and moments cuased by the interaction of the flexible skirt with the water surface.

The first category of hydrodynamic forces yields to theoretical analysis, whereas the second, in turn, consisting of components different in nature, cannot be subjected to theoretical analysis and can be determined approximately on the basis of test results.

Forces and Moments Created by the Interaction of the Air Cushion With the Water Surface (Belong to Category of Forces and Moments $\vec{R}_{a4}$, $\vec{M}_{a4}$, See §11, Chapter II).

The hovering of an ACV, as we know, is accompanied by continuous forcing of air into the high pressure region under the bottom. Air simultaneously escapes from the high pressure region. The escaping air, finding its way into the surrounding space (along the boundary between the two media--air and water) continuously transmits some of its energy to the water surrounding it

In the hovering mode, consequently, there is continuous perturbation of the water, which leads to the appearance of wave motions of the fluid. Thus, part of the power of the mechanical plant is expended in the hovering mode on the formation of waves.

During forward motion the interaction of the air in the air cushion with the surrounding water becomes complicated. In this case, wave drag appears (see Chapter IV), which can be represented as a force equivalent to the horizontal component of the pressure acting on the water surface in the direction of travel.

In our investigation of controllability we were interested in the forces of wave origin, which occur in the most complex case of ACV travel----during travel with drift angle β.

-306-

In connection with the fact that wave drag is a component of the forces of wave origin, acting in the direction of travel, in the system of coordinate axes rigidly connected to the vessel it will have the following components:

$$X_B = -R_{x_t} \cos \beta;$$
$$Z_B = -R_{x_t} \sin \beta, \tag{344}$$

where R_{x_1} is wave resistance at the angle of drift.

We will assume that the force of wave drag is applied at the center of gravity of the projection of the air cushion area onto the horizontal plane, and with respect to height, at the nozzle exit.

. If x_B, y_B, z_B. are the coordinates of the point of application of the force of wave resistance, the moments of this force of interest to us will be expressed through the following equations:

$$M_{x_B} = Z_B y_B;$$
$$M_{y_B} = Z_B x_B;$$
$$M_{z_B} = X_B y_B. \tag{345}$$

Thus, in order to determine the forces and moments of wave origin it is essential to know the magnitude of wave resistance R_{x_1} during ACV travel with an angle of drift.

The wave resistance of a floating vessel as it travels with drift angle β at the interface of the two media has not yet been analyzed. Therefore, and also because of the smallness of the angles of drift during travel of floating vessels, the influence of the angle of drift on wave resistance is usually either disregarded [2] or determined according to an approximate empirical formula [12].

The drift angles of ACVs during maneuvering, as we know, are considerably greater than those of floating vessels. · Therefore, it is worthwhile to determine the magnitude and character of the range of wave resistance of ACVs during travel with a drift angle.

In examining the problem of wave resistance of a rectangular system of constant pressure, moving on the open water surface with drift angle β [8], the expression for R_{x_1} remains the same as before (see Table IV), although the values of coefficients A, B, C and D are different.

In order to determine these coefficients in the case of travel of a rectangular constant pressure system with drift angle β we will introduce two systems of coordinate axes:

system of axes rigidly attached to rectangle Oxy and system of velocity axes Ox_1y_1 (Figure 151).
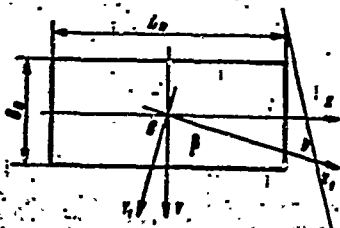
Figure 151. Systems of Axes Connected to Rectangle (XOY) and Velocity Axes (x_1Oy_1) in the Problem of Wave Resistance of Rectangular Constant Pressure System Moving with Drift Angle β

We will substitute the integration variables in the expressions for A, B, C and D on the basis of the following equations (Figure 151):

$$x_1 = x\cos\beta + y\sin\beta;$$
$$y_1 = y\cos\beta - x\sin\beta. \tag{346}$$

Using the definitions

$$a^* = vt\cos\beta;$$
$$b^* = vt\cos\beta;$$
$$c^* = vt\sqrt{i^2-1}\cos\beta; \tag{347}$$
$$d^* = vt\sqrt{i^2-1}\sin\beta.$$

we have

$$\cos vtx_1 = \cos a^*x\cos b^*y - \sin a^*x\sin b^*y; \tag{348}$$
$$\sin vtx_1 = \sin a^*x\cos b^*y + \cos a^*x\sin b^*y;$$
$$\cos vt\sqrt{i^2-1}\,y_1 = \cos c^*y\cdot\cos d^*x + \sin c^*y\cdot\sin d^*x;$$
$$\sin vt\sqrt{i^2-1}\,y_1 = \sin c^*y\cdot\cos d^*x - \cos c^*y\cdot\sin d^*x.$$

After substituting these values into expressions (183) and integrating, we obtain

$$A = 2p_n \cos^2\beta \left[\frac{\sin(a^* + d^*)\frac{L_n}{2}}{a^* + d^*} \cdot \frac{\sin(b^* - c^*)\frac{B_n}{2}}{b^* - c^*} + \right.$$
$$\left. + \frac{\sin(a^* - d^*)\frac{L_n}{2}}{a^* - d^*} \cdot \frac{\sin(b^* + c^*)\frac{B_n}{2}}{b^* + c^*} \right];$$

$$B = 0; \quad C = 0;$$

(349)

$$D = 2p_n \cos^2\beta \left[\frac{\sin(a^* + d^*)\frac{L_n}{2}}{a^* + d^*} \cdot \frac{\sin(b^* - c^*)\frac{B_n}{2}}{b^* - c^*} - \right.$$
$$\left. - \frac{\sin(a^* - d^*)\frac{L_n}{2}}{a^* - d^*} \cdot \frac{\sin(b^* + c^*)\frac{B_n}{2}}{b^* + c^*} \right].$$

Substitution of the expressions for the coefficients of (349) into equation (182) yields

$$R_{x_1} = \frac{8p_n^2 g^2}{\pi \rho V^6} \cos^4\beta \int_1^\infty \left[\frac{\sin^2(a^* + d^*)\frac{L_n}{2}}{(a^* + d^*)^2} \cdot \frac{\sin^2(b^* - c^*)\frac{B_n}{2}}{(b^* - c^*)^2} + \right.$$
$$\left. + \frac{\sin^2(a^* - d^*)\frac{L_n}{2}}{(a^* - d^*)^2} \cdot \frac{\sin(b^* + c^*)\frac{B_n}{2}}{(b^* + c^*)^2} \right] \frac{t^4 dt}{\sqrt{t^2 - 1}}.$$

(350)

Using relations (347), we obtain the following expression for R_{x_1}:

$$R_{x_1} = \frac{3p_n^2 g^2}{\pi \rho V^6 \gamma^4} \int_1^\infty \left\{ \frac{\sin^2\left[\frac{vtL_n}{2} \cos\beta (1 + \sqrt{t^2 - 1} \tan\beta) \right]}{(1 + \sqrt{t^2 - 1} \tan\beta)^2} \times \right.$$
$$\times \frac{\sin^2\left[\frac{vtB_n}{2} \cos\beta (\tan\beta - \sqrt{t^2 - 1}) \right]}{(\tan\beta - \sqrt{t^2 - 1})^2} +$$

(351)

$$+ \frac{\sin^2\left[\frac{\nu t L_n}{2}\cos\beta\left(1 - \sqrt{t^2-1}\, \mathrm{tg}\beta\right)\right]}{\left(1 - \sqrt{t^2-1}\, \mathrm{tg}\beta\right)^2} \times$$

$$\times \frac{\sin^2\left[\frac{\nu t B_n}{2}\cos\beta\left(\mathrm{tg}\beta + \sqrt{t^2-1}\right)\right]}{\left(\mathrm{tg}\beta + \sqrt{t^2-1}\right)^2}\Bigg\} \frac{dt}{\sqrt{t^2-1}}$$

After substituting g/V^2 for ν, where g is acceleration and V is velocity, and also using the definitions

$$k = \frac{1}{\mathrm{Fr}^2} = \frac{g L_n}{V^2}, \quad \mu_n = \frac{B_n}{L_n},$$

where Fr is Froude's number and B_n and L_n are the width and length of the pressure rectangle, we will obtain for R_{x_1} the following:

$$R_{x_1} = \frac{8 p_n^2 V^2}{\pi \rho g^2} \int_1^\infty \Bigg\{ \frac{\sin^2\left[\frac{kt}{2}\cos\beta\left(1 + \sqrt{t^2-1}\, \mathrm{tg}\beta\right)\right]}{\left(1 + \sqrt{t^2-1}\, \mathrm{tg}\beta\right)^2} \times$$

$$\times \frac{\sin^2\left[\frac{\mu_n k t}{2}\cos\beta\left(\mathrm{tg}\beta - \sqrt{t^2-1}\right)\right]}{\left(\mathrm{tg}\beta - \sqrt{t^2-1}\right)^2} + \quad (352)$$

$$+ \frac{\sin^2\left[\frac{kt}{2}\cos\beta\left(1 - \sqrt{t^2-1}\, \mathrm{tg}\beta\right)\right]}{\left(1 - \sqrt{t^2-1}\, \mathrm{tg}\beta\right)^2} \times$$

$$\times \frac{\sin^2\left[\frac{\mu_n k t}{2}\cos\beta\left(\mathrm{tg}\beta + \sqrt{t^2-1}\right)\right]}{\left(\mathrm{tg}\beta + \sqrt{t^2-1}\right)^2} \Bigg\} \frac{dt}{\sqrt{t^2-1}}.$$

Further, we will examine specific wave resistance

$$\frac{R_{x_1}}{G} = \frac{R_{x_1}}{p_n L_n B_n} = A_\beta(k, \mu_n) \frac{2 p_n}{\gamma L_n}. \quad (353)$$

The curves of coefficient A_β as a function of Froude's number are shown in Figures 152-157 for different drift angles β and coefficients μ_n, constructed on the basis of the results of calculations using equation (353). It follows from these graphs that the angle of drift β has a substantial influence of coefficient A_β, causing it not only to increase, but also to decrease.

Figure 152. Wave Resistance Coefficient A_β as a Function of Froude's Number for Various Drift Angles β and L_Π/B_Π = 5.

Figure 153. Wave Resistance Coefficient A_β as a Function of Froude's Number for Various Drift Angles β and L_Π/B_Π = 3.34.

Figure 154. Wave Resistance Coefficient A_β as a Function of Froude's Number for Various Drift Angles β and L_Π/B_Π = 2.5.

-311-
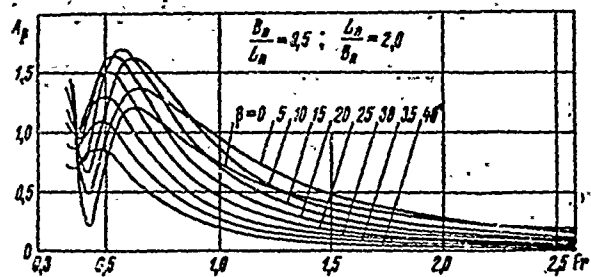
Figure 155.   Wave Resistance Coefficient A_β as Function of
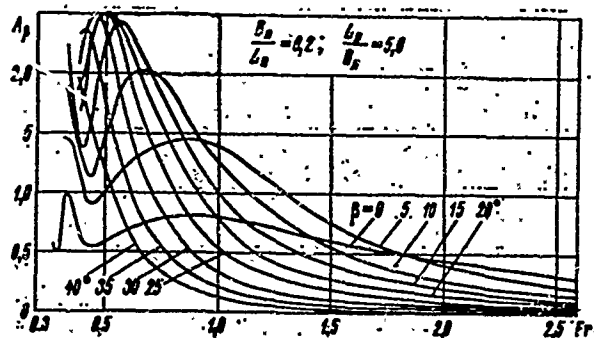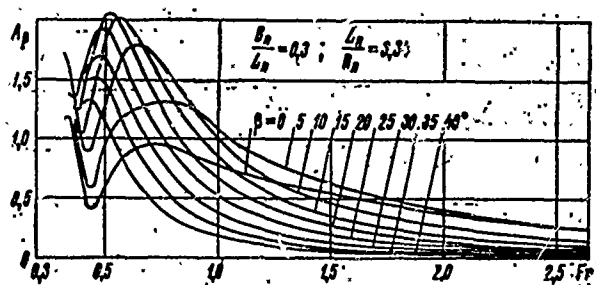Froude's Number for Various Drift Angles β and $L_\Pi/B_\Pi = 2$.
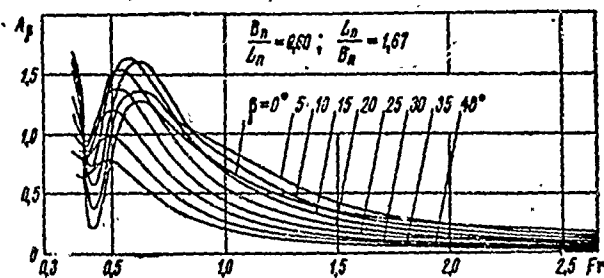
Figure 156.   Wave Resistance Coefficient A_β as a Function of
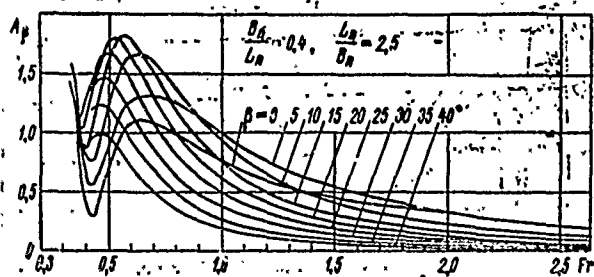Froude's Number for Various Drift Angles β and $L_\Pi/B_\Pi = 1.67$.
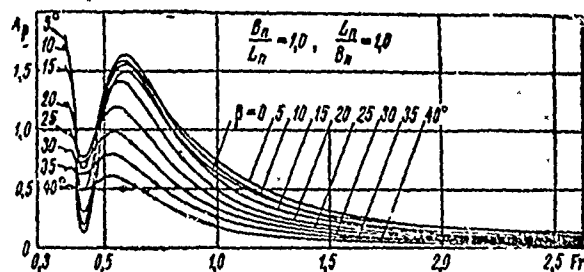
Figure 157.   Wave Resistance Coefficient A_β as a Function of
Froude's Number for Various Drift Angles β and $L_\Pi/B_\Pi = 1.0$.

-312-

The graphs (Figures 152-157), constructed for the most common air cushion elongations, show that wave resistance on the "hump" is much less for angle $\beta = 0$ than for other angles of drift; the exceptions are drift angles $\beta = 30$, 35 and 40°. This is evidence that the hump should be overcome by strictly holding to zero drift. At high speeds (Fr = 1.3-1.5) angle of drift $\beta > 10^\circ$ leads to reduced wave resistance, and only at angle of drift 5° is the resistance higher than during travel without drift.

Thus, we obtain

$$X_s = -A_\beta \frac{2p_n}{\gamma L_s} G;$$

$$Z_s = -A_\beta \frac{2p_v}{\gamma L_n} G\beta;$$

$$M_{x_s} = A_\beta \frac{2p_n}{\gamma L_n} G\beta y_s;$$

$$M_{y_s} = A_\beta \frac{2p_n}{\gamma L_n} G\beta x_s.$$

(354)

Forces and Moments Created by Interaction of a Flexible Air Cushion Skirt with Water Surface (Belong to Category of Forces and Moments $\vec{R}_r$ and $\vec{M}_r$, See §11, Chapter II)

Visual observations of the movement of ACV models with the various types of flexible skirts, and comparative analysis of the curves of tow drag, indicate that the flexible skirt qualitatively alters the tow characteristics of models.

A flexible skirt comes into direct contact with the water surface, with the result that components of the flexible skirt are awash in the stern part. The intensity of the washing of flexible skirt components depends on the following basic factors:

design and material of flexible skirt;

weight of ACV;

centering of ACV;

air flow rate;

speed of travel.

An extra component--skirt drag, is added to the drag of the model as a result of skirt washing. Moreover, spray resistance develops as a result of interaction of the escaping air jets with the water and reaction of water spray with the flexible skirt and hull of the vessel.

As pointed out in Chapter IV, there are presently no theoretical or experimental data for determination of the role of each component in the overall balance of this portion of hydrodynamic resistance. Therefore, it is determined as a whole as residual resistance

$$R_{r.o} = R_r - R_s \approx R_{ocr},$$ (355)

where R_r is the hydrodynamic drag according to the results of model tow tests, also including reactive drag.

During ACV travel with an angle of drift, especially at an angular velocity, the processes of reaction of the flexible skirt and air jets flowing from beneath it, with the surface of the water is substantially complicated, as we cannot determine the forces and moments created by this reaction, either component-wise or as a whole.

In order to approximate this force we may assume that residual resistance does not change at small angles of drift. In this case the residual resistance may be broken down into two components: longitudinal and lateral

$$X_{r.o} = -R_{r.o} \cos \beta;$$
$$Z_{r.o} = -R_{r.o} \sin \beta.$$ (356)

If $x_{r.o}$, $y_{r.o}$ are the coordinates of the point of application of the force, then the moments of interest to us are

$$M_{x_{r.o}} = Z_{r.o} y_{r.o};$$
$$M_{y_{r.o}} = Z_{r.o} x_{r.o}.$$ (357)

Thus, in order to determine the forces and moments created by the interaction of the flexible skirt with the water surface it is essential to know residual drag R_{ocr} and the coordinates of its point of application.

In this case we obtain

$$X_{r.o} = -R_{ocr};$$ (358)

-314-

$$Z_{\text{г.о}} = -R_{\text{ост}}\beta;$$

$$M_{x_{\text{г.о}}} = -R_{\text{ост}}\beta y_{\text{г.о}};$$

$$M_{y_{\text{г.о}}} = -R_{\text{ост}}\beta x_{\text{г.о}}. \tag{358}$$

§24. Differential Equations of Motion

In the most general case, the motion of an ACV as a freely moving solid body is determined by a system of six equations of the second order or by a system of twelve equations of the first order. Of these twelve equations, six represent kinematic equations and the other six are differential equations of solid dynamics, related to a system of coordinates axes rigidly attached to the vessel.

Kinematic Equations of Motion

The spatial motion of an ACV as a free body can be broken down into two simple components: translational--along with the pole (center of gravity) and rotational--around the pole. The rotational portion of ACV motion is completely defined if Euler's angles φ, ψ and θ are given (see §21). Therefore the equations

$$\varphi = \dot{\varphi}(t); \quad \psi = \dot{\psi}(t); \quad \theta = \theta(t)$$

are equations of rotation. From these are found the vector of angular velocity, equal to the geometric sum of three components:

$$\vec{\omega} = \dot{\vec{\varphi}} + \dot{\vec{\psi}} + \dot{\vec{\theta}}.$$

Each of these components characterizes the rate of change of Euler's angle and is directed along the corresponding axis of rotation. The projections of the angular velocity of rotation of the ACV around the center of gravity onto the axes are of the form

$$\omega_x = \dot{\theta} + \dot{\varphi}\sin\psi;$$

$$\omega_y = \dot{\psi}\sin\theta + \dot{\varphi}\cos\psi\cos\theta;$$

$$\omega_z = \dot{\psi}\cos\theta - \dot{\varphi}\cos\psi\sin\theta \tag{359}$$

or, solving the equations in terms of φ, ψ and $\dot{\theta}$,

$$\dot{\varphi} = \frac{\omega_y\cos\theta - \omega_z\sin\theta}{\cos\psi};$$

$$\dot{\psi} = \omega_y\sin\theta + \omega_z\cos\theta; \tag{360}$$

$$\dot{\theta} = \omega_x - \text{tg}\,\psi\,(\omega_y\cos\theta - \omega_z\sin\theta).$$

$$Z_{r.o} = -R_{ocr}\beta;$$

$$M_{x_{r.o}} = -R_{ocr}\beta y_{r.o};$$

$$M_{y_{r.o}} = -R_{ocr}\beta x_{r.o}. \tag{358}$$

§24. Differential Equations of Motion

In the most general case, the motion of an ACV as a freely moving solid body is determined by a system of six equations of the second order or by a system of twelve equations of the first order. Of these twelve equations, six represent kinematic equations and the other six are differential equations of solid dynamics, related to a system of coordinates axes rigidly attached to the vessel.

Kinematic Equations of Motion

The spatial motion of an ACV as a free body can be broken down into two simple components: translational--along with the pole (center of gravity) and rotational--around the pole. The rotational portion of ACV motion is completely defined if Euler's angles φ, ψ and θ are given (see §21). Therefore the equations

$$\varphi = \dot{\varphi}(t); \quad \psi = \dot{\psi}(t); \quad \theta = \theta(t)$$

are equations of rotation. From these are found the vector of angular velocity, equal to the geometric sum of three components:

$$\vec{\omega} = \dot{\vec{\varphi}} + \dot{\vec{\psi}} + \dot{\vec{\theta}}.$$

Each of these components characterizes the rate of change of Euler's angle and is directed along the corresponding axis of rotation. The projections of the angular velocity of rotation of the ACV around the center of gravity onto the axes are of the form

$$\omega_x = \dot{\theta} + \dot{\varphi}\sin\psi;$$

$$\omega_y = \dot{\psi}\sin\theta + \dot{\varphi}\cos\psi\cos\theta;$$

$$\omega_z = \dot{\psi}\cos\theta - \dot{\varphi}\cos\psi\sin\theta \tag{359}$$

or, solving the equations in terms of φ, ψ and $\dot{\theta}$,

$$\dot{\varphi} = \frac{\omega_y\cos\theta - \omega_z\sin\theta}{\cos\psi};$$

$$\dot{\psi} = \omega_y\sin\theta + \omega_z\cos\theta; \tag{360}$$

$$\dot{\theta} = \omega_x - \operatorname{tg}\psi\,(\omega_y\cos\theta - \omega_z\sin\theta).$$

-315-

Translational motion would best be determined, for clarity, with the aid of the coordinates of the center of gravity (x_g, y_g, z_g), called the principal parameters of translational motion, although this complicates the calculation of the aerodynamic forces. Therefore, translational motion is assigned by the vector of velocity of the center of gravity of the ACV, approximated relative to the axes Ox, Oy, Oz.

The parameters $V = V(t)$, $\alpha = \alpha(t)$, $\beta = \beta(t)$ (see §21) define the translational motion of the ACV and are auxiliary parameters of translational motion.

Here α and β are the angles of attack and drift, examined above.

The projections of the vector of velocity of translational motion of the center of gravity of the ACV onto the Ox, Oy, Oz axes are of the form

$$V_x = V \cos \beta \cos \alpha;$$
$$V_y = -V \cos \beta \sin \alpha;$$
$$V_z = V \sin \beta. \tag{361}$$

However, the parameters V, α and β, suitable for determination of the aerodynamic forces (for instance, in a wind tunnel or tank) give no representation of the character of translational motion. Hence it is necessary to relate the auxiliary parameters of translational motion to the principal parameters. This relation is found on the basis of the equations of point kinematics:

$$\frac{dz_g}{dt} = V_{z_g}, \quad \frac{dx_g}{dt} = V_{x_g}; \quad \frac{dy_g}{dt} = V_{y_g}; \tag{362}$$

where x_g, y_g, z_g are the coordinates of the center of gravity of the ACV;

V_{x_g}, V_{y_g}, V_{z_g} are the projections of the vector of translational velocity of the center of gravity of the ACV onto fixed axes.

These expressions are the fundamental equations of translational motion of ACV.

From expressions (362) we obtain:

$$x_g = x_{g_0} + \int_0^t V_{x_g} dt;$$

$$y_g = y_{g_0} + \int_0^t V_{y_g} dt;$$

(363)

$$z_g = z_{g_0} + \int_0^t V_{z_g} dt.$$

The projections of the vector of translational velocity of the center of gravity of the ACV onto fixed axes (V_{x_g}, V_{y_g}, V_{z_g}) are found by converting the projections of the vector of translational velocity of the center of gravity to rigidly connected axes (V_x, V_y, V_z) using the so-called direction cosines [34].

Differential Equations of Unsteady Unperturbed Motion of ACV in General Form

The derivation of the differential equations of spatial motion of ACVs in the system of coordinate axes Oxyz is generally based on the laws of the quantity of motion and moments of the quantity of motion. We know from hydrodynamics that motion of the region of high air pressure, which creates a depression in the water beneath the hull of the ACV (in the hovering mode, equal in volume to the volumetric displacement of water) under certain conditions, for instance, during travel at slow speeds, is practically the same as the motion of a solid in a liquid. Therefore, in order to derive the differential equations of motion of ACV in the most general form, we will regard it as a body moving in a fluid. As the differential equations of motion in a fluid, we can use the respective equations for a solid in a vacuum, but instead of kinetic energy T_1, we will consider the summary kinetic energy of the body--fluid system:

$$T_0 = T_1 + T_2,$$

where T_2 is the kinetic energy of the fluid.

From theoretical mechanics we know [30], that in equations of motion of a solid in a vacuum, related to axes connected to the solid, can be written in the following vector form:

$$\frac{d\vec{B}}{dt} + [\vec{\omega} \times \vec{B}] = \vec{R};$$

(364)

$$\frac{d\vec{N}}{dt} + [\vec{\omega} \times \vec{N}] + [\vec{V} \times \vec{B}] = \vec{M},$$

-317-

where $\vec{B}$ is the principal vector of the quantity of motion of the body;

$\vec{N}$ is the principal moment of the quantity of motion;

$\vec{R}$ is the principal vector of external forces;

$\vec{M}$ is the principal moment of external forces;

$\vec{V}$ is the vector of velocity of translational motion of the origin in coordinates system Oxyz, connected to the body;

$\vec{\omega}$ is the vector of velocity of rotational motion of coordinate system Oxyz, connected to the body.

Equations (364), in projections onto the axes of the coordinate system connected to the body, are of the form

$$\frac{dB_x}{dt} + \omega_y B_z - \omega_z B_y = X;$$

$$\frac{dB_y}{dt} + \omega_z B_x - \omega_x B_z = Y;$$ (365)

$$\frac{dB_z}{dt} + \omega_x B_y - \omega_y B_x = Z;$$

$$\frac{dN_x}{dt} + \omega_y N_z - \omega_z N_y + V_y B_z - V_z B_y = M_x;$$

$$\frac{dN_y}{dt} + \omega_z N_x - \omega_x N_z + V_z B_x - V_x B_z = M_y;$$

$$\frac{dN_z}{dt} + \omega_x N_y - \omega_y N_x + V_x B_y - V_y B_x = M_z.$$

The projections of the vectors $\vec{B}$ and $\vec{N}$ onto the fixed axes are expressed through kinetic energy T_c of the body--ambient medium system as follows:

$$B_x = \frac{\partial T_c}{\partial V_x}; \quad N_x = \frac{\partial T_c}{\partial \omega_x};$$

$$B_y = \frac{\partial T_c}{\partial V_y}; \quad N_y = \frac{\partial T_c}{\partial \omega_y};$$ (366)

$$B_z = \frac{\partial T_c}{\partial V_z}; \quad N_z = \frac{\partial T_c}{\partial \omega_z}.$$

With consideration of expressions (366), equations system (365) acquires the following form:

$$\frac{d}{dt}\left(\frac{\partial T_c}{\partial V_x}\right) + \omega_y \frac{\partial T_c}{\partial V_z} - \omega_z \frac{\partial T_c}{\partial V_y} = X;$$

$$\frac{d}{dt}\left(\frac{\partial T_c}{\partial V_y}\right) + \omega_z \frac{\partial T_c}{\partial V_x} - \omega_x \frac{\partial T_c}{\partial V_z} = Y;$$

$$\frac{d}{dt}\left(\frac{\partial T_c}{\partial V_z}\right) + \omega_x \frac{\partial T_c}{\partial V_y} - \omega_y \frac{\partial T_c}{\partial V_x} = Z;$$ (367)

$$\frac{d}{dt}\left(\frac{\partial T_c}{\partial \omega_x}\right) + \omega_y \frac{\partial T_c}{\partial \omega_z} - \omega_z \frac{\partial T_c}{\partial \omega_y} + V_y \frac{\partial T_c}{\partial V_z} - V_z \frac{\partial T_c}{\partial V_y} = M_x;$$

$$\frac{d}{dt}\left(\frac{\partial T_c}{\partial \omega_y}\right) + \omega_z \frac{\partial T_c}{\partial \omega_x} - \omega_x \frac{\partial T_c}{\partial \omega_z} + V_z \frac{\partial T_c}{\partial V_x} - V_x \frac{\partial T_c}{\partial V_z} = M_y;$$

$$\frac{d}{dt}\left(\frac{\partial T_c}{\partial \omega_z}\right) + \omega_x \frac{\partial T_c}{\partial \omega_y} - \omega_y \frac{\partial T_c}{\partial \omega_x} + V_x \frac{\partial T_c}{\partial V_y} - V_y \frac{\partial T_c}{\partial V_x} = M_z.$$

Considering that the ACV has a longitudinal vertical plane of symmetry, then for the principal axes of the coordinate system connected to the ACV and having its origin at the central point, the kinetic energy of the ACV can be written in the following form:

$$T_1 = \frac{1}{2}\left[m\left(V_x^2 + V_y^2 + V_z^2\right) + J_x\omega_x^2 + J_y\omega_y^2 + J_z\omega_z^2 - J_{xy}\omega_x\omega_y\right],$$ (368)

where   m is the mass of the ACV;

J_x, J_y, J_z are the principal moments of inertia of the ACV mass, taken relative to the axis with the appropriate subscript;

J_{xb} is the centrifugal moment of inertia relative to the Oz axis.

The kinetic energy of the medium can consist of the kinetic energy of the air and the kinetic energy of the water. The kinetic energy of air is considered, as we saw in the preceding sections, in the right-hand side of the equations in the form of various categories of forces and moments (Coriolis forces of inertia, forces and moments of reaction of intake air, etc.) and the kinetic energy of water in this case is determined by the following expression [2]:

-319-

$$T_2 = \frac{1}{2}\left[\lambda_{11}V_x^2 + \lambda_{22}V_y^2 + \lambda_{33}V_z^2 + 2\lambda_{12}V_xV_y + \lambda_{44}\omega_x^2 + \lambda_{55}\omega_y^2 + \right.$$
$$+ \lambda_{66}\omega_z^2 + 2\lambda_{45}\omega_x\omega_y + 2\lambda_{34}V_z\omega_x + 2\lambda_{35}V_z\omega_y +$$
$$\left. + 2\lambda_{16}V_x\omega_z + 2\lambda_{26}V_y\omega_z, \right. \tag{369}$$

where λ_{ik} are coefficients, called connected masses. They characterize the amount of motion and the moment of the amount of motion of the fluid (water) as the high air pressure region travels in it. Coefficients λ_{11}, λ_{12}, λ_{22}, λ_{33} have the dimension of mass, λ_{16}, λ_{26}, λ_{35}, λ_{34} the dimension of static moment, λ_{44}, λ_{45}, λ_{55}, λ_{66} the moment of inertia.

If now we take partial derivatives T_c in accordance with expressions (368) and (369) and substitute them into relations (367), we obtain:

$$\frac{dV_x}{dt}(m+\lambda_{11}) + \frac{dV_y}{dt}\lambda_{12} + \frac{d\omega_z}{dt}\lambda_{16} + \omega_yV_z(m+\lambda_{33}) +$$
$$+ \omega_y\omega_x\lambda_{34} + \omega_y^2\lambda_{35} - \omega_zV_y(m+\lambda_{22}) - \omega_zV_x\lambda_{12} - \omega_z^2\lambda_{26} = X;$$

$$\frac{dV_y}{dt}(m+\lambda_{22}) + \frac{dV_x}{dt}\lambda_{12} + \frac{d\omega_z}{dt}\lambda_{26} + \omega_zV_x(m+\lambda_{11}) +$$
$$+ \omega_zV_y\lambda_{12} + \omega_z^2\lambda_{16} - \omega_xV_z(m+\lambda_{33}) - \omega_x^2\lambda_{34} - \omega_x\omega_y\lambda_{35} = Y; \tag{370}$$

$$\frac{dV_z}{dt}(m+\lambda_{33}) + \frac{d\omega_x}{dt}\lambda_{34} + \frac{d\omega_y}{dt}\lambda_{35} + \omega_xV_y(m+\lambda_{22}) +$$
$$+ \omega_xV_x\lambda_{12} + \omega_x\omega_z\lambda_{24} - \omega_yV_x(m+\lambda_{11}) - \omega_yV_y\lambda_{12} - \omega_y\omega_z\lambda_{16} = Z;$$

$$\frac{d\omega_x}{dt}(J_x+\lambda_{44}) + \frac{d\omega_y}{dt}(\lambda_{45}-J_{xy}) + \frac{dV_z}{dt}\lambda_{34} + \omega_y\omega_z(J_z+\lambda_{66}) +$$
$$+ \omega_yV_x\lambda_{16} + \omega_yV_y\lambda_{26} - \omega_z\omega_y(J_y+\lambda_{55}) - \omega_z\omega_x(\lambda_{45}-J_{xy}) +$$
$$+ (V_y\omega_y - V_z\omega_z)\lambda_{35} + V_y\omega_z\lambda_{34} - V_z\omega_z\lambda_{26} = M_x;$$

$$\frac{d\omega_y}{dt}(J_y+\lambda_{55}) + \frac{d\omega_x}{dt}(\lambda_{45}-J_{xy}) + \frac{d\omega_z}{dt}\lambda_{35} + \omega_z\omega_x(J_x+\lambda_{44}) +$$
$$+ \omega_z\omega_y(\lambda_{45}-J_{xy}) + \omega_zV_z\lambda_{34} - \omega_x\omega_z(J_z+\lambda_{66}) - (\omega_xV_x - \omega_zV_z)\lambda_{16} -$$
$$- V_y\omega_x\lambda_{26} - V_x\omega_x\lambda_{34} - V_x\omega_y\lambda_{35} = M_y;$$

$$\frac{d\omega_z}{dt}(J_z+\lambda_{66}) + \frac{dV_x}{dt}\lambda_{16} + \frac{dV_y}{dt}\lambda_{26} + \omega_x\omega_y(J_y+\lambda_{55}) +$$
$$+ \omega_x^2(\lambda_{45}-J_{xy}) + \omega_xV_z\lambda_{35} - \omega_y\omega_x(J_x+\lambda_{44}) - \omega_y^2(\lambda_{45}-J_{xy}) -$$
$$- \omega_zV_z\lambda_{34} + V_x\omega_z\lambda_{35} - V_y^2\lambda_{16} - V_y\omega_x\lambda_{16} = M_z.$$

-320-

Equations (359), (362) and (370) jointly represent a system of twelve differential equations of the spatial motion of the ACV. In this system there are twelve unknowns:

$$V_x, V_y, V_z, \omega_x, \omega_y, \omega_z, \varphi, \psi, \theta, x_g, h, z_g.$$

In the aerodynamics of aircraft, the order of the equation system that describes the spatial motion of an aircraft is usually reduced by discarding equations (362). These equations can be disregarded in aircraft aerodynamics because coordinates x_g, y_g, z_g play no important role in the analysis of aircraft stability, since the aerodynamic forces and moments are generally independent of coordinates x_g and z_g, and the effect of change of coordinate y_g on the aerodynamic forces and moments can be disregarded.

In analyzing ACV, however, the effect of change of the coordinate y_g on the aerodynamic forces and moments obviously cannot be disregarded, and therefore the order of the equation system can be reduced only by excluding from the examination the first and third equations of (362).

Thus, in analyzing the dynamics of ACV we arrive at a system of ten differential equations. In view of the symmetry of ACV with respect to x0y, we can derive from the system of equations of spatial motion a system containing only those terms that characterize motion in plane of symmetry x0y, and which does not contain parameters of motion in the two other planes. The equations of motion in the plane of symmetry x0y, called longitudinal motion, can be derived from system (359), (362) and (370) assuming $\omega_x = \omega_y = V_z = \theta = 0$:

$$\frac{dV_x}{dt}(m + \lambda_{11}) + \frac{dV_y}{dt}\lambda_{12} + \frac{d\omega_z}{dt}\lambda_{16} - \omega_z V_y(m + \lambda_{22}) -$$

$$- \omega_z V_x \lambda_{12} - \omega_z^2 \lambda_{26} = X;$$

$$\frac{dV_y}{dt}(m + \lambda_{22}) + \frac{dV_x}{dt}\lambda_{12} - \frac{d\omega_z}{dt}\lambda_{26} + \omega_z V_x(m + \lambda_{11}) + \qquad (371)$$

$$+ \omega_z V_y \lambda_{12} + \omega_z^2 \lambda_{16} = Y;$$

$$\frac{d\omega_z}{dt}(J_z + \lambda_{66}) + \frac{dV_x}{dt}\lambda_{16} + \frac{dV_y}{dt}\lambda_{26} + V_x \omega_z \lambda_{26} - V_y^2 \lambda_{12} -$$

$$- V_y \omega_z \lambda_{16} = M_z;$$

$$\omega_z = \frac{d\psi}{dt};$$

$$\frac{dy_g}{dt} = V_{y_g}.$$

The kinematic parameters of longitudinal motion are ω_z, V, α, ψ, h.

ACV motion in planes xOz and yOz, when the center of gravity of the ACV remains in the horizontal plane, is called, lateral motion.

From aircraft aerodynamics we know that during small changes in the kinematic parameters of lateral motion (ω_x, ω_y, θ, β), the perturbed motion of the aircraft occurs in such a way that the kinematic parameters of longitudinal motion are not altered. Therefore the lateral motion of an aircraft can be examined separately from longitudinal, and the system of equations of spatial motion is divided into two independent systems.

In ACV analysis, such division is less justified, since the perturbation of lateral parameters, for instance the angle of roll θ leads to a change in certain longitudinal parameters, such as hovering altitude h.

If we assume that a change in the parameters of lateral motion causes no substantial change in the parameters of longitudinal motion, then we may derive the equations of lateral motion from systems (359), (362) and (370).

The differential equations of lateral motion correspond to the conditions V = const; α = const; ψ = const; $\omega_z = 0$, h = const and are of the following form:

$$\frac{dV_z}{dt}(m + \lambda_{33}) + \frac{d\omega_x}{dt}\lambda_{34} + \frac{d\omega_y}{dt}\lambda_{35} + \omega_x V_x \lambda_{12} -$$
$$- \omega_y V_x (m + \lambda_{11}) = Z;$$

$$\frac{d\omega_x}{dt}(J_x - \lambda_{44}) + \frac{d\omega_y}{dt}(\lambda_{45} - J_{xy}) + \frac{dV_z}{dt}\lambda_{34} + \omega_y V_x \lambda_{16} = M_x; \qquad (372)$$

$$\frac{d\omega_y}{dt}(J_y + \lambda_{55}) + \frac{d\omega_x}{dt}(\lambda_{45} - J_{xy}) + \frac{dV_z}{dt}\lambda_{35} - \omega_x V_x \lambda_{16} -$$
$$- V_x \omega_x \lambda_{34} - V_x \omega_y \lambda_{35} = M_y;$$

$$\omega_x = \frac{d\theta}{dt} + \frac{d\varphi}{dt}\sin\psi;$$

$$\omega_y = \frac{d\varphi}{dt}\cos\psi\cos\theta.$$

For further simplification of the equation system we turn our attention to the fact that with an increase in Froude's number during travel of the ACV, the water depression, moving along with the vessel, does not remain constant, but is deformed. At the limit for Froude's numbers of about 2.5, the water surface beneath the high pressure region during travel on calm water cannot be deformed and the water depression is not formed. In this case (in the absence of pressure oscillations in the air cushion), there is also no inertial action of the water on the traveling ACV, i.e., all connected masses are equal to zero.

Therefore, we may assume in the first approximation that all co-efficients of connected masses are equal to zero. Moreover, assuming that the coordinate axes coincide with the principal axes of inertia of ACVs, $J_{xy} = 0$.

In consideration of these assumptions the equations of lateral motion of ACVs acquire the form

$$m\left(\frac{dV_z}{dt} - \omega_y V_x\right) = Z;$$

$$J_x \frac{d\omega_x}{dt} = M_x;$$

$$J_y \frac{d\omega_y}{dt} = M_y;$$

$$\frac{d\theta}{dt} = \omega_x - \text{tg}\,\psi\omega_y \cos\theta;$$

$$\frac{d\varphi}{dt} = \sec\psi\cos\theta\omega_y.$$

(373)

The equation system (373) is inadequate for the solution of many problems of lateral ACV motion related to unsteady translatory motion. In this case it is necessary to add to it the first equation of system (370), which in consideration of the assumptions made acquires the form:

$$m\left(\frac{dV_x}{dt} + \omega_y V_z\right) = X.$$

(374)

Equations (373) and (374) represent the starting equations of unsteady, unperturbed ACV motion in the general form.

Equations of Perturbed Motion in Expanded Form

Perturbed motion of any dynamic system is motion caused by pulses which to some degree disrupt the dynamic equilibrium of the system. In order to derive the equations of perturbed motion, following the method of small perturbations, we will represent the kinematic characteristics of perturbed motion as the sum of values of these characteristics in the basic (unperturbed) motion and of perturbations, for example

$$V_x = V_{x_0} + \Delta V_x;$$
$$\beta = \beta_0 + \Delta\beta.$$

In accordance with the method of small perturbations, assuming deviations ΔV_x, ΔV_y to be small and disregarding terms of a higher order of smallness ($\Delta V_2 \Delta V_y$, etc.), we obtain the equations [for example the equation (374)] in the following form:

$$m\left(\frac{dV_{x_0}}{dt} + \frac{d\Delta V_x}{dt}\right) + m\left[V_{x_0}(\omega_{y_0} + \Delta\omega_y) + \Delta V_z \omega_{y_0}\right] = \tag{375}$$
$$= X_0 + \Delta X.$$

In the initial unperturbed motion, indeed, the following equation is valid:

$$m\frac{dV_{x_0}}{dt} + mV_{z_0}\omega_{y_0} = X_0. \tag{376}$$

$$m\frac{d\Delta V_x}{dt} + m\left[V_{z_0}\Delta\omega_y + \Delta V_z \omega_{y_0}\right] = \Delta X;$$

$$m\frac{d\Delta V_z}{dt} - m\left[\Delta V_x \omega_{y_0} + V_{x_0}\Delta\omega_y\right] = \Delta Z;$$

$$\tag{377}$$

$$J_x\frac{d\Delta\omega_x}{dt} = \Delta M_x;$$

$$J_y\frac{d\Delta\omega_y}{dt} = \Delta M_y;$$

$$\frac{d\Delta\theta}{dt} = \Delta\omega_x - \operatorname{tg}\psi_0\left[\cos\theta_0\Delta\omega_y - \omega_{y_0}\sin\theta_0\Delta\theta\right] - \sec^2\psi_0\omega_{y_0}\cos\theta_0\Delta\psi;$$

$$\frac{d\Delta\varphi}{dt} = \sec\psi_0\left[\cos\theta_0\Delta\omega_y - \omega_{y_0}\sin\theta_0\Delta\theta\right] + \operatorname{tg}\psi_0\sec\psi_0\omega_{y_0}\cos\theta_0\Delta\psi.$$

-324-

Thus, on the basis of the method of small perturbations, we have obtained differential equations with variable coefficients of relative unknown perturbations. Following the example of [35], we assume that the duration of transition processes during the action of perturbations is short, so that during the time of a transition process the kinematic parameters of the basic (unperturbed) motion change comparatively little. Under this assumption, during analysis of perturbed motion we may disregard change in the kinematic parameters of unperturbed motion compared to the change of the kinematic characteristics--perturbations (method of "frozen" coefficients). Here, the parameters of unperturbed motion are assumed to be constant and equal to their values at the beginning of perturbed motion. This permits us in the first approximation to consider system (377) a system of differential equations with constant coefficients. If we assume that the initial mode of travel is straight line, steady state motion without roll, but with constant drift, then

$$\theta_0 = \omega_{x_0} = \omega_{y_0} = 0,$$

(378)

and considering the smallness of angle β we obtain on the basis of expressions (371)

$$
\begin{aligned}
V_{z_0} &= V_0 \beta_0; \\
\Delta V_z &\approx V_0 \Delta \beta; \\
V_{x_0} &\approx V_0; \\
\Delta V_x &\approx \Delta V - \beta_0 V_0 \Delta \beta.
\end{aligned}
$$

(379)

Substituting expressions (379) into equations (377) and considering the function (378), we obtain

$$m \left[\frac{d\Delta V}{dt} - \left(\frac{d\Delta \beta}{dt} - \Delta \omega_y \right) \beta_0 V_0 \right] = \Delta X;$$

$$m V_0 \left[\frac{d\Delta \beta}{dt} - \Delta \omega_y \right] = \Delta Z;$$

$$J_x = \frac{d\Delta \omega_x}{dt} = \Delta M_x;$$

$$J_y = \frac{d\Delta \omega_y}{dt} = \Delta M_y;$$

$$\frac{d\Delta \theta}{dt} = \Delta \omega_x - \operatorname{tg} \psi_0 \Delta \omega_y;$$

$$\frac{d\Delta \varphi}{dt} = \sec \psi_0 \Delta \omega_y.$$

(380)

-325-

The increments of forces and moments in these equations depend, among other things, on change in the rate of travel ΔV.

Nonlinearity cannot be avoided in these equations (in the given case of the products of the variables). Thus, the problems related to consideration of the influence of change of rate of travel on the parameters of lateral motion must be solved in nonlinear form.

If we use the assumption that the initial mode is travel without roll and drift, then

$$\beta_0 = \theta_0 = V_{z_0} = \omega_{x_0} = \omega_{y_0} = 0.$$

In this case

$$\Delta V_z = V_0 \Delta \beta;$$
$$\Delta V_x = \Delta V \qquad \qquad (381)$$

and the second term in the left-hand side of the first equation of (380) is equal to zero. In this case the perturbations acting on the longitudinal plane of symmetry of the ACV cannot be reduced to the appearance of lateral forces and moments, and therefore the increments of lateral forces and moments are practically independent of perturbation of the kinematic parameters of longitudinal motion (in particular, of ΔV). For convenience we will omit the symbol Δ (with the exception of ΔV). Then, considering the expression $\omega = \bar{\omega}(V/L)$, equation system (380) can be converted to the following form:

$$\frac{d\Delta V}{dt} = n_{11}\beta + n_{15}\delta p + n_{16}\Delta V + n_{17}\delta\Lambda;$$

$$\frac{d\beta}{dt} = n_{31}\beta + n_{32}\bar{\omega}_y + n_{33}\theta + n_{34}\bar{\omega}_x + n_{35}\delta p;$$

$$\frac{d\bar{\omega}_x}{dt} = n_{41}\beta + n_{42}\bar{\omega}_y + n_{43}\theta + n_{44}\bar{\omega}_x + n_{45}\delta p; \qquad (382)$$

$$\frac{d\bar{\omega}_y}{dt} = n_{51}\beta + n_{52}\bar{\omega}_y + n_{54}\bar{\omega}_x + n_{55}\delta p + n_{57}\delta\Lambda;$$

$$\frac{d\theta}{dt} n_{73}\bar{\omega}_y + n_{74}\bar{\omega}_x;$$

$$\frac{d\varphi}{dt} = n_{83}\bar{\omega}_y.$$

Here the first digits of the subscripts of the coefficients n correspond to the ordinal number of the equation in the equation system of spatial motion of ACVs.

-326-

The coefficients $\mathbf{1}_{ij}$ have the following values:

$$n_{11} = \frac{qS\mathfrak{E}}{m}\left(c_{x_\kappa}^\beta + c_{x_\mathbb{B}}^\beta + c_{x_{on}}^\beta\right);$$

$$n_{15} = \frac{qS\mathfrak{E}}{m}c_{x_p}^\delta;$$

$$n_{16} = \frac{\rho VS\mathfrak{E}}{m}\left[c_{x_\tau} + \dot{c}_{x_\kappa} + c_{x_\mathbb{B}} + c_{x_{on}} - \right.$$
$$\left. - \frac{Q}{VS\mathfrak{E}} - \frac{X_\mathbb{B}^V}{\rho VS\mathfrak{E}} - \frac{X_{r.o}^V}{\rho VS\mathfrak{E}}\right];$$

$$n_{17} = c_{x_\tau}^{\delta\Delta}\frac{qS\mathfrak{E}}{m};$$

$$n_{31} = \frac{qS_{60\mathbb{K}}}{mV}\left(c_{z_\kappa}^\beta + c_{z_\mathbb{B}}^\beta + c_{z_{on}}^\beta\right) - \frac{\rho Q}{m} - \frac{Z_\mathbb{B}}{mV} - \frac{Z_{r.o}}{mV};$$

$$n_{32} = \frac{qS_{60\kappa}}{mV}\left(c_{z_\kappa}^{\bar\omega_y} + c_{z_\mathbb{B}}^{\bar\omega_y} + c_{z_{on}}^{\bar\omega_y}\right) + \frac{\rho Q}{m}\cdot\frac{x_\mathbb{B}}{L} + n_{74};$$

$$n_{33} = \frac{G\left(1 + Z_{R_1}^\delta\right)}{mV};$$

$$n_{34} = -\frac{\rho Q}{m}\left[\frac{y_{R_1}}{L} - \frac{2H_1}{L}\right];$$

$$n_{35} = \frac{qS_{60\kappa}}{mV}c_{z_p}^\delta;$$

$$n_{41} = \frac{qS_{60\kappa}L^2}{J_xV}\left[m_{x_\kappa}^\beta + m_{x_\mathbb{B}}^\beta + m_{x_{on}}^\beta\right] - \frac{\rho QLy_{R_1}}{J_x} + \frac{M_{x_\mathbb{B}}L}{J_xV} + \frac{M_{x_{r.o}}L}{J_xV};$$

$$n_{42} = \frac{qS_{60\kappa}L^2}{J_xV}\left(m_{x_\kappa}^{\bar\omega_y} + m_{x_\mathbb{H}}^{\bar\omega_y} + m_{x_{on}}^{\bar\omega_y}\right) - \frac{\rho Qx_{R_1}y_{R_1}}{J_x};$$

$$n_{43} = \frac{GB_nL}{J_xV}\left[m_{x_n}^\beta + Z_{R_\mathbb{B}}^\beta\frac{y_g + h_{r.o} + h_\mathbb{B}}{B_n}\right];$$

$$n_{44} = \frac{GB_nL}{J_xV}m_{x_n}^{\bar\omega_x} - \frac{\rho Q}{J_x}\left\{2H_1\left(y_{R_1} - h_1\right) - \right.$$
$$\left. - \frac{1}{2\pi}\left[3L_nB_n + \left(\frac{L_n^2}{2} + B_n^2\right)K_2\right]\right\} - \frac{\rho Q}{J_x}\left(y_{R_1}^2 + z_{R_1}^2\right);$$

(383)

-327-

$$n_{45} = \frac{q S_{60\text{к}} L^{3}}{J_x V}\, \dot{m}_{x_{\text{р}}}^{\delta};$$

$$n_{51} = \frac{q S_{60\text{к}} L^{3}}{J_y V}\left(\dot{m}_{y_{\text{к}}}^{\beta} + \dot{m}_{y_{\text{н}}}^{\beta} + \dot{m}_{y_{\text{оп}}}^{\beta}\right) - \frac{\rho Q L x_{R_1}}{J_y} -$$

$$- \frac{R_3 x_3 L}{J_y V} - \frac{R_{\text{оп}} x_{\text{г. о}} L}{J_y V};$$

$$n_{52} = \frac{q S_{60\text{к}} L^{3}}{J_y V}\left(m_{y_{\text{к}}}^{\bar{\omega}_y} + m_{y_{\text{н}}}^{\bar{\omega}_y} + m_{y_{\text{оп}}}^{\bar{\omega}_y}\right) - \frac{\rho Q}{J_y}\left(x_{R_1}^{2} + z_{R_1}^{2}\right) -$$

$$- \frac{\rho Q}{J_y}\left[6 L_{\text{п}} B_{\text{п}} + \left(\frac{1}{2} K_1 + K_2\right) B_{\text{п}}^{2} + \left(\frac{1}{2} K_2 + K_1\right) L_{\text{п}}^{2}\right];$$ (383)

$$n_{54} = \frac{\rho Q}{J_y} x_{R_1} y_{R_1} - \frac{\rho Q}{J_y} 2 H_1 x_{R_1};$$

$$n_{55} = \frac{q S_{60\text{к}} L^{3}}{J_y V}\, m_{y_{\text{р}}}^{\delta};$$

$$n_{57} = m_{y_{\text{т}}}^{\delta A}\frac{q S_{60\text{к}} L^{3}}{J_y V};$$

$$n_{72} = -\operatorname{tg}\psi n_{74};$$

$$n_{74} = \frac{V}{L}; \quad n_{82} = \sec\psi n_{74}.$$

It follows from the expressions (382) and (383) that the left and right-hand sides of equations (382) are linear functions of perturbations; this means that functions (382) are linear differential equations of perturbed motion of the ACV with constant coefficients.

Equations of Perturbed Motion in Consideration of Wind Action

Let V be the velocity vector of motion of the center of gravity of the ACV;

V_B is the wind velocity vector.

The relative air velocity in relation to the ACV (velocity of the incident flow) is determined by vector V_1 (see Figure 158). We will define φ_B as the angle between vectors V and V_B; γ is the heading of the wind, measured, for instance, by a compass; φ_K is the compass heading of the ACV; β_B is the angle of incidence of the air flow (true angle of air drift); β_T is the increment of the air drift angle due to wind; β is the angle of drift in relation to the water surface.
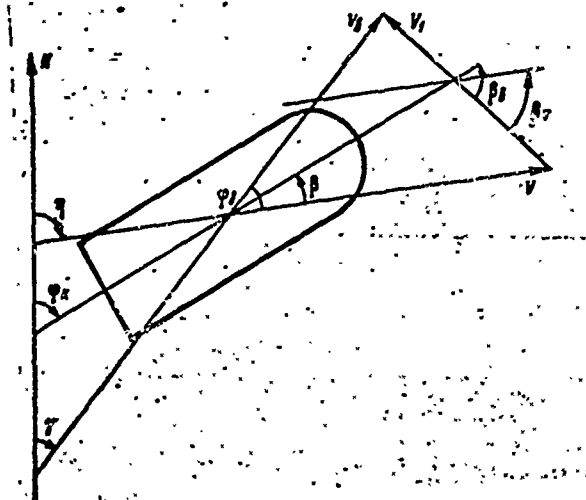
Figure 158. Summation of ACV Speed (V) and
Wind Speed V_B.

Then, on the basis of Figure 158, we obtain

$$\beta_{\mathrm{a}} = \beta + \beta_{\mathrm{T}};$$

$$\beta_{\mathrm{T}} = \arcsin\left[\frac{V_{\mathrm{B}}}{V_1}\sin\varphi_{\mathrm{a}}\right];$$

$$\varphi_{\mathrm{a}} = \beta + \varphi - \gamma; \tag{384}$$

$$V_1 = V\sqrt{1 + \left(\frac{V_{\mathrm{B}}}{V}\right)^2 - 2\frac{V_{\mathrm{B}}}{V}\cos\varphi_{\mathrm{a}}};$$

$$\beta_{\mathrm{T}} = \arcsin\left[\frac{V_{\mathrm{B}}\sin\varphi_{\mathrm{a}}}{V\sqrt{1 + \left(\frac{V_{\mathrm{B}}}{V}\right)^2 - 2\frac{V_{\mathrm{B}}}{V}\cos\varphi_{\mathrm{a}}}}\right];$$

$$\frac{d\beta_{\mathrm{T}}}{dt} = \frac{1}{\sqrt{1 - \left[\frac{V_{\mathrm{B}}\sin\varphi_{\mathrm{a}}}{\sqrt{1 + \left(\frac{V_{\mathrm{B}}}{V}\right)^2 - 2\frac{V_{\mathrm{B}}}{V}\cos\varphi_{\mathrm{a}}}}\right]}} \tag{385}$$

By substituting angle β in equations (380) by its value in expression
(384), we obtain for the equation of lateral forces

$$\frac{d\beta_{\mathrm{a}}}{dt} = \frac{\Delta Z}{mV} + \frac{V}{L}\bar{\omega}_y + \frac{d\beta_{\mathrm{T}}}{dt}. \tag{386}$$

-329-

The other equations in this case retain their prior form [see equations (380)].

Not all the lateral forces and moments are functions of air drift. Thus, the hydrodynamic forces and moments depend on the angle of drift relative to water β.

Recalling this circumstance, the equations of motion considering the action of the wind, can be reduced to the following form:

$$\frac{dV}{dt} = n_{11}\beta_{_\text{B}} + n_{15}\delta p + n_{16}\Delta V + n_{17}\delta\Lambda + \left(n_{11\;\text{B}} + n_{11\;\text{r.o}}\right)\beta_{_\text{T}};$$

$$\frac{d\beta_{_\text{B}}}{dt} = n_{31}\beta_{_\text{B}} + n_{32}\overline{\omega}_y + n_{33}\vartheta + n_{34}\overline{\omega}_x + n_{35}\delta p +$$

$$+ \frac{d\beta_{_\text{T}}}{dt} + \left(n_{31\;\text{B}} + n_{31\;\text{r.o}}\right)\beta_{_\text{T}};$$

$$\frac{d\overline{\omega}_x}{dt} = n_{41}\beta_{_\text{B}} + n_{42}\overline{\omega}_y + n_{43}\vartheta + n_{44}\overline{\omega}_x + n_{45}\delta p + \left(n_{41\;\text{B}} + n_{41\;\text{r.o}}\right)\beta_{_\text{T}}; \qquad (387)$$

$$\frac{d\overline{\omega}_y}{dt} = n_{51}\beta_{_\text{B}} + n_{52}\overline{\omega}_y + n_{54}\overline{\omega}_x + n_{55}\delta p + n_{57}\delta\Lambda +$$

$$+ \left(n_{51\;\text{B}} + n_{51\;\text{r.o}}\right)\beta_{_\text{T}};$$

$$\frac{d\vartheta}{dt} = n_{72}\overline{\omega}_y + n_{74}\overline{\omega}_x;$$

$$\frac{d\varphi}{dt} = n_{82}\overline{\omega}_y.$$

Equation system (387) is a system of differential equations of the induced perturbed motion of ACV. By equating δp, δΛ and β_T in equations (387) to zero we place the ACV in conditions under which no external perturbations act upon it and its motion is free perturbed motion. This occurs when pulse forces act upon the vessel in steady state motion. We will assume instantaneous initial perturbation Δβ in terms of angle of drift and instantaneous initial perturbation $\Delta\theta_0$ in terms of angle of roll to be the source of free perturbed motion. The appearance of $\Delta\theta_0$ causes angle of drift $\Delta\beta_{\theta_0} = \psi\Delta\theta_0$, which must be taken into account.

These initial perturbations can be regarded as the result of pulse actions at the initial moment of time t = 0

$$\Delta\beta_0\delta(t); \quad \Delta\beta_{\theta_0}\delta(t); \quad \Delta\theta_0\delta(t),$$

where δ(t) is the Dirac pulse function [35].

The action of perturbations in nonlinear plan can be analyzed by substituting in equations (387) the coefficients of these equations by nonlinearities. Analysis of the coefficient indicates that the category of forces and moments such as those that occur on the fan air intakes can be disregarded, since the coefficients n_{ijR} do not exceed 5% of the magnitude of the summary coefficients. The exceptions are the coefficients n_{34R} and n_{54R}. Coefficients n_{34} and n_{54} are themselves small, however, and they can also be ignored. We may also ignore the coefficient n_{32K} + + n_{32on} in the coefficient n_{32}.

In the category of hydrodynamic forces and moments, even when using an imperfect method of analysis, yields a coefficient that should not be ignored.

§25. Dynamic Stability of Lateral Motion of ACV

Transfer Functions of ACVs as Controlled Object in Lateral Perturbed Motion

We will examine a system of differential equations of lateral motion, discarding the first equation of (387). For the solution of these equations, we will use the methods of operational calculus. Applying the known laws of transition from the originals to the transforms, we write these equations in operator form

$$
\begin{aligned}
\beta_{\mathbf{n}}\,(p - n_{31}) - n_{32}\overline{\omega}_y - n_{33}\theta - n_{24}\overline{\omega}_x - n_{36}\delta p &= \\
&= \beta_\tau\,(p + n_{31\,r}) + \Delta\beta'_9; \\
\overline{\omega}_x\,(p - n_{44}) - n_{41}\beta_{\mathbf{n}} - n_{42}\overline{\omega}_y - n_{43}\theta - n_{45}\delta p &= n_{41\,r}\beta_\tau; \\
\overline{\omega}_y\,(p - n_{52}) - n_{51}\beta_{\mathbf{n}} - n_{54}\overline{\omega}_x - n_{55}\delta p - n_{57}\delta\Lambda &= n_{51\,r}\beta_\tau; \\
p\theta - n_{72}\overline{\omega}_y - n_{74}\overline{\omega}_x &= \Delta\theta_0; \\
p\varphi - n_{82}\overline{\omega}_y &= 0,
\end{aligned}
\tag{388}
$$

where p is a parameter of the Laplace transform.

The unknowns in these equations are the following transforms of the functions:

-331-

$$\beta_a(p) = L[\Delta\beta_a(t)];$$
$$\bar{\omega}_y(p) = L[\Delta\bar{\omega}_y(t)];$$
$$\varphi(p) = L[\Delta\varphi(t)];$$
$$\delta\Lambda(p) = L[\Delta\delta\Lambda(t)];$$
$$\bar{\omega}_x(p) = L[\Delta\bar{\omega}_x(t)];$$
$$\theta(p) = L[\Delta\theta(t)];$$
$$\delta p(p) = L[\Delta\delta p(t)],$$

(389)

where L [y(t)] is the integral Laplace transform.

Written in the right-hand side of equation (388) are the transforms
of perturbations, their derivatives and initial perturbations $\Delta\beta_0'$
= $\Delta\beta_0$ + $\Delta\beta_{\theta_0}$ and $\Delta\theta_0$, introduced with the aid of the Dirac pulse function

$\delta(t)$, the transform of which [35] is L [$\delta(t)$] = 1.

Therefore, the right-hand sides of equations (388) can also be
regarded as transforms. From these equations we will exclude the unknowns
$\bar{\omega}_x$ and $\bar{\omega}_y$.

After the corresponding transformations (considering expression
$\beta = \beta_B - \beta_T$) we obtain

$$\beta_a[p - n_{31}] + p\varphi\left[\frac{n_{34}n_{72}}{n_{82}n_{74}} - \frac{n_{32}}{n_{82}}\right] - \theta\left[n_{33} + \frac{n_{34}}{n_{74}}p\right] =$$

$$= n_{36}\delta p + \beta_T[n_{31\,r} + p] - \Delta\theta\frac{n_{34}}{n_{74}} + \Delta\beta_0';$$

(390)

$$-\beta_a n_{41} + p\varphi\left[\left(\frac{n_{44}n_{72}}{n_{82}n_{74}} - \frac{n_{42}}{n_{82}}\right) - p\frac{n_{72}}{n_{82}n_{74}}\right] +$$

$$+ \theta\left[-n_{43} - \frac{n_{44}}{n_{74}}p + \frac{p^2}{n_{74}}\right] = \delta p n_{45} + \beta_T n_{41\,r} +$$

$$+ \Delta\theta_0\left[\frac{p}{n_{74}} - \frac{n_{44}}{n_{74}}\right];$$

$$-n_{51}\beta_a + p\varphi\left[\left(\frac{n_{72}n_{54}}{n_{82}n_{74}} - \frac{n_{52}}{n_{82}}\right) + \frac{p}{n_{82}}\right] - p\theta\frac{n_{54}}{n_{74}} =$$

$$= n_{56}\delta p + n_{57}\delta\Lambda + \beta_T n_{51\,r} - \Delta\theta_0\frac{n_{54}}{n_{74}}.$$

-332-

Moreover, we will introduce the definitions

$$\frac{n_{34}n_{72}}{n_{82}n_{74}} - \frac{n_{35}}{n_{82}} = m_{32};$$

$$\frac{n_{34}}{n_{74}} = m_{33};$$

$$\frac{n_{34}n_{72}}{n_{82}n_{74}} - \frac{n_{42}}{n_{82}} = m_{42};$$

$$\frac{n_{44}}{n_{74}} = m_{43}; \tag{391}$$

$$\frac{n_{72}n_{54}}{n_{82}n_{74}} - \frac{n_{52}}{n_{82}} = m_{52};$$

$$\frac{n_{54}}{n_{74}} = m_{53}.$$

Then equation system (390) becomes:

$$\beta_a [p - n_{31}] + p\varphi [m_{32}] - \theta [n_{33} + m_{33}p] = Z(p);$$

$$\beta_a [-n_{41}] + p\varphi \left[m_{42} - \frac{n_{72}}{n_{82}n_{74}} p \right] + \theta \left[-n_{43} - pm_{43} + \frac{p^3}{n_{74}} \right] = M_x(p); \tag{392}$$

$$\beta_a [-n_{51}] + p\varphi \left[m_{52} + \frac{p}{n_{82}} \right] - \theta [m_{53}p] = M_y(p).$$

The right-hand sides of equation (392) are represented as the sums

$$Z(p) = Z_0(p) + Z'(p) \, p; \tag{393}$$

$$M_x(p) = M_{x_0}(p) + M'_x(p) \, p;$$

$$M_y(p) = M_{y_0}(p) + M'_y(p) \, p,$$

where

$$Z_0(p) = n_{35}\dot{\partial}p + \beta_r n_{31\,r} - \Delta\theta_0 m_{33} + \Delta\beta'_0;$$

$$Z'(p) = \beta_r;$$

$$M_{x_0}(p) = n_{45}\dot{\partial}p + \beta_r n_{41\,r} - \Delta\theta_0 m_{43} + \Delta\beta'_0; \tag{394}$$

$$M'_x(p) = \frac{\Delta\theta_0}{n_{74}};$$

$$M_{y_0}(p) = n_{55}\dot{\partial}p + n_{57}\dot{\partial}\Lambda + \beta_x n_{51\,r} - \Delta\theta_0 m_{53};$$

$$M'_y(p) = 0.$$

In terms of unknowns β, θ and φ these equations represent a system of the fourth order.

-333-

The complete solution of equation system (392) appears as follows:

$$\beta(p) = \frac{\Delta_\beta}{\Delta};$$

$$\theta(p) = \frac{\Delta_\theta}{\Delta};$$

$$p\varphi(p) = \frac{\Delta_{p\varphi}}{\Delta}.$$

(395)

where Δ is the determinant of system (392) and $\Delta\beta$, $\Delta\theta$ and $\Delta p\varphi$ are the partial determinants.

The determinant of system (392) is

$$\Delta = \begin{vmatrix} [p-n_{31}][m_{32}] - [pm_{33} + n_{33}] \\ [-n_{41}]\left[m_{42} - p\frac{n_{72}}{n_{72}n_{74}}\right]\left[\frac{p^2}{n_{74}} - n_{43} - m_{43}p\right] \\ [-n_{51}]\left[\frac{p}{n_{52}} + m_{53}\right][-m_{53}p] \end{vmatrix}$$

(396)

By expanding the determinant, we obtain its expanded expression in the following form:

$$\Delta = Ap^4 + Bp^3 + Cp^2 + Dp + E,$$

(397)

where

$$A = \frac{1}{n_{74}n_{52}};$$

$$B = -\frac{n_{51}}{n_{74}n_{52}} - \frac{n_{43}}{n_{52}} + \frac{m_{53}}{n_{74}};$$

$$C = \frac{m_{43}n_{51} - n_{43}}{n_{52}} + \frac{n_{51}m_{32} - n_{31}m_{52}}{n_{74}} - m_{43}m_{53};$$

(398)

$$D = \frac{n_{31}n_{43} - n_{33}n_{41}}{n_{52}} + m_{52}(m_{43}n_{31} - n_{43}) - m_{32}m_{43}n_{51};$$

$$E = n_{43}(n_{31}m_{52} - n_{51}m_{32}) + n_{33}(n_{51}m_{42} - n_{41}m_{52}).$$

The expressions for the partial determinants, which are the numerators of transforms $\beta(p)$, $p\varphi(p)$ and $\theta(p)$ [see functions (395)] are obtained on the basis of the determinant of system (396) by substituting the corresponding columns with the right-hand parts of equations (392).

-334-

Considering expressions (393) and (394), we can find the values of the partial determinants, given below. Determinant Δ_β is found from the following expression:

$$\Delta_\beta = r_{43} p^4 + r_{33} p^3 + r_{23} p^2 + r_{13} p + r_{03};$$ (399)

where

$$r_{43} = \frac{Z'(p)}{n_{74} n_{82}};$$

$$r_{33} = \frac{Z_0(p)}{n_{74} n_{82}} + Z'(p) m_1;$$ (400)

$$r_{23} = Z_0(p) m_1 + Z'(p) m_3 + M'_x(p) m_4 + M_{y_0}(p) m_2;$$
$$r_{13} = Z_0(p) m_3 - Z'(p) n_{43} m_{52} + M_{x_0}(p) m_4 + M_{y_0}(p) m_5 +$$
$$+ M'_x(p) m_{52} n_{33};$$
$$r_{03} = M_{x_0}(p) n_{33} m_{52} + M_{y_0}(p) m_6 - Z_0(p) n_{43} m_{52}.$$

In these expressions

$$m_1 = \frac{m_{52}}{n_{74}} - \frac{m_{43}}{n_{82}} - \frac{n_{73} m_{52}}{n_{74} n_{82}};$$

$$m_2 = \frac{n_{73} m_{33}}{n_{74} n_{83}} - \frac{m_{33}}{n_{74}};$$

$$m_3 = m_{42} m_{53} - m_{43} m_{52} - \frac{n_{43}}{n_{83}};$$

$$m_4 = \frac{n_{33}}{n_{83}} + m_{33} m_{52} - m_{53} m_{32};$$ (401)

$$m_5 = \frac{n_{73} n_{33}}{n_{74} n_{83}} + m_{43} m_{33} - m_{33} m_{43};$$

$$m_6 = m_{32} n_{43} - n_{33} m_{42}.$$

To determine Δ_θ we obtain the expression

$$\Delta_\theta = r_{31} p^3 + r_{21} p^2 + r_{11} p + r_{01},$$ (402)

where

$$r_{39} = M'_x(p)\frac{1}{n_{83}};$$

$$r_{29} = Z'(p)\,n_2 + M_{x_0}(p)\frac{1}{n_{83}} + M'_x(p)\,n_3 + M_{y_0}(p)\frac{n_{72}}{n_{74}n_{83}};$$

$$r_{19} = Z_0(p)\,n_2 + Z'(p)\,n_5 + M_{x_0}(p)\,n_3 + M'_x(p)\,n_6 + M_{y_0}(p)\,n_4; \tag{403}$$

$$r_{09} = Z_0(p)\,n_5 + M_{x_0}(p)\,n_6 + M_{y_0}(p)\,n_7.$$

In these expressions

$$n_2 = \frac{n_{72}}{n_{74}}\frac{n_{51}}{n_{82}} + \frac{n_{41}}{n_{82}};$$

$$n_3 = m_{52} - \frac{n_{31}}{n_{82}}; \tag{404}$$

$$n_4 = -m_{42} - \frac{n_{72}n_{31}}{n_{74}n_{82}};$$

$$n_5 = n_{41}m_{52} - m_{42}n_{51};$$

$$n_6 = m_{32}n_{51} - n_{31}m_{52};$$

$$n_7 = n_{31}m_{42} - m_{32}n_{41}.$$

For determinant $\Delta_{p\varphi}$ we find

$$\Delta_{p\varphi} = r_{3p\varphi}p^3 + r_{2p\varphi}p^2 + r_{1p\varphi}p + r_{0p\varphi}, \tag{405}$$

where

$$r_{3p\varphi} = Z'(p)\,q_1 + M'_x(p)\,q_2 + M_{y_0}(p)\frac{1}{n_{74}};$$

$$r_{2p\varphi} = Z_0(p)\,q_1 + Z'(p)\,q_4 + M_{x_0}(p)\,q_2 + M'_x(p)\,q_5 + M_{y_0}(p)\,q_3;$$

$$r_{1p\varphi} = Z_0(p)\,q_4 - Z'(p)\,n_{51}n_{43} + M_{x_0}(p)\,q_5 + M'_x(p)\,n_{33}n_{51} + \tag{406}$$
$$+ M_{y_0}(p)\,q_6;$$

$$r_{0p\varphi} = -Z_0(p)\,n_{51}n_{43} + M_{x_0}(p)\,n_{33}n_{51} + M_{y_0}(p)\,q_7.$$

In these expressions

$$q_1 = \frac{n_{51}}{n_{74}};$$

$$q_2 = m_{53};$$

$$q_3 = -\frac{n_{51}}{n_{74}} - m_{33}; \tag{407}$$

$$q_4 = m_{53}n_{41} - m_{43}n_{51};$$

$$q_5 = m_{33}n_{51} - m_{53}n_{31};$$

$$q_6 = n_{31}m_{43} - n_{43} - m_{33}n_{41};$$

$$q_7 = n_{31}n_{43} - n_{33}n_{41}.$$

Thus, the transforms of the desired kinematic parameters of lateral perturbed motion acquire the form of rational expressions

$$\Phi = \frac{r_4 p^4 + r_3 p^3 + r_2 p^2 + r_1 p + r_0}{A p^4 + B p^3 + C p^2 + D p + E}. \tag{408}$$

To facilitate the transition from such complex transforms to the originals we will expand this fraction into the sum of two simpler transforms:

$$\Phi = \frac{K_0 + K_1 p + K_2 p^2}{p^2 + 2\bar{h}_\kappa p + \bar{\omega}_\kappa^2} + \frac{D_0 + D_1 p}{p^2 + 2\bar{h}_\partial p + \bar{\omega}_\partial^2}. \tag{409}$$

The coefficients $2\bar{h}_K$, $\bar{\omega}_K^2$, $2\bar{h}_\partial$ $\bar{\omega}_\partial^2$ are expressed through the roots of the characteristic equation of system (392) as follows:

$$
\begin{aligned}
2\bar{h}_\kappa &= -(p_1 + p_2); \\
2\bar{h}_\partial &= -(p_3 + p_4); \\
\bar{\omega}_\kappa^2 &= p_1 p_2; \\
\bar{\omega}_\partial^2 &= p_3 p_4.
\end{aligned} \tag{410}
$$

Coefficients K_0, K_1, K_2, D_0, D_1 are found from the equation system obtained by equating (408) and (409). If we write the conditions of equality of the coefficients for identical powers of p in expressions (408) and (409), this system will acquire the form

$$
\begin{aligned}
K_2 &= \frac{r_4}{A}; \\
K_1 + D_1 &= \frac{r_3}{A} - \frac{r_4}{A} 2\bar{h}_\partial; \\
2\bar{h}_\partial K_1 + K_0 + D_0 + 2\bar{h}_\kappa D_1 &= \frac{r_2}{A} - \frac{r_4}{A}\bar{\omega}_\partial^2; \\
2\bar{h}_\partial K_0 + \bar{\omega}_\partial^2 K_1 + 2\bar{h}_\kappa D_0 + \bar{\omega}_\kappa^2 D_1 &= \frac{r_1}{A}; \\
\bar{\omega}_\partial^2 K_0 + \bar{\omega}_\kappa^2 D_0 &= \frac{r_0}{A},
\end{aligned} \tag{411}
$$

Above, we derived the transforms of the desired kinematic parameters of motion (output values) in the general case when perturbations δp and β_T occurred simultaneously and when initial perturbations $\Delta\beta_0'$ and $\Delta\theta_0$ differed from zero. Perturbed motion that occurs as a result of any one perturbation is an important special case in practice. To each form of perturbation (input value) and each output value correspond certain

-337-

expressions of the transfer function. The ratio of the transform of the output value to the transform of the input value at zero initial conditions is defined as the transfer function and it is denoted through $W(p)$.

The expressions of the transfer functions can be found if we retain any one perturbation in the general expressions of the transforms (399), (402) and (405), and then separate the expression obtained into the transform of this perturbation.

The transfer functions are of the following general form:

$$W(p)_i = \frac{L_i}{\Delta}, \tag{412}$$

where

$$i = \beta, \ \theta, \ p\varphi.$$

Specific values of the coefficients of the polynomials in the numerator of (412) are listed in Tables 14-16 for various perturbations.

The coefficients of the denominator in function (412) are determined through equations (398). The transforms of the kinematic values expressed through the transfer functions are found using the equation

$$y(p) = W(p) x(p),$$

where $x(p)$ symbolizes the perturbation transform in general form.

The presence of the expressions for the transfer functions makes it possible to solve a broad class of problems of ACV dynamics. In order, however, to use the transfer functions it is essential to find the roots of the characteristic equation of system (392). An example of the use of the transfer functions will be illustrated below.

Analysis of Dynamic Stability and Character of Natural Lateral Perturbed Motion of ACV

A. M. Lyapunov demonstrated [33], [55], that analysis of the problem of stability of motion in the first approximation, i.e., on the basis of the solution of a linearized differential equation system relative to variations, is permissible only under the condition that not one of the roots of the characteristic equation of the system be equal to zero or, if the roots are complex, not one of the roots have a real part equal to zero. Otherwise, in order to judge the stability of motion

it is essential to analyze a system of differential equations with higher powers of variations.

In solving the problem of stability of perturbed motion, and also of the suitability of a linearized system of differential equations for this purpose, it is possible also not to determine the roots of the characteristic equation, but to use the Raus-Gurvits criteria. In order that motion be dynamically stable it is essential and sufficient to have negative real parts in all roots of the characteristic equation.

The characteristic equation of lateral perturbed motion of ACV $\Delta = 0$ is an equation of the fourth power of the form

$$p^4 + a_3 p^3 + a_2 p^2 + a_1 p + a_0 = 0, \tag{413}$$

where

$$a_2 = \frac{B}{A} = [-n_{74}m_{43} - m_{53}n_{72} + n_{82}m_{52} - n_{31}];$$

$$a_3 = \frac{C}{A} [n_{72}(-n_{51}m_{33} - m_{53}n_{31}) + n_{74}(m_{43}n_{31} - n_{43} - m_{33}n_{41}) +$$
$$+ n_{82}(n_{51}m_{32} - n_{31}m_{52}) + n_{74}n_{82}m_{43}(-m_{52});$$

$$a_1 = \frac{D}{A} = [n_{74}(n_{31}n_{43} - n_{33}n_{41}) + n_{74}n_{82}m_{52}(m_{43}n_{31} - n_{43} - m_{33}n_{41}) + \tag{414}$$
$$+ n_{74}n_{82}m_{42}(n_{51}m_{33} - m_{53}n_{31}) + m_{52}n_{74}n_{82}(m_{53}n_{41} - m_{43}n_{51})];$$

$$a_0 = \frac{E}{A} [n_{74}n_{82}n_{43}(n_{31}m_{52} - n_{51}m_{32}) + n_{74}n_{82}n_{33}(n_{51}m_{42} - n_{41}m_{52})],$$

In the case of free perturbed motion

$$\beta_T = \delta p = \delta \Lambda = 0; \tag{415}$$
$$\beta_\lambda = \beta.$$

In addition the coefficients are

$$n_{34} = n_{54} = 0.$$

Under these conditions, coefficients (391) acquire the following values:

$$m_{32} = \frac{n_{32}}{n_{52}};$$

$$m_{33} = 0; \tag{416}$$

$$m_{42} = \frac{n_{44}n_{72}}{n_{42}n_{74}} - \frac{n_{43}}{n_{82}};$$

-339-

$$m_{43} = \frac{n_{44}}{n_{74}};$$

$$m_{52} = -\frac{n_{53}}{n_{52}};$$

$$m_{53} = 0, \tag{416}$$

and coefficients (414) of characteristic equation (413) will have the following form [in consideration of the values of (416)]:

$$a_3 = -n_{52} - n_{44} - n_{31};$$

$$a_2 = n_{44}n_{31} - n_{74}n_{74} - n_{51}n_{52} + n_{31}n_{52} + n_{52}n_{44};$$

$$a_1 = n_{74}n_{31}n_{43} - n_{74}n_{33}n_{41} - n_{52}n_{31}n_{44} + n_{74}n_{52}n_{43} + n_{33}n_{51}n_{44};$$

$$a_0 = -n_{74}n_{43}n_{31}n_{52} + n_{74}n_{43}n_{51}n_{32} + n_{33}n_{51}n_{44}n_{72} - $$
$$-n_{74}n_{33}n_{51}n_{42} + n_{74}n_{33}n_{41}n_{52}. \tag{417}$$

The approximate values of the coefficients of the characteristic equation are written as follows:

$$a'_3 = -n_{52} - n_{44} - n_{31} \quad \text{(in prior form)};$$

$$a'_2 \approx -n_{43}n_{74};$$

$$a'_1 = n_{74}n_{31}n_{43} - n_{74}n_{33}n_{41} + n_{74}n_{52}n_{43}. \tag{418}$$

In order that all roots of the characteristic equation have negative real parts it is necessary and sufficient to satisfy the following conditions [38], [55]:

$$a_0 > 0; \ a_1 > 0; \ a_2 > 0; \ a_3 > 0;$$

$$R = a_1 a_2 a_3 - a_3^2 a_0 - a_1^2 > 0; \tag{419}$$

$$a'_0 = -n_{74}n_{43}n_{31}n_{52} + n_{74}n_{43}n_{51}n_{32}.$$

Failure to satisfy the first conditions means aperiodic instability of the system, and failure to satisfy the last condition (plus sign of discriminate R) means oscillating instability of the system; furthermore, failure to satisfy any of the conditions may mean that one (or more) of the roots is equal to zero and has a real part equal to zero, and in this case it is essential to determine the roots of the characteristic equation.

Characteristic equation (413) for the ACV SKMR-1, for instance, has the   62]

$$p^4 + 0.0505p^3 + 2.857p^2 + 0.1175p + 0.0897 = 0. \tag{420}$$

-340-

TABLE 14. TRANSFER FUNCTION FOR ANGLE β

$$W_\beta = \frac{r_{4\beta}p^4 + r_{3\beta}p^3 + r_{2\beta}p^2 + r_{1\beta}p + r_{0\beta}}{Ap^4 + Bp^3 + Cp^2 + Dp + E}$$

After change of parameters

Coefficient	$\delta\rho$	$\delta\Lambda$	β_T	$\Delta\beta_\theta$	$\Delta\theta_\theta$
r_{43}	0	0	$\dfrac{1}{n_{74}n_{83}}$	0	0
r_{33}	$\dfrac{n_{33}}{n_{74}n_{83}}$	$n_{57}\dfrac{m_{33}}{n_{83}}$	$\dfrac{n_{31r}}{n_{74}n_{83}} + m_1$	$\dfrac{1}{n_{74}n_{83}}$	$\dfrac{1}{n_{74}n_{83}}$
r_{23}	$n_{23}m_1 + n_{43} \times \dfrac{m_{33}}{n_{83}} + n_{54}m_3$	$n_{57}m_3$	$n_{31r}m_1 + m_3 + n_{41r} \times \dfrac{m_{33}}{n_{83}} + n_{51r}m_3$	m_1	$(1-m_{33})\,m_1 - m_{43}\dfrac{m_{33}}{n_{83}} + \dfrac{m_4}{n_{74}} - m_{53}m_2$
r_{13}	$n_{33}m_3 + n_{43}m_4 + n_{54}m_5$	$n_{57}m_5$	$n_{31r}m_3 - n_{43}m_{33} + n_{41r}m_4 + n_{51r}m_5$	$m_3 + m_{54}m_5$	$(1-m_{33})\,m_3 - m_{43}m_4 + \dfrac{m_{33}n_{33}}{n_{74}} - m_{53}m_5$
r_{03}	$n_{43}n_{33}m_{83} + n_{54}m_5 - n_{53}n_{43}m_{83}$	$n_{57}m_5$	$n_{41r}n_{33}m_{83} + n_{51r}m_4 - n_{51r}n_{43}m_{83}$	$-n_{43}m_{33}$	$-m_{43}n_{33}m_{83} - m_{53}m_4 - (1-m_{33}) \times n_{43}m_{33}$

-341-

TABLE 15. TRANSFER FUNCTION FOR ROLL ANGLE θ

$$W_\theta = \frac{r_{3\theta}p^3 + r_{2\theta}p^2 + r_{1\theta}p + r_{0\theta}}{Ap^4 + Bp^3 + Cp^2 + Dp + E}$$

Coefficients After change of parameters

Coefficients	δp	$\delta\Lambda$	β_r	$\Delta\beta_\theta$	$\Delta\theta_\theta$
$r_{3\theta}$	0	0	0	0	$\dfrac{1}{n_{63}n_{74}}$
$r_{2\theta}$	$\dfrac{n_{43}}{n_{83}} + \dfrac{n_{53}n_{72}}{n_{74}n_{83}}$	$n_{53}m_8$	$n_3 + \dfrac{n_{41r}}{n_{83}} + \dfrac{n_{31r}n_{72}}{n_{74}n_{83}}$	0	$\dfrac{m_{43}}{n_{83}} + \dfrac{n_3}{n_{74}} - \dfrac{n_{12}m_{83}}{n_{74}n_{83}}$
$r_{1\theta}$	$n_{32}n_3 + n_{43}n_3 + n_{53}n_4$	$n_{53}m_6$	$n_{31r}n_4 + n_5 + n_{41r}n_3 + n_{51r}n_4$	n_3	$(1-m_{33})n_3 + \dfrac{n_6}{n_{74}} - m_{43}n_3 - m_{53}n_4$
$r_{0\theta}$	$n_{53}n_5 + n_{43}n_6 + n_{53}n_7$	$n_{53}n_7$	$n_{31r}n_5 + n_{41r}n_6 + n_{51r}n_7$	n_6	$(1-m_{33})n_6 - n_{43}n_6 - m_{53}n_7$

TABLE 16. TRANSFER FUNCTION FOR ANGULAR VELOCITY OF YAW φ

$$W_{p\varphi} = \frac{r_{3p\varphi}p^3 + r_{2p\varphi}p^2 + r_{1p\varphi}p + r_{0p\varphi}}{Ap^4 + Bp^3 + Cp^2 + Dp + E}$$

After change of parameters

Coefficients

	δp	$\delta\Lambda$	$\delta\tau$	$\Delta\vartheta_0$	$\Delta 0_0$
$r_{3p\varphi}$	$\dfrac{n_{35}}{n_{74}}$	$\dfrac{n_{57}}{n_{74}}$	$q_1 + \dfrac{n_{51r}}{n_{74}}$	0	$\dfrac{q_3}{n_{74}} - \dfrac{m_{33}}{n_{74}}$
$r_{2p\varphi}$	$n_{35}q_1 + n_{45}q_3 + n_{55}q_3$	$n_{57}q_3$	$n_{51r}q_1 + q_6 + n_{51r}q_3$	q_1	$(1 - m_{33})\,q_1 + \dfrac{q_3}{n_{74}} - m_{45}q_3 - m_{55}q_3$
$r_{1p\varphi}$	$n_{35}q_6 + n_{45}q_5 + n_{55}q_6$	$n_{57}q_6$	$n_{51r}q_6 - n_{51}n_{43} + n_{51r}q_5 + n_{51r}q_6$	q_6	$(1 - m_{33})\,q_6 + \dfrac{n_{33}n_{51}}{n_{74}} - m_{45}q_5 - m_{55}q_6$
$r_{0p\varphi}$	$-n_{35}n_{12}n_{43} + n_{45}n_{35}n_{11} + n_{55}q_7$	$n_{57}q_7$	$-n_{51r}n_{35}n_{53} + n_{51r}n_{35}n_{51} + n_{51r}q_7$	$-n_{51}n_{43}$	$(m_{33} - 1)\,n_{51}n_{43} - m_{45}m_{45}n_{51} - m_{55}q_7$

-343-

As seen from expression (420) all coefficients of the characteristic equation are positive. Furthermore, the Raus-discriminant

$$R = a_1 a_2 a_3 - a_3^2 a_0 - a_1^2$$

is also positive. This means that free perturbed motion of the ACV SKMR-1 is dynamically stable in relation to perturbations of the parameters β, θ and pφ.

To find the roots of the characteristic equation (413) we may use the method that is suitable in those cases when the roots of equation (413) are separated into two groups which differ substantially in terms of absolute value.[35], as is the case during lateral perturbed motion of ACV.

The solution of equation (420) gives the following values of the roots:

$$p_1 = +0{,}0208 + 0{,}1772i; \quad p_2 = -0{,}0208 - 0{,}1772i;$$
$$p_3 = +0{,}0045 + 1{,}681i; \quad p_4 = -0{,}0045 - 1{,}681i.$$

The roots of the characteristic equation are complex, and each pair is mutually conjugate. This means the following character of free perturbed motion: two attenuating oscillatory processes. Each pair of roots characterizes a certain oscillatory process, a certain form of motion, with its own frequency and degree of attenuation of oscillations.

If we denote a complex pair of roots as follows:

$$p = -\bar{h} \pm i\bar{\omega}^*, \tag{421}$$

then period T of oscillations is determined by the expression

$$T = \frac{2\pi}{\omega^*} \cdot t^* \text{ (sec)},$$

where

$$t^* = \frac{L}{V} \text{ (sec)}, \quad \bar{\omega}^* = \frac{L}{V} \omega^*.$$

-344-

The time during which the perturbation is cut in half is given by the expression

$$t_{yм} = \frac{\ln 2}{|\bar{h}|} t^* \text{ (sec)}.$$

The cycle of oscillations during which the perturbed value is cut in half is given by the equation

$$N_{yм} = \frac{t_{yм}}{t^* T} = 0{,}110 \frac{\bar{\omega}^*}{|\bar{h}|}.$$

For an approximate evaluation of the influence of dynamic coefficients on the roots of the characteristic equation we will simplify equation (413), omitting the first two terms. We will also use the approximate values of the coefficients according to the expressions (418).

Then one pair of roots will be determined by the equation

$$p^2 + \frac{a_1'}{a_2'} p + \frac{a_0'}{a_2'} = 0.$$

Hence

(422)

$$p_{1,2} = -\frac{1}{2} \frac{a_1'}{a_2'} \pm \sqrt{\frac{1}{4} \left(\frac{a_1'}{a_2'}\right)^2 - \frac{a_0'}{a_2'}},$$

but

$$4 \frac{a_0'}{a_2'} \gg \left(\frac{a_1'}{a_2'}\right)^2,$$

Therefore the first term of the radicand in equation (422) can be discarded. On the other hand, the value $a_1'/a_2' = -n_{31} + n_{33}/n_{43} (n_{41} - n_{52})$,

the product of coefficients $n_{33}/n_{43}\, n_{41}$ is comparatively small so that it can also be discarded. Then

$$\frac{a_1'}{a_2'} \doteq -n_{31}' - n_{32}',$$

-345-

and the first pair of roots will be given as follows:

$$p'_{1,2} = \frac{1}{2}[n_{31} + n_{32}] \pm i\sqrt{n_{31}n_{32} - n_{51}n_{33}}.$$ (423)

The equation for the approximate determination of roots $p_{1.2}$ gives an average of about 7% error, although it gives a graphic representation of the character of the oscillatory process it reflects. As shown by the set of dynamic coefficients in expression (423), roots $p_{1.2}$ reflect oscillations that depend on the dynamic coefficients characterizing yaw and drift, not related to oscillations in terms of roll. These oscillations are analogous to longitudinal short-period oscillations on aircraft, with the difference, however, that both the frequency of the oscillations and the degree of their attenuation are considerably smaller than for an aircraft.

Thus the values that typify the longitudinal short-period oscillations of an aircraft [59] are

$$T = 4{,}37 \text{ sec}; \quad t_{y_{H}} = 0{,}624 \text{ sec};$$
$$N_{y_{H}} = 0{,}143 \text{ } 1/\text{sec};$$
$$\bar{h} = -1{,}1' \div -2{,}2;$$
$$\bar{\omega}* = (1{,}5 \div 4{,}5)i.$$

The second pair of roots is found by expanding the characteristic polynomial for equation (413) into two quadratic expressions

$$p^4 + a'_3 p^3 + a'_2 p^2 + a'_1 p + a'_0 = (p^2 + \lambda_1 p + \mu_1)(p^2 + \lambda_2 p + \mu_2).$$ (424)

By equating the coefficients for p we obtain

$$a'_3 = \lambda_1 + \lambda_2;$$
$$a'_2 = \mu_1 + \lambda_1\lambda_2 + \mu_2;$$
$$a'_1 = \lambda_2\mu_1 + \lambda_1\mu_2;$$
$$a'_0 = \mu_1\mu_2.$$ (425)

-346-

Here $\lambda_1 = \dfrac{a_1}{a_2}$, $\mu_1 = \dfrac{a_0}{a_2}$ are from equations (425). We obtain from expressions (418) and (425)

$$\lambda_2 = a_2' - \lambda_1 = -n_{44}; \quad a_2' \gg \mu_1 + \lambda_1 \lambda_2.$$

Therefore we may assume [see function (425)]

$$\mu_2 \approx a_2' = -n_{43} n_{74}.$$

We now write

$$p^2 + \lambda_2 p + \mu_2 = 0, \tag{426}$$

Hence

$$p_{3,4} = -\frac{\lambda_2}{2} \pm \sqrt{\frac{\lambda_2^2}{4} - \mu_2}. \tag{'27}$$

Since $\mu_2 \gg \dfrac{\lambda_2^2}{4}$, we obtain

$$p'_{3,4} = \frac{n_{44}}{2} \pm i \sqrt{-n_{43} n_{74}}. \tag{428}$$

The set of dynamic coefficients in function (428) shows that this pair of roots characterizes its oscillations that depend on dynamic coefficients which determine roll and are not related to yaw. In lateral motion of an aircraft the combined pair of roots characterizes lateral oscillations or the "Dutch step," which does not occur in ACV motion.

The analogous result was obtained in [62] from analysis of the lateral motion of ACVs without flexible skirts over a solid screen.

For a more detailed analysis of natural perturbed motion we will determine what effect pulse perturbation of drift angle $\Delta\beta_0$ has on the kinematic parameters of lateral motion.

The sequence of calculations is shown for the example of the calculation of the transition process with respect to angle of drift β:

-347-

1. Using Tables 14-16, we find the values of the coefficients r_i of the transfer function W_β during perturbation $\Delta\beta_0$, which with consideration of functions (391) and (416) take on the following values:

$$r_{33} = \frac{1}{n_{74}n_{83}}$$

$$r_{23} = \frac{n_{83} + n_{44}}{n_{83}n_{74}};$$

$$r_{13} = \frac{n_{44}}{n_{74}} \cdot \frac{n_{83}}{n_{81}} - \frac{n_{43}}{n_{83}};$$

$$r_{03} = n_{43}\frac{n_{83}}{n_{83}}.$$

(429)

2. Further, we determine the roots of the characteristic equation (413) or, for example, their approximate values according to expressions (423) and (428).

3. Then by using equations (410) we determine the values of $2\bar{h}_k$, $\bar{\omega}_k^2$, $2\bar{h}_\partial$, $\bar{\omega}_\partial^2$.

4. From equations (411) we determine the coefficients D_0, D_1, K_0, K_1, K_2.

5. Using expression (409) we determine the transfer function of the drift angle during perturbation $\Delta\beta_0$

$$\frac{\beta(p)}{\Delta\beta_0} = W_\beta.$$

(430)

6. Using a glossary of transforms, we convert from the transforms to the originals:

$$\frac{\Delta\beta}{\Delta\beta_0} = f(t).$$

The results of typical calculation of the natural perturbed motion of ACVs with respect to drift angle β during pul 'perturbation of drift angle $\Delta\beta_0$ with consideration of the exact and app ximate roots of the characteristic equation are presented in Figure 159. We see from this figure that in examining the period of time sufficient for the completion of the transition processes the approximate equations yield comparatively small errors.

-348-

Figure 159. Natural Perturbed Motion of ACV with
Respect to Angle of Drift During Pulse Perturbation
of Drift Angle $\Delta\beta_0$. I, Short-period motion; II,
Long period motion; O, Exact formula. X, Approximate
formula.

The results of analogous calculations for perturbation of angle
of roll and angular velocity of yaw are presented in Figure 160 and
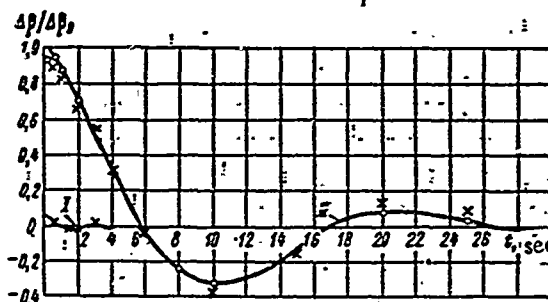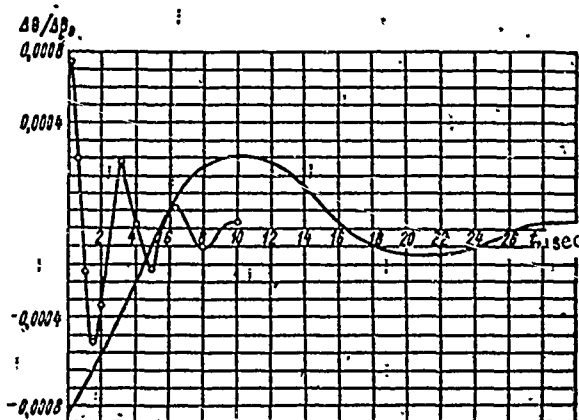161.

Figure 160. Natural Perturbed Motion of ACV with
Respect to Angle of Roll During Pulsed Perturbation
of Drift Angle $\Delta\beta_0$. -O-, Short period motion;
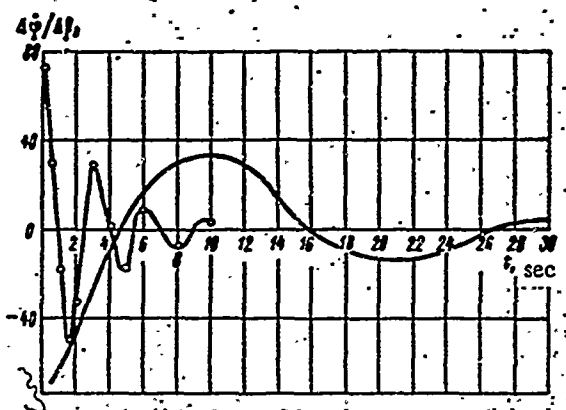——, Long period motion.

Figure 161. Natural Perturbed Motion of AC'/ with
Respect to Angular Velocity of Yaw During Pulsed
Perturbation of Drift Angle $\Delta\beta_0$. -0-, Short-period

motion; ———, Long-period motion.

As follows from examination of Figures 159 through 161, natural
perturbed motion with respect to each of the parameters of lateral
motion during perturbation of angle of drift $\Delta\beta_0$ represents a combina-

tion of two oscillatory processes that differ substantially from each
other with respect to period and time of attenuation of the oscillations.

By analogy with the terms used in aircraft dynamics these processes
can be called long-period and short-period processes. Thus, the first
term in equation (409) and in the equations derived from it expresses the
short-period motion and the second term, the long-period motion.

The denominators of the first and second terms in equation (409)
are the characteristic polynomials of short-period and long-period
motion, respectively. Equating it to zero and comparing with data in
Table 17 and equations (423) and (428), we obtain the roots in the
following form:

$$p_{1,2} = -\bar{h}_\delta \pm i \sqrt{\bar{\omega}_\delta^2 - \bar{h}_\delta^2};$$ (431)

$$p_{3,4} = -\bar{h}_\kappa \pm i \sqrt{\bar{\omega}_\kappa^2 - \bar{h}_\kappa^2}.$$ (432)

-350-

TABLE 17.   VALUES CHARACTERIZING SHORT-PERIOD AND LONG-PERIOD
FORMS OF MOTION OF SKMR-1.

Forms of motion	$\|\bar{h}\|$	$\bar{\omega}^\bullet$	$T = \dfrac{2\pi}{\bar{\omega}^\bullet}\,t^\circ \text{sec}$	$t_{y\text{и}} = \dfrac{0{,}69}{\|\bar{h}\|}\,t^\circ\text{sec}$	$N_{y\text{и}} = 0{,}110\,\dfrac{\bar{\omega}^\bullet}{\|\bar{h}\|}$ of oscillations
First $(p_{1,2})$	0,0208	0,093	35,4	17,4	0,49
Second $(p_{3,4})$	0,0045	0,882	3,7	80,5	21,6

Note: Commas indicate decimal points.

In equation (431) the value

$$\bar{\omega}_\partial = \omega_\partial \frac{L}{V} = \frac{\omega_\partial}{n_{74}}$$

(433)

is natural (dimensionless) frequency of long-periodic motion (in the absence of damping); it is expressed through the dynamic coefficients as follows:

$$\bar{\omega}_\partial \approx \sqrt{\frac{1}{4}\,(n_{31} + n_{52})^2 + (n_{31}n_{52} - n_{51}n_{32})}\,.$$

(434)

The value of equation

$$2\bar{h}_\partial = 2h_\partial \frac{L}{V} = \frac{2h_\partial}{n_{74}}\,,$$

(435)

is the coefficient of damping of long-period motion, and it can be expressed through the dynamic coefficients as follows:

$$\bar{h}_\partial \approx -\frac{1}{2}\,[n_{31} + n_{52}]\,,$$

(436)

for short-periodic oscillations we obtain

$$\bar{h}_\kappa = -\frac{1}{2}\,n_{44};$$

(437)

-351-

$$\bar{\omega}_{\kappa} = \sqrt{\frac{n_{44}^2}{4} - n_{43}n_{74}}. \qquad (438)$$

Comparing expressions (421), (431) and (432), we see that

$$\bar{\omega}_{\kappa}^{\bullet} = \sqrt{\bar{\omega}_{\kappa}^2 - \bar{h}_{\kappa}^2} \qquad (439)$$

$$\bar{\omega}_{\partial}^{\bullet} = \sqrt{\bar{\omega}_{\partial}^2 - \bar{h}_{\partial}^2}, \qquad (440)$$

where $\bar{\omega}_{k}^{\star}$, $\bar{\omega}_{\partial}^{\star}$ are the frequencies of oscillations in the transition process. They are lower than the frequencies of natural oscillations in the absence of damping.

With consideration of functions (439) and (440), the approximate expressions for the roots can be written as follows:

$$p_{1,2} = -\bar{h}_{\partial} \pm i\bar{\omega}_{\partial}^{\bullet}; \qquad (441)$$

$$p_{3,4} = -\bar{h}_{\kappa} \pm i\bar{\omega}_{\kappa}^{\bullet}. \qquad (442)$$

The expressions for the roots in this form were used in [62] for approximate analysis of the effect of the size and location of the tail assembly and nozzle width on the character of natural perturbed motion of ACV.

Figures 162 and 163 show, on the basis of calculations, how the elongation of the tail unit and location of the tail unit with respect to length, depending on the relative tail area, affect frequency $\bar{\omega}_{\partial}^{\star}$ and damping coefficient $\bar{h}_{\partial}$ of long-periodic oscillations of ACV SKMR-1.

These figures show that the change in the examined parameters has an effect on roots $p_{1,2}$, although this effect is slight, since these parameters cannot change in broad limits.
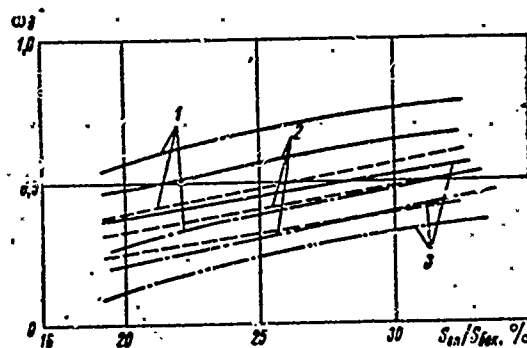
Figure 162. Effect of Relative Chord of Tail Group b_{on}/L and Position of Tail Group with Respect to Length x_{on}/L as Function of Change of Relative ARea of Tail Group $S_{on}/S_{бок}$ on Frequency $\bar{\omega}_{\partial}^{*}$ of Long-Periodic Oscillations of ACV SKMR-1.

$1 - x_{on}/L = 0.45;\ 2 - x_{on}/L = 0.35;\ 3 - x_{on}/L = 0.25.$
$b_{on}/L = 0.0323;$
$b_{on}/L = 0.0646;$
$b_{on}/L = 0.0968.$
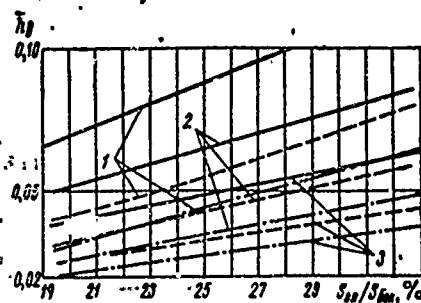
Figure 163. Effect of Relative Chord of Tail Group b_{on}/L and Position of Tail Group in Terms of Length x_{on}/L as Function of Change of Relative Area of Tail Group $S_{on}/S_{бок}$ on Damping Coefficient $\bar{h}_{\partial}$ of Long-Periodic Oscillations of ACV SKMR-1.

$1 - x_{on}/L = 0.45;\ 2 - x_{on}/L = 0.35;\ 3 -.$
$x_{on}/L = 0.25.$
$b_{on}/L = 0.0323;$
$b_{on}/L = 0.0646;$
$b_{on}/L = 0.0968$

Figure 164 shows the effect of relative nozzle width as a function of relative hovering altitude of ACV SKMR-1 over solid screen on frequency $\bar{\omega}_{k}^{*}$ of short-periodic oscillations. It is clear from Figure 164 that the frequency of oscillations $\bar{\omega}_{k}^{*}$ changes as a function of h and width b of nozzle, and here the change in the width of the vessel has negligible influence. When h and b decrease the frequency of oscillation $\bar{\omega}_{k}^{*}$ increases.

-353-

Figure 164. Effect of Relative Nozzle Width on Frequency ω_k^* of Short-Periodic Oscillations as a Function of Relative Hovering Altitude h/b of ACV SKMR-1 Over a Solid Screen.
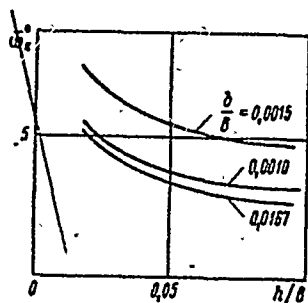
Figure 165 shows the effect of elongation of the tail group and width of nozzle as a function of relative tail group area on the damping coefficient $\bar{h}_k$ of short-periodic oscillations. It follows from the figure that the oscillations attenuate to a considerable extent when the area of the tail group is increased, and also when nozzle width and the chord of the tail group are reduced. It can be said, however, that the effect of the stated parameters on the character of motion both of short-periodic and long-periodic form, is small: very large changes in the geometrical parameters of the nozzle and tail group of the vessel are required in order to alter substantially the values of the roots[1].

We will see what conditions should be satisfied in order that both forms of motion be dynamically stable. For this purpose it is essential, as was stated earlier, that the roots of the characteristic equations (431), (432) be negative or have a negative real part.

Actually, the general solution of system (392) for four roots can be written in the following form:

$$\beta = \beta_1 e^{p_1 t} + \beta_2 e^{p_2 t} + \beta_3 e^{p_3 t} + \beta_4 e^{p_4 t};$$

$$b = \upsilon_1 e^{p_1 t} + \upsilon_2 e^{p_2 t} + \upsilon_3 e^{p_3 t} + \upsilon_4 e^{p_4 t}; \qquad (443)$$

$$\dot{\varphi} = \dot{\varphi}_1 e^{p_1 t} + \dot{\varphi}_2 e^{p_2 t} + \dot{\varphi}_3 e^{p_3 t} + \dot{\varphi}_4 e^{p_4 t}.$$

[1]The calculation does not take into account the coefficient of the damping moment of roll from the air cushion $m_x^{\tilde{\omega}x}$, but does consider the coefficient of damping moment of roll from the tail group $m_{x_{on}}^{\bar{\omega}x}$.
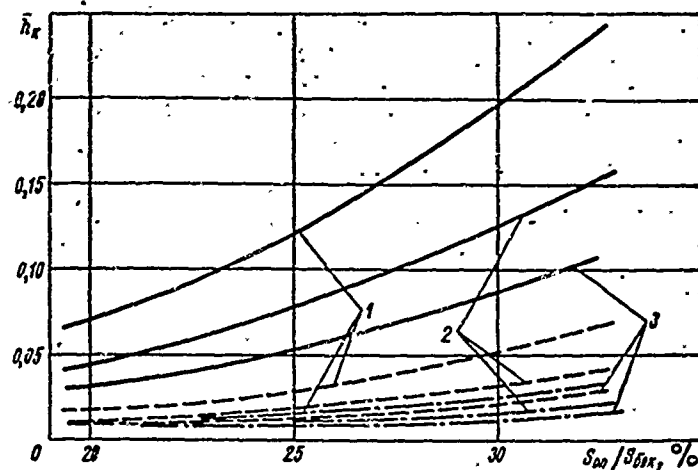
-354-

Figure 165. Effect of Elongation of Tail Group and Width of ACV SKMR-1 as Function of Relative Tail Group Area on Coefficient of Damping $\bar{h}_\kappa$ of Short-Periodic Oscillations.

$$1 - x_{on}/L = 0,45; \quad 2 - x_{on}/L = 0,35; \quad 3 - x_{on}/L = 0,25$$

$$\underline{\hspace{3cm}}\; b_{on}/L = 0,0323;$$

$$- - - - - -\; b_{on}/L = 0,0646;$$

$$-\cdot-\cdot-\cdot-\cdot-\; b_{on}/L = 0,0968.$$

If the roots are negative, all partial solutions contain factor $e^{p_i t}$ that diminishes with time and for $t \to \infty$ will diminish without bounds.

For four combined paired conjugate roots the general solution of system (392) can be written in the following form:

$$\vartheta = A_1 e^{-\bar{h}_\kappa t} \sin\left[\sqrt{\overline{\omega_\kappa^2 - \bar{h}_\kappa^2}}\, \overline{t + \tau_1}\right] +$$

$$+ A_2 e^{-\bar{h}_\partial t} \sin\left[\sqrt{\overline{\omega_\partial^2 - \bar{h}_\partial^2}}\, t + \tau_2\right];$$

$$\theta = B_1 e^{-\bar{h}_\kappa t} \sin\left[\sqrt{\overline{\omega_\kappa^2 - \bar{h}_\kappa^2}}\, t + \tau_3\right] +$$

$$+ B_2 e^{-\bar{h}_\partial t} \sin\left[\sqrt{\overline{\omega_\partial^2 - \bar{h}_\partial^2}}\, t + \tau_4\right]; \qquad (444)$$

$$\dot{\varphi} = C_1 e^{-\bar{h}_\kappa t} \sin\left[\sqrt{\overline{\omega_\kappa^2 - \bar{h}_\kappa^2}}\, t + \tau_5\right] +$$

$$+ C_2 e^{-\bar{h}_\partial t} \sin\left[\sqrt{\overline{\omega_\partial^2 - \bar{h}_\partial^2}}\, t + \tau_6\right].$$

-355-

The sinusoidal values in expressions (444) are harmonic functions of time t, so that the motion described by two pairs of complex roots will be attenuating or intensifying as a function of whether they are negative or positive values $-\bar{h}_k$ and $-\bar{h}_\partial$, representing the real parts of the combined roots.

Thus,

$$-\bar{h}_k < 0; \; -\bar{h}_\partial < 0 \tag{445}$$

or considering functions (423), (428), (431), (432)

$$n_{44} < 0; \; n_{31} + n_{52} < 0 \tag{446}$$

can be called the conditions of oscillatory dynamic stability.

The coefficient n_{44} is independent of hydrodynamic forces. Hence we conclude that the hydrodynamic forces have no effect on the coefficient of damping of short-periodic form of motion. The damping moment of roll created by the air cushion, plays the decisive role in this case. As regards coefficient of damping of long-periodic form of motion, the inequality

$$n_{31} + n_{52} < 0$$

can be satisfied only under certain conditions.

The coefficient n_{52} is not a function of the forces of hydrodynamic origin. It is determined basically by the forces of external, and even internal aerodynamics, and its sign cannot change for ACV. The coefficient n_{31} is a function of the forces of hydrodynamic origin. In connection with the fact that both aerodynamic n_{31a} and hydrodynamic n_{31h} components of the coefficient n_{31} have the same sign and are determining with respect to magnitude, the sign of the coefficient n_{31} cannot be changed for ACV. This means that alteration of the magnitude (and also point of application) of hydrodynamic forces cannot lead to oscillatory dynamic instability of long-periodic form of motion. It may be said, by and large, that the forces of hydrodynamic origin have a favorable effect on the oscillatory dynamic stability of lateral motion, since they increase the coefficient of damping of the long-periodic form of motion.

Conditions (446) are essential, but not sufficient for ensuring oscillatory dynamic stability. It is also necessary that roots (431) and (432) be combined conjugate. In order that roots (431) and (432) be combined conjugate with a negative real part, the following inequalities must be satisfied:

$$\bar{\omega}_\kappa^2 - \bar{h}_\kappa^2 > 0; \quad \bar{\omega}_\partial^2 - \bar{h}_\partial^2 > 0. \tag{447}$$

or in consideration of expressions (434), (436), (437) and (438)

$$n_{43} < 0; \tag{448}$$

$$n_{31} n_{52} - n_{51} n_{32} > 0. \tag{449}$$

The coefficient n_{43} is the coefficient of transverse static stability. Thus, in order that the short-periodic form of motion be dynamically stable the ACV must have transverse static stability $m_x^\theta < 0$.

Inequality (449) has a positive term $n_{31} n_{52}$, and moreover coefficient n_{32} is also positive. Thus, if the ACV is statically stable on course (coefficient of static stability on course $n_{51} < 0$), then inequality (449) is automatically satisfied, i.e., an ACV that is statically stable on course has a dynamically stable long-periodic form of motion. A slight degree of static instability on course does not necessarily mean that this form of motion is dynamically unstable.

The physical essence of condition (449) becomes clear if we write this inequality in the following form:

$$\frac{n_{43}}{n_{42}} < \frac{n_{51}}{n_{31}} \tag{450}$$

or, considering the expanded values of the coefficients (see §22 and 24),

$$\frac{m_y^{\bar{\omega}_y}}{c_z^{\bar{\omega}_y}} < \frac{m_y^\beta}{c_z^\beta}; \tag{451}$$

-357-

The value $\dfrac{m_y^{\bar{\omega}y}}{c_z^{\bar{\omega}y}} = l_{\text{жеипф}}$ is a dimensionless arm of action of reduced

forces of damping. The value $\dfrac{m_y^{\beta}}{c_z^{\beta}} = l_{\text{бокст}}$ is the dimensionless arm of

action of the transverse force. Hence the physical sense of condition (449) amounts to the requirement that the arm of action of the transverse force be longer than the arm of action of reduced damping forces.

We will also consider under what conditions the ACV will have aperiodic dynamic stability. In this case all roots should be real and negative. With positive values of $\bar{h}_k$ and $\bar{h}_\partial$ this can occur only if the following inequalities are satisfied:

$$\bar{\omega}_k^2 - \bar{h}_k^2 < 0; \quad \bar{\omega}_\partial^2 - \bar{h}_\partial^2 < 0; \tag{452}$$

for

$$\bar{\omega}_k^2 > 0; \quad \bar{\omega}_\partial^2 > 0 \tag{453}$$

or, considering the preceding expressions,

$$\frac{m_y^{\bar{\omega}y}}{c_z^{\bar{\omega}y}} > \frac{m_y^{\beta}}{c_z^{\beta}} \quad \text{for} \quad (n_{31} + n_{52})^2 > 4\,(n_{51}n_{33} - n_{31}n_{53}); \tag{454}$$

$$m_{x_{on}}^{\beta} > 0 \quad \text{for} \quad n_{44}^2 > 4n_{43}n_{74}.$$

Finally, we will examine under what conditions there will be no dynamic stability of lateral motion. This will occur, obviously, even in the case when only one of roots (431), (432) is positive. As we established earlier, the values $\bar{h}_k$ and $\bar{h}_\partial$ are always positive for ACV.

This means that ACV cannot have oscillatory dynamic instability. Dynamic instability of ACV may be only of an aperiodic character.

The conditions of dynamic instability are the inequalities

$$\bar{\omega}_k^2 < 0; \quad \bar{\omega}_\partial^2 < 0. \tag{455}$$

or, considering the expanded values,

$$n_{44}^2 < 4n_{43}n_{74};$$
$$(n_{31} + n_{52})^2 < 4\,(n_{51}n_{33} - n_{31}n_{53}). \tag{456}$$

§26. Static Stability on Course

The equations of straight-line steady state lateral motion, in which the forces acting on the ACV are in equilibrium, and the kinematic parameters of motion are constant, will be of the following form:

$$n_{31}\beta + n_{33}\theta + n_{35}\delta p = 0;$$
$$n_{41}\beta + n_{43}\theta + n_{45}\delta p = 0;$$
$$n_{51}\beta + n_{55}\delta p + n_{57}\delta\Lambda = 0.$$

(457)

We will determine the location of the point of application of the resultant of aerodynamic forces acting on the ACV in straight-line steady state motion.

The moment of the resultant relative to the vertical axis passing through the center of gravity of the vessel (moment of yaw) is

$$\dot{M}_y = \dot{Z}a,$$

(458)

where a is the distance between the center of application of the resultant of aerodynamic forces through the length of the vessel and the center of gravity of the vessel.

Steady state motion of ACV will be statically stable if during change of the angle of drift the moment of yaw tries to restore it to the initial angle of drift.

We know that the condition of static stability on course of a floating vessel means that the center of hydromechanical forces should be located sternward from the center of gravity of the vessel. By analogy, the condition of static stability on course of ACV will mean that the center of aerohydromechanical forces should be located sternward from its center of gravity.

From equations (457) and (458), assuming $\delta\Lambda = \delta p = 0$, we obtain

$$a = \frac{n_{31}}{n_{31}\left(1 - \frac{n_{33}n_{41}}{n_{31}n_{43}}\right)}.$$

(459)

Assuming arm a to be located sternward from the center of gravity, i.e., with a minus sign, the condition of static stability of ACV on course can be written as follows:

$$a < 0 \quad \text{or} \quad n_{s1} < 0. \tag{460}$$

This inequality can be written in expanded form as follows:

$$m_y^\beta < 0; \tag{461}$$

$$m_y^\beta = m_{y_a}^\beta + m_{y_R}^\beta + m_{y_\Gamma}^\beta; \tag{462}$$

$$m_{y_R}^\beta = -\frac{\rho Q x_{R_1} V}{q S_{60\kappa} L}; \tag{463}$$

$$m_{y_a}^\beta = m_{y_\kappa}^\beta + m_{y_H}^\beta + m_{y_{on}}^\beta; \tag{464}$$

$$m_{y_\Gamma}^\beta = m_{y_B}^\beta + m_{y_{\Gamma.o}}^\beta = -\frac{Z_B x_B}{q S_{60\kappa} L} - \frac{R_{\Gamma.o} x_{\Gamma.o}}{q S_{60\kappa} L}. \tag{465}$$

For aircraft the condition of static stability on course, as we know, is written as follows:

$$m_{y_a}^\beta < 0,$$

and for floating craft

$$m_{y_\Gamma}^\beta < 0.$$

If we assume that $m_{y_R}^\beta \doteq 0$, and that the ACV does not make contact with the water surface ($R_{\Gamma.o} = 0$) and moves at high speed ($Z_B = 0$), as has been assumed in investigations known to this date, then the condition of static stability of ACV on course can be written in the same way as for aircraft.

As follows from §25, the coefficient of static stability on course m_y^β plays an important role in insuring dynamic stability of the long--periodic form of motion, directly influencing the reserve of dynamic stability. It follows from expression (462) that in order to insure static stability on course it is advisable in ACV design to try to make the signs of all terms of expression (462) negative, and the values of the relative arms of application of each of the components of coefficient m_y^β maximum.

We will look at each component of inequality (461) individually.

-360-

Coefficient $m^\beta_{y_R}$. The sign of coefficient $m^\beta_{y_R}$ is determined by the location of the reduced arm x_{R_1}/L in relation to the center of gravity.

This fact can be used: coefficient m^β_y may change in the required direction, ensuring the distribution of the fans through the length of the vessel for which the reduced arm will be located sternward from the center of gravity.

Coefficient $m^\beta_{y_\Gamma}$. In examining the hydrodynamic coefficient of the moment of yaw $m^\beta_{y_\Gamma}$ the requirements set forth above lead to some contradiction. The lateral force of wave origin Z_B is applied at the center of the area of the air cushion, the location of which under normal operating conditions is rather stable. The center of gravity of the air cushion should be located ahead of the center of gravity of the vehicle, since through it passes the line of action of the lift from the air cushion, which creates in this location a positive (toward the stern) travel trim. The point of application of the lateral force of wave origin Z_B, and consequently coefficient $m^\beta_{y_B}$ are independent of change in trim if it does not involve a change in the centering of the vessel $x_g - x_\Pi/L$. Coefficient $m^\beta_{y_B}$ is directly dependent on centering. Thus, $m^\beta_{y_B}$ is additive to the coefficient of the moment of yaw, which has a negative effect on static stability on course.

In contrast, the point of application of the lateral force of hydrodynamic interaction of the flexible skirt with water $Z_{\Gamma.o}$ is extremely sensitive to change not only of the centering $x_g - x_\Pi/L$ but also of the travel trim of the ACV. Thus, a change in travel trim from positive to negative with a constant centering may change not only the magnitude, but also the sign of the coefficient $m^\beta_{y_{\Gamma.o}}$, whereas the value of $m^\beta_{y_B}$ here may remain the same as before.

Not only the arm, but also the magnitude of force $Z_{\Gamma.o}$ are exceedingly sensitive to changes in these parameters, since this has an effect on the wash area of the flexible skirt.

During travel at a constant positive travel trim, ensuring satisfactory travel qualities, the point of application of force $Z_{r.o}$ is located sternward from the center of gravity and thereby compensates (partially or completely, depending on the Froude number) the negative effect of the lateral force of wave origin on the static stability on course.

Coefficient $m_{y_a}^{\beta}$. The aerodynamic coefficient of static stability can be broken down into two parts:

$$m_{y_a}^{\beta} = m_{y_{a_0}}^{\beta} + m_{y_a}^{\beta} f(\sigma_p),$$
(466)

where $m_{y_{a_0}}^{\beta}$ is aerodynamic coefficient of static stability, not a function of the thrust load factor of the power plant;

$m_{y_a}^{\beta} f(\sigma_p)$ is an additive to it, a function of σ_p.

The coefficient $m_{y_{a_0}}^{\beta}$ can be expressed through the following equation:

$$m_{y_{a_0}}^{\beta} = m_{y_K}^{\beta} + m_{y_{on}}^{\beta}(\sigma_p = 0) + m_{y_n}^{\beta}(\sigma_p = 0),$$
(467)

This is the same coefficient of static stability on course that is found in the wind tunnel in testing of an ordinary schematic model without simulating the operation of the engine-fan complex.

The value $m_{y_a}^{\beta} f(\sigma_p)$ can be expressed as follows:

$$m_{y_a}^{\beta} f(\sigma_p) = m_{y_{on}}^{\beta} f(\sigma_p) + m_{y_n}^{\beta} f(\sigma_p).$$
(468)

Here the additive to the coefficient from the tail group is

$$m_{y_{on}}^{\beta} f(\sigma_p) = \sum c_{y_{on_l}}^{z} \frac{S_{on_l}}{S_{6ok}} \frac{x_{on_l}}{L} \Delta x_{b_l} +$$
$$+ \sum \mu_K \sigma_p \frac{S_{on_l}}{S_{6ok}} \frac{x_{on_l}}{L} x_{b_l} f(\sigma_p);$$
(469)
$$\Delta x_{b_l} = x_{b_l}(\sigma_p \neq 0) - x_{b_l}(\sigma_p = 0).$$
(470)

-362-

The additive from the shrouds is

$$m^3_{y_{_H}} f(\sigma_p) = \sum_i c^3_{z_{_{H_i}}} f(\sigma_p) \frac{x_{H_i}}{L} \cdot \frac{S_{H_i}}{S_{60\kappa}}.$$ (471)

This additive is determined according to the equations presented in §22.

The coefficient $m^{\beta}_{y_{a_0}}$ on a proposed vessel with the selected tail group depends only on the centering and trim. By and large, the dependence of the components of coefficient m_y on the principal parameters can be written as follows:

$$m^3_{y_R} = f(V);$$
$$m^3_{y_r} = f(V, \psi, h); \quad$$ (472)
$$m^3_{y_a} = f(\sigma_p, \psi, h)$$

for $\psi = f\left(\dfrac{x_g - x_n}{L}, \sigma_p\right).$

As we will see, the coefficient of the moment of yaw depends largely on the kinematic parameters of longitudinal motion--lift h and trim ψ. Herein is manifested the relationship between longitudinal and lateral motion of ACV. Hence it follows that analysis of the equations of lateral motion will not yield exhaustive information concerning the mechanism of phenomena related to static stability on course.

Imagine an ACV traveling on the open sea on calm water at infinitely increasing velocity. This motion will be accompanied by a slight keel, vertical jump and a reduction of travel trim due to increasing engine thrust.

The reduction of trim, and also each trim oscillation is primarily a change in the magnitude, and also the sign of $m^{\beta}_{y_{r.0}}$. When a certain velocity is reached this change of $m^{\beta}_{r.0}$ may change the sign of the entire coefficient m^{β}_y and its magnitude to such an extent that the reserve of dynamic stability m^{β}_y of the long-periodic form of motion of the ACV will vanish and the vehicle will go into an involuntary spin.

With a poorly designed flexible skirt, the bow portions of the flexible skirts will begin to disintegrate before this moment, and from the point of view of lateral motion this involves a substantially sharper change of $m_{y_{\Gamma.o}}^{\beta}$ due to a sharp increase in the area of wash of the flexible skirt. Part of the air cushion, toward the bow will break down and centering will be changed due to displacement of the center of gravity of the air cushion toward the stern. Here too, the restoring moment of roll $m_{x_{\Pi}}^{\theta}$ will decrease or vanish all together.

Thus, immediately following disintegration of the flexible skirt dynamic stability both of the long-periodic and short-periodic forms of motion will begin to be lost. Further behavior of the vessel will be determined by the nonlinearity of the hydrodynamic characteristics of spatial motion.

As shown by the experience of English researchers [81], breakdown of the flexible skirt during travel with drift can result in capsizing of the ACV.

To avoid emergency situations related to a loss of dynamic stability, attempts are made to standardize static stability and to determine experimentally the margin of static stability on course required for safe ACV operation.

The margin of static stability on course (value of m_y^{β}) will be minimal at top speed. This minimal margin is the criterion of static stability during ACV travel not only on calm water, but also on water of the prescribed degree of waviness, since top speed is reduced as the water becomes rougher as the coefficient of static stability on course increases as the speed is reduced.

Consequently, the basic factor adversely affecting the static stability on course of a traveling ACV is reduction of the travel trim as the speed of the vessel is increased. Different techniques are used to combat this phenomenon, chief among which are the use of horizontal aerodynamic rudders and control of centering.

As we have seen from (472), a change in centering effects both $m_{y_a}^{\beta}$ and $m_{y_{\Gamma}}^{\beta}$. Centering itself $x_g - x_{\Pi}/L$ may change the function of both arms x_g/L and x_{Π}/L.

A change of arm x_n/L, as we shall see, can occur only in an emergency situation; arm x_g/L changes regularly during the process of ACV operation. Therefore change of centering is considered to be a function of arm x_g/L. Displacement of the center of gravity of an ACV toward the stern leads to a reduction of $m^\beta_{y_{r.o}}$, but increases the trim on the stern, which leads to a twofold change of $m^\beta_{y_{r.o}}$: reduction of $m^\beta_{y_{r.o}}$ due to a reduction of the arm and an increase due to an increase in the area of washing of the flexible skirt. This complex dependence of m^β_y on centering leads to a situation where normal operation of ACV is possible only during strict observance of a certain range of change of centering, within which the ACV is not threatened by a loss of static stability on course.

In connection with the tremendous effect of centering and coefficient $m^\beta_{y_{r.o}}$ on static stability on course it is advisable to determine the coefficient $m^\beta_{y_{r.o}}$ through polling tests of ACV models with fans operating for different drift angles.

We will represent further the value m^β_y in the following form:

$$m^\beta_y = m^\beta_{y_{a_o}} + m^\beta_{y_a}(\sigma_p) + m^\beta_{y_s} + m^\beta_{y_{r.o}} + m^\beta_{j.g}.$$

The possibility during ACV operation of a combination of conditions of motion such that all components change for the worse (i.e., their change leads to a reduction of static stability), for example in the case of a tail wind, unfavorable trim and roll (or sudden disappearance of) thrust is not excluded. In this case the only value that is capable of insuring static stability on course is $m^\beta_{y_{a_0}}$, therefore it is advisable in the given stage to ensure a negative $m^\beta_{y_{a_0}}$, i.e., the ACV and its model should be statically stable in the aerodynamic sense.

If the vehicle is equipped with an automatic control system the absence of static stability can be compensated, but if the control system breaks down instability will be impossible with a positive $m_y^{\beta}{}_R$

§27. Circulation of ACV

We will examine controlled lateral motion of ACV created by rudder movement δ_p.

·We know from theoretical mechanics that in order to achieve a curvilinear trajectory of motion in a horizontal plane it is necessary to create a centripetal force that also lies in the horizontal plane. Such a force can be obtained for ACV in three ways:

by rolling (without drift);

by creating drift;

by means of simultaneous drift and roll.

Circulation as a Result of Rolling Without Drift

Let us examine the steady state circulation of an ACV in the horizontal plane, when the angle of roll is not changed and there is no drift. In aviation this maneuver is called "correct turning" [14] (Figure 166). The radius of curvature of the trajectory of the center of gravity of the vessel in this case is determined by the relation:

$$P_\text{ц} = m i_n,$$

where $P_\text{ц}$ is centripetal force;

    m is the mass of the ACV;

    i_n is the normal acceleration.

Since $i_n = V^2_\text{цирк}/R$ and $P_\text{ц} = Y \sin \theta$, then $Y \sin \theta = mV^2_\text{цирк}/R$.

It follows from Figure 166 that lift in this case is $Y = G/\cos \theta$.

Hence the radius of circulation is

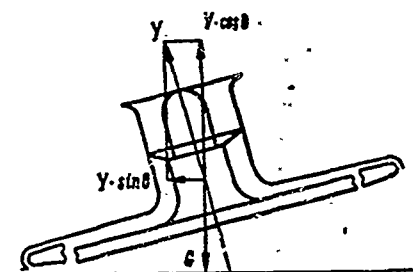$$R = \frac{V^2_\text{цирк}}{g \, \text{tg} \, \theta}. \tag{473}$$

Figure 166. Diagram of Action of
Forces During Steady State
Circulation of ACV as a Result
of Rolling Without Drift.

In steady state circulation the speed should be constant. Therefore it is essential that during the time of circulation the available thrust equal the thrust required for overcoming drag.

In order that the ACV enter into circulation in a given case it is essential to create roll to the side corresponding to the direction of circulation (internal roll). As soon as the vehicle begins to roll, the center of gravity begins to move in a curvilinear trajectory. If here the vessel is not made to turn in relation to the center of gravity at the same angular velocity at which the velocity vector of the center of gravity moves, then drift occurs.

To prevent this from happening it is necessary to deflect the vertical rudder to within circulation or to create the corresponding moment by some other means.

Figure 167 shows the curves, obtained by calculation using equation (473), of the radius of circulation achieved with roll only as a function of the angle of roll.
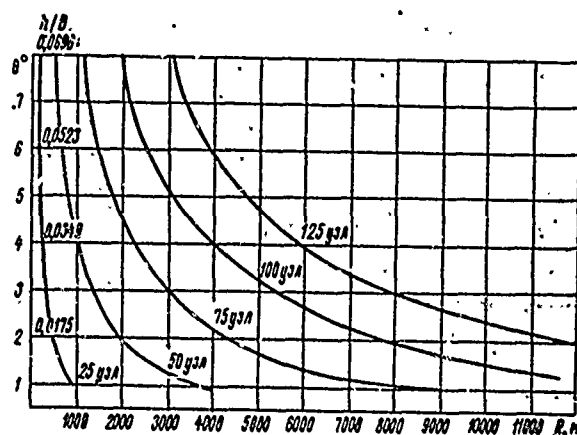

Figure 167. Radius of
Circulation Performed
With Roll Only as a
Function of Angle of
Roll θ.

To investigate circulation performed without drift, it is necessary to assume in equation (392) β (p) = 0, and also to consider that the sum of moments relative to the Oy axis is identically equal in this case to zero. Then system (392) will acquire the form

$$\theta\left[-n_{33}-m_{33}p\right]+$$
$$+ p\dot{\varphi}\left[m_{33}\right] = Z(p);$$
$$\theta\left[\frac{p^3}{n_{74}}-m_{43}p-n_{43}\right]+$$
$$+ p\dot{\varphi}\left[\dot{m}_{43}-\frac{n_{73}}{n_{33}n_{74}}p\right]=$$
$$= M_x(p). \tag{474}$$

The determinant of this system with consideration of the values of the dynamic coefficients according to expression (391) is equation

$$\Delta = Cp^2 + Dp + E, \tag{475}$$

where

$$C = -\frac{m_{33}}{n_{74}};$$

$$D = \frac{n_{72}n_{33}}{n_{74}n_{33}}+m_{43}m_{33};$$

$$E = m_{32}n_{43}-m_{42}n_{33}. \tag{476}$$

Partial determinants are found, as before, by substituting the corresponding columns with the right-hand sides of system (392).

For Δ_0

$$\Delta_\theta = r_{10}p + r_{09};$$
$$r_{10} = -\frac{n_{72}}{n_{32}n_{74}}Z(p);$$
$$r_{09} = m_{42}Z(p)-m_{32}M_x(p). \tag{477}$$

For $\Delta_{p\varphi}$

$$\Delta_{p\varphi} = r_{2p\varphi}p^2 + r_{1p\varphi}p + r_{0p\varphi};$$
$$r_{2p\varphi} = -\frac{1}{n_{74}}Z(p);$$
$$r_{1p\varphi} = r_{43}Z(p);$$
$$r_{0p\varphi} = n_{43}Z(p)-n_{33}M_x(p). \tag{478}$$

The transform of angle of roll θ and angular velocity of yaw $p\varphi$ are found using the expressions for

$$\theta(p) = \frac{\Delta_\theta}{\Delta};$$ (479)

$$p\dot{\varphi}(p) = \frac{\Delta_{p\varphi}}{\Delta}.$$ (480)

Expressions (479) and (480) permit analysis of the dynamic stability and transition processes of circulation without drift. We will be interested only in the parameters of steady state circulation.

If we assume that rotation of the rudder is accomplished instantaneously to some angle δp, then by converting from the transforms to the original for $t \to \infty$, then we obtain

$$\theta = \frac{r_{0\theta}}{E} = \delta p \frac{n_{32}n_{45}n_{74} + n_{33}(n_{44}n_{72} - n_{42}n_{74})}{n_{33}(n_{42}n_{74} - n_{44}n_{72}) - n_{32}n_{43}n_{74}};$$ (481)

$$\frac{1}{\varphi} = \frac{R}{L} = \frac{E}{r_{0p\varphi}} = \frac{n_{33}(n_{42}n_{74} - n_{44}n_{72}) - n_{32}n_{43}n_{74}}{n_{42}n_{74}(n_{43}n_{35} - n_{33}n_{45})} \cdot \frac{1}{\delta p},$$ (482)

where R/L is the relative radius of circulation.

In connection with the fact that rolling of the vessel in the given case is created only by reaction of lateral forces on the rudder, the balanced regime on circulation is insured by outside deflection of the rudder.

Circulation During Travel Only with Drift, Without Roll

In the given case there are two possible variants of curvilinear motion: with inside (toward the center of curvature of the trajectory) and with outside drift (away from the center of curvature of the trajectory).

We will examine motion of ACV in a curvilinear trajectory with inside drift. We see in Figure 168 that in the case of motion with inside drift a lateral force 7 and the projections of the force of thrust of the engines onto the normal to the trajectory of travel Z_T do not create centripetal forces, and travel with inside drift is not acceptable. During travel with outside drift, as seen in the Figure, the centripetal force develops and consists of lateral force Z and the projection of the engine thrust onto the normal to the trajectory of motion if the direction of the thrust does not coincide with the direction of the velocity of the center of gravity of the ACV.

What role does the vertical rudder of the ACV play in this case?
Rotation of the vertical rudder precedes steering of the ACV at some
angle to the incident flow, at which the centripetal force is developed.
As the vertical rudder is rotated in order to create outside drift
(rotation of the rudder toward the center of curvature of the trajectory)
a force is created on it, directed away from the center of curvature of
the trajectory of the center of gravity. This force reduces the centri-
petal force, but the moment of this force insures ACV travel with drift,
with the result that a lateral force builds up on the hull, which chiefly
governs the development of centripetal force.

However, if the vessel, during motion of the center of gravity of
the ACV on the curvilinear trajectory, should complete only translatory
motion, then the rotation of the trajectory of the center of gravity by
angle β would change the drift of the ACV by the same angle β--drift
would disappear and the centripetal force would also vanish. In order
that the angle of drift caused by the centripetal force remained constant
the vessel, in turn, must rotate around the center of gravity at the
same angular velocity as does the tangent to the trajectory of the center
of gravity of the ACV.
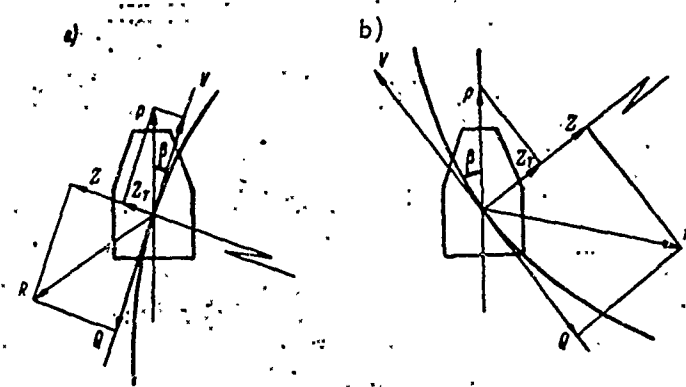
Figure 168. Diagram of Action of Forces in Steady State Circulation
of ACV in the Case of Motion with Drift Only: a, with inside drift;
b, with outside drift.

In order for an angular velocity of rotation around the center of
gravity to be developed the operator must create an angular acceleration
of the relative center of gravity until the angular velocity of rotation
around the center of gravity becomes equal to the angular velocity of
rotation of the center of gravity.

-370-

If the centripetal force is constant, then the angular velocity of rotation of the center of gravity relative to the center of curvature of the trajectory should also remain constant at constant translatory speed. During curvilinear motion with a constant angular velocity (steady state circulation) the ACV should be rotated around the center of gravity, also at constant angular velocity.

During rotational motion the ACV experiences resistance to motion from the medium--the effect of the damping moment. If the damping moment is not equalized, for instance, by deflecting the rudder, then rotation at a constant angular velocity is impossible. The angular velocity will decrease, approaching zero.

Thus, deflection of the rudder while bringing the ACV into steady state circulation is essential at first in order to create angular acceleration, and then in order that the magnitude of the angular velocity attained remains constant (i.e., in order that the damping moment be equalized). Here the rudder deflection required for createing angular velocity is the same in terms of direction as that which insures creation of the moment that equalizes the damping moment.

To analyze circulation accomplished without roll we must assume $\theta = 0$ in equation system (392), and also discard the equation of moments relative to the Ox axis. System (392) will acquire the following form:

$$\beta\left[-n_{31} + p\right] + p\dot{\varphi}\left[m_{32}\right] = Z(p);$$
$$-\beta\left[n_{51}\right] + p\dot{\varphi}\left[m_{52} + \frac{p}{n_{53}}\right] = M_y(p). \tag{483}$$

The determinant of this system in consideration of the dynamic coefficients according to dependence (391) is:

$$\Delta = Cp^2 + Dp + E, \tag{484}$$

where

$$C = \frac{1}{n_{53}};$$

$$D = m_{52} - \frac{n_{31}}{n_{53}}; \tag{485}$$

$$E = m_{32}n_{51} - m_{52}n_{31}.$$

The partial determinants are expressed through the following equations:

-371-

$$\Delta_3 = r_{13}p + r_{03};$$

$$r_{13} = \frac{Z(p)}{n_{32}};$$ (486)

$$r_{03} = Z(p)m_{52} - M_y(p)m_{32};$$

$$\Delta_{p\overline{\tau}} = r_{1p\overline{\tau}}p + r_{0p\overline{\tau}};$$

$$r_{1p\overline{\tau}} = M_y(p);$$ (487)

$$r_{0p\overline{\tau}} = n_{51}Z(p) - n_{31}M_y(p).$$

The transforms of angle of drift β and angular velocity of yaw are found through the expressions

$$\beta(p) = \frac{\Delta_\beta}{\Delta};$$ (488)

$$p\overline{\tau}(p) = \frac{\Delta_{p\overline{\tau}}}{\Delta}.$$ (489)

Expressions (488) and (489) enable us to analyze the dynamic stability and transition processes during circulation accomplished without roll. The parameters of steady state circulation will be determined by the expressions

$$\beta = \frac{n_{53}n_{33} - n_{33}n_{52}}{n_{52}n_{31} - n_{32}n_{51}}\delta p;$$ (490)

$$\frac{R}{L} = \frac{n_{52}n_{31} - n_{32}n_{51}}{n_{32}(n_{51}n_{33} - n_{31}n_{53})} \cdot \frac{1}{\delta p}.$$ (491)

Circulation as a Result of Simultaneous Drift and Roll

Circulation with inside drift, as seen in Figure 169a, will be accomplished in the horizontal plane, when

$$R\cos(\theta - \theta') = G.$$

Circulation with outside drift, as seen in Figure 169b will be accomplished in the horizontal plane when

$$R\cos(\theta + \theta') = G.$$
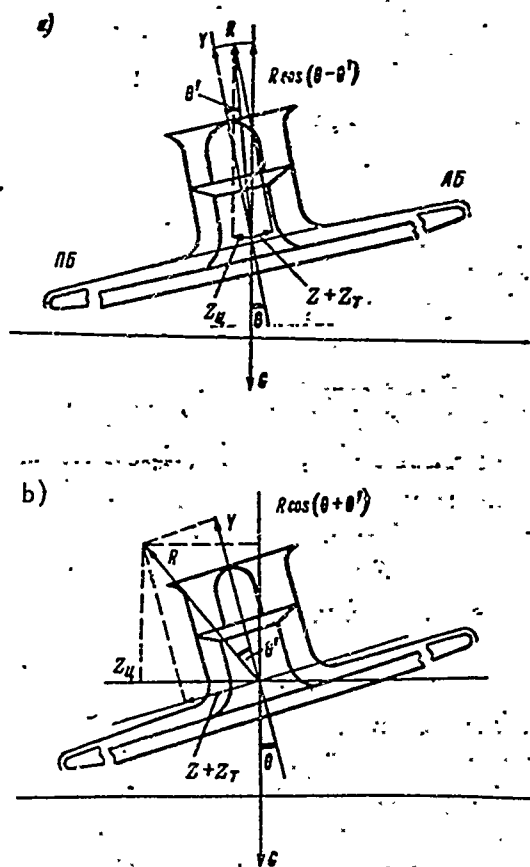
Figure 169. Diagram of Action of Forces in Steady
State Circulation of ACV as a Result of Simultaneous
Drift and Roll: a, Circulation with inside drift;
b, Circulation with outside drift. пб, Starboard;
лб, Port side.

It follows from the above that the same aerodynamic force R
equalizes with its projection onto the vertical, the weight of the ACV,
accomplishing circulation without side drift, with an angle of roll
smaller than in the case of circulation without drift. If circulation
is accomplished with inside drift, then the same magnitude of force R
equalizes the force of the weight with an angle of roll larger than in
the case of circulation without drift.

Thus, circulation with outside drift is also more suitable in this
case. To arrive at a quantitative evaluation of steady state circulation
during ACV travel with drift and roll we will write the transfer functions
for the kinematic parameters of lateral motion β, θ and φ with
perturbation δp.

-373-

We obtain from Tables 14-16, with considerations of expressions (401), (404), (407) and (416) for W_β:

$$r_{33} = \frac{n_{33}}{n_{74}n_{33}};$$

$$r_{23} = \left(-\frac{n_{33}}{n_{92}n_{74}} - \frac{n_{44}}{n_{74}n_{83}}\right)n_{35} + \left(\frac{n_{33}}{n_{83}n_{76}}\right)n_{55};$$

$$r_{13} = \left(-\frac{n_{44}n_{33}}{n_{74}n_{83}} - \frac{n_{43}}{n_{83}}\right)n_{35} + \left(\frac{n_{33}}{n_{83}}\right)n_{45} + \left(\frac{n_{73}n_{33}}{n_{82}n_{76}} - \frac{n_{33}n_{44}}{n_{83}n_{74}}\right)n_{55}; \qquad (492)$$

$$r_{03} = n_{45}n_{33}m_{52} + n_{55}m_6 - n_{35}n_{43}m_{52} = -n_{45}n_{33}\frac{n_{33}}{n_{83}} +$$
$$+ n_{55}\left[-n_{43}\frac{n_{33}}{n_{83}} - n_{33}\left(\frac{n_{44}n_{73}}{n_{83}n_{73}} - \frac{n_{43}}{n_{83}}\right)\right] + n_{35}n_{43}\frac{n_{33}}{n_{83}};$$

for W_θ:

$$r_{29} = -n_{35}(0) + \frac{n_{45}}{n_{83}} + \frac{n_{73}n_{55}}{n_{74}n_{83}};$$

$$r_{19} = n_{35}\left(\frac{n_{73}n_{51}}{n_{74}n_{83}} + \frac{n_{41}}{n_{83}}\right) + n_{45}\left(-\frac{n_{33}}{n_{83}} - \frac{n_{31}}{n_{83}}\right) + \qquad (493)$$
$$+ n_{55}\left(-\frac{n_{44}n_{73}}{n_{83}n_{74}} - \frac{n_{43}}{n_{83}}\right) - \frac{n_{73}n_{51}}{n_{74}n_{83}};$$

$$r_{09} = n_{35}\left[-n_{41}\frac{n_{33}}{n_{83}} - n_{51}\left(\frac{n_{44}n_{73}}{n_{83}n_{74}} - \frac{n_{43}}{n_{83}}\right)\right] +$$
$$+ n_{45}\left[n_{31}\frac{n_{33}}{n_{83}} - n_{51}\frac{n_{33}}{n_{83}}\right] + n_{55}\left[n_{31}\frac{n_{44}n_{73}}{n_{83}n_{74}} - \frac{n_{43}}{n_{83}}\right） + n_{41}\left(\frac{n_{33}}{n_{83}}\right)\right];$$

for $W_{p\varphi}$

$$r_{3p\varphi} = \frac{n_{33}}{n_{74}}; \qquad (494)$$

$$r_{2p\varphi} = n_{35}\frac{n_{51}}{n_{74}} + n_{55}\left(-\frac{n_{44}}{n_{74}} - \frac{n_{31}}{n_{74}}\right) + n_{45}(0);$$

$$r_{1p\varphi} = n_{35}\left(-n_{51}\frac{n_{44}}{n_{74}}\right) + n_{55}\left(n_{31}\frac{n_{44}}{n_{74}} - n_{43}\right) + n_{45}(0);$$

$$r_{0p\varphi} = n_{51}(n_{45}n_{33} - n_{35}n_{43}) + n_{55}(n_{31}n_{43} - n_{33}n_{41}).$$

-374-

In accordance with expression (408) we will determine the transfer functions W_β, W_θ and $W_{p\varphi}$ for perturbation δp and using expression (412) we will find the transforms themselves:

$$\beta(p) = W_\beta \delta p(p);$$
$$\theta(p) = W_\theta \delta p(p);$$
$$p\varphi(p) = W_{p\varphi} \delta p(p). \tag{495}$$

Here, in expression (408) the approximate coefficients of determinants (397) are:

$$A = \frac{1}{n_{74} n_{83}};$$
$$B = -\frac{n_{52} + n_{44} + n_{31}}{n_{74} + n_{83}};$$
$$C = -\frac{n_{43}}{n_{83}};$$
$$D = \frac{1}{n_{83}}(n_{31} n_{43} - n_{33} n_{41} + n_{52} n_{43});$$
$$E = \frac{1}{n_{83}}(n_{43} n_{51} n_{32} - n_{43} n_{31} n_{53}). \tag{496}$$

After finding the originals according to the transforms, we obtain expressions that are suitable for analyzing all three (maneuvering, evolutionary and steady state) periods of ACV circulation.

We will demonstrate the possibility of using these equations by way of example of analysis of the steady state circulation of ACV. During steady state circulation the kinematic parameters of motion acquire limiting values if, as before, time t approaches ∞. Here, toward the end of the transition process the kinematic parameters approach the following limiting values:

$$\Delta\beta(\infty) = \delta p \frac{r_{0\beta}}{E};$$
$$\Delta\theta(\infty) = \delta p \frac{r_{0\theta}}{E}; \tag{497}$$
$$\Delta\dot{\varphi}(\infty) = \delta p \frac{r_{0p\varphi}}{E}.$$

By substituting into expressions (497) the values entering into them we obtain

$$\vartheta = \delta p \left[\frac{n_{55}(n_{35} - n_{13}n_{31}) + n_{55}\left(n_{33}n_{42} - n_{43}n_{32} - n_{32}n_{56}\dfrac{n_{73}}{n_{76}}\right)}{n_{43}(n_{51}n_{33} - n_{31}n_{53})} \right]; \qquad (498)$$

$$\theta = \delta p \left[\frac{\left(n_{44}\dfrac{n_{72}}{n_{74}} - n_{42}\right)(n_{55}n_{31} - n_{35}n_{51}) + n_{41}(n_{53}n_{32} - n_{33}n_{52}) - n_{45}(n_{51}n_{32} + n_{31}n_{53})}{n_{43}(n_{51}n_{33} - n_{31}n_{53})} \right]; \qquad (499)$$

$$\frac{R}{L} = \frac{1}{\delta p} = \frac{\dfrac{n_{44}}{n_{54}}(n_{31}n_{32} - n_{31}n_{53})}{n_{51}(n_{44}n_{33} - n_{36}n_{43}) + n_{45}(n_{31}n_{43} - n_{33}n_{61})}. \qquad (500)$$

Analysis of the result obtained by calculating the elements of circulation of ACV of ordinary forms according to the equations presented above indicates that the angle of drift in steady state circulation is practical.y the same as during circulation with drift only and circulation with roll and drift, and the radius of steady state circulation in the former case is greater than in the latter. Despite the fact that the angle of roll during circulation with roll only is somewhat smaller than during circulation with roll and drift, the radius of the steady state circulation in the latter case is considerably smaller than in the former.

Circulation with drift only, and also with drift and roll, occurs in the direction of rudder deflection; circulation with roll only is in the direction opposite rudder deflection, since rolling in the given case occurs under the influence of lateral forces on the deflected rudder.

By an large the angle of roll on circulation is small. Allowance for the forces of hydrodynamic interaction leads to some enlargement of the radius of steady state circulation and reduction of the angle of roll and angle of drift on circulation.

Chapter VI.   Seaworthiness of Air Cushion Vehicles

It is known that seaworthiness is the total of all characteristics
which ensure smoothness and a small degree of roll (a favorable
characteristic considering the overflow and splashing of waves), and
also the suitability for long sea voyages.

Seaworthiness of ACV's is characterized by: vertical rolling,
pitching, side rolling, and by its so-called accelerations; loss of
speed in choppy sea conditions; yaw and drift; splashing on decks,
superstructures, and propelling agents; durability of the hull and
its specific construction; the possibility for maintenance of technical
equipment of the ACV while moving in choppy sea conditions; and the
general suitability of the ACV's to navigation in conditions of in-
creased choppy sea and winds.

To a considerable degree, the seaworthiness of an ACV is determined
by its rolling, which is itself the basic cause of lower operational
quality in moving over choppy seas. A number of these negative occur-
rences, called rolling, are attributed to:

A considerable loss of speed due to an increase of hydrodynamic
resistance with wash-off on the flexible skirts and hull and an increase
of reactively formed resistance with a great deal of pitching;

The possibility of a loss of local durability in the hull construc-
tion and overall durability, because of the appearance of additional
forces, called accelerations of vertical roll and pitch:

The possibility of the ACV overturning (especially while moving broadside to the waves with a great deal of drift, when the "slide" of the ACV on the waves may lead to blows on the lee side; and if the craft has considerable amplitude of side roll, then capsizing isn't excluded);

A deterioration of living conditions;

A sharp increase of overflow, hampering operation of the air screws and fans and promoting an intensive ice covering of the ACV at low temperatures; and a deterioration of control.

An ACV of the nozzle type, as already was noted, in the first phase of its development (until the invention and installation of flexible skirts) proved to be totally unseawothy because of intensive pitching and vertical rolling, accompanied by great accelerations and wash-off on the hull, sharply decreased its speed and made it unfit for operation in choppy sea conditions. Flexible skirts in the zone of the air cushions along the hull's perimeter (Class A) or in the extremities (Class B) permitted a considerable increase in clearance between the bottom of the ACV and the water's surface, which led to a considerable decrease in roll, a reduction of vertical acceleration, and a higher degree of seaworthiness. To the force of waves, the flexible skirts simply give way, resulting in considerably less wave resistance than an ACV without flexible skirts (Figure 170).
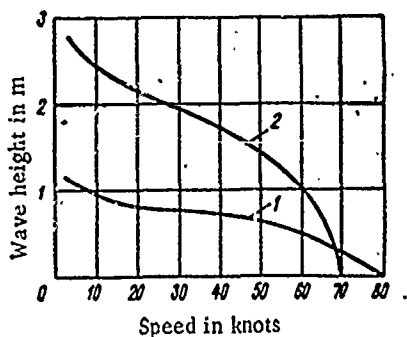

Figure 170. The Change in Seaworthiness of the SKMR-1 ACV with the Installation of Flexible Skirts; 1, Without flexible skirts; 2, With flexible skirts 1.2 meters high.

In such a way, flexible skirts opened new avenues of practical applications for ACV's in regions of increased choppiness of sea conditions. However, although flexible skirts decreased the subjection of an ACV to rolling, they could not eliminate it altogether. Every ACV is subject to rolling, and this remains a major problem for ACV's.

We note that, if the theory of rolling during the shift of a craft (one of the most complex disciplines of ship theory) has not been sufficiently worked out by now, then the theory of roll for ACV's only makes investigation of rolling in ACV's more difficult, since the interaction of the hull of the craft and the water across the air cushion is extremely complex and moments of force, acting on the ACV during rolling, appear, as a rule, as non-linear functions of the parameters of rolling and movement. The strict engineering organization of problems of rolling

2Nθ - damping moments.

In dividing the equation (501) by $J_x + \Delta J_x$, we get

$$\ddot{\theta} + 2v_\theta \dot{\theta} + n_\theta^2 \theta = 0, \tag{502}$$

where $v_\theta = N/J_x + \Delta J_x$ - coefficient of damping for side rolls.

Equations (501) and (502) are analogous equations for side roll in displacement-type craft on calm water, with resistance proportionate to the first degree of cornering speed with roll. The solution to this equation may be found in the form of

$$\theta = \theta_m e^{-v_\theta t} \cos(\omega_\theta t - \gamma_\theta), \tag{503}$$

where

$$\omega_0 = \sqrt{n_\theta^2 - v_0^2}; \quad \cos\gamma_\theta = \frac{1}{\sqrt{1 + \left(\frac{v_\theta}{\omega_0}\right)^2}}.$$

The expression (503) determines the dampening of fluctuation of movement with constant periods

$$T = \frac{2\pi}{\omega_\theta}$$

and with variable amplitude $\theta_m \cdot e^{-v_\theta t}$.
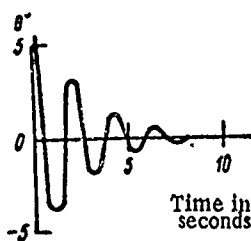
Figure 171. Damping of Side Fluctuations in the SKMR-1.

In Figure 171, the curve of the dampened side fluctuations in a model of the ACV SKMR-1 is set forth. As the drawing shows, the character of the side fluctuations agrees with equation (503).

In investigating an ACV's roll in average choppy sea conditions, one might take advantages of the method offered in a number of works, and substitute the wave surface with the surface of a hard screen moving at the speed of the waves, and the curve of the wave's profile. Then the perturbation forces, which act on the ACV, may be divided into two parts: the basic, determined by the supposition that the wave is not deformed by the ACV; and the hydrodynamic, with the stipulation of perturbation in introduction of the ACV to the dashing waves.

Perturbation moments, determined by the supposition that the wave is not deformed by the craft, the relative incline does not depart from the limits of linear length of the diagram Me = f(θ) and the width of the ACV, is small in comparison with the length of the waves, making

-380-

$$\dot{M}_{\text{возм}} = \frac{\partial M_\theta}{\partial \theta} \alpha_0 \sin \sigma t,$$

where α_0 - greatest angle of wave slope; and

σ - wave frequency.

In commensurability of the width of the ACV with wave length, the steepness of the wave to the full width of the craft will be altered. In theories on rolling in craft, this is accounted for by the introduction of the reduction coefficient x_0 in the expression of the amplitude of perturbation forces.

The hydrodynamic structure of the perturbation forces, in the first approximation, may also be accounted for by introduction of the correction factor k_1 in the expression of the amplitude of perturbation forces. Then the simplified equation for side roll in average choppy seas may be written as

$$(J_x + \Delta J_x)\ddot{\theta} + 2N\dot{\theta} + \frac{\partial M_\theta}{\partial \theta}\theta = \frac{\partial M_\theta}{\partial \theta} k_\theta \alpha_0 \sin \sigma t, \tag{504}$$

where $k_\theta = x_\theta \cdot k_1$ - correction factor depending on the expenditure of air, the height of the flexible skirts, the air pressure in the receiver and the cushions, the forms and relative measurements of the air cushions, and the relationship of the ACV's width to the length of the waves.

Testing of the models allows determination of the meaning of the correction factor. We note that equation (504) is correct, if the amplitudes of the rolling do not exceed the limits of the linear lengths of the diagram $M_\theta = f(\theta)$. In large amplitudes of rolling, the relationship of $M_\theta = f(\theta)$ may prove to be essentially non-linear and the differential equation of roll becomes complicated.

By dividing equation (504) by the coefficient, as a second derivative we get

$$\ddot{\theta} + 2\nu_\theta \dot{\theta} + n_\theta^2 \theta = k_\theta \alpha_0 n_\theta^2 \sin \sigma t. \tag{505}$$

Equations (504) and (505) are analogous to the shortened equations for side rolling, acquired in ship theory. A solution of equation (505) may be presented in the form of the sum of free and forced fluctuations

$$\theta = e^{-\nu_\theta t}\left(c_1 \cos \omega_\theta t + c_2 \sin \omega_\theta t\right) + \theta_m \sin\left(\sigma t - \delta_\theta\right), \tag{506}$$

where

$$\theta_m = \frac{k_\theta \sigma_0 n_\theta^2}{\sqrt{(n_\theta^2 - \sigma^2)^2 + 4v_\theta^2 \sigma^2}};$$

$$\tan \delta_\theta = \frac{2v_\theta \sigma}{n_\theta^2 - \sigma^2}; \quad \omega = \sqrt{n_\theta^2 - v_\theta^2} \approx n_\theta;$$

(507)

c_1 and c_2 - arbitrary constants, determined by primary conditions.

Free fluctuations in an ACV on actual choppy seas quickly fade, while forced fluctuations originate with frequency of perturbation forces: while moored, from wave frequency σ; and while moving, from so-called "apparent frequency," frequency of meeting with waves;

$$\sigma_\kappa = \sigma + \frac{\sigma^2}{g} V \cos \varphi,$$

where V - speed of the ACV in meters per second; and
ψ - course angle of the waves[1].

In Figure 172, data is set forth concerning the meanings of results of testing models for sweeps of side roll for a launch on air cushions, the SKMR-1, in moving broadside to waves at speeds up to 20-35 knots. As one can see from the drawing, the speed in practice does not influence the sweeps of roll. In higher waves (from 0.6-0.9 meters to 1.8 meters) the sweeps of side roll increase 1.5--2.2 times (from 10 to 16-22°). A change in wave lengths at h_V = 0.6-0.9 meters by 1.5 times does not lead to a considerable change in the sweeps of roll. At wave heights of 1.8 meters, an increase in their lengths from 20 to 30 meters leads to a decrease in the sweeps of roll by approximately 30% (from 22-23° to 16-18°).
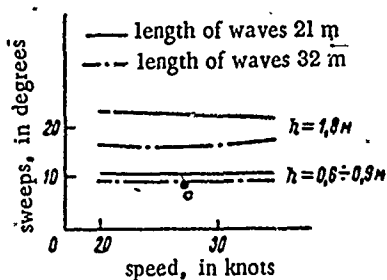
Figure 172. Side Roll in the SKMR-1 ACV in Average Choppy Sea Conditions.

The amplitudes of side roll in an ACV on average choppy seas reach maximum meaning in moving broadside to waves (course wave angle = 90°), as well as at sharp angles while moving at a speed, at which the period of meeting waves is close to the period of actual side fluctuations in the ACV.

Roll in an ACV on irregular choppy seas considerably differs from roll on average choppy seas and is characterized by a lack of visible regularity

---

[1]We note that Class A ACV's in crosswinds move with considerable drift angle, therefore, the angle under which waves are met by the ACV's differs from the course angle of the quantity of drift angle.

in alteration of amplitudes and periods of constant fluctuations.

In theories on roll in craft, it is establ.:ned that in frequency of perturbation moments, close to resonance, irregularity during periods of choppy sea condi: ons may lead to a decrease in total amplitude in comparison with computations in accordance wit'. theories of forced fluctuations or those measured in average choppy sea conditions. In frequency of perturbation moments, distant from resonance, irregularity of choppy seas may lead to an increase in total amplitude in comparison with that computed or measured in average choppy sea conditions.

It may be conjectured that this proposition is correct also in computing roll in ACV's.

Regarding investigations of roll in irregular choppy sea conditions, in current theories on roll methods in theory of stationary causal processes are being widely used. The craft is considered as a linear fluctuating system, the choppy sea conditions - as the entering causal process, resulting in the departing process of roll.

The basic tenets of the probability calculations of roll in craft apply also to calculations of roll in ACV's. We recall these tenets from [58]. As is known from the theories dealing with stationary causal processes, the entrance and departure processes, the depicted linear equations are bound by the theory of A. Ya. Khinchin relative to

$$S_{\text{out}}(\sigma) = |\overline{\Phi}|^2 S_{\text{in}}(\sigma),$$

(5'8)

where $S_{\text{out}}(\sigma)$ - spectral density of the departure process (rolling);

$S_{\text{in}}(\sigma)$ - spectral density of the entrance process (choppy sea conditions);

Φ - intermediate functions (dynamic reaction of the ship to a single harmonious perturbation).

As far as spectral density of choppy sea conditions, it has been well studied and may be expressed by well-known formulae (of Voznesenski, Firsov, Neiman, Derbyshire and others), with the probability calculation of roll problems leading to the determination of the intermediate functions. The intermediate function for side roll in an ACV moving broadside to waves may be acquired with the help of the expressions for amplitude of forced fluctuations (507), if one substitutes in the formula $\alpha_0 = \sigma^2/g \cdot h_v/2$

and it is assumed that $h_v/2 \approx 1.0,$

$$\overline{\Phi}_\theta = \frac{k_\theta n_\theta^2 \sigma^2 \cdot}{g \sqrt{(n_\theta^2 - \sigma^2)^2 + 4 v_\theta^2 \sigma^2}}.$$

-383-

With the movement of a craft at an angle ϕ toward the front of the waves, the intermediate function may be conceived relative to

$$\Phi_\theta = \frac{k_\zeta n_\theta^2 \sigma^2 \sin \phi}{g \sqrt{(n_\theta^2 - \sigma_\kappa^2)^2 + 4 v_\theta^2 \sigma_\kappa^2}}.$$

Consequently, the expression for the frequency spectrums of side roll in an ACV at all rates of movement may be written in the form of

$$S_\zeta(\sigma) = \frac{k_\zeta^2 n_\theta^4 \sigma^4 \sin^2 \phi}{g^2 [(n_\theta^2 - \sigma_\kappa^2)^2 + 4 v_\theta^2 \sigma_\kappa^2]} S_{y_B}(\sigma). \qquad (509)$$

According to the spectrum, dispersion D_θ and amplitudes of roll may be calculated, given the provision

$$D_\theta = \int_0^\infty S_\theta(\sigma)\, d\sigma; \qquad (510)$$

$$\theta_{n\%} = \frac{1}{4} \sqrt{D_\theta} \sqrt{2 \ln \frac{1}{n\%}}, \qquad (511)$$

where n% - the given provision.

Further, by the known relative theory of stationary causal processes, the spectral density of dispersion and amplitude meanings for speed and acceleration of roll (as well as the average frequencies and periods of roll) may be acquired.

Today, probability calculations of roll in an ACV may be considered only as highly conditional. It was already noted above that probability calculations are suitable only for examining the processes, depicted by linear differential equations. Regarding side roll in an ACV with considerable amplitudes, it is possible to have considerable non-linearity of the restored and damping moments, therefore, the limits of suitability for probability calculations require special investigation.

Of interest is becoming acquainted with the results of measurements of the parameters of roll for actual-size ACV's, during movement in irregular choppy sea conditions.

In the analysis of the craft's roll, two probability methods are employed: statistical and spectral
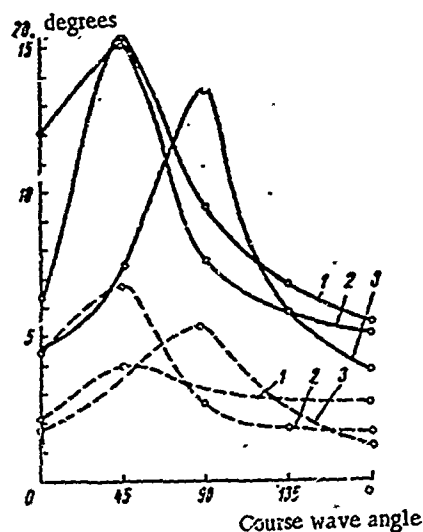
Figure 173. The Relationship of Maximum and Average Cycles of Side Roll in an ACV to the Course Angle of the Waves.

1, Without flexible skirts, waves of $h_{3\%}$ = 0.6 mmeters; V = 25 knots; 2, With flexible skirts, $h_{g \cdot o}$ = 0.4 meters, waves of $h_{3\%}$ = 0.7-1.0 meters, V = 30 knots; 3, With flexible skirts, $h_{g \cdot o}$ = 1 meter, waves of $h_{3\%}$ = 1 meter, V = 30 knots; ———————— maximum sweeps; ----------- average sweeps.

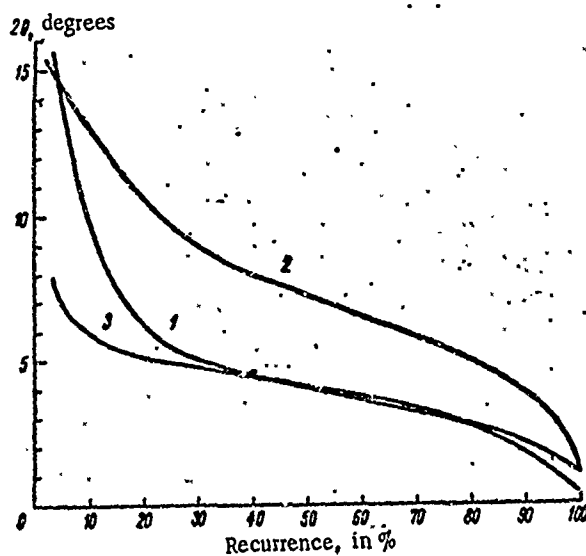
Figure 174. Curved Distributions of the Cycles of Side Roll, Course Wave Angle = 45°.

1, Without flexible skirts, waves of $h_{3\%}$ = 0.6 meters, V = 25 knots; 2, With flexible skirts, $h_{g \cdot o}$ = 0.4 meters, waves of $h_{3\%}$ = 0.7-1.0 meters, V = 30 knots; 3, With flexible skirts, $h_{g \cdot o}$ = 1 meter, waves of $h_{3\%}$ = 1 meter, V = 30-35 knots.

In the statistical method, cycles and half-cycles of roll are considered as a system of dual-correlated causal quantities. In quality of probability characteristics, these quantities are received as: the average and greatest meanings of cycles and half-cycles; the dispersion of cycles and half-cycles; the coefficient variations (variables) of cycles and half-cycles; the coefficient of the correlation between the cycles and the corresponding half-cycles.

Knowledge of these quantities, as a rule, is sufficient for quantitative estimations of the processes of rolling. In those cases, where it is necessary to present the choppy sea conditions and the roll as non-statistical totals of fluctuation elements, and in a form of a continuous physical process conforming to the spectral method of describing causal processes, the calculations are labor-consuming.

In Table 18, results are set forth for the determination of empirical functions for the distribution of cycles and half-cycles of side rolling, as well as showing calculations of the statistical characteristics of an air cushion launch with a displacement of 30 tons, moving broadside to the waves.

TABLE 18. CORRELATION TABLE OF DISTRIBUTION OF SWEEPS AND HALF-CYCLES IN SIDE-ROLL OF ACV's G = 30 TONS

Intervals $\Delta\tau$		Force and wave type $h_{3\%} = 1,0$ м, wind				
		Speed and wind force $v = 8$-10 meters per second				
		Intervals ΔH				
		0—0,1	0,1—0,2	0,2—0,3	0,3—0,4	0,4—0,5
		0,05	0,15	0,25	0,35	0,45
0—0,1	0,05					
0,1—0,2	0,15					
0,2—0,3	0,25	1	2		1	2
0,3—0,4	0,35	5	7	6	2	4
0,4—0,5	0,45	2	6	7	8	3
0,5—0,6	0,55		3	4	5	1
0,6—0,7	0,65				4	
0,7—0,8	0,75				1	
0,8—0,9	0,85				1	
0,9—1,0	0,95					
1,0—1,1	1,05					
Σn	I	9	18	17	22	10
P_H	II	0,084	0,168	0,159	0,206	0,094
$P_H \cdot H$	III	0,0042	0,0252	0,0396	0,072	0,0423
$H - \Sigma P_H \cdot H$	IV	—0,321	—0,221	—0,121	—0,021	0,079
$(H - \Sigma P_H \cdot H)^2$	V	0,104	0,049	0,0147	0,00045	0,0064
$P_H (H - \Sigma P_H \cdot H)^2$	VI	0,0087	0,0082	0,00234	0	0,0066
$\Sigma \tau \cdot n_H$	VII	3,25	8,1	9,15	13,7	5,90
$\dfrac{\Sigma \tau n_H}{n_H}$	VIII	0,365	0,45	0,54	0,623	0,59
$\Sigma \tau \cdot n_H \cdot H$	IX	0,16	1,22	2,29	4,80	2,66

continuation of Table 18

Intervals Δτ		Intervals ΔH						n_τ	P_τ
		0,5—0,6	0,6—0,7	0,7—0,8	0,8—0,9	0,9—1,0	1,0—1,1	1	2
		0,55	0,65	0,75	0,85	0,95	1,05		

Force and wave type $h_{3\%} = 1.0$ meters, wind — Speed V = 60 km per hour

Speed and wind force v = 8-10 meters/second — Course angle of waves 90°

Intervals Δτ		0,55	0,65	0,75	0,85	0,95	1,05	n_τ	P_τ
0—0,1	0,05							1	0,0093
0,1—0,2	0,15							9	0,0643
0,2—0,3	0,25			2				23	0,215
0,3—0,4	0,35		1		1			29	0,27
0,4—0,5	0,45		2	2				24	0,224
0,5—0,6	0,55	2	3					7	0,0655
0,6—0,7	0,65	3	3	3				5	0,0468
0,7—0,8	0,75	2	1					5	0,0468
0,8—0,9	0,85	3						4	0,0374
0,9—1,0	0,95	2	1			1			
1,0—1,1	1,05	2	1				1		
Σn_l	1	1ν	9	5	1	1	1	107	

P_H	II	0,131	0,084	0,0467	0,0094	0,0094	0,0094		
$P_H \cdot H$	III	0,072	0,0545	0,035	0,0072	0,00895	0,0099	0,371	
$H - \Sigma P_H \cdot H$	IV	0,179	0,279	0,379	0,479	0,579	0,679		
$(H - \Sigma P_H \cdot H)^2$	V	0,0321	0,078	0,144	0,23	0,335	0,46		
$P_H (H - \Sigma P_H \cdot H)^2$	VI	0,00421	0,0066	0,0067	0,0022	0,00314	0,00432	0,052	
$\Sigma \tau \cdot n_H$	VII	11,10	6,15	2,85	0,45	0,95	1,05		
$\dfrac{\Sigma \tau n_H}{n_H}$	VIII	0,8	0,685	0,572	0,45	0,95	1,05		
$\Sigma \tau \cdot n_H \cdot H$	IX	6,10	4,0	2,13	0,38	0,90	1,10	25,8	

Force and wave type $h_{3\%} = 1.0$ meters, wind — Greatest sweep $H_{max} = 13.6°$

Speed and wind force v = 8-10 meters/second — Greatest half-cycle $\tau_{max} = 6$ seconds

Intervals Δτ		$P_\tau \cdot \tau$	$\tau - \Sigma P_\tau \cdot \tau$	$(\tau - \Sigma P_\tau \cdot \tau)^2$	$P_\tau (\tau - \Sigma P_\tau \cdot \tau)^2$	$\Sigma (H \cdot n_\tau)$	$\dfrac{\Sigma H \cdot n_\tau}{n_\tau}$	$\Sigma H \cdot n_\tau \cdot \tau$
		3	4	5	6	7	8	9
0—0,1	0,05							
0,1—0,2	0,15							
0,2—0,3	0,25	0,00233	—0,336	0,113	0,00105	0,05	0,05	0,01
0,3—0,4	0,35	0,0295	—0,236	0,055	0,0047	0,95	0,105	0,33
0,4—0,5	0,45	0,0965	—0,136	0,0185	0,0039	7,25	0,333	3,26
0,5—0,6	0,55	0,15	—0,036	0,0013	0,0063	9,65	0,326	5,3
0,6—0,7	0,65	0,145	0,064	0,0041	0,0009	10,40	0,435	6,76
0,7—0,8	0,75	0,048	0,164	0,027	0,0017	3,15	0,45	2,35
0,8—0,9	0,85	0,040	0,264	0,070	0,0033	2,45	0,49	2,08
0,9—1,0	0,95	0,0445	0,364	0,133	0,0062	3,05	0,61	2,90
1,0—1,1	1,05	0,0375	0,463	0,214	0,006	2,80	0,70	2,94
Σn_l	1	0,593			0,028			25,80

			Sweeps H	Half-cycles τ
P_H	II			
$P_H \cdot H$	III	Parameters of Distribution	Sweeps H	Half-cycles τ
$H - \Sigma P_H \cdot H$	IV	Average Meaning	$\bar{H} = 5,3$	$\bar{\tau} = 3,55$
$(H - \Sigma P_H \cdot H)^2$	V	Dispersion	$D_H = 9,70$	$D_\tau = 1,01$
$P_H (H - \Sigma P_H \cdot H)^2$	VI	Coefficient	$U_H = 0,615$	$U_\tau = 0,28$
$\Sigma \tau \cdot n_H$	VII			
$\dfrac{\Sigma \tau n_H}{n_H}$	VIII			
$\Sigma \tau \cdot n_H \cdot H$	IX	Coefficient Correlations	$r_{H\tau} = 0,24$	

Data concerning the relationships of maximum and average cycles of side roll in this launch to the course wave angle is in Figure 173, and in Figure 174 - the curves of their distribution.

An analysis of the recorded side rolling of the ACV in irregular choppy sea conditions allows one to make the following basic conclusions:

a) At wave heights of 3%, exactly equal to the height of the flexible skirts, the sweeps of side roll reach a maximum 10-15° with course wave angle = 45-90°. In moving against the waves (course wave angle = 0°) and along the waves in conditions of 3-dimensional windy sea conditions, the sweeps of side roll do not exceed 5-6°;

b) In contrast to displacement-type craft, periods of side roll in ACV's almost coincide with periods of pitching:

c) Cycles of side roll in displacement-type craft may exceed the cycles in ACV's.

§29. Vertical Rolling

Acting in vertical fluctuations of an ACV are: inertial resilient forces of the air cushions, formed as a result of the inertial influence of the water; damping forces of the air cushions, proportionate speeds of linear shifts; resilient forces of the air cushions, proportionate quantities of linear shifts.

As experiments of model ACV's show, vertical rolling does not have a substantial influence on the keel, so that it is possible to examine vertical rolling clearly.

An equation for vertical rolling on calm water may be written in the form of

$$\left(\frac{G}{g} + \Delta M\right)\ddot{y} + 2N_y\dot{y} + \frac{\partial Y}{\partial h}y = 0 \qquad (512)$$

or

$$\ddot{y} + 2\nu_y \cdot \dot{y} + n_p^2 y = 0. \qquad (513)$$

Equation (513) is analogous to equation (502). Its solution may be written as

$$y = y_m e^{-\nu_y t} \cos(\omega_1 t - \gamma_y). \qquad (514)$$

Equation (514) determines the damping of the fluctuating movement with the period $2\pi/\omega_1$.

In Figure 175, the curves of damping of vertical fluctuations in models of the ACV SKMR-1 on calm water and over hard screens are set forth. From the drawing, one sees that vertical fluctuations over a hard screen dampen faster than over water, and the true period of fluctuation over the hard screen is less. This is explained by the great meaning of the coefficient of damping of vertical roll over a hard screen.

Observations of vertical rolling in an ACV on average choppy seas also may profit by assumption of substitution of wave systems with undeformed wavy surfaces, and subsequently in the acquired meanings of the perturbation forces to bring about the correction factor, taking into account the distinction between the water's surface and the undeformed surface.

Then the equation for vertical rolling on average choppy seas, with the ACV moving broadside to the waves, may be written as

$$\left(\frac{G}{g}+\Delta M\right)\ddot{y}+2N_y\dot{y}+\frac{\partial Y}{\partial h}\,y=\frac{h_z}{2}\,k_y\frac{\partial Y}{\partial h}\cos \sigma t, \tag{515}$$

where h_v - wave height;

k_y - correction factor, taking into account the limit of the relationship of the ACV's dimensions to the length of the waves.
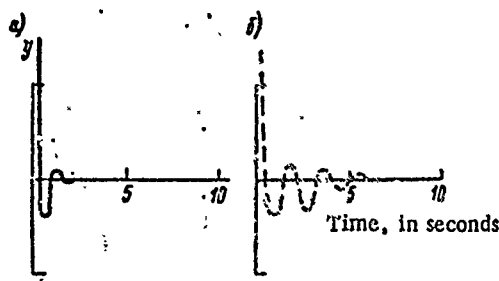

Figure 175. Damping of Vertical Fluctuations in the ACV SKMR-1. a, over a hard screen; b, over water.

Analogous to equation (505), the solution of equation (515) may be written as

$$y=e^{-\nu_y t}\,(c_1'\cos\omega_1 t+c_2'\sin\omega_1 t)+y_m\cos(\sigma t+\varepsilon). \tag{516}$$

-389-

In such a form, vertical rolling in an ACV on average choppy seas consists of free and forced fluctuations. Forced fluctuations occur with frequency perturbation forces.

In Figures 176b and 176c, data concerning the cycles of vertical roll in the SKMR-1, moving broadside to the waves, is set forth. An examination of the graphs allows one to conclude that, at increased wave heights the cycles of vertical roll increase proportionately to the wave height. An increase in wave lengths also leads to some increase in cycles of vertical roll, but up to a limit. The growth of speed in amplitude of roll is changed very little. In Figure 176a, the curves of cycles of vertical roll for a craft moving at 30 knots and at various course angles in relationship to waves, as well as five meanings of wave length, are set forth. From the graphs one sees that, in moving at sharp course angles, the amplitudes of vertical rolling may somewhat exceed the amplitudes during movements broadside to the waves.
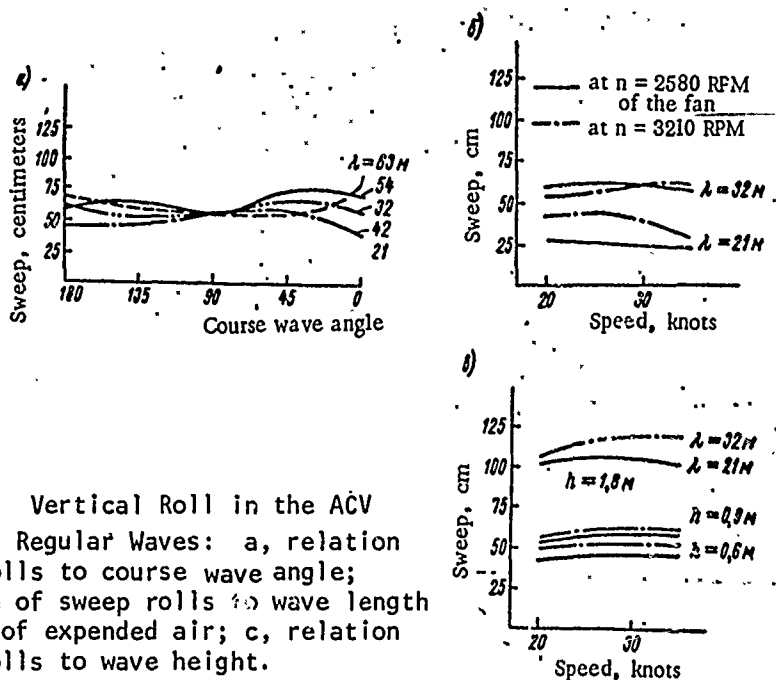

Figure 176. Vertical Roll in the ACV SKMR-1 over Regular Waves: a, relation of sweep rolls to course wave angle; b, relation of sweep rolls to wave length and volume of expended air; c, relation of sweep rolls to wave height.

In Figure 177, the relationships of maximum cycles of vertical roll to wave height are set forth, and in Figure 178 - curves of the distribution of cycles of vertical roll in an experimental craft on extremely rough seas. It might be noted that maximum cycles of vertical roll do not exceed 0.6-0.65 $h_{3\%}$.
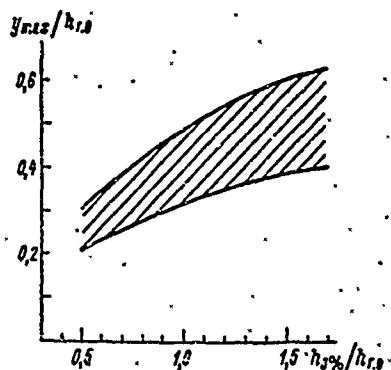
$y_{r.s}/h_{r.s}$

0,6

0,4

0,2

0,5   1,0   1,5 $h_{3\%}/h_{r.s}$

23,65

30 Course wave
angle = 0°

45°

20

135°

10 180°

0   20   40   60   80   100

Recurrence, %

Figure 177. Relation of Maximum
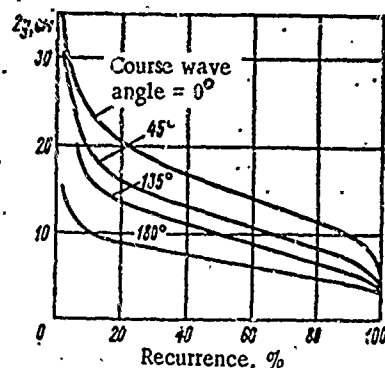Sweep Vertical Rolls to Wave
Height.

Figure 178. Uneven Distribution
of Sweep Vertical Rolls at $h_{3\%}$ =
= 0.8 meters.

§30. Pitching

Acting in angular fluctuations, relative to the axis 0_z of an
ACV, are: inertial moments of force, including moments of force of
the inertial influence of water transferred to the hull on account
of the redistribution of air pressure in the cushion (the inertial
makeup of resilient forces); moments of force conditional to the air
cushions (recovered moments proportionate to the angle of trim dif-
ference, and damping moments proportionate to the angle of speed of
the longitudinal fluctuations); moments of force from the interactions
of the pneumatic elements of the flexible skirts (or even the hull)
with the water's surface; moments of force from the reactions of the
intake of the fans and the escaping air, as well as the inertial influence of
air flowing through the air ducts of the ACV; moments of force arising
in the stern's horizontal tail unit; the gyroscopic moments from the
revolutions of the screws and the fans.

As tests in models show, pitching in an ACV influences it vertically,
therefore only conditionally may the equations for pitching be examined
in a "clear" view.

The equation for pitching in calm waters has the following form:

$$(J_z + \Delta J_z)\ddot{\psi} + 2N_\psi\dot{\psi} + \frac{\partial M_\psi}{\partial\psi}\psi = 0, \tag{517}$$

where ΔJ_z - inertial makeup of the resilient forces of the air cushions;

$2N_\psi\psi$ - damping moments;

$\partial M_\psi/\partial\psi\ \psi$ - recovered moments.

-391-

The division of $(J_z + \Delta J_z)$ in equation (517) leads to the form

$$\ddot{\psi} + 2\nu_\psi \dot{\psi} + n_\psi^2 \psi = 0. \tag{518}$$

Equation (518) is analogous to (502) and appears equal in damping fluctuations with constant periods and variables of amplitude. The solution for it may be written in the form

$$\psi = \psi_m e^{-\nu_\psi t} \cos(\omega_\psi t - \delta_\psi),$$

$$\omega_\psi = \sqrt{n_\psi^2 - \nu_\psi^2};$$

where

$$\cos \delta_\psi = \frac{1}{\sqrt{1 + \left(\dfrac{\nu_\psi}{\omega_\psi}\right)^2}}. \tag{519}$$

In Figure 179, results are set forth for a basic experiment for curves of damping fluctuations in models of the ACV SKMR-1 over a hard screen and in calm waters. From the drawing one sees that, the characteristic of damping fluctuations in the models corresponds to equation (519). Fluctuations over a hard screen are dampened considerably faster than in calm waters. The true period of fluctuation over a hard screen is somewhat less than the period in calm waters. In comparing Figures 171, 175 and 179, it may be noted that the true period of pitching in calm waters is larger than the periods of side roll and vertical roll.
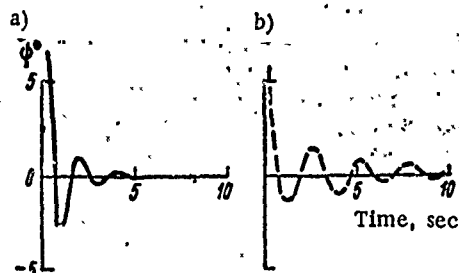

Figure 179. Damping of Fluctuations in the SKMR-1, Relative to the Transverse Axis:
a, Over a hard screen· b, over water.

In examining pitching of an ACV in average sea conditions, at rest or moving, against or along waves, one may again resort to the substitu-

tion of wave systems with undeformed wavy surfaces and come up with
perturbation forces on the ACV made up of two components: basic per-
turbation forces, attributed to the assumption that the wave is not
deformed by the craft (the ACV moves along the undeformed wavy surface);
hydrodynamic perturbation forces, conditional perturbation by intro-
ducing the ACV to the dashing of the waves.

The perturbation moments, attributed to the assumption that
the wave is not deformed by the craft and the length of the ACV is
small compared to the wave length, then will equal

$$M_{\text{возм}} = \frac{\partial M_{\psi}}{\partial \psi} \alpha_0 \sin \sigma t.$$

Commensurability of the length of the ACV with the wave length may be
computed by introducing the reduction factor x_{ψ} in the expression for
the amplitude of perturbation forces.

The hydrodynamic composition of the perturbation forces also may
be computed by introducing the correction factor k_2 in the expression
for the amplitude of perturbation forces.

The simplified equation for pitching in normal sea conditions is
written as

$$(J_z + \Delta J_z)\ddot{\psi} + 2N_{\psi}\dot{\psi} + \frac{\partial M_{\psi}}{\partial \psi}\psi = \frac{\partial M_{\psi}}{\partial \psi} k_{\psi}\alpha_0 \sin \sigma t \qquad (520)$$

or

$$\ddot{\psi} + 2\nu_{\psi}\dot{\psi} + n_{\psi}^2\psi = k_{\psi}n_{\psi}^2\alpha_0 \sin \sigma t, \qquad (521)$$

where $k_{\psi} = k_2 \cdot x_{\psi}$ - correction factor, the meaning of which may be
determined from a test of the known meanings of the coefficients in
the lift-hand part of the equations and the recorded pitch of the
models. The coefficient k_{ψ} depends upon the quantities of air expen-
diture, the pressure of air in the cushions and the flexible receiver,
and the forms and dimensions of the air cushions.

Equation (521) is correct as long as the amplitudes of pitching
do not deviate from the limits of the linear part of the diagram $M(\psi) = f(\psi)$. The solution to equation (521) may be presented in the form
of the total free and forced fluctuations

$$\psi = e^{-\nu_\psi t}(c_3 \cos \omega_\psi t + c_4 \sin \omega_\psi t) + \psi_m \sin(\sigma t - \delta_\psi); \quad (522)$$

$$\psi_m = \frac{k_\psi n_\psi^2}{\sqrt{(n_\psi^2 - \sigma^2)^2 + 4\nu_\psi^2 \sigma^2}};$$

$$\text{tg}\,\delta_\psi = \frac{2\nu_\psi \sigma}{n_\psi^2 - \sigma^2}. \quad (523)$$

True fluctuations of pitching quickly are eliminated and the ACV experiences only forced fluctuations, with periods equal to the periods of perturbation forces.

In Figure 180, graphs showing the cycles of pitch in the ACV SKMR-1 in normal sea conditions are set forth. An examination of the graphs allows one to make the following conclusions: the greatest cycles of pitch are found in moving against the waves (course wave angle = 0°); an increase in wave height leads to an intensive increase in amplitude of pitching; in increasing wave lengths to a certain limit, an increase in the amplitude of roll occurs, and in further lengthening of the waves, the amplitude of pitch is decreased. The greatest amplitude of pitching is attained in wave lengths, which exceed the length of the ACV by 1.5 times an increased expenditure of air leads to a considerable decrease of cycles of pitch. The influence of the changes in air expenditure is especially perceptible in moving over waves of "critical lengths ($\lambda \approx 1.5$ L_p); cycles of pitching depend on speeds of movement, but for waves of diverse lengths this relationship is different.

Testing of model ACV's in a basin allowed the establishment of the linear characteristics of recovered moments of force in a sufficiently wide-range angle of trim difference in an ACV with flexible skirts. Connected with this is the correct applicability of the probability computations of the parameters of pitching in the ACV in extremely rough sea conditions.

As was noted in §28, making probability computations of a problem leads to the determination of the intermediate function Φ, expressed by the dynamic reaction of the craft to singular harmonious perturbation. The intermediate function for pitching in an ACV with course wave angle = 0° and without movement may be written in the form of

$$\overline{\Phi}_\psi = \frac{k_\psi n_\psi^2 \sigma^2}{g\sqrt{(n_\psi^2 - \sigma^2)^2 + 4\nu_\psi^2 \sigma^2}}. \quad (524)$$

In the movement of a craft at an angle of ϕ toward the front of the waves, the intermediate function may be presented relative to

$$\overline{\Phi}_\psi = \frac{k_\psi n_\psi^2 \sigma^2 \cos \varphi}{g\sqrt{(n_\psi^2 - \sigma_\kappa^2)^2 + 4\nu_\psi^2 \sigma_\kappa^2}}.$$
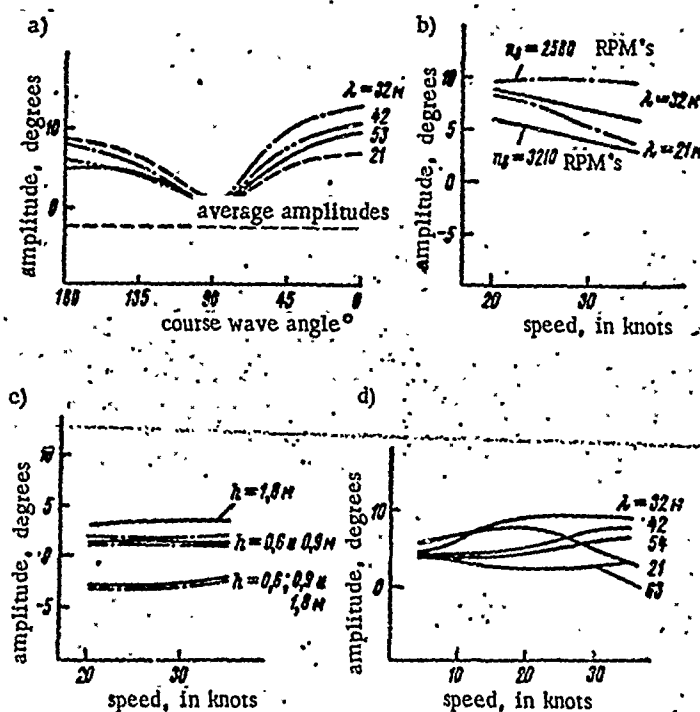
Figure 180. Pitch in the SKMR-1 in Normal Sea Conditions: a, The relation-
ship of the amplitude of roll to the course wave angle; b, The relationship
of the amplitude of roll to the output of the fans; c, The relationship of
the amplitude of roll to wave height; d, The relationship of the amplitude
of roll to speed and wave length.

According to Khinchin's theory, the expression for the frequency spec-
trum of pitch in an ACV, moving on an arbitrary course at a given speed,
may be written in the form

$$S_\psi = \frac{k_\psi^2 n_\psi^4 \sigma^4 \cos^2 \varphi}{g^2 \left[(n_\psi^2 - \sigma_\kappa^2)^2 + 4 \nu_\psi^2 \sigma_\kappa^2 \right]} S_{y_a}(\sigma), \qquad (525)$$

where $S_{y_v}(\sigma)$ - spectrum of the sea conditions.

According to the spectrum of (525), as was shown above, the following
may be computed: dispersion D_ψ and amplitude of roll of a given provision,

-395-

amplitude meanings for speed and accelerations of roll, and the average frequencies and periods of roll.

In such a way, from the results received from testing models in a basin (with meanings of coefficients k_ψ, n_ψ, v_ψ) the probability computation of the parameters of pitch in an ACV on extremely choppy seas may be accomplished.

Observations show that pitch in an actual-size ACV on extremely choppy seas has its own peculiarities. Thus, in moving in a private reservoir, with short, steep waves, the amplitude of roll is insignificant, but the periods are short and this creates an effect of constant fluctuation.

In the open sea, rolling changes considerably. In moving over waves of critical lengths ($\lambda \approx 1.2-2.0\ L_p$) with course wave angle = 0°, rolling becomes sharp, arousing lassitude and loss of capacity for work. Vertical blows are observed in some parts. A considerably abatement of the amplitude of rolling may be attained with increased air expenditure. In great wave lengths, their influence is decreased. With $\lambda = 6L$ in the ACV, the waves are hardly felt. Movement along the waves (course wave angle = 180°) is the smoothest, however, the control devices become almost ineffective.

In regard to the essential differences in the character of pitch of an ACV in a private reservoir and on the open sea, it is necessary to obtain from the probability computations first-rate calculations of the spectrum of the sea conditions, characteristic for its area, where the planned ACV will be operated.

To some degree, pitch in an ACV in extremely choppy sea conditions may be characterized by that data set forth in Table 19 for statistical analysis, as well as by the relationships of maximum and average cycles to course wave angle (Figure 181) and by the curves for distribution of the cycles (Figure 182).
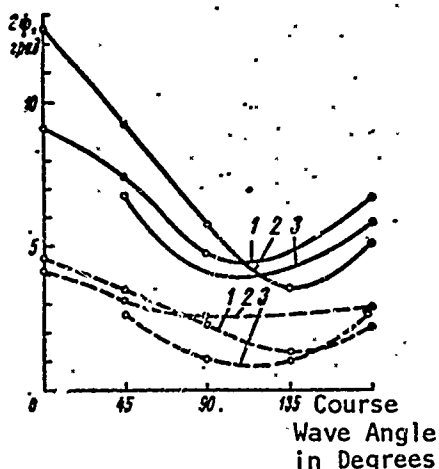

Figure 181. The Relationship of Maximum and Average Cycles of Pitch to Course Wave Angle; 1, without flexible skirts, waves of $h_{3\%} = 0.6$ meters, V = 25 knots; 2, with flexible skirt skirts, $h_{r \cdot o} = 0.4$ meters, waves of $h_{3\%} = 0.7-1.0$ meters, V = 30 knots; 3, with flexible skirts, $h_{r \cdot o} = 1$ meter, waves of $h_{3\%} = 1$ meter, V = 30--35 knots; ———— maximum cycles; ------ average cycles.

TABLE 19. CORRELATION TABLE OF DISTRIBUTION OF SWEEPS AND HALF-CYCLES IN PITCHING OF ACV'S G = 30 TONS

Force and wave type $h_{3\%} = 1,0$ м, wind

Speed and wind force v = 8-10 meters per second

Intervals Δτ		Intervals ΔH				
		0—0,1	0,1—0,2	0,2—0,3	0,3—0,4	0,4—0,5
		0,05	0,15	0,25	0,35	0,45
0—0,1	0,05					
0,1—0,2	0,15		1		1	
0,2—0,3	0,25	2	1	1	1	
0,3—0,4	0,35		5	4	2	
0,4—0,5	0,45		1	5	5	3
0,5—0,6	0,55			5	4	4
0,6—0,7	0,65			2	6	4
0,7—0,8	0,75			3		2
0,8—0,9	0,85				1	1
0,9—1,0	0,95					1
1,0—1,1	1,05					1
Σn_i	I	2	13	20	20	16
P_H	II	0,016	0,104	0,160	0,160	0,128
$P_H \cdot H$	III	1,0008	0,0156	0,0400	0,0460	0,0576
$H - \Sigma P_H \cdot H$	IV	−0,425	−0,325	−0,225	−0,125	−0,025
$(H - \Sigma P_H \cdot H)^2$	V	0,1800	0,1080	0,0502	0,0156	0,0007
$P_H (H - \Sigma P_H \cdot H)^2$	VI	0,0029	0,0112	0,0080	0,0025	—
$\Sigma(\tau \cdot n_H)$	VII	0,50	4,95	10,20	10,30	10,50
$\dfrac{\Sigma \tau n_H}{n_H}$	VIII	0,25	0,37	0,51	0,45	0,67
$\Sigma \tau \cdot n_H \cdot H$	IX	0,03	0,74	2,55	3,6	4,72

Force and wave type $h_{3\%} = 1,0$ м, wind   Speed v = 60 kilometers per hour

Speed and wind force v = 8-10 meters per second   Course angle of waves 180°

Intervals Δτ		Intervals ΔH						n_τ	P_τ
		0,5—0,6	0,6—0,7	0,7—0,8	0,8—0,9	0,9—1,0	1,0—1,1	i	2
		0,55	0,65	0,75	0,85	0,95	1,05		
0—0,1	0,05								
0,1—0,2	0,15		1					2	0,016
0,2—0,3	0,25							6	0,048
0,3—0,4	0,35				2			12	0,096
0,4—0,5	0,45	1	4	1	3			25	0,200
0,5—0,6	0,55	4	5	1	2	1		32	0,257
0,6—0,7	0,65	9		3		1	1	29	0,232
0,7—0,8	0,75	5	3	2				9	0,072
0,8—0,9	0,85	2						6	0,048
0,9—1,0	0,95	1			1			2	0,016
1,0—1,1	1,05	1						2	0,016
Σn_i	I	23	13	7	8	2	1	125	
P_H	II	0,184	0,104	0,056	0,064	0,016	0,008		
$P_H \cdot H$	III	0,1010	0,0676	0,0408	0,0544	0,0228	0,0084	0,475	
$H - \Sigma P_H \cdot H$	IV	0,0785	0,175	0,275	0,375	0,475	0,575		
$(H - \Sigma P_H \cdot H)^2$	V	0,0056	0,0305	0,076	0,1400	0,2250	0,330		
$P_H (H - \Sigma P_H \cdot H)^2$	VI	0,0010	0,0030	0,0042	0,0090	0,0026	0,0026	0,0470	
$\Sigma(\tau \cdot n_H)$	VII	13,75	8,25	4,45	4,80	1,200	0,65		
$\dfrac{\Sigma \tau n_H}{n_H}$	VIII	0,73	0,64	0,64	0,60	0,60	0,65		
$\Sigma \tau \cdot n_H \cdot H$	IX	7,6	5,36	3,34	4,08	1,14	0,68	33,0	

		$P_\tau \cdot \tau$	$\tau - \Sigma P_\tau \cdot \tau$	$(\tau - \Sigma P_\tau \cdot \tau)^2$	$P_\tau(\tau - \Sigma P_\tau \cdot \tau)^2$	$\Sigma(H \cdot n_\tau)$	$\frac{\Sigma H n_\tau}{n_\tau}$	$\Sigma H n_\tau \cdot \tau$
Intervals $\Delta \tau$		3	4	5	6	7	8	9
0—0,1	0,05	0,0004	—0,504	0,2540	0,0041	0,50	0,25	0,06
0,1—0,2	0,15	0,012	—0,404	0,1740	0,0064	1,50	0,25	0,38
0,2—0,3	0,25	0,0536	—0,304	0,0930	0,0069	3,00	0,35	1,05
0,3—0,4	0,35	0,0900	—0,204	0,0416	0,0063	9,75	0,35	4,40
0,4—0,5	0,45	0,1430	—0,104	0,0108	0,0028	16,40	0,51	9,15
0,5—0,6	0,55	0,1510	—0,004	0,00002	—	16,35	0,57	10,65
0,6—0,7	0,65	0,0560	0,096	0,0093	0,0007	4,30	0,48	3,22
0,7—0,8	0,75	0,0408	0,196	0,0386	0,0019	3,30	0,55	2,80
0,8—0,9	0,85	0,0015	0,296	0,0880	0,0014	1,30	0,65	1,23
0,9—1,0	0,95	0,0168	0,396	0,157	0,0025	1,00	0,50	1,06
1,0—1,1	1,05							
Σn_τ	1	0,847			0,0390			33,0

P_H	II				
$P_H \cdot H$	III	Parameters of distribution		Sweep H	Half-cycles
$H - \Sigma P_H \cdot H$	IV	Average meaning		$\bar{H} = 2.75$	$\bar{\tau} = 3.30$ сек
$(H - \Sigma P_H \cdot H)^2$	V				
$P_H(H - \Sigma P_H \cdot H)^2$	VI	Dispersion		$D_H = 1.08$	$D_\tau = 1.40$
$\Sigma(\tau \cdot n_H)$	VII				
$\frac{\Sigma \tau n_H}{n_H}$	VIII	Coefficient variance		$U_H = 0.435$	$U_\tau = 0.36$
$\Sigma \tau n_H \cdot H$	IX	Coefficient correlations		$r_{H\tau} = 0.23$	

Header of table:

Force and wave type $k_{3\%} = 1.0$ м. wind   **Greatest sweep** $H_{max} = 5.80$

Speed and wind force $v = 8$-10 meters/second   **Greatest half-cycle** $\tau_{max} = 6$ seconds

These statistical relationships are set forth for ACV's with displacements of approximately 30 tons and are attributed to tests made in high waves with 3% provision, equal to 0.8-1.0 meters.

Of interest is the equation for the parameters of roll in an ACV without flexible skirts and with skirts of various heights. A craft without flexible skirts, even in moving over calm waters at a set rate of speed, had pitching with cycles of 3-4°, accompanied by damping in the air cushions of the blows to the hull by the water. At increased speeds, the roll vanished. In conditions of very little choppiness, rates of movement along the waves were shown to be highly unfavorable for a craft without flexible skirts when, at insignificant speeds, the frequency of perturbation was close to the true frequency and the craft experienced a drop in resonance, accompanied by partial blows to the bow extremity by the water. Installation of flexible skirts, even at small heights (up to 0.5 meters) led to considerable decreases in pitching in highly choppy sea conditions. In moving over gently sloping and long waves, the characteristics of roll were different from those in highly choppy sea conditions. In moving against waves with lengths of $\lambda = 1.2$-1.5 L_p and within a fixed range of speed, the launch fell sharply in rate of resonance of pitching with great sweeps and often by actions of considerable vertical accelerations. In moving along the waves, the craft went smoothly, not falling in rate of resonance.
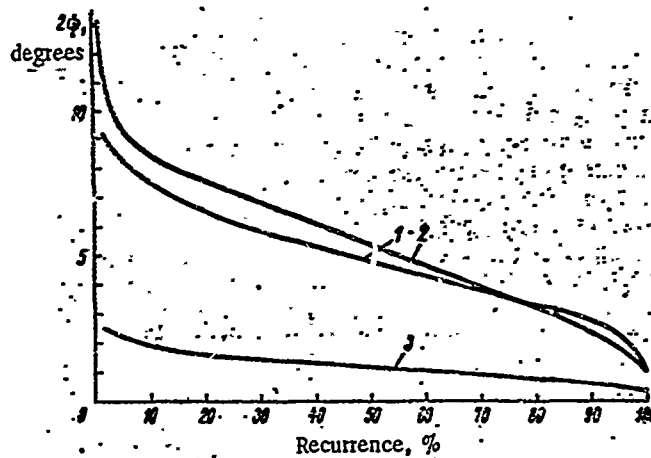
Figure 182. Curves of the Distribution of Cycles of Pitching, Course
Wave Angle = 0°.
1, Without flexible skirts, waves of $h_{3\%}$ = 0.6 meters, V = 25 knots;
2, With flexible skirts, $h_{r \cdot o}$ = 0.4 meters, waves of $h_{3\%}$ = 0.7-1.0
meters, V = 30 knots; 3, With flexible skirts, $h_{r \cdot o}$ = 1 meter, waves
of $h_{3\%}$ = 1 meter, V = 30-35 knots.

By further increasing the height of the flexible skirts (up to
1 meter), the characteristic of pitching in extremely choppy sea condi-
tions did not change, but the vertical accelerations were decreased
appreciably. The greatest amplitudes of pitching are observed in
moving against waves at low speeds. The cycles of pitch may reach
15-18° in this case. At increased speeds, the rolling becomes less
intensive with the cycles not exceeding 5°.

In moving along the waves, the cycles of rolling are considerably
less, however, poor construction of the bow elements of the flexible skirts
may lead to the "bending under" or buckling" of these elements which
in turn, leads to a quick increase to trim difference in the bow of
dangerous proportions (loss of longitudinal stability). Buckling of
the bow elements of the flexible skirts may also occur in moving against
the waves at high speeds when the elements, bent under by the waves,
do not have time to smooth out before the approach of the next wave.
In order to avoid this, constructive measures must be provided for
eliminating the possibility of the bow elements buckling anywhere in
the speed range and the centering of the ACV in moving both on calm
waters and in choppy sea conditions.

Division of vertical rolling and pitching of an ACV and examination
of them, independent of each other, is possible only to the first approxi-
mation. Large angles of trim difference usually reveal a loss of lift
forces and, as a result, a decrease in lift height, as well as a shift
of the center of gravity in the ACV. Thus, pitching is effected vertically
as a rule, and it is more correct, therefore, to examine longitudinal
rolling of an ACV, determined by the equation:

-399-

$$\left(\frac{G}{g}+\Delta M\right)\ddot{y}+2N_{v}\dot{y}+\frac{\partial Y}{\partial h}y=\frac{h_{\imath}}{2}h_{v}\frac{\partial Y}{\partial h}\cos{(\sigma t-\delta_{g})};$$

$$(J_{z}+\Delta J_{z})\ddot{\psi}+2N_{\psi}\dot{\psi}+\frac{\partial M_{z}}{\partial \psi}\psi=\frac{\partial M_{z}}{\partial \psi}k_{\psi}\alpha_{0}\cos{(\sigma t-\delta_{\psi})}.$$

(526)

Calculations of the parameters of longitudinal rolling and their amplitude-frequency and phase-frequency characteristics may be accomplished on the basis of the experimental data acquired in the testing of models.

First, a few words about the problem of stabilization of an ACV in choppy sea conditions. The statistics concerning the parameters of rolling in an ACV are set forth above and are convincing enough to prove that an air cushion vehicle, moving in choppy sea conditions, experiences intensive side and longitudinal rolling. It is entirely logical that a statement of the problems of restraining roll in an ACV should arise in connection with this.

There are three known methods for stabilization of craft: con-structive stabilization, attained by the selection of rational dimensions and forms; natural stabilization, ensured by maneuvering the craft (by changing the speed and course angle); and artificial stabilization or the calming of roll.

Constructive stabilization of an ACV, to a great degree, depends on the dimensions of the craft, its displacement, the height and con-struction of the flexible skirts, as well as the means of sectioning the cushions and the volume of air expenditure. The range of variance of these elements and the parameters in the design are highly limited, therefore, constructive stabilization also has limited possibilities. The most reliable way of resolving the problem is the calming of roll.

Calming of roll in an ACV does not exist in the navigation and building of the craft, however, familiarization with patent information provides a basis for maintaining that the problems of stabilization for ACV's are being studied seriously.

In accordance with classification [58], calming of roll is divided into: active or passive, in relation to the possibilities of their control and their consumption of external energy; gravitational, hydro-dynamic, and gyroscopic - in relation to the source of forces implementing the stabilization; damping (increase of damping forces), equilizing (balancing of perturbation forces), and frequency (change in frequency of free fluctuations of the craft) - in relation to the change in receptivity of the craft to perturbation; and calming of side and vertical rolling and pitching - in relation to the planes of activity.

It may be assumed that, in ACV's, there are applications for active and, to a lesser degree, passive calming of roll. It is unlikely that a use for gravitational calming, utilizing liquid tanks, will arise. The

greatest prospect, apparently, is the use of the following means of calming rolling:

1) Aerodynamically controlled horizontal rudders, prescribed for air screws and working in the stream of air from the screws. In symmetry, relatively diametric planed aerodynamic rudders are able to ensure effective restraint of side rolling. In placing the aerodynamic rudders in the stern, they may also be used for first-rate calming of pitch.

Aerodynamic horizontal rudders, in rational dispositions and in keeping with a system of control, may become universal calming agents, ensuring the restraint of cycles of side rolling and pitching.

2) Calming of roll, based on the regulation of pressure in various sections of the air cushions. Regulation of the feeding of air from the fans to the sections of the air cushions may create recovered moments, compensating moments of external forces acting both in longitudinal and transverse planes.

This type of calming agent[1] appears universal and also provides for restraint of side rolling and pitching. The basis for its advantage appears to be its use in first-rate operation of an established supercharger. External energy is required only for the drive of the regulating damper in the air-distribution ducts.

3) Hydrodynamic calming of roll - controlled or uncontrolled rudders, appearing as foils of small lengths, working in the running stream of liquid. These calming agents may be used in special ACV combined schemes, with the basic part of the lift forces used for creating the air cushions and the foil system used for improving stability in moving and abatement of roll.

Hydrodynamic calming agents for rolling may also be applied to ACV's in Class B, with their drive placed in the side of the craft. In this case, the design of the rudder may be close to that of the side rudder in displacement-type craft.

It is expected that, in the next few years, stabilization of ACV's will be given a great deal of attention.

§31. Increase in Resistance and Decrease in Speed in Moving Over Waves

An increase in resistance, while moving in choppy sea conditions, depends on the interaction of the ACV's hull and its flexible skirts coming into contact with waves, as well as the circumstance of the reactive composition of the resistance to movement (appearing in the form of horizontal projection of the resultant pressure of air on the bottom) with great cycles of pitch periodically changing the mark, determining the irregularity

---

[1]The first of this type of calming agent for rolling in an ACV was proposed by Yu. Yu. Benya. Also, see the French patent classification B60 #1476633, 1967.

of translational movement. The interaction of the ACV's rigid hull with the waves may occur in moving over waves of great height or in undergoing a drop in resonance of rolling, as is the case also when, because of the flexible skirts' small heights, their design is a failure or due to insufficient output of the craft's fans while passing over waves, "losing" the cushion and causing escape of air along the perimeter and especially in the area at the foot of the waves, considerably exceed the quantity of air being received from the fans. In such cases, strong blows are possible on the hull from the water's surface and a sharp increase in resistance to movement.

The height of the flexible skirts and the output of the fans are selected for a design, with such calculations which exclude blows on the hull by water and its interaction with waves in given sea conditions. Then an increase in resistance occurs only by interactions of the flexible skirts with waves and the characteristic influence of the reactive composition.

Moving in choppy sea conditions, the flexible skirts are deformed elastically under the action of the waves. It is practically impossible to avoid mechanical contact of the flexible skirts with the waves, but with the right design it is possible to significantly decrease the arising of such interacting forces of resistance to movement. Theoretically, resistance arising from the interaction of the flexible skirts with the water isn't determined, therefore, during planning this resistance is considered as made up of the remaining hydrodynamic resistance, evaluated in the transition from models to actual ACV's according to the law of mechanical similarities in equalities of Froude numbers.

In isolated cases, with sufficient experimental material on hand, one may single out the resistance of interactions between the flexible skirts and the water from the overall resistance. Thus, in 1964-65 on the basis of testing the VA-3 ACV, the Republic firm set forth the empirical formula for determining the coefficient of resistance to the flexible skirts

$$C_{x\,r.o} = 6.6 \left(\frac{h_a - 2t}{L_n} \right)^{1.2}.$$

The formula was suitable in conditions of

$$0.005 < \frac{t}{L_n} < \frac{1}{2} \frac{h_a}{L_n} \quad \text{и} \quad \frac{h_a}{L_a} < 0.1,$$

where h_v - wave height, in meters;

    t - midpoint clearance between the flexible skirts and the screen, in meters;

    L_p - length of air cushions, in meters.

of translational movement. The interaction of the ACV's rigid hull with the waves may occur in moving over waves of great height or in undergoing a drop in resonance of rolling, as is the case also when, because of the flexible skirts' small heights, their design is a failure or due to insufficient output of the craft's fans while passing over waves, "losing" the cushion and causing escape of air along the perimeter and especially in the area at the foot of the waves, considerably exceed the quantity of air being received from the fans. In such cases, strong blows are possible on the hull from the water's surface and a sharp increase in resistance to movement.

The height of the flexible skirts and the output of the fans are selected for a design, with such calculations which exclude blows on the hull by water and its interaction with waves in given sea conditions. Then an increase in resistance occurs only by interactions of the flexible skirts with waves and the characteristic influence of the reactive composition.

Moving in choppy sea conditions, the flexible skirts are deformed elastically under the action of the waves. It is practically impossible to avoid mechanical contact of the flexible skirts with the waves, but with the right design it is possible to significantly decrease the arising of such interacting forces of resistance to movement. Theoretically, resistance arising from the interaction of the flexible skirts with the water isn't determined, therefore, during planning this resistance is considered as made up of the remaining hydrodynamic resistance, evaluated in the transition from models to actual ACV's according to the law of mechanical similarities in equalities of Froude numbers.

In isolated cases, with sufficient experimental material on hand, one may single out the resistance of interactions between the flexible skirts and the water from the overall resistance. Thus, in 1964-65 on the basis of testing the VA-3 ACV, the Republic firm set forth the empirical formula for determining the coefficient of resistance to the flexible skirts

$$C_{x_{r.o}} = 6,6 \left(\frac{h_\text{в} - 2l}{L_\text{n}} \right)^{1,2}.$$

The formula was suitable in conditions of

$$0,005 < \frac{l}{L_\text{n}} < \frac{1}{2} \frac{h_\text{в}}{L_\text{п}} \text{ и } \frac{h_\text{в}}{L_\text{п}} < 0,1,$$

where h_v - wave height, in meters;

l - midpoint clearance between the flexible skirts and the screen, in meters;

L_p - length of air cushions, in meters.

-402-

For the VA-3 L_p = 15 meters, t = 0.02 meters, and h_v = 1.0 meters $c_{x_{r \cdot o}}$ = 0.25. The speed of the VA-3 equalled 115 kilometers per hour (31 meters per second), corresponding to an increase in the forces of resistance of 1170 kilograms.

In research for designing of a foreign ACV, another formula was applied

$$\frac{R_{r.o}}{G} = \frac{\rho g}{2} (Fr)^2 \cdot 3,3 \left(\frac{G \cdot h_\text{в}}{L_\text{ц}}\right)^{1,2} \cdot \left(\frac{p_\text{п}}{L_\text{ц}}\right)^{-1},$$

where Fr - Froude number;

p_p - pressure in the air cushion, in foot pounds^2;

G - weight of the ACV, in tons;

L_p - length of air cushions, in feet;

h_v - wave height in feet.

Resistance to movement of an ACV on choppy seas depends on the length and height of the waves, the course angle, the speed, and quantity of air expenditure. In Figure 183, the relation of resistance in the SKMR-1 ACV in average sea conditions to the calculated parameters (obtained as a result of tests made in a basin) is set forth. An examination of this relationship allows one to make the following conclusions: a sharp increase in resistance occurs in moving against waves and at sharp course angles; the greatest amount of resistance comes in moving waves with lengths of λ = 1-2 L_p; by increasing the wave length, the resistance to moving is decreased and becomes roughly equal to the resistance encountered in moving broadside to the waves; in moving over waves, where λ = 1-2 L_p, resistance increases intensively at increased speeds; an increase in wave height leads to proportionate growth of resistance; an increase in air expenditure permits a sharp decrease in resistance to movement on choppy seas.

Resistance to movement on choppy seas, to a great degree, depends on both the construction of the flexible skirts and the centering in the ACV. In Figure 184, designs for experimental ACV's with relationships of relative additional resistance on choppy seas to wave heights at various Froude numbers are set forth. These relationship are characteristic only for a definite design of flexible skirts, a definite volume of air expenditure, and where the relationship of pressure in the flexible receiver to the pressure in the cushion is ~1.2.

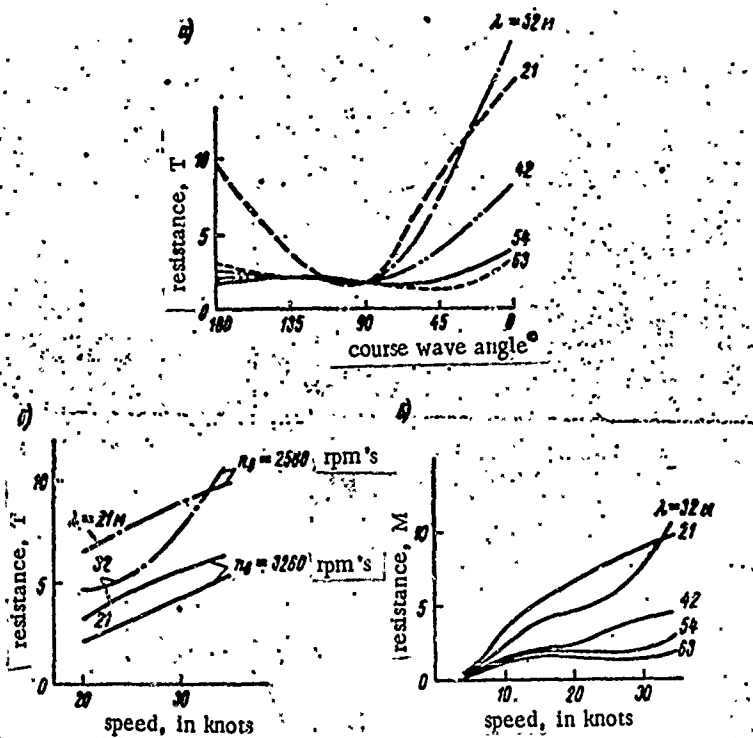An increase in resistance leads to significantly lower speeds in choppy sea conditions.

Figure 183. Relationship of Resistance to Movement in the SKMR-1 on Choppy Seas to Various Parameters: a, to course wave angle; b, to the output of the fans and speed; c, to wave length and speed.
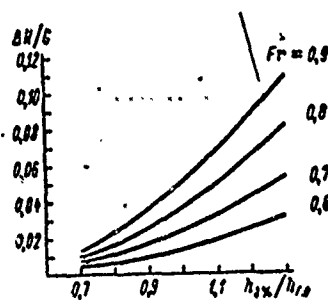

Figure 184. Relationship of Relative Additional Resistance in Choppy Sea Conditions to Wave Height and Speed.
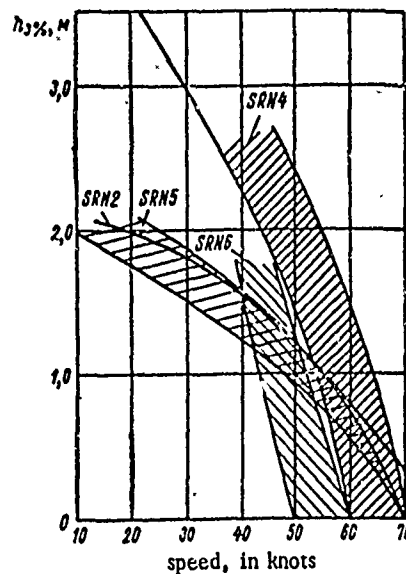

Figure 185. Seaworthiness of Air Cushion Vehicles.

-404-

Set forth in Figure 185 are the relationships of speed of an ACV to the intensity of choppy sea conditions, showing that, in State 3 sea conditions, speed in the SRN5 and SRN6 drops 20-30%. In State 3-4 sea conditions, speed in the SRN4 (largest of the foreign ACV's) also is lowered considerably.

In Figure 186a, the relationships of resistance in moving to speed and wave height are set forth, calculated for prospective ACV's with displacements of 1000 tons, and in Figure 186b the relationships of resistance for prospective ACV's with displacements of up to 10,000 tons.

§32. Vertical Accelerations Which Act on ACV's in Moving Over Waves

In moving over even short waves, making up only part of the length of the air cushions, ACV's are tested for the influence of acceleration of small amplitudes and large frequencies. The air cushion, as was mentioned, must dampen small perturbations and absorb the accelerations of small amplitudes, transferring them to the hull. This somewhat unexpected phenomenon was explained by Cockerell [64].

We observe, for example, movement of the craft at right angles, when the pressure of the cushion consists of 300 kilograms force per meter^2. The craft is moving against waves with lengths of $\lambda = 0.4\ L_p$. One moment there might be three crests and two feet of waves along the air cushion under the craft, and the next moment of wave system might consist of two crests and three feet. If, during this shift, the volume in the cushions is changed only by 1%, then this leads to a change of absolute pressure in the cushions of 1% (we compute the contour of the air cushions with reserve), i.e. by 106 kilograms force/meter^2 10330 + 300/100. But 106 kilograms force/ /meter^2 consists of 1/3 the pressure in the cushion, and the appearance of this pressure leads to accelerations arising and acting on the craft, equal to 1/3 G. By changing the form of the ACV, making the transition from a right-angled to a sharp bow extremity and rounded stern, perceptibility of the craft to perturbation, giving rise to short waves, is decreased. In moving over longer waves, the changes in volume of the air cushions is some instances may be great, and the accelerations increase. Accelerations, acting on an ACV, depend on not only changes in volume of the cushions and, subsequently, pressure, but also on the parameters of longitudinal roll.

As is known, there are physiological thresholds for sensations of accelerations of roll, when a person begins to develop symptoms of seasickness which grow progressively worse. Usually, intensive seasickness develops during vertical accelerations of more than 0.1G and rotary accelerations of more than 3° per second^2. The quantity of possible vertical accelerations is set in relation to the extent of the route and frequency of accelerations. In England, the possible level of accelerations for a passenger ACV were equal to 0.1 G at a frequency of 2 hertz and not more than 0.2 G at a frequency of less than 1 hertz. If the extent of the route does not exceed 8 miles, possible vertical accelerations are calculated up to 2 G's. For military-type ACV's, the possible level of accelerations may also be raised up to 2 G's.
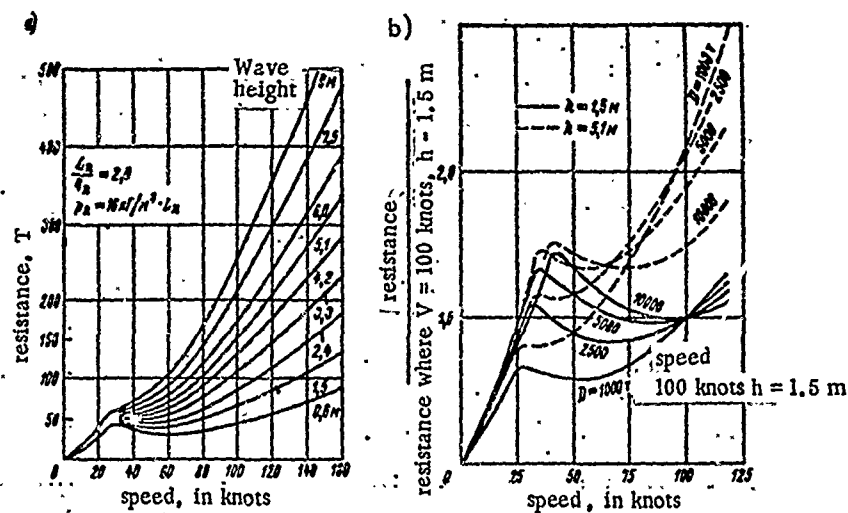
-405-

Figure 186. Relationship of Resistance in Moving of Prospective Class B
  ACV's to Wave Height and Speed.
a., An ACV with displacement of 1000 tons, b, An ACV with displacement of
from 1000 to 10,000 tons.

The prospect of passenger air cushion vehicles, to a great degree,
depends on the successful resolution of the problem of rolling in these
craft and the ensuring of normal accelerations, making for conditions of
comfort. In England, in connection with this, investigations were carried
out concerning the relationships of accelerations to the displacements and
dimensions of craft, heights of the flexible skirts, power of the fans,
and speed [64]. The results of these investigations are set forth in
Figure 187, as well as Figure 188-192.

In Figure 187, the lift height of the hull's bottom from the base
surface, in relation to speed and parameters of waves in conditions where
vertical accelerations of the ACV must not exceed 0.5 G, is shown.

It may be concluded that, to ensure a given level of accelerations,
the minimum lift height in moving over any waves with lengths up to 300
meters must be 3 meters at speeds of 100 knots, 1.8 meters at speeds of 50
knots, and 1.2 meters at speeds of 25 knots. Just as in conditions for
ensuring stability the lift height may not exceed 1/6 the width of the ACV,
then the heights of 3, 1.8, and 1.2 meters will correspond to the width of
the ACV accordingly - 18, 11, and 7.2 meters. In a first-rate ACV prototype
with regard to L:B = 2, it is not difficult to determine the length of the
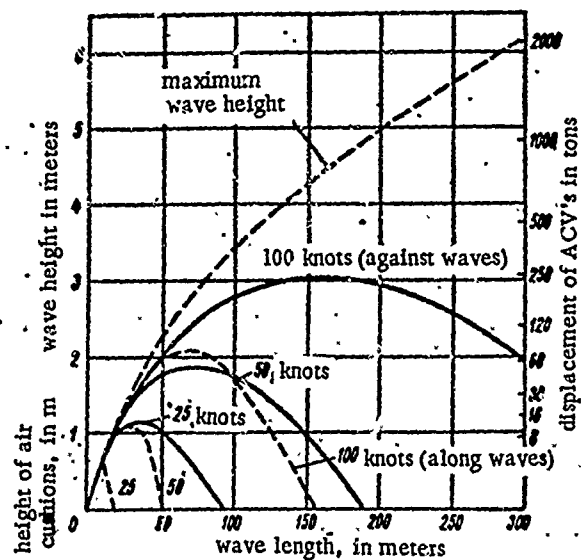ACV and, according to law, subsequently to find the similarities and displace-
ment.

-406-

Figure 187. Lift Height of the ACV's Hull from the Water's Surface, Necessary to Ensure Normal Accelerations W ≤ 0.5 G's.

As a result, it was established that a permissible level of vertical accelerations of roll of 0.5 G may be ensured: at speeds up to 100 knots for ACV's with displacements of 250 tons at lift heights of 3 meters; at speeds up to 50 knots for ACV's with displacements of 60 tons at lift heights of 1.8 meters; and at speeds up to 25 knots for ACV's with displacements of 20 tons at lift heights of 1.2 meters.
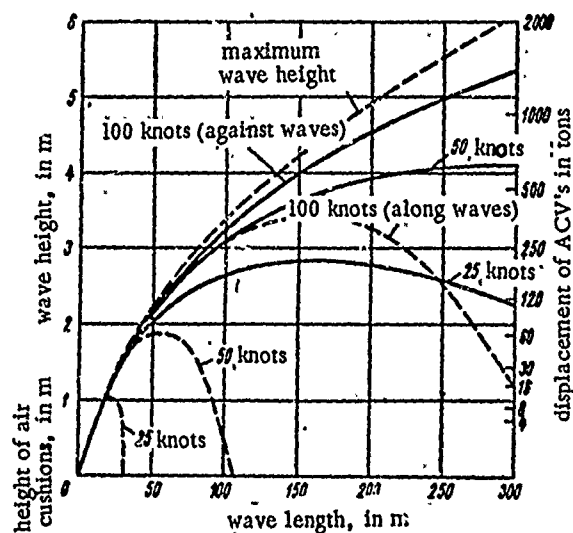

Figure 188. Lift Height of the Hull of an ACV from the Water's Surface, Necessary to Ensure Normal Accelerations W ≤ 0.1 G's.

-407-

In Figure 188, the relationships are the calculated results of the possible level of accelerations of 0.1 G's. In ACV's with displacements of over 1000 tons, this level of accelerations may be ensured at speeds up to 100 knots with lift heights of the hulls above 5 meters; in ACV's with displacements of more than 500 tons - at speeds up to 50 knots with lift heights of about 4 meters; and in ACV's with displacements of about 150 tons - at speeds of 25 knots.

However, to reach given levels of vertical accelerations, it isn't enough to select the dimensions of the ACV and the lift height in accordance with the recommendations set forth in Figures 187 and 188.

The form of the hull, the internal air ducts, the correlation of pressure in the receiver and in the cushion, and the design and materials of the flexible skirts must be selected so as to ensure sufficient rigidity and, at the same time, pliability of all lift systems. What is really important, is ensuring a sufficiently large volume of air expenditure to compensate for the loss during rolling.
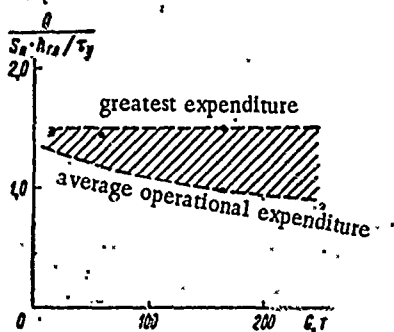

Figure 189. Relationship of Relative Air Expenditure to Displacement of the Craft.

In the first stage of designing an ACV, the volume of air expenditure was determined as a result of ensuring better quality of operation of the craft over calm waters.

As was mentioned in Chapter IV, the curve in the relationship of the resistance to movement of a craft over calm waters to the expenditure of air has its own optimum. Experimentally, it was established that this optimum, for an ACV with flexible skirts (where the flexible jet conforms to the mid-point of the perimeter), in quantity of clearance between the base surface and the flexible skirts was equal to 0.004 L_p. For ACV's with transverse, open-formation elements, the optimum relative quantity of clearance to the bottom of the ACV may prove considerably less, therefore, to ensure first-rate operation of the ACV it is not necessary to increase the clearance to increase displacement.

Following the selection of the force-pump equipment, it then becomes necessary to ensure the volume of air expenditure to meet the conditions of seaworthiness. This expenditure must be sufficient to compensate the periodic escape of air during rolling of the ACV.

In Figure 189, data is set forth, characterizing the volume of air expenditure for ACV's of various displacements. It may be noted that, non-dimensional parameters are themselves, in the relationship of the volume of air expended to the volume of the air cushions, divided into

periods of true vertical fluctuations of the ACV, independent of the displacement. The greatest volume of air expenditure may be determined by the following formula:

$$Q = 1,5 S_n h_{r.o} \frac{1}{2\pi} \sqrt{\frac{g}{h_{r.o}}} \approx 0,75 S_n \sqrt{h_{r.o}}, \; \text{м}^3/\text{сек.}$$ (527)

Investigations, carried out in England, permitted the establishment of the relationships between the output of the fans and the level of vertical accelerations in the movement of an ACV in various sea conditions at various speeds.
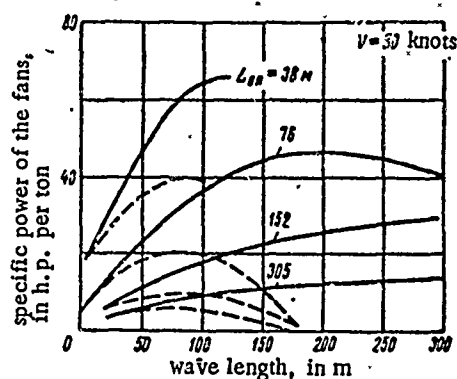

Figure 190. Specific Power of the Fans of an ACV, Necessary to Ensure a Given Level of Normal Accelerations in Moving at a Speed of 50 Knots.
——————— accelerations W ≤ 0.1 G's;
---------- accelerations W ≤ 0.5 G's.

These relationships are set forth in Figures 190 and 191, and an examination of them allows one to make the following conclusions: at speeds of 50 knots, for craft with cushions about 40 meters in length and displacements of about 250 tons, the accelerations do not exceed 0.5 G's if the specific power of the fans is 40 h.p. per ton; to ensure accelerations of 0.1 G's, it is necessary to increase the specific power of the fans to 65 h.p. per ton; for craft with displacements of about 2000 tons and cushion lengths of about 80 meters, the specific power of the fans decreases accordingly to 20 and 45 h.p. per ton; at speeds of 100 knots, the specific power of the fans needed to ensure a given level of accelerations sharply increases - - 100-120 h.p. per ton for an ACV with a length of about 40 meters (G = = 250 tons) and 60-90 h.p. per ton for one with a length of about 80 meters (G = 2000 tons).

It is quite obvious that the power of the fans, necessary to ensure a given level of vertical accelerations at speeds of 100 knots, is beyond technical means. In an ACV, at such speeds, only a considerably small specific power of the fans would be provided and, consequently, the ACV would be restricted to speeds in relationship to intensity of sea conditions.

-409-

One cannot help but note that the characteristics of the fans' power, necessary to ensure vertical accelerations for the ACV and not exceeding 0.5 G's (Figure 190), even at speeds of 50 knots prove to be higher than those received in practical designs.

Thus, the specific power of the fans installed on the English SRN6 and SRN4, are, respectively, 28 h.p. per ton and 25-40 h.p. per ton.
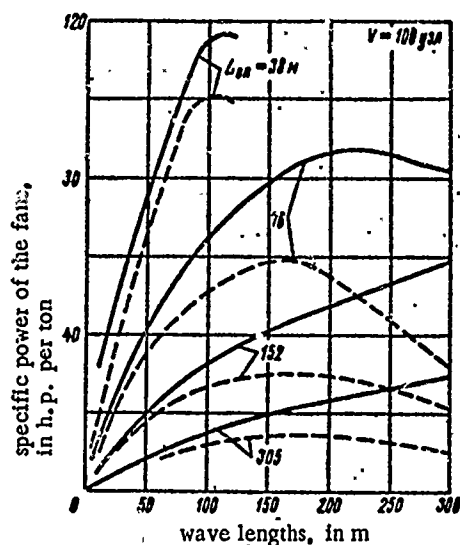

Figure 191. Specific Power of the Fans of an ACV, Necessary to Ensure a Given Level of Normal Accelerations in Moving at a Speed of 100 Knots.
——————— accelerations $W \leqslant 0.1$ G's;
----------- accelerations $W \leqslant 0.5$ G's.

Considering that the specific power, necessary to ensure a given level of accelerations, is decreased with the increase of linear measurements of the ACV, it is possible to compute the power of the fans required for an ACV. This would consist of about 60 h.p. per ton for the SRN6 and about 50 h.p. per ton for the SRN4.

However, this substantial decrease, according to the equation from the calculations for ensuring accelerations $W \leqslant 0.5$ G's, did not lead to a significant deterioration in seaworthiness of the SRN6 and SRN4. In connection with these relationships, set forth in Figures 190-191, it is possible to observe the desirable maximum.

Using the law of similarities, and based on data from testing model ACV's on extremely choppy seas, it is possible to predict the seaworthy capabilities of prospective ACV's. Such investigations were conducted in England, and they permitted the establishment of the relationship of sea-worthiness in ACV's to displacements and speeds with a permissible level of vertical accelerations of 0.5 G's and an energy supply of about 100 h.p. per ton (Figure 192).

An examination of these relationships allows one to make the following conclusions: at a given level of permissible accelerations for ACV's with displacements up to 120 tons, it is possible to go to sea in sea conditions up to State 4 inclusive: in more intensive sea conditions (State 5), their being at sea is permissible in conditions of safety, but the level of vertical accelerations for this exceeds 0.5 G's; craft with displacements of 250-500 tons might move at speeds up to 60-80 knots in State 3 sea conditions, and the accelerations for this would not exceed 0.5 G's; only large craft with displacements of about 2000 tons will move at great speeds in the open sea during storm conditions.
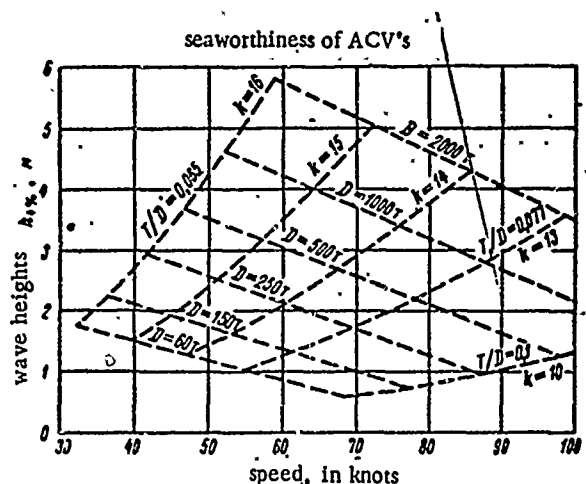

Figure 192. Seaworthiness of Prospective ACV's (Normal Accelerations W ≤ 0.5 G's).

We note that there are relationships of designs for vertical accelerations of rolling of 0.5 G's and they do not characterize in full measure the seaworthiness of ships and ACV's. The limits of safe navigation for ACV's lie in considerably higher cited curves, therefore, in some deviations from levels of permissible accelerations (up to 1-2 G's) characteristics of seaworthiness may be considerably improved. Serving to confirm this, are the graphs set forth in Figure 185 on the seaworthiness of ACV's. Still another observation is: the relationships in Figure 192 are designs for most unfavorably rates of movement against waves. In moving at other course angles, the characteristics of seaworthiness will significantly improve.

More detailed characteristics for expected seaworthiness in prospective ACV's are set forth in the well-known work of R. Stenton-Jones [75] - the relationships of seaworthiness (characterized by wave heights of 4% assurance, over which an ACV may travel at 50 knots) to the displacement and energy supply (Figure 193), as well as the graph of changes in energy supply for an ACV as the displacement is increased (Figure 194). In making these graphs,

-411-

it was assumed that an ACV, using air propelling agents, may be created with
a displacement up to 400 tons; for ACV's with large displacements, water
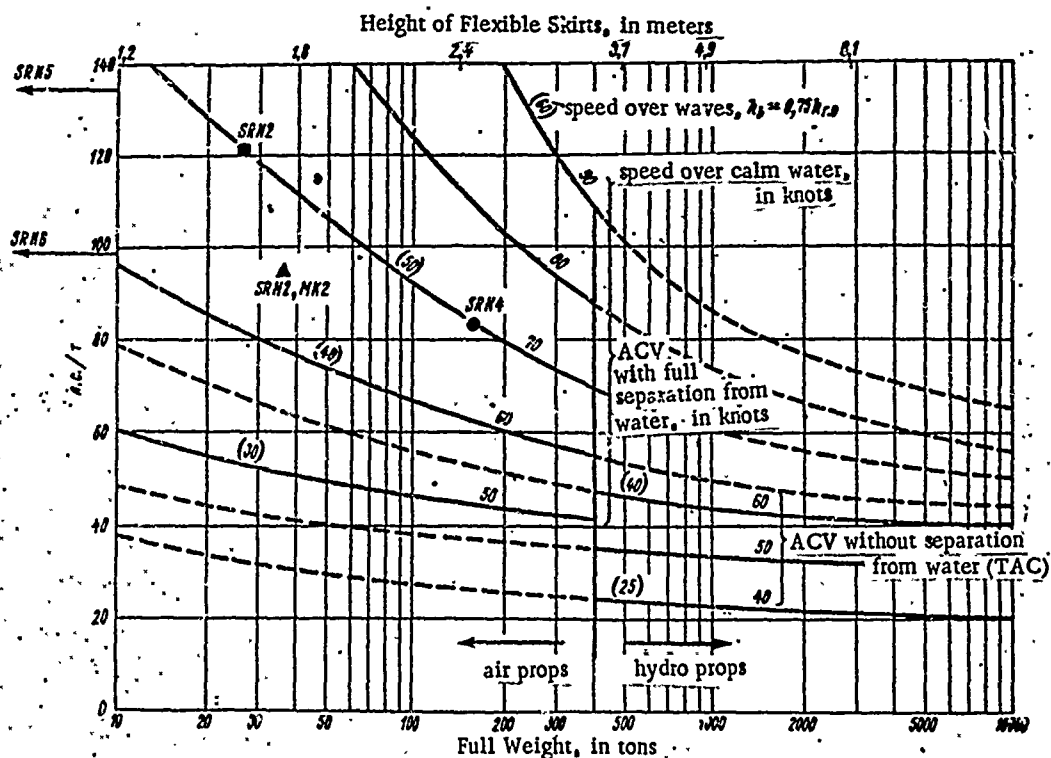propelling agents (screws, water-jets) must be installed.

Figure 193. Change in Energy-supply of ACV's in Relation to Water Displace-
ment and Speed Over Calm Water and Over Waves.

The graph in Figure 193 allows one to make the following conclusions:
for ACV's with displacements up to 400 tons, a rise in energy supply from
60-to 100 h.p. per ton leads to a proportionate rise in seaworthiness; to
increase the speed in sea conditions from 50-to 60 knots, it is necessary
to increase the energy supply of the ACV by 1 1/2 times.

In Figure 194, the relationship of the required energy supply of
prospective ACV's to displacements and speeds is set forth. In the graph,
points are plotted for the corresponding energy supplies, speeds, and sea-
worthiness of contemporary ACV's. From the graph, one sees that the required
energy supply of an ACV decreases considerably with the increase of displace-
ment. Thus, to ensure speeds of 70 knots over calm water, the energy supplies
of ACV's with displacements of 20, 200, and 1000 tons must reach 130, 80
and 60 h.p. per ton, respectively. In moving against waves, the height of
which makes up 3/4 of the height of the flexible skirts ($h_{4\%} = 0.75$ $h_{g.o}$)
a speed of 20-30 knots less than in moving over calm water is assured.
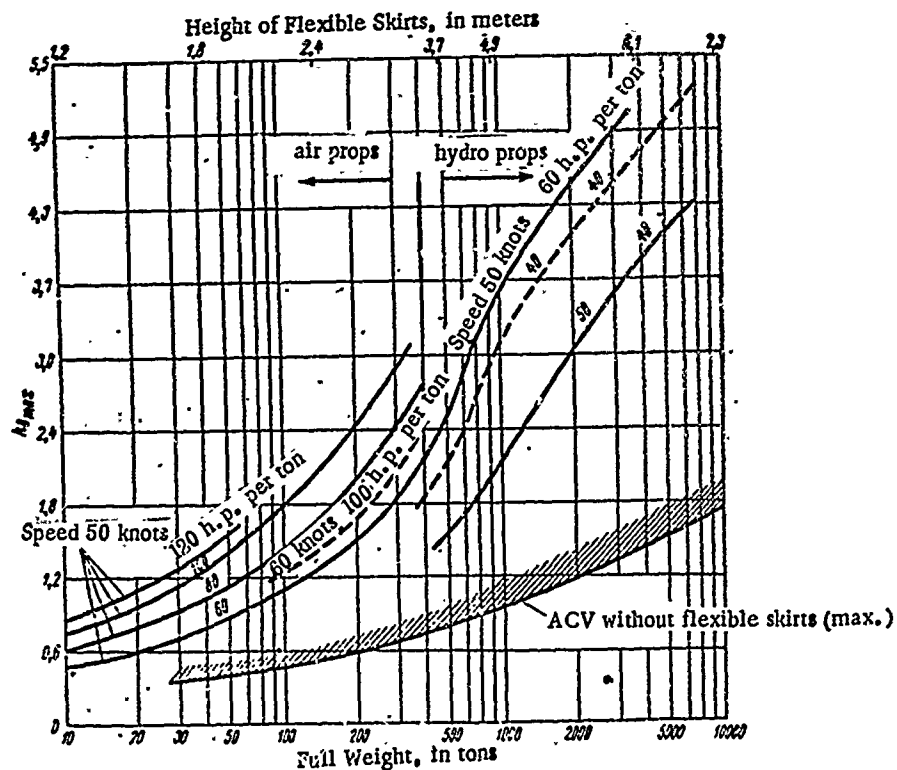
-412-

Height of Flexible Skirts, in meters

Figure 194. Seaworthiness of Prospective ACV's.

§33. Overflow and Splashing in ACV's

Overflow and splashing in displacement-type craft is caused, on the whole, by pitching, accompanied by blows to the bow extremities by waves and masses of water falling on the deck. In contrast to overflow and splashing in displacement-type craft, the basic source of spray-formations in the movement of an ACV appears to be the escape of air from zones of rising pressure, leading to the formation of shrouds (curtains) of spray around the ACV. In rate of suspension, for a stationary ACV, this shroud is almost vertical. In moving at a rowing rate, the spray curtain in the bow extremities gradually disappears. At a rowing rate, with increases in speed, the spray curtain moves to the stern and becomes more gentle. At high speeds, the spray shroud remains in the form of a narrow train, beginning approximately at the middle. During movement in a cross-wind, the spray curtain on the windward side is carried by the wind to the stern sections of the ACV.

Splashing increases considerably when the ACV moves against the waves and the wind at low speeds, where intensive pitching leads to a great vertical shift in the bow extremities and promotes the break-through of a large air-mass forward. At increased speeds, for craft in choppy sea conditions, splashing decreases considerably.

-413-

At low temperatures, spray-formation leads to icing-over of the hull and projecting parts. The air screws, fans, and flexible skirts, as a rule, do not ice-over in these conditions.

Spray formation intensively increases with increased pressure in the cushions. We note that the process of spray formation isn't modelled, therefore, it is impossible to determine the intensity of spray formation from test-model data. In Figure 12, one can see the spray trail formed during the operation of the SRN3.

§34. Features of Seaworthiness in Test Model ACV's

Special significance is given to the design of actual-size ACV's from model experiments, since testing models allows one to study their behavior in operating in average and extremely choppy sea conditions with various speeds on various courses relative to the waves. The influence of wave height and wave length on the parameters of moving models is investigated, as well as the relationship of the ACV's seaworthy qualities to the volume of air expenditure, centering of the craft, construction, materials and dimensions of the flexible skirts. In testing the models, the accuracy of solutions pertaining to architectural design and correlation of the chief dimensions also is checked.

The scales of models may vary-from 1/20 to 1/2. Not only geometirc similarity is observed in creating the models, but similarity of mass distribution, air pressure in the receiver and air cushions, and volume of air expenditure through the fans are sought.

Tests are conducted on tow-type or self-propelled models. The modelling is carried out in observance of the equality of Froude numbers of the models and the actual-size craft. Since resistance is stipulated partially by the friction of the flexible skirts making contact with the water, modelling according to Froude is not accurate.

In testing tow-type models, 3 degrees of freedom are ensured; this allows the possibility of fluctuations vertically and around the axes Ox and Oz. Self-propelled models have 6 degrees of freedom, therefore, their tests provide the most reliable and complete information.

It follows that, if, in testing the self-propelled models, the stop vector changes direction during pitching, then, in testing tow-type models, this vector retains its direction. Thus, in tow-type tests the conditions of modelling are broken considerably. If one considers that, while moving in choppy sea conditions, resistance of an ACV changes as much as the passing waves and , consequently, also change speed, then it is obvious that in tow--type tests, at constant speeds, the conditions of modelling are broken according to the quantity of stop and its direction relative to the models.

All this leads to considerably different kinematics for operation of tow-type and self-propelled models in identical test conditions. Thus, cycles of pitching and vertical roll in tow-type tests prove significantly greater than in self-propelled tests.

Therefore, in order to get sufficiently reliable data about roll of an ACV and to estimate its seaworthiness, it is necessary to conduct self--propelled tests of models on extremely choppy seas.

In conducting seaworthy tests of large-scale, self-propelled models, specific problems arise, the solution of which requires the creation of special measuring devices and exploitation of special techniques of measuring.

The first such problem is the measurement of speed. An ACV's speed, relative to water and air, differ in actual conditions. Considering that aerodynamic forces (including impulse resistance) acting on an ACV depend on speeds relative to air, and hydrodynamic forces depend on speeds relative to water, it is necessary to know the meaning of these speeds to get a true determination of the forces. The measuring device must fix the quantity and direction of the vectors of speeds relative to water and air.

In practical seaworthy tests, speed relative to water is determined by Doppler gauges, which fix the speed of translational movement of an ACV along the axes Ox and Oz. The speed also may determined by using systems of external measuring: coastal theodolite-filming posts, a pilot's synchronous survey of the ACV in trajectory of movement, or aerial survey of the shift of the ACV relative to a fix on water bases.

Considering the great influence of drift of the ACV, relative to the water's surface, on forces which act on the craft (equal to $\arctan V_z/V_x$), it is necessary to measure the angle of drift with great accuracy. It was learned from tests that, the angle of drift must be maintained by the driver within the limits of $\pm 2\text{-}5°$ and the accuracy for determining the make-up of speeds along axes Ox and Oz must ensure determination of the drift angle with an error of not more than $1°$.

Speed relative to air may be measured only by devices mounted on the side of an ACV. The usual air speed gauges, used on aircraft, are useless for determining an ACV;s speed, because they only fix the make-up of speed along axis x and do not permit the determination of air speed vectors. Therefore, in testing an ACV, it is necessary to install special devices to measure speeds and directions of the air flow on the ACV. Special attention must be given to the choice of site for installing the devices to measure the air speed, because it is necessary to exclude the influence of the hull and the air streams in the region of the screws and the air gates of the fans on the receptors of these devices.

Higher demands must be made for accuracy in measuring angle of trim difference. It is known that a change in trim difference of $1°$, means a change in resistance to movement equal to $G_\psi = 0.0175G$. If one considers that, in moving at cruise speed, the hydrodynamic quality of the ACV constitues roughly 7-10 and, subsequently, resistance equals 0.14-0.10 G, so it is obvious that a change in trim difference of $1°$ means a change in resistance of 12-18%. Therefore, to determine the forces acting on an ACV, with an accuracy of 1-2%, it is necessary to measure the trim with an accuracy of 0.05-0.1%.

Since it is impossible to ensure similarity of hydrodynamic and aerodynamic forces simultaneously, the conditions of balance in tow-type models are different from the conditions of balance in self-propelled models and actual-size ACV's, and the angles of operational trim difference in situations of balance are not equal (the influence of draught of propelling agents is compensated by a shift in the center of gravity for models).

REFERENCES

1. Basin, A. M., and I. Ya. Minovich, *Teoriya I Rachet Grebnykh Vintov* [Theories and Calculations on Screw Propellers], Leningrad, State All-Union Publishing House of the Shipbuilding Industry, 1965.

2. Basin, A. M., *Teoriya Ustoychivosti Na-Kurse I Povorotlivosti Sudna* [Theories on Stability and Maneuverability of Vessels], State Publishing House of Tactical-Technical Literature, 1949.

3. Basin, A. M., et al., "Speed of Craft With Air Blown Under the Bottom," *Sudostroeniye*, No. 1, 1968.

4. Benya, Yu. Yu., and V. M. Korsakov, *Suda Na Vozdushnoy Podushke* [Air Cushion Vehicles], Leningrad, State All-Union Publishing House of the Shipbuilding Industry, 1962.

5. Biryulin, A. P., "Some Results of Experimental Research on the Static Stability of Air Cushion Devices," The work of the Central Institute of Aerohydrodynamics, copy 889, Moscow, 1963.

6. Blagoveschenski, S. N., *Kachka Korablya* [Ship's Pitch], Leningrad, State All-Union Publishing House of the Shipbuilding Industry, 1954.

7. Bol'shakov, V. P., "Wave Resistance in Systems of Surface Pressure," A report to the 13th Science-Technical Conference of the Scientific and Technical Society of the Shipbuilding Industry on ship theories (Hydrofoil Readings). The work of the Scientific & Technical Society of the Shipbuilding Industry, Ship Theories, copy 49, 1963.

8. Bol'shakov, V. P., and V. A. Litvinenko, "Wave Resistance in Right-Angled Systems of Constant Pressure, Moving Along Freely on the Water's Surface with a Drift Angle," A report to the 16th Science-Technical Conference of the Scientific & Technical Society of the Shipbuilding Industry on Ship Theories (Hydrofoil readings), 1966.

9. Bushel', A. P., "Investigation of Short Radial and Combined Diffusers," Industrial Aerodynamics, copy 28, *Mashinostroeniye*, 1966.

10. Bashkevich, K. P., "Controls for Movement with an Automatic Pilot," The work of the Central Institute of Aerohydrodynamics, copy 889, 1963/

53. Khanzhonkov, V. I., "Inleakage of the Annular Jets on a Screen," Industrial Aerodynamics, Central Institute of Aerodynamics, Issue 23, State Scientific and Technical Publishing House of Literature on Defense, 1962.

54. Tsiolkovski, K. E., *Soprotivleniye Vozdukha i Skoryy Poezd* [Air Resistance and the Express Train], Kaluga, 1927.

55. Chetayev, N. G., "Stability in Movement," Science, 1965.

56. Shadrin, V. P., "Influence of Speed on the Characteristics of ACV's," From the collection: "Hydrodynamics of Hydrofoils and ACV's. An exchange of experience by members of the Scientific and Technical Society of the Shipbuilding Industry, Issue 61, Leningrad, 1964.

57. Shmyrev, A. N., V. A. Morenshildt and S. G. Ilina, *Uspokoyiteli Kachki Sudov* [The Calm Rolling of Craft], Leningrad, State All-Union Publishing House of Shipbuilding Industry, 1965.

58. Shmyrev, A. N., *Kachka i Stabilizatsiya Korablya na Bolnenii.* [Rolling and the Stabilization of Ships on Waves], a textbook published by the Leningrad Shipbuilding Institute, 1968.

59. Ehtkin, B., "Dynamics of Flight," Mechanical Engineering, 1964.

60. Alexander, A. I., "The Effect of Forward Speed on Hovercraft with Particular Reference to Cushion Breakdown," Hovering Craft and Hydrofoils, Vol. 3, No. 10, 1964.

61. Be , J., P. Guienne and Ch. Marchetti, "Present Prospects for Cushion Vehicles," *Zeitschrift fuer Flugwissenschaft*, Vol. 14, No. 8, 1966.

62. Bluston, H. S., "The Lateral Stability of the Hydroskimmer Craft," TRC report NTRG-158-SR-1, 1962, January. in: International Shipbuilding Progress, Vol. 12, No. 135, p. 136, 1965.

63. duCane, P., "High Speed Small Craft," (Third Edition), Temple Press Books, London, 1964.

64. Cockerell, "On Seaworthiness and Economics," ACV, N. 64, 1967.

65. Crewe, P. R. and W. J. Egginton, "The Hovercraft, a New Concept in Maritime Transport," Quarterly Transation of the Royal Institution of Naval Architects, Vol. 102, No. 3, 1960.

66. Daley, R. E. and J. U. Kordenbrock, "Experimental Trials of Surface Effect Vehicle SKMR-1," AIAA Paper, No. 66-729, New York, 1966.

38. Pontryagin, L. S., "Common Differential Equations," *Nauka*, 1965.

39. Richardson, .Eh., "Dynamics of Practical Fluids," *Mir*, Moscow, 1965.

40. Ruzhitski, E. I., "Cross-Country Air Vehicles," *Mashinostroeniye*, 1964.

41. Sabinin, G. Kh. and V. I. Sergeev, "Influence of the Screw in the Stability of the Path of an Aircraft," Technical Report of the Central Institute of Aerodynamics, 1944.

42. Sedov, L. I., "Methods of Similarities and Regularities in Mechanics," State Publishing House for Tactical-Technical Literature, 1957.

43. Stepanov, G. Yu., "Hydrodynamic Theory of ACV's," State Scientific and Technical Publishing.House of Literature on Machinery Manufacturing, 1963.

44. Semenov-Tyan-Shanski, V. V., *Statika I Dinamika Korablya* [Statics and Dynamics of Ships], State All-Union Publishing House of the Ship-building Industry, Leningrad, 1960.

45. Skripach, B/ K. and dN. N. Fomina, "Aerodynamic Characteristics for Several Types of Ships' Rudders," Office of Scientific Information of the Central Institute of Aerodynamics, 1959.

46. Sobolev, G. V., "Some Problems in Control," (Thesis), Leningrad Shipbuilding Institute, 1954.

47. Sobolev, G. V., "Control of Ships," Leningrad Shipbuilding Institute, 1959.

48. Targ, S. M., "A Short Course on Theoretical Mechanics," State Publishing House of Literature on Physics and Mathematics, 1961.

49. Redyaevski, K. K., "Tests for Classification of Bodies of Extremely Small Lengths," A Report to the XIV Scientific-Technical Conference of the Scientific and Technical Society of the Shipbuilding Industry On Ship Theory "Readings on Hydrofoils," 1964.

50. Fedyaevski, K. K., and G. V. Sobolev, *Upravlyaemost' Korablya* [Control of Ships], State All-Union Publishing House of the Shipbuilding Industry, Leningrad, 1963.

51. Fedyaevski, K. K. and Ya. T. Pugachev, "Lectures on Theories of Ship Control," Naval "Order of Lenin" Academy, 1958.

52. Khanzhonkov, V. I., "Aerodynamic and Power Characteristics of ACV's Which Utilize Jets," Work of the Central Institute of Aerodynamics, Issue 889, 1963.

23. Klichko, V. V., "Hydrodynamic Resistance in ACV's," *Sudostroenie*, No. 5, 1965.

24. Kovalev, M. A., and R. M. Rublevskaya, "Experimental Research in Control of the NACA-0018 With Foils," Aerodynamic Laboratory of Leningrad State University, 1963.

25. Kozlyakov, V. V., "On a Rational Structure Formula for Determination of Statistical Characteristics of Wave Loads," *Sudostroenie*, No. 8, 1966.

26. Kochin, N. E., I. A. Kirel and Roze, *Teoreticheskaya Gidromekhanika* [Theoretical Hydromechanics], Vol. I, State Publishing House of Literature on Physics and Mathematics, 1963.

27. Kravets, A. S., *Kharakteristiki Vozdushnykh Vintov* [Characteristics of Air Screws], State Scientific and Technical Publishing House of Literature on Defense, 1941.

28. Kulikov, S. V. and M. F. Khramkin, *Vodometnye Dvizhiteli* [Hydrodrive Propelling Agents], Leningrad, *Sudostroenie*, 1965.

29. Lamb, G., *Gidrodinamika* [Hydrodynamics], State Publishing House for Tactical-Technical Literature, Moscow-Leningrad, 1947.

30. Landau, L. D. and E. M. Livshits, "Mechanics," *Nauka*, 1965.

31. Loitsyanski, L. G., "Mechanics of Fluids and Gases," State Publishing House for Tactical-Technical Literature, 1957.

32. Lyubomirov, I. P., K. V. Zharinov, and V. F. Petukhov, "Research on Moments of Force in ACV's During Suspension Over the Water's Surface," Work of the Central Institute of Aerodynamics, Issue 889, 1963.

33. Lyapunov, A. M., "The General Problem of Stability During Movement," State Publishing House of Literature on Physics and Mathematics, 1959.

34. Ostoslavski, I. V. and I. V. Strazheva, "Dynamics of Flight," "Stability and Control of Flying Machines," *Mashinostroeiiye*, 1965.

35. Ostoslavski, I. V., "Aircraft Aerodynamics," State Scientific and Technical Publishing House of Literature on Defense, 1957.

36. Pashin, V. M., "Economical Indices of ACV's," *Sudostroenie*, No. 3, 1965.

37. Pletneva-Machabeli, L. I., "On Systems for Equalization of Rolling in Ships, Taking Into Consideration the Connection Between Vertical, Horizontal, and Side Roll," Work of the Leningrad Shipbuilding Institute, Issue 22, 1958.

11. Vojtkunski, Ya. I., "The Flowing Hydrodynamic Feature Situated Above the Surface Divided by Fluids of Various Density," Engineering Journal of the Academy of Science of the USSR, Vol. III, Copy 2, 1963.

12. Vojtkunski, Ya. I., R. Ya. Pershits, and I. A. Titov, *Spravochnik Po Teoriy Korablya* [A Reference Book of Ship Theories], Leningrad, State All-Union Publishing House of the Shipbuilding Industry, 1960.

13. Girs, I. V., A. A. Rusetski and Yu. A. Netsvetaev, *Islytaniya Morekhodnykh Kachestv Sudov* [Tests of Seaworthy Qualities in Vessels], Leningrad, "Shipbuilding," 1965.

14. Goroschenko, B. T., *Dinamika Poleta Samoleta* [Dynamics of Aircraft Flight], State Scientific and Technical Publishing House of Literature on Defense, 1954.

15. Grechin, M. A., "Calculations of Lift Forces and Power of Air Cushion Vehicles," The work of the Central Scientific Research Institute of the Maritime Fleet, Hydromechanical Engineering in Boats, Copy 49, "Sea Transport," 1963.

16. Dorfman, A. Sh. and M. I. Sajkovski, "A Rough Method for Calculation of Loss in Curvilinear Diffusers with a Cut-Off of Flow," *Promyshlennaya Aerodinamika*, Issue 28, *Mashinostroenie*, 1966.

17. D'Yachenko, V. K., "Wave Resistance to Systems of Surface Pressure During Movement," Work of the Leningrad Shipbuilding Institute, Hydromechanics and Ship Theorgy, Issue 52, 1966.

18. Eger, S. M., "The Designing of Passenger Jet Aircraft," *Mashinostroenie*, 1964.

19. Egerov, A. A. and B. M. Shojkhet, "Transport ACV's Abroad," Science Research Institute of Information for the Automobile Industry, 1967.

20. Zhukovski, N. E., *O Reaktsii Vtekayushchey I Vytekayushchey Zhidkosti* [On Reactions to Discharge and Leakage of Fluids], Collected Works, Vol. III, State Publishing House for Tactical-Technical Literature, 1949.

21. Kabanski, V. V., "Design of a Craft of Balloon-Type Construction and Outfitted with an Envelope of Air," Joint Scientific and Technical Publishing House, 1936.

22. Kalitievski, L. F., *K Aercdinamicheskomu Raschety Apparatov Na Vozdushnoy Podushke* [Aerodynamic Calculations for ACV's], From the collection "Aircraft Engineering and Mechanics of the Air Force," Published by the Kharkov State University at Kharkov, Issue 6, 1966.

67. Everest, I. T., "Factors Affecting Hovercraft Performance at Low Speed over Water," Hovering Craft and Hydrofoil, Nol. 3, No. 11--12, 1964.

68. Hayward, L. H., "The History of Air Cushion Vehicles," London, 1963.

69. Jones, D. J. G., "Hovering Performance of Plenum Chamber GEMs Over Land and Water," J. Aircraft, Vol. 3, No. 4, 1966.

70. Kuhn, R. E., A. W. Carter and R. O. Schade, "Over-Water Aspects of Ground-Effect Vehicles," IAS Paper, No. 60, 1960.

71. Keiler, L. L., "Hovercraft Research at Royal Aircraft Establishment," Bedford, Hovering Craft and Hydrofoil, Vol. 6, No. 12, 1967.

72. Mair, W. A., "The Physical Principles of Hovercraft," in Hovering Craft and Hydrofoil, Vol. 4, No. 3, 1964.

73. Neuman, I. N. and F. A. P. Poole, "The Wave Resistance of a Moving Pressure Distribution in a Channal," Schiffstechnik, Vol. 9, No. 45, 1962.

74. Postle, R. S. and H. Mankuta, "Performance Comparisons of Propulsion Systems for a Peripheral-Jet GEM," Proc. of the Nat. Meeting on Hydrofoils and ACV's, Washington, September 17-18, 1962, New York, 1962.

75. Stanton Jones, R. S., "Hovercraft Skirt Development," an Engineering, and Performance Review, Quarterly Transactions of the Royal Institution of Naval Architects, October 1968.

76. Thomson, G. J., "The Design and Development of Hovercraft Machinery," Hovering Craft and Hydrofoil, Vol. 7, No. 3, 1967.

77. Walker, N. K., "Some Notes on the Lift and Drag of GEMs," Proc. of the National Meeting on Hydrofoils and ACV's, Washington, Sept. 17-18, 1962, New York, 1962.

78. Walker, N. K., "The Influence of the Fan. and Ducting Characteristics on the Stability and Performance of GEM," Journal Aircraft, Vol. 2, No. 1, 1965.

79. "Symposium on Ground Effect Phenomena," The Princeton University Conference at the Department of Aeronautical Engineering in Co-operation with U. S. Army TRECOM, 1959.

80. "Janes Surface Skimmer Systems," London, 1967.

81. "Air-Cushion Vehicles," Vol. 6, No. 39, 1965.

82. "Air Cushion Vehicles," Vol. 8, No. 49, p. 52, 1966.

83. "Air Cushion Vehicles," Vol. 6, No. 42, 1965.

84. "Air Cushion Vehicles," Vol. 4, No. 20, 1964.

85. "Air Cushion Vehicles," Vol. 10, No. 63, 1967.

86. "Air Cushion Vehicles," Vol. 5, No. 25, 1964.

87. "Air Cushion Vehicles," Vol. 6, No. 37, p. 33, 1965.

88. "Aerospace Engineering," Vol. 20, No. 2, 1961.

89. "Aerospace Engineering," Vol. 21, No. 4, 1962.

90. "Astronautics and Aeronautics," No. 10, 1965.

91. "Bureau of Ships Journal," Vol. 12, No. 12, 1963.

92. "Engineering," Vol. 205, No. 5313, 1968.

93. "Hovering Craft and Hydrofoil," Vol. 3, No. 11-12, 1964.

94. "Hovering Craft and Hydrofoil," Vol. 3, No. 10, 1964.

95. "Hovering Craft and Hydrofoil," Vol. 4, No. 3, 1964.

96. "Hovering Craft and Hydrofoil," Vol. 4, No. 8; Vol. 5, No. 2, 1965.

97. "Hovering Craft and Hydrofoil," Vol. 3, No. 2-3, 1963.

98. "Hovering Craft and Hydrofoil," Vol. 7, No. 1, 1967.

99. "Hovering Craft and Hydrofoil," Vol. 4, No. 3-4, 1965-66.

100. "Hovering Craft and Hydrofoil," Vol. 2, No. 9, 1963.

101. "Hovering Craft and Hydrofoil," Vol. 7, No. 10, 1968.

102. "Hovering Craft and Hydrofoil," Vol. 4, No. 1, 1964.

103. "Marine Engineer and Naval Architect," Vol. 86, No. 1051, 1963.

104. "Marine Engineering/Log;" Vol. 71, No. 4, 1966.

105. "Naval Engineers Journal," Vol. 78, No. 3, 1966.

106. "Naval Engineers Journal," Vol. 79, No. 4, 1967.

107. "Shipbuilding and Shipping Record," Vol. 122, No. 10, 1968.

108. "Journal Aero/Space Sci.," Vol. 28, No. 1, 1961.